Expeditions in Siberia in 1999

Edited by Volker Rachold

Russian-German Cooperation SYSTEM LAPTEV SEA 2000:
The Expedition LENA 1999

by the participants of the expedition
edited by Volker Rachold and Mikhail N. Gregoriev

EURASIAN ICE SHEETS:
German-Russian Expedition Polar Ural '99

by Wolf-Dieter Hermichen, Anette Gierlichs, Frank Wischer and Dmitry Bolshiyanov

Ber. Polarforsch. 354 (2000)
ISSN 0176 - 5027

Volker Rachold, Wolf-Dieter Hermichen & Frank Wischer, Alfred-Wegener-Institute for Polar and Marine Research, Research Department Potsdam, PO Box 60 01 49, D-14401 Potsdam, Germany

Anette Gierlichs, Alfred-Wegener-Institute for Polar and Marine Research, Columbusstrasse D-27568 Bremerhaven

Mikhail N. Grigoriev, Permafrost Institute, Russian Academy of Sciences 677018 Yakutsk, Yakutia, Russia

Dmitry Bolshiyanov, Arctic and Antarctic Research Institute, Bering St. 38, 199397 St. Petersburg, Russia

Contents

Russian-German Cooperation SYSTEM LAPTEV SEA 2000:

The Expedition LENA 1999

by the participants of the expedition

edited by Volker Rachold and Mikhail N. Grigoriev

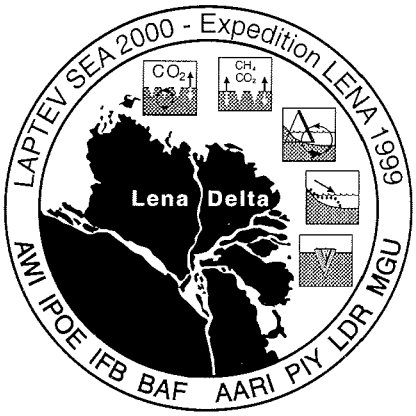

Volker Rachold, Alfred-Wegener-Institute for Polar and Marine Research,
Research Department Potsdam, PO Box 60 01 49, D-14401 Potsdam,
Germany

Mikhail N. Grigoriev, Permafrost Institute, Russian Academy of Science
677018 Yakutsk, Yakutia, Russia

Contents

1 Introduction

(V. Rachold and M. N. Grigoriev)

Our knowledge of the Arctic climate system has been significantly improved through multi-disciplinary investigations carried out in the Siberian Arctic during previous Russian-German projects, such as THE LAPTEV SEA SYSTEM (1994-1997) and TAYMYR (1994-1997). The results are presented in a collection of papers published by Kassens et al. (in press).

Detailed climatic reconstructions of the late Quaternary and important information concerning the complex modern system were obtained and form the basis for the prediction of future climate changes. The investigations documented that the closely coupled land-ocean system of the Laptev Sea with the East Siberian hinterland and its complex connections, such as the Lena Delta, represent a key region for understanding environmental changes. Our present knowledge indicates that environmental changes in this area not only affect the Arctic Ocean but also contribute to variations in the global system.

The Project SYSTEM LAPTEV SEA 2000 is based on these results but addresses completely new scientific problems as well. The following subjects are studied:

A. Seasonal variability of modern fluxes in permafrost areas
   - balance of greenhouse gases (carbon dioxide and methane) and process studies of the methane cycle
   - water and energy flux in permafrost soils
   - microbial communities and carbon dioxide flux in permafrost soils

B. Environmental reactions of the terrestrial-marine system of the Siberian Arctic during the last 100 years
   - marine environmental reactions and material balance
   - atmospheric input of radio-nuclides
   - sensibility of marine Arctic ecosystems

C. Land-ocean interactions and the influence on the sediment budget of the Laptev Sea
   - environmental and climatic history of the Lena Delta
   - particle transport in the delta-shelf system

D. Terrestrial system: short- and medium-term climatic trends in the Siberian Arctic
   - terrestrial climatic signals in ice-rich permafrost deposits

E. Marine system: long-term climatic trends in the Siberian Arctic
   - causes and consequences of short- and medium-term climatic trends in permafrost regions
   - acoustic signatures of submarine permafrost

Within the framework of the project SYSTEM LAPTEV SEA 2000 the first terrestrial expedition to the Lena Delta was performed during summer 1998

(Rachold and Grigoriev, 1999). Based on the experiences and results of this first expedition, the second expedition LENA 99 was carried out from April 26 to September 19, 1999. A multi-disciplinary, Russian-German team of 42 scientists worked in the Lena Delta, on the New Siberian Islands and in the Laptev Sea coastal region (Figure 1-1). The expedition LENA 99 was organized by the AWI-Potsdam in close co-operation with the Arctic and Antarctic Research Institute, St. Petersburg, the Permafrost Institute, Yakutsk, and the Lena Delta Reserve, Tiksi.

The scientific program of the expedition covered the terrestrial research objectives of the project SYSTEM LAPTEV SEA 2000, i.e.:

A. Seasonal variability of modern fluxes in permafrost areas (→ *Chapter 3: Modern Processes in Permafrost Affected Soils*)

C. Land-ocean interactions and the influence on the sediment budget of the Laptev Sea (→ *Chapter 4: Coastal Processes in the Laptev Sea and the Environmental History of the Lena Delta*)

D. Terrestrial system: short- and medium-term climatic trends in the Siberian Arctic (→ *Chapter 5: Paleoclimate Signals of Ice-rich Permafrost*)

References

Kassens, H., Bauch, H., Dmitrenko, I., Eicken, H., Hubberten, H.-W., Melles, M., Thiede, J. and Timokhov, L. (1999), Land-Ocean systems in the Siberian Arctic: dynamics and history. Springer, Berlin, 711pp.

Rachold, V. and Grigoriev, M. N. (1999): Russian-German Cooperation SYSTEM LAPTEV SEA 2000: The Lena Delta 1998 Expedition. Rep. Polar Res. 316, 1-259.

Acknowledgments

The success of the expedition LENA 99 would have not been possible without the support by several Russian, Yakutian, and German institutions and authorities. In particular, we would like to express our appreciation to the Tiksi Hydrobase and the Lena Delta Reserve, special thanks to D. Melnichenko and D. Gorokhov. The members of the expedition wish to thank the captain of RV Dunay and his crew and the staff of the biological station Samoylov.

The expedition was funded by the German and Russian Ministries of Science and Technology (BMBF-Verbundvorhaben SYSTEM LAPTEV-SEE 2000, LAPEX).

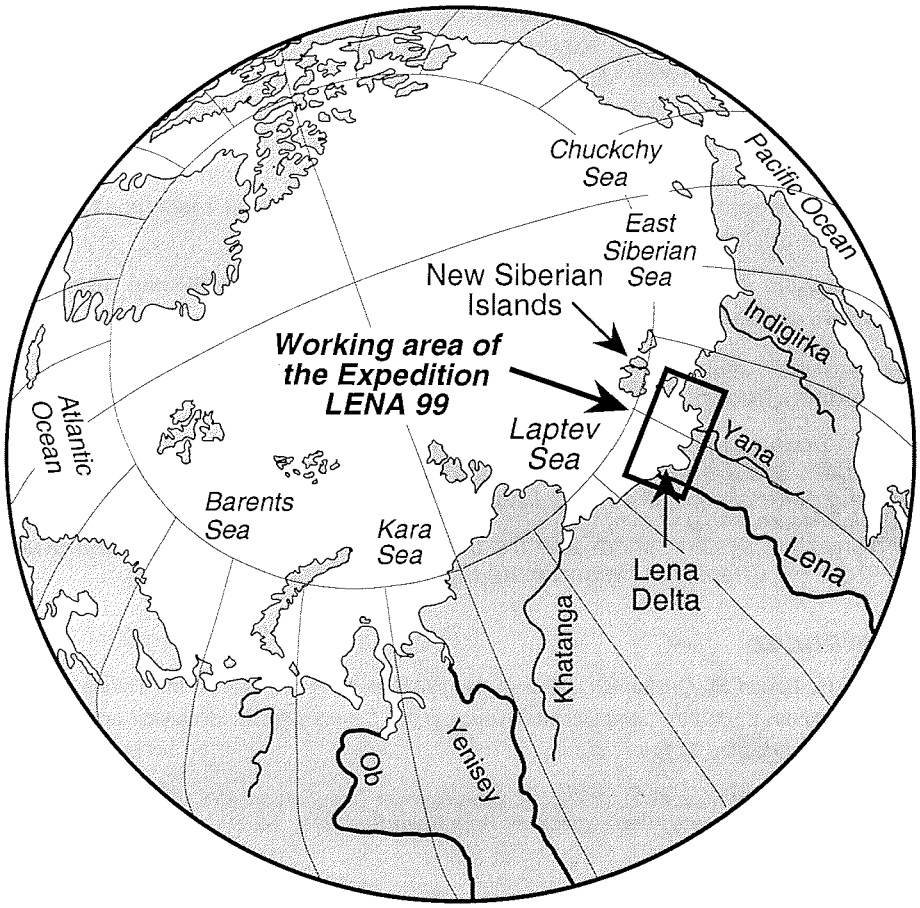

Figure 1-1: Map showing the location of the working area of the expedition LENA 99.

2 Expedition Itinerary

(V. Rachold and M. N. Grigoriev)

2.1 Selection of working areas

With respect to the scientific program, the expedition group had been divided into several teams prior to the expedition. For each team specific working areas, shown in Figure 2-1, had been selected.

Team 1 (Samoylov Island), which concentrated on modern processes of permafrost affected soils, used a biological station of the Lena Delta Reserve on the island Samoylov in the central part of the Lena Delta. The field work was carried out close to the station on Samoylov Island. In order to cover both winter and summer conditions, continuous measurements were carried out from the beginning of May to the beginning of September. For that reason, the Samoylov team was divided into three sub-teams (team 1 a-c).
Samoylov station is equipped with a kitchen, a dining room, some living rooms that were used as laboratories and a sauna. The participants lived in small tents during the expedition. A cook was provided by the Lena Delta Reserve.

(→ *Chapter 3: Modern Processes in Permafrost Affected Soils).*

Team 2 a (Arga Island) and **2 b (RV Dunay)** focused on modern and ancient sedimentation in the Lena Delta and the Laptev Sea coast. The objectives were to understand the genesis of deep lakes of the Arga Island in the western Lena Delta (Team 2a: Arga Island) and to quantify the material input to the Laptev Sea by coastal erosion (Team 2b: Dunay).
The field work of team 2a was carried out during winter conditions in early May in order to carry out lake sediment coring and ground penetrating radar studies from the ice-cover of the lake. A tractor sledge including a bullock with living rooms for the participants was used for transportation.
Team 2 b was based aboard the vessel Dunay. During the summer season coastal erosion studies were performed around the Lena Delta and along the coastline of the eastern Laptev Sea. The vessel Dunay, which was chartered from the Tiksi Hydrobase, is constructed for navigation work in the delta and in the coastal regions of the Laptev Sea. The participants of the expedition lived in one of the cabins of the ship. The ship is provided with a dining room, a cook and a shower. Two motorboats for the work in shallow regions were available.

(→ *Chapter 4: Coastal Processes in the Laptev Sea and the Environmental History of the Lena Delta*)

For their paleoclimatic/paleoecological work program carried out during the summer season **team 3 (Lakhovsky Island)** had chosen an outcrop at the southern coast of the Island Bolshoy Lyakhovsky. The 2 km wide and 30 m high ice-complex was studied and sampled in detail. The Lyakhovsky team lived in a field camp.

(→ *Chapter 5: Paleoclimate Signals of Ice-rich Permafrost*)

Team 4 (Olenyokskaya Channel) carried out paleogeographical investigations along the Olenyokskaya Channel in the western part of the Delta during the summer season. Rubber boats were used for transportation and the participants lived in a field camp.

(→ *Chapter 4: Coastal Processes in the Laptev Sea and the Environmental History of the Lena Delta*)

Team 5 (Bykovsky Peninsula) completed the paleontological work on Bykovsky Peninsula, which was started during the expedition LENA 98. The team lived in a field camp on Bykovsky Peninsula during summer.

(→ *Chapter 5: Paleoclimate Signals of Ice-rich Permafrost*)

2.2 General logistics and transport

The general logistics of the LENA 1999 Expedition were jointly organized by the Permafrost Institute (Yakutsk), the Arctic and Antarctic Research Institute (St. Petersburg) and the Research Unit Potsdam of the Alfred Wegener Institute. Logistic operations in Tiksi (renting of busses, trucks, helicopters etc.) were organized by the Tiksi Hydrobase.

Due to the long duration of the field work and the large number of participants very complex logistic operations had to be organized. Figure 2-2 shows the timetable and the transport logistics.

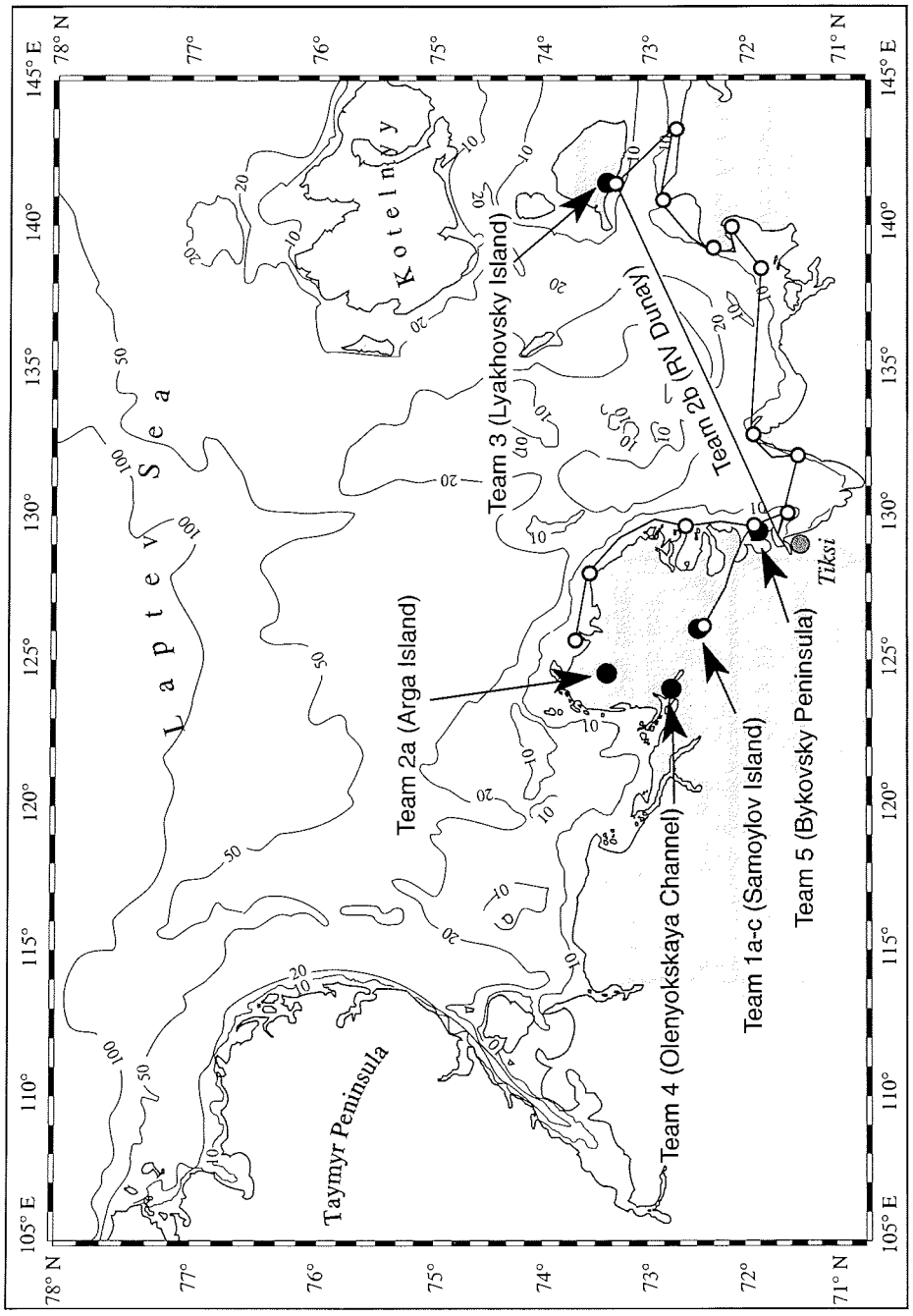

Figure 2-1: Location map of the expedition LENA 99.

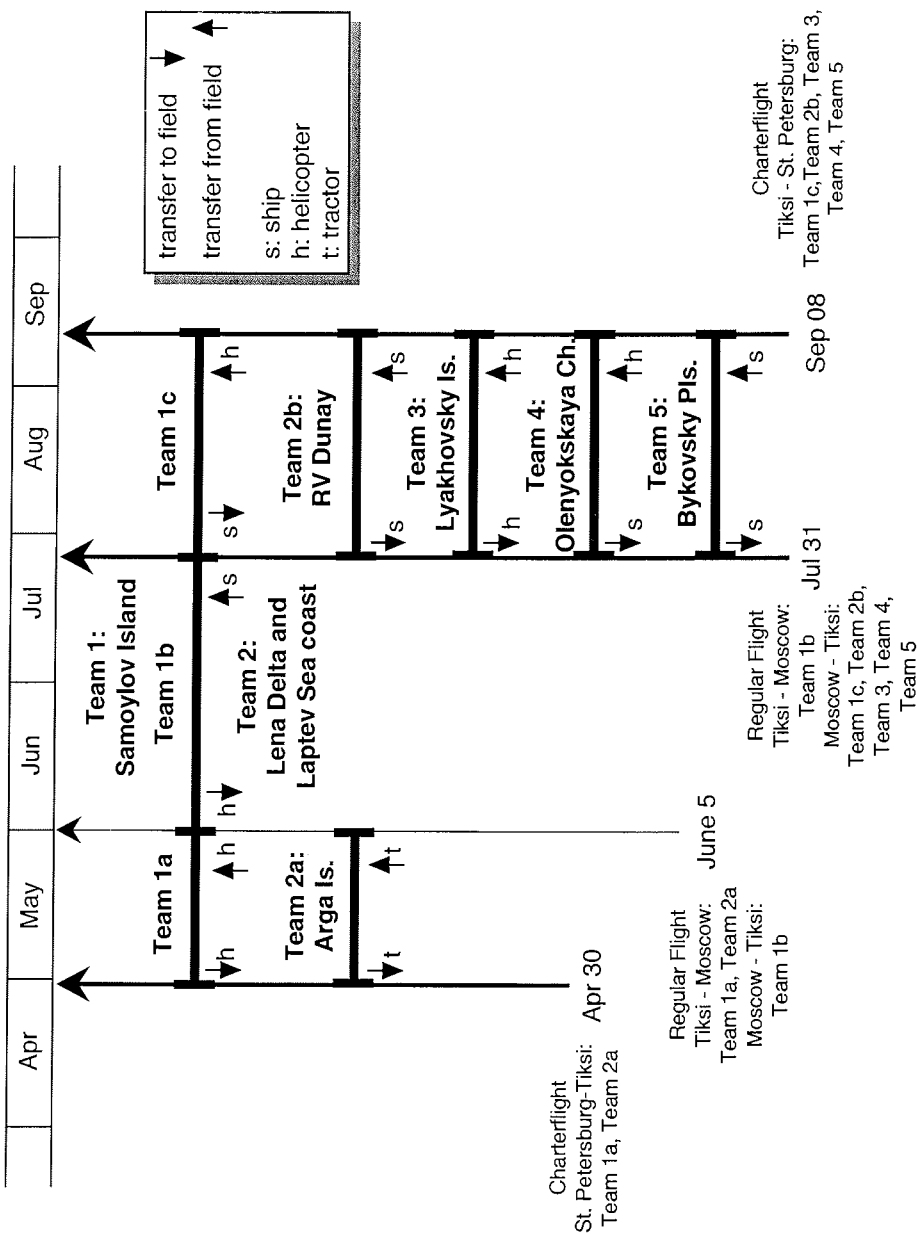

Figure 2-2: Timetable and transport logistics of the expedition LENA 99.

2.3 Timetables of individual working groups

2.3.1 Team 1 (Samoylov Island)

Team 1a

May 2	transport of equipment to Samoylov with two trucks; return to Tiksi
May 3-6	waiting in Tiksi
May 7	flight to Samoylov by military helicopter
May 8	set up of laboratory; check of automated soil and climate stations on Samoylov
May 9 –25	field work: data collection on soil thermal and hydrologic dynamics; snow, soil, gas and water sampling, snow surveys
May 22:	arrival of team 2a (Schwamborn & Schneider) on Samoylov
May 23-24	drilling of permafrost cores
May 26	packing of equipment and samples and waiting for helicopter
May 27	flight to Tiksi by helicopter

Team 1b

June 05	transfer Tiksi-Samoylov by helicopter, first inspection of the investigation sites
June 06	beginning daily gas sampling for CH_4 andCO_2 emission, daily soil monitoring at plot 3 (temperature, water table, permafrost table); checking the sites and the instruments
June 07	installation of the gas chromatograph, calibration of FID-detector and first analysis of gas samples; taking samples from plot 2, logger start; test measurements with the GPR-system, installing a polygon measuring field
June 08	calibration of the WLD-detector; starting the routine measurements (depth of active layer, TDR- and temp.-data); starting GPR with 500MHz
June 09	each second day analysing of gas samples by gas chromatography; taking samples from plot 3 (nuncs and vacutainer)
June 10	calibration of the gas exchange system
June 11	taking samples from plot 2; GPR along the transect t (500MHz), installing new measureing field close to plot 2
June 12	starting gas exchange analysis every second day; start of weekly GPR measurments at both investigation sites
June 13	beginning TDR and temperature monitoring each second day at plot 2 and 4
June 14	working as lumerjack for the banja; first GPR measurments at 800 MHz
June 15	taking samples from plot 2 and 4 (vacutainer)
June 17	beginning gas sampling for analysis CH_4 and CO_2 emission at plot 4 each second day
June 18	beginning of water sampling (tundra lake) once a week and inspection of automatic weather and soil station (plot 3)
June 19	taking samples from plot 3
June 20	taking samples from plot 3; new transect from permafrost cellar to the edge of the island, investigating it with both antennas
June 21	first mosquito attacks, taking samples from plot 3; GPR: transect t at 800 MHz
June 22-23	measuring the thawing depth at polygon site used for GPR measurements
June 25	determination of soil respiration; new GPR high center investigation site, using both antennas
June 26	expedition to Stolb mountain; thawing depth measurements at GPR site close to plot 2
June 27	beginning of 3 day digging for a new profile at plot 3 for temperature measurements
June 28	installation of automatic station for redox potential measurements at plot 3

June 30	beginning of hourly monitoring of redox potential, monitoring of methane emission, air and soil temperature as well as polygon water concentrations within a day
July 01	Soil repiration determination
July 02	beginning of water sampling from suction lysimeter at plot 2,3 and 4 once a week; finalising temperature profile at plot 3; starting 3 days of GPR measurements with 100 MHz
July 05	determination of in situ CH_4 production activity at plot 3; start of 5 days sample taking at plot 2 and 3
July 10	CMP at 100 MHz
July 11	trip to the grave of the famous American DeLong
July 12	installation and start of CH_4 production and emission measurements from a polygon lake
July 13	preparing the laboratory for the third part of the expedition
July 14	soil respiration determination
July 15	determination of in situ CH_4 production activity at plot 4; taking samples from plot 2; measuring the active layer at the GPR polygon site
July 17	measuring the active layer at GPR site close to plot 2
July 19	taking samples from plot 3
July 20	sandstorm; vacutainer sample taking
July 24	GPR (800 MHz) on transect t
July 25	ship transfer to Tiksi

Team 1c

August 2	Start of the transfer Tiksi/Samoylov with Dunay
August 3	Heavy storm on the Laptev Sea and get stuck on a sandbank
August 4	Arrival on Samoylov, first excursion, installation of the camp, start of the daily methane and carbon-dioxide monitoring and regular water sampling.
August 5-9	Digging of Profile EP1 and sampling
August 9-13	Digging of Profile EP1 and sampling
August 7	Start of lake emission measurements
August 8	Excursion to America Khaya
August 16	Transfer of E.-M. Pfeiffer to Tiksi on board the MS Brise
August 17	Start of the zero degree production/oxidation experiment
August 21	Excursion to Kuringnyakh Sise
August 26-28	Digging of profile near plot 3, sampling
August 27	Visit of RV Dunay
August 28	Short excursion with the group from Dunay on Samoylov
August 29	Excursion to Stolb, leaving of Dunay.
September 3	Digging of profile 4, sampling
September 5	deinstallation of automatic station for redox potential measurements at plot 3
September 7	deinstallation of several instruments and packing of samples and equipment
September 8	return to Tiksi by helicopter

2.3.1 Team 2a (Arga Island)

May 1	departure from Tiksi (21.00h local time) by sledge transport
May 6	arrival at Lake Nikolay (Western Lena Delta)
May 7-9	drilling of core A1, radar profiling r1-r6 (25-MHz-antennae), lake sediment sampling with gravity corer (AARI activities)
May 10-11	bad weather conditions
May 12-16	drilling of cores A2-A5, radar profiling r9-r13 and CMP measurements (100-MHz-antennae), lake sediment sampling with gravity corer (AARI activities)
May 17	departure from Lake Nikolay

May 19	radar profiling r20 and CMP measurements (100-MHz-antennae) at the mouth of Trofimofskaya channel
May 21	radar profiling r30+r31 (100-MHz-antenna) at the mouth of Bykowsky channel and on Mammontovy Khayata
May 22	radar profiling r40 and CMP measurements (100-MHz-antennae) in Ivashkina Laguna (Bykovsky Peninsula)
May 22	drilling of lagoon deposits in Ivashkina Laguna (Bykovsky Peninsula)
May 22	arrival in Tiksi and departing for Samoylov Island (vehicle transport)
May 23	arrival on Samoylov Island
May 24	radar profiling r50 and CMP measurements (100-MHz-antennae)
May 25-26	activities with the Samoylov group (Team 1a)
May 27	departure from Samoylov Island and arrival in Tiksi (by helicopter)

2.3.1 Team 2b (RV Dunay)

August 6	loading RV Dunay
August 7	transfer of Team 5 to Bykovsky Peninsula
August 8	cruise to Kuba Island (northern Lena Delta)
August 9-12	geodetic measurements on Kuba Island, shallow seismic profiles and sediment sampling off the coast
August 12	cruise to Tumat Bay, bad weather conditions (fog)
August 13	impossible to reach the coast due to very strong wind, cruise to Sardakh Channel
August 14	good weather conditions, seismic profiles and sediment sampling across the Sardakh Channel and in the Laptev Sea, geodetic measurements on nameless island near the mouth of Sardakh Channel
August 15	cruise to Bykovsky Channel, geodetic measurements on small island, visit of the Bykovsky Team, cruise to Muostakh Island
August 16	geodetic measurements on Muostakh Island, cruise to Tiksi
August 17	transfer of two participants (H.-W. Hubberten and E.M. Pfeiffer) to Tiksi airport
August 18	cruise to Buorchaya Bay with Dunay
August 18-19	geodetic measurements along the coastline, seismic profiles of the coast, cruise toVankina Bay
August 20	seismic profiles and sediment sampling in the Vankina Bay
August 21	cruise to Makar Island, geodetic measurements on the island
August 22	cruise to Sherokastan Peninsula, geodetic measurements along the coast
August 23	bathymetric studies off Sherokastan Peninsula
August 24-25	cruise to Svetoy Nos, waiting for ice-breaker to Kotelnyy
August 26	cruise to Dmitry Laptev Strait, seismic profiles and sediment sampling in the strait
August 27	cruise to Bolshoy Lyakhovky Island, visit of team 3, geodetic measurements
August 28	cruise back to Svetoy Nos to meet ice-breaker
August 29	radio-information that ice-breaker will not go to Kotelnyy, cruise back to Tiksi
August 30	arrival in Tiksi
August 31	meeting of visitors (J. Thiede, W. Benz, H. Bauch) at Tiksi airport, cruise to Bykovsky Peninsula and after that to Samoylov Island
September 1	visit of Samoylov team, collecting water samples
September 2	excursion to Stolb Island
September 3	visit of Lena-Nordensheld station, collecting water samples, cruise to Bykovsky Peninsula, in the evening meeting with the Marine Group on board RV "Yakov Smirnitskiy"
September 4	visit of the Bykovsky team, in the night cruise to Muostakh Island
September 5	visit of Muostakh Island, cruise back to Tiksi

2.3.3 Team 3 (Lyakhovsky Island)

August 4: Transfer from Tiksi to Bol'shoy Lyakhovsky Island via Nishneyansk with 2 Helicopters, camp installation

August 5: Installation of the camp and the radio station; first overview trip to the western part of the study area (section R)

August 6: First overview trip to the eastern part of the study area (section L); installation of markers along the coastal and shore lines in distances of 100 m; start of precipitation sampling for stable isotope study

August 7: Survey of markers with GPS and theodolith

August 8: Detailed reconnaissance of section R; determination of the main units and the special study points; survey and sampling of ice wedges for stable isotope and hydrochemistry analysis at section R 19, study and sampling of the subaerial "Kuchchuguy" in section R 6+70

August 9-10: Collecting fire wood for the next weeks by the whole expedition group; cleaning of section R 17 by water pump; geocryological and cryolithological survey and sampling of sediments and for OSL-dating of section R 17; survey and sampling of ice wedges with ice screws and chain saw at the upper boundary of "Kuchchuguy" in section R6, R 8, R 9 and R 17

August 11-13: Geocryological and cryolithological survey and sampling of sediments and for OSL-dating in the first, second and third thermo-erosional cirque; survey and sampling of ice wedges in section R 7 and in the second thermo-erosional cirque; start of laboratory work for hydrochemistry studies (pH, conductivity, separation of samples for anion/cation and stable isotope analysis); sampling of surface water; screening of big samples for insect and rodent studies; survey of the outcrop in section R with the theodolith

August 14: Camp and lab day; separations and saving of sediment samples

August 15: Field studies of ice wedge and texture ice samples, survey and sampling of ice wedges in the second thermo-erosional cirque; screening for insect studies section R 8

August 16: Survey and sampling of section R 17+30 ("Olyor"/"Kuchchuguy") with the whole group; sampling of an old peat profile near the sea level in section R 8+50; continuation of working on ice wedges of the second thermo-erosional cirque, thermokarst studies of alas deposits in section R 33

August 17: Geocryological and cryolithological survey and sampling of sediments sedimentological studies and for OSL-dating in the first thermo-erosional cirque; termination of ground ice study in the second thermo-erosional cirque; preparation of the first general scheme of section R

August 18: Collecting fire wood for the following weeks; geocryological and cryolithological survey and sampling of alas deposits and taberites in section R 22+60; excavation and survey of recent soil profiles, sampling of ground water

August 19: Geocryological and cryolithological survey and sampling of alas deposits in section R 33; survey and sampling of ice wedges in section R 10

August 20: Lab day; continuation of ice wedge study in section R 10; ground ice sampling for Be-isotope study with the chain saw; description of section L

August 21: Geocryological and cryolithological survey and sampling of the boundary "Kuchchuguy"/Ice Complex in section R 9+85; survey and sampling of ice wedges in section R 22 ("Kuchchuguy" and taberites)

August 22-24: Three days foot-trip of three members of the expedition (Kunitsky, Grosse, Schirrmeister) to Khaptagai Tas hill; study of recent snow patch area; survey and sampling of ice wedges in the third thermo-erosional cirque and in section R 20 (log); ice structure analysis; description of the far area of the sections L and R

August 25-26: Camp and lab day; sampling for OSL-Dating in section R 9+95; Geocryological and cryolithological survey and sampling of valley deposits (log) in section R 19; ice structure analysis; thermokarst study of alas deposits in section L

August 27: Visit of the "Dunay" team; documentation of the whole coastal profiles in section R and L and recovery of big bones by motor boat, Transfer of first complete sample series to Tiksi

August 28: Sampling of paleosols in section R; Mapping of the most important geomorphologic units in the area of section R; determination of the main units and the special study points in section L; survey and sampling of ice wedges and ice structure analysis in section L 21 (alas)

August 29: Geocryological and cryolithological survey and sampling of two alas profiles in section L 11 - L 14; sampling for OSL-dating; termination of ice wedge study in section L 21 and study of section L 2 (fluvial deposits)

August 30-31: Lab day; geocryological and cryolithological survey and sampling of an alas profile in section L 21+50

September 1: Final overview-trip to section R, exkursion to a known location of well preserved mammoth remains on the Zimov'e River bank; geocryological and cryolithological survey and sampling of fluvial deposits in section L 3; installation of an ice cellar for large ice samples; description of the Ice Complex in Section L

September 2-4: Packing up of samples and equipment, sawing of mammal bones; Modulation of sampling co-ordinates and lists, completion of the general profile schemes, preparation of a columnar section for the study area; sampling of a peat profile below the Ice Complex in section L 9

September 5: Description of section R with new and better outcrop conditions after a big storm, sampling of the weathering crust in section R 13+50

September 6: Dismantling of the camp

September 7: Transfer to Tiksi via Nishneyansk with two Helicopters

2.3.1 Team 4 (Olenyokskaya Channel)

August 3-4 tranfer from Tiksi to Samoylov Island by RV Dunay

August 5 preparation of rubber boat and motor and packing of equipment and foodstuffs for cruise by Olenyokskaya Chanel. Pollen trap station L-3 was taken off on Samoylov Island.

August 6 cruise from Samoylov Island to Gusinca - a biological station of the Lena Delta Reserve on the Kuogastakch-Aryta Island in south-west part of Lena Delta. By the way preliminary survey of the shore outcrops of Olenyokskaya Chanel in locality Buor-Kchaya.

August 7 geological and geomorphological investigations of banks of Tyuerenkey-Tebyulege Chanel and Arynskaya Chanel and preliminary survey of the shore outcsops of norht part of Jangylakch-Sis Island.

August 8-9 geological and geomorphological investigations of the high flood plain in south part of Jangylakch Island, sampling of lake sediments.

August 10 geological and geomorphological investigations of shores of the small chanels around Jangylakch-Sis Island. Studies and sampling of one permafrost section in north part of Jangylakch-Sis Island

August 11 packing of equipment and cruise from Gusinca to south-west part of Kchardang-Sise Island

August 12-13 delivery of equipment to Byracan-Kyuele Lake (south-west part of Kchardang-Sise Island), sampling of lake sediments and geomorphological investigations in the vicinity of Byracan-Kyuele Lake.

August 13 cruise from Kchardang-Sise Island to Nagym in the west part of Lena Delta - Kyuryuelyakch-Sis Island

August 14	levelling along the line and placing hydrologikal post for measuring of water level in Olenyokskaya Chanel
August 15-16	hourly observations for level of water on the hydrologikal post, geological and geomorphological investigations in the west part of Kyuryuelyakch-Sis Island
August 17	sampling of one permafrost section along Olenyokskaya Chanel, packing of equipment and samples for cruise from Nagym to Gusinca.
August 18	cruise from Nagym to Gusinca, sampling for 14C-dating from the shore outcrops of first above the flood plain terrase by the way
August 19	sampling of permafrost section of the first above the flood plain terrace in the vicinity of Gusinca
August 20-21	delivery of equipment to Jangylakch-Sisin-Kyuele Lake (Jangylakch-Sis Island) and sampling of lake sediments and geomorphological investigations in the vicinity of Jangylakch-Sisin-Kyuele Lake.
August 22	packing of equipment and samples for cruise from Gusinca to Buor-Kchaya
August 23	stay in Gusinca because of bad weather conditions. Pollen trap station L-2 was taken off by employee of the Lena Delta Reserve in Sagastyr Is.
August 24	cruise from Gusinca to Buor-Kchaya, sampling for 14C-dating from the shore outcrops of first above the flood plain terrase by the way, camp construction in Buor-Kchaya, visit of Samoylov Island
August 25	team was divided into two groups in twos members in every group for geological and geomorphological investigations in the vicinity of Buor-Kchaya and cruise from Samoylov Island to Yugus-Yie (Yeppiries Is.) - central part of Lena Delta. Pollen trap station L-1 was taken off in Yugus-Yie.
August 26	geological studies of the shore outcsops of right bank of Olenyokskaya Chanel in the vicinity of Buor-Kchaya, studies and sampling of permafrost section of second above the flood plain terrace in the right bank of MalayaTumatskaya Chanel.
August 27-29	for geological and geomorphological investigations in the vicinity of Buor-Kchaya (Olenyokskaya Chanel) and by chanels of central parrt of Lena Delta from Malaya Tumatskaya Chanel to Arynskaya Chanel with sampling for 14C-dating from the shore outcrops of the high flood plain and the first above the flood plain terrase by the way
August 30	work wasn't possible because of bad weather conditions (very strong wind - sandy storm)
August 31	end of cruise from Yugus-Yie to Samoylov Is., visit of Samoylov Is.
September 1	sampling of the ice wedge of ice-complex for methane concentration and for stable isotope analysis in Buor-Kchaya. Work was carried out together Samoylov Group.
September 2	sampling of one permafrost section in Buor-Kchaya, packing of samples and equipment, dismanting of the camp, return tc Samoylov Is., loading of the equipment on the board of the vessel Dunay.
September 3	leaving Samoylov Is. on the board of Dunay for excursion to Bykovsky Peninsula
September 4	excursion to Bykovsky Peninsula
September 5	excursion to Muostakch Island, shipping back to Tiksi

2.3.4 Team 5 (Bykovsky Peninsula)

August 7-8	shipping by 'Dunay' from Tiksi to the Bykovsky Peninsula (Siegert/Kunitsky '98 camp site), loss of part of the team's equipment and food (later compensated by the team 2b) in the landing accident under stormy weather, camp construction
August 9	emergency revision, drying, and repair of equipment and food supply, camp construction
August 10	first overview inspection of the Mamontovy Khayata cliff exposure, search of poorly preserved '98 landmarks and realising that a new survey is necessary

August 11-12	storm and rain, planning the site survey, preparation of the land markers, visit and emergency staying on by P.Nikolskiy and A.Basilyan with their experimental 6-wheel cross-country vehicle
August 13-14	theodolite survey of the NW half of the Mamontovy Khayata cliff, selection of the profile for detailed study at the topmost part of the cliff, test sampling for macrofossils in the upper part of Ice Complex, fossil bone collecting
August 15	calculation of the survey and building of the new site plan and profile, correlated with the old one, test screening for macrofossils, brief visit by 'Dunay' and the AWI-Potsdam Chief with the team 2b, excursion across the site area and the Ice Complex with Prof. H.-W. Hubberten
August 16	storm and rain, sampling and screening for macrofossils in the upper level of Ice Complex
August 17-21	investigation of the Ice Complex profile from the top of the Mamontovy Khayata cliff to the depth 17 m (Sartanian and end-Karginian) along the sequence of baidzherakhs H-F - description and sediment sampling, primary sample processing, bone collecting at the cliff and low-tide bars
August 22	excursion along the coast to the NW edge of the Mamontovy Bysagasa alass and the next Yedoma, bone collecting and search for a white whale modern carcass
August 23	completing of regular sampling of the main sequence (H-F), control instrumentary levelling of the profile
August 24-25	processing of the collected samples (sampling for pollen, drying, sampling for AMS)
August 26	sampling of the main sequence for plant, insect, and other macrofossils, selection of additional profiles to fill the gap in the main one (ice wedge crossing), study of soil profiles on top of the Yedoma (description, sampling) on Dr. E.-M. Pfeiffer request
August 27	processing of the collected samples (sampling for pollen, drying, sampling for AMS), search for bones in the upper part of the Mamontovy Khayata Ice Complex
August 28	photographic survey (documentation) of the Mamontovy Khayata section, excursion to the exposures in 2.2 km SE from the Camp, screening of macrofossil samples
August 29-31	processing of the collected samples (sampling for pollen, drying, sampling for AMS), screening of macrofossil samples, search for bones in the upper part of the Mamontovy Khayata Ice Complex, additional detailed study of the main profile and its photographic survey
August 31	arrival of 'Dunay' and landing of the Team 2b (Erosion Group)
September 1	sampling and description of the additional profile of baydzherakh E to fill the gap in the main profile, taking more samples for macrofossil screening in the main profile, discovery of in situ bones in baydzherakhs Ma1 and Ma2 (near '98 RP 4.9)
September 2	processing of the collected samples, screening of macrofossil samples, discovery of baby mammoth skull in baydzherakh Ma1
September 3	processing of the collected samples, screening of macrofossil samples, excavation of baby mammoth skull, meeting with the Marine Group on board RV "Yakov Smirnitskiy"
September 4	excavation of baby mammoth skull, lecture and excursion to the Mamontovy Khayata Ice Complex with the German visitors (Prof. J.Thiede, Dr. H.Bauch, Dr. W. Benz, sample and bone packing
September 5	sample and bone packing, shipping by 'Dunay' back to Tiksi

2.4 Appendix

Table A2-1: List of participants.

Name	email	Institution	Team
Irina Akhmadeeva	tikzap.sakha@rex.iasnet.ru	LDR	3
Felix Are	but@peterlink.ru	PSUMOC	2b
Martin Antonow	antonow@geo.tu-freiberg.de	TU-BAF	1a
Henning Bauch	hbauch@geomar.de	GEOMAR	2b
Holger Becker	hbecker@awi-potsdam.de	AWI-P	1c
Winfried Benz		Wiss.Rat	2b
Julia Boike	jboike@awi-potsdam.de	AWI-P	1a
Dmitry Bolshiyanov	bolshiyanov@aari.nw.ru	AARI	2a
Alesksey Bortsov	asher@orc.ru	MGU-G	5
Alexander Derevyagyn	dereviagin@glasnet.ru	MGU-G	3
Victor Dobrobaba		HB-Tiksi	2a, 2b
Marina Dorozhkina	bolshiyanov@aari.nw.ru	AARI	2a, 4
Mikhail Grigoriev	m.n.grigoriev@sci.yakutia.ru	PIY	2a, 2b
Guido Grosse	guido76grosse@yahoo.com	TU-BAF	3
Hans-Wolfgang Hubberten	hubbert@awi-potsdam.de	AWI-P	2b
Dmitry Kozlov	bolshiyanov@aari.nw.ru	AARI	4
Wolfram Kloss	wkloss@ipoe.uni-kiel.de	IPOE	1b
Victor Kunitsky	v.v.kunitsky@sci.yakutia.ru	PIY	3
Anna Kurchatova	a.n.kurchatova@sci.yakutia.ru	PIY	1c
Lars Kutzbach	L.Kutzbach@ifb.uni-hamburg.de	IFB	1c
Svetlana Kuzmina	skuz@orc.ru	SIEE	3
Tatyana Kuznetsova	esin@sgm.ru	MGU-P	3
Hanno Meyer	hmeyer@awi-potsdam.de	AWI-P	3
Dmitry Melnichenko		HB-Tiksi	2a
Elena Pavlova	bolshiyanov@aari.nw.ru	AARI	2a, 4
Eva-Maria Pfeiffer	empfeiffer@awi-bremerhaven.de	AWI-Brhv	1c
Ivan Parmusin	asher@orc.ru	MGU-G	5
Wladimir Pozdnyakov	sterh@yacc.yakutia.su	IBS-LN	4
Wiebke Quass	wquass@ipoe.uni-kiel.de	IPOE	1a
Volker Rachold	vrachold@awi-potsdam.de	AWI-P	2b
Sergey Rasumov	m.n.grigoriev@sci.yakutia.ru	PIY	2b
Andrey Sher	asher@orc.ru	SIEE	5
Lutz Schirrmeister	lschirrmeister@awi-potsdam.de	AWI-P	3
Waldemar Schneider	wschneider@awi-potsdam.de	AWI-P	2a, 2b
Björn Schulz	bschulz@ipoe.uni-kiel.de	IPOE	1c
Georg Schwamborn	gschwamborn@awi-potsdam.de	AWI-P	2a
Igor Syromyatnikov	v.v.kunitsky@sci.yakutia.ru	PIY	3
Jörn Thiede	jthiede@awi-bremerhaven.de	AWI-Brhv	2b
Julia Tsherkasova	tikzap.sakha@rex.iasnet.ru	LDR	1b
Wladimir Tumskoy	tumskoy@orc.ru	MGU-G	3
Aleksey Vlasenko	root@bssys.com	MGU	1c
Bianca Wächter	waechter@merkur.hrz.tu-freiberg.de	TU-BAF	1b
Dirk Wagner	d.wagner@awi-potsdam.de	IFB	1b

Table A2-2: Participating institutions.

AARI	Arctic and Antarctic Research Institute Bering St. 38 199397 St. Petersburg Russia
HB-Tiksi	Tiksi Hydrobase 678400 Tiksi, Yakutia Russia
IBS-LN	International Biological Station "Lena-Nordensheld" 3/1 Dzerzhinsky St. 67700 Yakutsk Yakutia, Russia
LDR	Lena Delta Reserve 28 Academician Fyodorov St. Tiksi 678400 Yakutia, Russia
MGU-G	Moscow State University Faculty of Geology 119899 Moscow Russia
MGU-P	Moscow State University Faculty of Paleontology 119899 Moscow Russia
PIY	Permafrost Institute Russian Academy of Science 677018 Yakutsk Yakutia, Russia
PSUMOC	St. Petersburg State University of Means of Communications 9 Moskovskii 190031 St. Petersburg Russia
SIEE	Severtsov Institute of Ecology and Evolution Russian Academy of Sciences 33 Leninskiy Prospect 117071 Moscow Russia
AWI-Bhrv	Alfred Wegener Institute PO Box 120161 D-27515 Bremerhaven Germany
AWI-P	Alfred Wegener Institute Research Unit Potsdam PO Box 60 0149 D-14401 Potsdam Germany
GEOMAR	Geomar Research Center Wischhofstrasse 1-3 D-24148 Kiel Germany
IPOE	Institute for Polar Ecology University of Kiel Wischhofstrasse 1-3 D-24148 Kiel Germany
IFB	Institute of Soil Science University of Hamburg Allende-Platz 2 D-20146 Hamburg Germany
TU-BAF	Freiberg Academy of Mining and Technology Institute of Geology Bernhard-von-Cotta-Str. 2 D-09596 Freiberg Germany
Wiss.Rat	Wissenschaftsrat Brohler Strasse 11, D-50968 Köln Germany

3 Modern Processes in Permafrost Affected Soils

(E.-M. Pfeiffer, D. Wagner, H. Becker, A. Vlasenko, L. Kutzbach, J. Boike, W. Quass, W. Kloss, B. Schulz, A. Kurchatova, V. I. Pozdnyakov and I. Akhmadeeva)

3.1 General objectives of the soil related investigations

(E.-M. Pfeiffer)

The investigations of the modern processes are focused on the energy an hydrological dynamics and trace gas fluxes (CH_4 and CO_2) of permafrost affected soils in the Lena Delta / Northeast Siberia. The main field works - having started in 1998 - could be finished in the different parts (winter/spring, spring/summer and summer season) of the 99-Expedition. Additional sediment, soil, water, ice and plant samples could be taken for more necessary analysis. The seasonal emission of methane and carbon dioxide from different polygon tundra sites were studied by field experiments and combined with biochemical and microbial process experiments under defined field laboratory conditions. The methane generation in tundra cryosols at near zero temperatures in different soil horizons as well as the influence of the vegetation on gas emission were investigated by special field experiments. The results show the importance of the trace gas emission from permafrost soils for the regional / global methane budget.

The soil related investigations in the Lena Delta are necessary to understand the modern processes of these sensitive ecosystems and to estimate the impact on possible global climate changes. The soil processes will supply the necessary data base for further investigations like studies on permafrost associated gas hydrates or special research on the surviving ability of microorganisms in extreme habitats

3.2 The distribution of soils on Samoylov Island and other comparison sites of the Lena Delta

(I. Akhmadeeva, A. Kurchatova and E.-M. Pfeiffer)

During the Lena Delta Expedition 1999, the soil survey on Samoylov Island and other sites was completed. Soil mapping was carried out by the description of typical landscape units in dependence of vegetation, relief position, water

regime, the parent material and other parameters. Soil and plant samples were taken for additional analysis in Yakutsk and Germany.

The soil distribution is shown in Figure 3-1. The soils were classified according to the classification of Yelovskaya (Table 3-1). The soil map and patterned ground map of the island after the international classification is in progress and will be presented after processing of all analytical and morphological data.

The first terrace in the western part of the island is dominated by weak developed and wet soil without any pattern ground structure (soil type: Permafrost Alluvial Layered Poorly Developed). The main soils of the island are wet soils, which are dominated by humus accumulation and cryoturbation (Permafrost Peat Gley). The general description of the island and of the investigation area were given in the last year`s report (Pfeiffer et al., 1999).

The main soil investigations are focused on the active layer and their correlated processes. To get more information to the associated deeper buried soils and the permafrost sediments two deep soil profiles (ice wedge polygon soil, 5 m depth; peat soil 7.5 m depth) on southeastern part of Samoylov Island were investigated. Soil and plant samples were taken for additional peat/pollen studies and ^{14}C-analysis. These studies are necessary for the co-operation with the other projects on paleoenvironmental and paleoclimatic studies of the Laptev Sea program.

Table 3-1: Classification of soils of Samoylov Island.

Section	Order	Type	Subtype	Index
Poorly Developed (Primitive)	Primitive Alluvial	Permafrost Alluvial Layered Poorly Developed (Primitive)		APr
Alluvial	Alluvial Typical	Permafrost Alluvial Turfness	Permafrost Alluvial Turfness Typical	AT
			Permafrost Alluvial Turfness Gley	ATG
		Permafrost Alluvial Peat-Gley	Permafrost Alluvial Muddy-Peatish-Gley	AMPshG
			Permafrost Alluvial Muddy-Peat-Gley	AMPG
			Permafrost Alluvial Muddy-Gley	AMG
Gley	Humus-Gley	Permafrost Turfness-Gley	Permafrost Turfness-Gley Typical	TG
		Permafrost Peat-Gley	Permafrost Peat-Gley	PG
			Permafrost Peatish-Gley	PshG
Accumulative-Humus	Accumulative-Humus Typical	Permafrost Straw	Permafrost Straw	S

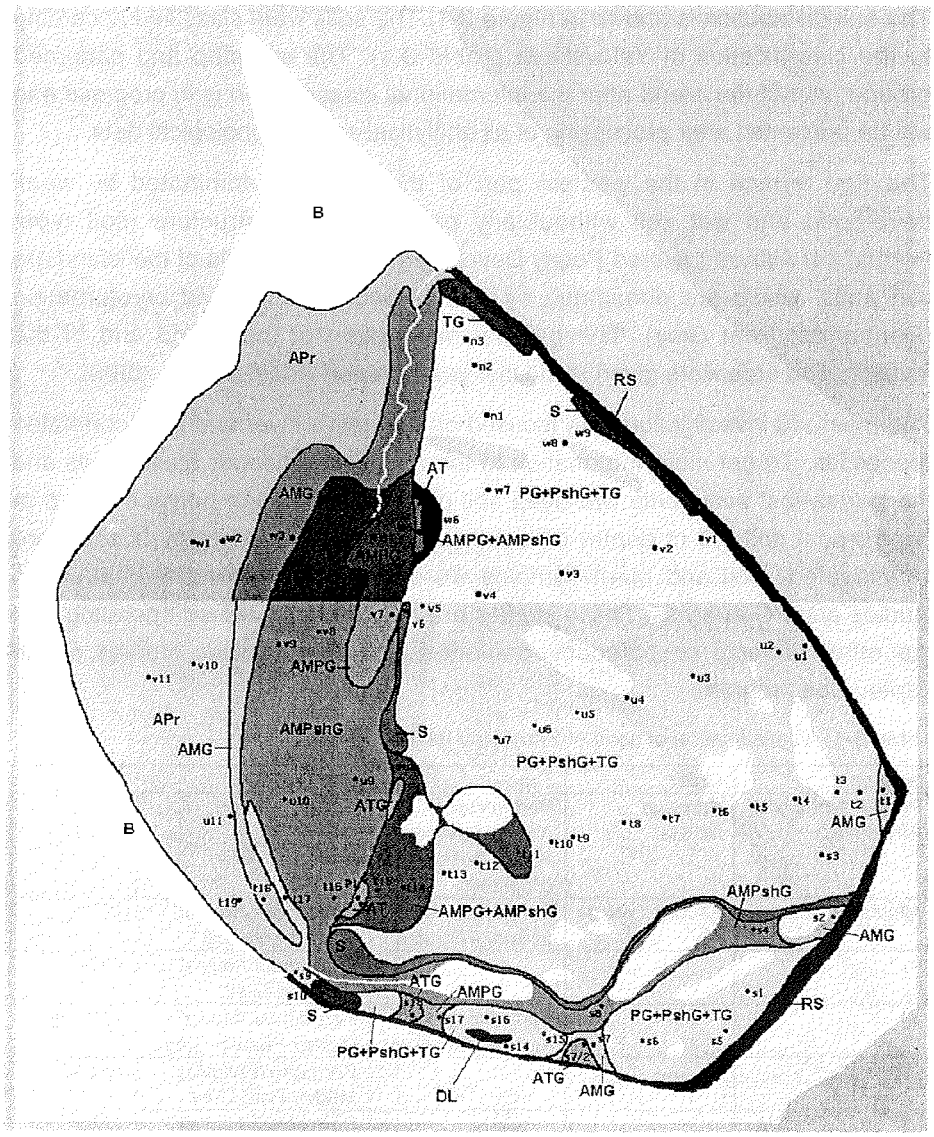

Figure 3-1: Soil map of Samoylov Island (for legend see Table 3-2).

Table 3-2: Legend of soil map of Samoylov Island.

Color and index	
APr	Permafrost Alluvial Layered Poorly Developed (Primitive)
AT	Permafrost Alluvial Turfness Typical
ATG	Permafrost Alluvial Turfness Gley
AMPshG	Permafrost Alluvial Muddy-Peatish-Gley
AMPG	Permafrost Alluvial Muddy-Peat-Gley
AMG	Permafrost Alluvial Muddy-Gley
AMPG+AMPshG	Soil complex
TG	Permafrost Turfness-Gley Typical
PG+PshG+TG	Soil complex
S	Permafrost Straw
B	Beach
RS	Zones of retreat shores
DL	Drained lake
	Channels and lakes
v3	Soil pits

3.3 Thermal and hydrologic dynamics of the active layer

(J. Boike and H. Becker)

Microclimate and soil temperature were continuously logged using automated stations from August 1998 to September 1999 at the low centered polygon site. A summary of instruments and methods is provided in Friedrich & Boike (1999). Soil moisture and temperature were recorded and soil water from suction lysimeters sampled manually every other day at sites 1 and 2 from May to September 1999. Between May 7 and May 27, 1999, snow pits were dug to permit determination of snow physical characteristics (structure, temperature, density, grain size and form).

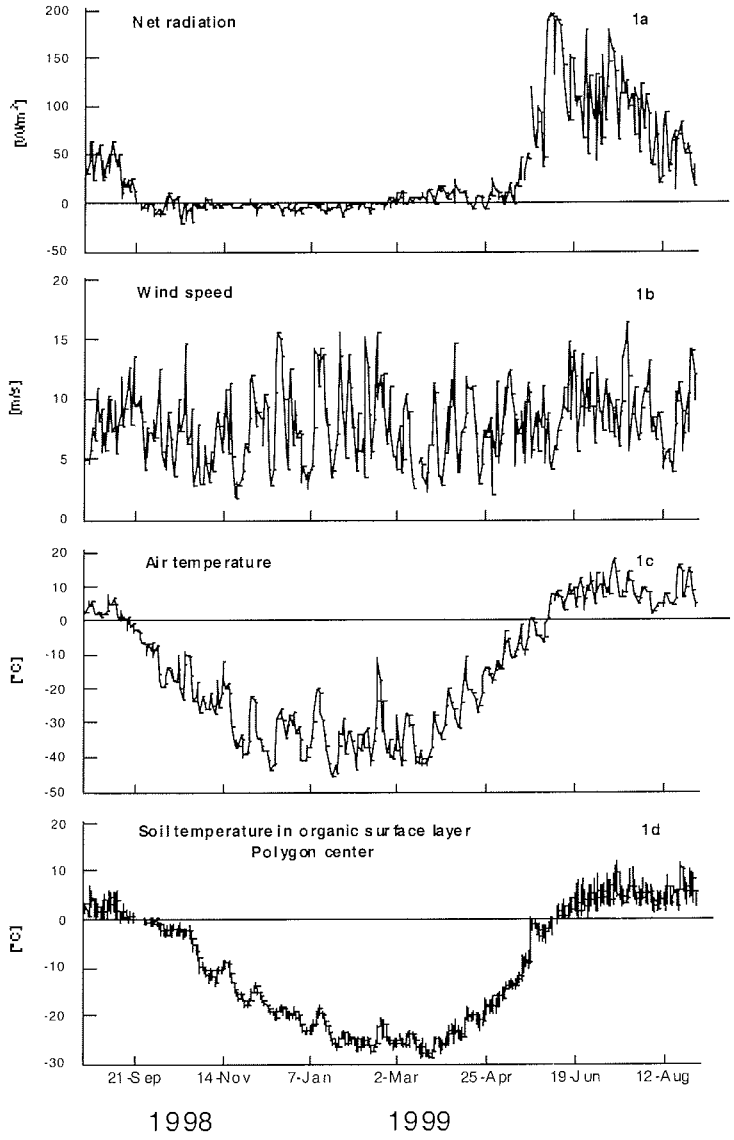

Figure 3-2: Weather and soil temperature for the period August 20, 1998 to September 3, 1999, Samoylov Island, Lena River Delta, Siberia.

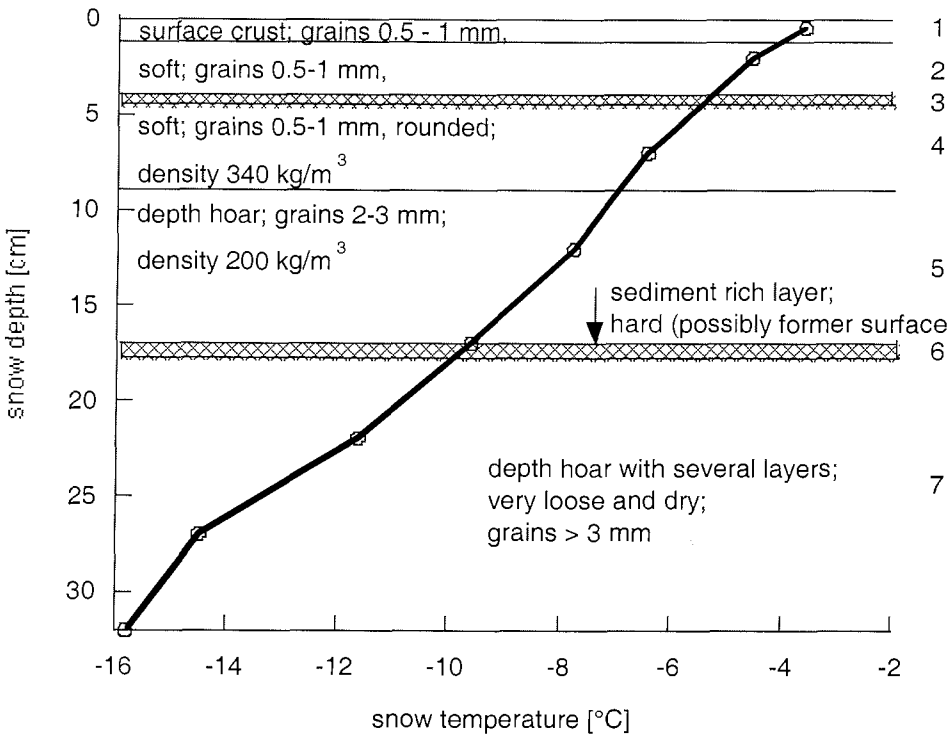

Figure 3-3: Stratigraphy and physical properties of the snow cover of the polygon center before snowmelt (May 10, 1999).

All water and snow samples were analyzed for pH and electrical conductivity; a 30 ml sub sample was kept cool for stable water isotope ($d^{18}O$, dD) and geochemical analyses.

Microclimate data for the period August 20, 1998 to September 3, 1999 is shown in Figures 3-2a to 3-2c. Net radiation first turned positive around the end of February. After disappearance of the snow cover at the end of May, the net radiation rapidly increased (Figure 3-2a). Wind speeds were generally high with maxima of up to 16.4 m/s (Figure 3-2b). The average air temperature for the entire period was –14.7 °C with a minimum of –47.8 °C on January 22, 1999 and a maximum of 18.3 °C on July 3, 1999 (Figure 3-2c).

Soil temperature changes for one sensor installed in the organic surface layer in the polygon center site are depicted in Figure 3-2d. Soil temperatures in the organic surface layer closely followed air temperature fluctuations. Progressive

decreases in air temperature at the end of September initiated the phase change in the soil. During fall and spring the phase change occurred rapidly and no zero curtain effect (temperature stabilization around 0 °C) was observed.

Snow depth was very heterogeneous spatially and varied between 40 cm in the polygon centers and 0 to 5 cm on the apex. A surface crust and hardened layers within the snow profile contained a large amount of aeolian sediments and indicated high wind speeds (Figure 3-3). Large depth hoar crystals with grain sizes larger than 3 mm were the result of steep temperature gradients between soil and air and their associated vapor pressure gradients. In addition, the long grass tundra vegetation promoted depth hoar formation by preserving a loose, aerated layer at the snow cover base. Figure 3-3 shows the snow temperature, stratigraphy and physical properties of the initially cold, dry snow period. Around May 23, the snow cover started to become isothermal and phase change was initiated.

3.4 Seasonal variability of trace gas emission (CH_4, CO_2) and in situ process studies

(D. Wagner, L. Kutzbach, H. Becker, A. Vlasenko and E.-M. Pfeiffer)

3.4.1 Methods and field experiments

The investigations on Samoylov Island, a representative island in the Lena delta (N 72°, E 126°) includes field measurements of the methane and carbon dioxide emission of a typical ice-wedge tundra and the process studies of methane fluxes (production, oxidation, emission).

Daily measurements of trace gas emission (CH_4, CO_2), thaw depth, water level and soil temperature were carried out from the beginning of June 1999 to the end of August 1999 at the low centre polygon site. The CH_4 and CO_2 release from the floodplain site and from a polygon lake were also periodically monitored. The used method (close chamber system) and the investigation sites had been described previously (Pfeiffer et al. 1999). Furthermore, the CH_4 and CO_2 concentration in the backwater of the polygon centre as well as the pore water concentration of all investigation sites was periodically analyzed.

A series of field experiments were conducted to investigate the plant-mediated methane flux. Special glass bottles (500 or 1000 ml) were used to enclose single tillers of *Carex concolor* (Figure 3-4). In the bottom of the flask was a round hole, which could be fitted by a rubber stopper. The stopper was drilled out and cut open on one side. The prepared rubber stopper was wrapped

around the base of an individual plant tiller and then the system was closed by placing the bottle over the plant onto the rubber stopper. The top of the bottle was closed with a screw cap with septum. Gas samples were taken after 30 or 60 min of incubation with a gastight syringe and analyzed for the concentration of CH_4 and CO_2 by gas chromatography. The experiments were carried out at the same site (site 3) where the seasonal variation of CH_4 and CO_2 flux was measured.

The in situ CH_4 production and oxidation was investigated considering the natural soil temperature gradient. Fresh soil material (20 g) from different soil layers was weight into 100-ml glass jars and closed with a screw cap with septum. To determine the in situ CH_4 production the samples were evacuated and flushed with N_2. In the case of CH_4 oxidation the samples were incubated under a methane/air atmosphere (approx. 200 ppm CH_4). The prepared soil samples were re-installed in the same layers of the soil profile from which the samples had been taken (site 3 and 4). The CH_4 production at zero and negative (-3 °C) temperatures were carried out in the permafrost cellar (Lednik) of the biological station. For these experiments soil samples were taken from the permafrost boundary of the polygon centre and periphery at site 3. Gas samples were taken from the headspace with a gastight syringe and analyzed for the concentration of methane by gas chromatography.

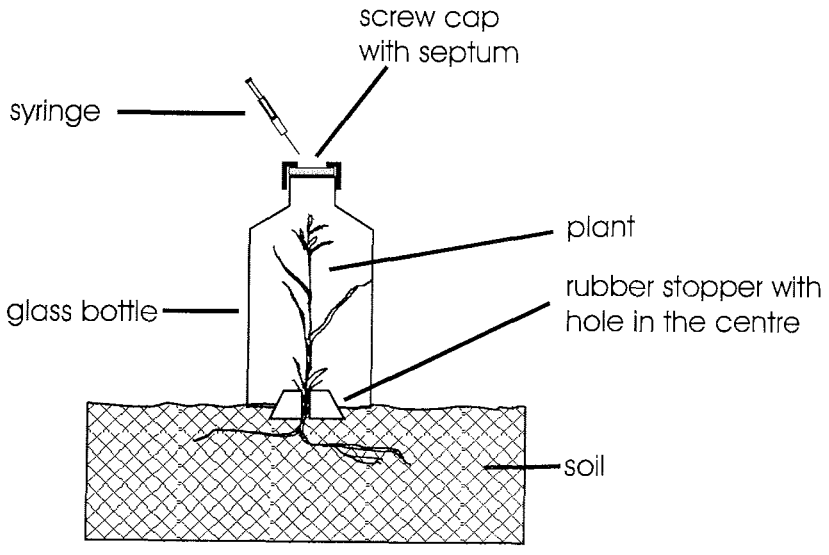

Figure 3-4: *Scheme of the experiment for plant mediated flux measurements.*

An automatic station for longtime recording of redox potentials (Fiedler and Fischer, 1994) was installed along a transect through a low centre polygon. The redox potential was determined in the top and bottom zone of the active layer in intervals of one hour at 16 measuring points.

CH_4 and CO_2 concentrations were determined with a Chrompack (GC 9003) gas chromatograph in the field laboratory. The instrument was equipped with a Poraplot Q and a Molesieve 5A capillar column connected with a switching valve. CH_4 was analyzed by a flame ionization detector (FID) and CO_2 by a hot wire detector (HWD). All gas sample analyses were done after calibration with standards of known concentrations of the respective gases. Helium was used as carrier gas.

3.4.2 Preliminary Results

The closed chamber measurements of CH_4 emission from the centre of a wet polygon tundra showed right from the start of soil thawing a relatively high CH_4 emission rate (> 15 mg h^{-1} m^{-2}) at the beginning of June, which increased with continuing thawing of the active layer (Figure 3-5b). The highest CH_4 emission was observed during July with a rate between 70 - 80 mg CH_4 d^{-1} m^{-2}.

The maximum thaw depth of the soil was reached in August (Figure 3-5a). During this period, the CH_4 emission decreased again and showed a rate on an average of 24.8 ± 6.8 mg CH_4 d^{-1} m^{-2}. In contrast to the polygon centre the CH_4 emission from the border was lower than 10 mg CH_4 d^{-1} m^{-2} during the whole season.

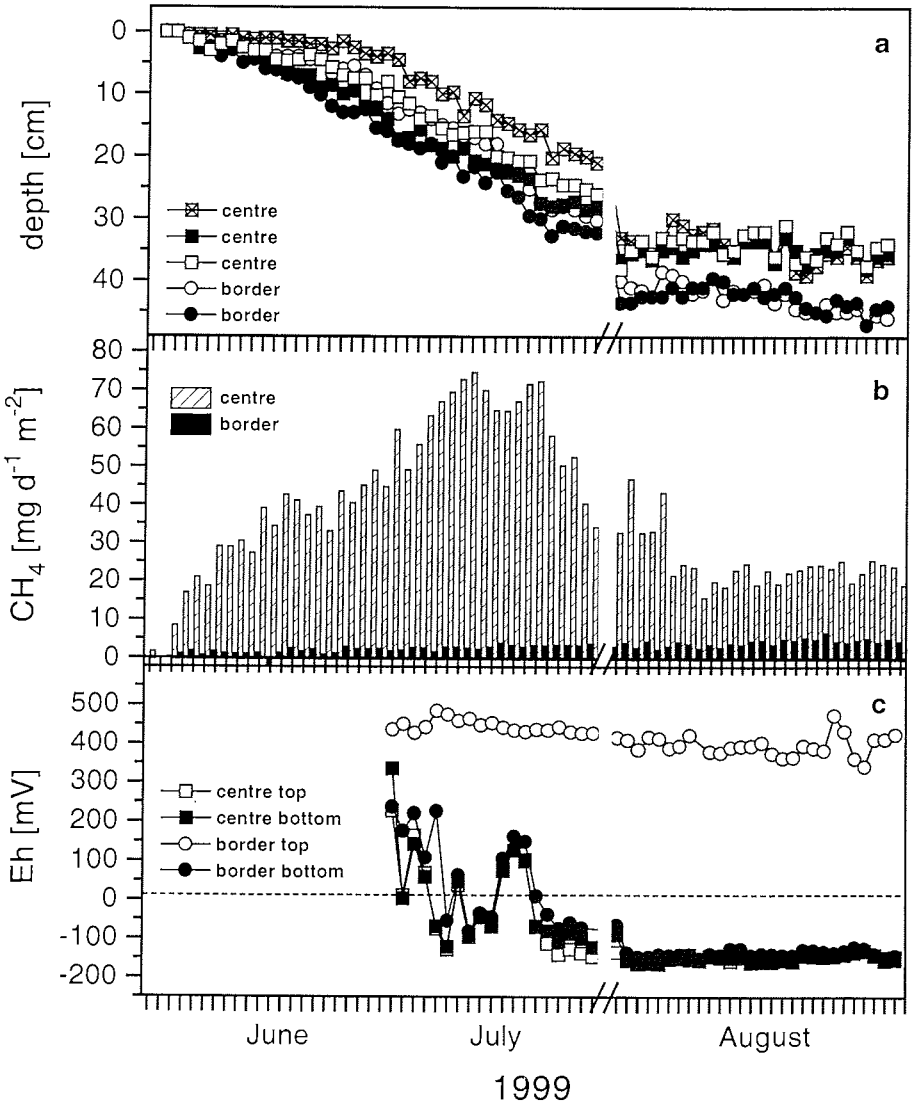

Figure 3-5: Thaw depth (a), CH_4 emission (b) and redox potential (c) of the polygon centre and border for the season 1999.

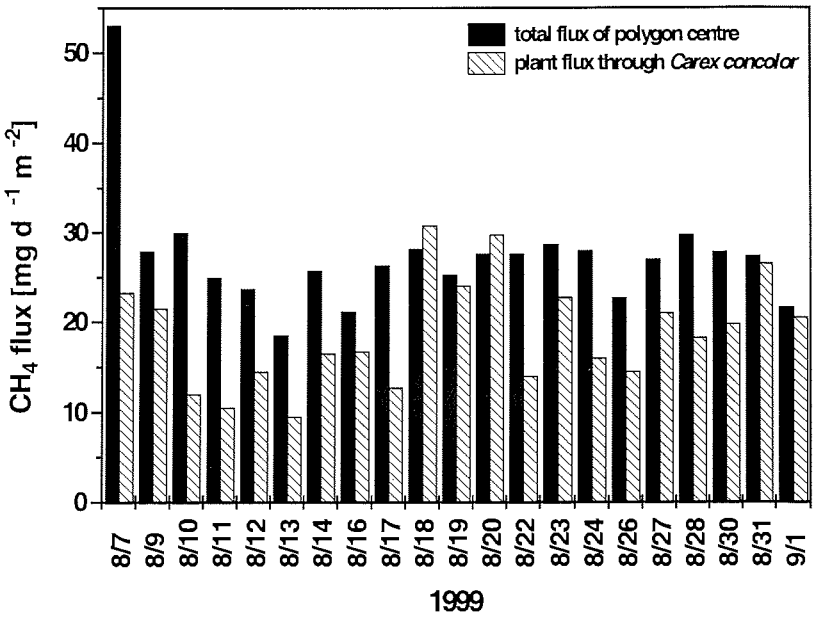

Figure 3-6: Total and plant-mediated CH_4 flux from the polygon centre in August 1999.

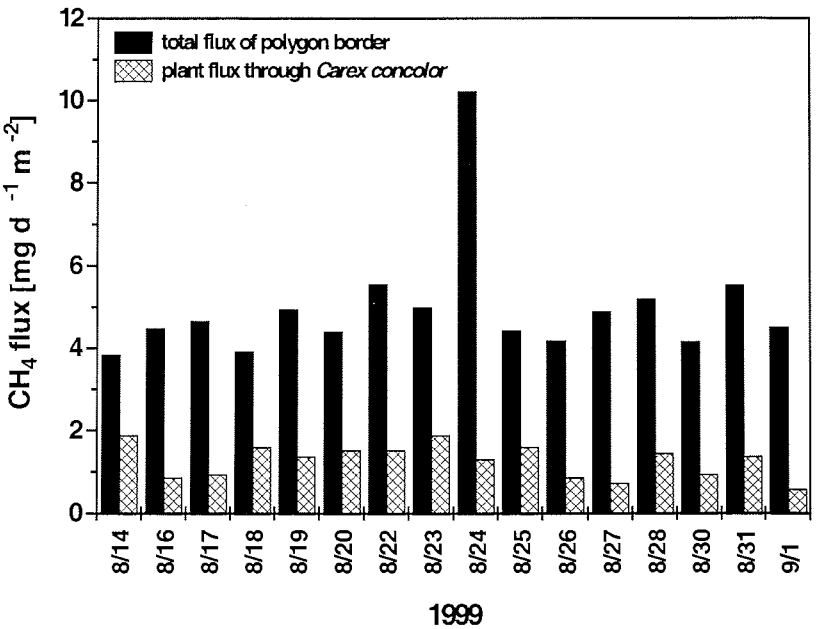

Figure 3-7: Total and plant-mediated CH_4 flux from the polygon border in August 1999.

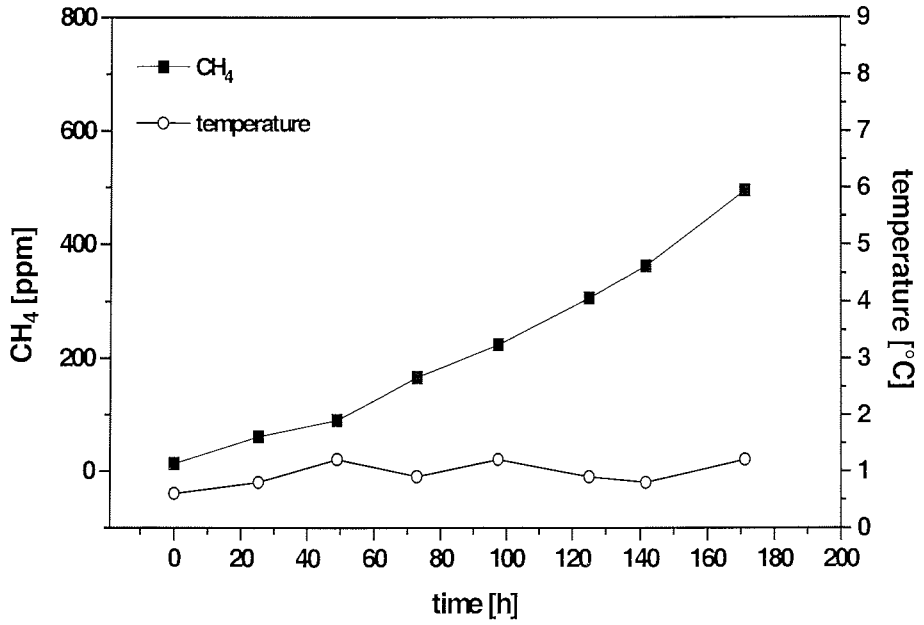

Figure 3-8: CH_4 production of the bottom zone of the active layer for the polygon centre.

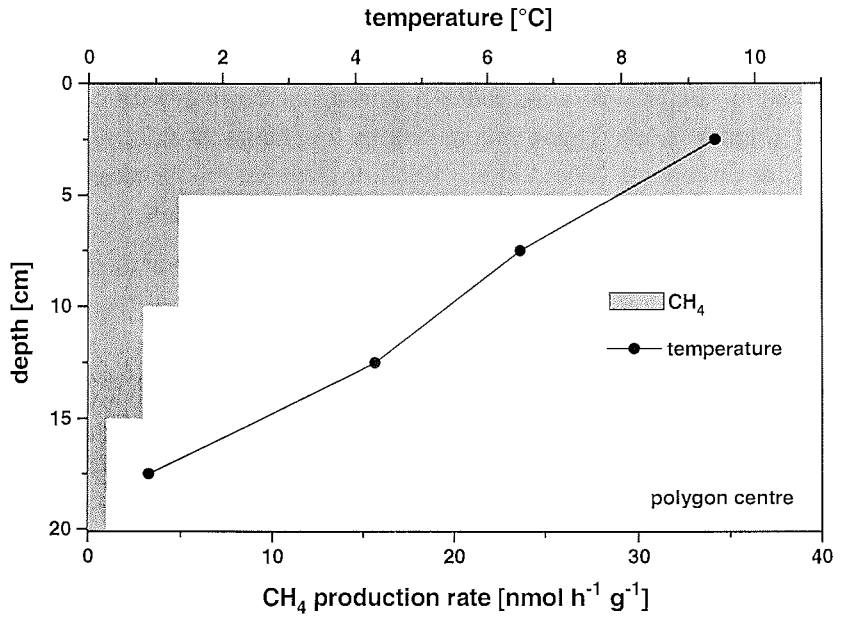

Figure 3-9: Vertical profile of in situ CH_4 production and soil temperature for the polygon centre.

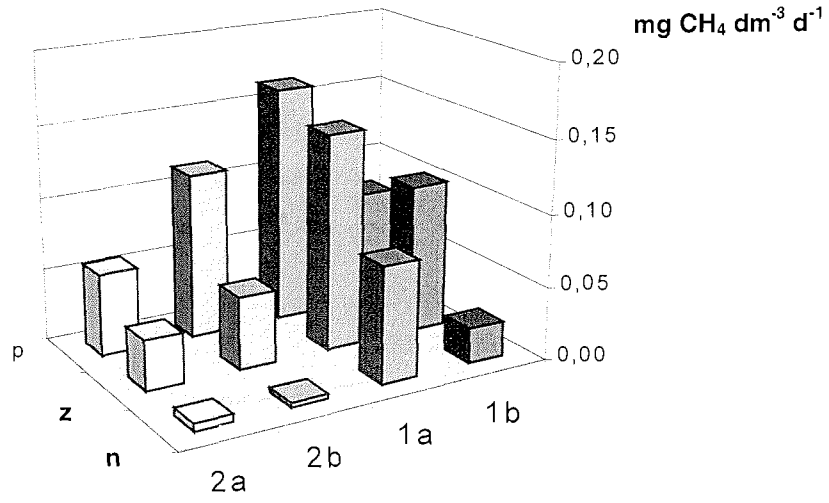

Figure 3-10: CH_4 production of the bottom zone of the active layer at positive (p), zero (z) and negative (n) temperatures (1, 2 – number of a series, a - polygon periphery, b - polygon centre).

The redox potential of the centre and of the bottom layer of the border showed during the period of soil thawing in July more fluctuations between +200 and -100 mV as in August where the redox potential was more or less constant at -160 mV (Figure 3-5c). These values are in the range of natural methane producing environments (Wang et al., 1993). In contrast the redox potential of the top layer of the border was relatively high with about +450 mV.

The results indicate that under these conditions the CH_4 oxidation became more important and therefore the CH_4 emission decreased in the course of the season.

The plant-mediated CH_4 flux ranged between 38 - 236 µg CH_4 d^{-1} from the polygon centre and 8 - 26 µg CH_4 d^{-1} from the border of polygon (Figure 3-6 and 3-7). The calculated CH_4 flux through single tillers of *Carex concolor* accounted to 74 ± 19 % of the total CH_4 emission from the centre, whereas the plant-mediated CH_4 emission from the border of the polygon accounted only to 27 ± 10 % of the total CH_4 emission. The CH_4 emission through *Carex concolor* correlated significantly with the plant biomass ($r = 0.91$) and also a strong correlation was found between the stocking density of *Carex concolor* and the release of CH_4 ($r = 0.87$, results are not shown).

The investigation of in situ CH_4 production activity showed that methane formation occurred already at the bottom of the active layer at temperatures between 0.6 and 1.2 °C (Figure 3-8). The vertical profiles of in situ CH_4 production and soil temperature of the polygon centre showed a rate of 1.0 nmol h^{-1} g^{-1} in the bottom zone of the active layer, which had a temperature of about 1 °C (Figure 3-9). The highest CH_4 production rate was determined in the top layer of the polygon with 38.9 nmol h^{-1} g^{-1} at an average temperature of 10 °C. Even the incubation experiment at zero and negative temperatures showed a significant CH_4 production (Figure 3-10). Therefore we assume that in cryosols a methanogenic community exist, which is adapted to the low in situ temperatures. This would be of great ecological significance because methane formation is the last step of anaerobic decomposition of soil organic matter. The results indicated that CH_4 production will occur in the active layer until the soil is completely refreezed in late autumn.

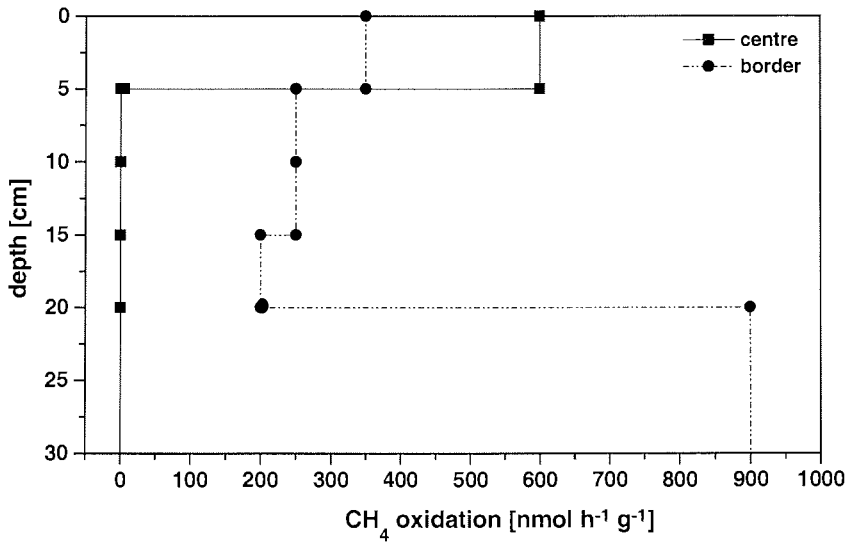

Figure 3-11: Vertical profile of in situ CH_4 oxidation for the polygon centre.

The border of the polygon showed methane oxidation activity down to a soil depth of 30 cm (Figure 3-11). The rate of methane oxidation was in the range between 0.2 - 0.9 nmol h^{-1} g^{-1}, whereas the highest rate was analyzed in the bottom layer (20 - 30 cm soil depth) of the profile. In contrast methane oxidation of the polygon centre was only detectable in the upper 5 cm. The soil

temperature ranged from about 6 °C in top layer to about 2.4 °C in the bottom layer of the border. This demonstrates that there is no significant correlation between soil temperature and methane oxidation activity.

The isolation and characterization of methanogenic and methane oxidizing bacteria, which is still in progress, should clarify the physiological potential and ecological significance of these microorganisms.

The differences in CH_4 fluxes between centre and border of the polygon were due to widely differing ecological conditions. The type of vegetation and the distribution of roots are considered to be an important factor. In the centre a waterlogged, organic-rich and extremly strong rooted horizon was situated directly at the soil surface. Anaerobic conditions combined with sufficient substrate availability stimulated methanogenesis. The dense mat of rhizomes and roots implied an effective uptake and transport of CH_4 by the aerenchyma of *Carex concolor*. On the border the soil was deeper thawed than in the centre. Because of drainage to the polygon centre the water table on the border was distinctly below the soil surface. Water-saturated conditions permitting methanogenesis occurred not in the organic-rich, strongly rooted surface horizon but in deeper horizons characterized by sandy sediments and a low organic content. Thus, substrate availability for methanogenesis was lower than in the centre. The coverage of vascular plants was small on the border and most of the roots were found in the aerobic surface horizon. Root density in the zone of methanogenesis was low and, therefore, the potential of CH_4 uptake by plant aerenchyma was limited. On the border most of the CH_4 had to diffuse through the soil and to pass zone of CH_4 oxidation.

3.5 CO_2 - Fluxes in permafrost affected soils

(W. Quass, W. Kloss and B. Schulz)

To investigate the seasonal variability of CO_2-fluxes, three expedition teams visited Samoylov Island from April to September. The first group started at the end of April and finished the field part at the 27th of May. The second group started the field investigations on the 6th of June, end of this field studies were the 24th of July. The third and last group did their investigations between the 5th of August and 6th of September.

3.5.1 Team 1 A (winter)

(W. Quass)

3.5.1.1 Introduction

In recent years, scientists found evidence of a carbon loss in form of CO_2 at high latitudes during the winter months (Clein et al. 1995; Zimov et al. 1996; Oechel et al. 1997; Mast et al. 1998; Grogan and Chapin 1999). Two mechanisms can be used as explanations for the observed winter efflux: metabolic processes of cold tolerant soil microorganisms and/or CO_2 loss during ice formation in the freezing soil (Coyne and Kelley 1971).

The hypothesis of Zimov (1993) emphasizes that during the freezing process much of the free soil water is attracted to the freezing front, creating a relatively warm, caused by the release of latent heat, and well-aerated microenvironment. Supported by the exothermic process of soil respiration, heat is produced which might be enough heat to retard the soil freezing and enable further decompositions even at temperatures below 0°C.

Changes of soil physical properties due to the freezing process might be another explanation for winter CO_2 effluxes. A release of CO_2 may arise from the freezing of soil water (Coyne and Kelley 1971).

The freezing process leads, in dependence of the soil substrate and the actual soil water content, to the formation of cracks in the permafrost by differential expansion and contraction of the permafrost-soil system, which occurs throughout the arctic cold season. The mechanical disturbances by the freezing process creates conduits for the release of trapped, subsurface CO_2 (Oechel et al. 1997).

The early start of the expedition offered the possibility to get more information about the CO_2 fluxes in wintertime.

3.5.1.2 Field studies

The first group was able to experience the arctic winter conditions on Samoylov Island. The field investigations began at the 7th of May, they were based on the sites set-up in 1998 (see Pfeiffer et al. 1999). The whole island was still snow-covered.

The investigation started with the mapping of snow heights at Plot 3 and at the surrounding polygons, in order to get more knowledge about winter conditions, especially snow-coverage and ice content of the polygon centers.

Soil temperature profiles at Plot 2 (thermistor pearls were installed at the end of last summer) were taken every 30 minutes between May and September, in 5 to 10 cm steps down to a depth of 60 cm.

No thaw depth was determined in this early period. A temperature rise above 0°C was not noticed before the end of May. For estimating further variations in thaw depth, a transect through a polygon field was created. This transect is 18 m long with 15 gauge points and it includes the apex, cracks and the centre of one polygon.

For determination of the soil CO_2 – flux two different methods were used:

A: The determination of carbon dioxide evaluation was performed with the CO_2 gas-exchange system (Walz–Germany). Measurements were carried out with soil samples in the closed system of the minicuvette. The track modus of the system enabled respiration measurements with respect to outside temperatures.

Measurements were carried out at frozen and thawing samples. Thawing happened at different temperature steps during the test.

B: The second method was carried out with the help of vacutainers and medical drain tubes (Becton-Dickinson). This method is not destructive and collects 12 ml of air samples, which are analyzed in a gas chromatograph in the laboratory in Kiel. Special interest was put on the boundary layer between snow cover and soil surface.

The O-layer of the soils at the measurement sites were also sampled, as well as exposed sites near the thermokarst lake. Sampling became more frequent as soon as the snow cover started to decrease.

Interannual differences in soil temperatures, especially surface temperatures, and varying soil water contents account for changes in the net CO_2 efflux. Temperature and TDR data were investigated in the year 1998 and 1999 by the automatic climate station of AWI-Potsdam. This device gives a good opportunity to estimate the thermal properties of the soil, especially during thawing and freeze-back. Thermocouples and TDR-probes at the sampling sites for gas measurements give necessary data for the prediction of microenvironmental properties.

And with the help of these data, laboratory test on soil respiration under controlled conditions should give more information about CO_2 fluxes in frozen soils.

3.5.2 Team 1 B (spring)

(W. Kloss)

3.5.2.1 Introduction

On the 5th of June the second team arrived expectantly on Samoylov Island by helicopter. The river break-up had happened just a few days ago and the rising water level and high amounts of floating ice made an outside camping for the first days impossible.

3.5.2.2 Field studies

Daily temperature and TDR measurements continued. Sampling of gas probes with the help of vacutainers needed to be varied because of the snow-free and thawing soil surface. For sampling the upper soil horizon, the atmosphere had to be excluded. Therefore liquid Agar-Agar was poured for sealing on the soil surface. At sites with high vegetation, it was cut of before.

With a continuing thawing-depth, deeper soil horizons were sampled with needles of various defined lengths. Particular horizons of profiles at site 2 and 3 were sampled with this method.

In this early thawing period, samples of Site 2 and 3 were measured in the gas exchange system with track modus. A well-aerated slope near a thermokarst lake and Plot 4 was included in these measurements. TDR measurements control the volumetric water content at the sampling sites. At Site 3 TDR measurements started after the 2nd of July in an organic and in a mineral part of the apex. The temperature measurements at Site 2 and 3 were continued in

time steps of 30 min, as well as thawing depths measurements (Figure 3-13). Measurements of the active layer were as well extended on site 4.

At Plot 3 the depths of the active layer were measured at the transect with 18 gauge points. The distance between the gauge points was between 80 and 200 cm. Differences of thaw-depth between the apex, including cracks, and the centre part of the low-centre polygon were well determined (Figure 3-12).

3.5.3 Team 1 C (summer)

(B. Schulz)

3.5.3.1 Introduction

Soil bacteria decompose organic material and so they produce gases (e.g., CO_2, CH_4), which play an important role in climate change. For these reasons soil microbiota and the gaseous emissions were investigated.

Soil bacteria are found in all horizons of permafrost affected soils even beneath the permafrost table, but from horizon to horizon the microbial community structure differs in a wide range. Because soil properties can change on small spatial scales in wet tundra ecosystems, it is necessary to investigate all types of sites.

The objective of this study is to describe the abundances and the distribution of bacteria in different sites of a low-center-polygon. Another aim is to investigate the soil chemical and soil physical characteristics in order to find out, which parameters control the presence of soil bacteria and their metabolic processes.

3.5.3.2. Methods and first results of field work

In 1998 and 1999 samples were taken at different sites of a low-center-polygon in a typical wet tundra ecosystem. In 1998, only the border of a polygon was sampled. In order to investigate the exact distribution of bacteria with depth, samples were taken in 2 cm steps. In 1999 a transect through a low-center-polygon was dug (digging and pedological descriptions were done together with L. KUTZBACH of TP1), so that all sites of a polygon (border, slope and the polygon centre) with its characteristics of microbial habitats and microbial community structure can be analyzed (Table 3-3 to 3-5). This was done to be able to transfer the results to whole polygons. For an overview on bacterial communities at the time of maximum thaw-depth, sampling in 1999 took part at the end of August. Further information on the polygon sites were noticed, e.g. botanical descriptions and pedological information.

Additional to these investigations the routine measurements of soil water content, soil temperature and thaw-depth continued. A back-freeze in August was expected but high air temperatures and long sunshine periods prevented this. On the contrary to this, we measured the soil continuing to thaw until our departure on September 4th. The sampling of soil air by vacutainer and of soil water as exchange analysis continued as well, differences of CO_2-content in soil air and CO_2-production of soil bacteria between summer and fall are expected.

3.5.4 Description of the sites and profiles

Site 1: "low-center polygon, apex":

100 % total plant coverage

dominating species (vascular plants with > 1 % coverage): *Dryas punctata, Carex aquatilis, Salix spec., Astragalus hirculus, Astragalus frigidus, Luzula nivalis*

other species: *Saxifraga hirculus, Saxifraga nelsoniana, Lagotis glauca, Polygonum viviparum, Orthilia obtusata, Papaver spec., Luzula multiflora, Stellaria spec., Alopecurus alpinus*

Table 3-3: Description of the soil at the apex (symbols according to AG BODENKUNDE, 1994).

depth [cm]	**description**
+5 – 0	plant coverage and organic layer
0 – 4	sandy loam, very strong rooted, medium content of organic material (fSu2, w5, h3)
4 – 8	sandy loam, strong rooted, low content of organic material (fSu2, w4, h2)
8 – 11	sand, very strong rooted, mS, w5, h0
11 – 16	sandy loam, strong rooted, high content of organic material (fSu2, w4, h2)
16 – 18	sandy loam, medium rooted, low content of organic material (Sl2, w3, h2)
18 – 24	sandy loam, medium rooted, medium content of organic material (Sl2, w3, h3)
24 – 32	sandy loam, medium rooted, medium content of organic material (Sl2, w3, h3)
32 – 40	sand, mS, very weak rooted, w1, ho
40 – 45+	loamy sand, very weak rooted, medium content of organic material (Su3, w1, h3 (h5))

Site 2: "low-center polygon, slope":

100 % total plant coverage (40 % vascular plants, 60 % lichen and bryophytes)

dominating species (vascular plants with > 1 % coverage): *Carex aquatilis, Polygonum vivipara, Orthilia obtusata, Parrya nudicaulis, Astragalus spec., Luzula spec., Salix glauca,*
other species: *Salix reptans, Valeriana capitata, Saxifraga hirculus, Saxifraga nelsoniana, Dryas punctata, Lagotis glauca, Pedicularis spec., Equisetum variegatum*

Table 3-4: Description of the soil at the slope.

depth [cm]	**description**
+9 – 0	plant coverage and organic layer
0 – 4	sand, very strong rooted, very low content of organic material (mS, w5, h1)
4 – 9	sand, very strong rooted, low content of organic material (mS, w5, h2)
9 – 19	sandy loam, strong rooted, low content of organic material (Su2, w4, h2)
19 – 24	sand, weak rooted (mS, w2, h0)
24 – 35+	sand, weak rooted, high content of organic material (mS, w1, h4)

Site 3: "low-center polygon, center":
100 % total plant coverage (30 % vascular plants, 70 % bryophytes)
dominating species (vascular plants with > 1 % coverage): *Carex aquatilis, Carex lugens*
other species: *Salix reptans, Salix glauca, Carex spec., Caltha palustris, Pedicularis spec., Polygonum vivipara, Arctagrostis spec., Saxifraga cernua, Saxifraga spec., Equisetum variegatum*

Table 3-5: Description of the soil at the center.

depth [cm]	**description**
+9 – 0	plant coverage and organic layer
0 – 15	organic material with low content of sand, very strong rooted (mS, w6, h6-h7)
15 – 20	sand, medium rooted (mS, w3, h0)
20 – 45	organic material with low content of sand ((mS), w0)
45 – 50	sand (w0)
50 +	organic material with low content of sand ((mS), w0)

The complete description of sites and the analysis of microbial communities at the different sites is in progress.

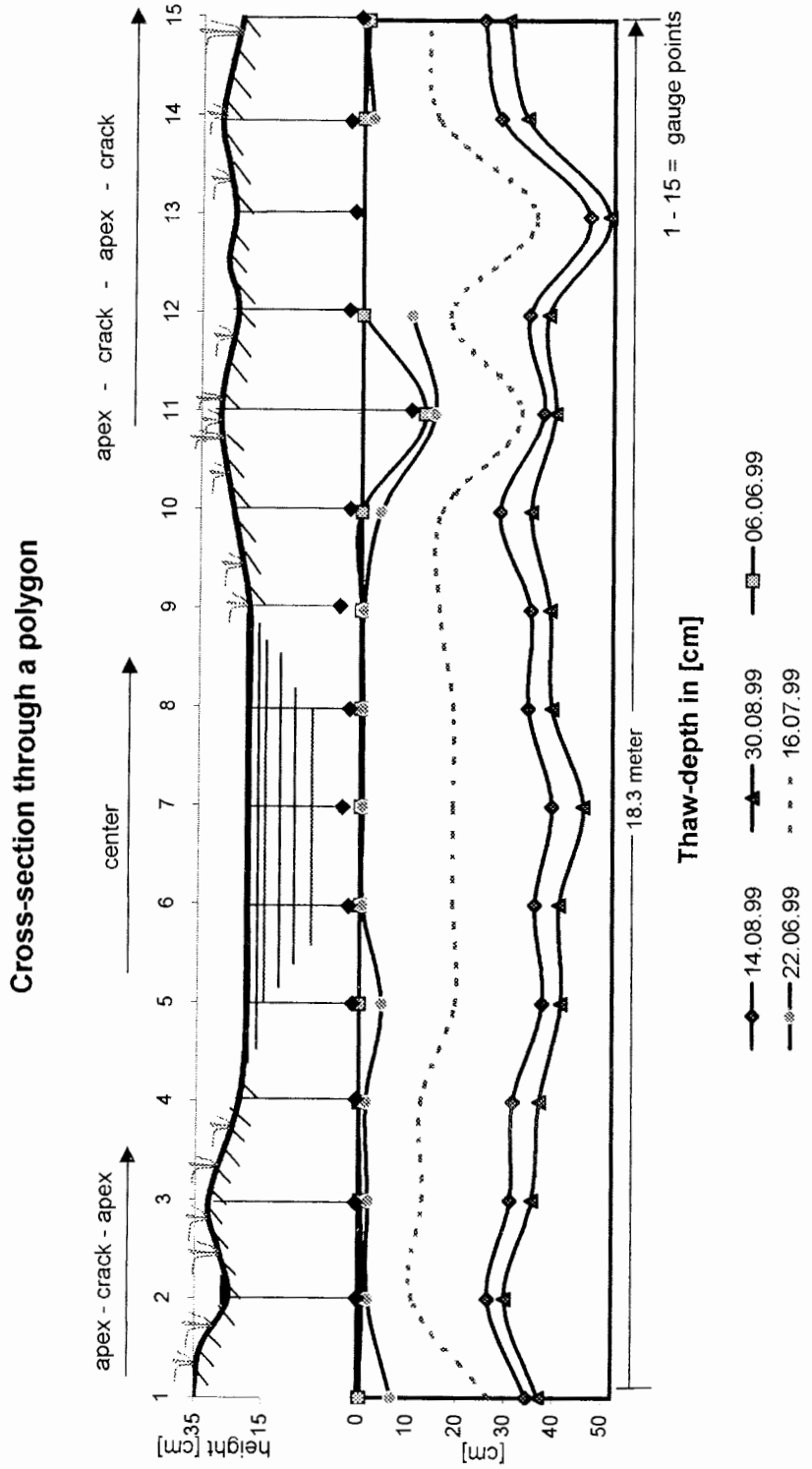

Figure 3-12: Transect of thaw-depth at Plot 3 between 6. June – 30. August 1999.

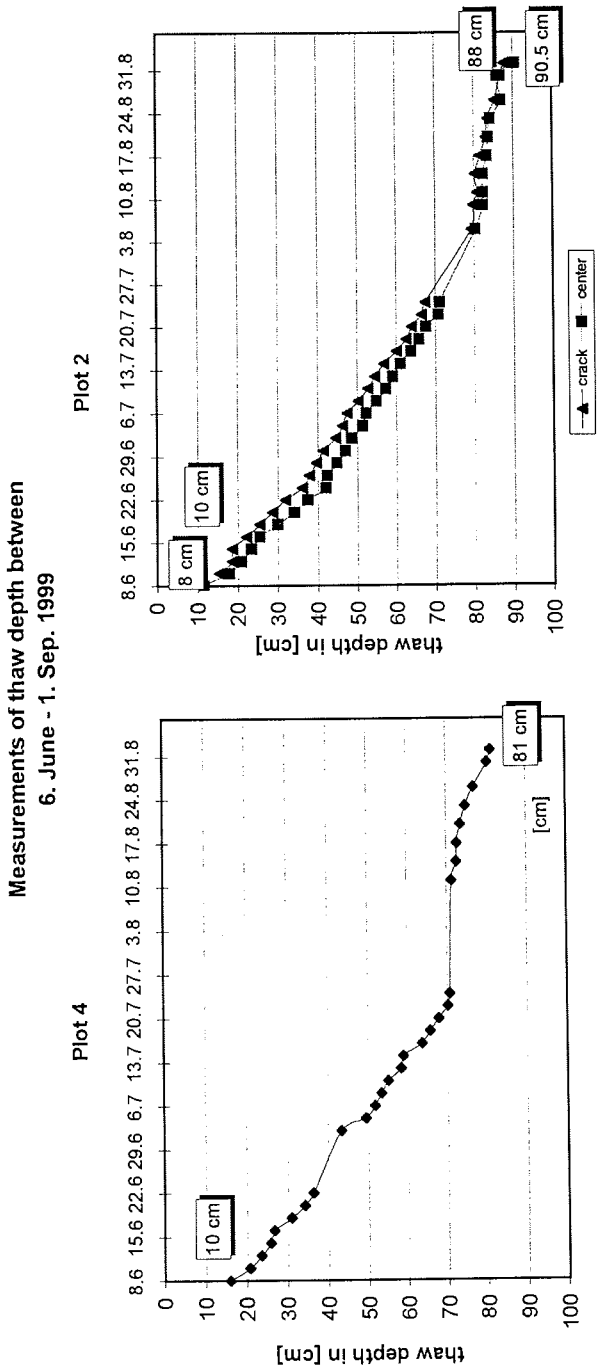

Figure 3-13: Thaw-depth at Plot 4 and Plot 2 between 8 June and 31 August 1999.

3.6 Monitoring for bird populations in the Lena Delta

(V.I. Pozdnyakov)

In 1999 investigations of the status of bird populations in the Lena Delta in accordance with the program of 1998 were continued (Pozdnyakov, 1999; Solovieva, 1999). We studied character of seasonal distribution on territory and abundance, characteristic of breeding success of various groups of birds per year and characteristic of fall migration period.

3.6.1 Methods and materials

The observations were conducted from June 29 till September 23 mainly in the southern part of the Delta. Like in 1998, a motor boat was used on the main channels (Pozdnyakov, 1999). The total length of registration routes was 2823 km. We inspected a few nesting colonies of birds. Unfortunately, the observations of nested biology were limited because the work had begun in the late nesting period. Therefore breeding success was estimated as positive mainly by meetings of broods or young birds after the nesting period.

The inspected region was divided into sites, which corresponded to sites of 1998 and have received the same numbers. The records were not conducted on sites 5, 6, 8 and 9 in 1999, and on sites 12-15 in 1998.

1. Channel sites in the southern part of the Lena Delta, joining the principal channel of the Lena River 72°24' - 72°36' N; 125°25' - 127°O' E. Total length of routes was 249 km.

2. The southern part of the Arynskaya Channel up to 72°50' N. The length of routes was 187 km.

3. The channels between the southern parts of the Arynskaya and the Malaya Tumatskaya Channels up to 72°54' N. The length of routes was 126 km.

4. The channels between the southern parts of the Malaya and the Bolschaya Tumatskaya Channels up to 72°54' N. The length of routes was 126 km.

7. The southern part of the Bolschaya Tumatskaya Channel up to 72°54' N. The length of routes was 26 km.

10. The channels between the Bolschaya Trofimovskaya and Bykovskaya Channels, south from 72°45' N. The length of routes was 117 km.

11. The Bykovskaya Channel. The length of routes was 1005 km.

12. Southern part of the Olenekskaya channel up to 72°40' N. The length of routes was 197 km.

13. Channels between the southern parts of Olenekskaya and Arynskaya Channels up to 72°50' N. The length of routes was 129 km.

14. Channels between the Bolschaya Tumatskaya and Bolschaya Trofimovskaya Channels, south from 73° N. The length of routes was 494 km.

15. Western part of the Bolschaya Trofimovskaya Channel up to 128°25' E. The length of routes was 167 km.

The period of observations was divided into three parts appropriate to main parameters of seasonal activity of birds (Table A3-2 – A-3-4):

- nesting period, till July 15;
- brood period, July 16 - August 15;
- fall migration period, from August 16 till completion of works.

3.6.2 Results and discussion

During the whole observation period 48 bird species were registered, 37 of them during the records on the channels (Table A3-2 to A3-4). In addition the following species could be observed earlier: Brent Goose (*Branta bernicla*), Golden Eagle (*Aquila chrysaetos*), Gyrfalcon (*Falco rusticolus*), Ptamigan (*Lagopus mutus*), Turstone (*Arenaria interpres*), Red-necked Stint (*Calidris ruficollis*), Snipe (*Gallinago gallinago*), Pintail Snipe (*G. stenura*), Swallow (*Hirundo rustica*), Redpoll (*Acanthis flammea*), Rosy Finch (*Leucosticte arctoa*). The average density of birds on the channels of the Lena Delta was 20.43 individuals per 10 km channel.

In 1999 the breeding success of majority of bird species in the Lena Delta appeared high. The warm and fast spring promoted concerted beginning of nesting. Nesting success depended on lemming density. After one year with high depression of lemmings number, the number of Arctic Fox was very low. We did not register destruction of eggs and nests by Arctic Fox. In 1999 on all territory of the Delta happened rapid lemming's number growth.

Loons. We observed only usual for the Delta Black-throated Loon (*Gavia arctica*) and Red-throated Loon (*G. stellata*). Both species were successfully breeding. In the brood of a Red-throated Loon, observed on August 25, the young birds were not able to fly yet. The flocks of Black-throated Loon from 6-10 birds preparing to fall migration were observed in late August - beginning of September in the central part of the Delta on sites 4 and 7.

Geese. The breeding of the geese in 1999 was successful. In colonies of Brent Geese the hatch of chicks began on July 7-8. The average size of clutch at this time was 4.24 eggs (n = 41). From 48 examined nests only 2 (4.1 %) were destroyed by large gulls.

All young White-fronted Geese (*Anser albifrons*) could fly on August 20. The large flocks of birds, preparing for fall migration, were met on sites 3, 4, 7. The average amount of birds in flocks was 27.8 (n = 28), maximum 130.

On August 10 we observed the flock (44 birds) from the molting adults of Bean Geese (*Anser fabalis*) with chicks on site 2. During preparation for fall migration the average of the observed flocks was 14.4 (n=20) and maximum 100.

In fall migration period on the feeding's places the White-fronted Geese and Bean Geese were derivated by the mixed congestions. The maximum number (99.13 individuals/10 km) of these two species together was marked on site 3.

Swans. Bewicks Swan (*Cygnus bewickii*), which is common in the Lena Delta, was observed. The greatest abundance (10.96 individuals/10 km) was marked in the nesting period on site 15. Flocks of non-breeding birds were observed here. First broods, abandoning the nests, were observed on July 9. The average of brood for all period of observations was 3.93 (n = 14). The fall migration passed in September. Bred swans flied by families (adults with young birds).

Ducks. The breeding of Long-tailed Duck (*Clangula hyemalis*), King Eider (*Somateria spectabilis*) and Steller's Eider (*Polysticta stelleri*) was successful. At the end of the incubation period of King Eider an average of 4.82 eggs (n = 11) was determined. The earliest beginning of hatching in nests of this species was marked on July 10. In the middle of August a high number of Pintail (*Anas acuta*) was observed in the central part of the delta (site 14). The flocks reached 500 birds and the abundance was 26.99 individuals/10 km of channel. In the same region we observed the flock of 28 Teals (*Anas crecca*) on August 14.

Predators. Rough-legged Buzzard (*Buteo lagopus*) and Peregrine (*Falco peregrinus*) nested on all sites which were known from previous years. Flying young Buzzards were observed since August 10 and Peregrines from the beginning of September. Gyrfalcon (*Falco rusticolus*) and Golden Eagle (*Aquila chrysaetos*) were observed in the Olenekskaya channel on August 23. Both birds were young. In 1999 the Snowy Owl (*Nyctea scandiaca*) did not breed in the Lena Delta. Only once (August 26) a single adult bird was seen on site 4.

Waders. All species of this bird group observed in the investigation area were successfully breeding. But on channels of the delta they were appreciable only

in the fall migration period. The greatest abundance was marked on site 14. By August 20 the fall migration of waders in the delta was completed.

Skuas. In the investigation area the abundance of skuas was low. Arctic Skua (*Stercorarius parasiticus*) and Long-tailed Skua (*S. longicaudus*) were breeding.

Large gulls. Distribution and abundance of large gulls on channels of the Delta in 1999 corresponded to 1998. The flying young birds were seen after August 20.

Small gulls and terns. Sabine's Gall (*Xema sabini*) in the southern part of the delta was not breeding. The breeding of Ross's Gull (*Rhodostethia rosea*) and Arctic Tern (*Sterna paradisaea*) was successful. The emerging of chicks in the nest of Ross's Gall was observed on July 10. On July 23 a few migrating birds of this species were observed on the Bykovskaya Channel (site 11). First flying young of Arctic Terns were seen on August 8. The departure of terns from the Delta proceeded until August 17.

Passerines. Except for Snow Banting (*Plectrophenax nivalis*), which nests in peat breakaways of islands, Passerines were observed on channels of the Delta in nesting and hatching periods very seldom. The autumnal migration of Northern Wheatear (*Oenanthe oenanthe*), Lapland Bunting (*Calcarius lapponicus*) and Pipit (*Anthus sp.*) was observed on Olenekskaya (site 12) and Bykovskaya (site 11) Channels in the last third of August.

3.7 References

Clein J.S and J.P. Schimmel (1995): Microbial Activity of Tundra and Taiga Soils at Sub-Zero Temperatures, Soil Biol. Biochem. Vol. 27, No. 9, 1231-1234

Coyne, P.I. and J.J. Kelley (1971): Release of carbon dioxide from frozen soil to the arctic atmosphere, Nature 234, 407-408

Grogan, P. and F.S. Chapin III (1999): Artic Soil Respiration: Effects of Climate and Vegetation Depend on Season, Ecosystem 2: 451-459

Mast, M.A.; K.P.Wickland, R.T. Striegl, and D.W. Clow (1998): Winter fluxes of CO2 and CH4 from subalpine soils in Rocky Mountain National Park, Colorado, Global Biogeochemical Cycles, Vol. 12, No. 4, 607-620

Oechel, W.C.; G. Voulitis, and S.J. Hastings (1997): Cold season CO2 emission from arctic soils, Global Biogeochemical Cycles, Vol. 11, No. 2, 163-172

Pfeiffer, E.-M.; Akhmadeeva, I.; Becker, H.; Friedrich, K.; Wagner, D.; Quass, W.; Zhurbenko, M.; Zöllner, E. (1999): Modern processes in permafrost affected soils. In: Rachold, V. (eds.) Russian-German Cooperation SYSTEM LAPTEV SEA 2000: The Lena Delta 1998 Expedition. Reports on Polar Research 315, 19-79.

Pozdnyakov, V.I. (1999): Distribution and Abundance of Birds on the Channels of the Lena Delta. Reports of the Polar Research, Volume 315, p.48-51.

Solovieva, D.V. (1999): Ornithological observations. Reports of the Polar Research, Volume 315, p.46-48

Wang, Z.P.; DeLaune, R.D.; Masscheleyn, P.H.; Patrick Jr., W.H. (1993): Soil redox and pH effect on methane production in a flooded rice soil. Soil Sci. Soc. Am. J. 57, 382-385.

Yelovskaya (1987): Classification and diagnosis of permafost soils in Yakutia. Publ. Yakutian Section of the Siberian Branch of the Academy of Science USSR: 172 p. (in Russian).

Zimov, S.A., G.M. Zimova, S.P Davidov, O.V. Prosiannikova, I.V. Semiletova, and I.P. Semiletov (1996): Winter biotic activity and production of CO2 in siberian soils, J. Geophys. Res. 98, 5017-5023

3.8 Appendix

Table A3-1: List of soil samples.

Number	Samples	Planned Analysis
LD99 6182-6185	soil samples P10	^{14}C analysis
LD99 6187-6189	soil samples P11	chemical
LD99 6200-6202	plant material	^{13}C analysis
LD99 6203-6221	soil samples P11	chemical
LD99 6223-6250	soil samples P10	chemical
LD99 6251-6253	plant material	^{13}C analysis
LD99 6254-6261	peat samples	^{14}C analysis
LD99 6166-6170	soil samples	chemical
LD99 6171-6174	soil samples	chemical
LD99 6357-6361	soil samples P8	chemical, microbiological
LD99 6362-6370	soil samples P6	chemical, microbiological
LD99 6371-6376	soil samples	chemical, microbiological
LD99 6381-6389	undisturbed soil samples	physical
LD99 6390-6394	soil samples P8	microbiological
LD99 6395-6400	soil samples P6	microbiological
LD99 6416-6420	soil samples P9	chemical, microbiological
LD99 6421-6424	undisturbed soil samples	phisical
LD99 6428-6432	soil samples P9	microbiological
LD99 6456-6473	soil samples Arga	microbiological
LD99 6474-6479	sediments Nikolay Lake	microbiological
LD99 6480-6487	sediments Nikolay Lake	microbiological
LD99i 001-003	gas samples	chemical
LD99i 005-006	gas samples	chemical
LD99i 008-009	gas samples	chemical
LD99i 013-017	gas samples	chemical
LD99i 022-024	gas samples	chemical
LD99i 026-029	gas samples	chemical
LD99i 032	gas samples	chemical
LD99i 037-040	gas samples	chemical
LD99i 061-066	gas samples	chemical
LD99i 128a-131a	gas samples	chemical
LD99i 143a-146a	gas samples	chemical
LD99i 152-164	gas samples	chemical
LD99i 175-178	gas samples	chemical

Table A3-1: continuation.

Number	Samples	Planed Analysis
LD99i 190-199	gas samples	chemical
LD99i 230-349	gas samples	chemical
LD99i 007	ice samples	chemical
LD99i 010-012	ice samples	chemical
LD99i 041-059	ice samples, frozen	chemical
LD99i 018-021	soil samples	chemical, microbiological
LD99i 025	soil samples	chemical, microbiological
LD99i 030-031	soil samples	chemical, microbiological
LD99i 033-036	soil samples	chemical, microbiological
LD99i 060	soil samples	chemical, microbiological
LD99i 080-140	soil samples	chemical, microbiological
LD99i 165-174	soil samples	chemical, microbiological
LD99i 180-189	soil samples	chemical, microbiological
LD99i 200-222	soil samples	chemical, microbiological
LD99i 120a-127a	soil samples	chemical, microbiological
LD99i 132a-142a	soil samples	chemical, microbiological
LD99i 141-151	soil samples	chemical, microbiological
LD99i 067-077	undisturbed soil samples	physical
LD99i 078-079	soil samples	chemical, microbiological

Table A3-2: Abundance of birds on the channels of Lena Delta in the nesting period (ind./10 km).

Sites	**10**	**11**	**14**	**15**
km	**117**	**465**	**127**	**94**
Gavia arctica	0.17	0.02	0.39	0.21
Gavia sp.	0.0	0.02	0.0	0.0
Cygnus bewickii	0.77	0.04	3.54	10.96
Clangula hyemalis	0.34	0.11	0.24	0.21
Somateria spectabilis	0.26	0.04	0.31	0.0
Polysticta stelleri	0.0	0.0	0.39	0.74
Phalaropus fulicarius	0.09	0.0	0.0	0.0
Wader sp.	0.09	0.0	0.71	0.43
Stercorarius parasiticus	0.0	0.15	0.08	0.0
Stercorarius longicaudus	0.43	0.15	0.0	0.0
Stercorarius sp.	0.0	0.06	0.0	0.0
Larus argentatus	2.05	2.24	0.94	1.06
Larus hyperboreus	1.03	0.80	0.87	0.43
Larus sp.	0.34	0.0	0.0	0.0
Xema sabini	0.43	0.0	0.16	0.0
Rhodostethia rosea	0.17	0.0	0.47	0.0
Sterna paradisaea	1.03	1.27	0.24	0.0
Plectrophenax nivalis	0.77	0.09	0.31	0.0
Total birds	**8.21**	**4.99**	**8.66**	**14.0**

Table A3-3: Abundance of birds on the channels of Lena Delta in the brood period (ind./10 km).

Sites	**1**	**2**	**11**	**12**	**13**	**14**
km	**78**	**68**	**240**	**73**	**129**	**193**
Gavia arctica	0.13	0.44	0.42	0.14	0.70	0.41
Gavia stellata	0.0	0.0	0.0	0.0	0.08	0.05
Gavia sp.	0.13	0.29	0.04	0.0	0.78	0.98
Anser albifrons	0.0	0.74	0.0	0.0	0.78	1.04
Anser fabalis	0.0	4.26	0.0	0.0	0.31	0.0
Anser sp.	0.0	2.65	0.0	0.0	0.70	0.0
Cygnus bewickii	0.0	0.0	0.0	0.0	0.0	0.93
Anas acuta	0.0	0.0	0.0	0.0	0.0	26.99
Buteo lagopus	0.0	1.32	0.0	0.0	0.78	0.0
Falco peregrinus	0.0	0.29	0.0	0.0	0.0	0.0
Pluvialis fulva	0.0	0.0	0.0	2.47	0.0	2.44
Phalaropus fulicarius	0.0	0.0	0.0	0.0	0.0	0.0
Calidris minuta	0.0	0.44	0.0	0.0	0.23	3.37
Calidris tamminckii	0.0	0.15	0.0	0.0	0.08	0.16
Calidris alpina	0.0	2.94	0.0	0.0	0.0	0.83
Calidris melanotos	0.0	0.0	0.0	0.0	0.0	0.16
Wader sp.	1.03	2.06	0.13	0.0	0.62	4.82
Stercorarius parasiticus	0.0	0.0	0.08	0.0	0.08	0.05
Stercorarius longicaudus	0.0	0.29	0.04	0.0	0.08	0.0
Larus argentatus	3.72	4.56	1.04	1.10	2.17	2.59
Larus hyperboreus	0.38	1.03	0.42	0.27	1.47	1.30
Larus sp.	1.28	0.0	0.54	0.0	0.0	0.0
Rhodostethia rosea	0.0	0.0	0.21	0.0	0.0	0.0
Sterna paradisaea	0.0	0.88	0.0	0.82	0.47	0.52
Corvus corax	0.0	0.0	0.0	0.0	0.08	0.0
Motacilla alba	0.0	0.15	0.0	0.0	0.08	0.0
Oenanthe oenanthe	0.0	0.0	0.0	0.0	0.08	0.0
Plectrophenax nivalis	0.0	42.35	0.04	0.0	9.61	0.98
Calcarius lapponicus	0.0	0.44	0.0	0.0	0.23	0.10
Total birds	**6.67**	**65.29**	**2.63**	**4.79**	**24.03**	**47.70**

Table A3-4: Abundance of birds on the channels of Lena Delta in the fall migration period (ind./10 km).

Sites	1	2	3	4	7	11	12	14	15
km	171	119	126	126	26	300	124	174	73
Gavia arctica	0.0	0.0	3.49	2.96	0.0	0.03	0.08	0.46	0.0
Gavia stellata	0.0	0.17	0.08	0.0	0.0	0.0	0.0	0.0	0.0
Gavia sp.	0.12	0.59	2.14	0.63	0.77	0.13	0.24	0.98	0.27
Anser albifrons	0.0	0.0	38.3	10.2	0.0	0.0	0.0	1.55	0.0
Anser fabalis	0.0	1.51	5.63	0.87	0.0	0.0	1.05	0.0	0.0
Anser sp.	7.89	15.5	55.2	11.2	44.2	0.0	1.77	0.0	0.0
Cygnus bewickii	0.29	0.50	1.03	0.16	0.0	0.0	0.0	0.06	0.0
Anas acuta	0.0	0.0	0.0	0.0	0.0	0.0	0.0	1.90	4.11
Anas crecca	0.0	0.0	0.0	0.0	0.0	0.0	0.0	0.0	3.84
Buteo lagopus	0.06	0.25	0.71	0.48	0.38	0.0	0.08	0.06	0.0
Falco peregrinus	0.06	0.0	0.0	0.08	0.0	0.10	0.16	0.0	0.0
Lagopus lagopus	0.0	0.76	0.0	0.0	0.0	0.0	0.0	0.0	0.0
Pluvialis squatarola	0.0	0.0	0.08	0.0	0.0	0.0	0.0	0.0	0.0
Phalaropus fulicarius	0.0	0.0	0.08	2.22	0.0	0.0	0.0	2.87	0.0
Charadrius hiaticula	0.0	0.08	0.16	0.0	0.0	0.0	0.0	0.0	0.0
Philomachus pugnax	0.0	0.0	0.0	0.0	0.0	0.0	0.0	0.40	1.10
Calidris minuta	0.0	0.0	0.0	0.0	0.0	0.0	0.0	3.56	0.0
Calidris temminckii	0.0	0.0	0.0	0.0	0.0	0.0	0.0	0.40	0.96
Calidris alpina	0.0	0.0	0.0	0.0	0.0	0.0	0.0	0.34	0.0
Calidris melanotos	0.0	0.0	0.0	0.0	0.0	0.0	0.0	1.09	0.0
Wader sp.	0.0	0.0	0.0	0.0	0.0	0.0	0.0	4.83	2.33
Stercorarius pomarinus	0.0	0.0	0.0	0.0	0.0	0.0	0.0	0.06	0.0
Stercorarius parasiticus	0.0	0.0	0.0	0.0	0.0	0.0	0.0	0.06	0.0
Larus argentatus	2.75	1.85	3.57	3.17	5.77	1.33	2.34	2.36	0.55
Larus hyperborus	1.05	0.25	0.63	1.35	0.77	0.70	0.56	1.03	0.68
Larus sp.	0.0	0.0	0.0	0.0	0.0	0.0	0.0	0.0	1.78
Sterna paradisaea	0.0	0.0	0.0	0.0	0.0	0.0	0.0	0.57	0.0
Nyctea skandiaca	0.0	0.0	0.0	0.08	0.0	0.0	0.0	0.0	0.0
Corvus corax	0.0	0.17	0.0	0.0	0.0	0.07	0.0	0.0	0.0
Motacilla alba	0.0	0.0	0.0	0.0	0.0	0.13	0.24	0.0	0.0
Oenanthe oenanthe	0.0	0.0	0.0	0.0	0.0	0.43	0.0	0.0	0.0
Plectrophenax nivalis	0.0	1.26	1.03	2.64	0.0	0.33	0.24	0.86	0.0
Calcarius lapponicus	0.0	0.0	0.32	0.0	0.0	1.43	4.68	0.0	0.0
Anthus sp.	0.0	0.0	0.0	0.0	0.0	0.40	1.05	0.0	0.0
Total bird	**15.09**	**22.86**	**112.5**	**35.95**	**51.92**	**5.00**	**12.50**	**23.45**	**16.03**

4 Coastal Processes in the Laptev Sea and the Environmental History of the Lena Delta

4.1 Introduction

(V. Rachold and M. N. Grigoriev)

Accumulation and erosion in the coastal zone are of major importance for the modern and ancient sediment budget of the Laptev Sea. The amount of sediment transported by the Siberian rivers is relatively well quantified. However, the portion of sediment that is deposited in the river deltas, mainly the Lena Delta, and, therefore, never actually reaches the Laptev Sea is not known. Furthermore the amount of material delivered to the Laptev Sea through the erosion of ice-rich coastlines has not been accurately quantified (Rachold et al., in press).

The Lena Delta is a large Arctic delta and the conditions are very different from that of delta regions in lower latitudes. It is the main connection between interfering continental and marine processes within the Laptev Sea. The sedimentation history of the Lena Delta, its importance as a fossil accumulation area as well as the processes that control the lateral extension, are poorly understood. While the main part of the eastern Lena Delta is assumed to be an actual „active" delta the western part consists of mainly of sandy deposits (Arga Island) and Ice Complexes of different origin (Rachold et al., 1999).

Shore dynamics directly reflecting the complicated land-ocean interactions play an important role in the balance of sediments, organic carbon and nutrients in the Arctic Basin. Formerly the rivers were considered as the main suppliers of sediments into the World Ocean. However, the results of recent investigations showed pronounced regional differences in the ratio between riverine and coastal erosion sediment input. Thus, Are (1999) suggested that the amount of sediment supplied to the Laptev Sea by rivers and shores is at least of the same order but probably the coastal erosion input is considerably larger than the input of the rivers.

Our working group consisting of three individual teams focussed on the reconstruction of the sedimentation history of the Lena Delta and the quantification of coastal sediment input to the Laptev Sea. The working areas visited during the LENA 99 expedition are shown in Figure 4-1.

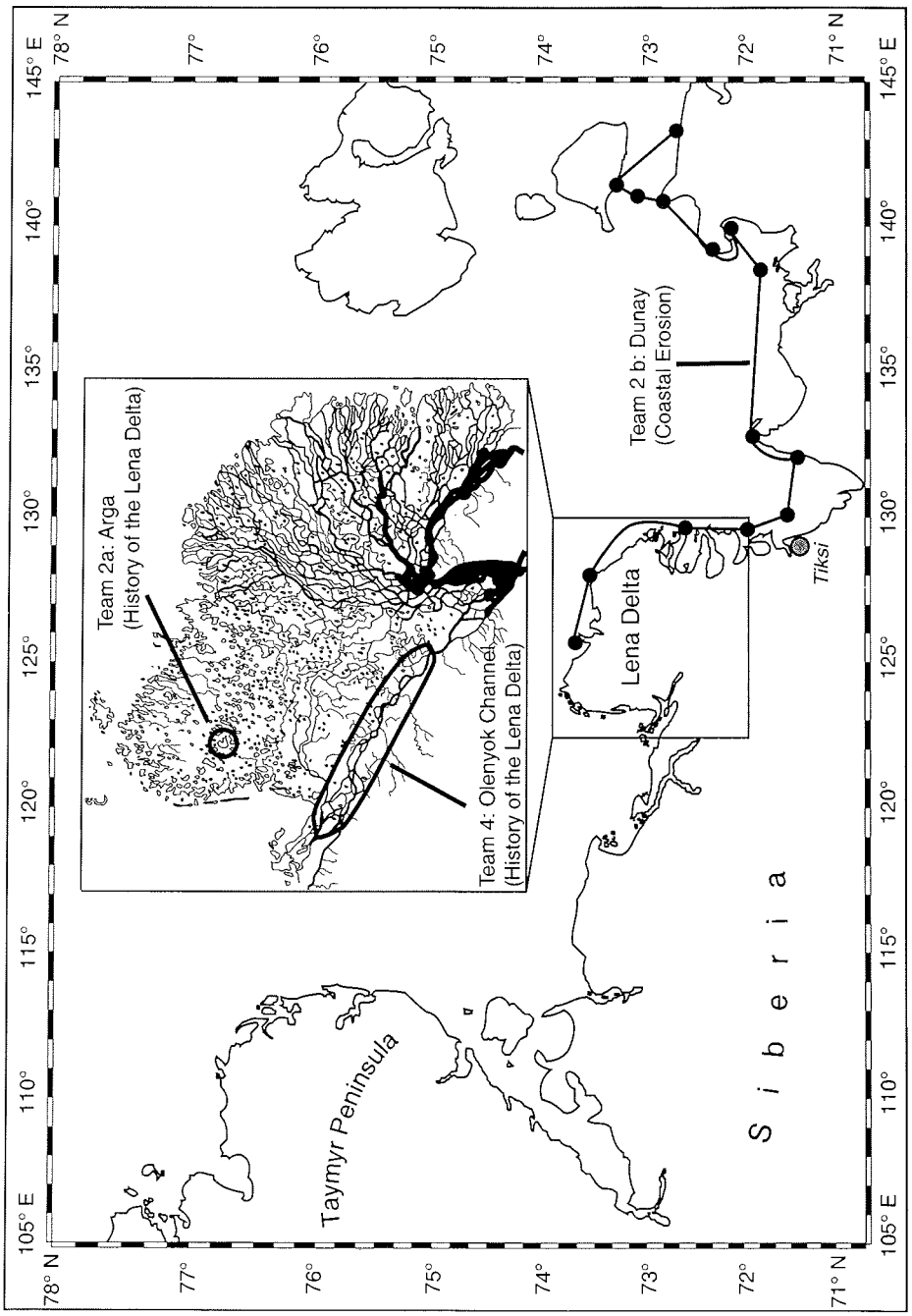

Figure 4-1: Working areas of research groups focussing on coastal processes in the Laptev Sea and the environmental history of the Lena Delta (Team 2a: Chapter 4.2, Team 2b: Chapter 4.3, Team 4: Chapter 4.4).

4.2 Lake Sediment Studies on Arga Island

(G. Schwamborn, D. Yu. Bolshiyanov, M. Dorozhkina, M. N. Grigoriev, E. Yu. Pavolva, W. Schneider and V. E. Tumskoy)

4.2.1 Introduction

The Lena River draining to the Siberian Arctic is considered to be the main sediment source for the Laptev Sea. Nevertheless, the Lena Delta - occupying an area of 28.000 km^2 - is a poorly studied and complicated region of land-ocean-interactions in the Arctic. There are many unsolved questions concerning the environmental and sedimentation history, geomorphology, genesis of deposits, permafrost distribution and climatic variability in that area.

There are different opinions on the genesis and age of the second sandy terrace (north-western sector of the Lena Delta). Its lower horizons may be apparently identified with sandy deposits underlying the south-western Delta Ice Complex. The upper horizon is an accumulative layer of channel alluvium accumulated after active lower Holocene erosion. The sandy terrace is penetrated by a dense net of ice wedges, related to the Holocene or, possibly, the pre-Holocene. Furthermore, sheet ice up to 2 m thickness is found here. The volumetric ice content of the upper horizon of the sandy terrace is about 25 %. These layers are supposed to contain larger ice bodies. This may explain the formation processes of numerous large thermokarst lakes and active contemporary thermokarst processes on the second terrace.

To survey and quantify the stratigraphic sequence of Lake Nikolay (western Delta Lena) ground penetrating radar studies (25 MHz and 100 MHz antennas) from the winterly ice cover have been applied in connection with drilling activities to determine the geologic composition. The '99 activities complement shallow seismic studies and first sediment sampling at the same site from summer '98 (Schwamborn et al., 1999) and help to solve questions concerning the environmental and sedimentation history, geomorphology, and genesis especially for the second terrace deposits in western Delta Lena.

Major concerns guiding this 99´s campaign have been as follows:

- what is the origin and age of the second terrace sandy deposits (Arga Island) of western Delta Lena?
- what is the origin and age of Arga Island`s lakes, i.e. Lake Nikolay?

The following methods have been applied:

- radar sounding

- to determine suitable sites for coring lake sediments
- to find possible ground ice occurrences
- to identy the talik - permafrost boundary below the water body

- lake sediment coring
  - for identifying the lithofacies of the subground
  - for providing material for age determination by the radiocarbon method
- comparison of radar sounding (25 MHz and 100 MHz) with shallow seismic data (frequencies in the range of 1.5 - 11.5 kHz), which had been obtained in the year before
- water and ground temperature measurement
  - for identifying the talik boundary and
  - for heat flow determination.

4.2.2 Samples and methods

Ground Penetrating Radar (GPR) analyses produced the data necessary to outline the subsurface stratigraphy of Lake Nikolay area. The commercially available impulse radar equipment used for these observations was a RAMAC/GPR System, which consists of a control unit, a field PC and 25 and 100 MHz antenna units containing both transmit and receive antennas. The control unit generates timing signals to key the transmitter on and off and synchronizes this keying with the receiver. Digital commanding and recording in the field was managed on a HUSKY field PC along with the packaged signal processing software. General settings of the software when collecting data have been chosen in the following way:

	25 MHz antenna	**100 MHz antenna**
samples	1024	1536
stacks	128	128
horizontal spacing interval	2.00 m	1.00 m
vertical resolution	ca. 1.00 m	ca. 0.30 m

The time window was set to record in a length of 2000 ns. This allowed receiving signals through a water column of about 30 m at maximum and from the sedimentary environment below the deeper basins. Radar wave velocity in water is 33 m/µs and in unconsolidated sediments about 60 m/µs. For the permafrost sediments a value of 110 m/µs is assumed. Estimates for sediment thicknesses are based on these values (Davies and Annan, 1989).

A total number of 13 profiles have been collected with data for about 30 km of subsurface profiling (see Figure 4-2, Table A4-1, appendix). This was done out

of a diesel vehicle which pulled a textile sheet 45 m behind where the antennas were mounted on. The 25 MHz antennas have been fixed with an offset of 4 m, the 100 MHz antennas with an offset of 1 m, respectively. Additionally, 4 CMP measurements yielded velocity information for the radar waves. They have been recorded at shallow lake areas, deep basins and on land. The CMP measurements covered a distance of 30 or 50 m to both sides with antenna spacing intervals of 25 cm or 100 cm, respectively. Along with subsurface profiling the thickness of lake ice and the water depth have been measured conventionally for certain key sites.

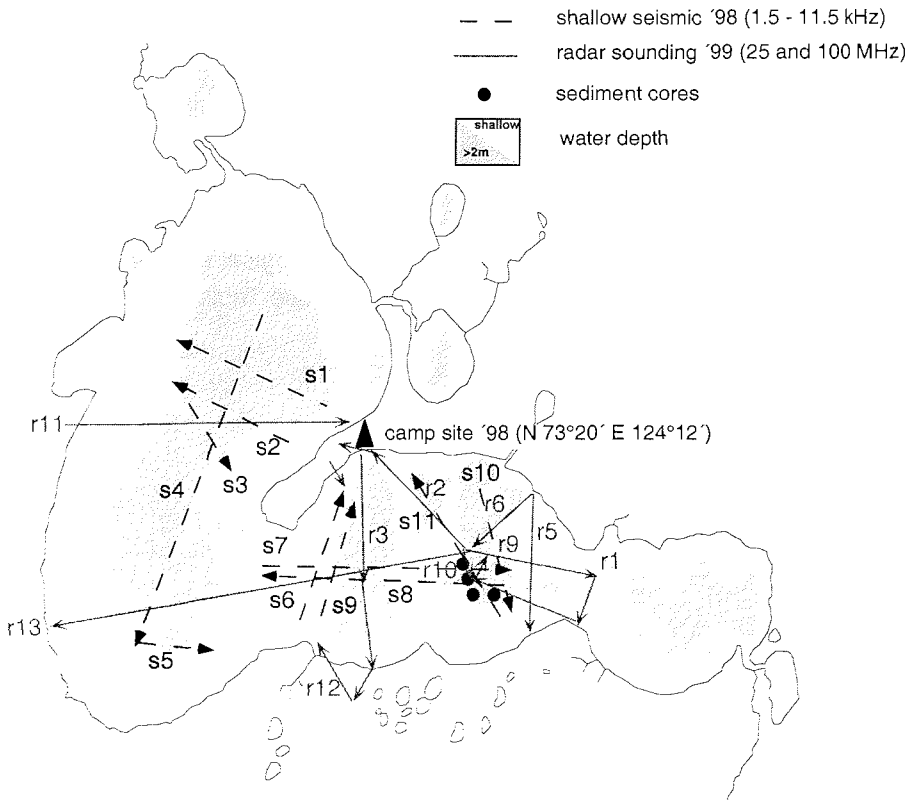

Figure 4-2: Localities of radar profiles on Lake Nikolay. Since one primary objective of the radar profiling was to compare characteristics of the 25 MHz and 100 MHz records with acoustic data the shallow seismic profiles gained in the summer '98 are shown, too. They have been recorded with the "GeoChirp" system, a sediment echosounder, which sends out and processes a sweep of signals in the range of 1.5 - 11.5 kHz. Analog printouts are provided already in the field.

After profiling the 16 bit data have been loaded into GRADIX software that provides radar processing with a variety of filtering functions and data display formats.

In some cases high quality sub-bottom information was obtained without data processing. This is valid especially for profiles of deeper basins where lake sediments can be found. However, signal processing substantially improved the records when signal-to-noise ratios were low, i.e. the shallow areas of Lake Nikolay where sediments are object to permafrost conditions.

Based on the results of the radar studies, lake sediment sampling was carried out by gravity corer and permafrost drilling equipment, respectively. The drilling locations are shown in Figure 4-2 and Table A4-1 (appendix). A total number of 5 sediment cores (up to 7 m length) were recovered from Nikolay Lake by permafrost drilling. In addition one 5,90 m long core was retrieved from Ivashkina Laguna, Bykovsky Peninsula (see Figure 4-3 and 4-4). Furthermore, 12 lake sediment cores (up to 95 cm) were obtained by gravity coring. The recovered sediments will be analyzed for sedimentological and geochemical properties and used for AMS-C^{14} age determinations (see Table A4-2).

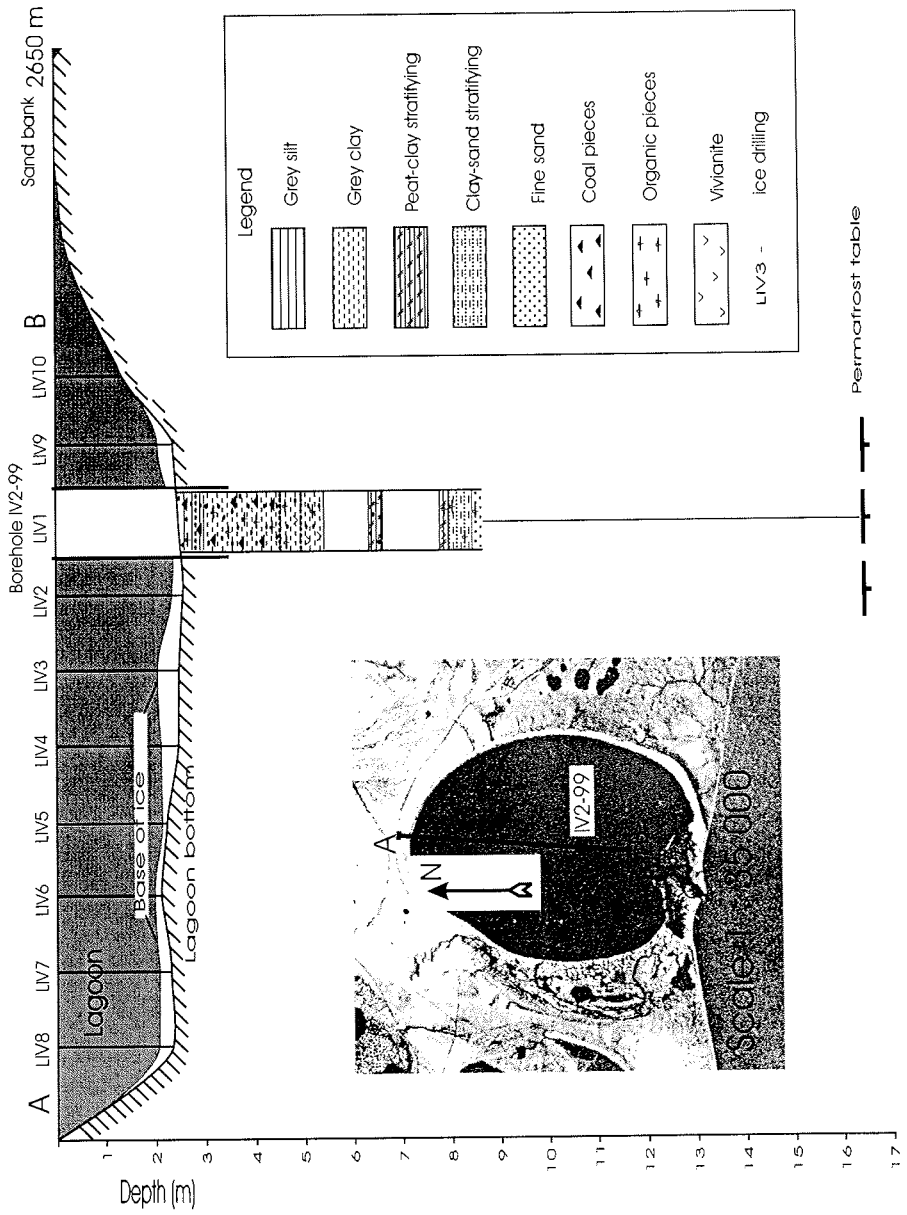

Figure 4-3: Location and profile of borehole IV2-99 drilled in Ivashkina Laguna, Bykovsky Penisula.

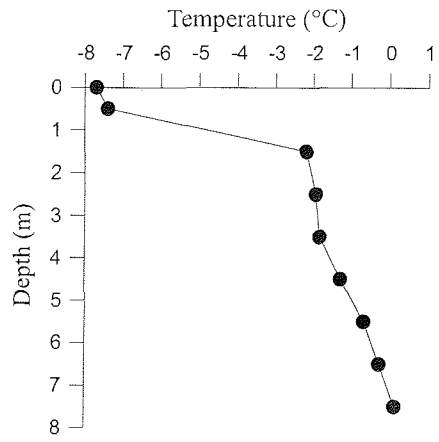

Figure 4-4: Temperature profile of borehole IV2-99 drilled in Ivashkina Laguna, Bykovsky Penisula.

4.2.3 Preliminary results

Not all of the survey results are shown here, rather one example is displayed where certain geophysical features are verified by sediment drilling (see Figure 4-5). The field results can be summed up as follows:

- Both the 25 MHz and the 100 MHz antenna are suitable for stratigraphic investigations of lake sediments.
- The bathymetry of the lake can clearly be lined out having a water depth of 30 m at maximum.
- The thickness of the lake sediments in the deeper basins is ca. 2.5 m deduced from a 100 MHz radargram as far as signal penetration reveals. This corresponds well with results of the shallow seismic measurements. However, drilling results show that just the upper 0.9 m of the lake sedimentation can be regarded as of lacustrine origin. They consist of organic rich silty sand. The material below is composed purely of fine to silty sand indicating a fluvial origin.
- Having a winterly ice cover on Lake Nikolay of 1.2 - 2.6 m the radar sound penetration is about 20 m down into the permafrost with the 25 MHz antenna, and about 15 m with the 100 MHz antenna. This stays in contrast to the seismic surveys where the seismic waves have been reflected almost totally by the frozen sand. It is valid for the shallow parts of the lake only where sediments are lying directly beneath the ice cover and are thoroughly frozen.

- Inclined reflectors in these shallow areas are interpreted to represent fluvial layering of the sandy subground. They are equally inclined towards the deeper basins.
- Since radar waves are absorbed in the saturated lake sediments there are no possibilities to detect the talik-permafrost boundary below the deeper basins.
- The occurrence of ice bodies and other types of ground ice cannot be observed in the radar charts.
- The fluctuations in ice cover thickness cannot be observed in the radargrams at first, either.
- All radar charts are affected by strong multiple occurrence created by the lake ice – lake water interface.
- Organic samples from drilling cores no. A1 and no. A5, and gravity cores no. CN 2 and no. CN 6 have been prepared to be dated by the radiocarbon method to reveal the age of the lake deposits.
- Temperature measurements, which were conducted in the boreholes drilled from lake ice, allowed to determine the position and dynamics of the sublake permafrost table (see Table A4-3, appendix). Ground and water temperature show that the table of subwater permafrost has a very steep angle of incidence from shallow to deep water. Sometimes the permafrost table is characterized by an adverse gradient (concave) towards land near the steep lake bottom slope.
- Large ice bodies under lake shallows within the second sandy terrace of the Lena Delta were not found by drilling. The existence of such ice bodies could be documented by deeper seismic and drilling methods. Nevertheless, we assume that large inclusions of ice or ice rich deposits occur in the Arga Island sandy horizons and that the numerous deep lake depressions of the Arga Island were formed mainly in Holocene as a result of thermokarst land subsidense.

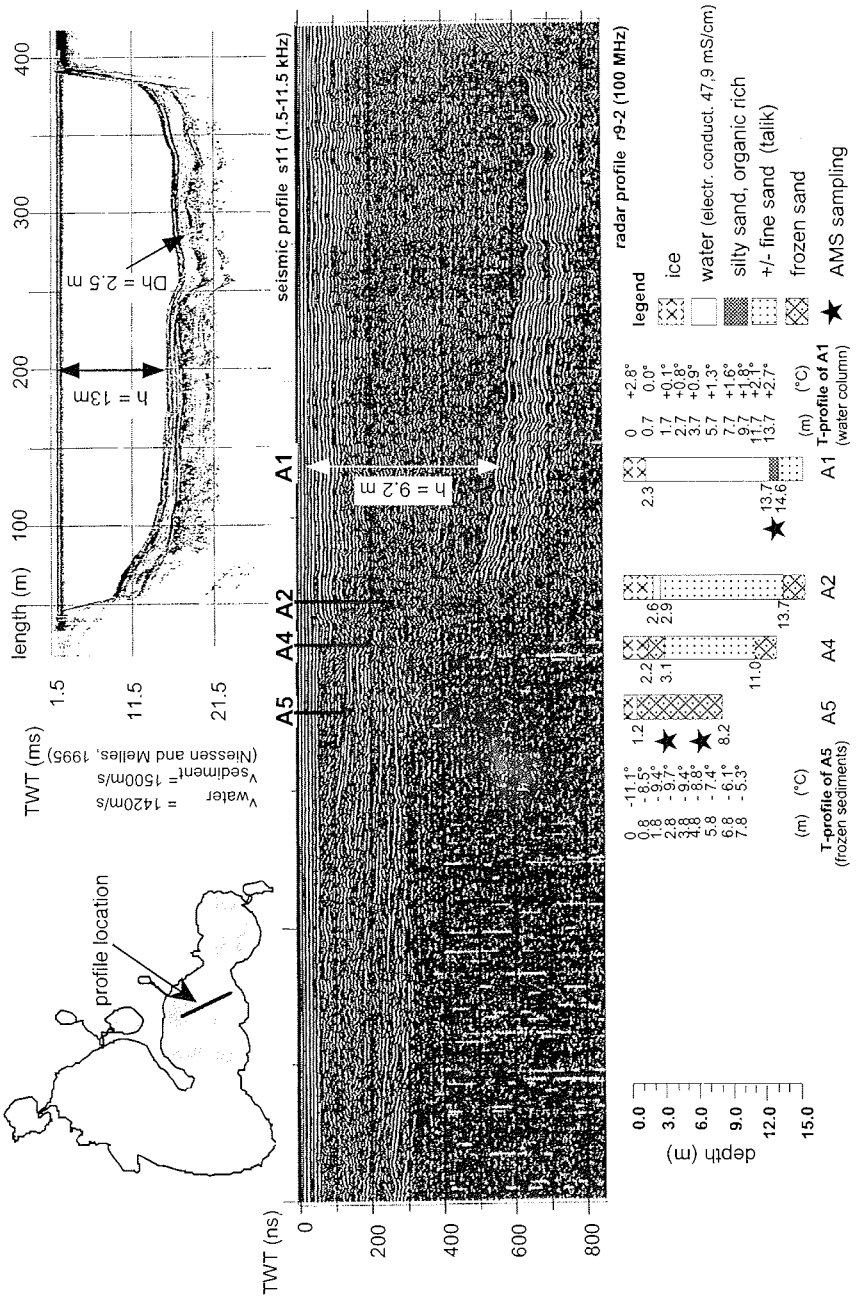

Figure 4-5: The seismic and the radar profile have been gained over the same lake basins and are complementing one another since the geologic situation does not change decisively. Drilling results are to scale with the radar chart. Temperature profiles for frozen sediments (A5) and the water column (A1) are added.

4.3 Coastal erosion studies in the Laptev Sea

(F. E. Are, M.N. Grigoriev, H.-W. Hubberten, V. Rachold, S. O. Rasumov and W. Schneider)

4.3.1 Introduction

The main goal of investigations was a quantitative evaluation of coastal dynamics through three parameters:

- Land loss or accretion,
- Amount of coastal erosion products entering the sea,
- Amount of sediments consumed for delta advance into the sea.

Obtaining values of the land loss or accretion is simple in principle. For that it is enough to measure the displacement of the shoreline during definite time. These measurements may be carried out (1) by the comparison of aerial photographs, maps and space images taken in various times, (2) using results of long-run monitoring of coastal dynamics or (3) by means of field measurements of modern shore line position and subsequent comparison of results with old maps etc.

Evaluation of the second parameter is much more complicated. The coastal erosion takes place both above the sea level (cliff destruction) and under the sea level (shoreface erosion). The cliff geometry may be easily measured, but it is not the case with the shoreface because its outer boundary often is not pronounced either morphologically or lithologically or otherwise. This situation is especially often observed in shallow Arctic seas along coasts composed of very fine-grained sediments. Thus, a special scientific problem arises: how to determine the outer boundary of the shoreface. The scarce factual data available suggest that in shallow seas the sediment type plays an important role in shoreface formation. Therefore, the morphology and the bottom sediment lithology of the shoreface in different coastal environments are studied as a first step for solving this problem.

In addition to bathymetrical profiling and bottom sediment sampling, shallow seismic studies were included in the program of field work in order to identify the boundary between modern coastal erosion sediments and underlying non-eroded sediments as well as the upper boundary of ice bonded permafrost. Essentially, both boundaries are the paleo-climatic signals. Furthermore, shallow seismic profiling also produces high quality bathymetrical profiles.

4.3.2 Methods

Investigations were carried out on several key sections of the coast (Figure 4-6 and Table A4-4, appendix), situated in various environments and consisted of five main parts:

1 Geodetic measurements were performed on land to obtain the modern horizontal and vertical position of the shores. On erosional shores the position of the cliff base and the cliff upper edge was measured. On accretional shores the subject of measurements was the shoreline. Characteristic terrestrial features, which could be identified on arial photographs as well, such as sharp turns of small streams, small water bodies, boundaries of different types of vegetation etc., served as natural marks. Measurements were carried out using a laser theodolite Elta 50 R. During good weather conditions 3.2 km of shoreline could be measured from one theodolite position with an accuracy of some millimeters. The geodetic measurements are indicated as (c) "coastal studies" in Figure 4-6 and Table A4-4 (appendix).

2 Shoreface profile measurements were carried out from the shoreline across the outer boundary of the shoreface. At water depth > 2 m these measurements were carried out using the echo sounder on board of the vessel Dunay, which has a resolution of about 2 cm. A small portable echo sounder on board of a motor boat with 10 cm resolution was used in near shore shallows with water depths < 2 m. During the measurements the position of the vessel Dunay was fixed by GPS. The location of the motor boat in shallows up to 1.5 km from the shore was measured using a theodolite and an on-shore range marked by poles. Shoreface measurements are indicated with (s) "shallow water profiling" and (d) "deep water profiling".

3 Bottom sediment sampling along the shoreface profiles was carried out in intervals of 0.1-1.0 km using a light grab sampler (indicated by (b) "bottom sediment sampling"). A list of samples is presented in the appendix (Table A4-5).

4 For shallow seismic profiling a sediment echo sounder (Geoacoustics GeoChirp 6100A) was used (see chapter 4.2 and Schwamborn et al., 1999). Shallow seismic studies are indicated by (g) "geophysics" in Figure 4-6 and Table A4-4).

5 Additionally, temperature profiles in the sea water column were recorded at several stations marked by (t) "temperature measurements". Sea water

temperature measurements were carried out at 14 stations from Dunay. Two thermal cables with temperature sensors were used for measurements of water temperature on a vertical water profile. The depth of the bottom sensor was checked by echo sounding. Air temperature, wind direction and speed, characteristics of currents and wave regime were determined as well (see Table A4-6, A4-7 appendix).

6 About 1000 aerial photographs (scales 1:30,000-80,000) and 150 topographic maps (scales 1:25,000-300,000) were purchased for study of the Laptev Sea coast dynamics by remote methods. The remote material was produced in 1951 - 1991 and covers all key sites listed below. Theodolite profiles and bench marks recorded in the field could be identified in the remote material. Furthermore, arial photos and maps are used for long-term analysis of coastal dynamics of the key sites by computer techniques, which allow to estimate an average rate of shoreline retreat and long-term trends of the Laptev Sea coast quite precisely.

The following key sections have been selected (see Figure 4-6):

1 Arga Island, north-east coast of the Lena Delta (Stations 1,2,3), a sea dominated, erosional, 10 m high coast composed of fine-grained sands with low ice content (ca. 20-30 %)

2 Amerika-Kuba Island (Station 4) in the northern part of modern Lena Delta, which is bounded by a 3 m high cliff, composed of loams, sands and peat

3 A nameless island in the Sardakh Channel mouth (Station 5), which is an accretional flood plain, 0-1 m high, composed of silt, fine-grained sand and peat, ice contents 25-40 %

4 Orto-Yuos Island in the Bykovsky Channel mouth (Station 7), the first terrace of the Lena Delta, 1-3 m high, smoothly turning into an accretional flood plain, composed of silt, fine-grained sand and peat, ice contents 25-40 %

5 Muostakh Island located at the entrance to Tiksi Bay (Station 8), a remnant of the coastal plain, 20 m high, 500 m wide and 7 km long, composed of small polygonal ice wedges (ice contents 60-85 %), characterized by a steep angle after thawing

6 West coast of Buor-Khaya Peninsula (Station 10) and Shirokostan Peninsula (Station 13), a sea dominated, erosional coast, bordering a coastal plain up to 30-40 m high, composed of large polygonal ice wedges

(ice contents 60-85 %), characterized by a steep angle after thawing, with vast lake-thermokarst depressions

7 North-west coast of Makar Island (Station 12), an up to 40 m high remnant of the coastal plain situated at the off-shore edge of a vast marsh, which is composed of small polygonal ice wedges (ice contents 60-85 %), characterized by a small angle after thawing

8 West coast of Buor-Khaya Peninsula (Station 9), south coast of Dmitry Laptev Strait (Station 16), south coast of Bolshoy Lyakhovsky Island (Station 17) and west coast of Bykovsky Peninsula (Station 20 and 21), all of which are erosional coasts, 30-40 m high, composed of small polygonal ice wedges (ice contents 60-85 %), characterized by a small angle after thawing

9 Vankina Guba Bay (Station 11), penetrating 30 km into the land, which is a subject to wind surges up to 6-10 m high (Tarakanov and Biryukov, 1974), representing a complicated coastal system with vast marshes and erosional cliffs, ice contents 60-85 %

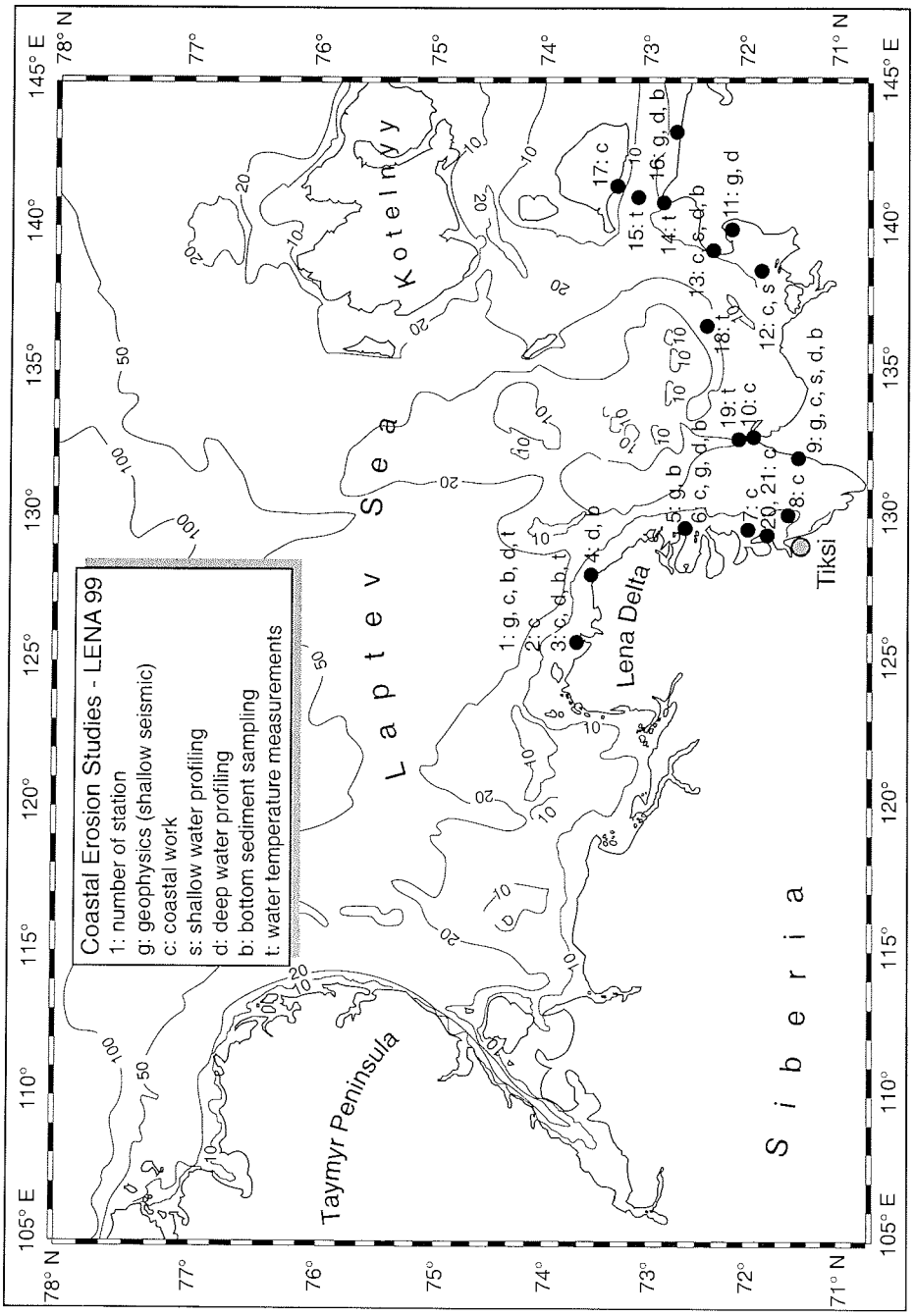

Figure 4-6: Working areas and stations of the coastal erosion team (2b: Dunay).

4.3.3 Preliminary results

Geodetic survey of 55 km shores lines has been carried out. Seven shoreface profiles of a total length of 46 km were measured using echo sounder and partly shallow seismic. Eleven profiles of a total length of 240 km were obtained from bathymetrical maps of 1:25 000 - 1:200 000 scale. 70 samples of bottom sediments were taken.

Shoreface profiles obtained during field season indicate significant diversity and complicity of Laptev Sea shoreface morphology. Figure 4-7 shows an example of a shoreface profile measured at station 3. On the other hand some general features and peculiarities can be recognized.

- All shoreface profiles of erosional shores are concave; this reveals non-equilibrium state of the coasts and allows to forecast continuation of intensive coastal erosion during the next century,
- The off-shore boundary of the erosional shorefaces is situated mainly in the 10 m isobath area,
- The shoreface of river delta advancing coasts usually has one or two shallow benches in its upper part, as wide as 20 km, with sharp increase of inclination in the 1 or 2 m isobath area,
- Local depressions created by strudel-scour could be observed on the 2-m bench in the mouth region of the Sardakh Channel (Station 5) both in the bathymetrical and in the shallow seismic profile (Figure 4-7),
- A buried ice-complex, which is overlain by marine sediments, could be identified in the shallow seismic profile recorded in the Dmitry Laptev Strait (Station 6, see Figure 4-8).

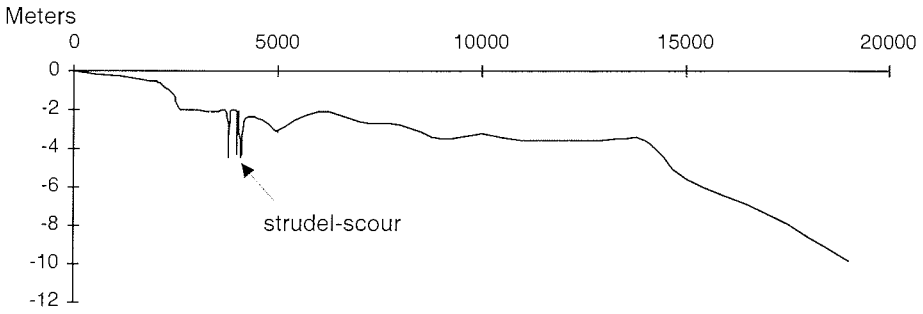

Figure 4-7: Shoreface profil of station 5 (nameless island in the Sardakh Channel mouth). Accretional flood plain, 0 - 1 m high, consisting of silt, fine-grained sand and peat. Start point: E 129°37.1', N 72°33.3', Az. 90°.

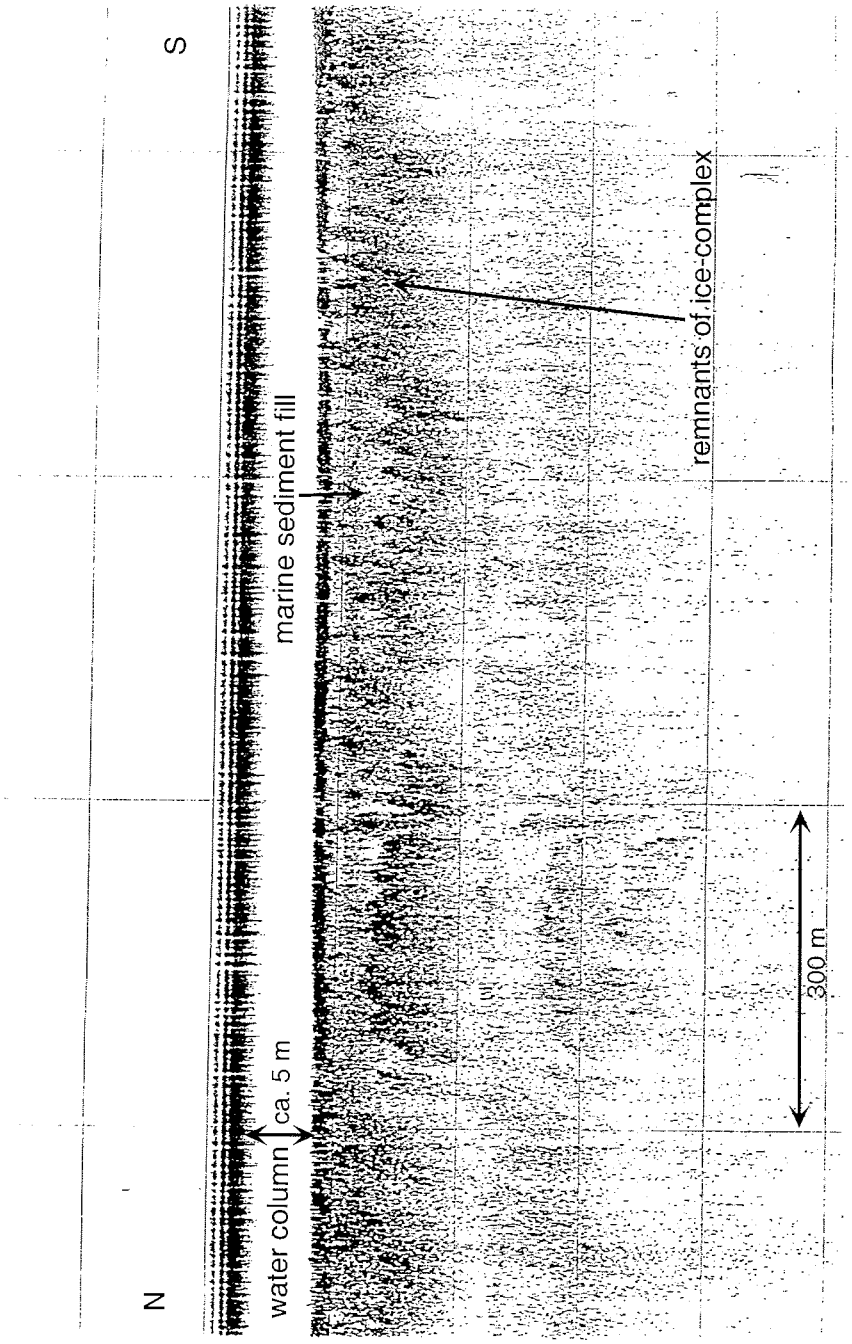

Figure 4-8: Shallow seismic profile across Dmitry Laptev Strait. The buried ice-comples, which is overlain by marine sediments, is indicated.

The results of our laser theodolite survey carried out during the field season 1999 and the subsequent comparison with aerial photos taken between ca. 1950 and 1980 show that the average coastal retreat rate for the long-term period is:

- Station 1 (Arga Island): 1971-99 - 1.5 m • year^{-1}
- Station 2 (Arga Island): 1971-99 - 2.5 m • year^{-1}
- Station 3 (Arga Island): 1971-99 - 2 m • year^{-1}
- Station 5 (Sardakh Channel Mouth): 1969-99 - 2 m • year^{-1}
- Station 7 (Orto-Yuos Island in the Bykovsky Channel mouth): 1951-99 - 0.7 m • year^{-1}
- Station 8 (northern coast Muostakh Island): 1951-99 - 4.7 m • year^{-1}
- Station 9 (western coast Buor-Khaya Peninsula): 1974-99 – 1.9 m • year^{-1}
- Station 10 (western coast Buor-Khaya Peninsula): 1974-99 - 1.7 m • year^{-1}
- Station 12 (western coast Makar Island): 1973-99 - 4.8 m • year^{-1}
- Station 13 (western coast Shirokostan Peninsula): 1974-99 - 4.4 m • year^{-1}
- Station 20 (northeast coast Bykovsky Peninsula): 1951-99 -
- 2 m • year^{-1}
- Station 21 (northeast coast Bykovsky Peninsula): 1951-99 – 2.7 m • year^{-1}

According to the results of our research we can evaluate the average shoreline and cliff top retreat rate for all Laptev Sea coastal sites, which consist of ice-rich sediment. This rate is approximately 2-2,5 m • year^{-1}. The shoreline retreat rate of small islands covered by ice-reach deposits is almost twice faster than that of continental sites or large islands. The shoreline retreat rate of the sandy Arga Island coast is almost comparable with that of coasts formed by an Ice Complex, which was unexpected for us. The maximum rate of coastal erosion was observed on the Northern Cape of Muostakh Island: 650 m during 48 years or 13.5 m • year^{-1} (Station 8, see Figure 4-9). The obtained data on the average coastal retreat rate will allow us to estimate the volume of coastal mineral material entering the Laptev Sea shelf more precisely.

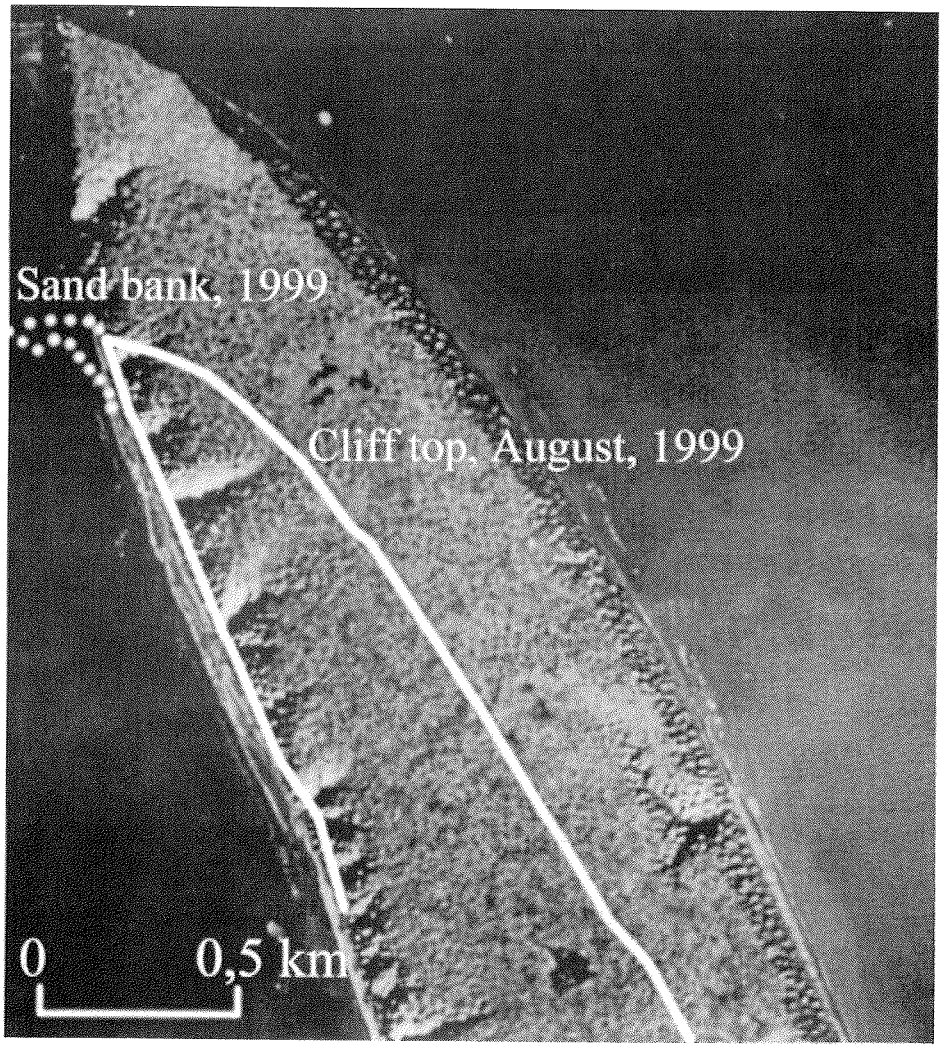

Figure 4-9: Arial photograph of Muostakh Island taken in September 1951 and the modern position of the cliff recorded in August 1999.

The temperature measurements on vertical sea water profiles show that temperature below zero near sea bottom is a quite regular phenomenon even in the coastal zone (Figure 4-10). This fact is very important for understanding the development of subsea permafrost along the nearshore shelf. The vast distribution of near bottom summer temperatures below zero indicates that subsea permafrost can be preserved on a shallow shelf for a long time. The

temperature regime of water mainly depends on the local hydrometeorological conditions (see Table A4-6, and A4-7, appendix).

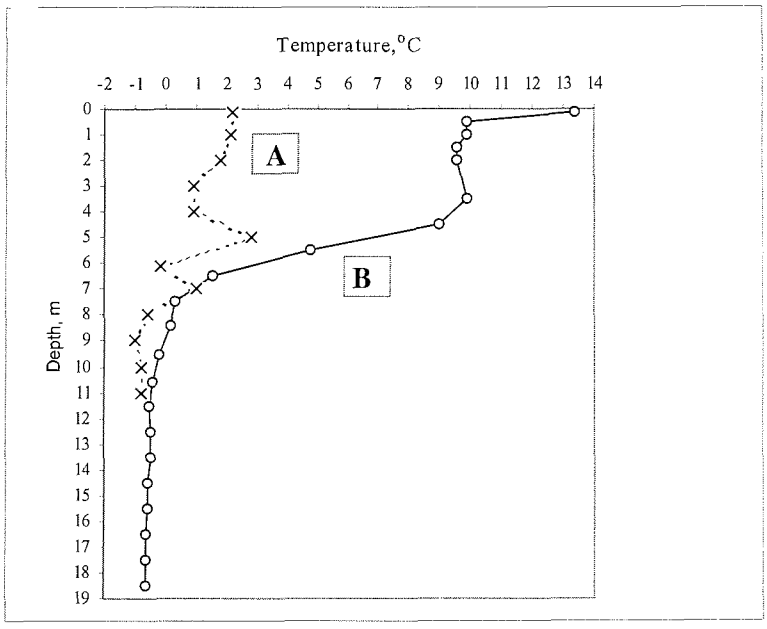

Figure 4-10: Water temperature profiles at (A) station 4 (Kuba Bay) and (B) station 19 (Buor Khaya Bay).

(A) - intensive water mixing during a strong north-eastern wind-induced surge

(B) - calm conditions.

4.4 Geological-Geomorphological studies in the western and central sectors of the Lena Delta

(E. Yu. Pavlova and M. Dorozhkina)

4.4.1 Introduction

The 1999 expedition activities continued the 1998 field season studies on reconstruction of the paleogeographic conditions for the development of the natural environment in the Lena River Delta during the Pleistocene and Holocene with obtaining quantitative paleoclimatic characteristics (Pavlova and Dorozhkina, 1999).

The 1999 field studies aimed to collect field data necessary for characterizing the present state and for paleogeographic reconstruction of the natural environment evolution in the western and central Lena Delta and for creating a geomorphologic 1:200 000 scale map.

The main objectives of field studies included:

- to reveal and trace the main delta terrace levels with special sampling for radiocarbon dating of terrace levels;
- to study the current cryogenic and channel relief features;
- to investigate shore exposures in the branches and lakes with detailed sampling;
- to study lacustrine bottom sediments with detailed sampling;
- to recover the pollen traps set up in summer 1998.

4.4.2 Methods

The methods of field studies are presented in the 1998 Report (Pavlova and Dorozhkina, 1999), a list of samples is presented in the appendix (Table A4-8).

4.4.3 Study area

The field studies were carried out in the western and central Lena Delta sectors on the segment along the Olenyokskaya Channel from Samoylov Island to the Ebe-Basyn-Sise Island on Kurungnakh-Sise, Jangylakh-Sise, Khardang-Sise and other islands and along the small branches of the central delta area from Samoylov Island to the Gerasim-Tebyulege branch – eastern part of Jeppiries Island (Figure 4-11). The total route length under study comprised about 400 km.

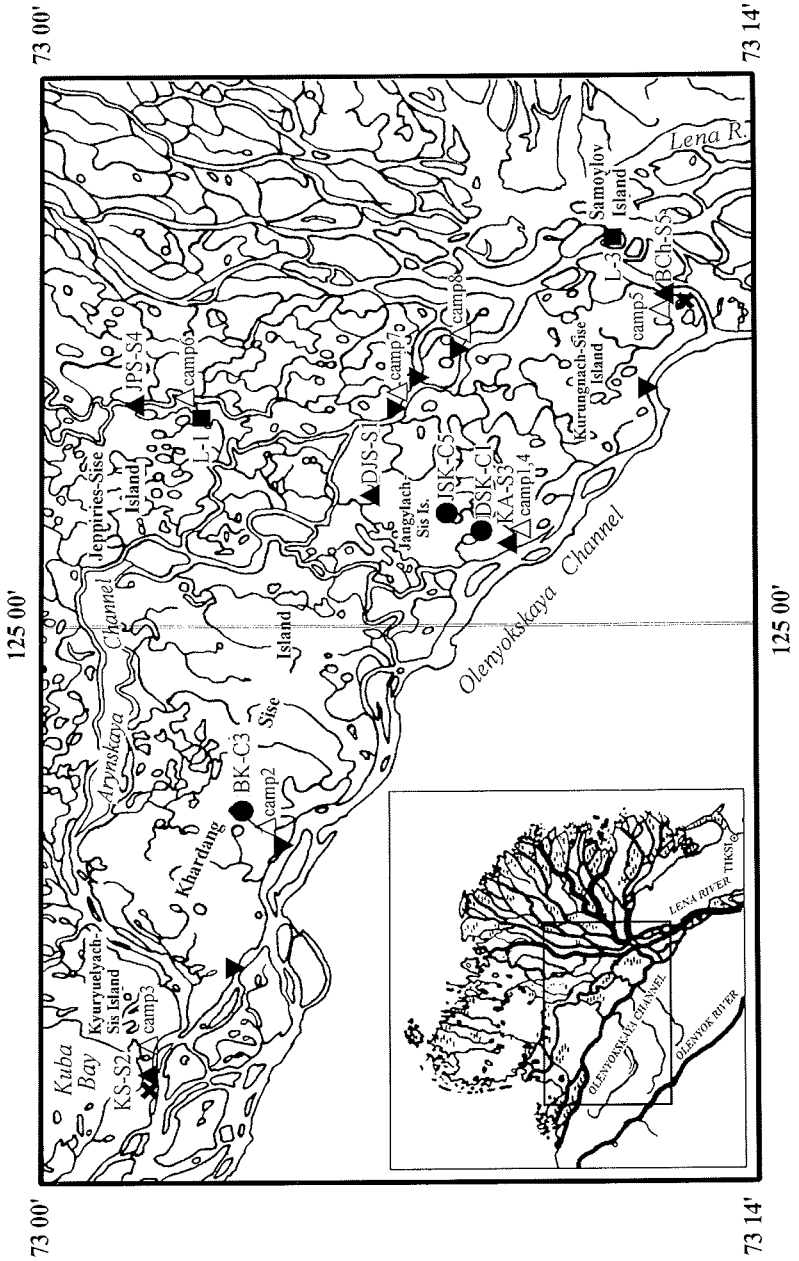

Figure 4-11: Location map of the western and central parts of the Lena Delta.
▲ section sampling, ▼ location sampling for 14 C –dating, Δ field camp
● lake sediment sampling, × bones samples, ■ pollen trap station

The Olenyokskaya Channel is the south-westernmost branch of the Lena River Delta. It is oriented in the sub-latitudinal direction. The left-hand branch shore is mainly bedrock being formed by the mountain slopes of the Chekanovsky range system. The right-hand shore of the branch consists of numerous delta islands. The length of the Olenyokskaya Channel is 229 km. It has a meandering channel with a width ranging between 0.25 and 2.4 km at the exit. The water depth is between 1.5 m and 11.3 m. The lowest depths (1.5-1.6 m) are observed in the upstream reaches over the first 95 km. There are 5 bars with a total length of 17.5 km. The current speed comprises 0.3 to 0.7 m/s. With moving westward, the current speed decreases. The segment from the Batyyalakhsky bar to the exit to the Olenyok Bay is subjected to the action of wind surges.

There is a developed polygonal- ridge and flat-hillocky complex of tundra bog lowland and tundra peat- and peat-gley soils belonging to a permafrost tundra-arctic type within the study area (Atlas of the Arctic, 1985).

The vegetation communities of the study area are represented by dwarf shrub and herbaceous-dwarf shrub (Dryas octopetata, Cassiope tetragona, Salix nummularia, Salix reptans, Luzula confusa, Poa arctica, Papaver pulvinatum, Saxifraga hirculus, Valeriana capitata), moss (Tomenthyphnum nitens) and lichen of northern and Arctic East Siberian tundra in combination with herbaceous-hypno and polygonal bogs.

4.4.4 Results of the field studies

The following geomorphologic levels were identified in the study area:

- low floodplain and a complex of modern channel features (1-4 m a.s.l.) of modern age;
- high floodplain (4-8.5 m a.s.l.) of Late Holocene age;
- first above the floodplain terrace (9-12 m a.s.l.) of Early-Middle Holocene age;
- second above the floodplain terrace (13-29 m a.s.l.) of Late-Pleistocene-Early Holocene age.
- third above the floodplain terrace (30-60 m a.s.l.) of Late-Pleistocene age;

The data obtained agree in general with a complex of earlier identified terrace levels for the Lena Delta (Korotayev, 1984; Grigoriev, 1993; Pavlova and Dorozhkina, 1999).

The **low floodplain** is traced by segments of different width (some meters to 3.5-4 km) along the branches. The low floodplain surface is sparsely covered

with vegetation. The low floodplain is annually flooded with water during the floods and frequent wind surges.

The low floodplain deposits are represented by alluvial fine- and medium grained sands and the sand-silt-clayey alternation strata with plant macro-remains. Active accumulation processes forming the strata of sand alternation and silt-clayey deposits with plant macro-remains occur during wind surges at the periodical flooding of the low floodplain areas covered with vegetation. Active accumulation of sand material with the formation of wide near-channel sandy shoals (Diring-Ayan-Belkeye Island, sands of Kukula-Kumaga, Butun-Kumaga, etc.), alluvial longshore ridges and spits occurs in the areas of large bends near the convex shores of the branches. The surface of sand shoals is flat and devoid of vegetation. Sands are undulated-layered.

The complex of current channel features includes channel bars and islets comprised of alluvial sands (Kel'tegey-Bel'key Island, sands of Byrakan-Kumaga, etc.) They are up to 7 m high. Their active formation occurs during the flood period. When the water level in the branches reaches the low water level, the islets and the near-channel shoals dry. At this time, eolian processes are active at their surface with the formation of the eolian relief features (sand ripples, hillocky sands, and barkhans). The surface is devoid of vegetation.

The lake ratio coefficient for the low floodplain surface comprises 0-37 %. The low floodplain is characterized by the development of mort lakes, that have an elongated shape and a meandering coastline.

As a result of the influence of the channel flow, a thermo-erosion recess up to 4 m high and up to 3-10 m deep forms in some places near the rear seam of the low floodplain.

Cryogenic processes within the low floodplain are manifested in the presence of separate frost cracks without a pronounced polygonal character. Sometimes, separate areas of developed bar concave polygons with small bogs in the center are observed.

The **high floodplain** (4-8.5 m) is developed everywhere throughout the entire length of the branches presenting a flooded surface during the flood only in some rare years. The high floodplain along the Olenyokskaya Channel is represented by areas of different width (up to 1 km), that are attached to the relics of the first above the floodplain terrace. In the central delta area along the Arynskaya, Balaganakh-Uesya branches, etc., the high floodplain is represented by a complex of large delta islands.

In general, the sediments of the high floodplain level in the western delta area are similar to the high floodplain deposits developed in its northern area (Pavlova and Dorozhkina, 1999) being represented by layered silty-sandy peat deposits.

The following datings were obtained for the deposits comprising the high floodplain:

- 2850±200 BP (LU-4414) for a sample of observation point 80-1 (72°48'06.5" N, 123°37'28" E) at a height of 2.10-2.15 m above the waterline of the Olenyokskaya Channel
- 3930±90 BP (LU-4413) for a sample of observation point 127-1 (72°36'50" N, 125°53'30"E) at a height of 5.15-5.20 m above the waterline of the Arynskaya Channel.

These datings indicate that the time of formation and the age of the high floodplain in the western delta area are determined as Late Holocene, which is in agreement with previous data (Pavlova et. al., 1999).

The high floodplain deposits have a high ice content with a developed lens-shaped, layered and reticulate structure. The outcrops of ice veins are observed everywhere in the high floodplain shore exposures. The ice vein width reaches 5-7 m with visible vertical thickness of up to 3.5 m. The distance between the veins is 5-8 m. A polygonal and polygonal-bar micro-relief is widespread on the high floodplain surface. The polygons are characterized by a tetragonal shape reaching 10-11 m in the cross-section. The central depressed polygon areas are swampy.

Thermo-erosion processes cause an intense decay of the high floodplain shores. The shore decay results from a downfall of large (3-8 m) soil blocks that separate along the cracks and thermo-erosion ruts bedding along the ice veins. The formation of a thermo-erosion recess contributes to a more rapid process of the downfall of blocks.

The lake ratio coefficient for the high floodplain surface comprises 12.5-17.2%. The high floodplain is characterized by a wide spreading of mort and thermokarst lakes. The mort lakes have an elongated shape with a meandering coastline reaching 2-2.5 km in length. The thermokarst lakes formed as a result of melting of ice saturated deposits and multiple ice veins are characterized by a rounded shape.

The investigated nameless thermokarst lake located in the southeastern area of Jangylakh-Sis Island is confined to the height level of the high floodplain. The lake area is 0.5 km^2, the coastline length is 2.2 km and the prevailing depth is 5

m. The southeastern lake shore is low and swampy whereas the northwestern shore is high and precipitous with a typical hillocky, small raviney relief presenting a bench of the third above the floodplain terrace with a relative elevation of 3 m. During high floods, river water penetrates into the lake.

A 0.80 m long bottom sediment core (DSK-C1) was retrieved from the deepest northeastern lake area (72° 32' 15" N, 125° 26' 10" E) (see Figure 4-11). Lacustrine sediments are represented by clayey silts of dark-grey color with non-uniform organic matter interlayers with a thickness between 0.1 to 2 mm.

The **first above the floodplain accumulation terrace** (9-12 m a.s.l.) is observed along the branches presenting local island segments of different width. The deposits of the first above the floodplain terrace are similar in composition to the high floodplain sediments being represented by silty-sandy-peaty deposits. One of the typical sediment sections of the first above the floodplain terrace is section KA-S3 (72° 29' 33" N, 125° 18' 45" E), located on the left bank of the Tyuerenkey-Tebyulege branch (see Figure 4-11). The absolute height of the shore exposure lip is 12.5 m a.s.l. The KA-S3 section deposits were described and sampled and are represented from the waterline down as follows (see Figure 4-12):

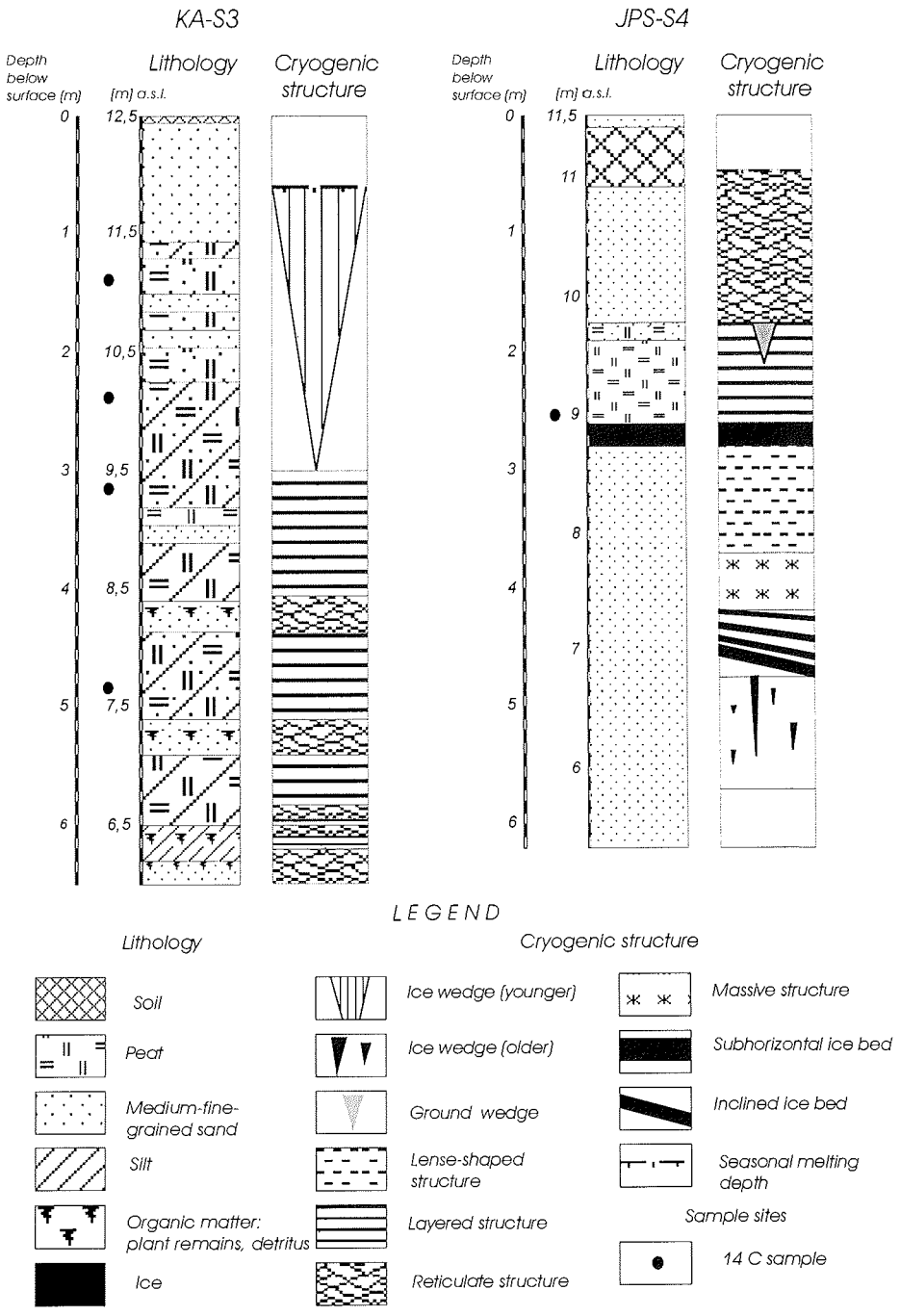

Figure 4-12: Cryolithological sections of the first (KA-S3) and second (JPS-S4) above the flood plain terraces.

12.50-12.45 m - Soil-vegetation layer
12.45-11.45 m - Pale-yellow-reddish-colored, fine-, close-grained, ferruginated and horizontally layered sand. Lamination is governed by the interlayers of strongly decomposed organic matter.
11.45-11.30 m - Silty-sandy-peaty alternation strata. The silt interlayers are dark-grey colored with a thickness of 1 cm. Fine-grained sand interlayers of a pale-yellow color up to 1. 2 cm thick. The interlayers of brown-colored fibrous peat are 1.4 cm thick.
11.30-11.00 m - Strongly sandy peat, fine-, close-grained sand.
11.00-10.85 m -Fine- and close-grained sand of a pale-yellow color with plant macro-remains.
10.85-10.70 m - Peat with a large content of fine- and close-grained sand.
10.70-10.55 m - Pale-yellow colored fine- and medium-grained sand
10.55-10.25 m - Peat with a large content of fine-grained sand.
10.25-9.20 m - Silty-sandy-peat alternation strata. Silty interlayers of a dark-grey color up to 1.5 cm thick. Interlayers of fine-and medium-grained pale-yellow sand up to 2.5 cm thick. Interlayers of loose carton-like brown-colored peat with a thickness of 2-3 cm. In the 11.10-11.05 interval, there is a fragment of wood 14 cm in diameter.
9.20-9.05 m - Reddish carton-like peat with a large ice content.
9.05-8.80 m - Fine-grained sand of a pale-yellow color with fine fibrous plant macro-remains.
8.80-8.30 m - Silt and peat alternation strata. Silt interlayers of a dark-grey color with a thickness of 0.7-1 cm. Interlayers of brown-colored carton-like peat with wood fragments up to 2-3 cm thick.
8.30-8.15 m - Yellowish-grey, fine-, close- and medium-grained ferruginated sand with plant macro-remains.
8.15-7.40 m - Silty-sand-peat alternation strata. Silty interlayers of a dark-grey color 0.7-1 cm thick. interlayers of fine-and medium-grained pale-yellow sand up to 1 cm thick. Interlayers of brown-colored peat with a thickness of 0.3-1 cm. The character of lamination is horizontally-undulated.
7.40-7.10 m - Brownish-grey colored fine-, close- and medium-grained sand with a very large content of plant macro-remains.
7.10-6.50 m - Silt and peat alternation strata of a grey-brown color. Peat is fibrous, slightly decomposed with separate twigs and roots.
6.50-6.20 m - Grey-colored silt with plant macro-remains and ice interlayers 0.1-0.2 cm thick.
6.20-6.00 m - Yellowish-grey, fine-grained ferruginated sand with plant macro-remains.
6.00-0.0 m - Talus.

The following datings were obtained for the deposits comprising the first above the floodplain terrace along the Olenyokskaya Channel:

- 6870±230 BP (LU-4409) for a sample of KA-S3-5 (6.60-6.65 m)
- 5100±140 BP (LU-4411) for a sample of observation point 81-1 (72°45'26" N, 124°05'26.5"E) at a height of 2.00-2.05 m above the waterline.

These datings indicate that the time of formation and the age of the first above the floodplain terrace in the western delta area are determined as Middle Holocene, which is in agreement with previous data (Pavlova et. al., 1999).

The first above the floodplain terrace deposits with a large ice content are characterized by the developed massive, lens-shaped and reticulate cryogenic

structures. Ice veins are widespread in the deposits. The outcrops of ice veins are observed in the shore exposures of the first above the floodplain terrace. The width of the ice veins in the upper portion is 1.5 to 2.5 m, the visible vertical thickness is up to 3-5 m and the distance between the individual veins is up to 11-13 m. The ice veins are frequently overlapped with laminated peat-silt deposits.

The flat hummocky surface of the first above the floodplain terrace is characterized by the developed polygonal and polygonal-bar micro-relief. In general flat polygons are most developed. The polygons often have a regular rectangular shape with a size up to 12-15 m in the cross-section. The central areas of the polygons are swampy being often occupied by small lakes.

Along the shores of the branches, bedding of thermo-erosion ruts occurs along the ice veins. The process of shore destruction of the first above the floodplain terrace is similar to the character of destruction of the high floodplain shores.

The lake ratio coefficient is between 7.5 to 15.6%. Thermokarst lakes of a round shape with smooth coastline contours and mort elongated lakes are developed at the surface of the first above the floodplain terrace.

The **second above the floodplain terrace** has a fragmentary development in the form of erosion remnant with absolute top marks of 13-19 m a.s.l. The relics of the second above the floodplain terrace sharply differ from the other terrace levels by the lithological composition of the deposits, the geomorphologic surface habit and the character of the vegetation cover. The deposits are characterized by a uniform composition and structure. They are mainly represented by quartz fine-, close- and medium-grained, sub-horizontally and obliquely-laminated sands.

The deposits of the second above the floodplain terrace are described in the section JPS-S4 (72°54' 43" N, 125°52' 50" E) of the sand remnant (16 m a.s.l.) on the left shore of the Malaya Tumatskaya Channel (see Figure 4-11). The absolute height of the shore exposure lip is 11.5 m a.s.l. The description is from the top down (see Figure 4-12) :

0.0-0.1 m - Fine-grained pale yellow polymict sands;

0.1-0.6 m - Turf;

0.6-1.75 m - Fine-grained, pale yellow horizontally undulated-laminated sands with a polymict-quartz composition. Lamination is determined by alternation of grey interlayers 0.3-1.5 cm thick enriched with organic matter and sand interlayers 1-12 cm thick. The bottom portion contains ferrugination spots and interlayers. The contact with lower strata is clear, undulated and stressed with the ferrugination interlayer 0.4-2 cm thick.

1.75-1.90 m - Peat-sand alternation strata. The thickness of brown colored peat interlayers is 0.5-0.7 cm. The thickness of pale-yellow sand interlayers is 0.5-1.5 cm. The strata is broken by a vertical frost crack (with a visible thickness of 35 cm) going deep to the lower lying strata. The crack is filled with fine-grained sand. Intense ferrugination is observed along the crack sides, the sides are irregular and lacerated. The crack width is 10-13 cm. The vertical displacement along the crock of the northern and southern blocks comprises 7 cm;
1.90-2.60 m - Brown-colored well decomposed peat with lenses of fine-grained yellow colored sand;
2.60-2.80 m - Ice is in layers. The layer sloping angle is 10°. The contact with the above lying strata is uniform and with the lower strata – pockety;
2.80-3.70 m - Fine-grained yellowish-grey colored quarts sands with reddish ferrugination spots and streaks. The spots are elongated along the long axis from bottom to top. At the contact with the lower strata, there is a thin ferrugination interlayer with a thickness of 0.3-0.4 cm.
3.70-4.20 m - Fine-grained pale-yellow undulated-horizontally-laminated sands. The character of the cryogenic structure is massive.
4.20-4.75 m - Fine-grained pale-yellow colored quartz undulated-horizontally-laminated sands. The strata contain the oblique ice veins with the sloping angles of 10°, 20°, 30° and 45°. The thickness of ice veins increases downward the section comprising between 0.5 to 25 cm;
4.75-5.75 m - Fine-grained pale-yellow colored quartz undulated-horizontally-laminated sands with subvertical ice veins and veinlets 0.3 –5 cm thick.
5.75-11.00 m - Talus.

The character of the cryogenic microrelief of relics of the second above the floodplain terrace and the thermo-erosion, eolian modern relief-forming processes are described in (Pavlova and Dorozhkina, 1999). The lake coefficient is 12.5-60.9 %.

The **third above the floodplain terrace** presents large erosion remnants located in the southwestern zone of the study territory – along the right-hand shore of the Olenyokskaya Channel (Kurungnakh-Sise, Jangylakh-Sis, Khardang-Sise and Kyuryuelyakh-Sis Islands). The absolute top marks of the relics comprise 30-60 m a.s.l. A typical feature of the third above the floodplain level is widespread deposits of the ice complex in the upper section portion of the relics. The deposits comprising the relics of the third above the floodplain level were investigated and described at three locations: Kurungnakh-Sise, Jangylakh-Sis and Kyuryuelyakh-Sis Islands.

The deposits investigated in the shore exposure (the absolute height of the shore exposure lip is 36 m a.s.l.) in the northern part of Jangylakh-Sis Island on the left-hand shore of the Arynskaya Channel – section DJS-S1 (72°38' 40" N, 125°30' 58" E) (see Figure 4-11) - are presented from the waterline:

0.0-2.0 m - Talus;
2.0-4.5 m - Brown carton-like, horizontally laminated peat with lamination stressed by thin interlayers of close-grained sand.

4.5-5.5 m - Fine-grained pale-yellow undulated-horizontally layered sand with a quartz-feld spar composition. Lamination is emphasized by dark interlayers enriched with organic matter;
5.5-9.0 m - Brown-colored laminated peat. Lamination is determined by interlayers of fine-, close-grained sand;
9.0-24.2 m - Fine-, close-grained horizontally layered sand with a quartz-feldspathic composition. Lamination is governed by alternation of thin interlayers of fine-grained sand with interlayers of close-grained sand. Organic remains in the form of fibers and twigs appear in the upper 0.6 m in the 23.6-24.2 m interval. Permafrost sand with lenses and veins of massive large bubbly ice;
24.2-36.0 m - Ice complex deposits represented by a laminated sandy peat-loam alternation strata broken by multiple ice veins. The visible vein width is up to 6 m.
Above the outcrop lip to an absolute height of 41 m a.s.l, the slope is turf-covered being represented by a complex of hillocky relief.

The description of the section is in agreement with the previous description (Galabala, 1987). The obtained 14C-dating in the 2.0-4.5 m intervals revealed an age of more than 32000 years BP (MAG-539) and in the 5.5-9.0 m interval – 39000±3400 years BP (MAG-538) (Galabala, 1987).

The composition and structure of the third above the floodplain terrace investigated along the right-hand shore of the Olenyokskaya Channel in the vicinity of Buor-Khaia, BCh-S5 (72° 19' 31" N, 126° 16' 07" E) and in the vicinity of Nagym, KS-S2 (72° 52' 51" N, 123° 11' 58" E) (see Figure 4-11) agree in general with those described before (Kunitsky, 1989; Schwamborn et al., 1999). In section BCh-S5 the base of the ice complex is located at a height of 24 m a.s.l. with an ice complex thickness of 11-12 m. In section KS-S2 the base of the ice complex is observed at a height of 10-11 m above the waterline with an ice complex thickness of 7-8 m. For determining the age of the onset of the formation of the ice complex, samples for radiocarbon analysis were collected from all sections studied from the base of the Yedoma deposits (see Table A4-9, appendix).

In the vicinity of Buor-Khaia in the talus, bone remains of the mammoth complex fauna were detected that have melt from the Yedoma deposits. The bone remains of the mammoth fauna were found in the lake shore exposure south of Kuba Bay with an absolute mark of 16.8 m above the waterline (see Table A4-9, appendix).

In August 1997 A. Ye. Paselsky, a fisherman from Taimylyr, found an in-situ mammoth scull in the ice complex deposits of the third above the floodplain terrace of the Olenyokskaya Channel 3.6 km downstream from Nagym. In July 1998, the scull was frozen out from the deposits containing it. I. I. Vinokurov, a fisherman from Taimylyr working in the Nagym fishery area, informed us about the unique finding for the western delta sector. The well-preserved scull, with

the size of 0.65 x1.05 m, was found not far from the place of observation near the fisherman' house and supplemented to the collection of bone remains from the ice complex of the western delta sector.

The surface of the third above the floodplain terrace, which's upper cocle is represented by Yedoma deposits with a high ice content, is characterized by the most active development of cryogenic processes. In the flattened water divide areas under the conditions of conservation of the ice veins, general surface planation occurs with the formation of a polygon-free micro-relief or flat often hexagonal polygons with leveled bars and overgrown small bogs. A bar micro-relief with concave swampy polygons is often developed at the swampy gentle slopes of the third above the floodplain terrace. Near the terrace lip under the conditions of drained slopes, a thermokarst polygonal bar micro-relief is formed with melting rills between the bars. Steep benches of the third terrace are characterized by a hillocky relief.

Alas troughs with round thermokrast lakes and pingos confined to their bottoms are widespread over the terrace surface. The lake sizes vary between some meters and 1-2 km in the cross-section, with pingos reaching a height of 28-30 m. Sometimes the alas depressions combine forming a general alas trough complicated in configuration and significant in area (up to 10 km wide).

A strongly branched thermo-erosion network is observed on Khardang-Sise, Jangylakh-Sis and Kurungnakh-Sise Islands with ravines entrenched here to the ice complex deposits to a depth of 35 m at the mouth width of up to 70 m. The cross profile of the ravines is V-shaped, with the bottom becoming flatter and the profile attaining a box-like form closer to the mouth.

Flat bottom dells without a channel and sometimes with rudimentary channels, along which melt and rainwater is discharged are widely developed at the terrace surface. The length of dells varies between some meters and 4.5 km.

The lake ratio coefficient changes from 0 to 14.4%. Thermokarst lakes are confined to the height level of the third above the floodplain terrace. Lakes Byrakan-Kyuele (Khardang Island) and Jangylakh-Sisin-Kyuele (Jangylakh-Sis) were studied. Lake Byrakan-Kyuele has an area of 2.4 km^2. Its coastline length is 4.6 km and the waterline mark is 23.4 m a.s.l. The lake basin presents a calicular-shaped trough. A sand shoal with depths of 0.5-1.6 m gently sloping towards the lake center is traced along the southern shore over 400 m. At a depth of 2 m there is a dramatic depth increase to 6.5-7 m. The largest depth reaches 9 m being observed closer to the northern lake shore (see Figure 4-13). The northern underwater trough slope is more steep.

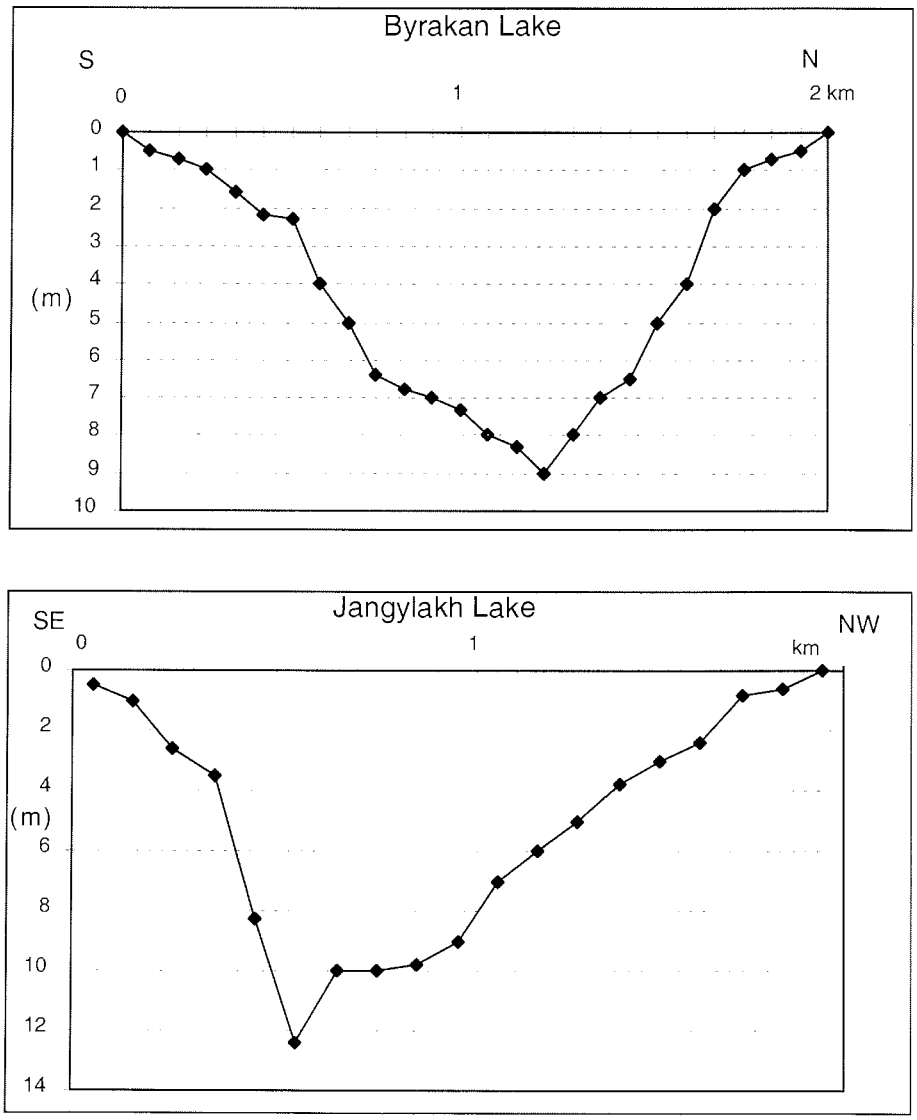

Figure 4-13: Bottom profiles of lake troughs of the thermokarst lakes of the third above the floodplain terrace

A 0.68 m long bottom sediment core (BK-C4) was retrieved in the deepest lake area (72° 47' 23" N, 124° 14' 59"E) (see Figure 4-11). The lacustrine sediments are represented by clayey silt of a dark-grey color with separate plant macro-remains and interlayers of fine-grained sand. The interlayers of fine-grained sand with a thickness between 2 to 9 mm are observed in the 0.20-0.08 m interval.

The area of Lake Jangylakh-Sisin-Kyuele comprises 1.8 km^2, the coastline length is 4 km and the waterline mark is 13.6 m a.s.l. The prevailing depths, comprising 9.5-10 m at the maximum lake depth of 12.3 m, are observed in the lake center (see Figure 4-13). A sand shoal with a depth of 0.5 m and a width of 300 m extends along the northern-northwestern shore.

A 0.58 m long bottom sediment core (JSK-C5) was retrieved in the deepest central area of the lake (72° 33' 23" N, 125° 26' 31"E) (see Figure 4-11). The lacustrine sediments are represented by clayey silt of a greenish-brown color with a mixture of fine-grained laminated sand. The lamination is determined by a different content of organic matter and fine-grained sand.

The shores of the thermokarst lakes of the third above the floodplain terrace are characterized by relative elevations of up to 11-18 m, steep slopes up to 20-25° and a wide development of hillocky-raviney relief.

Three spore-pollen traps were recovered in the Lena Delta:

- L-1 in the Yugus-Jie area with coordinates: 72° 50' 17" N, 125° 49' 15" E;
- L-2 on Sagastyr Island with coordinates: 73° 23' 14" N, 126° 36' 53" E;
- L-3 on Samoylov Island with coordinates: 72° 22' 43" N, 126° 31' 08"E.

A herbarium was collected along the study traverse in the Lena Delta.

4.4.5 Preliminary Conclusions

The main geomorphologic levels were revealed and followed within the western delta sector as a result of field studies. Each height level was characterized by a representative section of Quaternary deposits and the composition and structure of the upper strata of bottom lacustrine sediments were determined. Sampling for spore-pollen and diatom analyses, analysis of plant macro-remains and dating was undertaken from the sections and lacustrine Quaternary sediment cores. The spore-pollen traps were recovered for revealing the character of pollen transfer in the Lena River Delta.

For revealing the specific geological-geomorphologic structure and the relief formation history of the Lena River Delta, geomorphologic maps of the major delta segments at 1:100 000 and 1:200 000 scales were compiled based on field observations and interpretation of aerial survey data (Pavlova and Dorozhkina, 1999). A comparison of the maps of major segments and an analysis of earlier obtained and published data on the available sections of quaternary deposits (Korotaev, 1984; Tomirdiaro et. al., 1985; Galabala, 1987; Kunitsky, 1989; Grigoriev, 1993; Nagaoka, 1994; Kuptzov and Lisitzin, 1996;

Pavlova and Dorozhkina, 1999; Pavlova et. al., 1999; Siegert et al., 1999; Schwamborn et.al., 1999) allow the following conclusions:

- The thickness of the ice complex deposits in the eastern delta sector is 2-3-fold greater compared to that in the western sector.
- The base of the ice complex declines from 10 to 28 m a.s.l. in the western area to –8 to -10 m a.s.l. in the eastern area.
- A sharp decrease of the base level of the ice complex is observed east of the Malaya and Bolshaya Tumatskaya Channels.
- The eastern delta sector is mainly characterized by young datings (10-30 kyr) whereas the western sector – by more ancient datings (older than 30 kyr) located at similar hypsometric marks.
- A full complex of terraces is developed in the western delta area while only two floodplain levels and relics of the third above the floodplain level are observed in the eastern area.

The established typical features testify to the tectonic regime change and the modification of the hydrographic network of the Lena River Delta during the Late Pleistocene and Holocene.

- Submerging of the base of the ice complex deposits from west to east and increasing thickness in the same direction, as well as the radiocarbon dating distribution indicates that from the Late Pleistocene the western and eastern delta areas developed in different directions under the conditions of the prevailing steady tectonic rise of the western delta sector and lowering or stabilizing of the eastern sector.
- The boundary between the two delta areas has a submeridional strike and is located between the Malaya and Bolshaya Tumatskaya Channels.
- The differences in the tectonic regimes of the western and eastern delta sectors account for the development of the entire complex of terraces in the western delta area while only two floodplain levels and relics of the third above the floodplain level are observed in the eastern area.
- The absence of the terrace levels of Late Pleistocene-Early Holocene and Early-Middle Holocene age in the geomorphologic series in the eastern delta area indicates that the onset of more active neotectonic motions took place at the end of the Late Pleistocene-Early Holocene.
- The development of the first above the floodplain terrace of Early-Middle Holocene age within the southwestern delta area indicates that this part of the delta was a sedimentation area in the Early-Middle Holocene. The main runoff of the Lena River at that time was in the northwestern direction along the Olenyokskaya Channel.

- The predominant development of the high floodplain of Late Holocene age in the northeastern delta area indicates a change in the main Lena runoff direction during the second half of the Holocene to the northeast-eastern due to tectonic causes.

The data obtained will serve as a basis for further detailed paleogeographic reconstructions of the environmental evolution of the Lena Delta in the Pleistocene and Holocene.

Acknowledgements: The authors are grateful to D. Kozlov (Department of Polar Geography Countries, RF SRC AARI), V. Pozdnyakov (International Biological Station "Lena-Nordensheld") and to V. Achikasov and V. Dormidontov (State Reserve Ust'-Lensky) who directly took part in the field studies.

The authors express their gratitude to the expedition participant A. Sher, senior scientist of the Institute of the Problems of Ecology and Evolution, RAS for determining the collection of bone remains.

The authors would also like to thank all who provided help and support during the field studies.

4.5. Observations of water level oscillations in the Olenyokskaya Channel

(E. Pavlova., M. Dorozhkina and D. Kozlov)

Observations of water level oscillations in the Olenyokskaya Channel in the area of a MINILOG-sensor LD98M02 (with coordinates (72° 52,941' N, 123° 14,580' E)) set up in 1998 (Antonow et al., 1999), were carried out for linking the automated MINILOG sensor data on the water level oscillations with the absolute marks.

A hydrological station with a visual readout was set up on the right-hand shore of the Olenyokskaya Channel, 2.4 km downstream from Nagym, in the area of the triangulation point 106 of the Main Administration of the NSR (24.8 a.s.l.) as a result of leveling on August 14, 1999. The coordinates of the hydrological station are 72° 53' 10" N, 123° 14' 28" E.

The observations at the hydrological station were performed every hour from 0 h on August 15 to 21 h on August 16, 1999. The diagram of water level oscillations is presented in Figure 4-14. The minimum water level values comprised –250 mm (for 16 h on August 16, 1999) and the maximum value was +115 mm (for August 18, 1999).

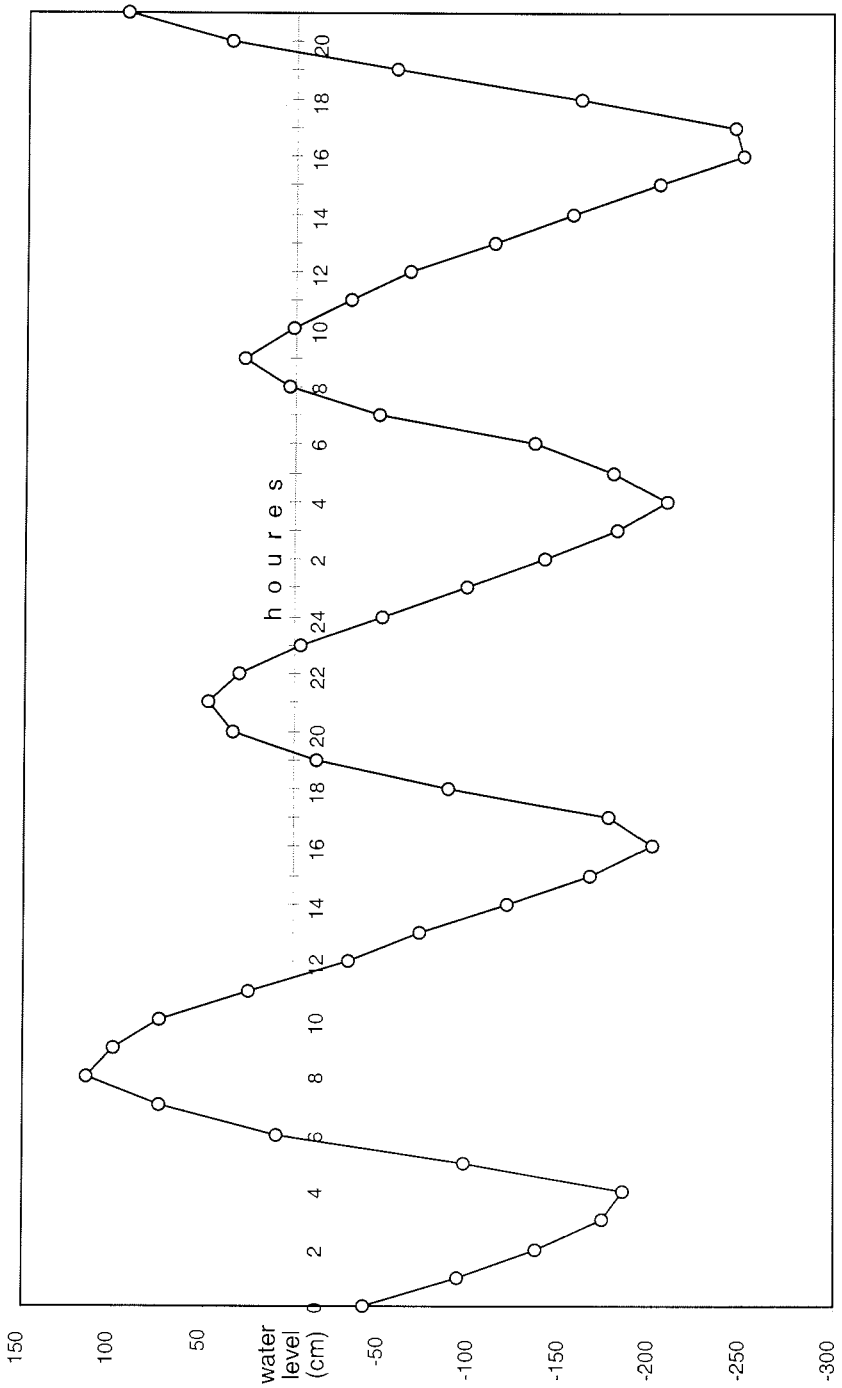

Figure 4-14: Diagram of water level oscillations in the Olenyokskaya Channel from August 15 to 16, 1999.

4.6 Aeolian sedimentation processes in the Lena Delta

(M. Antonow and J. Boike)

During the short Arctic summer season sediment is mainly transported by the Lena River. Wind also affects the particle transport of the delta region, strongly stressing the vegetation or wiping it out. As a result of the aeolian activity, many deflation plains were observed mainly in the Arga region (NW-delta). Although large meteorological data sets and climatic models exist, the magnitude of aeolian mass transport from the Siberian hinterland via the Lena delta towards the Laptev Sea is poorly understood. After break-up, the sediment-laden river ice supplies a large amount of (former) aeolian particles to the Lena river bed and the Laptev Sea shelf. A Campbell Scientific automatic weather station installed on Samoylov during July 1998 continuously recorded meteorological parameters. The wind speed during the winter months averaged around 4 m/s. Maximum wind speeds with up to 10 m/s occurred between December to January and originated from the south-west as well as from the north (see Figure 4-15).

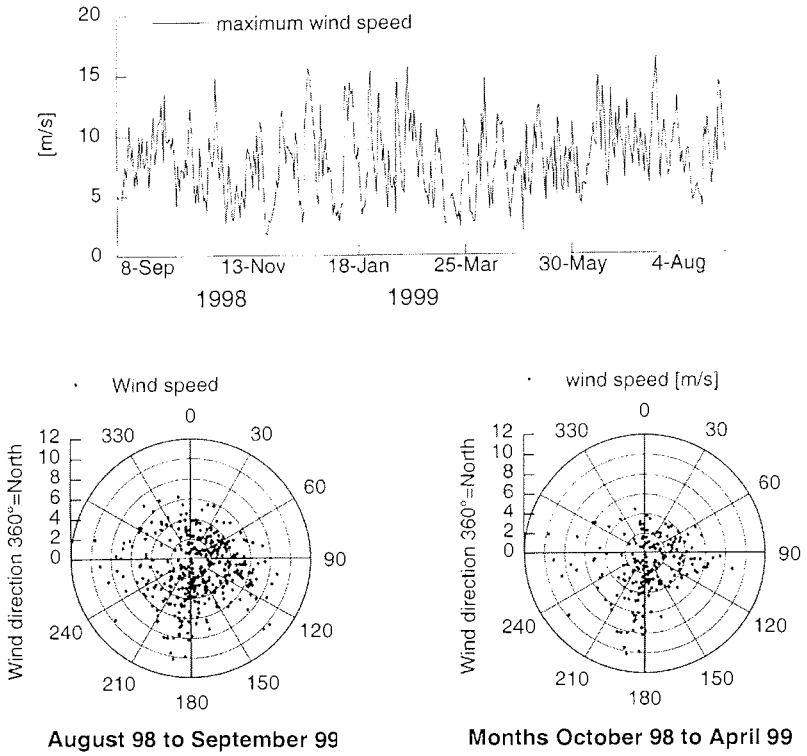

Figure 4-15: Near bottom wind activities (speed and direction) of the investigations area during the field period 1998/1999.

Environmental studies have been performed on the island Samoylov (N 72°22'/ E 126°30; area ~ 1,200 ha) at the end of the winter season in 1999. This island is one of about 1500 islands of that region and is representative for the south-western part of the delta. Due to seasonal changes of river water levels, four terraces were shaped with an elevation maximum of 12 m above sea level. Water and wind action formed an (thermo)abrasion coast with nearly vertical cliffs and a very narrow beach at the eastern and southern banks.

During May and June the thickness of snow was measured on the island along 19 transects (see Figures. 4-16 and 4-18). 54 surface snow samples (each of 20x20x2.5cm) were melted and filtered (0.45 micron HVLP filters by Millipore) to determine the amount of aeolian particles. The deposited aeolian sediment is remarkable high during the onset of the Arctic spring and depicts the meteorological conditions during the field period. The particle content of the surface snow samples ranges from a few mg/l of fine-grained material to about 10 g/l of aeolian particles (Figures 4-15 and 4-17). The grain-size of the aeolian material even reaches the sand fraction greater than 63 microns .

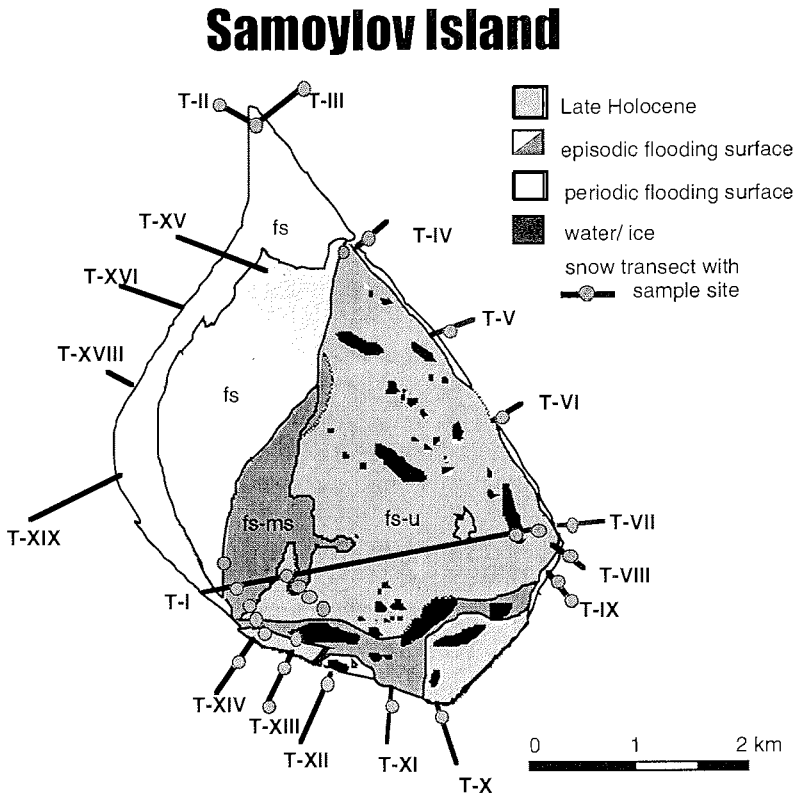

Figure 4-16: Location of snow sampling during the expedition Lena 99/Team 1a. For snow transects see Figure 4-18.

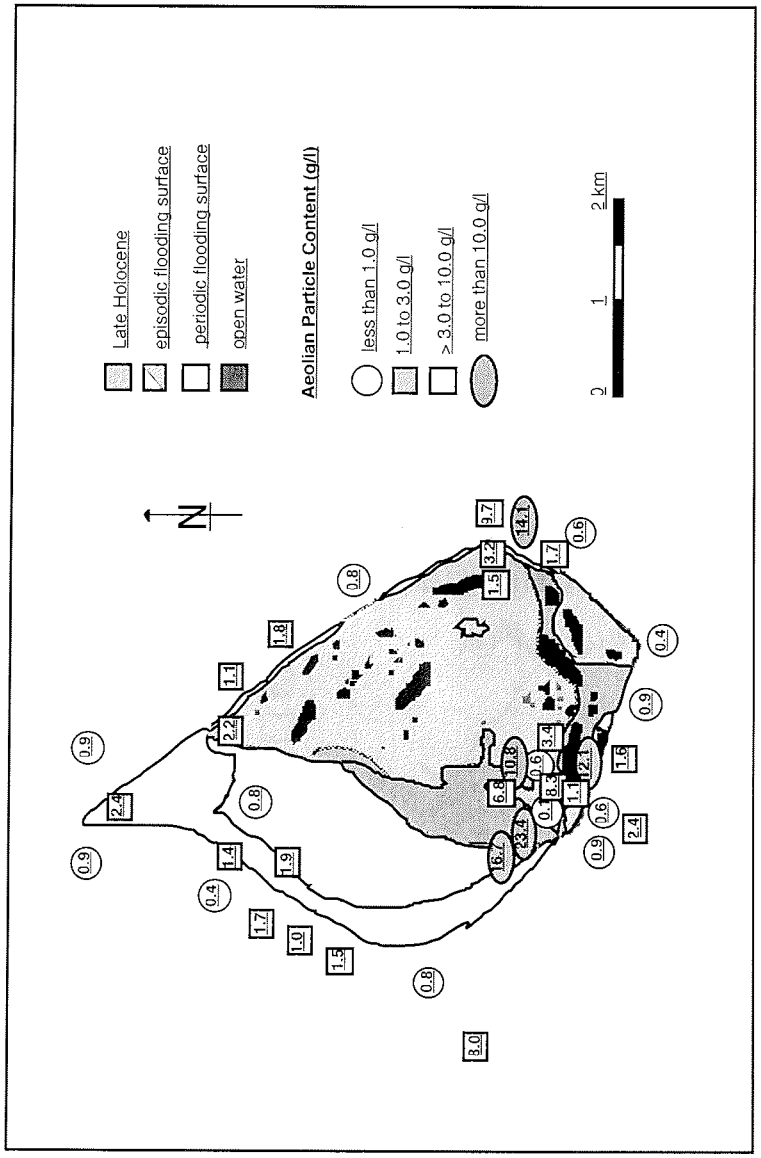

Figure 4-17: Aeolian particle distribution in the area of Samoylov Island. The concentration of particles in the snow samples is given in g/l.

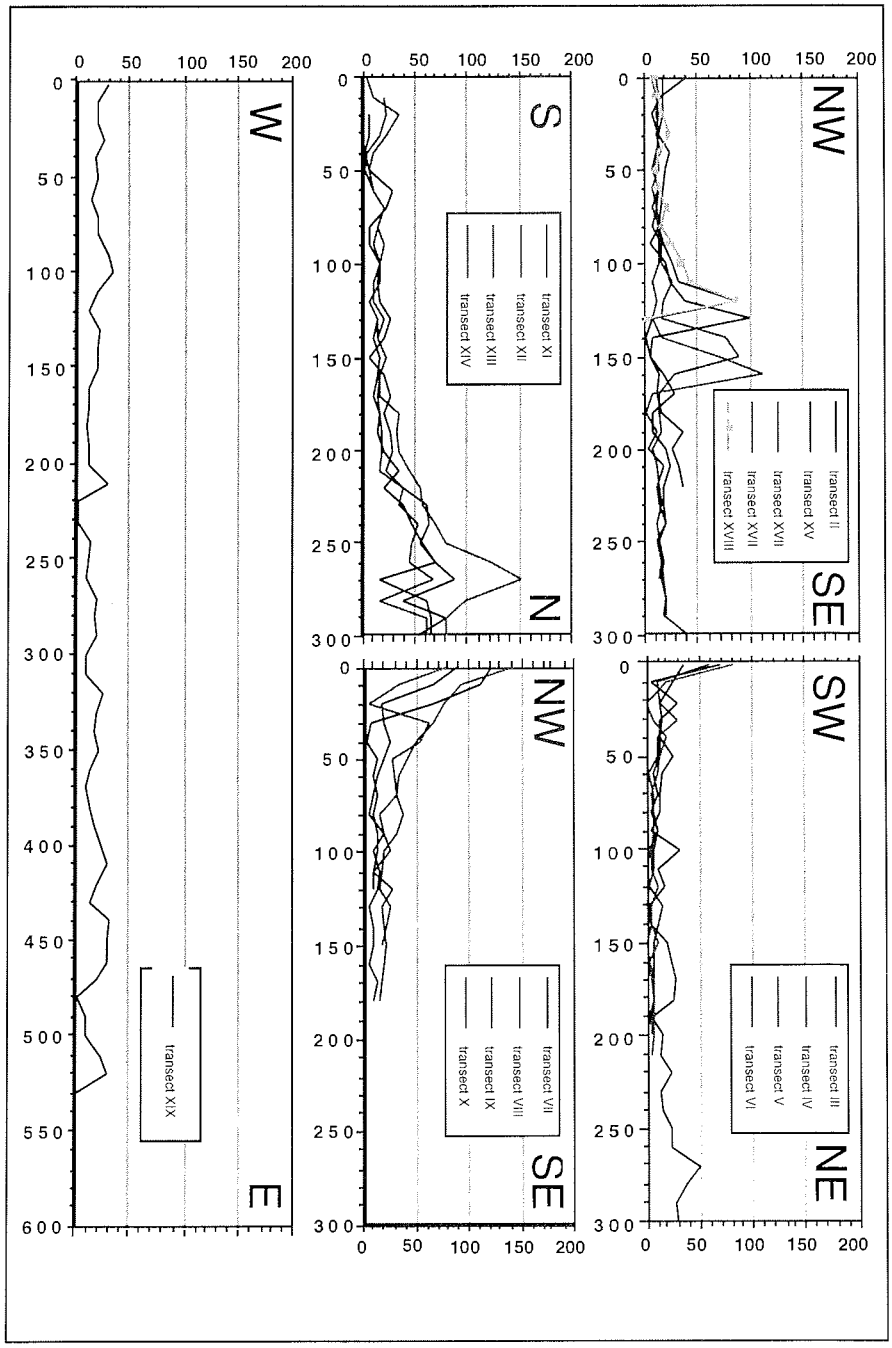

Figure 4-18: In-situ snow coverage (cm) on and around Samoylov Island. For the positions of transects see Figure 4-16.

4.7 References

Antonow, M., Grigoriev, M.N., Rachold, V. and Reimnitz, E. (1999): Seasonal changes of water level in the Lena Delta region. In: Rachold (ed.): Expeditions in Siberia in 1999. Rep. Polar. Res. 315, 92-93.

Are, F.E. (1999) The role of coastal retreat for sedimentation in the Laptev Sea. In: Kassens H, Bauch H, Dmitrenko I, Eicken H, Hubberten HW, Melles M, Thiede J and Timokhov L (eds) Land-Ocean systems in the Siberian Arctic: dynamics and history. Springer, Berlin, 287-299

Atlas of the Arctic (1985): GGUK, Moscow, 204 pp. (in Russian).

Davies, J.L. and Annan, A.P., 1989. Ground-Penetrating-Radar for High-Resolution Mapping of Soil and Rock Stratigraphy, Geophysical Prospecting, Vol. 37, 531-551.

Galabala, R.O. (1987): New data on the Lena Delta structure. In: The Quaternary period of North East Asia. Magadan, DVO AN SSSR, 152-170 (in Russian)

Grigoriev, M.N. (1993): Cryomorphogenesis of the Lena River mouth area. Yakutsk, SO AN SSSR, 176 pp. (in Russian).

Korotaev, V.N. (1984): The formation of the hydrographic network of the Lena Delta in the Holocene. Vestnic MGU, Ser. 5, No. 6, 39-44 (in Russian)

Kunitsky, V.V. (1989): Cryolithology of the Lena lower reaches. Yakutsk, SO AN SSSR, 162 pp. (in Russian).

Kuptsov, V.M. and Lisitsin, A.P. (1996): Radiocarbon of Quaternary along shore and bottom deposits of the Lena and the Laptev Sea sediments. Mar. Chem. 53, 301-311.

Nagaoka, D. (1994): Properties of Ice-complex Deposits in Eastern Siberia. - In; Proceedings of the Second Symposium on the Joint Siberian Permafrost Studies between Japan and Russia in 1993, Tsukuba.

Niessen, F. and Melles, M., 1995. Lacustrine sediment echosounding and physical properties, Berichte zur Polarforschung, Vol. 174: Die Expedition ARKTIS-X/2 mit FS Polarstern 1994, Hubberten, H.-W. (ed.), pp. 69.

Pavlova, E. and Dorozhkina, M. (1999). Geological-Geomorphological Studies in the Northern Lena River Delta. In: Rachold (ed.): Expeditions in Siberia in 1999. Rep. Polar. Res. 315, 112-126.

Pavlova. E., Dorozhkina, M. and Rachold, V. (1999). - Geomorphological structure of the western sector of the Lena River Delta. Fifth workshop on Russian-German Cooperation, Laptev Sea System 2000, St.Petersburg, Russia, 25-29 November 1999.

Rachold, V., Grigoriev, M.N. and Antonow, M. (1999): Modern sedimentation and the environmental history of the Lena Delta. In: Rachold (ed.): Expeditions in Siberia in 1999. Rep. Polar. Res. 315, 81-144.

Rachold, V., Grigoriev, M.N., Are, F.E., Solomon, S., Reimnitz, E., Kassens, H. and Antonow, A. (in press): Coastal Erosion vs. Riverine Sediment Discharge in the Arctic Shelf Seas. Geol. Rundsch.

Schwamborn, G., Schneider, W., Grigoriev, M.N., Rachold, V. and Antonow, M. (1999): Sedimentation and environmental history of the Lena Delta. In: Rachold (ed.): Expeditions in Siberia in 1999. Rep. Polar. Res. 315, 94-111.

Siegert, C. et al. (1999): Paleoclimate signals of ice-rich permafrost. In: Rachold (ed.): Expeditions in Siberia in 1999. Rep. Polar. Res. 315, 145-190.

Tarakanov, L.V. and Biryukob, V.Yu. (1974): Geomorphologic evidence of Laptev Sea modern ingression in Shirokostan Peninsula area. – Geomorphology 4, 98-100.

Tomirdiaro, S.V., Arslanov, K.H. and Chernenkiy, B.I. et. al. (1985): Geochronology of key sections of arctic and subarctic types of ice-complex. - In: Geochronology of the Quaternary period. Tallinn, 62 (in Russian)

4.8 Appendix

Table A4-1: List of stations for lake sediment studies on Arga Island.

Station	Date	GMT	Position		Description	Sampling	Field Device	Recovery
LD99-A01	07 05 99	2:00	N 73°19´31´´	E 124°15´00´´	Nikolay Lake	Lake sediments	drilling	335 cm
LD99-A02	13 05 99	2:00	N 73°19´35´´	E 124°14´18´´	Nikolay Lake	Lake sediments	drilling	180 cm
LD99-A03	14 05 99	2:00	N 73°19´37´´	E 124°14´50´´	Nikolay Lake	Lake sediments	drilling	52 cm
LD99-A04	14 05 99	2:00	N 73°19´37´´	E 124°14´50´´	Nikolay Lake	Lake sediments	drilling	58 cm
LD99-A05	15 05 99	2:00	N 73°19´39´´	E 124°14´50´´	Nikolay Lake	Lake sediments	drilling	700 cm
LD99-CN1	07 05 99	2:00	N 73°19´31´´	E 124°15´04´´	Nikolay Lake	Lake sediments	gravity coring	77 cm
LD99-CN1D	07 05 99	3:00	N 73°19´31´´	E 124°15´04´´	Nikolay Lake	Lake sediments	gravity coring	80 cm
LD99-CN2	07 05 99	4:00	N 73°19´31´´	E 124°15´04´´	Nikolay Lake	Lake sediments	gravity coring	83 cm
LD99-CN3	07 05 99	5:00	N 73°19´31´´	E 124°15´04´´	Nikolay Lake	Lake sediments	gravity coring	84 cm
LD99-LS-10-1	08 05 99	2:00	N 73°19´31´´	E 124°15´04´´	Nikolay Lake	Lake sediments	gravity coring	32 cm
LD99-LS-10-2	08 05 99	3:00	N 73°19´31´´	E 124°15´04´´	Nikolay Lake	Lake sediments	gravity coring	33 cm
LD99-CNPP-1	08 05 99	4:00	N 73°19´31´´	E 124°15´04´´	Nikolay Lake	Lake sediments	gravity coring	31 cm
LD99-CNPP-2	13 05 99	2:00	N 73°20´36´´	E 124°10´12´´	Nikolay Lake	Lake sediments	gravity coring	28 cm
LD99-CNPP-3	13 05 99	3:00	N 73°20´36´´	E 124°10´12´´	Nikolay Lake	Lake sediments	gravity coring	32 cm
LD99-CN4	13 05 99	4:00	N 73°20´36´´	E 124°10´12´´	Nikolay Lake	Lake sediments	gravity coring	98 cm
LD99-CN5	13 05 99	5:00	N 73°20´36´´	E 124°10´12´´	Nikolay Lake	Lake sediments	gravity coring	85 cm
LD99-CN6	13 05 99	6:00	N 73°20´36´´	E 124°10´12´´	Nikolay Lake	Lake sediments	gravity coring	95 cm
LD99-Iv.2	22 05 99	2:00	N 71°44´38´´	E 129°24´03´´	Ivashkina Laguna	Lagoonal sediments	drilling	590 cm
LD99-R01	08 05 99	2:00	N 73°19.842´	E 124°13.939´	Nikolay Lake	Radar profiles	25-MHz-ant.	-
LD99-R02	08 05 99	4:00	N 73°19.195´	E 124°17.166´	Nikolay Lake	Radar profiles	25-MHz-ant.	-
LD99-R03	08 05 99	6:00	N 73°20.208´	E 124°12.452´	Nikolay Lake	Radar profiles	25-MHz-ant.	-
LD99-R05	09 05 99	2:00	N 73°19.527´	E 124°15.004´	Nikolay Lake	Radar profiles	25-MHz-ant.	-
LD99-R06	09 05 99	6:00	N 73°20.167´	E 124°14.212´	Nikolay Lake	Radar profiles	25-MHz-ant.	-
LD99-R09	12 05 99	2:00	N 73°19.619´	E 124°14.229´	Nikolay Lake	Radar profiles*	100-MHz-ant.	-
LD99-R10	13 05 99	2:00	N 73°19.633´	E 124°14.222´	Nikolay Lake	Radar profiles*	100-MHz-ant.	-
LD99-R11	14 05 99	2:00	N 73°20.719´	E 124°06.952´	Nikolay Lake	Radar profiles	100-MHz-ant.	-
LD99-R12	16 05 99	2:00	N 73°18.997´	E 124°12.870´	Arga Island	Radar profiles*	100-MHz-ant.	-
LD99-R13	16 05 99	6:00	N 73°19.619´	E 124°14.229´	Nikolay Lake	Radar profiles	100-MHz-ant.	-
LD99-R20	19 05 99	2:00	N 72°58.488´	E 129°39.166´	Trofimofsky Ch.	Radar profiles*	100-MHz-ant.	-
LD99-R30	21 05 99	2:00	N 71°47.241´	E 129°25.354´	Bykowsky Ch.	Radar profiles	100-MHz-ant.	-
LD99-R31	21 05 99	4:00	N 71°47.167´	E 129°25.018´	Mammontovy Kh.	Radar profiles	100-MHz-ant.	-
LD99-R40	22 05 99	2:00	N 71°44.633´	E 129°24.050´	Ivashkina Laguna	Radar profiles*	100-MHz-ant.	-
LD99-R50	25 05 99	2:00	N 72°22.220´	E 126°28.720´	Samoylov Island	Radar profiles*	100-MHz-ant.	-

*CMP-measurements

Table A4-2: List of samples for lake sediment studies on Arga Island.

sample site	depth	sediments	type of analyses			
recovered by drilling (D) or gravity coring (G)			grain size	ice / water content	TC,TOC, N,S	^{14}C (AMS)
LD99-A01 (D)	0-90 cm	fine-silty sand, organic rich	x	x	x	x
	90-335 cm	fine-silty sand, (talik)	x	x	x	x
LD99-A02 (D)	0-180 cm	fine-silty sand, (talik)	x	x	x	
LD99-A03 (D)	52 cm	fine-silty sand, (talik	x	x	x	
LD99-A04 (D)	58 cm	fine-silty sand, (talik)	x	x	x	
LD99-A05 (D)	700 cm	fine-silty sand, (permafrost)	x	x	x	x
LD99-CN1 * (G)	77 cm	fine-silty sand, organic rich				
LD99-CN1D ** (G)	80 cm	fine-silty sand, organic rich				
LD99-CN2 (G)	83 cm	fine-silty sand, organic rich	x	x	x	x
LD99-CN3 • (G)	84 cm	fine-silty sand, organic rich				
LD99-LS-10-1 * (G)	32 cm	fine-silty sand, organic rich				
LD99-LS-10-2 * (G)	33 cm	fine-silty sand, organic rich				
LD99-CNPP-1 * (G)	31 cm	fine-silty sand, organic rich				
LD99-CNPP-2 * (G)	28 cm	fine-silty sand, organic rich				
LD99-CNPP-3 * (G)	32 cm	fine-silty sand, organic rich				
LD99-CN4 * (G)	98 cm	fine-silty sand, organic rich				
LD99-CN5 * (G)	85 cm	fine-silty sand, organic rich				
LD99-CN6 (G)	95 cm	fine-silty sand, organic rich	x	x	x	x
LD99-lv.2 * (D)**	590 cm	lagoonal sediments				

* provided for AARI, St. Petersburg
** provided for IFB, University Hamburg
*** provided for MGU-P, Moscow State University

Table A4-3: Boreholes temperature measurments in Nikolay Lake (Arga Island) and Ivashkina lagoon, May 1999.

Bore-holes №	Date	Water (+ice) thick-ness, m	Bore-holes bot-tom, m	Depth, m --- Temperature, °C												
A1	May 07	13.7	17,4	0,0 3.0	0.7 0.0	1.7 0.1	2.7 0.8	3.7 0.9	5.7 1.3	7.7 1.6	9.7 1.8	11.7 2.1	13.7 2.7			
A1	May 09	13.7	17.4	4 1.1	5 1.2	7 1.2	8 1.5	9 1.6	10 1.7	12 1.9	14 2.4	16 2.5	16.5 2.7	17 2.5		
Hole-10	May 11	13.7	13.7	0 -0.1	1.7 -0.2	1 0.2	2 -0.2	3 0.9	4 1.2	5 1.3	7 1.5	9 1.7	11 2.0	11.5 2.0	12 1.8	13.7 2.0
A5	May 15	1.2	3.6	0 -5.2	0.4 -7.2	2.4 -8.1	2.9 -7.4	3.4 -7.3								
A5	May 16	1.2	3.6	0 -2.5	0.6 -7.6	2.6 -7.3	3.1 -8.3	3.6 - 8.5								
A5	May 17	1.2	8.2	0 -11.4	1 -9.2	3 -9.7	5 -8.1	5.5 - 7.5	6 - 7.3							
A5	May 17	1.2	8.2	0 -11.1	0.8 -8.5	1.8 -9.4	2.8 -9.7	3.8 - 9.4	4.8 - 8.8	5.8 -7.4	6.8 -6.1	7.8 - 5.3				
IV2-99	May 23	2.5	8.7	0 -8.1	1.5 -2.2	2.5 -2.0	3.5 -1.8	4.5 - 1.3	5.5 - 0.7	6.5 -0.3	7.5 0.1					

Table A4-4: List of stations for coastal erosion studies.

station LD99-CR...	date	location	*shallow seismic*	*coastal studies*	*bottom sediment sampling*	*deep water bathymetry*	*shallow water bathymetry*	*water temperature measurements*
1	09 08 99	Arangastakh-Tumula Peninsula (Arga Island)	x	x	x	x		
2	10 08 99	Gerasim Island (Kuba Bay)		x				
3	11 08 99	Kuba-Aryta Island		x	x	x		x
4	12 08 99	Tumat Bay (near America-Kuba Island)			x	x		x
5	14 08 99	Hans-Aryta Island (mouth region of Sardakh	x	x	x		x	
6	14 08 99	mouth region of Sardakh Channel	x		x	x		
7	15 08 99	Orto Yuos Island near Bykovsky Cape		x				
8	15 08 99	Muostakh Island		x				
9	18 08 99	Buor-Khaya Peninsula (Hargy Lake)	x	x	x	x	x	
10	19 08 99	Buor-Khaya Peninsula (Alas site)		x				
11	20 08 99	Vankina Guba Bay	x			x		x
12	21 08 99	Makar Island		x			x	x
13	22 08 99	Shrokostan Peninsula		x	x	x	x	x
14	24 08 99	Svyatoy Nos Cape						x
15	25 08 99	Dmitry Laptev Strait						x
16	26 08 99	Dmitry Laptev Strait (Oiyagoskiy Yar,	x		x	x		
17	27 08 99	Bolshoy Lyakhovky Island (Zimovie River Mouse)		x				
18	29 08 99	Yana Bay						x
19	30 08 99	Buor-Khaya Cape						x
20	2 09 99	Bykovsky Peninsula (Hotu-Hapsagay-Khayata)		x				
21	3 09 99	Bykovsky Peninsula (Mamontovy-Khayata)		x				

Table A4-5: List of samples for coastal erosion studies.

station LD99-CR...	type of sampling	no. of samples	start coordinates	end coordinates
1	marine surface samples, profile	5	73°39.117´ 125°32.076´	73°36.831´ 125°28.750´
3	marine surface samples, profile	10	73°41.090´ 126°01.445´	73°44.189´ 126°14.518´
	cliff samples	6	73°39.183´ 125°51.250´	
4	marine surface samples, profile	11	73°37.742´ 127°51.624´	73°42.306´ 127°55.889´
5	marine surface samples, profile	6	72°35.483´ 129°28.037´	72°34.419´ 129°32.826´
	coast samples	2	72°36.290´ 129°32.350´	
6	marine surface samples, profile	18	72°33.324' 129° 37.139'	72°33.003´ 130°13.573´
9	marine surface samples, profile	7	71°25.258´ 131°59.169´	71°25.229´ 132°05.448´
	cliff samples	3	71°24.270´ 132°05.650´	
13	marine surface samples, profile	8	72°12.150´ 139°09.040´	72°12.624´ 138°57.633´
	cliff samples	4	72°12.100´ 139 09°980´	
14	cliff samples	4	72°47.970´ 140°46.820´	
16	marine surface samples, profile	5	72°42.771´ 143°38.126´	72°48.717´ 143°36.153´

Table A4-6: Water temperature profiles (°C) along the Laptev Sea coast.

Hori-zon,	Stations													
m	3	4	11	12	13	14a	14b	15a	15b	18a	18b	19a	19b	19c
0	5.3	2.2	5.1	5.3	5.3	4.2	-	4.8	5.0	85	8.6	9.9	13.4	9.8
1	4.1	2.1	4.9	4.7	5.8	4.0	-	3.5	5.9	7.2	8.3	10.2	9.9	10.1
2	2.5	1.8	4.5	3.9	5.8	4.0	4.2	2.5	4.5	6.7	7.9	9.3	9.6	9.0
3		0.9	4.3	2.6	5.4	3.8	4.3	2.2	3.0	6.8	7.6	8.0	9.9	7.6
4		0.9	4.2	-0.9		3.7	4.3	2.1	2.8	6.7	7.5		9.0	
5		2.8	4.0			3.7	4.0	2.0	3.0	5.9	5.2		4.8	
6		-0.1	3.9			3.7	4.1	1.9	2.5	4.8	4.6		1.5	
7		1.0	2.7				4.5	2.1	2.1	4.0	4.3		0.3	
8		-0.6	2.5				4.7	1.9	1.9	3.8	4.1		0.1	
9		-1.0	1.9				4.6	1.8	1.9	2.8	2.9		-0.2	
10		-0.8	1.8				3.7	1.7	1.8	1.7	1.3		-0.4	
11		-0.8					2.9	1.4		0.5	1.1		-0.5	
12							2.0	0.4		0.4	0.8		-0.5	
13							1.4	0.4		0.2	0.3		-0.5	
14							0.8	0.4		0.2	0.3		-0.6	
15							0.3	0.4		0.1	0.3		-0.6	
16							0.1			0.1	0.3		-0.6	
17							0.0			0.1	0.3		-0.6	
18											0.3		-0.6	

Table A4-7: Hydrometeorological characteristics along the Laptev Sea coast (bottom water temperature - Tb , air temperature - Ta).

№ St.	Date	Latitude, N ° '	Altitude, E ° '	Wind direction	Wind velocity, m/sec	Wave height, m	Wave lenght, m	T_a, °C	Depth, m	T_b, °C
3	10. 08	73 35,95	125 23,00	N	6-8	0.5	7	5.5	2.7	2.0
4	12. 08	73 44,88	126 17,00	NE	8-10	1.0	12	6.7	11.0	-0.8
11	20. 08	72 05,29	139 25,97		0	0	0	3.5	10.0	1.8
12	21. 08	71 51,91	138 21,00	S	1-3	0.1	0.5	6.9	4.0	-0.9
13	23. 08	72 12,15	139 07,60	SE	6-8	0.6	7	9.1	3.6	5.4
14a	24. 08	72 49,73	140 43,22	SE	1-3	0.2	1	8.7	6.0	3.7
15a	25. 08	73 06,10	140 49,00		0	0	0	8.6	15.0	0.4
15b	25. 08	73 09,03	141 32,83		0	0	0	11.7	10.0	1.8
14b	29. 08	72 53,82	140 44,35		0	0	0	8.0	17.0	0.0
18a	29. 08	72 09,71	133 53,58		0	swell	swell	9.2	21.0	-
18b	29. 08	72 07,05	133 53,73		0	swell	swell	12.8	18.5	0.3
19a	29. 08	71 57,31	132 46,11	S	1-2	0	0	11.6	3.3	8.0
19b	30. 08	71 47,12	131 29,24	S	3-5	0.1	1	12.8	18.5	-0.6
19c	30. 08	71 38,70	128 50,07	S	0-2	0.1	0.5	10.8	3.5	7.6

Table A4-8: List of samples for geological-geomorphological studies in the Lena Delta (abbreviations see end of table).

Study site DJS-S1: Arynskaya Channel (72° 38' 40" N, 125° 30' 58" E).

Sample no	Depth (m)	Sediment	PA	DA	PR	D
DJS-S1 - 1	23,5-23,6	fine sand with plant remains		x	x	x
DJS-S1 - 2	23,6-23,7			x		
DJS-S1 - 3	23,7-23,8			x	x	
DJS-S1 - 4	23,8-23,9			x		
DJS-S1 - 5	23,9-24,0			x	x	
DJS-S1 - 6	24,0-24,1			x		
DJS-S1 - 7	24,1-24,2			x	x	
DJS-S1 - 8	24,2-24,25			x		
DJS-S1 - 9	24,25-24,30	peat with clay interbeds		x	x	x
DJS-S1 - 10	24,30-24,35			x		
DJS-S1 -11	24,35-24,40			x	x	
DJS-S1 - 12	24,45-24,50			x		
DJS-S1 - 13	24,55-24,60			x	x	
DJS-S1 - 14	24,65-24,70			x		
DJS-S1 - 15	24,75-24,80			x	x	x

Study site KS-S2: Olenekskaya Channel, Nagym (72° 52' 51" N, 123° 11' 58" E).

Sample no	Depth (m)	Sediment	PA	DA	PR	D
KS-S2-1	6,24-6,31	fine sand with plant remains			x	
KS-S2-2	6,93-7,13				x	
KS-S2-3	7,67-7,70				x	
KS-S2-4	7,61-7,64				x	
KS-S2-5	10,96-11,01	peat				x
KS-S2-6	11,30-11,35					x

Study site KA-S3: Tyuerenkey-Tebyulege Channel (72° 29' 33" N, 125° 18' 45" E).

Sample no	Depth (m)	Sediment	PA	DA	PR	D
KA-S3-1	6,00-6,05	fine sand with plant remains	x		x	
KA-S3-2	6,15-6,20			x		
KA-S3-3	6,30-6,35	silt with plant remains	x		x	
KA-S3-4	6,45-6,50			x		
KA-S3-5	6,60-6,65	alternating bedding of peat and silt	x		x	x
KA-S3-6	6,75-6,80			x		
KA-S3-7	6,90-6,95		x		x	
KA-S3-8	7,05-7,10			x		
KA-S3-9	7,20-7,25	fine sand with plant remains	x		x	
KA-S3-10	7,35-7,40	medium sand with plant remains		x		
KA-S3-11	7,50-7,55	alternating bedding of peat, fine sand , silt	x		x	
KA-S3-12	7,65-7,70			x		
KA-S3-13	7,80-7,85		x		x	

Table A4-8: continued.

KA-S3-14	7,95-8,00			x		
KA-S3-15	8,10-8,15		x		x	
KA-S3-16	8,25-8,30	fine, medium sand with plant remains		x		
KA-S3-17	8,40-8,45	alternating bedding of peat, silt	x		x	
KA-S3-18	8,55-8,60			x		
KA-S3-19	8,70-8,75		x		x	
KA-S3-20	8,85-8,90			x		
KA-S3-21	9,00-9,05	fine sand with plant remains	x		x	
KA-S3-22	9,15-9,20	peat		x		
KA-S3-23	9,30-9,35	alternating bedding of peat, fine sand , silt	x		x	
KA-S3-24	9,45-9,50			x		
KA-S3-25	9,60-9,65		x		x	
KA-S3-26	9,75-9,80			x		
KA-S3-27	9,90-9,95		x		x	
KA-S3-28	10,05-10,10			x		
KA-S3-29	10,20-10,25		x		x	
KA-S3-30	10,35-10,40	peat with fine sand		x		
KA-S3-31	10,50-10,55		x		x	
KA-S3-32	10,65-10,70	fine, medium sand		x		
KA-S3-33	10,80-10,85	peat with fine sand	x		x	
KA-S3-34	10,95-11,00	fine sand with plant remains		x		
KA-S3-35	11,10-11,15	peat with fine sand	x		x	
KA-S3-36	11,25-11,30			x		
KA-S3-37	11,40-11,45	alternating bedding of peat, fine sand , silt	x		x	
KA-S3-38	11,55-11,60	fine horizontal laminated sand		x		
KA-S3-39	11,70-11,75		x		x	
KA-S3-40	11,85-11,90			x		
KA-S3-41	12,00-12,05		x		x	
KA-S3-42	12,15-12,20			x		
KA-S3-43	12,30-12,35		x		x	
KA-S3-44	12,45-12,50			x		
KA-S3-45	subresent		x		x	

Study siteBCH-S5: Olenekskaya Channel, Buor-Khaia (72° 19' 31" N, 126° 16' 07" E).

Sample no	Depth (m)	Sediment	PA	DA	PR	D
BCh-S5-1	2,85-2,90	silt		x		x
BCh-S5-2	2,95-3,00			x		x
BCh-S5-3	3,10-3,15	sandy peat		x		x
BCh-S5-4	3,20-3,25	peat		x		x
BCh-S5-5	3,61-3,62			x		x
BCh-S5-6	4,08-4,09			x		x

Table A4-8: continued.

Study siteJPS-S4: Malaya Tumatskaya Channel, Djeppiries-Sise (72° 54' 43" N, 125° 52' 50" E).

Sample no	Depth (m)	Sediment	PA	DA	PR	D
JPS-S4-1	1,95-2,00	sandy peat	x			
JPS-S4-2	2,00-2,05			x		
JPS-S4-3	2,55-2,60		x			x
JPS-S4-4	3,00-3,05	fine sand		x		
JPS-S4-5	3,30-3,35		x			
JPS-S4-6	3,65-3,70			x		
JPS-S4-7	4,10-4,15		x			
JPS-S4-8	4,50-4,55			x		
JPS-S4-9	4,95-5,00		x			
JPS-S4-10	5,60-5,65			x		

Study site DSK- CI: Central part of Anonymous Lake (72° 32' 15" N, 125° 26' 10" E).

Sample no	Depth (m)	Sediment	PA	DA	PR	D
DSK-C1-1	0,80-0,78	pelitic silt with organic interbeds	x			x
DSK-C1-2	0,78-0,76					
DSK-C1-3	0,76-0,74		x			
DSK-C1-4	0,74-0,72	fine sand	x			
DSK-C1-5	0,72-0,70	pelitic silt with organic interbeds				
DSK-C1-6	0,70-0,68		x			
DSK-C1-7	0,68-0,66					
DSK-C1-8	0,66-0,64		x			
DSK-C1-9	0,64-0,62					
DSK-C1-10	0,62-0,60		x			
DSK-C1-11	0,60-0,58					
DSK-C1-12	0,58-0,56		x			
DSK-C1-13	0,56-0,54					
DSK-C1-14	0,54-0,52		x			
DSK-C1-15	0,52-0,50					
DSK-C1-16	0,50-0,48		x			
DSK-C1-17	0,48-0,46					
DSK-C1-18	0,46-0,44		x			
DSK-C1-19	0,44-0,42					
DSK-C1-20	0,42-0,40		x			
DSK-C1-21	0,40-0,38					
DSK-C1-22	0,38-0,36		x			
DSK-C1-23	0,36-0,34					
DSK-C1-24	0,34-0,32		x			
DSK-C1-25	0,32-0,30					
DSK-C1-26	0,30-0,28		x			
DSK-C1-27	0,28-0,26					
DSK-C1-28	0,26-0,24		x			
DSK-C1-29	0,24-0,22					
DSK-C1-30	0,22-0,20		x			

Table A4-8: continued.

DSK-C1-31	0,20-0,18		
DSK-C1-32	0,18-0,16		x
DSK-C1-33	0,16-0,14		
DSK-C1-34	0,14-0,12		x
DSK-C1-35	0,12-0,10		
DSK-C1-36	0,10-0,08		x
DSK-C1-37	0,08-0,06		
DSK-C1-38	0,06-0,04		x
DSK-C1-39	0,04-0,02		
DSK-C1-40	0,02-0,00		x

Study siteJSK-C5: Central part of Djangylakh-Kyuele Lake (72°33' 23" N, 125°26' 31"E).

Sample no	Depth (m)	Sediment	PA	DA	PR	D
JSK-C5-1	0,58-0,56	pelitic silt with organic interbeds	x	x		x
JSK-C5-2	0,56-0,54		x	x		x
JSK-C5-3	0,54-0,52		x	x		
JSK-C5-4	0,52-0,50		x	x		
JSK-C5-5	0,50-0,48		x	x		
JSK-C5-6	0,48-0,46		x	x		
JSK-C5-7	0,46-0,44		x	x		
JSK-C5-8	0,44-0,42		x	x		
JSK-C5-9	0,42-0,40		x	x		
JSK-C5-10	0,40-0,38		x	x		
JSK-C5-11	0,38-0,36		x	x		
JSK-C5-12	0,36-0,34		x	x		
JSK-C5-13	0,34-0,32		x	x		
JSK-C5-14	0,32-0,30		x	x		
JSK-C5-15	0,30-0,28		x	x		x
JSK-C5-16	0,28-0,26		x	x		
JSK-C5-17	0,26-0,24		x	x		
JSK-C5-18	0,24-0,22		x	x		
JSK-C5-19	0,22-0,20		x	x		
JSK-C5-20	0,20-0,18		x	x		
JSK-C5-21	0,18-0,16		x	x		
JSK-C5-22	0,16-0,14		x	x		
JSK-C5-23	0,14-0,12		x	x		
JSK-C5-24	0,12-0,10		x	x		
JSK-C5-25	0,10-0,08		x	x		
JSK-C5-26	0,08-0,06		x	x		
JSK-C5-27	0,06-0,04		x	x		
JSK-C5-28	0,04-0,02		x	x		
JSK-C5-29	0,02-0,00		x	x		x

Table A4-8: continued.

Study site BK-C2: Central part of Byrakan-Kyuele Lake (72° 47' 23" N, 124° 14' 59"E).

Sample no	Depth (m)	Sediment	PA	DA	PR	D
BK-C3-1	0,68-0,66	pelitic silt with plant remains	x			x
BK-C3-2	0,66-0,64					
BK-C3-3	0,64-0,62		x			
BK-C3-4	0,62-0,60					
BK-C3-5	0,60-0,58		x			
BK-C3-6	0,58-0,56					
BK-C3-7	0,56-0,54		x			
BK-C3-8	0,54-0,52					
BK-C3-9	0,52-0,50		x			
BK-C3-10	0,50-0,48					
BK-C3-11	0,48-0,46		x			
BK-C3-12	0,46-0,44					
BK-C3-13	0,44-0,42		x			
BK-C3-14	0,42-0,40					
BK-C3-15	0,40-0,38		x			
BK-C3-16	0,38-0,36					
BK-C3-17	0,36-0,34		x			
BK-C3-18	0,34-0,32					
BK-C3-19	0,32-0,30		x			
BK-C3-20	0,30-0,28					
BK-C3-21	0,28-0,26		x			
BK-C3-22	0,26-0,24					
BK-C3-23	0,24-0,22		x			
BK-C3-24	0,22-0,20					
BK-C3-25	0,20-0,18	pelitic silt with fine sand interbeds and plant remains	x			
BK-C3-26	0,18-0,16					
BK-C3-27	0,16-0,14		x			
BK-C3-28	0,14-0,12					
BK-C3-29	0,12-0,10		x			
BK-C3-30	0,10-0,08					
BK-C3-31	0,08-0,06		x			
BK-C3-32	0,06-0,04					
BK-C3-33	0,04-0,02		x			
BK-C3-34	0,02-0,00					

PA - pollen analysis; DA - diatom analysis; PR - analysis of plant remains; D - dating

Table A4-9: List of bone samples for geological-geomorphological studies in the Lena Delta.

Data-base No.	Field label	Taxon	Skeleton element	Preservation	Locality	Notes**)
1	2	3	4	5	6	7
301	A 1-1	Equus caballus L.	radius	damaged	Lena R. Delta, Olenyokskaya Channel, Kurungnakh Island, Buor-Khaya area	out
302	A 1-3	Lepus sp.	tibia	complete	Lena R. Delta, Olenyokskaya Channel, Kurungnakh Island, Buor-Khaya area	
303	A 1-4	Mammuthus primigenius (Blum.)	ulna	fragment	Lena R. Delta, Olenyokskaya Channel, Kurungnakh Island, Buor-Khaya area	out
304	A 1-5	Rangifer tarandus (L.)	antler	fragment	Lena R. Delta, Olenyokskaya Channel, Kurungnakh Island, Buor-Khaya area	out
305	A 1-6	Bison priscus (Boj.)	tooth (heavily worn)	damaged	Lena R. Delta, Olenyokskaya Channel, Kurungnakh Island, Buor-Khaya area	out
306	A 1-7	Equus caballus L.	radius	damaged	Lena R. Delta, Olenyokskaya Channel, Kurungnakh Island, Buor-Khaya area	
307	A 1-8	Mammuthus primigenius (Blum.)	pelvis	fragment	Lena R. Delta, Olenyokskaya Channel, Kurungnakh Island, Buor-Khaya area	out
308	A 2-1	Rangifer tarandus (L.)	shed antler	fragment	Lena R. Delta, Olenyokskaya Channel, Kurungnakh Island, Buor-Khaya area	out
309	A 3-1	Lepus timidus L.	skull	recent	Lena R. Delta, Olenyokskaya Channel, Kurungnakh Island, Buor-Khaya area	
310	A 4-2	Mammuthus primigenius (Blum.)	rib	fragment	Lena R. Delta, Olenyokskaya Channel, Kurungnakh Island, Buor-Khaya area	out
311	A 4-3	Mammuthus primigenius (Blum.)	vertebris	damaged	Lena R. Delta, Olenyokskaya Channel, Kurungnakh Island, Buor-Khaya area	out
312	A 4-4	? Equus sp.	patella	complete	Lena R. Delta, Olenyokskaya Channel, Kurungnakh Island, Buor-Khaya area	
313	A 4-5	Rangifer tarandus (L.)	tibia	distal fragment (recent ?)	Lena R. Delta, Olenyokskaya Channel, Kurungnakh Island, Buor-Khaya area	out
314	A 5-1	Bison priscus (Boj.)	femur	fragment	Lena R. Delta, Olenyokskaya Channel, Kurungnakh Island, Buor-Khaya area	out

Table A4-9: continued.

315	A 5-2	Bison priscus (Boj.)	tibia	fragment	Lena R. Delta, Olenyokskaya Channel, Kurungnakh Island, Buor-Khaya area	out
316	A 5-3	Equus caballus L.	metatarsal	fragment	Lena R. Delta, Olenyokskaya Channel, Kurungnakh Island, Buor-Khaya area	out
317	A 5-4	Equus caballus L.	scapula	damaged	Lena R. Delta, Olenyokskaya Channel, Kurungnakh Island, Buor-Khaya area	
318	A 6-1	? Equus sp.	scapula	two fragments	Lena R. Delta, Olenyokskaya Channel, Kurungnakh Island, Buor-Khaya area	out
319	A 6-3	Equus caballus L.	scapula	fragment	Lena R. Delta Olenyokskaya Channel, Kurungnakh Island, Buor-Khaya area	
320	A 9-1	Bison priscus (Boj.)	femur	fragment	Lena R. Delta, Olenyokskaya Channel, Kurungnakh Island, Buor-Khaya area	out
321	IN 2-8	Rangifer tarandus (L.)	vertebris	damaged	Lena R. Delta, Olenyokskaya Channel, Kurungnakh Island, Buor-Khaya area	out
322	IN 2-2	Bison priscus (Boj.)	metatarsal	damaged	Lena R. Delta, Olenyokskaya Channel, Kurungnakh Island, Buor-Khaya area	
323	IN 2-3	Rangifer tarandus (L.)	radius	fragment	Lena R. Delta, Olenyokskaya Channel, Kurungnakh Island, Buor-Khaya area	out
324	IN 2-5	Equus caballus L.	humerus	fragment	Lena R. Delta, Olenyokskaya Channel, Kurungnakh Island, Buor-Khaya area	
325	IN 2-6	Equus caballus L.	metatarsal	fragment	Lena R. Delta, Olenyokskaya Channel, Kurungnakh Island, Buor-Khaya area	
326	IN 2-7	?	unident. fragment		Lena R. Delta, Olenyokskaya Channel, Kurungnakh Island, Buor-Khaya area	out
327	IN 76-1	Rangifer tarandus (L.)	humerus juv.	fragment	Lena R. Delta, Olenyokskaya Channel, Kyuryelyakh-Sis Island	out
328	IN 76-3	Rangifer tarandus (L.)	atlas	complete	Lena R. Delta, Olenyokskaya Channel, Kyuryelyakh-Sis Island	
329	IN 76-4	Equus caballus L.	phalanx I	complete	Lena R. Delta, Olenyokskaya Channel, Kyuryelyakh-Sis Island	out
330	IN 76-5	Alopex lagopus (L.)	Mandible	damaged	Lena R. Delta, Olenyokskaya Channel, Kyuryelyakh-Sis Island	out
331	IN 76-6	Rangifer tarandus (L.)	antler	fragment	Lena R. Delta, Olenyokskaya Channel, Kyuryelyakh-Sis Isl.	out

Table A4-9: continued.

332	IN 76-7	? Lepus sp.	?	bone fragment	Lena R. Delta, Olenyokskaya Channel, Kyuryelyakh-Sis Island	
333	no number	Mammuthus primigenius (Blum.)	pelvis	fragment	Lena R. Delta, Olenyokskaya Channel, Kyuryelya-Sis Island	out
334	no number	Rangifer tarandus (L.)	antler	fragment	Lena R. Delta, Olenyokskaya Channel, Kyuryelyakh-Sis Island	out
335	no number	Rangifer tarandus (L.)	antler	fragment	Lena R. Delta, Olenyokskaya Channel, Kyuryelyakh-Sis Island	out

5 Paleoclimate Signals of Ice-Rich Permafrost Deposits

5.1 Quaternary Deposits of Bol'shoy Lyakhovsky Island

5.1.1 Introduction

(V. Kunitsky and L. Schirrmeister)

Ice-rich permafrost deposits, called „Ice Complex" and their associated thermokarst formations are the most important archives of the Quaternary climatic and environmental history in the nonglaciated areas of North Siberia. Large parts of Bol'shoy Lyakhovsky Island are covered by such permafrost deposits.

The cliffs of the south-coast of the Bol'shoy Lyakhovsky Island contain deposits of the Lower, Middle and Upper Quaternary. In summer 1999, a group of Russian and German scientists studied 6 km of the coastal outcrops east and west of the Zimov'e river (Figure 5-1) in order to record different characteristics for the reconstruction of the paleoclimatic and paleoenvironmental conditions in the Laptev Sea region.

Main topics of the field work were:

- Geological and cryolithological mapping and facies differentiation of the deposits;
- Sampling of frozen sediments and measurement of ice contents;
- Characterisation of different types and generations of ice wedges;
- Investigation of ice crystal structure;
- Detailed sampling of typical ice wedges for stable isotope and hydrochemistry analyses;
- Sampling of recent waters like rain, surface water, snow patches, ground water;
- Measurement of pH and electrical conductivity of ice and water samples;
- Sampling for age determination: Conventional radiocarbon dating, AMS, Optical Stimulated Luminescence (OSL); Paleomagnetics, Uran/Thorium-dating;
- Collection of fossil mammal bones;
- Screening of sediments for rodents and insect studies
- Sampling for paleobotanical analyses (especially carpological and palynological studies)

- Mapping of different types of recent soils in the study area; description of paleosols
- Determination and collection of recent tundra vegetation
- Study of the past and present thermokarst processes
- Sampling for thermo-physical analysis of permafrost deposits.

This expedition to Bol'shoy Lyakhovsky Island continues the studies of permafrost sequences at the Bykovsky Peninsula in 1998 in order to compare paleoclimatic and paleoenvironmental archives of two different locations in the Laptev Sea region.

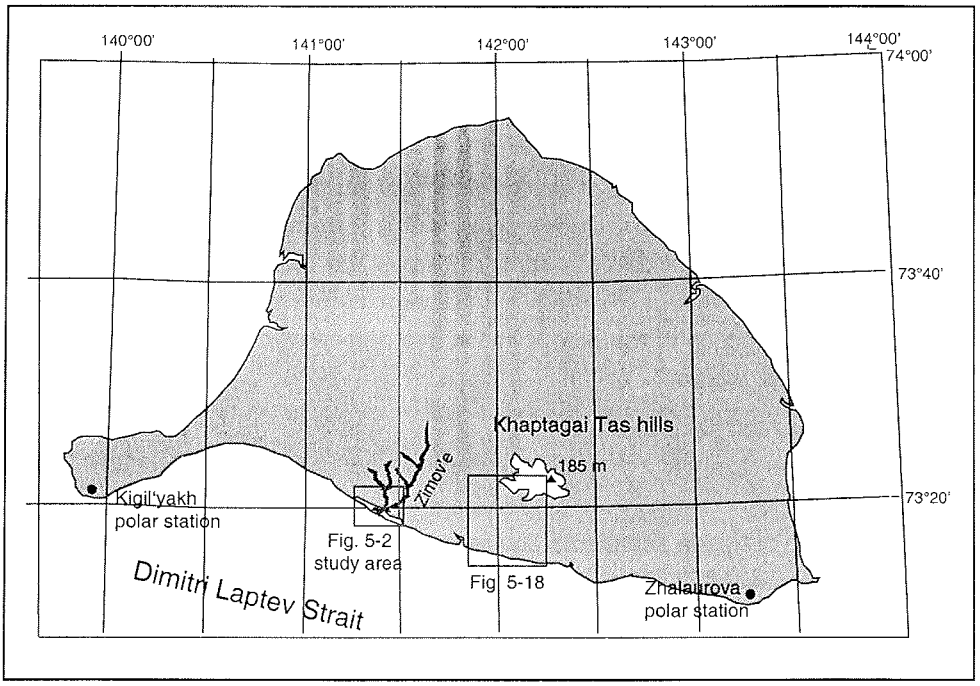

Figure 5-1: General map of Bol'shoy Lyakhovsky Island and the locations of the study areas.

5.1.2 Geological-geomorphological situation

(V. Kunitsky, L. Schirrmeister)

Bol'shoy Lyakhovsky Island is the southern part of New Siberian Island Archipelago. The Island is situated at the eastern boundary of the Laptev Sea between 139°90' - 143°30' E and 73°10' - 75°55' N (Figure 2-1). The north and the south rime of the island consist of hills with altitudes of about 100 to 300 m a.s.l. which act as bifurcations. The central part and the coastal regions have altitudes up to ca 40 m a.s.l.. River mouths, Ice Complex elevations (Edoma), big thermokarst depressions (alases), wide flat valleys (logs), gullies or ravines (ovrags) form the south coast of Bol'shoy Lyakhovsky Island.

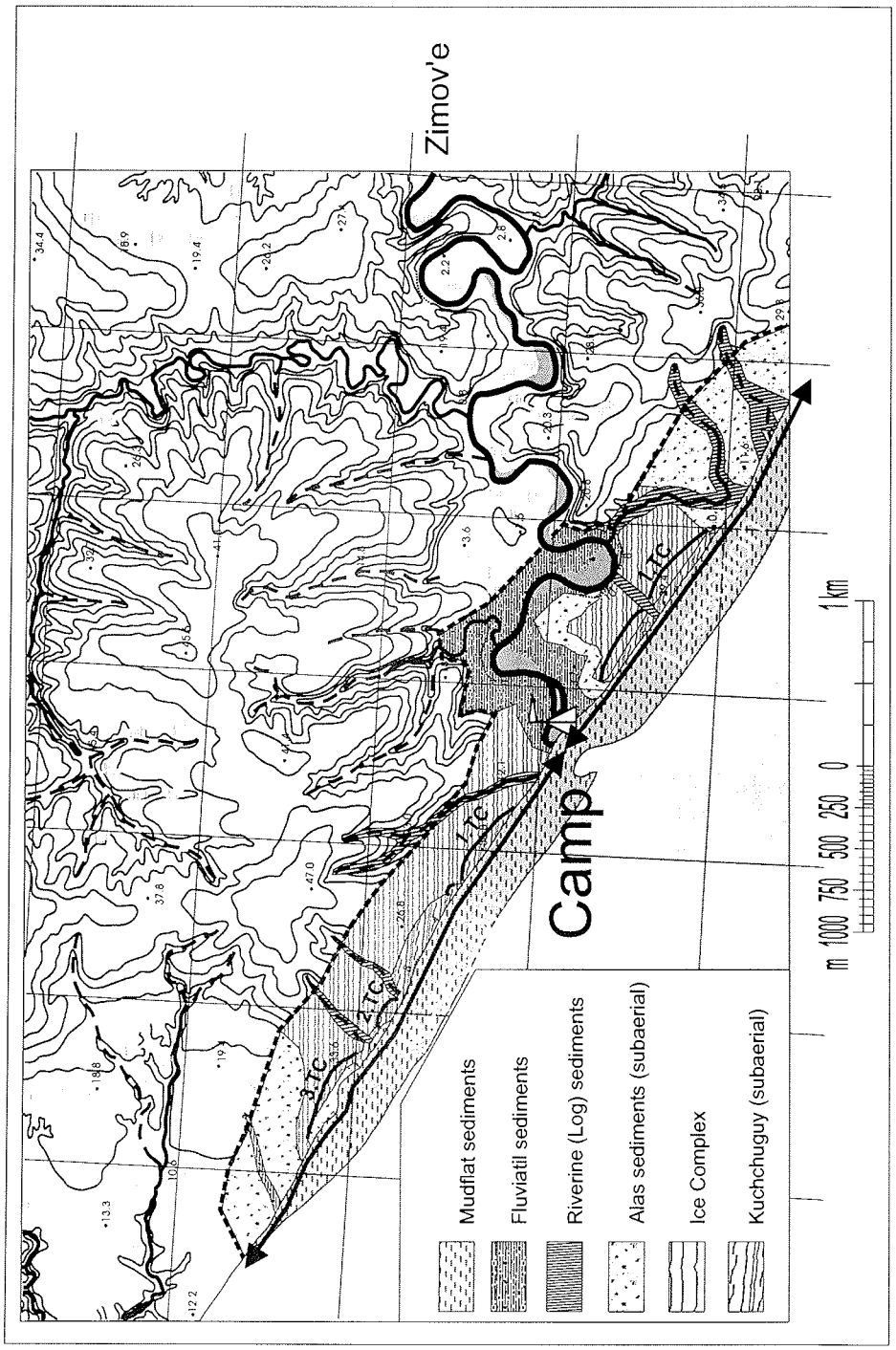

Figure 5-2: Detailed geomorphological map of the study area.

The oldest rocks of the Island are Proterozoic amphibolites and crystalline slates. They are exposed at the Emii-Tas hill, the most eastern part of the Island (Krasnyi 1981). Palaeozoic rocks like Permian sandstones and phyllitic slates of the Burustasky Series (P_1Bt) are visible at the slopes of Emii-Tas and Khaptagai-Tas hills. Mesozoic sandstone, siltstones and clay stones of Upper Jurassic and Lower Cretaceous were drilled down to 70 m depth at the Bol'shoy Lyakhovsky Island (Telepnev 1981). Some fissures of these rocks were filled by ice. In addition a Cretaceous or Paleogenic weathering crust on Pre-Cenozoic rock consisting of debris and clay was drilled to 16 m thickness (Alekseev et al. 1991).

While Eocene sands and gravels were drilled in depths of about 27 to 60 m at the north part of the island, Miocene silts, sands and gravel were found in depths of about 7 to 36 m at the east part. Miocene deposits contain the Khapchansky Horizon which is characterized by a pollen spectrum typical for colder conditions (Pinus, Betula, Alnus) (Grinenko at al. 1998 a). Eocene and Miocene deposits are part of the cryolithozone of Bol'shoy Lyakhovsky Island. Upper Pliocene deposits (N_2^3) were determined by Arkhangelov et al. (1996) in the south part of the island near the mouth of Zimov'e river. These peaty silts were dated by thermoluminescence between 950±250 ka and 980 ±250 ka (Table 5-3). The horizon contains syngenetic ice wedges, which are 2 to 3 m wide. It was called „Olyor-Suite" by Arkhangelov et al. (1996). The same author designate the following horizon as „Kuchchuguy-Suite" with a TL-age of 360±90 ka (Table 5-3). Both names were provisionally used for this report in order to describe the several cryolithological units.

One of the problems of the study area is the absence of a general usable scale of Quaternary stratigraphy. Therefore we used different scales:

- Stratigraphic scheme of Ivanov (1968, 1970, 1972)
- Unified regional stratigrafic scheme of Quaternary deposits of the Yana Indigirka Lowland and its mountainous surroundings and the decision of the expert commission of Quaternary (Sher et al. 1987)
- Stratigraphic scheme of Alekseev (1989)
- Regional stratigraphic scheme of Paleogene and Neogene deposits of east Yakutia (Grinenko et al. 1998a/b)

Table 5-1: Stratigraphic scheme of Bol'shoy Lyakhovsky Island.

Upper Quaternary ,Holocene (deposits of thermokarst forms, fluvial sands)
Middle and Upper Quaternary (silts with lenses of sand, clay and peat) „Ice Complex"; „Krest-Yuryask-Suite"
Upper Pliocene/Lower Quaternary (peaty silts with debris, sands) - „Olyor-Suite"; „Kuchchuguy-Suite", „Kanarchasky Layer"
Miocene (sands, silts , gravels) - with „Khapchansky Horizon"
Eocene (sands gravels)
Upper Cretaceous/Paleogene; (Weathering crust)
Lower Cretaceous; Upper Jurassic (sandstone, siltstone, claystone)
Permian (sandstones, phyllitic slates)
Proterozoic (amphibolites, crystalline slates)

Quaternary deposits of the south coast of Bol'shoy Lyakhovsky Island were firstly described in detail by Romanovsky (1958a-c). According to him the Quaternary consists of flood plain deposits in different terrace levels and ages with thermokarst lakes and fluvial deposits. Whereas Kunitsky (1998) explains the Quaternary deposits of the south coast as formations connected with Pleistocene perennial snow patches (snezhniki) on cryoplanation terraces, the Japanese scientists consider especially the Ice Complex deposits as formations of a big swampy marshland on the Pleistocene Laptev Sea Shelf (Nagaoka 1994; Nagaoka et al. 1995).

5.1.3 Methods of field study

(L. Schirrmeister)

The expedition to the Bykovsky Peninsula in 1998 showed that the cooperation between the different scientific disciplines should be closer concerning the survey and sampling of important profiles. At first numerous markers were established in distances of 100 m as simple orientations at the shore or coastal line depending on the coastal stability. The marker R 1 to R 35 stood in the west section R (right) (Figure 5-6) and the markers L 1 to L 25 in the east section L (left) (Figure 5-7). The exact appellation of the single profile consists of the number of the nearest marker and the distance of the study point to this marker. For instance the profile R 17+30 is located 1730 m west of the Zimov'e river mouth. The altitude of study points and characteristic locations was surveyed by

theodolith or also by tape measure near the sea. The bigger profiles were cleaned with the help of a water pump. The appendant ice wedges were separately sampled and only cleaned after sampling. Furthermore the water pump was used in order to screen big sediment samples for rodent study (50 kg, 1 mm mesh) and insect study (20 kg, 0,5 mm mesh). Special important methods for different scientific disciplines are described within the several chapters.

5.1.4 Description of the outcrop

(V. Kunitsky, L. Schirrmeister; G. Grosse, T. Kuznetsova, S. Kuz'mina, V. Tumskoy, A. Dereviagin, H. Meyer)

The study area of the summer 99 expedition is located on the Dimitri Laptev Strait about 2.5 km to the east and 3.5 km to the west of the Zimov'e river at the south coast of Bol'shoy Lyakhovsky Island (Figure 5-1). The following geomorphologic elements can be distinguished: the mouth and the valley with flood plain of the Zimov'e river; Ice Complex elevations (Edoma) (about 40 m a.s.l.), big thermokarst depressions with gentle slopes (alases, diameter: 1-2 km, altitude: 12-15 m a.s.l.), wide and flat, U-shaped thermo-erosional valleys (log, altitude: 20 to 10 m a.s.l.), deep (until 5 m), strait (50-100 m) and V-shaped thermo-erosional ravines or gullies (ovrags). The wide and flat valleys (logs) occur on Ice Complex elevations as well as in alas depressions. Thermal abrasion destroys the Ice Complex elevations at the bank of Dimitri Laptev Strait and forms so called thermo-erosional cirques, semicircular outbreaks of the coastal line and about 50 m wide thermoterraces (10 m a.s.l.) with thermokarst mounds (baydzharakhs, 2 to 5 m high) in front of the Ice Complex wall (Figure 5-3).

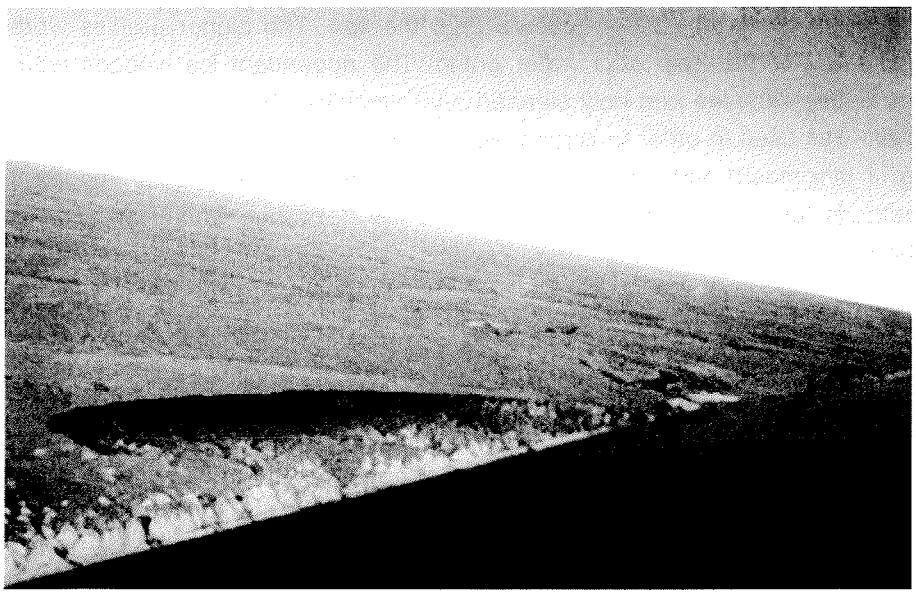

Figure 5-3: South coast of Bol'shoy Lyakhovsky Island at the mouth of the Zimov'e river with big thermo-erosional cirques and thermoterraces in front of the Ice Complex wall.

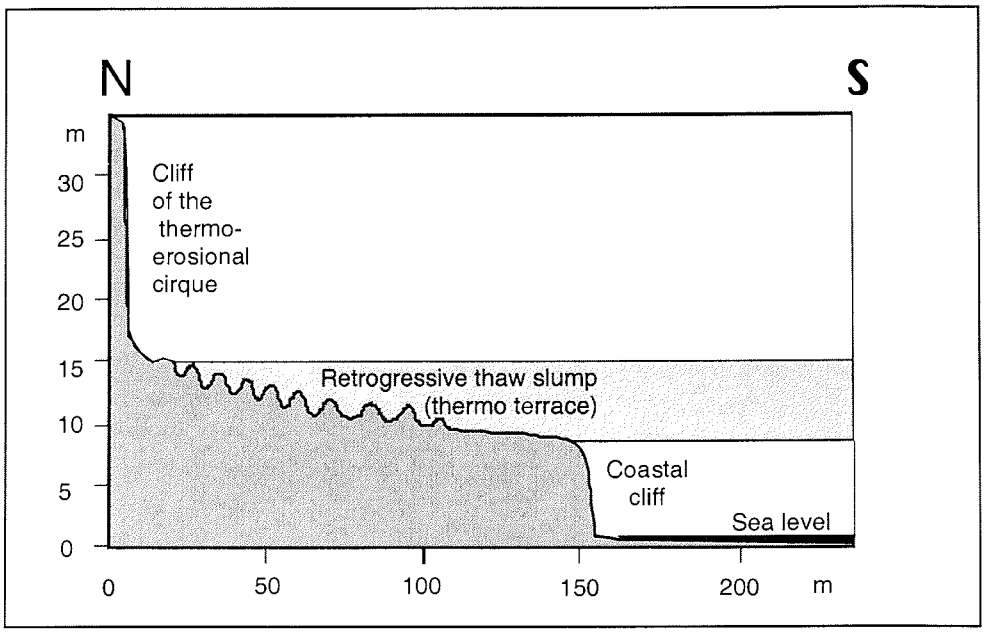

Figure 5-4: Schematic coastal cross profile from south coast of Bol'shoy Lyakhovsky Island.

Altogether eleven different geological cryolithological units were found. The rocks of the basement, like Permian quartzitic sandstone, slates, basalt, granites, quartz-pebbles, porphyry were found as debris or as solid rock on the beach in some cases. Bigger stones show phenomena of parallel frost shattering. A well developed (matured), yellowish to greenish-grey zonated weathering crust forms the first visible horizon. An ice-rich, coarse clastic deposit with stones of reworked basement, peat inclusions, peat horizons and paleosols, which are provisionally named „Olyor-Suite" followed the weathering crust. The next unit, provisionally named „Kuchchuguy-Suite", consists of two facies: a dryer subaerial silty-sandy series with many vertically orientated grass roots and subaquatic sediments with molluscs. The so called "subaquatic Kuchchuguy" consists again of two horizons, divided by a layer of ice wedge pseudomorphs. Some authors (V. Tumskoy, T. Kuznetsova, S. Kuzmina) consider the upper horizon of the "subaquatic Kuchchuguy" as a separate unit named "Krest-Yuryask-Suite" after Ivanov (1968) (see Chapter 5.1.7 and 5.1.9 and Appendix A5-2 to 5-2-3). So called taberites - thawed and refrozen permafrost deposits were visible below various subaquatic deposits.

The Late Pleistocene Ice Complex formed the big ice walls at the coast. It contains big ice wedges and many peat inclusions and paleosols in the upper level. The Ice Complex deposits are partly destructed by thermokarst. These thermokarst depressions are filled by Holocene subaerial and subaquatic alas deposits. Latter are underlain by talik formations (taberites). Additional Holocene deposits occur on thermo-erosional wide flat valleys (log) and ravines or gullies (ovrag). At last recent fluvial, alluvial and slope deposits close the sedimentary history of the study area (Figure 5-3). All these units are characterized by different types of ice wedges, distinguished in size, shape, colour, ice structure and ice-crystal size and texture, gas and sediment contents (Chapter 5.1.8).

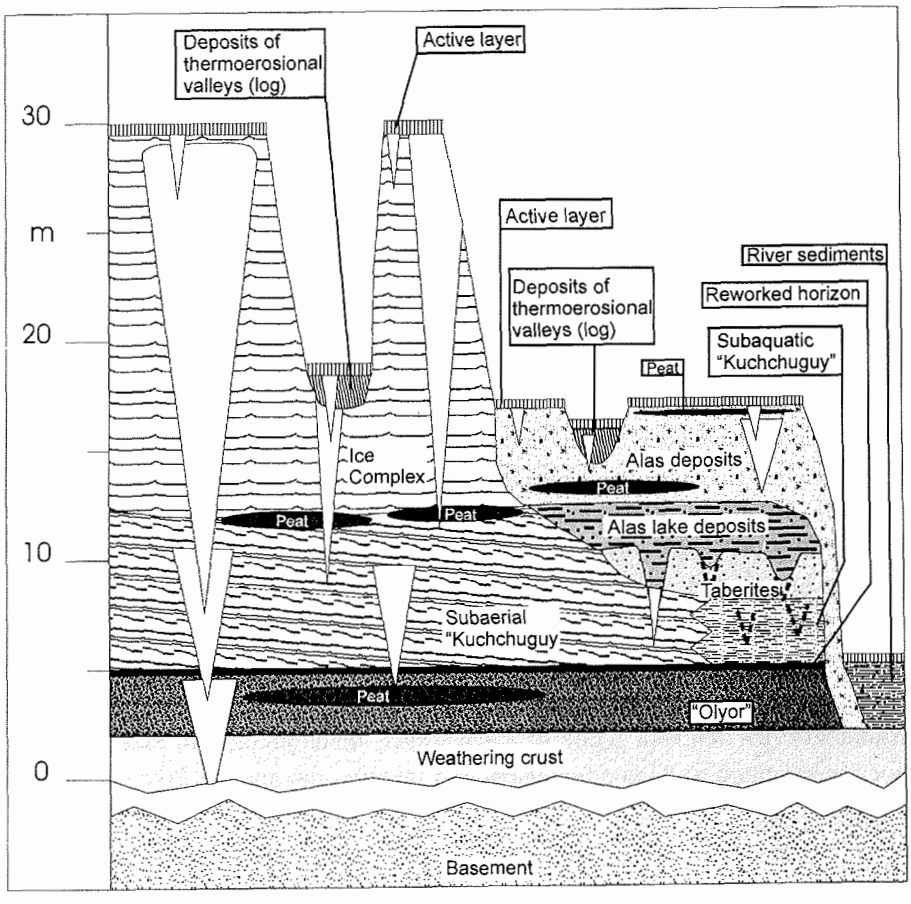

Figure 5-5: Columnar section of the studied permafrost deposits on Bol'shoy Lyakhovsky Island (see also A5-2).

The section R west of the Zimov'e river mouth consists of three big thermo-erosional cirques and a smaller one. They are separated each other by wide and flat thermo-erosional valleys (logs). The end of the western part is formed by a thermo-erosional ravine (ovrag) followed by a big thermokarst depression (alas) (Figure 5-6). This alternation of Ice Complex elevations and thermokarst depressions continues to the interior of the coastal region. The coastal cliff in front of the 20 m high Ice Complex walls form a step of about 5 to 10 m a.s.l. (Figure 5-4). The thermoterraces consist of dryer deposits than the Ice Complex. Thermoterraces are intersected by numerous brooks, which were supplied by the melted ice from the Ice Complex walls.

Section L east of the Zimov'e river mouth starts with fluvial deposits of the river valley within an alas depression. Following a big thermo-erosional cirque divided in to parts by a flat thermo-erosional valley is visible. The study area of the section L also concludes with a wide extended alas thermokarst depression (Figure 5-7). This depression contains a system of connected thermo-erosional valleys

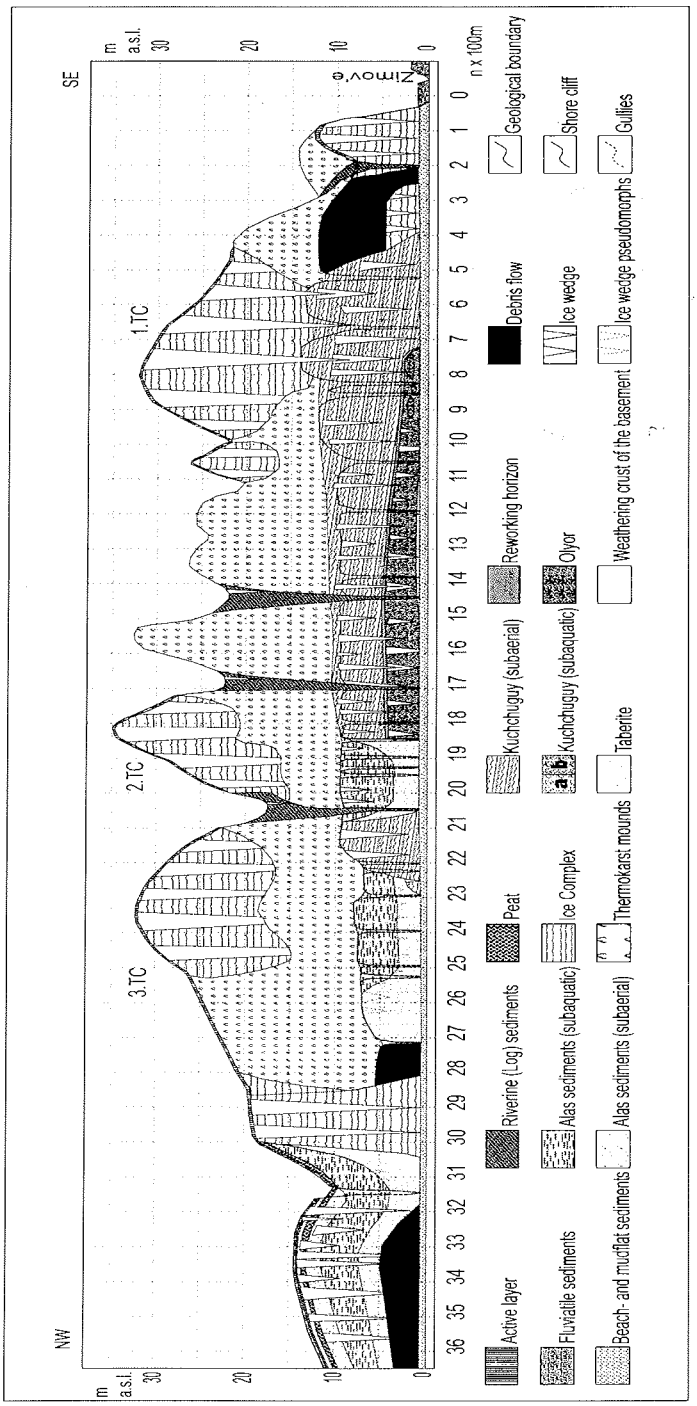

Figure 5-6: Schematic outcrop profile of section R (see also A5-2).

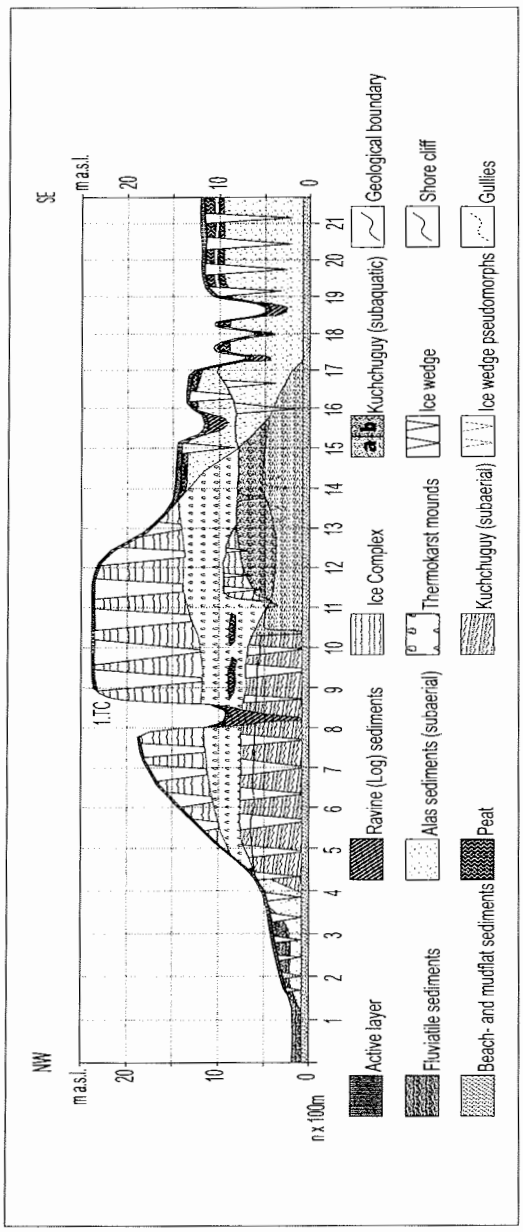

Figure 5-7: Schematic outcrop profile of section L (see also A5-2).

5.1.5 Cryolithological and sedimentological studies

(L. Schirrmeister, G. Grosse, V. Kunitsky)

The different genetic units numerated above (chapter 5.1.4) were characterized during the field studies in ice content (gravimetric), cryostructure, colour, organic remains, sedimentary structures, grain size and carbonate content. Their typical sedimentological and cryological features are summarized in Table 5-2. The special attention of survey and sampling was directed to the boundaries of important units like „Olyor"/„Kuchchuguy", „Kuchchuguy"/Ice Complex and to the bottom of alas deposits. The sediments were mostly frozen, and samples were taken with small hatchets and a hammer. In the camp the samples were divided into two small parts for palynological and micropaleontological analyses and a larger part for sedimentological studies. Firstly, after thawing water was sucked off for stable isotope and hydrochemical analyses.

Table 5-2: Sedimentological and cryological characteristics of typical permafrost deposits of Bol'shoy Lyakhovsky Island.

genetic units	sedimentological description	cryological description of sediment
Fluvial deposits	- brownish grey to light brown - fine to medium grained sands, cross and ripple bedding - layers of peaty plant detritus	- no cryostructures visible - ice content 30-90 %
Valley deposits (log)	- grey, brownish spotted - strongly rooted upper part	- banded, lenslike reticulated - ice content 40-100 %
Alas deposits	- grey, stratified, peaty soil horizons - several grass roots, twigs, peat covers	- banded, lens like reticulated - ice content 80-120 %
Alas lake deposits	- grey, brown, ochre; carbonate rich - sandy silt, ripple and fine bedding - shells horizons, sapropel layers with plant detritus, peat inclusions - pseudomorphosis with wood remains	- dotted distributed ice - ice content 30-60 %
Ice Complex	- grey brown - silty fine-sand (alevrit) - peaty paleosols, brown spotted - peat inclusions (10-20 cm), vertical grass roots, small twigs	- banded, alternation of ice band (3-5 cm) and sediment interlayers - fine to coarse lens like reticulated - ice content 60-170 %
Taberites	- grey with small black sulphide patches - dense; laminated; without grass roots	- some finely distributed ice - i ce content 25-50 %

subaquatic „Kuchchuguy" (older alas lake deposits)	- blue grey to light grey, black sulphide patches, brownish oxidation zones - fine-dispers distributed organic material, bituminous - twigs, shells, peat inclusions - laminated; carbonate rich	- some dotted distributed ice - ice content 20-30 %
subaerial „Kuchchuguy"	- grey-brown, with black sulphide patches - laminated, partly cryoturbated - silty fine-sand (alevrit) - carbonatic; many grass roots	- some dotted distributed ice -ice content 30-40 % - small ice wedges 0,5 m wide
„Olyor"	- grey-brown; carbonate free - unrounded stones in several layers and irregularly distributed - fine-sandy to silty matrix - peat inclusions (2-5 cm); peat horizon (1 m)	-banded - lens like reticulated interlayers - ice lenses 2-3 cm wide and 3-5 cm long - ice content 60-150 %
weathering crust	- yellowish to greenish-grey, zonated -unrounded stones (1-5 cm) in silty matrix	- lens like reticulated

5.1.6. Geochronometric age determination

(G.Grosse, L.Schirrmeister, V. Kunitsky, A. Dereviagin, T. Kuznetsova)

There are only few data of age determinations so far available for the Bol'shoy Lyakhovsky outcrop locality. The Pre-Cenozoic basement of the outcrop area consists of Permian sandstones. Further, there are some dykes belonging to Cretaceous granitic intrusions in the whole region (Drachev and Savostin 1993). On this basement a Cretaceous/Paleogene weathering crust and different Quaternary sediment sequences are situated. These sediments where dated in different ways by Russian and by Japanese scientists. It is important to note that the results of age determinations from Russian and Japanese scientists are quite different. To disclaim or confirm these data our team took samples for OSL (Optically Stimulated Luminescence)-, paleomagnetics-, radiocarbon dating and U/Th-dating.

Arkhangelov (1996) dated eight samples of the outcrop west of the Zimov'e river by thermoluminescence method (TL). The determined ages range from 57 ± 15 ka in the upper part of the Ice Complex (second thermo-erosional cirque) up to 980 ± 245 ka in the lower part of the „Olyor" suite near the weathering crust of Permian sandstone. Arkhangelov (1996) did some paleomagnetic measurements with „Olyor" sediments, too. The age was dated near the

Brunhes-Matuyama boundary. We could not locate exactly the position of sample RTL-758 (s. Table 5-3) but it must be somewhere in the Ice Complex. The samples RTL-755 and RTL-757 contain fluviatil sediments which could not be found again by our team. According to Arkhangelov (1996), the Ice Complex sediments are much older than those dated by Kunitsky (1996, 1998) and Nagaoka (1995). The limnic sediments could be part of the Kazanzev (equivalent to Eem). Between „Kuchchuguy" and „Olyor" there is a big span of time by some 100.000 years which has to be explained.

Kunitsky (1996, 1998) also dated samples by TL. The ages ranging from 61 ± 15 ka up to 114 ± 28 ka. Some pieces of wood found in alas sediments were dated by Kunitsky (1998, 1999b) with about 7.000 years by conventional radiocarbon dating. A young lake sediment west of the third thermo-erosional cirque was dated with 7.993 ± 183 years. A peat horizon laying above had an age of 6.436 ± 174 years. Japanese scientists dated six samples from peat layers in the Ice Complex Formation by radiocarbon method (Nagaoka et al. 1995). The range of those data is from 7.370 ± 820 years, near the top of the Ice Complex elevation up to >42.240 years at almost 25 m depth below the surface.

As shown above there are some problems with age determinations at this outcrop. Data are correct within sampling of one field team but often controversial in comparison with results of other teams. Additionally, the punctual sampled TL data of Arkhangelov (1996) have a huge range in age, and geological consequences cannot clearly be reproduced. A source for errors may be methodical problems in used definite age determination techniques accepted in the international science community. In general, it has to be mentioned that TL-ages above about 150 ka are reliable only under certain conditions (quartz dates from well bleached very low radioactive sediments). This is not the case in the region investigated. For instance, in case of the thermoluminescence method the signal needs 15 to 20 h of direct sunlight to bleach the sediment to a level which can be reconstructed in the laboratory. But sediments in these regions are often transported in suspension with water, so water and suspended sediment reduce the bleaching of minerals. Furthermore by the lack of sunlight in polar regions during long times the bleaching effect is reduced. Both problems can cause overestimated ages by TL.

Table 5-3: Previous age determinations on Bol'shoy Lyakhovsky Island

Sample number (year of sampling)	Sequence	Depth below surface	Determined age (method of dating)
Drachev and Savostin (1993)			
	Granitic intrusions in the basement		110-90 ± 5 Ma (K/Ar)
Arkhangelov (1996, pers. comm.)			
RTL-755 (pers. comm.)	upper Ice Complex		57 ± 15 ka (TL)
RTL-757 (pers. comm.)	Ice Complex		110 ± 28 ka (TL)
RTL-758 (pers. comm.)	?		113 ± 28 ka (TL)
RTL-753 (pers. comm.)	Lower Ice Complex		122 ± 30 ka (TL)
RTL-756 (pers. comm.)	Limnic sediments		136 ± 34 ka (TL)
RTL-754 (1996)	Sands „Kuchchuguy"		360 ± 90 ka (TL)
RTL-751 (pers. comm.)	„Olyor"		951 ± 240 ka (TL)
RTL-750 (1996)	„Olyor"		950 ± 250 ka (TL)
RTL-752 (1996)	„Olyor" near weathering crust		980 ± 250 ka (TL)
Kunitsky			
RTL-741 (1996)	Alevrit, „Kuchchuguy"		61±15 ka (TL)
RTL-821 (1998)	„Kuchchuguy"		35±10 ka (TL)
RTL-822 (1998)	„Kuchchuguy"		36±10 ka (TL)
RTL-740 (1996)	„Kuchchuguy"		94±26 ka (TL)
RTL-742 (1996)	Taberit		114±28 ka (TL)
PI-1197 (1998)	Alas (lake sediment)	5 m	7.993 ± 183 a (^{14}C)
PI-1198 (1998)	Alas (peat layer)	0.8 m	6.456 ± 174 a (^{14}C)
PI-1196 (1999a)	valley deposits (log) (roots, twigs)		7594 ± 255 (^{14}C)
Nagaoka et al. (1995)			
NUTA-2840	Ice Complex	~ 1m	7.370 ± 820 a (^{14}C)
NUTA-3532	Ice Complex	~ 5m	28.710 ± 400 a (^{14}C)
NUTA-2841	Ice Complex	~ 6m	30.980 ± 350 a (^{14}C)
NUTA-2797	Ice Complex	~ 7m	34.210 ± 1850 a (^{14}C)
NUTA-2842	Ice Complex	~ 21m	>39.650 a (^{14}C)
NUTA-2798	Ice Complex	~ 25m	>42.240 a (^{14}C)

Because of the problems mentioned above, we have chosen the **Optical Stimulated Luminescence method** for absolute dating. The minerals which can be dated by OSL need only a very short time (a few minutes) to become bleached. So there will be much less problems with overestimated ages. Altogether we sampled 16 single points for dating sediments by OSL and in respect to the problems of reduced bleaching effects 1 sample of recent sediment too. We have chosen most of those points with the knowledge of layer boundaries for fixing them with an absolute age.

We sampled in two different ways. The first was by hammering an opaque PVC cylinder horizontally into the sediment sequence chosen for sampling (used for unfrozen sediments). The second way was by coring with similar PVC cylinders and a hand drilling machine with accumulator (used for frozen sediments). To decrease the exposure to light we used opaque plastic bags while handling the samples. For most of the samples we did additionally in situ Gamma ray measurements which are used for laboratory correction of the radioactive history of the sample. A second sample of the same sediment is used for moisture content determinations, one precondition of correct dating. The range for the OSL method actually is from 1.000 up to 200.000 years BP.

With **radiocarbon dating** we can obtain additional information about the Late Pleistocene evolution of the study area. Several in situ bones and wood pieces were found in different altitudes of the outcrop. We can determine time ranges in which certain mammalian species existed on Bol'shoy Lyakhovsky with bones which were found not in situ at the beach or reworked in the outcrop. Bones will be dated in the Geological Institute of the Russian Academy of Science in Moscow. Radiocarbon AMS dating will be used for exact age determination of separated small plant remains like roots, moss-plants, twigs and seeds, which are presumed to be in situ. This material will be dated in the Leibniz Laboratory for age determination and isotopic studies in Kiel. Samples of bigger peat horizons and bigger wood remains will be dated by conventional radiocarbon dating at the Permafrost Institute in Yakutsk.

Whereas conventional radiocarbon dating is useful only for the last 40 ka and AMS dating perhaps for the last 60 ka, the OSL dating reaches the last 200 ka. Older deposits will be dated by **U/Th method,** which should be useful up to 500 ka. For dating by U/Th method we sampled a frozen peat horizon in the „Olyor-Suite" near the sea level (section R8+50) by sawing out a cube measuring 30x30x30 cm. This frozen cube was taken to the laboratory of Lower Saxon Survey of Soil Research in Hannover.

Paleomagnetic investigations have been carried out in section R where the sediments were dated N_2^3 (Arkhangelov 1996). Sediments presented the provisionally named „Olyor-Suite" and „Kuchchuguy-Suite". Samples were collected with a sheet-steel cube (45 mm) from flat surfaces into special cardboard boxes (24x24 mm) taking into consideration the accurate orientation to the North. The sample equipment was constructed by P. Minyuk. Ten samples (each in 6 specimen) from different levels of the „Olyor-Suite" were collected (8 samples from thawed dry sediment, 2 samples from frozen sediment). Additionally, a bigger monolith of sediment was taken which was

conserved with paraffin. It was very difficult to take non-disturbed samples because of the very high ice contents of the sediments. Further investigations are being provided in the Laboratory of Main Geomagnetic Field and Magnetic Petrology (Institute of Physics of the Earth, Russian Academy of Science).

5.1.7. Thermokarst Processes

(V. Tumskoy)

Thermokarst is defined as an integral set of physico-geological processes and phenomena including thawing of ground ice inclusions and deposits, subsidence of thawed ground and formation of negative forms of micro- and mesorelief (Grechichshev et al. 1980). The initial concept of thermokarst embraced only the relief forms but subsequently it was extended to processes generating these forms (Katasonov 1979).

The shapes of thermokarst formations are largely dependent on the morphology of thawing ice inclusions. This thesis underlies the existing classifications of thermokarst. Specifically, they differentiate the thermokarsts developing in texture-forming, massive, intrusive and wedge ices. Due to these factors, the thermokarst processes develop at different rates, have zonal and regional peculiarities and lead to differing relief forms of thermokarst. The largest and most significant in its manifestation is the thermokarst induced by the thaw of thick syngenetic ice wedges and high-ice deposits of the Ice Complex. Its development leads to the formation of relatively deep thermokarst lakes, their subsequent expansion and drainage. As a result, high-ice deposits are degraded leaving depressions called alases in Siberia. The above-mentioned processes are accompanied by transformation of initial deposits and accumulation of new ones reflecting conditions of their formation. The set of the deposits formed due to the occurrence of the above processes will further be called „alas complex". A typical region of the Ice Complex occurrence and the thermokarst development is the north of Yana–Indigirka Lowland and the Novosibirsk Islands.

The aim of studying alas deposits in Bol'shoy Lyakhovsky Island was to establish their relationship with embedding rocks and to reconstruct the time and conditions of their formation and development. The possibility of the occurrence of analogous but more ancient deposits was also investigated.

Nowadays, large alases occur widely in Bol'shoy Lyakhovsky Island. The thermokarst lakes proper are rare and have insignificant sizes. Alases are found mostly in the western part of the island where they are confined to a subsided

tectonic block (Neotectonic map 1984; Romanovsky 1961a, 1961b). They include residual lakes preserved after the drainage of thermokarst lakes. Here, the absolute heights of these 1–2-m deep lakes are 2–6 m above sea level. Nearer to the elevations constituted of bedrocks, the quantity and the size of alas depressions are decreased. In the area of Zimov'e river estuary, the 15–30-m deep alas depressions 4–5 km in diameter have a rounded isometric shape. The absolute height of the floor of alases varies from 2–3 to 14–15 m. The alas floor is flat and has a low-center polygons topography, while its central parts are swamped. In some places, alases are cut by the valleys of thermoerosion ravines („log") 10–25 m wide and 5–15 m deep. These ravines drain alas depressions and control the occurrence of lakes and swamped alases. Near such ravines the surface of alases is dry, and in winter the snow cover is thinner at their edges.

In the area of Zimov'e river estuary, the structures of four alases have been described. The first alas is situated 2.9–7 km westward of the Zimov'e river estuary (Figure 5-2). The absolute height of its surface is 12–15 m above sea level. The second alas is cut today by the Zimov'e river valley and its surface stretching 2–4 m above sea level. The two other alases are situated 1.3–2.85 and 3.35–4.4 km eastward of the Zimov´e river estuary, respectively. The heights of their surfaces range from 13 to 15 m. The profiles of all alases are well stripped in coastal exposures and accessible for examination.

The structure of the first alas (Figure 5-8) was studied most thoroughly. The profile of alas deposits was investigated along its entire length of 4.1 km. Their relationship with the lining rocks was described and the taberal, lake and intrinsic alas deposits constituting the alas profile were differentiated. Their lithology and cryolithology were also studied. The profile situated in the eastern part (3.2–3.3 km westward of the Zimov'e river estuary) was sampled for comprehensive analysis and radiocarbon dating (Table A5-5). A. Dereviagin and H. Meyer sampled the Holocene alas ice wedges for the stable isotope analysis (Chapter 5.1.8).

As regards other exposures of the alas complex, their profiles and relationships with the embedding rocks were described and their structures were established. All the profiles were investigated along the entire length of their vertical and horizontal strike.

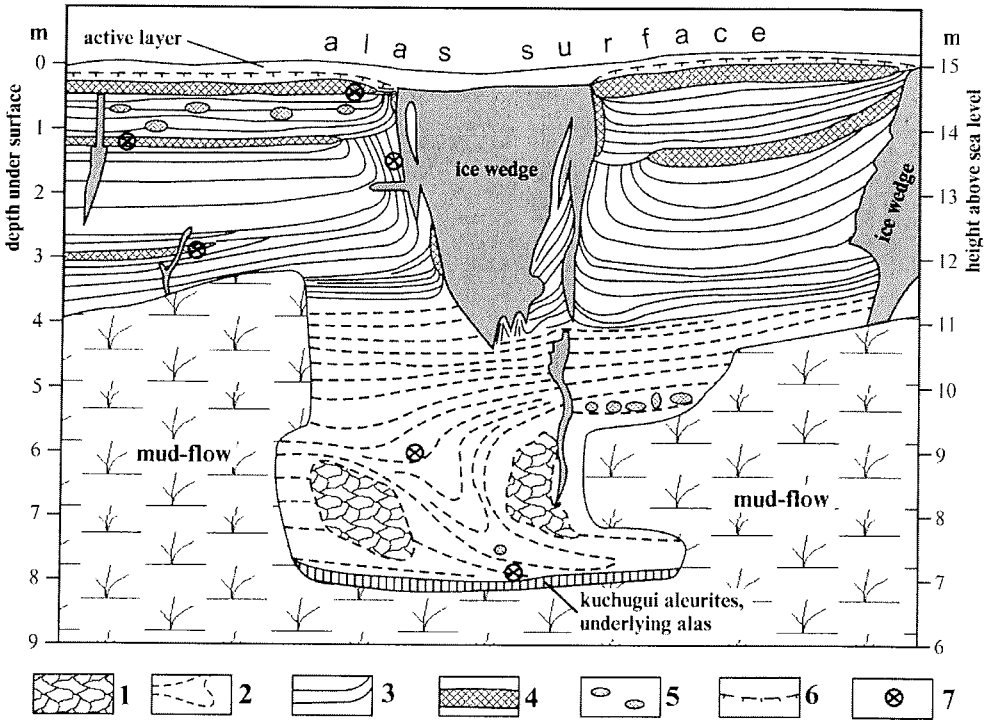

Figure 5-8: The structure of the first alas situated to the west of the Zimov'e River estuary.

1 - taber alevrites with reticulated cryostructure
2 - layered loamy silts of lake sediments with medium-scale lense like cryostructure
3 - alas peaty alevrites with syngenetic belt like cryostructure
4 - alas peaty horizons 5 - allochtonous peat inclusions
6 - boundary of active layer 7 - ^{14}C-dating samples

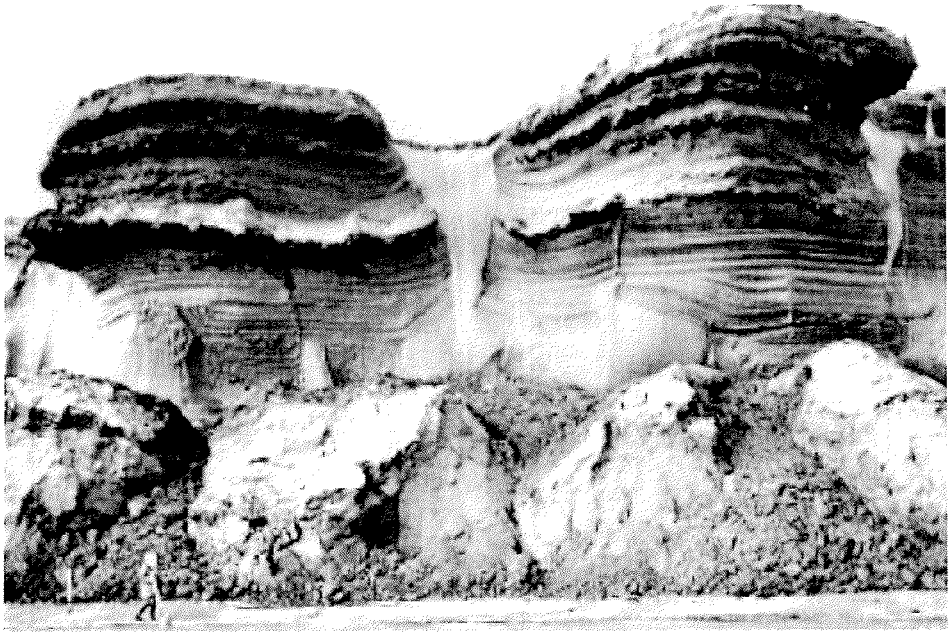

Figure 5-9: Inclusion of alas deposits in the Ice Complex (L-section; L 28-29)

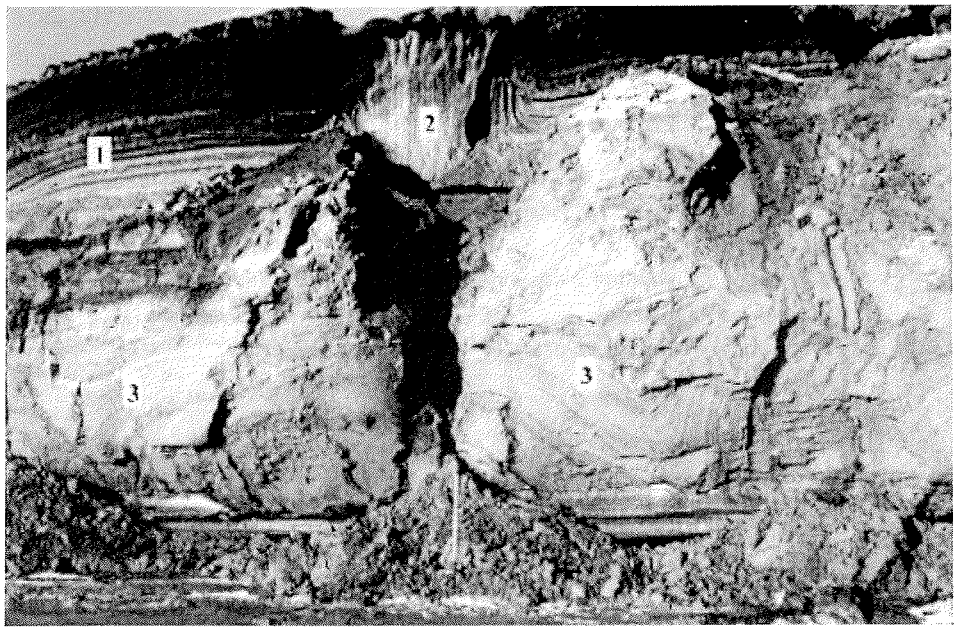

Figure 5-10: The outcrop of alas sediments (1) with an ice wedge (2) and underlain by deposits of "Krest-Yuryakhsk-Suite" with ice wedge pseudomorphs (3)

First Results

The results of field work suggest the following conclusions relative to the development of thermokarst in Bol'shoy Lyakhovsky Island.

1. Thermokarst was widely developed on the island territory. The consequence of this is a vast actual occurrence of alas depressions.
2. Alases are predominantly confined to negative tectonic structures. They fuse here with each other and form an alas plain with small individual outliers of the ice complex. Nearer to elevations, the number and the size of alas depressions go on the decrease. Alases are separated by interalas elevations constituted by the ice complex.
3. Thermokarst developed along the ice wedges of the ice complex with formation of thermokarst lakes under which the ice complex deposits thawed and formed depressions that were subsequently drained and transformed into alases. This is seen from the structure of the alas profiles, the base of which is composed of thin taberal deposits overlain with lacustrine lamellar alevrites and loams and crowned with the alas deposits proper including peat interlayers.
4. The relationship between the alas deposits and the enclosing and lining rocks is determined by conditions of the ice complex occurrence. For instance, in the area of Zimov'e river estuary the floor of the ice complex was below sea level. For this reason, the absolute height of an alas formed here does not exceed 2–4 m above sea level, whereas the floor of the alas deposits is below modern sea level. In other profiles the ice complex floor was found to lie 13–15 m above sea level and to be lined with low-ice alevrites of the „Kuchchuguy Suite". Therefore, the absolute heights of the surface of alas depressions are not less than 14–15 m. At the edges of alases one can see everywhere inclusions of alas deposits into the ice complex that lines them to a stretch of 100–200 m (Figure 5-9). A lake did not exist here for a relatively long time and was relatively shallow and hence the ice complex did not have enough time to thaw completely. In their middle part, the alas deposits overlie directly the deposits belonging to the „Krest-Yuryakhsk Suite".
5. The profile of the alas complex deposits has a regular structure. Its base includes in some places taberal deposits composed of greenish-grey alevrites with a large-scale reticulate cryogenic texture. These are the thawed ice complex deposits partially transformed by bottom processes. Often there is no clear-cut interface between the taberal deposits and the lake sediments, which substitute them up the profile. The latter are represented by silty loams

with a poorly distinct horizontal stratification. They are characterized by the irregular reticular and broken lenticular cryogenic textures. In some places one observes the mudflow structures characteristic of bottom conditions (Figure 5-8). After a partial or total drainage of a thermokarst depression, the floor of the alas formed becomes the site of frost-cracking of lake deposits, growth of ice wedges and formation of a surface with small intrapolygonal bogs. There occurs accumulation of the alas deposits proper with characteristic peat layers 0.2–0.5 m thick. The size of penta- and hexagons in Bol'shoy Lyakhovsky Island ranges from 12 to 15 m with the width of ice wedges reaching 2–2.5 m. In the peripheral part of alases their ice wedges penetrate into the bulk of ice complex, whereas in their central parts the ice wedges insert themselves into deposits of the „Krest-Yuryakhsk Suite" (Figure 5-10) and, sometimes, of the „Kuchchuguy Suite"; the vertical stretch of ice wedges can reach 4-4.5 m. The freezing deposits are becoming ice-rich. The alas deposits proper have a ice-belt cryogenic texture pointing to their syngenetic freezing.

6. The layer, which lines the alas complex and which was also found to occur under the ice complex remaining frozen until now, may apparently be regarded as formed by sediments of ancient thermokarst lakes. This stratum was first differentiated in 1956–1957 by Romanovsky (1958a-c) in Bol'shoy Lyakhovsky Island and soon after by O.A. Ivanov (1972) in the north of Yana–Indigirka Lowland and was subsequently called the „Krest-Yuryakhsk Suite". Deposits of this suite form pseudomorphs along the ice wedges in the roof of „Kuchchuguy Suite" (enveloping structures) and are represented by bluish-grey silty loams with inclusions of plant macroresidues, filamentous rootlets and bivalvular shells (Figure 5-10). They are also characterized by a manifest thin stratification. After their accumulation, these sediments were covered by the ice complex. The occurrence of the „Krest-Yuryakhsk Suite" deposits under the still unthawed ice complex implies that this thickness is not constituted by the thawed „Kuchchuguy Suite" deposits which were subsequently refrozen under the Holocene thermokarst lakes. The accumulation of this stratum took place under subaqual lacustrine conditions and was accompanied by the thawing of the lining frozen deposits with ice wedges, as indicated by the presence of pseudomorphs in the base of this stratum (Figure 5-10). Thus, the available data imply that the deposits of the „Krest-Yuryakhsk Suite" are associated with the formation of ancient thermokarst lakes and possibly „thermokarst lagoons", as maintained by N.N. Romanovsky and O.A. Ivanov.

5.1.8 Ground ice and water

(H. Meyer, A. Dereviagin & I. Syromyatnikov)

Introduction

Field work was carried out on the south coast of Bol´shoy Lyakhovsky Island in the area around Zimov´e River. The section consists of eleven stratigraphic units, which were subdivided by sedimentary and cryolithological aspects (see Figures 5-4 to 5-7 and Table 5-5). The oldest stratigraphic unit is Permian sandstone, that is found in the working area as Tertiary weathering crust only. The next younger units are the provisionally named "Olyor" and "Kuchchuguy" as well as the Late Pleistocene Ice Complex with steep ice walls reaching 35 m a.s.l.. All younger facies such as alas, proluvial-deluvial (or log) and fluvial deposits are presumably of Holocene age. Its deposition is related to the destruction of the older units by processes like thermal erosion or thermal denudation.

The cryolithological differentiation of the section is different compared to a common sedimentological subdivision. In the field, especially ice wedges cannot easily be attributed to a discrete sedimentary unit. Firstly, ice wedges grow perpendicular to the sedimentation, secondly, they may traverse sedimentological boundaries. A younger ice wedge may enter an older stratigraphic unit. This phenomenon has to be taken into account for a stratigraphic subdivision of a working area.

Two types of ground ice were studied in the working area: ice wedges and segregated ice. The sources of segregated ice formation can be suprapermafrost ground water of the active layer (mainly in syngenetic type of freezing), and also pore and free water in epigenetic type of freezing (Popov 1967; MacKay 1983). The source of ice wedge ice formation is mainly snowmelt water (Shumsky 1960; Romanovsky 1977). The stable isotope composition of ice wedges reflects mean annual winter temperatures (Vaikmae 1991). Therefore, ice wedges are perspective archives for paleoclimatic research, especially when ice wedges of different age and different geneses are available.

Different types of ice wedges as well as mostly fine dispersed segregated ice occur in all stratigraphic units. The oldest generation of ice wedges enters from so called "Olyorian" deposits into the weathering crust of Permian sandstone. The youngest generation is found in the recent active layer characterized by modern ice wedge growth.

The combination of last year´s sampling site, the Bykovsky Peninsula, and this year's working area Bol´shoy Lyakhovsky Island extends considerably the understanding of the regional paleoclimate. Ice complex, alas and log deposits can be found in both areas, enabling us to identify these deposits and their respective types of ground ice easily during the 1999 expedition. The main difference between the two areas is the occurrence of sediment and ground ice, which are much older than the Ice Complex on Bol´shoy Lyakhovsky Island. According to thermoluminescence data by Arkhangelov (1989), "Olyorian" sediments are about 950 ka old, "Kuchchuguy" sediments have been dated 350 ka (see also section 5.1.6). Additionally, Bol´shoy Lyakhovsky Island has been closer to the sea compared to the Bykovsky Peninsula. Thus, gradients of continentality and winter temperatures between both sites should be expected. This hypothesis may be proved by stable isotope method and different sources of (winter) precipitation may be identified.

Sampling and methods

Sampling was performed as described in last year's field report (Meyer et al. 1999). In total, 670 samples of ground ice, surface water, ground water, rain water and of snow patches were collected in the area around Zimov´e River. An overview of the sampling sites for ground and surface water, snow patches and active layer ice is given in Figure 5-11, excluding ground ice samples. Rainwater was collected close to the camp (see flag).

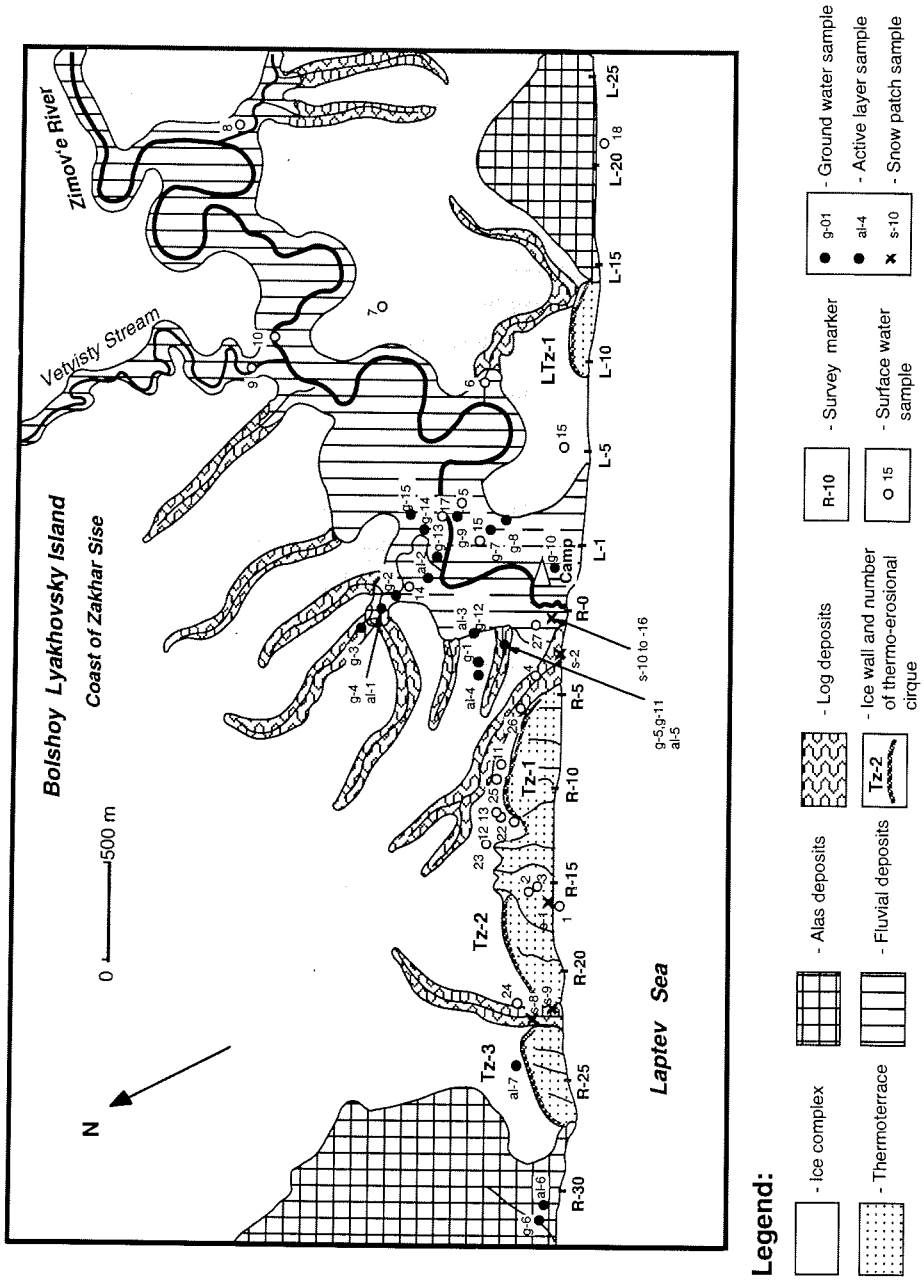

Figure 5-11: Overview of the working area inclusive sampling sites for ground and surface water, snow patches and active layer ice

Generally, the same sampling strategy as last year has been applied to ground ice. Ice wedges and segregated ice were sampled in all stratigraphic units. The locations of ground ice samples can be deduced from Figures A5-1 to 5-1-3 and Table 5-4. In order to get a complete vertical profile of all stratigraphic units, we sampled ice wedges in different heights of the outcrop (Table 5-4). The lateral position is given in three parts: the letter R or L defines the section of the outcrop, the numbers give the distance from the mouth of Zimov´e River. For example R32+20 signifies: right section, 3220m from the mouth of Zimov´e River in a NW-SE striking profile (see also Figures 5-11 and 5-2).

In total, 28 ice wedges were described and sampled. The most intensive sampling was carried out for ice wedge LYA-R-10-1 in the Ice complex, which is cut by coastal erosion perpendicularly to its growth structure and easily to reach and to sample. Some ice wedges were sampled, because they contain two or more generations of ice wedges. R-17-1 shows i. e. the contact between "Kuchchuguy" and "Olyor" and sections R-8 and R-9 the contact between Ice Complex and "Kuchchuguy".

Table 5-4: Sampled ice wedges including colour of ice, lateral position in the outcrop and respective height above sea level (see also Table 5-5)

ICE WEDGE	Stratigraphic unit	Number of samples	Colour of Ice	Lateral position	Height a.s.l. (Top outcrop)
LYA-R-1-1	Log?	3	grey, transparent	R1+40	8.0 m
LYA-R-8-1/2	Ice complex/Kuchchuguy	19	grey, transparent and Polosatic*	R8+50	15.4 m
LYA-R-6-1	Ice complex/Kuchchuguy	18	light grey, transparent and Polosatic*	R6+90	6.5 m
LYA-R-9-1	Ice complex/Kuchchuguy	28	grey, transparent	R9+90	9.0 m
LYA-R-7-1	Kuchchuguy	30	light grey and transparent	R7+40	6.5 m
LYA-R-10-1	Ice complex	82	yellowish grey and transparent	R10+90	22.0 m
LYA-R-10-2	Ice complex	6	grey, transparent	R10+60	23.0 m
LYA-R-17-1	Kuchchuguy/Olyor	48	grey, transparent and Polosatic*	R17+0	7.0 m
LYA-R-17-2	Kuchchuguy/Olyor	32	grey, transparent and Polosatic*	R17+30	3.0 m
LYA-R-19-1	Log	6	white and milky	R20+40	16.0 m
LYA-R-20-1	Log?	13	yellowish grey and milky	R20+60	3.0 m
LYA-R-22-1	Kuchchuguy	3	grey, transparent and Polosatic*	R22+60	2.0 m
LYA-R-32-1	Modern ice wedge	1	white and milky	R32+0	14.0 m
LYA-R-32-2	Alas	34	yellowish grey and milky	R32+20	14.0 m
LYA-R-32-3	Modern ice wedge	1	white and milky	R33+0	14.0 m
LYA-R-32-4	Modern ice wedge	1	white and milky	R33+20	14.0 m
LYA-R-32-5	Modern ice wedge	2	white and milky	R32+40	14.0 m
LYA-TZ-2-1	Log?	1	grey, transparent	R20+10	18.5 m
LYA-TZ-2-2	Ice complex	34	light grey and transparent	R20+5	19.0 m
LYA-TZ-2-3	Log?	4	grey, transparent	R20+0	18.5 m
LYA-TZ-2-4	Ice complex	19	yellowish grey and transparent	R18+30	19.0 m
LYA-TZ-2-5	Ice complex/Kuchchuguy	10	yellowish grey and transparent, Polosatic*	R18+30	16.8 m
LYA-TZ-2-6	Ice complex	2	yellowish grey and transparent	R18+10	15.0 m
LYA-TZ-3-1	Ice complex	36	yellowish grey and transparent	R21+60	27.5 m
LYA-L-21-1	Alas	45	white and milky	L21+10	9.0 m
LYA-L-15-1	Modern ice wedge	1	white and milky	L15+10	15.0 m
LYA- L-2-1	Fluvial deposits	15	colourless and transparent	L2+90	3.0 m
LYA- L-6-1	Ice complex	11	yellowish grey and transparent	L6+10	9.0 m
Total :	**28 ice wedges**	**505**	**samples**		

* Polosatic: very sediment-rich zebra-striped subvertical structures interrupted by ice veinlets

Segregated ice was described and sampled as vertical profile including ice belts and active layer ice. After complete melting, supernatant water was sucked off with a syringe. Samples from different modern surface waters (small streams, thermokarst lakes, ice wedge ponds, Laptev Sea) and precipitation (rain, snow patches) and suprapermafrost ground water were collected in order to compare data from fossil ice to actual hydrochemical and climatic conditions.

In order to reconstruct paleoclimatic changes and paleoenvironmental conditions of Bol'shoy Lyakhovsky Island, sampling for stable isotope ($\delta^{18}O$ and δD), ^{10}Beryllium, Tritium and hydrochemistry (pH, electrical conductivity, anions, cations) were carried out for ground ice. Samples were collected simultaneously for all types of analyses except ^{10}Be, where larger samples were needed. All ice wedge samples were taken with an ice screw or a chain saw, and were thawed in the field laboratory. The melt water was separated for stable isotope, Tritium and hydrochemical (anion/cation) analyses (Meyer et al. 1999). Anions will be measured by ion-chromatograph type Eppendorf IC 2001, cation measurements will be undertaken with a Perkin-Elmer ICP-OES Optima 3000 XL. pH and electrolytical conductivity were measured directly in the field laboratory with WTW instruments. Stable isotopes $\delta^{18}O$ and δD will be determined with a Finnigan Delta-S mass spectrometer at AWI-Potsdam. Finally, ^{10}Be as an indicator for variations in solar activity and climate (Beer et al. 1985) will be measured by AMS at the ETH Zurich. The preparation of the samples will be done at the Institute for Environmental Physics in Heidelberg.

Tritium as indicator of moisture transportation processes is a radioactive component of the water molecule and reflects the content of modern (younger than 1953 - the beginning of hydrogen bomb tests) water in permafrost.

There is a lot of information in geocryology on cryogenic ground features and cryogenic processes as a result of energy and mass exchanges in freezing, frozen and thawing deposits. Nevertheless the mechanism of these processes is usually invisible and insufficiently understood. The application of Tritium analyses allows the study of the processes of modern ice formation in the cryolithozone. The combination of Tritium analyses with other methods, especially stable isotopes enables us in some cases to understand the processes of modern ice formation. The knowledge of modern ice formation processes is the key for the understanding of Pleistocene ice formation. Thus, the main object of our investigations is the upper part of permafrost, including the seasonal thawing layer and recent waters such as rain water, surface water or ground water. 105 samples were collected for Tritium analyses (see Table A5-6). The measurements will be performed in the department of

Radiochemistry of Moscow State University using a liquid-scintillation spectrometer Trycarb-1600.

Cryogenic construction of the working area

The cryogenic construction of eleven different genetic units from the weathering crust to Holocene ground ice is described below. Table 5-5 gives a brief summary of the most important ground ice features, which occur in the working area.

Table 5-5: Description of the ground ice of eleven stratigraphic units with their respective approximate age. The terms "subaquatic" and "subaerial" refer to the deposition of the sediments and not to the conditions during ice wedge formation.

Stratigraphic unit	**Approximate age** (* after Arkhangelov 1989)	**Description**
11. Fluvial deposits	Holocene to recent	Syngenetic ice wedges, maximum width about 1.5 m, modern heads, layered cryogenic structure.
10. Log deposits	Holocene (about 1 ka)	Epi- and syngenetic ice wedge growth, maximum width about 1.2 m, reticulate to layered subhorizontal cryogenic structure
9. Alas deposits - subaerial facies	Holocene (<8 ka)	Epigenetic ice wedges, maximum width about 3 m, many modern heads, reticulate to layered cryogenic structure. L-section with multiple ice wedge generations within the alas.
8. Alas deposits - subaquatic facies		Ice wedge pseudomorphs only.
7. Ice complex	Pleistocene (<80 ka)	Huge syngenetic ice wedge polygons (Ø = 25 m), maximum ice wedge width about 6 m, forming thermo-erosional cirques and steep, up to 15 m high ice walls with very high ice content, characteristic are massive subhorizontal ice belts, reticulate to layered cryogenic structure.
6. Taberites	???	Ice wedge pseudomorphs only.

5. "Kuchchuguy" - subaerial facies	~350 ka*	Epigenetic ice wedges, maximum width about 2.5 m, may occur isolated, generally more than one head per ice wedge which may reach 0.2 m in width, typical is the occurrence of epigenetic subvertical yellowish to grey striped ice-sediment wedges called "Polosatic". Low ice content in the sediment, finely distributed, high sediment content in the ice wedges. Low number of ice wedges.
4. "Kuchchuguy"- subaquatic facies	~350 ka*	Ice wedge pseudomorphs only.
3. "Olyor"	~950 ka*	Syngenetic ice wedges, max. width about 3 to 3.5 m, may contain rock fragments, high ice content in the sediment with subhorizontal ice belts, occurrence of subvertical epigenetic ice-sediment wedges called "Polosatic", which may probably be associated to younger Kuchchuguy. Layered to reticulate cryogenic structure with ice lenses.
2. Weathering crust	Paleogene?	Epigenetic ice wedges continuing under sea level, maximum width about 0.5 m. reticulate cryogenic structure.
1. Permian Sandstone (basement)	Perm	not found in the working area

The **basement** of Permian sandstone is not found in the working area but its weathering crust, which outcrops in the R-section between R11 and R19. Small ice wedges are generally more narrow than 0.5 m entering the **weathering crust** from the overlying stratigraphic unit provisionally named "Olyor". This presumably represents the oldest permafrost found in the working area. It can be assumed that the "tails" of the ice wedges continue beneath sea level. The absolute maximum height of the weathering crust does not exceed 1 m a.s.l. in the working area. The weathering crust consists of eluvial clay and silt with numerous poorly rounded rock fragments and is characterized by basal and cellular structure. (Features of chemical weathering are found, which may indicate a warmer period (like the Paleogene) for the weathering.)

Ice wedges in "**Olyor**ian" sediments are about 3.5 m wide. We never saw any whole "Olyorian" ice wedge in the working area, but best outcrops were observed around section R-17. The maximum height of "Olyorian" ice wedges can roughly be estimated as more than 5 m. A peculiarity is that they are characterized by inclusions of underlying weathering crust such as yellowish clay and silt as well as numerous rock debris. Ice wedges in "Olyorian"

sediments may be subdivided into two parts which may occur side by side: an ice-rich part with low sediment content, light grey transparent ice with a great number of gas bubbles ≥1mm and poorly developed subvertical structures and ice-soil-wedges provisionally named "polosatic". Polosatics probably belong to the next younger genetic unit "Kuchchuguy", and thus, are explained there. The question whether the two parts represent different generations of ice wedges may be solved by stable isotope method.

Horizontally orientated ice belts predominate the cryogenic structure of the „Olyor". The thickness of the ice belts is about 15 mm in the upper part of the profile and not more than 5 mm in the lower part of the profile. The growth of ice wedge was probably both syngenetic, as shown by the subvertical flexure of ice belts close to ice wedges, and epigenetic (the "polosatic" part) to the sedimentation. Paleomagnetic investigations conducted in the upper part of "Olyorian" suite allow us to associate these sediments with the magnetic inverse episode Jaramillo about 990-1070 Ka BP (Kravchinsky et al. 1998).

The "**Kuchchuguy**" unit is characterized by relatively low ice content in the mostly massive-structured sediment. Ice wedges are epigenetic and rather rare compared to other units. The ice wedges in "Kuchchuguy" sediments have different width from 1 m to 2.5 m and show some specific features:

In most cases "Kuchchuguy" ice wedges contain ice-soil-wedges "**polosatic**" (see Figure 5-12). "Polosatic" is a phenomenon of very sediment-rich zebra-striped vertical bands interrupted by (elementary?) ice veinlets. The thickness of ice veins is generally about 1 to 3 mm, but may reach up to 1 cm. Ice in "polosatic" is dirty, turbid and yellowish, but may be also clear and transparent. The thickness of mineral layers is normally about of 1-2 mm, but it may be significantly higher. The genesis of "Polosatic" is unknown, but the entering of "polosatic" into older "Olyorian" ice wedges is certainly associated with "Kuchchuguy" cryolithological unit. The contact with "Olyorian" ice wedges could clearly be seen in section R-17, where "Kuchchuguy" ice wedges cross the sedimentary boundary between the two units. Vertical striped "polosatic"-structures can be found between 1 m and 17 m a.s.l., even in contact or adjacent to overlying Ice Complex.

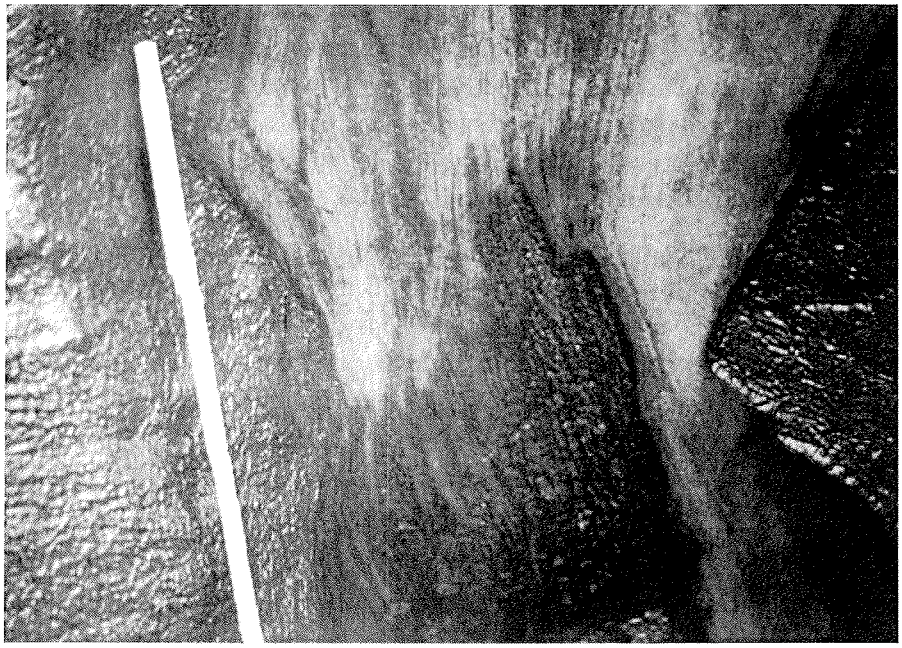

Figure 5-12: "Polosatic" – vertically banded ice-sediment wedge typical for Kuchchuguy deposits in direct contact with the lowest part ("tail") of Ice Complex ice wedge.

Generally, we observe more than one vertical extension or "head" in the upper part of "Kuchchuguy" ice wedges. The width of heads may reach up to 20 cm and in some cases, they are buried under "Kuchchuguy" sediments, and should therefore be of "Kuchchuguyan" age. In other cases, we observe isolate "Kuchchuguy" ice wedges without any contacts to other ice wedges or genetic units (R-7). The phenomenon of ice wedge heads may be due to a sudden rise in the sedimentation rate. Additionally "Kuchchuguy" ice wedges generally have an uneven upper surface. Melting processes may have caused a degradation of the ice wedge from above prior to the growth of ice wedge heads. The contact between "Kuchchuguy" and Late Pleistocene Ice Complex is not clearly defined and not uniformly at the same height above sea level. The heads of "Kuchchuguy" ice wedges cross the boundary to the next younger genetic unit, the Ice Complex. "Polosatic"- structures can sometimes even be found in direct contact to the lower part (or "tails") of ice wedges (see Figure 5-12) attributed to the Late Pleistocene Ice Complex (R-8, R-9).

Some parts of permafrost profile of "Kuchchuguy" sediments have visible marks of thawed ice wedges. These ice wedge pseudomorphs belong to the subaquatic sediment facies of "Kuchchuguy" unit and are usually associated with alas depressions.

The **Ice Complex** is characterized by huge syngenetic ice wedge polygons, which may reach 25 m in diameter. A single ice wedge may attain widths up to 6 m and vertical dimensions up to 25 m. The colour of ice wedges is usually yellowish-grey and has well-defined subvertical structures such as elementary ice veins, oval gas bubbles and orientated thin mineral layers. The mean thickness of elementary veins is generally about 1-4 mm. The cryogenic structure of the Ice Complex has been formed by syngenetic freezing of deposits in landscapes with a thin active layer (Siegert & Romanovsky 1996). Other typical cryolithological features in the sediment are massive subhorizontal 2 to 4 cm thick ice belts, which are always bound upward close to the ice wedges. The ice of ice belts is clean, transparent and includes numerous bubbles of air. Thermal erosion of the Ice Complex causes typical geomorphological forms such as up to 15 m high and about 70 to 75° steep ice walls (Figure 5-13) as well as semicircles called "thermo-erosional cirques". The extension of thermo-erosional cirques is about 400-700 m (Figure 5-3) and they are characterized by 50 m to 100 m wide thermoterraces with numerous baydzharahks (or thermokarst mounds) formed by melting processes. Four thermo-erosional cirques (TZ-1, TZ-2 and TZ-3 and L-TZ-1) were studied during the field work.

Figure 5-13: Thermo-erosional cirque TZ-2 with a 15 m high steep wall of Late Pleistocene Ice Complex

Three younger facies - likely of Holocene age - overlie the Ice Complex and older deposits. Alas deposits are located to the easternmost and westernmost part of the investigated area in basins, where the ancient surface has been lowered by thermal denudation. Deluvial-proluvial sediments of small streams (or logs) occur in the whole section as thermo-erosive channels. Fluvial deposits are found in the area around Zimov´e River only.

Alas deposits were best studied in sections R-32 and L-21. The cryogenic construction is determined by a system of thick epigenetic polygonal ice wedges and ice-rich alas sediments usually with horizontally layered to reticulate structure. Thin ice belts were observed to be bound upward near the contacts with ice wedges. Ice wedge polygons normally attain 10-15 m in diameter. Alas ice wedges may reach heights of 6 to 8 m, maximum widths of about 3.5 m and show subvertical structures such as 3 mm thick elementary ice veins and orientated very small gas bubbles. The ice wedges are white and milky and contain a lot of datable organic material (small leaves, blades and peat). Alas ice wedges near thermo-erosional cirque L-TZ-1 could be differentiated into several (up to four) ice wedge generations. At this site, no sampling was possible because of the steep wall with overhanging peat layers. In alas deposits, modern ice wedge growth ("heads") with width of 1 to 4 cm is very common.

Logs or shallow small streams and their respective thermo-erosive channels are typical features in the whole working area (see Figures 5-4 to 5-6 and 5-11). Both epigenetic and syngenetic ice wedges with a maximum width of about 1.5 m are found. Generally, log deposits are in direct contact with the Ice complex. Log ice wedges are characterized by white to gray, milky ice with subvertically orientated and elongated gas bubbles ≥ 1 mm resembling a string of beads. The elementary ice veinlets are between 1 to 4 cm thick but not easily identified.

The Holocene **fluvial deposits** are characterized by ice wedge polygons with small diameter. In the working area, they are found in the Holocene fluvial terrace in the mouth of Zimov'e river only. The maximum height of the fluvial deposits is about 5 m, the width of ice wedges may reach 1.5 m. The ice wedges have modern heads in the upper part and show subvertically orientated 2 to 6 mm thick ice veins, very thin layers of sediment and elongated gas bubbles. The ice is relatively clear, colourless and transparent. Enclosed sediments are characterized by a layered cryogenic structure bound upward near ice wedges.

Additionally, active ice wedges with widths of 1 to 4 cm have been observed in some parts of the section, especially in the alas near R-32. All these modern "heads" of ice wedges were sampled because they may be useful as standards for paleotemperature reconstruction.

Ice wedges are neither found in the taberites, which are thawed and refrozen sediments of former taliks, nor in the subaquatic parts of both "Kuchchuguy" and alas deposits. Here, ice wedge pseudomorphs display a former existence of ice wedges. The higher heat capacity of episodically open water bodies causes melting and talik formation.

Investigations of the crystalline structure of ground ice

In addition to geochemical investigations of ground ice, the ice structure was studied using polarising lenses. The method of crystalline structure analyses is widely used in geocryological investigations of ground ice and most generally employed in studies of polygonal ice wedges. The crystalline structure of ice wedges largely depends on the conditions of ice wedge formation. It is based on specific characteristics of ice crystal size, shape and orientation, which represent the conditions of crystallisation (Solomatin 1974).

During the field season, ice wedges of five different genetic units ("Olyor", "Kuchchuguy", Ice Complex, alas and log) were sampled. Both, studies of crystalline structure of "Olyorian" and "Kuchchuguy" ice wedges as well as the

combination of ice crystallography with isotopic investigations of ground ice were carried out for the first time.

The standard method of field crystal-optics investigations was applied. At first, a monolith of ice of 20x20x20 cm was cut out of an ice wedge using a chain saw. Two 1-2 cm thick slices of ice were sawn. One of slices was orientated lengthways to elementary ice veins and the other one crossing the veins. Both slices were manually polished to a width of about 1 mm (transparent microsection). The microsections were described, photographed and analysed under special polarisation filters. Maximum, minimum and mean area of ice crystals (respectively S_{max}, S_{min} and S_m) as well as maximum, minimum and mean size of crystals (respectively L_{max}, L_{min}, L_m) were determined.

Table 5-6: Morphometric characteristics of ice wedge crystallography. Maximum, minimum and mean area of ice crystals (S_{max}, S_{min} and S_m) and maximum, minimum and mean diameter of crystals (L_{max}, L_{min}, L_m)

Study subject	Section	Orien-tation	Smax (mm2)	Smin (mm2)	Sm (mm2)	Lmax (mm)	Lmin (mm)	Lm (mm)
"Olyorian" ice wedge	R-17+30-1	horizontal	-	-	-	8x12	1x2	4x5
"Olyorian" ice wedge	R-17+30-1	vertical	-	-	-	6x10	4x4	1x1
"Kuchchuguy" ice wedge	R-9+85-2	horizontal	-	<1	1	4x2.5	-	1x1
"Kuchchuguy" ice wedge	R-9+85-2	vertical	7	<1	1.5	4x2.5	-	1.5x1
Ice Complex, bottom part	R-9+85-1	horizontal	6	<1	1.5	3.5x3	-	1.2x1.3
Ice Complex, bottom part	R-9+85-1	vertical	14	-	4	4x4	-	2x2
Ice Complex, middle part	R-10+55-1	horizontal	24	1	4	3.5x3	-	1.2x1.3
Ice Complex, middle part	R-10+55-1	vertical	14	-	4	4x4	-	2x2
Ice Complex, upper part	TZ-3-1	horizontal	-	-	-	6x6	-	4x4
Ice Complex, upper part	TZ-3-1	vertical	40	-	16	12x6	-	-
Ice wedge in alas	L-21+10-1	horizontal	9.5	<1	3	4x3.5	-	2x1.5
Ice wedge in alas	L-21+10-1	vertical	19	<1	4	6x4	-	2x2
Ice wedge in log	R-20+50-1	horizontal	10	<1	2	5x3	-	2x1.5
Ice wedge in log	R-20+50-1	vertical	5.5	<1	2	2x3	-	1.5x1.5

The basic morphometrical characteristics of ice wedge crystalline structure of Bol´shoy Lyakhovsky Island are presented in Table 5-6. Results of field measuring show that the ice of "Olyorian" ice wedges (around R-17) is characterized by rather large sizes of isometrical crystals. Small isometrical crystals of ice and numerous spherical bubbles of air are observed in "Kuchchuguy" ice wedges (R9+85). The diameter of bubbles is generally less than 1 mm. The crystal-optic analyses of Ice Complex ice wedges were conducted in three different height levels: 10 m a.s.l. (R-9-1), 22 m a.s.l. (R-10-

1) and 27 m a.s.l. (TZ-3-1). The biggest sized crystals were observed in the upper part of Ice Complex. Crystals have an elongated form and both spherical and cylindrical bubbles of gas were observed. Cylindrical bubbles have vertical orientation reaching 5 mm. The diameter of gas bubbles is about 1 mm. The middle part of the Ice Complex profile is characterized by slightly smaller size of crystals. Bubbles of gas mostly have a cylindrical form and their vertical size reaches to 12 mm. The horizontal size of air bubbles is not more than 1 mm. The bottom part of Ice Complex is characterized by small size of crystals and small spherical (diameter about 0.5 mm) bubbles of gas.

Ice wedges in alas and log deposits also have a different crystalline structure of ice (Table 5-6). Size of spherical gas bubbles both in alas and log ice wedges is less than 1 mm. The data handling will be continued and photographs will supplement visual observation. It is expected to make statistical analysis of obtained data.

5.1.9 Paleontological research at the southern coast of Bol'shoy Lyakhovsky Island

(T. Kuznetsova and S. Kuzmina)

Stratigraphic and paleontological studies were one of important components of the multidisciplinary research of the Pleistocene deposits at the southern coast of Bol'shoy Lyakhovsky Island. These studies included the search and collecting of large and small fossil vertebrate remains, fossil and modern insects, plant macrofossils, and fossil molluscs.

Large mammal fossils

The famous Russian Novosibirsk Expedition of 1886, led by A.Bunge and E.Toll, collected nearly 2000 bones and discovered many species of fossil mammals, previously not known in the Arctic, such as saiga antelope, a large lion-like panther, woolly rhino, and many others (Cherskiy 1891). This collection was made mostly at the southern coast of the island, which became one of the most important Pleistocene sites in whole Siberia. In 1956, a few hundred bones were collected by V.D.Lebedev and N.N.Romanovsky at the same site (Vangengeim 1963). In recent years, a few occurrences of woolly mammoth with preserved soft tissues were recorded here (Lozhkin 1977; Arkhangelov 1996; Lazarev in press). The site also became a rich field for ivory hunters and illegal bone collectors. That has been for the first time since the last century, when mammal bones were collected here professionally, and exposed in relation to the study of the sediments.

when mammal bones were collected here professionally, and exposed in relation to the study of the sediments.

During our work in 1999, with the active help of all the team members, we collected 1028 bones and bone fragments of large mammals (Table A5-7). The collecting was rather thorough - all of the found identifiable fragments were registered, to obtain as complete statistics of species composition as possible. The bones were collected from an about 10 km long segment of the island southern coast - 4 km west of the Zimov´e River mouth (side "R"), and 6 km east of it (side "L"), both on the shore and within the coastal cliffs. As 1998 on the Bykovsky Peninsula, the major part of the collection unfortunately comes from the shore, which is common in permafrost regions. Strictly *in situ* in the sediments, 33 bones were found (group "a"), 20 of them belonging to an articulated skeleton of bison (sample BL-O193-R).

The second group ("b") includes 54 bones found within the exposures, mostly in the thermo-erosional cirques I, II, and III on the R side, beneath almost vertical walls of Ice Complex exposed. By their finding locations, it is possible to define the area, where the bones came from, with more or less certainty. These areas are marked as "the bone fields", and the altitude of their lower boundaries was instrumentally defined as the level of minimum height of the original position of the bones. Group "c" (134 samples) incorporates the bone specimens found at the exposures, but in or on the scree. For these bones, it is not always possible even to infer from which member of the section they came. They can only be related to the particular station of the cliff, and to the sediments occurring not lower than the finding location.

The most of the material has been collected on the shore. It was divided into two groups - the bones, picked up on the L side (group "d", 226 specimens), and those collected on the R side (group "e", 442 specimens). Such a subdivision was potentially important, since on the side R the earliest deposits (of the "Olyorian" age) are exposed, and correspondingly, the most ancient bones could be encountered. On the L side, the earliest are the deposits of the middle member ("Kuchchuguy"), and the occurrence of the Early Pleistocene bones is less likely. During our work, we could several times observe the transportation of bones by the coastal waves along the shore R from the landmark R-25 (the cape) to the landmark R-0. However, bones from beyond the cape were never seen to be transported closer to the camp. The coastal bone transport along the L shore was also observed, but we never recorded the transport from the L to the R shore, and vice versa. We can assume, that the Zimov´e River mouth is an obstacle for such transportation. Whether these sets

of bones have some real difference in taxonomic or other composition can only be concluded after detailed morphological study of the collection.

One more small group of bones recorded separately (group "f", 38 specimens) comes from the Zimov´e River floodplain. They have been redeposited into the modern river deposits from the sediments, eroded by the river. This group includes the bones with some remains of soft tissues, found at the site, where a partial skin and foot of mammoth was found in 1995. We registered the bones scattered around the camp site as a completely separate group (group "g", 96 specimens). These bones were collected in various areas of the island by previous expeditions and bone hunters, and left behind near the camp, so their provenance can be recorded as "the Bol'shoy Lyakhovsky Island" only.

Table 5-7 summarizes the present taxonomic composition of the collection. The 1999 collection, by its size and taxonomic composition is comparable with the 1886 collection by A. Bunge. The latter, however, as reconstructed from Cherskiy (1891), had abnormally low percentage of mammoth bones (1.7%) and very high number of hare bones (17.6%), with reindeer bones dominating the sample (39%). That looks like possible collecting biases. From that point, our collection seems more adequately corresponding to the other Late Pleistocene local faunas. It is dominated by mammoth and horse fossils (25.1% and 24.7% respectively), followed by bison (19.5%) and reindeer (18%). Unusually high is the number of muskox fossils (7.2%). Hare bones are only 2.3%. Woolly rhino, carnivores (panther and wolf), and saiga antelope each are less than 1% of the whole collection. It should be noted that these calculations are based on the preliminary identification only, and may have undergone some minor changes in the course of the detailed study of this huge collection. In particular, we have not yet found bones of red deer (*Cervus elaphus*), known from the 1896 collection; identification of *Praeovibos sp.* (an Early Pleistocene muskox) is still to be confirmed, and if so, it would be a very important novelty. There are some other interesting features of this collection (e.g., very large size of panther and most bison bones), but this is a matter of more detailed morphological studies.

Table 5-7: Preliminary list of vertebrate taxa identified in the Bol'shoy Lyakhovsky collection*.

Class AVES - birds**
- Order Anseriformes
  - *Clangula hyemalis* L. (moryanka)

Class MAMMALIA- mammals
- Order Lagomorpha
  - *Lepus sp.* (hare)
  - *Lepus tanaiticus Gur.* (Pleistocene hare)
- Order Rodentia
  - Microtinae gen. (Voles and lemmings)
- Order Carnivora
  - Family Canidae
    - *Alopex lagopus* (L.) (Arctic fox)
    - *Canis sp.* (wolf and dog?)
    - *Canis lupus* L. (wolf)
  - Family Felidae
    - *Panthera spelaea* (Gold.) (Pleistocene "lion")
- Order Proboscidea
  - *Mammuthus primigenius* (Blum.) (woolly mammoth)
- Order Perissodactyla
  - Family Rhinoceratidae
    - *Coelodonta antiquitatis* (Blum.) (woolly rhinoceros)
  - Family Equidae
    - *Equus sp.* (horse)
    - *Equus caballus* L. (small Late Pleistocene horse)
- Order Artiodactyla
  - Family Cervidae
    - *Rangifer tarandus* (L.) (reindeer)
  - Family Bovidae
    - *Saiga tatarica* L. (saiga antelope)
    - *Praeovibos sp.* (extinct muskox)
    - *Ovibos moschatus* Zimm. (muskox)
    - *Bison priscus* (Boj.) (Pleistocene bison)
- Mammalia gen.***

* Identification of large mammal bones from this collection was made with the help of Andrei Sher.

** Birds identified by A. Karkhu (Paleontological Institute RAS, Moscow).

*** Mammalia gen. - non identifiable fragments of bones of large mammals.

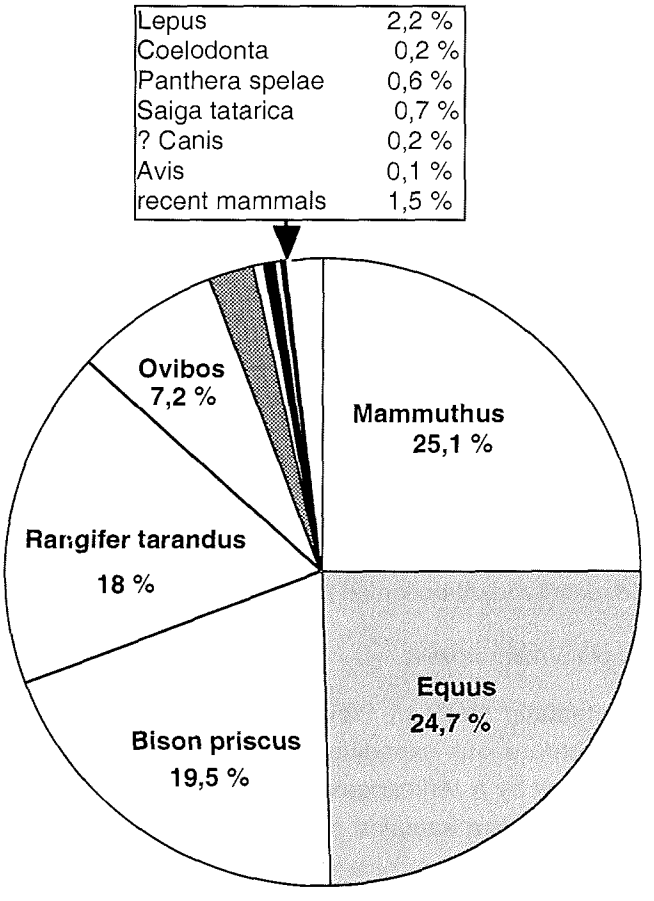

Figure 5-14: Composition of mammal bones collection from Bol'shoy Lyakhovsky Island, 1999, total number: 1032 specimens.

An interesting and rather rare find was a partial skeleton of bison in natural articulation; several bones had some soft tissues preserved (ligaments) and bone marrow inside them. At the site of the earlier find of partial skin and leg of mammoth (Zimov'e River floodplain) we collected fragments of soft tissues and hair, which have been forwarded to the Institute of Zoology and Wildlife Research (Berlin) for further study.

Some of especially large mammoth limb bones and tusks were studied (measured) in the field, photographed, and then the samples for conventional ^{14}C dating were cut out of them. In Moscow, we selected 80 bone samples from

the whole collection and sent them to the Radiocarbon Laboratory of the Geological Institute RAS. There are only a few ^{14}C dates on mammal bones available from the whole Novosibirsk Archipelago, so the dating of our collection is very important to determine the time of occurrence of certain mammal species on the islands.

Small mammal fossils

Because of limited time, the search and screening for small mammal fossils has been carried out in the lowermost ("Olyorian") part of the section. Six samples, 50 to 80 kg each, were screened from 4 sites in this member (Figures A5-2 to A5-2-3; Table A5-8). As this member is very poorly exposed and frozen, and the thawing was very slow, we were not able to take more samples. The screening was performed by the hand sieve with 1 mm mesh, and with water supply by a motor pump in a special screening box (constructed by A. Sher), also with 1 mm mesh. For the reference collection, we screened one sample (BL-O-1001-L) from the beach, quite rich for small mammal bones, skull fragments, and teeth, and also collected recent rodent bones on the island.

Fossil insects and plant macrofossils

There was no systematic study of Pleistocene fossil insects on Bol'shoy Lyakhovsky Island before our expedition, except three isolated samples, collected in different time by A. Arkhangelov and V. Kunitsky and studied by S. Kiselyov (manuscript). Those samples contained a rather small number of fossils, and gave only a very approximate idea on the insect fauna composition.

We sampled all the accessible horizons of the section, giving preference to the facies, most potential for preservation of insect fossils in sufficient quantities. Usually these fossils are most abundant in fine-grained sands and silts, enriched with plant detritus. If the plant organic is represented mostly by thread-like roots, these sediments usually contain few insect fossils. The latter are not found in heavily decomposed peat and pure moss autochthonous peat, but can be abundant at the base and top of the peat layer. Relatively rich insect assemblages can come from slightly decomposed allochthonous peat, in the sediments with alternating thin layers of organic (peat) and mineral composition. Sometimes insect fossils are very abundant in coarser facies, such as coarse-grained sand and gravel rich with plant detritus, but in these cases the species composition of the assemblage can be misrepresented because of the enrichment of the sample with the most resistant larger elements of the insect

skeleton. Most Pleistocene insect fossils are represented by beetles (Coleoptera).

Different members of the studied section on Bol'shoy Lyakhovsky Island are not equally characterized by insect fossils. Large and representative fossil assemblages have been obtained from the "Krest-Yuryakh" member and from the Holocene deposits. Fossil assemblages from the "Olyorian" member are less rich, and from the "Kuchchuguy" and "Yedoma" members - even smaller.

The sample size for insect fossils varies from 10-20 kg for the sediments, rich with plant detritus (and usually containing abundant insect fossils), to 100 kg for those containing few plant detritus; on the average, the amount of screened sediment was 40-50 kg. Since the technical problem of extracting frozen sediment from the exposure has not been solved since 1998 (Siegert et al. 1999), we had to sample only a thin, freshly thawed cover of the sediment, still remaining in its original position. To obtain such a large volume of thawed matrix, we had to take each sample from a strip up to 0.4 m high and up to 2 m long (along the strike of the sediment layer). All the samples were screened with a hand sieve with 0.5 mm mesh.

In the practice of the Russian paleoecological studies, the samples for plant macrofossils are most commonly obtained by the screening, similar to the described above, and have similar volume. In 1999, however, we used a different method, suggested by our German colleagues. Samples of up to 0.5 kg were taken every 30 cm along the vertical profile, and no screening was used in the field. One or two carpological samples were always taken from the same layer, where an insect sample was taken from, and then upward and downward from it with 30 cm intervals. This difference in methods should be taken into account when comparing the future results with the previously obtained paleocarpological evidence from the Russian Arctic.

Both insect screening residual and the carpological samples were taken in fabric bags to facilitate the necessary sample drying.

In total, 25 samples for insect fossils were screened from the Bol'shoy Lyakhovsky Island sections, and 67 carpological samples taken (Table A5-8). From the lower member ("Olyorian") only one sample was screened and one carpological sample taken (Figures A5-2 to A5-2-3; Table A5-8), but some insect fossils will be also obtained from 6 samples that were screened for small mammals (sieve 1.0 mm), with special precautions to provide the preservation of insect remains.

The next member ("subaerial Kuchchuguy") was sampled at three sites (Figures A5-2 to A5-2-3; Table A5-8) totally 5 insect and 25 carpological samples. The first site was at the bottom of the "Kuchchuguy", immediately above the boundary with the "Olyorian" (Figure 5-15a). At the second site (R-6+70 m, the Third creek, or Volodya's burrow), the lower and middle parts of this member were sampled (Figure 5-15b). At the third site, the upper part of the "Kuchchuguy" was sampled (Figure 5-15c), beneath its contact with the "Yedoma", in the thermo-erosional cirque II. Three insect and 6 carpological samples were taken from the "subaquatic Kuchchuguy". All the sections studied are in the coastal cliffs, both on the L and the R sides.

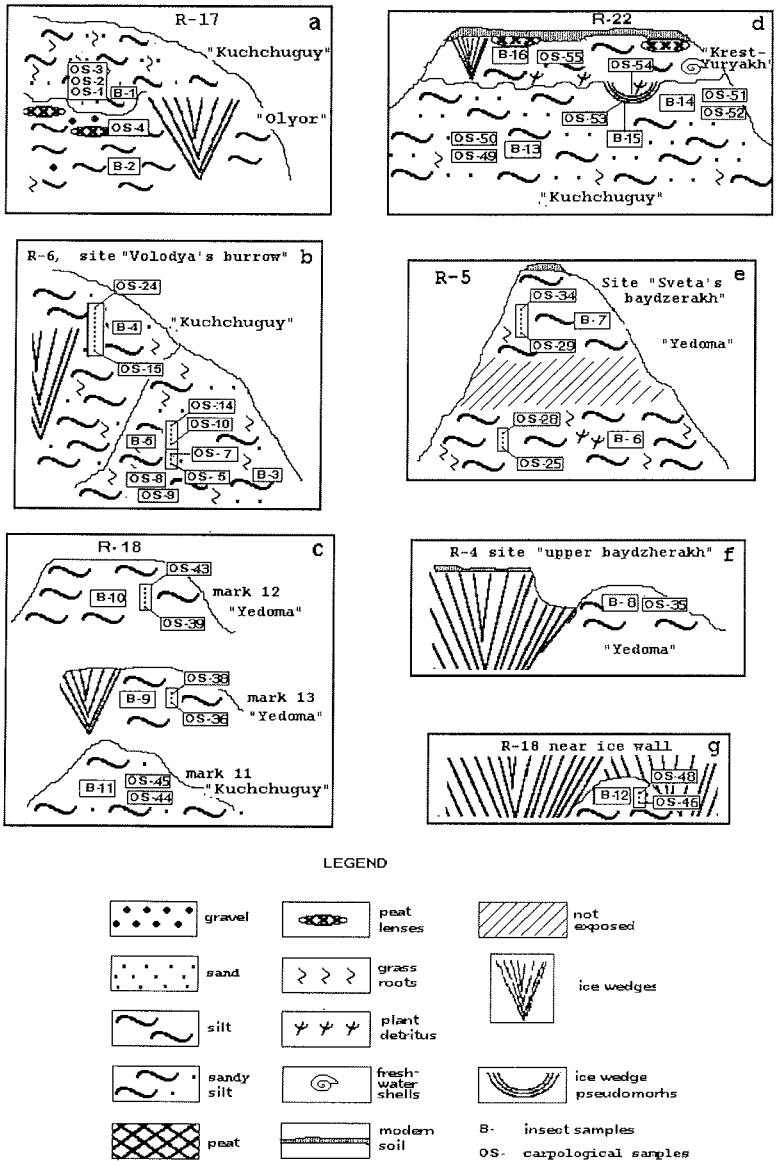

Figure 5-15: (a-g) Fossil insect and carpological sampling sites at the right side (R) from the camp (west of the Zimov´e River mouth).

The "Krest-Yuryakh" deposits overlie the "subaquatic Kuchchuguy" with a sharp unconformity. From the "Krest-Yuryakh" member, 4 insect and 7 carpological samples were taken (Figures 5-15d, 5-16d). The upper Ice Complex (the "Yedoma Suite") has been sampled insufficiently, because its sections were hardly accessible. In total, 6 insect and 22 carpological samples have been collected from the sections on the L side. From the Holocene alas deposits (side L), 3 insect and 3 carpological samples were taken (Figure 5-16b). Fluvial sediments of the Holocene age were sampled in the section of the low terrace of the Zimov´e River near the camp (Figure 5-16c) - 3 insect and 3 carpological samples.

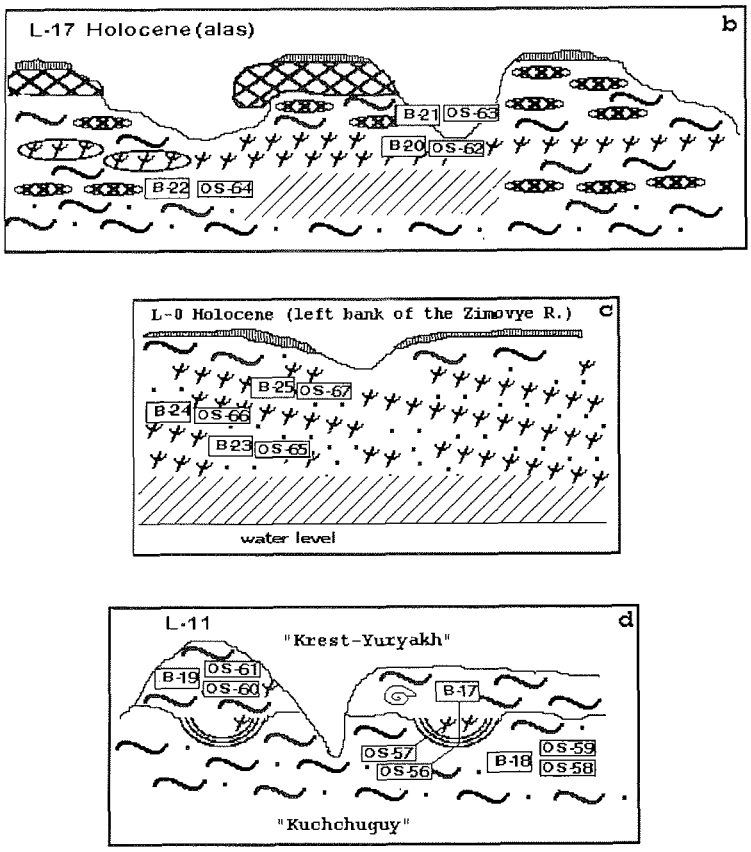

Figure 5-16: (b-d) Fossil insect and carpological sampling sites at the left side (L) from the camp (west of the Zimov´e River mouth).

The modern insect fauna of Novosibirsk Islands is very poorly known (the last extensive collection was obtained by the Bunge Expedition in 1896), so modern beetles were also collected in 1999. This collection is necessary for comparison with the fossil species, but also has an independent importance. It includes water tigers *Agabus nigripalpis* Shlb. (59 specimens), a catopid beetle *Cryocatops poppiusi* Jeann. (1), staphylin beetles *Tachinus arcticus* Motsch. (109), leaf beetles *Chrysolina* (67), including such rare species as *C. wollosowiczi* Tcbs. and *C.bungei* Tbst., ground beetles *Pterostichus agonus* Horn. (1), *Curtonotus alpinus* Pauk (1), *Bembidion sp.* (1), and *Pterostichus (Cryobius) spp* (43 specimens of 2-3 species). A comparative sample of modern plant detritus was taken from the surface of the Zimov´e River left bank. General low species diversity in combination with high numbers of individual species is very typical for the harsh conditions of the High Arctic. It is interesting to note that some beetles, belonging to different families (ground beetles, leaf beetles), demonstrate similar deformations of their chitin (the wrinkling, narrowing of the upper ends of elytra), that is caused by the effect of low temperatures on young beetles at the stage of their transformation from the puparian to imago. Large numbers of fossils with these kinds of deformations can be an indirect evidence of low summer temperature in the past.

Collecting of seeds of modern plants, also for comparative purpose, has been attempted, but only very few plants could be found with ripe seeds before we left the island: *Salix sp., Potentilla sp., Draba sp., Cochlearia sp., Ranunculus sp., Polygonum sp., Saxifraga sp., Sausuria sp.* Some more plants with seeds were also collected during the short stop in Nizhneyansk (*Oxytropus sp., Senecio sp., Artemisia sp., Eriophorum sp.*).

In course of the study and description of the sections, both on the L and the R side, T. Kuznetsova and V. Tumskoy collected 6 peat samples to analyse their botanical composition (Figures A5-2 to A5-2-3, Table A5-9). These samples have been sent for identification to the Botanical Institute RAS.

Fossil molluscs

A few shells and their fragments were determined only as *Pisidium sp.* from this region (Kunitsky, 1998). New samples with great number of Gastropoda and Bivalvia were collected from "Krest-Yuryakh" deposits to analyze taxonomic composition and paleoecological conditions of their inhabitation (Table A5-10).

5.1.10 Recent and fossil soils of the south coast of Bol'shoy Lyakhovsky Island

(I. Akhmadeeva)

During the 1999 expedition soils of the southern coast of the Bol'shoy Lyakhovsky Island, district of the mouth of Zimov'e river were studied. The topographic map 1:25.000 was used as cartographic basis. During this study 93 descriptions of soil pits and 3 descriptions of geologic profiles were made, in one which of the tracks of ancient soils were detected. Soil pits were produced by the generally accepted methods. 103 samples for carrying out a standard set of chemical analysis in soil-analytical lab of Yakutsk were taken from pits and denudations and 69 samples are going to be processed in Germany. The position of several pits are shown in Figure 5-17. A soil map of a scale 1:10.000 is in preparation. Except for soil research, on each pit the geobotanical descriptions were fulfilled. The herbarium is assembled and contain 66 species of plants. One of them is new for the Arctic islands. For classifying soils we used the classification of Yelovskaya (1987).

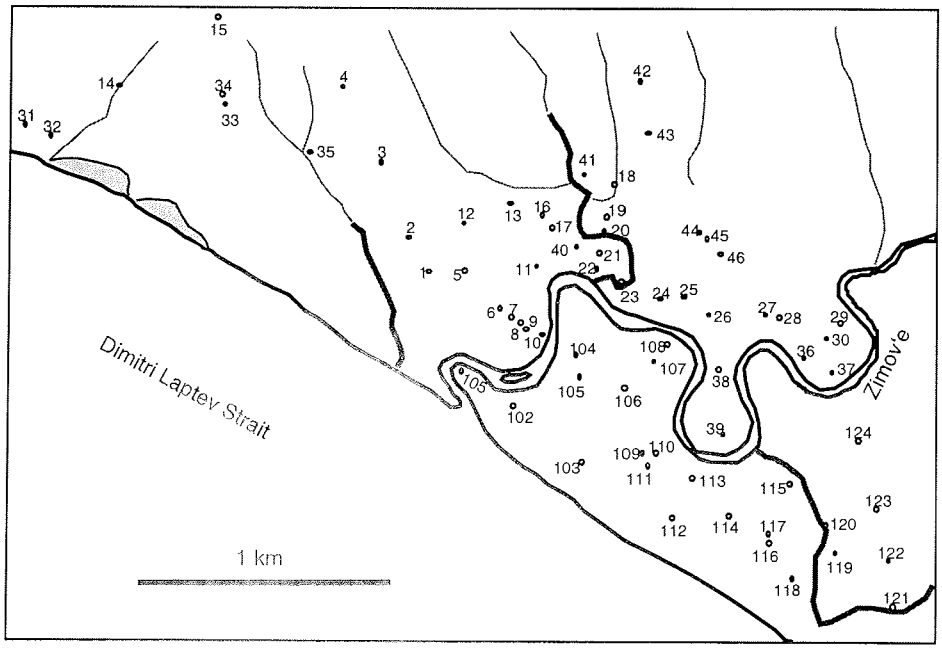

Figure 5-17: Position of soil pits.

The mapped area covers the river flat of Zimov'e from its mouth up to 3.5 km upstream and adjoining non-flood-plain territories representing slope-undulating ovals with hollows between them. The river worked out a channel and has derivated flood plains on the bottoms of the alas system. All soils, including alluvial, are cryoturbated in different degrees . Classification and characteristics of soil-subtypes of the studied area is given below and in appendix A5-12.

Section: Poorly developed, primitive; Order: Primitive alluvial.
Type: Permafrost alluvial layered poorly developed (primitive) soil

This type occupies completely the first terrace and partially also the second terrace, especially closer to marine coast. On granulometrical composition it is difficult to refer them to the particular type, as the stratified strata in pits with alternation of mudded loamy, sandy and peated stratums is usually uncovered. This type of soils melts deeper than all the others, because it is not protected by vegetation.

Section: Alluvial; Order: Purely alluvial;
Type: Permafrost alluvial sod soils

This type occupies terrace 2, which is flooded not every year and where there are conditions for derivation almost of continuous plant cover. The type is represented by a subtype „Permafrost alluvial sod-gley".

The type „Permafrost alluvial peat- soils" occupies all swamps on the river flat. These swamps are widely distributed on the river flat and their expansion is comparable with the length of a nowadays channel of the river. The depth of thaw changes from 23 up to 30 cm. The thickness of peat horizon ranges from 17 to 24 cm, therefore, according to the classification of Yelovskaya (1987), the soil of these swamps belong to two subtypes: „Permafrost alluvial muddy-peaty-gley" (at a thickness of peat from 8 up to 20 cm) and „Permafrost alluvial muddy-peat-gley" (peat horizon is 20-50 cm). However, in this case this division appears formal, as all of the soils of this type are shaped here in similar conditions, and the dispersion in thickness of peat is very insignificant, only 7 cm. The mudding of peat increases with depth, the peat is spread also by strongly mudded grey gleyic horizons containing clusters of peat and plant remains.

The relief strongly influences the formation of non-river-flat soils of this district, especially the micro- and the nanorelief. Soils of the section „Gley", order „Humus-gley" are formed under conditions of constant or, anyway of durably strong humification on the negative forms of the relief (depressions between baydzharakhs and hillocks, hollows). The profile of these hydromorphic soils

looks like the profile of „Permafrost alluvial peat-gley", also formed in conditions of strong humification. However, there is also one essential difference. Soil of river-flat swamps exists in rather quiet conditions, almost without input of particles from outside. The natural arrangement of peat horizon on gleyic soils was observed within the profiles. We observed diversities in gley soils. The hollows with steep sides gain permanently material from steep inclines, especially during spring snow melt. Therefore the profile represents alternation of more or less peaty muddy stratums. The upper horizon is conventional muddy peat. The depth of thaw varies from 27 up to 45 cm. Soils of depressions between baydzharakhs differ from soils of hollows a little by the greater regulation. Soils of one subtype „Permafrost peatish-gley" which is included in the type „Permafrost peat-gley" are mapped in the study area.

The largest square in the research area is covered by soil of the section „Permafrost cryoturbated", divided into two orders depending on the intensity of cryoturbations. These are „Permafrost cryoturbated with destructive profile", with the completely destroyed profile, and „Permafrost cryoturbated with distorted profile", with broken positions of soil horizons, isolated in the profile.

The order „Permafrost cryoturbated with destructive profile" includes only the type „Permafrost effused". These soils of mud circles (pyatny medallion) of the spotted tundra are not distinguished in different genetic horizons. The profile is homogeneous in colour and granulometrical composition (loamy sand or loam). Sometimes gleying is observed at the bottom of the profile.

Some types of soils concern the order „Permafrost cryoturbated distorted". The classification of them is difficult, is mixed and needs further development.

During work on Bol'shoy Lyakhovsky Island also fossil soils were studied. A small amount of buried humus were found in some outcrop profiles (Appendix A5-12).

5.1.11 Trip to Khaptagai Tas hills - study of recent snow patch phenomena

(V. Kunitsky, L. Schirrmeister, G. Grosse)

Satellite pictures of the Khaptagai Tas hills SE of Bol'shoy Lyakhovsky Island show a continuous occurrence of snow patches over some years until August. In order to study the area of these snow patches, a three days trip took place from August 22 to 24. However, this year there were no snow patches at all on Khaptagai Tas hills. Anyway, it was possible to study the specific periglacial geomorphologic structures, the zonality of deposits in the snow patch area and surface and sediment phenomena in the whole snow patch location.

The entire study area is located between the coast of the Dimitry Laptev Strait in the south, the Khaptagai Tas hills in the north and between the river Vankina in the west and the Dymnaya river in the east. In a distance of about 15 km from the sea the country surface gradually rises to the hills of 200 m a.s.l.. Surface structures are dominated by a net of thermo-erosional valleys (log) and separate gullies or ravines (ovrag) and different small thermokarst forms (Figure 5-18).

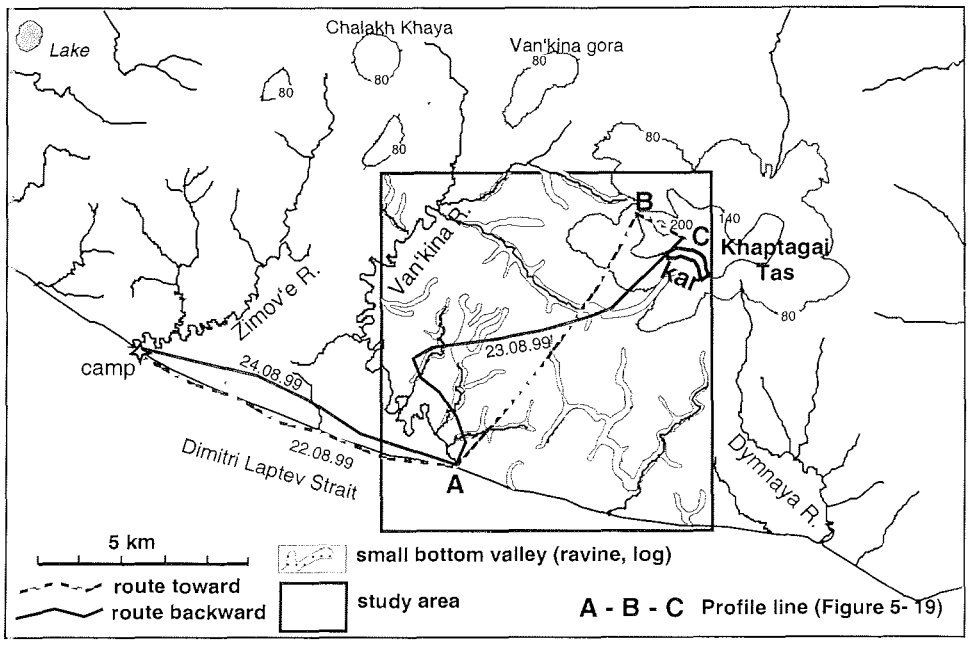

Figure 5-18: Schematic geomorphologic map of the study area of Khaptagai Tas hills characterized by thermo-erosional landscape and cryoplanation terraces

The slopes of the Khaptagai Tas hills are superimposed by cryoplanation terraces. The hills are covered by meter sized granite blocks, which get rare towards the feet of the slopes. Pebbles of sandstones and slates were found in larger distances in fluvial deposits. The Khaptagai Tas hills are part of a mesozoic granite intruding Permian sandstones and slates. Large kar-like formations with features of repeated snow patch positions occur in sites where the snow patches were located on the northern and southern slopes.

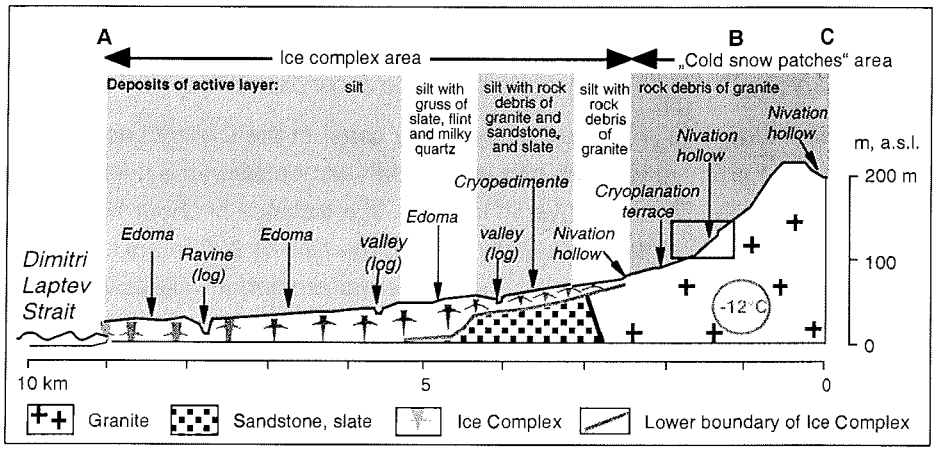

Figure 5-19: Schematic profile of geocryological and geomorphological elements of Khaptagai Tas hills (in frame details of the snow patch area, Figure 5-20)

A gradual enlargement of surface sediments are visible when approaching the hills. The surface material of larger distances consists of loamy, silty fine sand without any small stones or gravels. But near the hills the frequency and size of stones in the dominated fine grained silty material increase gradually. Most of the granite blocks are covered by black lichens. Only stones on the snow patch locations show a light grey colour without any black lichens. Many wet sediment patches occur between the granite. They are settled by various plants and contain a lot of fine roots. This sediment looks like the fine grained rooted silty material of the Late Pleistocene Ice Complexes.

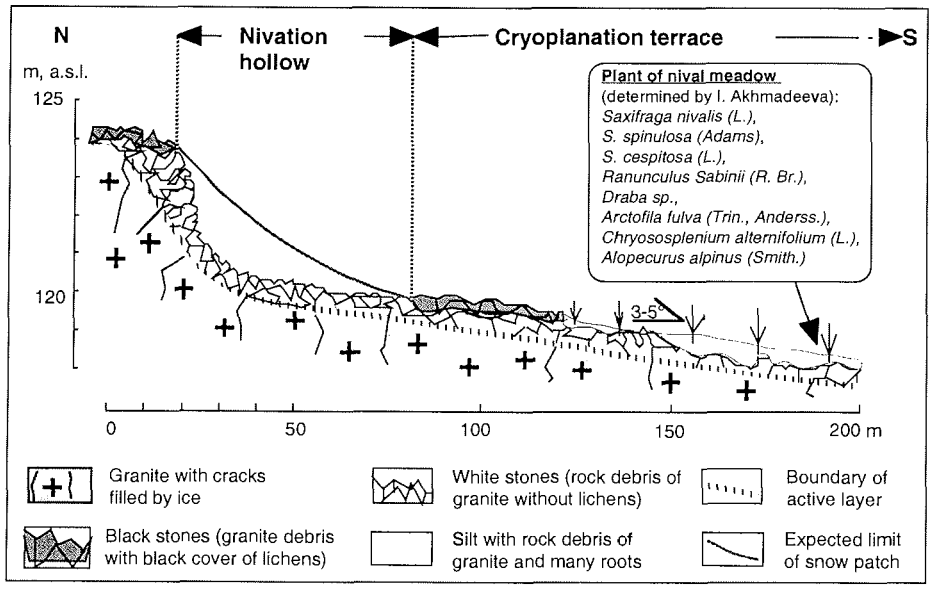

Figure 5-20: Schematic profile of a part of the snow patch area

Corresponding satellite pictures and photos of landscape, parts of Khaptagai Tas hills are considered as areas of regularly developed single forms of embryonic glaciation and they belong to the type of „cold" snow patches. The other part of the hills belongs to the area of Ice Complex. Their boundary generally runs along the 80 m-isohypse of the south slope.

Nival kars and niches (nivation hollows) are traces of snow patches. Areas of nival niches of former snow patch positions are well identified by fields of „white stones" (Figure 5-20). The bottom of a nival niche usually changes down the slope to less inclined places of the cryoplanation terrace with nival meadows. Therefore, a meadow vegetation grows in freshly accumulated silt patches in these areas. Tundra vegetation covers the distal part of the cryoplanation terrace and also the cryopediment which is followed downward to the study area.

The cryopediment of Khaptagai Tas hills between 80 and 60 m a.s.l. becomes complicated by thermokarst mounds and belongs to the Ice Complex area (Edoma). The active layer of the cryopediment consists of silt (alevrite) with granite debris. The active layer contains less debris with increasing distance to the snow patch positions down the slope and besides of granite debris of sandstones and slates occurs.

The Ice Complex area comprises not only the cryopediment but also a less inclined plain with polygonal patterns trenched by ravines. The altitude of this plain gradually decreases towards Dimitri Laptev Street. At the boundary to the cryopediment the active layer of Edoma consists of silt (alevrite) with single inclusions of gruss (flint, hornfels and milky quartz). But close to the sea the active layer consists only of silt, exposed in mud circles and thermokarst mounds (Figure 5-19).

The special feature composition and fabric of the upper horizons of the cryolithozone along the studied profile permits to consider the important role of nivation and cryoplanation processes for the formation of Ice Complex deposits at the south slope of Khaptagai-Tas hills. Snow patches are possibly more important for the genesis of Quaternary ice-rich permafrost deposits of Northern Siberia than presumed until now. A number of geocryological phenomena described in the Ice Complex and the underlain older Quaternary deposits are found again in the area of snow patches of Khaptagai Tas hills.

5.2 Ice Complex on Bykovsky Peninsula

(A. Sher, I. Parmuzin and A. Bortsov)

5.2.1 Research aims

In 1998, the Russian-German team led by Drs. C.Siegert and V.Kunitsky conducted a very interesting and successful field research on the Bykovsky Peninsula, mainly on the famous Ice Complex site Mamontovy Khayata. That research, aimed at the multidisciplinary study of a long succession of Ice Complex, resulted in an unparalleled collection of geological, sedimentological, geocryological, paleoecological, and paleontological data, which should provide a detailed analysis of paleoclimatic signals from ice-rich permafrost during the last 50-60 thousand years (Siegert et al., 1999). A thorough chronological control was insured by a unique number of samples for ^{14}C dating, both of microscopic plant organic for AMS, and mammal bone and bulk peat samples for conventional dating.

The sampling, most detailed in the middle part of this almost 40-m high cliff (between about 9 and 24 m a.s.l.), was, however, rather sparse at the foot of the cliff (covered by slope sediments) and in its upper part, which was hardly accessible in the summer of 1998, as a steep frozen wall being actively destroyed. The team managed to collect some samples near the top line of the cliff, but a vertical gap about 10 m (24-34 m a.s.l.) remained undated, and the interval between 27 and 33 m a.s.l. could not be studied at all. That manifested in the AMS date succession obtained, which revealed a time gap of about 12-15 ka, corresponding to the most of the last "glacial" (Sartanian) (Schirrmeister et al., submitted). Since this gap roughly corresponded to the unsampled interval of the existing sediment, it was evidently caused by the sampling bias, but not by the break in sedimentation.

To fill that gap, a small additional team was organized in the Lena Delta 99 Expedition (Team 5, Bykovsky), which included the three authors of this report chapter. Initially, the field team was organized by the Severtsov Institute of Ecology and Evolution RAS, to fulfil the tasks of the RFBR project 98-04-48084 "Evolution of continental arctic biota at the borderlands of north-eastern Asia (shelf land of the Laptev and East Siberian Seas)" and the related (additional) expedition grant RFBR 99-04-63067. However, those grants were quite small, and our field work would not be possible without the financial and logistic support of the Russian-German Lena Delta 99 Expedition.

5.2.2 Site survey and geomorphologic observations

The team was based on the same camp spot as in 1998, so there is no need to repeat here the general site descriptions, maps and profiles published in the 98' report (Siegert et al., 1999). In accordance with the original goal, the team work was concentrated in the upper third of the cliff, which was being actively destroyed by thermal denudation. Precise correlation with the 98' landmarks and sampling sites was absolutely necessary, but unfortunately no old landmarks were found preserved on the top line of the cliff. Only one marked stick was found in mud not very far down from its original position (RP 5.5), while the few others - quite far down in the mud flows. Some 98' sampling marks preserved on tops of baydzherakhs were useful (B1, R8, B15), but that did not solve the whole problem of correlation. Additional sampling could not be started without a new theodolite survey of the cliff. The new survey covered the SE side of the alas (from the Camp Creek to the foot of the yedoma), the NW slope of the Mamontovy Khayata (MKh) yedoma hill, its top, and the upper part of its SE slope. Another theodolite line was laid off along the beach, to make correction for the distances measured.

The results of the survey were quite satisfactory, and showed a good correlation with the 98' survey results, for instance, in the maximum height of the MKh yedoma hill, in the position and altitude of some inactive baydzherakhs, etc. By the "MKh yedoma hill" we mean the NW part of the Mamontovy Khayata, between the camp alas and the first erosional valley to the south-east; here, at the distance between ca 300 and 1000 m from the camp, the studies were concentrated both in 98' and in 99'. On the other hand, the survey revealed some interesting topographic features, confirmed by further observations, and important for the site geomorphology (Figure 5-21).

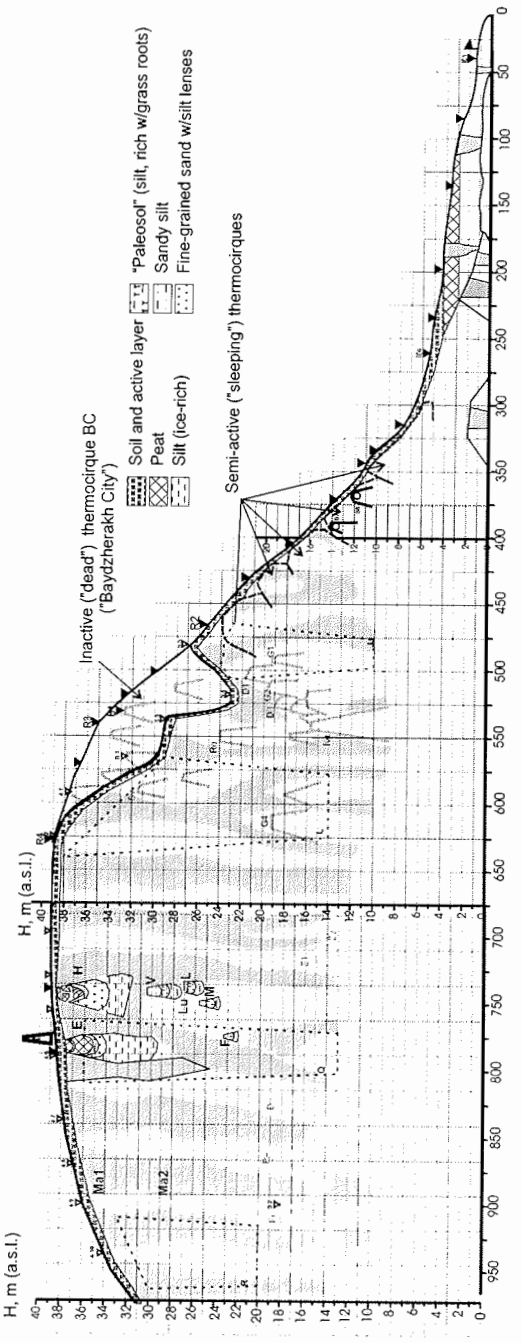

Figure 5-21: Central and NW sectors of the Mamontovy Khayata Exposure, according to 1999 instrumental survey, with the position of the main study sites. Combined results of 1998 and 1999 field seasons

The MKh yedoma hill has a flat, essentially horizontal top part, which is about 100-150 m wide (in NW-SE direction) and positioned at about 39 m a.s.l. The only morphological features of this flat top, except normal polygonal, are very shallow elongated grooves near the cliff edge, corresponding to the large ice wedges of the Ice Complex beneath the soil. On the NW side (facing the camp alas), the surface of the hill gently descends to the alas surface. The WNW slope of the MKh hill (towards the alas) is somewhat steeper in the middle part (8 to 34 m a.s.l.) and more gentle in the upper part (34-39 m) and at its foot (6-8 m), where the slope denudation products accumulate and creep over the alas surface. This slope shows no additional erosional forms on its surface. In the upper part of the NW flank of the MKh hill a large ancient thermocirque can be observed (between the 98' landmarks 5.5 and 4.2). The cirque is totally inactive and covered with lash herbs. A few inactive baydzherakhs 2-3 m high tower above the cirque floor, each fixed by herbaceous vegetation, more stable than that on the baydzherakhs within the active cliff. This dead thermocirque (labelled as the "Baydzherakh City" (BC) was faced almost straight North. From the side of the main cliff, the cirque is being intensively destroyed by thermal denudation, and forms very steep frozen walls. The undercut edge of the ancient cirque should not be taken for the top line of the main cliff, as it was pictured in the 98' report (Siegert et al., 1999, Figure 5-9 b,c).

We dwell at length on these newly documented morphological features because of their importance for the interpretation of stratigraphy of the NW flank of the MKh hill. Our survey and observations do not allow to agree with the assumption (Schirrmeister et al., submitted) that some "valley deposits" are present on the top of the Ice Complex at this flank of the MKh hill. Unlike the SE flank, where the runoff valleys are well developed morphologically and confirmed by the corresponding sediment sections, at the NW flank of the MKh hill only superimposed thermocirques can be found. Repeated cycles of thermocircue formation can be easily observed at the present MKh cliff, which has relatively low activity due to an insufficient removal of the denudation products accumulating at the cliff foot (the sand bar blocking the shore, the thermo-terrace protecting effect, etc.). Because of general low activity of the MKh cliff in the recent years, many active thermocirques get covered with a thick layer of frozen mud, and the cirque becomes inactive ("dead"). But from time to time, new thermodenudation centres appear near the "dead" cirque, and the latter becomes either involved in the active denudation process again (rejuvenate), or undercut by a new active cirque. In both cases, newly emerging baydzherakhs (no matter if they inherited the old ones, or cut out anew) may include in their upper part the remnants of the old frozen mud formed during the

previous denudation cycle. It is very important to distinguish between the original baydzherakh core (presenting the sediment in undisturbed position) and the top part, which includes the mixture of all kinds of material, transported by mud flows from the upper levels. As we could observe, this top part is often frozen, and looks quite similar to the main baidzherakh's core.

The survey has also provided a more detailed picture of the alas topography. The geodesic profile from the camp to the foot of the MKh hill revealed the following elements in the alas surface (cf. Figure 5-21):

1. the lowest central part (1-2 m a.s.l.), corresponding to the camp creek valley;
2. the main alas surface (3-3.5 m a.s.l.), very slightly sloping from its periphery to the centre;
3. peripheral part (4 m a.s.l.), build by the peat mounds, encircling the alas and corresponding to the thick marginal peat outcrop in the cliff;
4. the marginal part (4-6 m a.s.l.), transitional to the yedoma slope, were the yedoma denudation products creep over the alas surface.

5.2.3 Sampling sites

In summer 1999, the weather conditions kept the MKh cliff in a moderate activity. The most evident was the thawing out of the ice wedges immediately beneath the upper edge of the active exposure. The blocks of the surface soil (mostly moss sod) or separate hummocks were torn away in great numbers, and slid down the ice. That resulted in the visible retreat of the upper edge above the wide ice wedges, while the baydzherakhs of the uppermost level were destroyed evidently slower. Consequently, in the highest part of the cliff, a series of baydzherakhs developed, that looked like the "capes" of the cliff top line, keeping the upper soil on their top. These capes were still the part of the hill top surface, joining it on the back side, while the three other sides were rather steep and well exposed for 5-6 m down the cliff. These baydzherakhs of the topmost level allowed rather easy descent of the researchers with the minimum safety measures, and presented very suitable sites for the studying the uppermost 5-6 m of the section. In this condition, the top baydzherakhs persisted until they were separated from the main yedoma surface, at least for two weeks, which gave enough time for the section study and sampling. Further down, the steep faces of the baydzherakhs passed to more gentle slope of the exposed icy sediment or to the thawing ice wedges of longitudinal (parallel to the top edge) orientation. In this zone, the products of thermodenudation of the upper layer periodically accumulated as a liquid mud, but they could be cleared, and the original frozen sediment could be reached.

The next level of baydzherakhs down the cliff was found within the interval between 7-9 to 11-12 m from the top. Those did not rise much above the slope in their back part, but had rather steep and actively destroyed sea-side faces 2-3 m high. Further down, two-three levels of baydzherakhs of similar kind could be found separated by bare eroded ice wedges and the mud flows running over them. In 14-16 m from the top of the highest portion of the cliff, accumulation of mud flows was much more extensive, with few scattered baydzherakhs towering over them, usually lacking fresh exposures (weathered).

For the main study profile, we were able to select almost continuous chain of baydzherakhs, starting from a very impressive one of the top level (baydzherakh "H"), and following down to the depth of 17 m through baydzherakhs "V", "L", "M", and "F". The gap in this succession above "V", related to a longitudinal ice wedge exposure, was covered in the neighbouring baydzherakh "E" (Figures 5-22a, 22b). The main profile was positioned in the highest part of the MKh hill, straight above the horizontal landmark of 750 m from the camp creek, and in 30-50 m NW from the navigation signal. It corresponds to the 99' landmark R5, and is supposed to be located between the 98' landmarks RP4.4 and RP4.5.

Additional profile was studied 150 m further SE (cf. Figure 5-22a), where the baby mammoth skull was found (baydzherakhs "Ma1" and "Ma2", approximately corresponding to the 98' landmark RP4.9). According to our survey, the yedoma surface at this point is 36 m a.s.l.

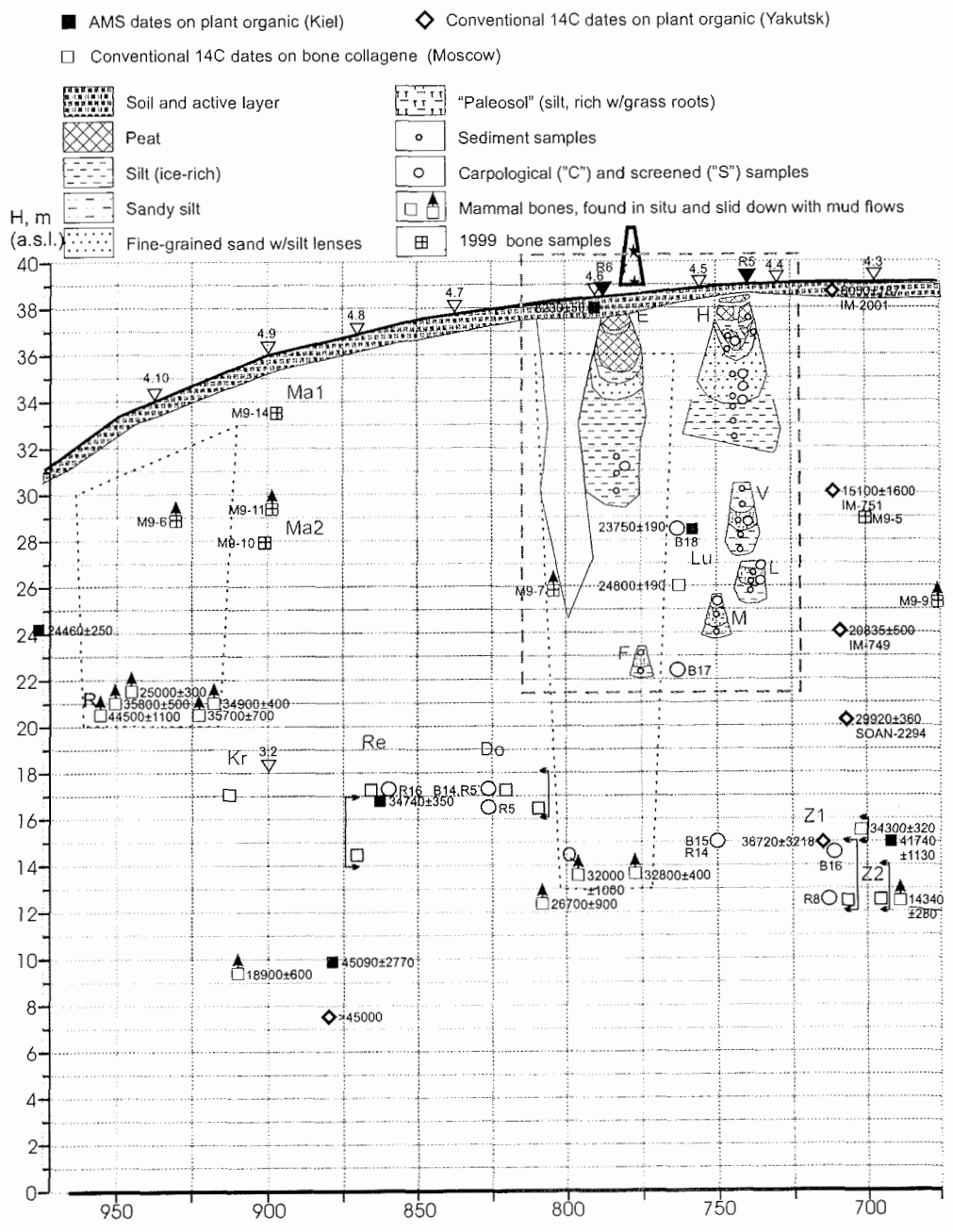

Figure 5-22a: Mamontovy Khayata Exposure, Zone 3 (675-975 m from the Camp). Combined results of 1998 and 1999 field seasons. Dashed rectangle - detailed sampled part (cf. Figure 5-23).

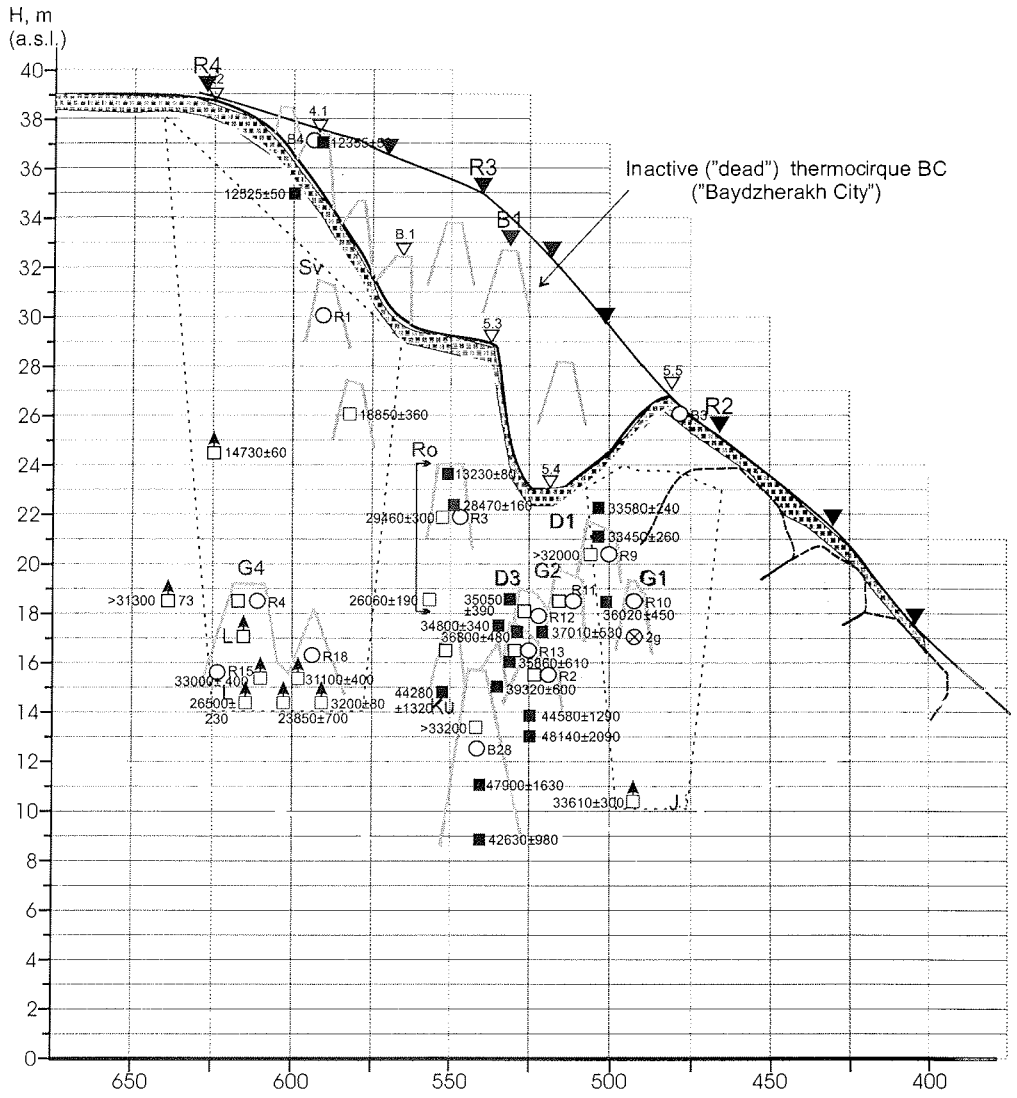

Figure 5-22b: Mamontovy Khayata Exposure, Zone 2 (375-675 m from the Camp). Combined results of 1998 and 1999 field seasons. See legend for Figure 5-22a.

5.2.4 Stratigraphic and sedimentological observations

Several stratigraphic units can be recognized in the upper part of the MKh yedoma hill. Some of them can be traced for 100-200 m along the strike, and for that reason can be considered as the general elements of the yedoma section.

- The top soil layer, overlying Ice Complex and cutting large ice wedges, is usually 0.5-0.7 m thick (Figure 5-23) - altitude ca. 39.2-38.5 m a.s.l. in the main profile.
- The upper "peat layer". The baydzherakhs of the topmost level have the core, highly enriched with poorly decomposed plant remains. Strictly speaking, they do not form a true peat layer, but numerous separated inclusions of peat ("peat hummocks") in the ice-rich silty sediment. They consist mostly of perfectly preserved sphagnum moss and sedges, and are quite likely of the autochthonous origin. In course of the baydzherakh thawing, these plant remains form large hanging fringe, and from the distance they appear to be a continuous peat layer. The sediment, including the "hummocks", is ice-saturated silt, with large inclusions of very pure ice. Since these peat accumulations build the core of the baydzherakhs, occur between the large ice wedges, and have lateral deformations (bent upward along the contact with the ice wedges), they most evidently form a part of Ice Complex, and are not superimposed on it. The thickness of this unit is up to 2.3-3.0 m. (altitude ca. 38.5-36.0 m a.s.l. in the main profile.
- The upper sand layer. The base of the baydzherakhs of the topmost level consists of fine to medium-grained silty sand with vaguely pronounced bedding, possibly with some fine cross-bedding. The sand has massive cryo-structure and relatively low ice content, but the latter increases to the bottom of the unit, where thick (1-2 cm) horizontal ice bands occur. The layer contains relatively few grass roots, but is rather rich for insect and plant macrofossils. The thickness of the sand layer varies from 1 to 2 m - altitude ca. 36.0-34.0 m a.s.l. in the main profile.
- Ice-rich silt. It is exposed between the baydzherakhs of the topmost level and the next level downward, on a gently sloping surface under thermodenudation, locally covered by mud flows from thawing baydzherakhs above it. This sediment contains enormous amount of structure-forming ice (lens-like and reticulated cryostructure), and is rather rich with grass roots and tiny woody sticks (dwarf shrubs ?), though not visible in the section. The thickness of this unit is estimated as up to 4 m (in the main profile it includes a longitudinal ice wedge) - altitude ca. 34.0-30.0 m a.s.l. in the main profile.

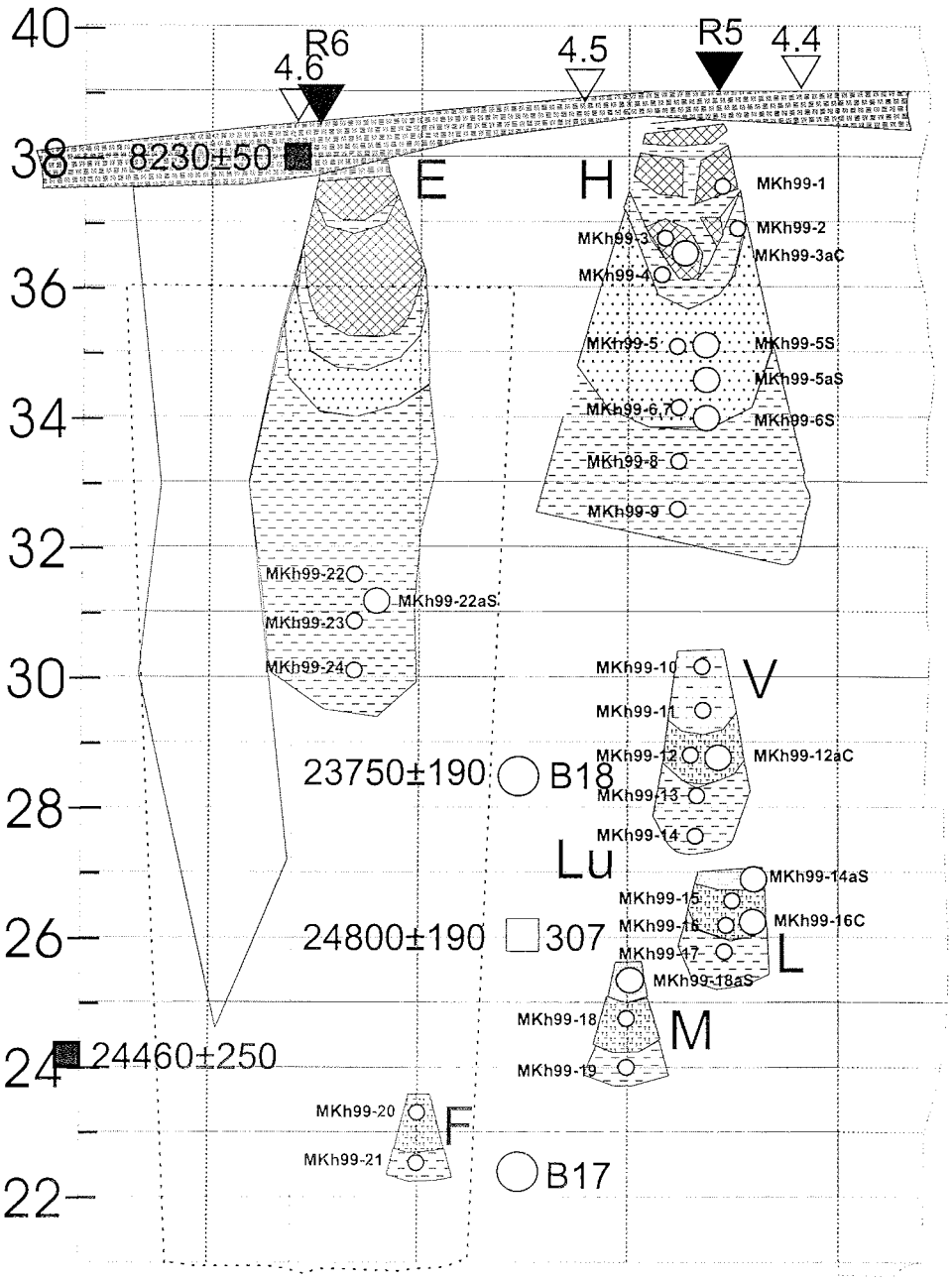

Figure 5-23: Mamontovy Khayata Exposure. The main profile sampled in 1999. See legend for Figure 5-22a.

Further down the section, four more levels of baydzherakhs have essentially similar structure to each other. Their core is presented by a layer of less than 1 m thickness, permeated by numerous grass roots. For some reasons (partly because of their relatively low ice content), these layers support a steeper (almost vertical) slope, actually forming the sea-side exposure of a baydzherakh. It seems that the whole network of baydzherakhs is pre-defined by the occurrence of these layers. Due to the shape of mini-cliffs and their slightly darker color, they can often be traced across several neighboring baydzherakhs of the same altitude. They are always underlain by silt with a very rich ice content (at the foot of each particular baydzherakh and between them in the vertical profile) and overlain by seemingly more sandy layer. The middle layer is especially rich for grass roots, sometimes forming furcating systems (branches); it also includes woody sticks (twigs or roots of dwarf shrubs), usually without any traces of rounding. Woody roots are even more common in the upper sandy layer, but grass roots also present there.

These three units - the lower ice-rich silt, the middle grass root layer, and the upper sandy layer - form a cycle, repeating in each baydzherakh in the studied part of the section. Since our colleagues who made more detailed '98 work at the MKh section concluded that the whole Ice Complex section represents a succession of paleosols, marked by vertical grass roots and shrub remains (Siegert et al., 1999; Schirrmeister et al., submitted), quite arbitrarily, we called the middle layer "paleosol". It should be, however, noted, that the buried soils, described up to the fine details in the middle part of the cliff ('98), seem different from what we could observe in the upper part. For instance, we failed to observe pronounced brown spots, or peat inclusions, or general peaty composition of our "soils" in the interval of 23 to 30 m a.s.l. Neither we observed any cryoturbations, typical for buried soils. Finally, the frequent alteration of soil and mineral horizons, such as described in baydzherakhs KB 2, KB 3, KB 4, KB 6 (13-20 m a.s.l.) (Siegert et al., 1999, Tab. A5-2) is quite different from what we observed in the upper part. A few soil horizons described in the top part of the section in '98 (op. cit.) presumably come from our upper "peat layer". So, it is possible that the buried soils change their character through the MKh section from its middle to the upper part. Hopefully, that can be solved after the analytic work is done through the whole section.

Thus, in the interval 23-30 m a.s.l. we recognized four horizons as possible subaerial surfaces, which we currently label as paleosols "V" (28.5-29.2 m a.s.l.), "L" (26.0-26.7 m), "M" (24.2-25.0 m), and "F" (23.0-23.7 m). It is possible that at least one more soil horizon is present in the interval of 31.0-32.5 m a.s.l.,

poorly exposed in the main profile, but it was not clearly seen in the profile R6 as well.

5.2.5 Cryolithological observations

The whole upper part of the MKh section contains a system of thick ice wedges of a presumably single generation. They have been described many times before, but a few cryolithological features that we observed are worth mentioning. First, it seems possible that the conclusion about the extreme width of the ice wedges in MKh - up to three times wider than the ground columns (Tomirdiaro, 1984) - can be to some extent exaggerated. Such an impression can be partially related to the oblique cross-cuttings of the wedges in the cliff, partially to a sharp widening of the ice wedges in the very top part of the cliff, which is the best exposed and impressive. While the conic or pyramidal shape of the baydzherakhs in the middle part of the cliff seems primarily due to their thermal denudation, the topmost level of the baydzherakhs, as we observed, originally has such a shape. That is due to the fact that in the uppermost 2-3 m of the cliff the ice wedges are really much wider than the ground columns, but at 5-6 m from the top they are already almost equal to each other in their width.

A possible explanation of this fact is that the Pleistocene (yedoma) ice wedges are subjected to the recent epigenetic frost cracking and the formation of younger wedges, entering the older ones from the top. We observed some vertical off-shoots of ice, raising from the middle of a large ice wedge into the top soil up to the bottom of the active layer. It is possible that the corresponding portion of the large wedge is actually represented by a younger generation of ice (some vertical stripes of more white ice were observed). But this phenomenon requires further special study by permafrost experts.

Our observations did not confirm the earlier statement (Tomirdiaro & Chernen'ky, 1987) that the Ice Complex sediments in MKh display strong upward bending at the contacts with ice wedges only in the lower part of the section, while in the upper these deformations are much less pronounced, to which these authors attach important genetic meaning. Throughout the whole upper part of the section studied by us, lateral deformations in the ground blocks are extremely strong. They are most clearly outlined by a layer of silt with very high ice content and fine lens-like cryogenic structure, occurred in the basal parts of most baydzherakh sections. In the lateral zones of the ground column this layer bends up along the contact with the ice wedge for up to one meter or more, acquiring almost vertical position.

5.2.6 The sampling methods and the samples collected

In the studied 17-m interval of the section (22 to 39 m a.s.l.) we took 24 basic (sediment) samples (Table A5-13, appendix), from which we separated 24 pollen samples and picked 17 samples of grass roots and twigs for the AMS-dating from them (some more have been picked later in Potsdam). All basic samples were taken from frozen sediment. Also, 10 samples were taken from freshly melted sediments on steep baydzherakhs walls for small mammal remains, insect and plant macrofossils. Almost all samples contained visible insect fossils. As the previous experience showed, even using the sieve of 0.5 mm mesh can result in the loss of some smallest plant and insect fossils. To avoid that, we tried a new method of sample processing. A sample was repeatedly floatated in the bucket, and then the silty suspension with many floating organic remains was poured into fabric bags, slightly squeezed, left to drain and dried. Much of silt particles went out with water through the fabric pores, but hopefully all the smallest fossils were preserved. Although some mineral remained in the sample, with this reservation we labelled these parts of the sample as "light fraction". The heavy fraction, which remained in the bucket, was either processed in the same way (through another fabric bag), or screened through the 0.5 mm sieve. The methods applied to particular samples are listed in Table A5-13.

5.2.7 Mammal bone collecting

In addition to about 600 bones, collected in the MKh area in 1998, we found and identified 300 more bones, about 220 of them have been preserved and transported to Moscow (Table A5-14 and A5-15). As in 1998, most bones were collected on the shore and sand bars. Only 16 bones were found within the exposure itself (there is some information that before our arrival to the site, the bones, recently appeared in the mud flows, have been picked up by a team of illegal bone collectors). Among those few bones, however, there are some important findings, especially wanted in the upper part of the cliff.

In a frozen wall of baydzherakh Ma1 (Station 900 m from the Camp, height 33.5 m a.s.l.) a partial skull of baby mammoth was found. Besides the fact that almost no bones have been found *in situ* in the upper part of the MKh cliff before (and they are very much needed for the dating), this one is actually a very rare paleontological find because of the juvenile age of this mammoth. The specimen is a facial fragment of skull with milk teeth and two still unerupted tusks of the permanent generation, each about 10 cm long. The baby was probably about 1 year old. Also *in situ*, on the other side of the same

baydzherakh another fragment of a baby mammoth skull was found (occipital), which can belong to the same individual. A few meter down from this site, at ca 28 m a.s.l., a humerus of a baby mammoth was found in the mud, that possibly may belong to the same individual.

Another interesting find is a shed antler of a young deer, found in the top soil layer (the first find of an *in situ* bone in this unit). Unfortunately, because of the young individual age, it is hard to decide whether it belongs to reindeer, or to moose, but the bone can be used for the AMS dating, and also is interesting because of its peculiar preservation.

A bone of hare was found in baydzherakh Ma2 (28 m a.s.l.), and a bone of reindeer on the slope of a baydzherakh at Stn. 700 (29 m a.s.l.). Because of their high position in the section, these bones, as well as a few other bones, found in the upper part of the MKh cliff, may be useful for the AMS dating.

The bones collected on the shore and bars almost do not change the 98' mammal species list, with one important exception. For the first time on Bykovsky Peninsula a bone is found that can be older than the Late Pleistocene. This is a fragment of a lower jaw of a very large horse. As far as we know, during the time of deposition of the main Ice Complex (late Middle to Late Pleistocene) horses in this region were represented by small caballine forms. The horses of such a large size like a fragment found were known in the Early and Middle Pleistocene (large caballine forms) and in the Late Pliocene - Early Pleistocene (large plesippine forms, such as *Equus verae* Sher). This find, though rather poor (no teeth preserved, so the exact taxonomic position cannot be solved) and possibly redeposited from the sediments, currently not exposed at this site above the sea level, may confirm the existence of the Middle or even Early Pleistocene sediments in this area (cf. Slagoda, 1991).

5.2.8 Conclusion

A small size of the '99 Bykovsky team (as compared with '98) did not allow to carry out the study of the isotopic composition of fossil ice, and a more detailed research of the geocryological features of various sedimentary facies. But as a whole, the main research tasks were fulfilled, and it is clear that when the analytical studies and other laboratory work are completed, the combined evidence, obtained in 1998 and 1999 will make the Mamontovy Khayata section a unique and most detailed interdisciplinary archive of the Late Pleistocene (Kargin-Sartan) time not only for the Laptev Sea area, but for the whole Siberian Arctic.

5.3 References

Alekseev (1989): Quaternary stratigraphy of the Novosibirsk Island.- In: Yanshin, A.L. (ed.): Quaternary Period.- International Geological Congress, XXVIII Session; Moscow: Nauka, 1989: 159-16 (in Russian).

Alekseev, M.N.; Arkhangelov, A.A.; Ivanonova, N.M.; Patyk-ara, N.G.; Plakht ,I.V.; Sekretov, S.B.; Shkarubo, S.I. (1991): Laptev Sea and East-Sibirian Cenozoic - Atlas of paleogeographic map of Eurasian shelf during the Mesozoic and Cenozoic.- volume 1: Moscow, Inst. of Geology, Russian Academy of Science: 1-20 (In Russian).

Arkhangelov, A. A., Konishev, V. N., Rozenbaum, G. E. (1989): Primorsko-Novosibirsky Region, Regional cryolithology, In: Popov, A. I. (Ed.), Moscow University Press, p. 128-151 (In Russian).

Arkhangelov, A.A., Mikhalev, D.V., Nikolaev, V.I. (1996): Reconstruction of formation conditions of permafrost and climates in Northern Eurasia. In: Razvitie oblasti mnogoletney merzloty i periglyatsial'noy zony Severnoy Evrazii i usloviya rasseleniya drevnego cheloveka., M., 85-109 (In Russian).

Arkhangelov, A.A.; Mikhalev, D.V. & Nikolaev, V.I. (1996): Reconstruction of formation conditions of permafrost and climates in Northern Eurasia.- In: Velichko, A.A., Arkhangelov, A.A., Borisova, O.K. et al. (eds.): History of permafrost regions and periglacial zones of northern Eurasia and conditions of old human settlement; Moscow, Institute of Geography, Russian Academy of Science , 1996: 85-109 (in Russian).

Beer, J., M. Andree, H. Oeschger, B. Stauffer, R. Balzer, G. Bonani, C. Stoller, M. Suter, W. Wolfli, & R. C. Finkel (1985): Be-10 variations in polar ice cores. Greenland Ice Core; Geophysics, Geochemistry and the Environment, 33, p. 66-70.

Cherskiy, I.D. (1891): The description of the collection of post-Tertiary mammals, collected by New Siberian expedition of 1885-86. Zapiski Imper. Akademii Nauk (Prilozhenie k LXV tomu), 65, 1, 1-707 (In Russian).

Drachev,S.S. and Savostin, L.A., (1993): Ophiolites of the Bol`shoi Lyakhov Island (Novosibirsk Islands). Geotektonika, 6: 33-51 (in Russian).

Grechichshev, S.E.; Chistinov L.V., Shur, Yu. L. (1980): Kryogenesis of physico-geological processes and their prognosis.- Moscow: Nedra, 1980: 324 p. (in Russian).

Grinenko, O.V.; Sergeenko, A.I.. Belolubsky I,N. (1998a): Paleogene and Neogene of North-East Russia. Part I.: Regional stratigrafic scheme of Paleogene and Neogene deposits of North-East Russia and Explanatory note.- Publications of Yakutian Centre of Science Siberian Branch, Section of the Russian Academy of Science 1998: 22 p., Yakutsk (in Russian).

Grinenko, O.V.; Sergeenko, A.I.. Belolubsky I,N. (1998b): Paleogene and Neogene of North-East Russia. Part I.: Regional stratigrafic scheme of Paleogene and Neogene deposits of Eastern and Explanatory note.- Publications of Yakutian Centre of Science Siberian Branch, Section of the Russian Academy of Science, 1998: 36 p., Yakutsk (in Russian).

Ivanov (1968):Stratigraphy and correlation of Neogene and Quaternary deposits in the subarctic plain of north-east USSR.- In: Problems of study of Quaternary. III. All-Union conference for Quaternary study (Khabarovsk, 1968), thesis.- Publication of Khabarovsk branch of the Geographic Society of USSR: 70-72 (in Russian).

Ivanov (1970): The fundamental stage of the development of subarctic plain.- In: Northern Ice Sea and his coast during the Cenozoic; Leningrad, Hydrometeorological Publ., 1970: 474-479 (in Russian).

Ivanov, O.A. (1972): Stratigraphy and correlation of Neogene and Quaternary deposits in the subarctic part of East Yakutia.- Problems of study of Quaternary period.- Moscow, Nauka: 202-211 (in Russian).

Katasonov, E.M. (1979): About the terms „thermokarst" and „thermokarst forms of the relief".- In: Structure and absolute geochronology of alas deposits in Central Yakutia. - Nauka, 1979: 4-7 (in Russian).

Krasny, L Y. (1981): Geology of Yakutia ASSR: Nedra: 300 p. Yakutsk (in Russian)

Kravchinsky, V. A., Pek, J., Cakhan H. et al., (1998): Magnetostratigraphic scale of Late Cenozoic of central Asia according to data of deep drilling at Baikal; In: Global changes of nature, Dobrecov, N. L. and Kovalenko V. I. (Eds.), Novosibirsk RAN (In Russian).

Kunitsky, V. V. (1996): Chemical composition of continuous grown ice wedges of the Ice Complex.- In: Cryolithozone anf groundwater of Siberia, part I.: Morphology of the cryolithozone, Publ. of Melnikov Permafrost Institute Yakutsk, Russian Academy of Science, Siberian Branch: 93-117, Yakutsk (in Russian).

Kunitsky, V. V. (1998): The Ice Complex and cryoplanation terraces on Big Lyakhovsky Island,.- In: Kamensky R.M.; Kunitsky, V.V.; Olovin, B.A. & Shepelev, V.V. (eds.): Problems of geocryology (collected paper)., Publ. of Melnikov Permafrost Institute Yakutsk, Russian Academy of Science, Siberian Branch: 60-72, Yakutsk (in Russian).

Kunitsky, V. V. (1999a): Ice complex and hypothesis of the sartan glaciation in Northern Yakutia.- Quaternary Environment of the Eurasien North (QUEEN). Third workshop, Oystese, 16-18 April 1999, abstracts , p. 30.

Kunitsky V. V. (1999b): Study of Ice Complex deposits with methods of monitoring of natural outcrops.- International conference „Monitoring of Cryoshere", Pushchino, 20-23 April 1999, abstracts: 124-125 (in Russian).

Lazarev, P. A. (in press): On the new findings of mammoth remains with soft tissues on Novosibirsk Islands. Proc. Of Paleontological Institute, RAS

Lozhkin, A. V. (1977): Radiocarbon dating of Upper Pleistocene deposits on Novosibirsk islands and age of the Yedoma Suite of Northeast USSR. Doklady AN SSSR, 235, 2, 435-437 (In Russian).

MacKay, J. R. (1983): Oxygen isotopic variation in permafrost, Tuktoyaktuk peninsula area, NWT. Geol. Surv. Can. Pap., B, **18**, p. 67-76.

Meyer, H., Dereviagin A. & Syromyatnikov I. (1999): Ground ice studies. – In: Rachold, V. (Ed.): Expeditions in Siberia in 1998, Reports on Polar Research **315**, p. 155-163

Nagaoka, D. (1994): Properties of Ice Complex deposits in Eastern Siberia. In: Inoue, G. (ed.): Proceedings of the Second Symposium on the Joint Siberian Permafrost Studies between Japan and Russia in 1993, Isebu Tsukuba-Japan, p. 14-18.

Nagaoka, D., Saijo, K., Fukuda, M. (1995): Sedimental environment of the Edoma in high Arctic eastern Siberia. In: Takahashi, K., Osawa, A., and Kanazawa, Y. (eds.): Proceedings of the third Symposium on the Joint Siberian Permafrost Studies between Japan and Russia in 1994, Tsukuba, Japan, p. 8-13.

Neotectonic map (1984): Neotectonic map of SSSR 1: 4.000.000 (in Russian).

Popov, A.I. (1967): Cryolithology. - Moscow University Press, 304 p. (in Russian).

Romanovsky, N.N. (1958a): Permafrost structures in Quaternary deposits.- In: Science College report, Geological-geographical Serie, No. 3; Moscow: 185-189 (in Russian).

Romanovsky, N.N. (1958b): Paleogeographic conditions of formation of the Quaternary deposits on Bol'shoy Lyakhovsky Island (Novosibirsky Islands).- In: Questions of Physical Geography of Polar region: Publications of Moscow State University, 1958: 80-88 (in Russian).

Romanovsky, N.N. (1958c): New data about teh construction of Quaternary deposits on Bol'shoy Lyakhovsky Island (Novosibirsky Islands) .- In: Science College report, Geological-geographical Serie, No. 2; Moscow: 243-248 (in Russian).

Romanovsky, N.N. (1961a): Erosional-thermokarst kettles in the north of the coastal lowland of Yakutia and Novosibirsky Islands.- In: Permafrost studies, issue 1: 124-144 (In Russian).

Romanovsky, N.N. (1961b): About the construction of Yana-Indigirka Coastal Lowland and its forming conditions.- In: Permafrost studies, issue 2: 129-139 (In Russian).

Romanovsky, N.N. (1977) Ice wedges system formation. - Novosibirsk, 216 p. (in Russian).

Schirrmeister, L., Siegert, Ch., Kunitzky, V., Grootes, P., Erlenkeuser, H. (2000): Late Quaternary ice-rich permafrost sequences as an archive for the Laptev Sea Region paleoenvironment. Geologische Rundschau (submitted).

Sher, A.V.; Kaplina, T.N.; Ovander, M.G.; (1987): Unified regional stratigraphic scheme for Quaternary deposits in the Yana-Kolyma Lowland and ita mountain surroundings. (Scheme I). - In: Resolution of the Joint Stratigraphic Conference on Quaternary of the East USSR (Magadan 1982). Note of explanation to the regional stratigraphic diagrams of Quaternary of the East USSR. Magadan, Northeastern Complex Research Institute, Far-Eastern Branch, Siberian Department of the Academy of Sciences of USSR. p. 29-69 (In Russian).

Shumsky, P.A. (1960): About the genesis of ice wedges. - Works of INMERO **26**, p. 81-97 (in Russian).

Siegert, C. & Romanovsky, N.N. (1996): The Late Pleistocene "Ice Complex" – a phenomenon of the non-glaciated areas of Northern Eurasia. QUEEN Workshop, Strasbourg, November 1996.

Siegert, C., et al. (1999): Paleoclimate signals of Ice-rich Permafrost – In: Rachold, V. (Ed.): Expeditions in Siberia in 1998, Reports on Polar Research **315**, p. 145-259.

Slagoda, E.A. (1991): Microstructure features of the deposits of Ice Complexes in Northern Yakutia (by the example of Bykov Peninsula). In: Gilichinskiy D.A., Ed. Kriologiya pochv. Pushchino, IPFS PNTs AN SSSR, 38-47 (In Russian)

Solomatin, V.I. (1974): The structure and genesis of the polygonal ice wedges in the Pleistocene deposits of Northern Yakutia. - In: Popov, A. I. (Ed.): Problems of Cryolithology, Vol. 4, Moscow University Press, p. 7-29. (In Russian).

Telepnev (1981): Subaquatic frozen zone of the coastal part of Bol'shoy Lyakovsky Island.- Kryolithozone of the arctic shelf; C: 44-53; Permafrost Institute Yakutsk, Section of the Russian Academy of Science.

Tomirdiaro, S.V. (1984): Periglacial landscapes and loess accumulation in the Late Pleistocene Arctic and Subarctic. In: A. A. Velichko, H. E. Wright,Jr. and C. W. Barnosky, Eds., Late Quaternary environments of the Soviet Union, London, The University of Minnesota Press, Longman, 1984, 141-146.

Tomirdiaro, S.V. & Chernen'kiy, B.I. (1987): Cryogenic deposits of East Arctic and Subarctic. AN SSSR Far-East Science Centre, 196 p. (in Russian).

Vaikmae, R. (1991): Oxygen-18 in Permafrost Ice.- International Symposium of the Use of Isotope Techniques in Water Resources Development. – International Atomic Energy Agency, Vienna, 11-15 March 1991.

Vangengeim, E.A. (1963): Fauna of Quaternary mammals from the Bol'shoy Lyakhov Island. In: Novosibirskie ostrova. Trudy Arkticheskogo i Antarkticheskogo nauchno-issledovatel'skogo instituta, 224, 73-87 (In Russian).

Yelovskaya (1987): Classification and diagnosis of permafrost soils in Yakutia.- Publ. Yakutian Section of Sibirian Branch of Academy of Science USSR: 172 p. (in Russian).

5.4 Appendix

A5-1: Profile map of sample positions (German version).
A5-1-1: Legend.
A5-1-2: R-section.
A5-1-3: L-section.

A5-2: Profile map (Russian version).
A5-2-1: Schematic profile of permafrost deposits. South coast of Bol´shoy Lyakhovsky Island.
A5-2-2: Bol´shoy Lyakhovsky Island, south coast, R-side exposure.
A5-2-3: Bol´shoy Lyakhovsky Island, south coast, L-side exposure.

A5-3: List of sediment samples collected on Bol´shoy Lyakhovsky Island.
A5-4: List of OSL-samples.
A5-5: List of alas samples.
A5-6: List of water and ice samples collected on Bol´shoy Lyakhovsky island during field season 1999.
A5-7: List of bone samples.
A5-8: List of small fossil samples (rodents, insects, ostracodes, seeds).
A5-9: List of peat samples for botanical analysis.
A5-10: List of mollusc samples.
A5-11: List of samples for paleomagnetics.
A5-12: Description of soil profiles.
A5-13: List of samples collected by the Bykovsky team at the upper part of MKh main section in 1999.
A5-14: The composition of the mammal bone collection (Bykovsky Peninsula, 1999).
A5-15: Mammal bones, found in 1999 within the Mamontova Khayata cliff (Bykovsky Peninsula).

A5-1: Profile map of sample positions (German version).
A5-1-1: Legend.

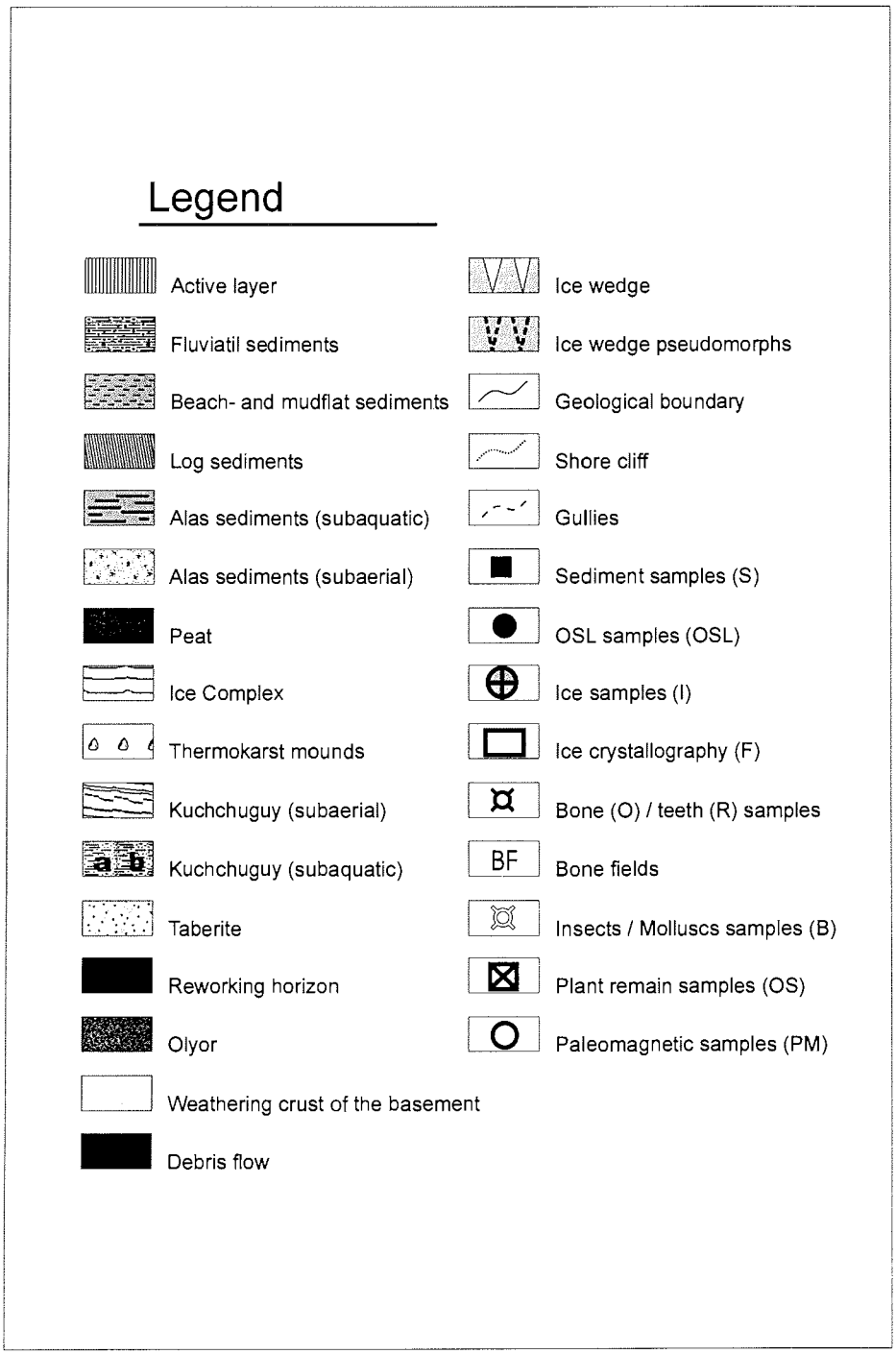

A5-1: Profile map of sample positions (German version).

A5-1-2: R-section

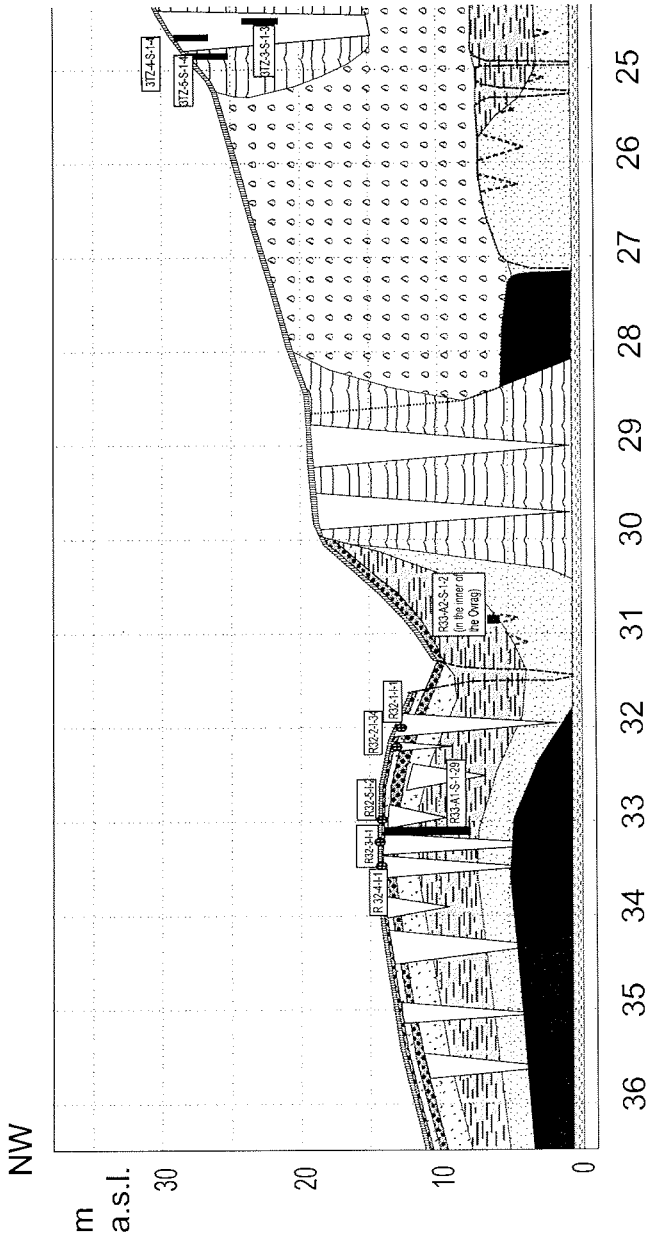

A5-1-2: continuation.

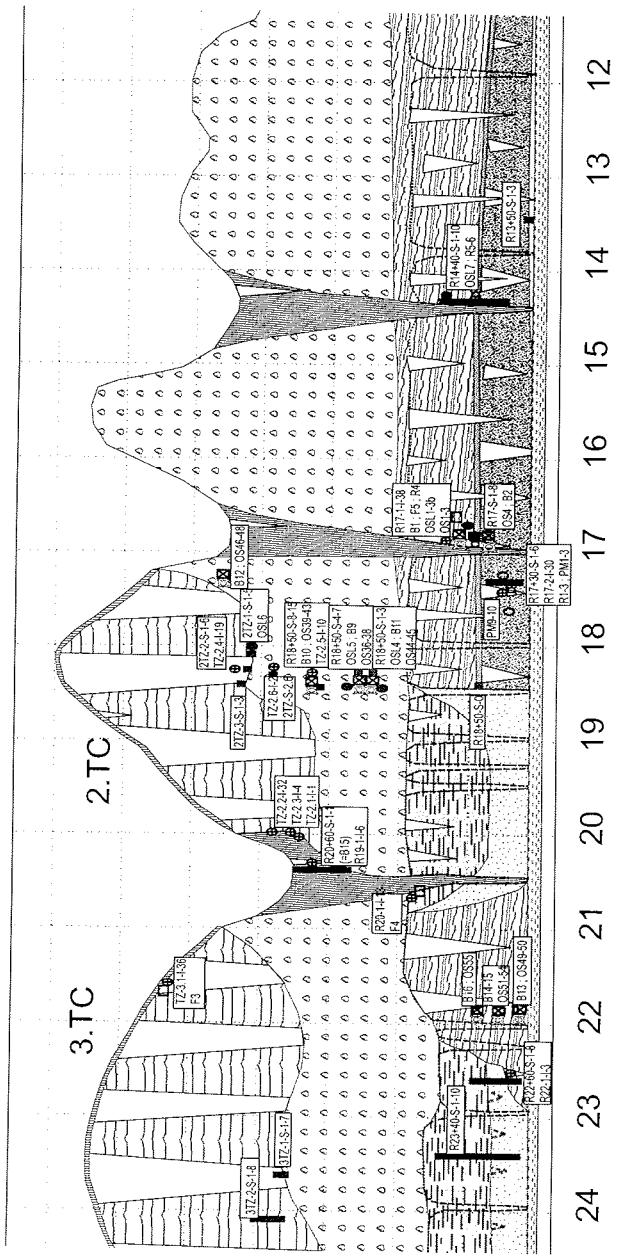

A5-1-2: continuation.

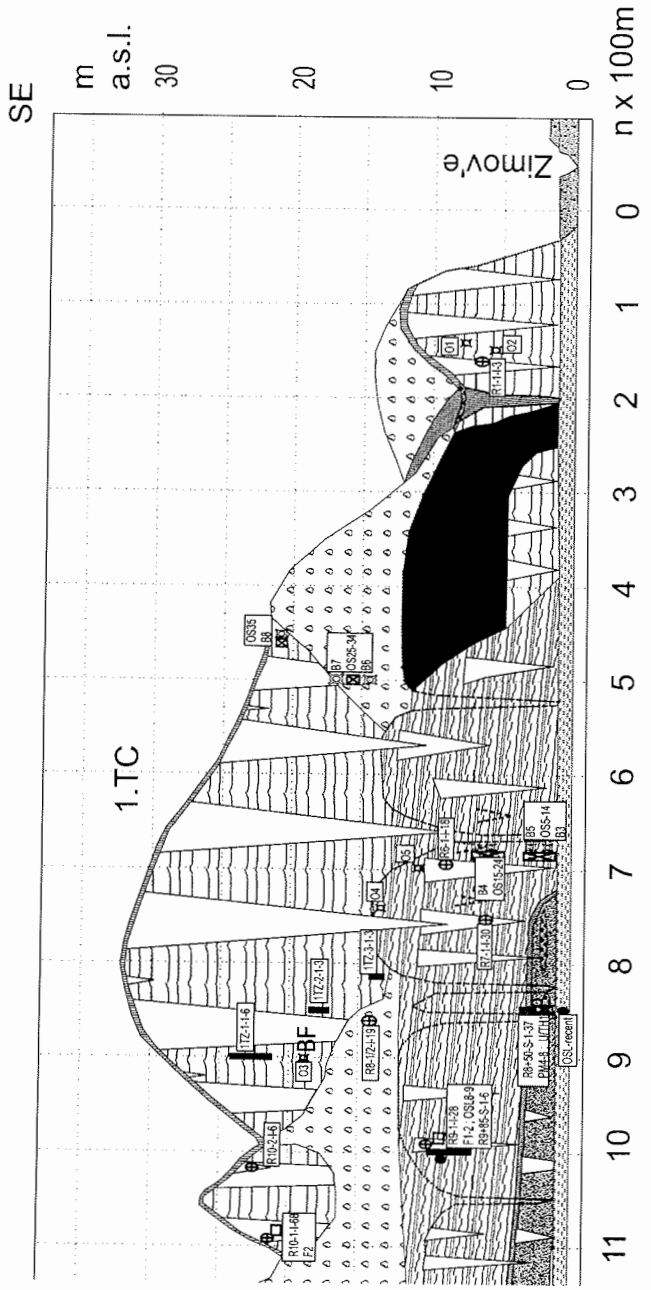

A5-1: Profile map of sample positions (German version).

A5-1-3: L-section.

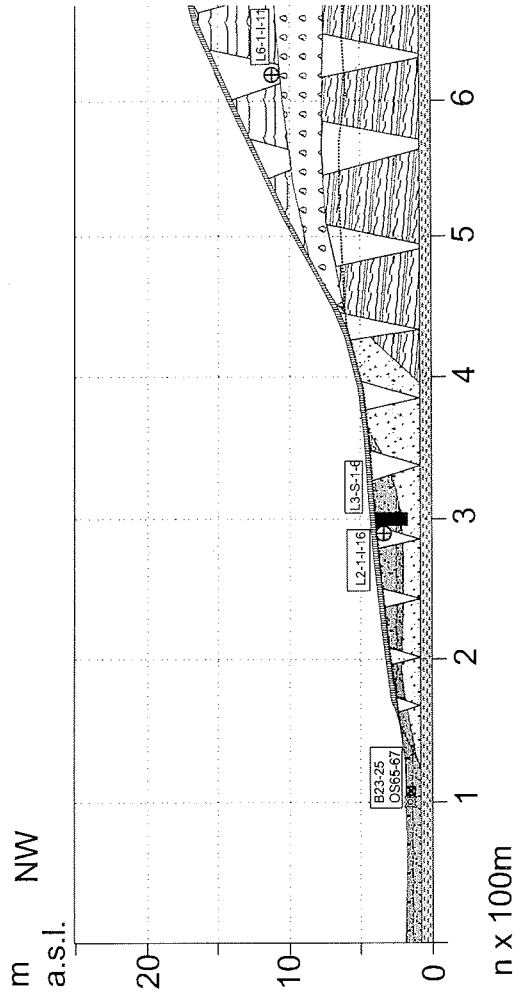

A5-1-3: continuation.

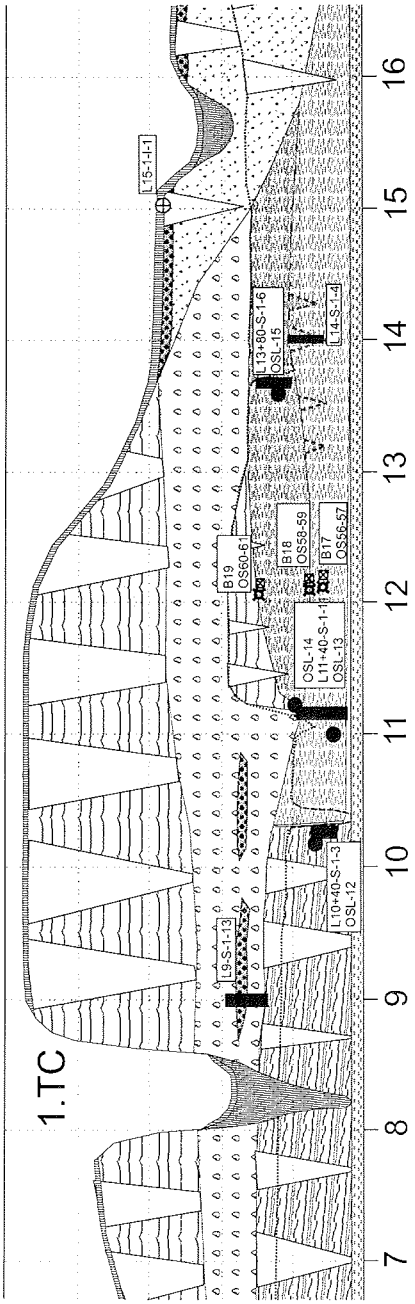

A5-1-3: continuation.

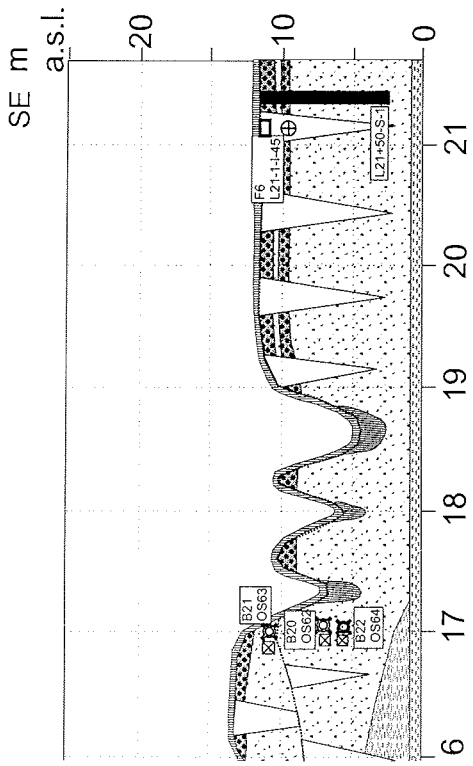

A5-2: Profile map (Russian version).

A5-2-1: Schematic profile of permafrost deposits. South coast of Bol´shoy Lyakhovsky

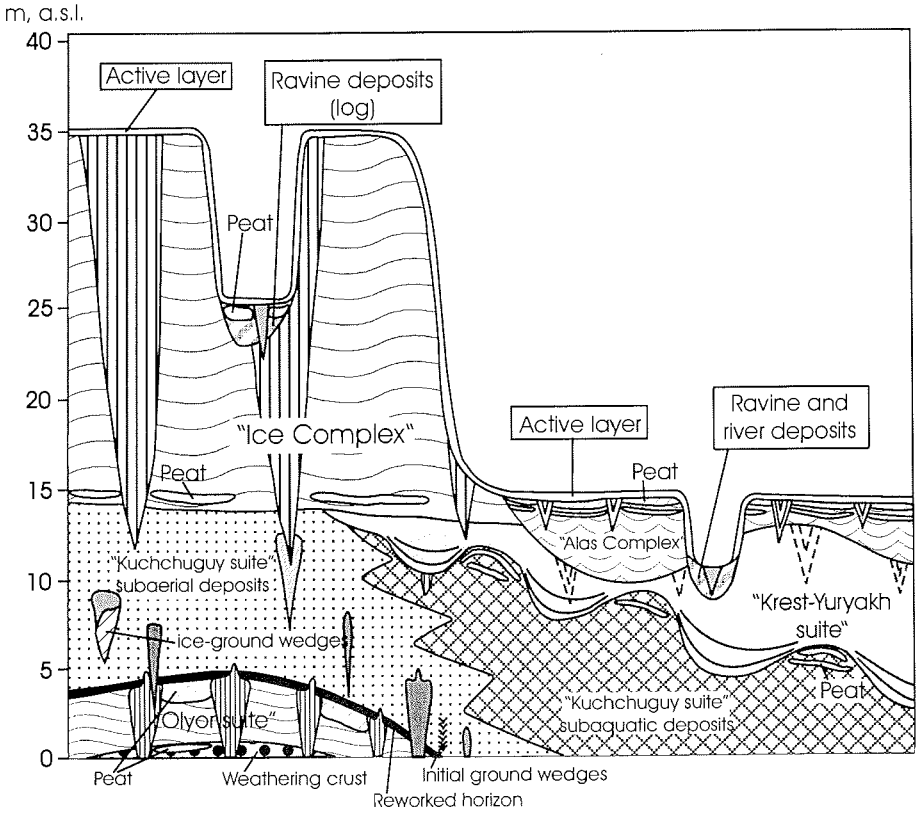

A5-2: Profile map (Russian version).

A5-2-2: Bol´shoy Lyakhovsky Island, south coast, R-side exposure.

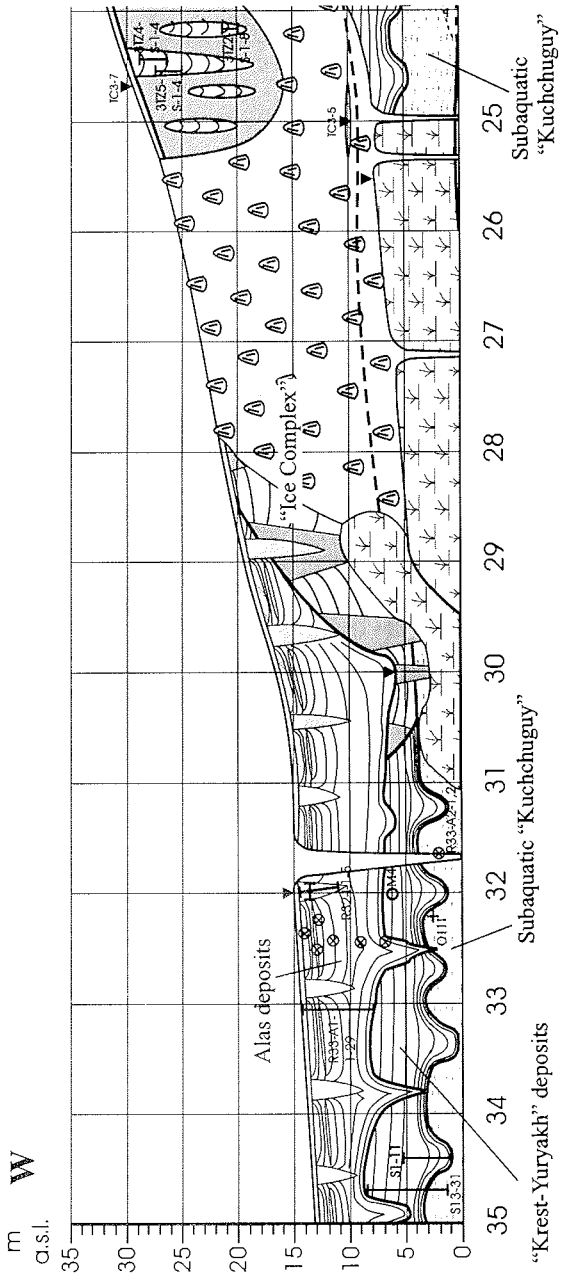

A5-2-2: continuation.

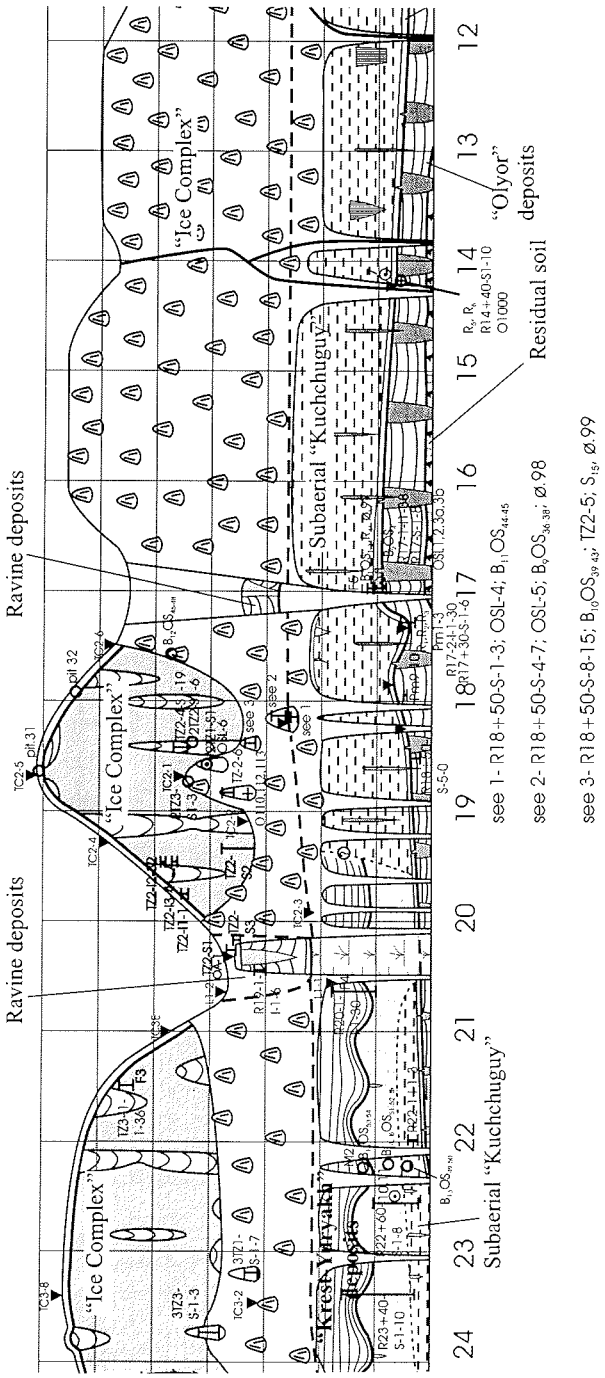

Table A5-2-2: continuation.

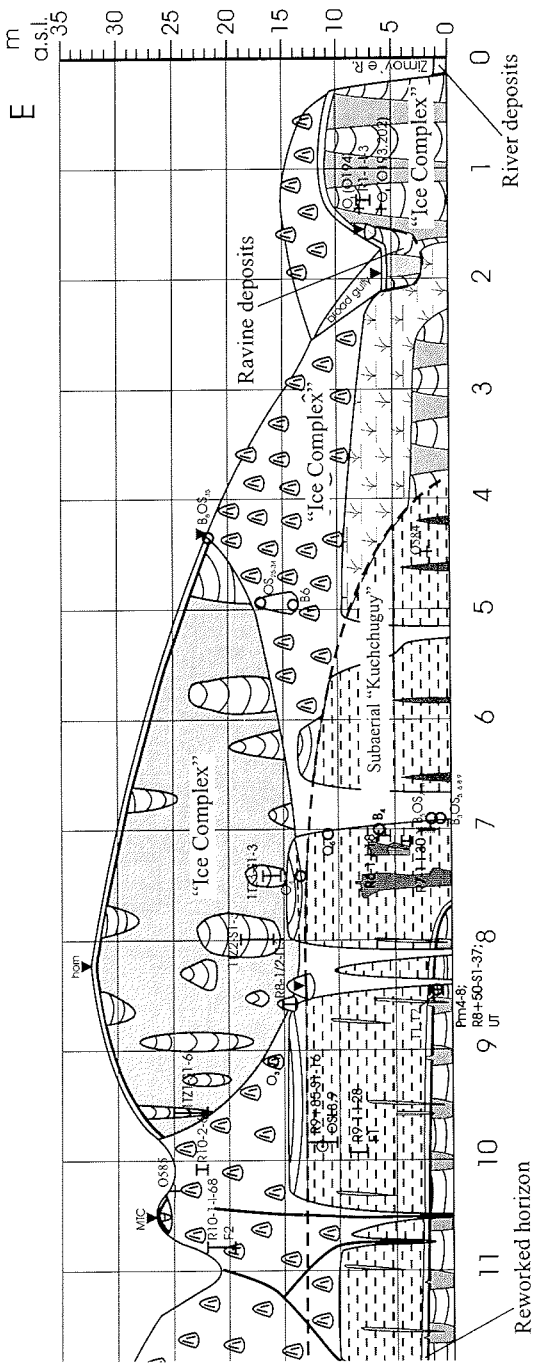

A5-2: Profile map (Russian version).

A**5-2-3:** Bol´shoy Lyakhovsky Island, south coast, L-side exposure.

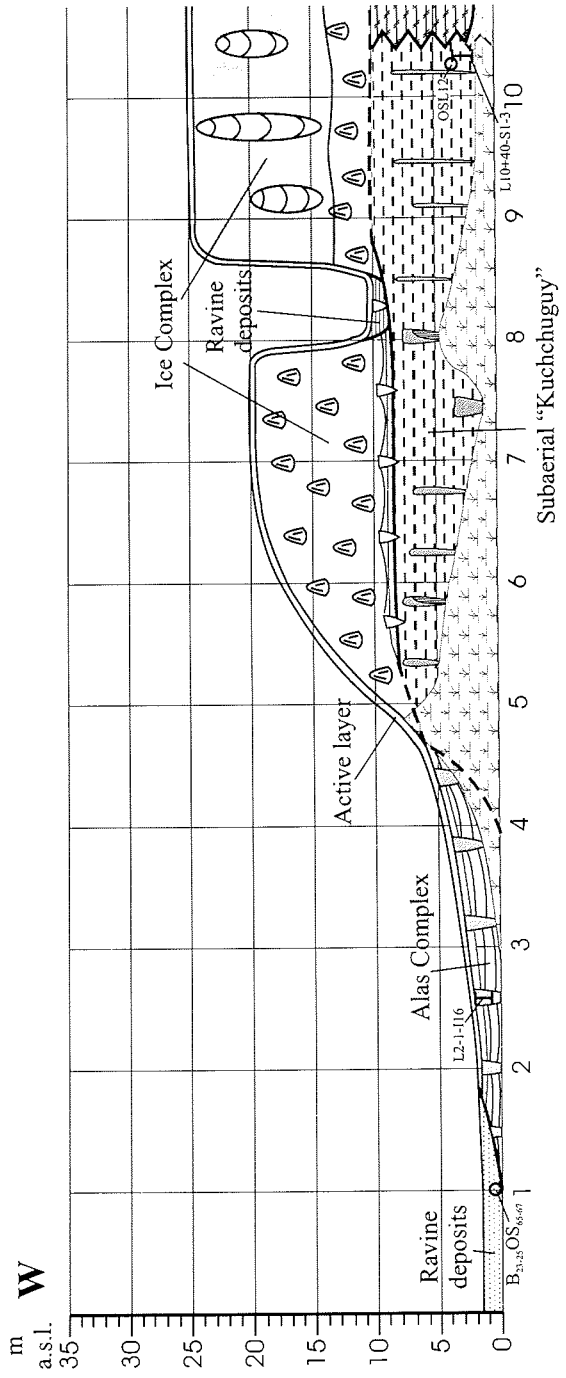

A5-2-3: continuation.

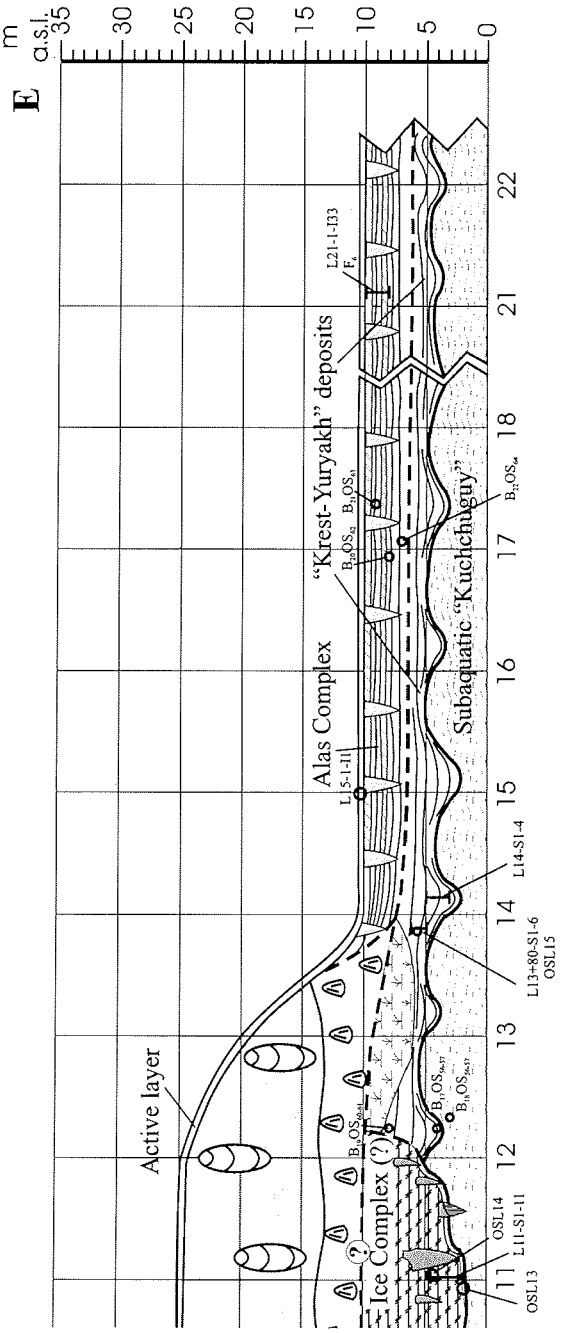

A5-3: List of sediment samples collected on Bol´shoy Lyakhovsky Island.

no.	sample	Sediment typ	hight [m] profile	altitude [m, a.s.l.]	horizontal position	remarks	ice content gravim. [%]	carb.
1	R17-S-0					?= R18+50-S-0 ?	32,2	-
2	R17-S-1	weathering crust	0,8	0	R 1700		46,5	-
3	R17-S-2	Olyor	1,6	0,4	R 1700		62,1	+
4	R17-S-3	peat inclusion	2	1	R 1700		98,8	-
5	R17-S-4	Olyor	3,7	2,7	R 1700		62	-
6	R17-S-5	peat inclusion	3,8	2,8	R 1700		94,8	-
7	R17-S-6	peat inclusion	5,7	4,7	R 1700			
8	R17-S-7	reworked horizon	6	5	R 1700	near R-17-OSL-2	43,9	-
9	R17-S-8	Kuchchuguy	6,7	5,7	R 1700	near R17-OSL-3a	49,4	-
10	R17-BC-2				R1700	Polosatic		
11	R18+50-S-0	weathering crust			R 1850	Bach Nr. 11		
12	R18+50-S-1	Kuchchuguy	0,4	11,8	R 1850	Baydzh. 11	41	-
13	R18+50-S-2	Kuchchuguy	1,3	12,7		Baydzh. 11; 12,9 m a.s.l. R18+50-OSL-4	33,7	-
14	R18+50-S-3	Kuchchuguy	2,1	13,5		Baydzh. 11	43,2	+
15	R18+50-S-4	alevrite	0,3	13,4		Baydzh. 13; base 13,1 m a.s.l.	53,2	-
16	R18+50-S-5	cryoturbated soil, gray	0,6	13,7		Baydzh. 13	75,7	-
17	R18+50-S-6	cryoturbated soil, dark brown	0,65	13,75		Baydzh. 13	76,1	
18	R18+50-S-7	alevrite	1,15	14,25		Baydzh. 13	82	-
19	R18+50-S-8	alevrit with gravels	0,3	13,5		Baydzh. 12, east side	74,1	-
20	R18+50-S-9	cryoturbated soil	0,75	13,75		Baydzh. 12, east side	53,6	
21	R18+50-S-10	alevrit	1,1	14,1		Baydzh. 12, east side	116,9	+
22	R18+50-S-11	cryoturbated soil	1,4	14,4		Baydzh. 12, east side	51,8	+
23	R18+50-S-12	alevrite	2	15		Baydzh. 12, south side	57,7	
24	R18+50-S-13	alevrite	3,1	16,1		Baydzh. 12, south side	44,6	+
25	R18+50-S-14	alevrite	3,4	16,4		Baydzh. 12, south side	42,4	-
26	R18+50-S-15	alevrite	3,8	16,8		Baydzh. 12, marker, in situ bone	53,2	(+)

A5-3: continuation.

no.	sample	Sediment typ	hight [m] profile	altitude [m. a.s.l.]	horizontal position	remarks	ice content gravim. [%]	carb.
27	2TZ-1-1	peaty soil	0,7	20,3	R 1806		165,9	(+)
28	2TZ-1-2	alevrite	0,85	20,45			97,5	+
29	2TZ-1-3	peaty soil	1,2	20,8			139,5	-
30	2TZ-1-4	alevrite	1,75	21,35			46,7	-
31	2TZ-1-5	alevrite	1	20,6		marker 20,6 m a.s.l., 2TZ-OSL-6	61,1	-
32	2TZ-2-1	alevrite	0	21,8	R 1820	marker 21,8 m a.s.l.	74,4	-
33	2TZ-2-2	alevrite	0,5	22,3			83,9	-
34	2TZ-2-3	alevrite	1,3	23,1			50	-
35	2TZ-2-4	alevrite	2,3	24,1			59,7	+
36	2TZ-2-5	alevrite	3	24,8			46,7	-
37	2TZ-2-6	alevrite	3,7	25,5			51,4	+
38	2TZ-3-1	alevrite	0	22	R 1845	marker 22,0 m a.s.l.	132,5	-
39	2TZ-3-2	alevrite	1,3	23,3			40,1	+
40	2TZ-3-3	alevrite	2,4	24,4			45,1	+
41	2TZ-S-2.6	alevrite		19	R 1830	between Baydzh. 12 and ice wall	82,4	+
42	3TZ-1-1	alevrite	*1,8	16,8	R 2360	*below the top, base of Baydzh. marker TC3-4 16,8 m a.s.l.	78,5	-
43	3TZ-1-2	soil	*1,5	17,1		*below the top	75,1	-
44	3TZ-1-3	alevrite	*1,4	17,2			107,1	-
45	3TZ-1-4	peat	*1,2	17,4			115,9	-
46	3TZ-1-5	peat	*1,25	17,45			164,3	-
47	3TZ-1-6	peat	*0,8	17,8			89,6	-
48	3TZ-1-7	alevrite	*0,7	17,9			78,6	-
49	3TZ-2-1	alevrite	0,1	16,6	R 2370	base marker TC3-9; 16,5 m a.s.l.	91,5	-
50	3TZ-2-2	soil	0,4	16,9			161,1	-
51	3TZ-2-3	alevrite	0,9	17,4			80,4	-
52	3TZ-2-4	soil	1,1	17,6			72,9	-
53	3TZ-2-5	soil	1,5	18		immature	85,4	-

A5-3: continuation.

no.	sample	Sediment typ	hight [m] profile	altitude [m, a.s.l.]	horizontal position	remarks	ice content gravim. [%]	carb.
54	3TZ-2-6	alevrite	1,8	18,3			60,8	-
55	3TZ-2-7	alevrite	2,4	18,9			62,1	-
56	3TZ-2-8	alevrite	2,8	19,3			66,2	-
57	3TZ-3-1	soil	0,15	21,45	R 2380	two brothers	66,2	-
58	3TZ-3-2	alevrite	0,6	21,9			74,8	-
59	3TZ-3-3	alevrite	1,3	22,6			42,8	(+)
60	3TZ-4-1	alevrite	0	23,6	R 2380		53,1	-
61	3TZ-4-2	soil	0,6	24,2			72,9	+
62	3TZ-4-3	alevrite	1,2	24,8			89,9	+
63	3TZ-4-4	alevrite	1,9	25,5			59	+
64	3TZ-5-1	alevrite	0,3	25,8	R 2400		141,4	+
65	3TZ-5-2	soil	0,8	26,3			112,8	-
66	3TZ-5-3	soil	1,1	26,6			96,3	-
67	3TZ-5-4	alevrite	1,3	26,8			80,1	+
68	R17+50-S-1	Olyor		2,8	R 1750	gehört zu R17+30		
69	R17+30-S-1	Olyor		1	R 1730	a.s.l.	107,2	
70	R17+30-S-2	Olyor		1,9			101,5	(+)
71	R17+30-S-3	peat inclusion		2,4		reworking horizon	25,1	-
72	R17+30-S-4	peat inclusion		2,45		reworking horizon		
73	R17+30-S-5	sand		2,5		reworking horizon	31,9	+
74	R17+30-S-6	Kuchchuguy		3,1			27,1	(+)
75	R14+40-S-1	Olyor	0,1	3,1	R 1440	brook no. 8	148,9	-
76	R14+40-S-2	peat	1	4			115,2	-
77	R14+40-S-3	Olyor	1,3	4,3			138,1	(+)
78	R14+40-S-4	peat inclusion	1,7	4,7		peaty soil, U/Th !!	360,6	-
79	R14+40-S-5	Olyor	1,8	4,8			57,6	-
80	R14+40-S-6	sand	2	5		reworking horizon, marker 5 m a.s.l.	60,6	(+)

A5-3: continuation.

no.	sample	Sediment typ	hight [m] profile	altitude [m, a.s.l.]	horizontal position	remarks	ice content gravim. [%]	carb.
81	R14+40-S-7	Kuchchuguy	2,6	5,6			33,1	+
82	R14+40-S-8	Kuchchuguy	3,6	6,6			27,7	-
83	R14+40-S-9	Kuchchuguy	4,3	7,3		thawed, dry, R14+40-OSL-7		
84	R14+40-S-10	Kuchchuguy	5	8		thawed, dry		
85	R8+50-S-1	peat	0,05	0,05	R 850	frozen		
86	R8+50-S-2	peat	0,1	0,1		frozen		
87	R8+50-S-3	peat	0,13	0,13		frozen		
88	R8+50-S-4	peat	0,16	0,16		frozen		
89	R8+50-S-5	peat	0,19	0,19		frozen		
90	R8+50-S-6	peat	0,22	0,22		frozen		
91	R8+50-S-7	peat	0,25	0,25		frozen		
92	R8+50-S-8	peat	0,28	0,28		frozen		
93	R8+50-S-9	peat	0,31	0,31		frozen		
94	R8+50-S-10	peat	0,34	0,34		frozen		
95	R8+50-S-11	peat	0,37	0,37		frozen		
96	R8+50-S-12	peat	0,4	0,4		frozen		
97	R8+50-S-13	peat	0,43	0,43		frozen		
98	R8+50-S-14	peat	0,46	0,46		frozen		
99	R8+50-S-15	peat	0,49	0,49		frozen		
100	R8+50-S-16	peat	0,52	0,52		frozen		
101	R8+50-S-17	peat	0,55	0,55		frozen		
102	R8+50-S-18	peat	0,58	0,58		frozen		
103	R8+50-S-19	peat	0,61	0,61		frozen		
104	R8+50-S-20	peat	0,64	0,64		frozen		
105	R8+50-S-21	peat	0,67	0,67		frozen, U/Th-sample		
106	R8+50-S-22	peat	0,7	0,7		frozen, U/Th-sample		
107	R8+50-S-23	peat	0,73	0,73		frozen, U/Th-sample		
108	R8+50-S-24	peat	0,76	0,76		frozen, U/Th-sample	403,1	-

A5-3: continuation.

no.	sample	Sediment typ	hight [m] profile	altitude [m, a.s.l.]	horizontal position	remarks	ice content gravim. [%]	carb.
109	R8+50-S-25	peat	0,79	0,79		frozen, U/Th-sample		
110	R8+50-S-26	peat	0,82	0,82		frozen, U/Th-sample		
111	R8+50-S-27	peat	0,85	0,85		frozen, U/Th-sample		
112	R8+50-S-28	peat	0,9	0,9		frozen, U/Th-sample		
113	R8+50-S-29	peat	0,95	0,95		unfrozen		
114	R8+50-S-30	peat	1	1		unfrozen		
115	R8+50-S-31	peat	1,05	1,05		unfrozen		
116	R8+50-S-32	peat	1,1	1,1		unfrozen		
117	R8+50-S-33	peat	1,15	1,15		unfrozen		
118	R8+50-S-34	peat	1,2	1,2		unfrozen		
119	R8+50-S-35	peat	1,25	1,25		unfrozen		
120	R8+50-S-36	Olyor	2,5	2,5			47,1	-
121	R8+50-S-37	Kuchchuguy	3	3				
122	1TZ-1-1	alevrite	0,2	22	R 900	marker 22 m a.s.l.	162,5	-
123	1TZ-1-2	alevrite	0,45	22,25			72,1	(+)
124	1TZ-1-3	peat inclusion	0,55	22,35			49,8	(+)
125	1TZ-1-4	alevrite	1	22,8			111,3	-
126	1TZ-1-5	peat inclusion	1,6	23,4			76,7	-
127	1TZ-1-6	alevrite	1,9	23,7			96,9	-
128	1TZ-2-1	alevrite	0,1	17	R 850	marker 17 m a.s.l.	79,8	-
129	1TZ-2-2	alevrite	0,75	17,65		roots, Fe-impr.	48,9	-
130	1TZ-2-3	alevrite	1,4	18,3			76,7	+
131	1TZ-3-1	alevrite	0,1	13	R 820	marker 13 m a.s.l.	101,4	-
132	1TZ-3-2	peat inclusion	0,3	13,2			75,7	-
133	1TZ-3-3	alevrite	0,8	13,7			85,2	-
134	R22+60-S-1	Kuchchuguy	1	1	R 2260	OSL-10	24,4	+ +
135	R22+60-S-2	Kuchchuguy, peat incl.	1,05	1,05		OSL-11		
136	R22+60-S-3	Taberit	2	2				

A5-3: continuation.

no.	sample	Sediment typ	hight [m] profile	altitude [m, a.s.l.]	horizontal position	remarks	ice content gravim. [%]	carb.
137	R22+60-S-4	Taberit	2,35	2,35			24,2	+ +
138	R22+60-S-5	ice wedge pseudom., peat inclusion	3	3				
139	R22+60-S-6	ice wedge pseudom., lake sediment	3,05	3,05			32,7	+ +
140	R22+60-S-7	Taberit	4	4			50,5	+ +
141	R22+60-S-8	alas lake deposits	4,8	4,8				
142	R33-A2-1	ice wedge pseudom.		7	R 3200	twig		
143	R33-A2-2	subarerial Kuchuguy				roots		
144	R33-A1-S1	Taberit	7	7	R 3300			-
145	R33-A1-S2	alevrit, ice complex		7,1			35,7	-
146	R33-A1-S3	peat inclusion in lake sediment		8		5 m western R33-A1-S2	32	-
147	R33-A1-S4	Taberit ?		8,05		12 m western R33-A1-S3	102,4	+
148	R33-A1-S5	alas lake sediment		8,2		base of alas lake	39,8	+
149	R33-A1-S6	alas lake sediment		8,5		twigs, shells, gastropods	37,5	-
150	R33-A1-S7	alas lake sediment		8,8			35,2	-
151	R33-A1-S8	alas lake sediment		9,2			41,3	-
152	R33-A1-S9	alas lake sediment		9,5			40,2	+
153	R33-A1-S9a	alas lake sediment		9,52		leaves layer		
154	R33-A1-S10	alas lake sediment		9,6			35	+
155	R33-A1-S10a	alas lake sediment		9,62		plant detritus		
156	R33-A1-S11	alas lake sediment		9,8			39,2	+ +
157	R33-A1-S12	alas lake sediment		10,1		shells	45	+ +
158	R33-A1-S12a	alas lake sediment		10,12			49,5	+ +
159	R33-A1-S13	alas lake sediment		10,5			80	+
160	R33-A1-S14	alas lake sediment		10,8			44,7	- / +
161	R33-A1-S15	alas lake sediment		11,3			71,4	-

A5-3: continuation.

no.	sample	Sediment typ	hight [m] profile	altitude [m, a.s.l.]	horizontal position	remarks	ice content gravim. [%]	carb.
162	R33-A1-S16	alas lake sediment		11,7			90,3	+
163	R33-A1-S17	alas lake sediment		12		shells	69,4	+
164	R33-A1-S18	alevrit		12,4		without shells	103,9	+
165	R33-A1-S19	alevrit		12,9		grass roots	79,6	+
166	R33-A1-S20	peaty soil		13,7		twigs	165	-
167	R33-A1-S21	silt		14			129,8	-
168	R33-A1-S22	peat		14,3				
169	R33-A1-S23	peat	0,1	14,1		7 m western R33-A1-S22, same horizon	205,2	-
170	R33-A1-S24	peat	0,17	14,17				
171	R33-A1-S25	peat	0,25	14,25				
172	R33-A1-S26	peat	0,33	14,33				
173	R33-A1-S27	peat	0,4	14,4				
174	R33-A1-S28	peat	0,48	14,48				
175	R33-A1-S29	peat	0,56	14,56			88,9	-
176	R9+85-S-1	alevrit	*0,8	10,2	R 985	*below surface of the thermo terrace, OSL-9	31,7	-
177	R9+85-S-2	alevrit	*2	8,95			67,8	-
178	R9+85-S-3	alevrit	*1,8	9,25		discordance	57,7	-
179	R9+85-S-4	Kuchuguy	*2,05	9		R9+85-OSL-8, measurement of F 1 (ice photo)	38,4	(+)
180	R9+85-S-5		*1,5	9,5			67,2	+
181	R9+85-S-6	Kuchuguy	*3,5	7,5			32,6	(+)
182	R23+40-S-1	alas sediment		1,75	R 2340	sand		
183	R23+40-S-2	alas sediment		2,75		twigs, gravels		
184	R23+40-S-3	alas sediment		3,75		deformed		
185	R23+40-S-4	alas sediment		4,25		shells, sandy		
186	R23+40-S-5	alas sediment		4,75		sand		
187	R23+40-S-6	alas sediment		5,25				
188	R23+40-S-7	alas sediment		5,5		alternation of silt and peat layers		
189	R23+40-S-8	alas sediment		5,75		alternation of silt and peat layers		

A5-3: continuation.

no.	sample	Sediment typ	hight [m] profile	altitude [m, a.s.l.]	horizontal position	remarks	ice content gravim. [%]	carb.
190	R23+40-S-9	alas sediment		6,5		alternation of silt and peat layers		
191	R23+40-S-10	alas sediment		7,25		alternation of silt and peat layers		
192	B15-1	peat inclusion, alevrite	5	13,6	R 2065	below the surface; marker L1-2; 18,6 m a.s.l. , brook 15	114,9	-
193	B15-2	alevrite	4,9	13,7			89	-
194	B15-3	alevrite, soil	4,6	14		with wood remains	78,6	-
195	B15-4	valley deposit (log)	3,9	14,7			42,3	-
196	B15-5	valley deposit (log)	3,1	15,5			100,6	-
197	B15-6	valley deposit (log)	2,5	16,1			78,2	-
198	B15-7	valley deposit (log)	2	16,6		roots	69,8	-
199	B15-8	valley deposit (log)	1,2	17,4		roots	61,3	-
200	B15-9	soil	0,7	17,9		C-horizon		
201	B15-10	soil	0,5	18,1		B-horizon		
202	B15-11	soil	0,1	18,5		A-horizon		
203	L10+40-S-1	Kuchchuguy		1,5	L 1040	grass roots	38,1	+
204	L10+40-S-2	Kuchchuguy peat inclusion		3,5			45,8	+
205	L10+40-S-3	Kuchchuguy		1,7				
206	L11-S-1	older alas lake deposit, peat inclusion		0,5	L 1140	twigs	27,8	+
207	L11-S-2	peat inclusion		1				
208	L11-S-3	older alas lake deposit		1,01		subaquatic Kucheguy	25,8	+ +
209	L11-S-4	older alas lake deposit		1,4		subaquatic Kucheguy	29,4	(+)
210	L11-S-5	older alas lake deposit		2		subaquatic Kucheguy	25,7	(+)
211	L11-S-6	older alas lake deposit		2,6		subaquatic Kucheguy	26,9	+
212	L11-S-7	older alas lake deposit		2,8		subaquatic Kucheguy	27,7	+ +
213	L11-S-8	older alas lake deposit		3,3		subaquatic Kucheguy	24,4	-
214	L11-S-9	alevrite, soil ?		3,4		brownish weathering horizon ?	65,8	-

A5-3: continuation.

no.	sample	Sediment typ	hight [m] profile	altitude [m, a.s.l.]	horizontal position	remarks	ice content gravim. [%]	carb.
215	L11-S-10	alevrite		4		grass roots	72,4	-
216	L11-S-11	alevrite		4,3		LYA-L11-OSL-14	71,4	-
217	L14-S-1	alas lake deposit with peat inclusion		3	L 1200	ice wedge pseudomorphosis	33,3	+ +
218	L14-S-2	peat inclusion		4,1		ice wedge pseudomorphosis, twigs	37	+
219	L14-S-3	older alas lake deposit		4,12		subaquatic Kucheguy	26	+ +
220	L14-S-4	alas lake deposit		5,4		ice wedge pseudomorphosis		
221	L13+80-S-1	older alas lake deposit		5	L 1380	subaquatic Kucheguy	26	+ +
222	L13+80-S-2	peat incl. , younger alas lake deposit		5,4				
223	L13+80-S-3	younger alas lake deposit		5,42			41,7	(+)
224	L13+80-S-4	younger alas lake deposit		5,8		L13+80-OSL-15	49,5	(+9
225	L13+80-S-5	younger alas lake deposit		6			45	+
226	L13+80-S-6	younger alas lake deposit		6,3		many twigs	30,1	+ +
227	L3-S1	alevrite		1,4	L 300	cross bedded	92	-
228	L3-S-2	fluvial sand		1,7		ripples	60,2	-
229	L3-S-3	fluvial sand		2		ripples	86	-
230	L3-S-4	fluvial middle grained sand		2,25		ripples	34,2	-
231	L3-S-5	fluvial sand		2,9		ripples. alternations of sand and plant detritus	93	-
232	L3-S-6	fluvial sand					62,3	-
233	L21+50-S-1	older alas lake deposit		2,5	L 2150	subaquatic Kucheguy	30	+ +
234	L21+50-S-2	older alas lake deposit		3,1		subaquatic Kucheguy	24,6	+ +
235	L21+50-S-3	older alas lake deposit		3,6		subaquatic Kucheguy	24,6	+
236	L21+50-S-4	younger alas lake deposit		4,3			26	+ +
237	L21+50-S-5	peat incl., younger alas lake deposit		5			30,4	+
238	L21+50-S-6	younger alas lake deposit		5,6			34,7	-

A5-3: continuation.

no.	sample	Sediment typ	hight [m] profile	altitude [m, a.s.l.]	horizontal position	remarks	ice content gravim. [%]	carb.
239	L21+50-S-7	younger alas lake deposit		6,2			47,9	-
240	L21+50-S-8	younger alas lake deposit		6,9			63,4	+
241	L21+50-S-9	younger alas lake deposit		7,5		shells	34,3	+
242	L21+50-S-10	younger alas lake deposit		8,2			37,6	+ +
243	L21+50-S-11	alevrite		8,5			51,1	-
244	L21+50-S-12	peat layer		9,5			114,3	(+)
245	L21+50-S-13	peat		10,3		unfrozen, lower part		
246	L21+50-S-14	peat		10,4		unfrozen, middle part		
247	L21+50-S-15	peat		10,5		upper part	706,8	-
248	L21+50-S-16	alevrite intelayer		10,7			99	-
249	L21+50-S-17	peat		11		second peat horizon, lower part, cryoturbated, twigs	613,9	-
250	L21+50-S-18	peat		11,2		second peat horizon,	962,1	-
251	L21+50-S-19	peat		11,4		second peat horizon, upper part	133,1	-
252	L21+50-S-20	peat		11,6		unfrozen, second peat horizon, middle part		-
253	L21+50-S-21	peat		11,8		unfrozen fresh peat, top of a baydzherakh		-
254	L9-S-1	Kutchuguy		6,1	L 900	grass roots		
255	L9-S-2	sand layer		6,5				
256	L9-S-3	alevrite		7,1				
257	L9-S-4	peat inclusion		7,7				
258	L9-S-5	alevrite with peat incl.		8				
259	L9-S-6	peat inclusion (small)		8,2				
260	L9-S-7	peat		8,8				
261	L9-S-8	peat		9				
262	L9-S-9	peat		9,1				
263	L9-S-10	peat		9,2				
264	L9-S-11	peat		9,3				
265	L9-S-12	peat		9,4				

A5-3: continuation.

no.	sample	Sediment typ	hight [m] profile	altitude [m, a.s.l.]	horizontal position	remarks	ice content gravim. [%]	carb.
266	L9-S-13	alevrite		9,7				
267	R13+50-grau	weathering crust		1	R 1350			
268	R13+50-gelb	weathering crust		1,2				
269	R13+50-grün	weathering crust		1,4				
270	Rezent 1	recent sample of waters bottom						
271	Rezent 2	recent sample of waters bottom						
272	Rezent 3	recent sample of waters bottom						
273	KGT-1-1	recent alevrit				Khaptagai Tas, pyatny medalion		
274	KGT-1-2	alevrite				Khaptagai Tas, between granite blocks		
275	KGT-1-3	aeolian material (?)				Khaptagai Tas, between granite blocks		

stones of Khaptagai Tas region

	Lya-Y	granit				Khaptagai Tas		
	Lya-X	sandstone				Khaptagai Tas		

sample for structure analyse

	R8+50	Olyor over the peat		2,5		2 samples		
	R8+50	Kuchchuguy		3,1		2 samples		
	R9+85	ice complex (?)				perhaps only active layer of the thermo terracce		
	R22+50	Kuchchuguy		1				
	R22+50	taberite or lake deposit		1,5				
	R25	lake deposit		1,5		shells		

A5-4: List of OSL-samples.

no.	sample	sediment typ	hight [m] profile	altitude [m, a.s.l.]	horizontal position	remarks
1	R17-OSL-1	Olyor	3,2	2,2	R 1700	
2	R17-OSL-2	alevrite	6	5	R 1700	reworked horizon
3	R17-OSL-3a	Kuchchuguy	6,7	5,7	R 1700	
4	R17-OSL-3b	Kuchchuguy	7,5	6,5	R 1700	
5	R18+50-OSL-4	Kuchchuguy		12,9	R 1850	Baydzh. 11
6	R18+50-OSL-5	alevrite	1,6	14,7	R 1850	Baydzh 13;
7	2TZ-1-OSL-6	alevrite		20,6	R 1860	base of the ice wall
8	R14+40-OSL-7	Kuchchuguy		5	R 1440	brook no. 8
9	R9+85-OSL-8	Kuchchuguy		9	R 985	9 m a.s.l. measurement of F 1 (ice photo)
10	R9+85-OSL-8-alt	Kuchchuguy		9	R 985	
11	R9+85-OSL-9	alevrite		10,2	R 985	
12	R22+60-OSL-10	Kuchchuguy		1	R 2260	
13	R22+60-OSL-11	taberite		2	R 226ß	
14	L10+40-OSL-12	Kuchchuguy		2,5	L 1040	
15	L11-OSL-13	old lake deposits		1,8	L 1100	
16	L11-OSL-14	alevrite		4,3	L 1100	
17	L13+80-OSL-15	younger lake deposits		5,8	L 1380	
18	Rezent-OSL-R8+50	beach sediment		0	R 850	recent surface sediment

A5-5: List of alas samples.

Site: First alas westward of the Zimov'e river estuary R33 – sampling of Holocene alas. Date: 16.08.99 R35 - sampling of ancient alas sediments. Date: 28.08.99				
Sample number	Sediment description	Depth, m under the surface	Altitude, m a.s.l.	Notes
R33-A1-D1	piece of wood	1.6		for dating
R33-A1-D2	piece of wood	6		for dating
R33-A1-D3	piece of wood	3		for dating
R33-A1-D4	piece of wood	7.9		for dating
R33-A1-D5	peat	0.4		for dating
R33-A1-D6	piece of wood	1.2		for dating
R35-S1	silty loam's		5.2	„Krest-Yuryakhsk suite"
R35-S2	silty loam		4.8	
R35-S3	silty loam		4.4	
R35-S4	silty loam		4.0	with gastropods
R35-S5	silty loam		3.6	with gastropods
R35-S6	silty loam		3.2	
R35-S7	silty loam		2.8	
R35-S8	silty loam		2.4	
R35-S9	silty loam		2.0	
R35-S9D	remnants of sprigs		2.0	for dating
R35-S10	silty loam		1.6	
R35-S11	silty loam		1.2	
R35-S11D	remnants of thin sprigs		1.0	for dating
R35-S12	aleurite		1.8	taberal (?) deposits under cast
R35+5-S13	lacustrine brown loam		8.5	„Krest-Yuryakhsk suite"
R35+5-S14	lacustrine brown loam		8.1	
R35+5-S15	lacustrine brown loam		7.7	

A5-6: List of water and ice samples collected on Bol´shoy Lyakhovsky island during field season 1999.

				Isotopes				Chemistry		
Nr.	date	sample	type	18 O	2 H	3 H	10 Be	anion/cation	pH	LF
1	06.08.1999	LYA 99/01	RW	X	X	X	-	X	6,69	1763?
2	08.08.1999	LYA 99/02	RW	X	X	X	-	X	6,39	151
3	08.08.1999	LYA-R17-1-I1	IW	X	X	X	-	X	6,69	47
4	08.08.1999	LYA-R17-1-I2	IW	X	X	-	-	-	6,79	45
5	08.08.1999	LYA-R17-1-I3	IW	X	X	-	-	-	6,10	24
6	08.08.1999	LYA-R17-1-I4	IW	X	X	-	-	-	5,84	37
7	08.08.1999	LYA-R17-1-I5	IW	X	X	-	-	X	5,91	35
8	08.08.1999	LYA-R17-1-I6	IW	X	X	-	-	-	5,92	32
9	08.08.1999	LYA-R17-1-I7	IW	X	X	-	-	-	6,00	44
10	08.08.1999	LYA-R17-1-I8	IW	X	X	-	-	-	6,06	37
11	08.08.1999	LYA-R17-1-I9	IW	X	X	-	-	-	-	41
12	08.08.1999	LYA-R17-1-I10	IW	X	X	-	-	X	6,62	88
13	08.08.1999	LYA-R17-1-I11	IW	X	X	-	-	-	-	-
14	08.08.1999	LYA-R17-1-I12	IW	X	X	-	-	-	7,9	490
15	08.08.1999	LYA-R17-1-I13	IW	X	X	-	-	-	-	-
16	08.08.1999	LYA-R17-1-I14	IW	X	X	-	-	-	7,36	133
17	08.08.1999	LYA-R17-1-I15	IW	X	X	-	-	X	-	-
18	08.08.1999	LYA-R17-1-I16	IW	X	X	-	-	-	7,44	96
19	08.08.1999	LYA-R17-1-I17	IW	X	X	-	-	-	-	-
20	08.08.1999	LYA-R17-1-I18	IW	X	X	-	-	-	7,99	464
21	08.08.1999	LYA-R17-1-I19	IW	X	X	-	-	-	-	-
22	08.08.1999	LYA-R17-1-I20	IW	X	X	-	-	X	6,82	50
23	08.08.1999	LYA-R17-1-I21	IW	X	X	-	-	-	-	-
24	08.08.1999	LYA-R17-1-I22	IW	X	X	-	-	-	7,01	102
25	08.08.1999	LYA-R17-1-I23	IW	X	X	-	-	-	-	-
26	08.08.1999	LYA-R17-1-I24	IW	X	X	-	-	-	7,20	77
27	08.08.1999	LYA-R17-1-I25	IW	X	X	X	-	X	-	-
28	08.08.1999	LYA-R17-1-I26	IW	X	X	-	-	-	7,19	104
29	08.08.1999	LYA-R17-1-I27	IW	X	X	-	-	-	-	-
30	08.08.1999	LYA-R17-1-I28	IW	X	X	-	-	-	8,02	44
31	08.08.1999	LYA-R17-1-I29	IW	X	X	-	-	-	-	-
32	08.08.1999	LYA-R17-1-I30	IW	X	X	-	-	X	6,70	44
33	08.08.1999	LYA-R17-1-I31	IW	X	X	-	-	-	-	-
34	08.08.1999	LYA-R17-1-I32	IW	X	X	-	-	-	6,84	131
35	08.08.1999	LYA-R17-1-I33	IW	X	X	-	-	-	-	-
36	08.08.1999	LYA-R17-1-I34	IW	X	X	-	-	-	7,29	161
37	08.08.1999	LYA-R17-1-I35	IW	X	X	-	-	-	-	-
38	08.08.1999	LYA-R17-1-I36	IW	X	X	-	-	-	7,49	172
39	08.08.1999	LYA-R17-1-I37	IW	X	X	-	-	-	-	-
40	08.08.1999	LYA-R17-1-I38	IW	X	X	-	-	-	7,38	148
41	09.08.1999	LYA-R9-1-I1	IW	X	X	-	-	X	7,35	-
42	09.08.1999	LYA-R9-1-I2	IW	X	X	-	-	-	6,37	-
43	09.08.1999	LYA-R9-1-I3	IW	X	X	-	-	X	-	-
44	09.08.1999	LYA-R9-1-I4	IW	X	X	-	-	-	-	48
45	09.08.1999	LYA-R9-1-I5	IW	X	X	-	-	X	6,24	-
46	09.08.1999	LYA-R9-1-I6	IW	X	X	-	-	-	-	48
47	09.08.1999	LYA-R9-1-I7	IW	X	X	X	-	-	-	67
48	09.08.1999	LYA-R9-1-I8	IW	X	X	-	-	-	7,34	63
49	09.08.1999	LYA-R9-1-I9	IW	X	X	-	-	-	-	56
50	09.08.1999	LYA-R9-1-I10	IW	X	X	-	-	X	6,72	-
51	09.08.1999	LYA-R9-1-I11	IW	X	X	-	-	-	-	59
52	09.08.1999	LYA-R9-1-I12	IW	X	X	-	-	-	7,27	64
53	09.08.1999	LYA-R9-1-I13	IW	X	X	-	-	-	-	56
54	09.08.1999	LYA-R9-1-I14	IW	X	X	-	-	-	7,20	79
55	09.08.1999	LYA-R9-1-I15	IW	X	X	-	-	X	6,38	-
56	09.08.1999	LYA-R9-1-I16	IW	X	X	-	-	-	7,22	-
57	09.08.1999	LYA-R9-1-I17	IW	X	X	-	-	X	-	-
58	09.08.1999	LYA-R9-1-I18	IW	X	X	-	-	-	6,78	-
59	09.08.1999	LYA-R9-1-I19	IW	X	X	-	-	-	-	-
60	09.08.1999	LYA-R9-1-I20	IW	X	X	-	-	X	6,89	-
61	09.08.1999	LYA-R9-1-I21	IW	X	X	-	-	-	-	-
62	09.08.1999	LYA-R9-1-I22	IW	X	X	-	-	-	6,69	-
63	09.08.1999	LYA-R9-1-I23	IW	X	X	-	-	-	-	-
64	09.08.1999	LYA-R9-1-I24	IW	X	X	-	-	-	7,05	-
65	09.08.1999	LYA-R9-1-I25	IW	X	X	-	-	-	-	-
66	09.08.1999	LYA-R9-1-I26	IW	X	X	-	-	-	6,69	-
67	09.08.1999	LYA-R9-1-I27	IW	X	X	-	-	X	-	-
68	09.08.1999	LYA-R9-1-I28	IW	X	X	-	-	-	6,95	-
69	09.08.1999	LYA-R17-97/01	SP	X	X	-	-	-	-	-
70	09.08.1999	LYA-96/01	SW	X	X	X	-	X	7,52	4910
71	09.08.1999	LYA-R17-97/02	SP	X	X	X	-	X	6,97	27
72	10.08.1999	LYA-R17-1-Be1	IW	X	X	-	-	-	-	-
73	10.08.1999	LYA-R17-1-Be2	IW	X	X	-	-	-	-	-
74	10.08.1999	LYA-R17-1-Be3	IW	X	X	X	-	-	-	-
75	10.08.1999	LYA-R17-1-Be4	IW	X	X	-	-	-	-	-

A5-6: continuation.

				Isotopes				Chemistry		
Nr.	date	sample	type	18 O	2 H	3 H	10 Be	anion/cation	pH	LF
76	10.08.1999	LYA-R17-1-Be5	IW	X	X	-	-	-	-	-
77	10.08.1999	LYA-R8-97/01	SP	X	X	X	-	X	7,24	11
78	10.08.1999	LYA-R8-97/02	SP	X	X	X	-	X	7,35	36
79	10.08.1999	LYA-R8-1-I1	IW	X	X	-	-	-	7,69	22
80	10.08.1999	LYA-R8-1-I2	IW	X	X	-	-	X	7,01	23
81	10.08.1999	LYA-R8-1-I3	IW	X	X	-	-	-	-	-
82	10.08.1999	LYA-R8-1-I4	IW	X	X	-	-	-	7,69	20
83	10.08.1999	LYA-R8-1-I5	IW	X	X	-	-	X	-	-
84	10.08.1999	LYA-R8-1-I6	IW	X	X	-	-	-	7,48	32
85	10.08.1999	LYA-R8-1-I7	IW	X	X	-	-	X	-	-
86	10.08.1999	LYA-R8-1-I8	IW	X	X	-	-	-	7,84	33
87	10.08.1999	LYA-R8-1-I9	IW	X	X	-	-	X	-	-
88	10.08.1999	LYA-R8-1-I10	IW	X	X	-	-	-	7,90	24
89	10.08.1999	LYA-R8-2-I1	TI	X	X	-	-	X	7,09	567
90	10.08.1999	LYA-R8-2-I2	IW	X	X	-	-	-	-	68
91	10.08.1999	LYA-R8-2-I3	IW	X	X	-	-	-	7,39	33
92	10.08.1999	LYA-R8-2-I4	IW	X	X	-	-	X	-	446
93	10.08.1999	LYA-R8-2-I5	IW	X	X	-	-	X	8,79	21
94	10.08.1999	LYA-R8-2-I6	IW	X	X	-	-	-	-	-
95	10.08.1999	LYA-R8-2-I7	IW	X	X	-	-	X	7,45	84
96	10.08.1999	LYA-R8-2-I8	IW	X	X	-	-	X	7,76	54
97	10.08.1999	LYA-R8-2-I9	IW	X	X	-	-	-	-	-
98	10.08.1999	LYA-R17-1-I39	TI	X	X	-	-	X	6,33	13
99	10.08.1999	LYA-R17-1-I40	TI	X	X	-	-	X	6,74	36
100	10.08.1999	LYA-R17-1-I41	TI	X	X	X	-	X	6,46	48
101	10.08.1999	LYA-R6-1-I1	IW	X	X	-	-	-	-	-
102	10.08.1999	LYA-R6-1-I2	IW	X	X	-	-	X	7,44	42
103	10.08.1999	LYA-R6-1-I3	IW	X	X	-	-	-	8,08	54
104	10.08.1999	LYA-R6-1-I4	IW	X	X	-	-	X	-	-
105	10.08.1999	LYA-R6-1-I5	IW	X	X	-	-	X	8,17	49
106	10.08.1999	LYA-R6-1-I6	IW	X	X	-	-	X	-	-
107	10.08.1999	LYA-R6-1-I7	IW	X	X	-	-	X	7,65	55
108	10.08.1999	LYA-R6-1-I8	IW	X	X	-	-	X	-	-
109	10.08.1999	LYA-R6-1-I9	IW	X	X	-	-	-	7,76	67
110	10.08.1999	LYA-R6-1-I10	IW	X	X	-	-	-	-	-
111	10.08.1999	LYA-R6-1-I11	IW	X	X	-	-	-	7,57	55
112	10.08.1999	LYA-R6-1-I12	IW	X	X	-	-	X	-	-
113	10.08.1999	LYA-R6-1-I13	IW	X	X	-	-	X	7,37	41
114	10.08.1999	LYA-R6-1-I14	IW	X	X	-	-	X	-	-
115	10.08.1999	LYA-R6-1-I15	IW	X	X	-	-	-	7,58	51
116	10.08.1999	LYA-R6-1-I16	IW	X	X	-	-	X	-	-
117	10.08.1999	LYA-R6-1-I17	IW	X	X	-	-	-	7,99	67
118	10.08.1999	LYA-R6-1-I18	IW	X	X	-	-	-	-	-
119	11.08.1999	LYA-R7-1-I1	IW	X	X	-	-	X	7,17	78
120	11.08.1999	LYA-R7-1-I2	IW	X	X	-	-	-	-	137
121	11.08.1999	LYA-R7-1-I3	IW	X	X	-	-	-	-	-
122	11.08.1999	LYA-R7-1-I4	IW	X	X	-	-	-	7,16	66
123	11.08.1999	LYA-R7-1-I5	IW	X	X	-	-	X	7,33	-
124	11.08.1999	LYA-R7-1-I6	IW	X	X	-	-	-	-	-
125	11.08.1999	LYA-R7-1-I7	IW	X	X	-	-	-	7,42	225
126	11.08.1999	LYA-R7-1-I8	IW	X	X	-	-	-	-	171
127	11.08.1999	LYA-R7-1-I9	IW	X	X	-	-	-	-	107
128	11.08.1999	LYA-R7-1-I10	IW	X	X	-	-	X	-	-
129	11.08.1999	LYA-R7-1-I11	IW	X	X	-	-	-	7,62	111
130	11.08.1999	LYA-R7-1-I12	IW	X	X	-	-	-	7,54	91
131	11.08.1999	LYA-R7-1-I13	IW	X	X	-	-	-	-	-
132	11.08.1999	LYA-R7-1-I14	IW	X	X	-	-	-	-	101
133	11.08.1999	LYA-R7-1-I15	IW	X	X	-	-	X	7,67	-
134	11.08.1999	LYA-R7-1-I16	IW	X	X	-	-	-	-	72
135	11.08.1999	LYA-R7-1-I17	IW	X	X	-	-	-	7,66	97
136	11.08.1999	LYA-R7-1-I18	IW	X	X	-	-	-	-	89
137	11.08.1999	LYA-R7-1-I19	IW	X	X	-	-	-	7,97	129
138	11.08.1999	LYA-R7-1-I20	IW	X	X	-	-	X	-	105
139	11.08.1999	LYA-R7-1-I21	IW	X	X	-	-	-	7,79	-
140	11.08.1999	LYA-R7-1-I22	IW	X	X	-	-	-	-	141
141	11.08.1999	LYA-R7-1-I23	IW	X	X	-	-	-	-	-
142	11.08.1999	LYA-R7-1-I24	IW	X	X	-	-	-	7,73	124
143	11.08.1999	LYA-R7-1-I25	IW	X	X	-	-	X	8,10	-
144	11.08.1999	LYA-R7-1-I26	IW	X	X	-	-	-	-	104
145	11.08.1999	LYA-R7-1-I27	IW	X	X	-	-	-	7,41	200
146	11.08.1999	LYA-R7-1-I28	IW	X	X	-	-	X	7,7	-
147	11.08.1999	LYA-R7-1-I29	IW	X	X	-	-	-	-	-
148	11.08.1999	LYA-R7-1-I30	IW	X	X	-	-	X	8,05	159
149	12.08.1999	LYA-R17-S2	TI			-	-	X	7,67	1900
150	12.08.1999	LYA-R17-S3	TI	X	X	-	-	X	6,00	2060

A5-6: continuation.

				Isotopes				Chemistry		
Nr.	date	sample	type	18 O	2 H	3 H	10 Be	anion/cation	pH	LF
151	12.08.1999	LYA-R17-S5	TI	X	X	-	-	X	5,55	532
152	12.08.1999	LYA-R17-S7	TI	X	X	-	-	X	5,25	3250
153	12.08.1999	LYA-R18+50-S4	TI	X	X	-	-	X	7,36	6050
154	12.08.1999	LYA-R18+50-S5	TI	X	X	-	-	X	-	-
155	12.08.1999	LYA-R18+50-S6	TI	X	X	-	-	X	7,53	3530
156	12.08.1999	LYA-R18+50-S7	TI	X	X	-	-	X	7,61	3520
157	12.08.1999	LYA-R18+50-S8	TI	X	X	-	-	X	7,72	1730
158	12.08.1999	LYA-R18+50-S9	TI	X	X	-	-	X	7,48	3990
159	12.08.1999	LYA-R18+50-S10	TI	X	X	-	-	X	7,64	2600
160	12.08.1999	LYA-R18+50-OSL5	TI	X	X	-	-	X	-	-
161	12.08.1999	LYA-R17-OSL1	TI	X	X	-	-	X	5,78	297
162	12.08.1999	TZ-2-1-I1.	IW	X	X	X	-	-	6,64	48
163	12.08.1999	LYA 96/02	SW	X	X	X	-	X	8,82	584
164	12.08.1999	LYA 96/03	SW	X	X	X	-	X	8,37	1088
165	13.08.1999	TZ-2-2-I1	IW	X	X	-	-	X	6,59	58
166	13.08.1999	TZ-2-2-I2	IW	X	X	-	-	-	-	86
167	13.08.1999	TZ-2-2-I3	IW	X	X	-	-	-	6,26	65
168	13.08.1999	TZ-2-2-I4	IW	X	X	-	-	-	-	72
169	13.08.1999	TZ-2-2-I5	IW	X	X	-	-	X	6,45	59
170	13.08.1999	TZ-2-2-I6	IW	X	X	-	-	-	-	-
171	13.08.1999	TZ-2-2-I7	IW	X	X	-	-	-	-	-
172	13.08.1999	TZ-2-2-I8	IW	X	X	-	-	-	-	77
173	13.08.1999	TZ-2-2-I9	IW	X	X	-	-	-	6,96	103
174	13.08.1999	TZ-2-2-I10	IW	X	X	-	-	X	-	89
175	13.08.1999	TZ-2-2-I11	IW	X	X	-	-	-	6,77	71
176	13.08.1999	TZ-2-2-I12	IW	X	X	-	-	-	-	57
177	13.08.1999	TZ-2-2-I13	IW	X	X	-	-	-	6,78	141
178	13.08.1999	TZ-2-2-I14	IW	X	X	-	-	-	-	87
179	13.08.1999	TZ-2-2-I15	IW	X	X	-	-	X	6,69	68
180	13.08.1999	TZ-2-2-I16	IW	X	X	-	-	-	-	138
181	13.08.1999	TZ-2-2-I17	IW	X	X	-	-	-	7,03	80
182	13.08.1999	TZ-2-2-I18	IW	X	X	-	-	-	-	75
183	13.08.1999	TZ-2-2-I19	IW	X	X	-	-	-	6,75	67
184	13.08.1999	TZ-2-2-I20	IW	X	X	-	-	X	-	55
185	13.08.1999	TZ-2-2-I21	IW	X	X	-	-	-	6,45	65
186	13.08.1999	TZ-2-2-I22	IW	X	X	-	-	-	-	-
187	13.08.1999	TZ-2-2-I23	IW	X	X	-	-	-	-	-
188	13.08.1999	TZ-2-2-I24	IW	X	X	-	-	-	-	-
189	13.08.1999	TZ-2-2-I25	IW	X	X	-	-	X	6,77	78
190	13.08.1999	TZ-2-2-I26	IW	X	X	-	-	-	-	79
191	13.08.1999	TZ-2-2-I27	IW	X	X	-	-	-	6,48	49
192	13.08.1999	TZ-2-2-I28	IW	X	X	-	-	-	-	-
193	13.08.1999	TZ-2-2-I29	IW	X	X	-	-	X	6,43	57
194	13.08.1999	TZ-2-2-I30	IW	X	X	-	-	-	-	-
195	13.08.1999	TZ-2-2-I31	IW	X	X	-	-	X	6,87	102
196	13.08.1999	TZ-2-2-I32	IW	X	X	-	-	-	-	-
197	13.08.1999	TZ-2-2-I33	MW	X	X	X	-	-	7,03	167
198	13.08.1999	TZ-2-2-I34	IW	X	X	-	-	-	-	-
199	13.08.1999	TZ-2-3-I1	IW	X	X	X	-	-	-	-
200	13.08.1999	TZ-2-3-I2	IW	X	X	-	-	-	6,45	52
201	13.08.1999	TZ-2-3-I3	IW	X	X	-	-	-	-	-
202	13.08.1999	TZ-2-3-I4	IW	X	X	-	-	-	6,53	58
203	14.08.1999	LYA-96/05	SW	X	X	X	-	X	6,85	350
204	14.08.1999	LYA-96/06	SW	X	X	X	-	X	6,72	364
205	14.08.1999	LYA-96/07	SW	X	X	X	-	X	6,41	119
206	14.08.1999	LYA-96/08	SW	X	X	X	-	X	7,09	134
207	14.08.1999	LYA-96/09	SW	X	X	X	-	X	7,62	11090
208	14.08.1999	LYA-96/10	SW	X	X	X	-	X	7,54	9040
209	14.08.1999	R18+50 S2	TI	X	X	-	-	X	-	-
210	14.08.1999	2TZ-1-1	TI	X	X	-	-	X	7,34	1526
211	14.08.1999	2TZ-1-2	TI	X	X	-	-	X	7,49	639
212	14.08.1999	2TZ-1-3	TI	X	X	-	-	X	5,88	563
213	14.08.1999	2TZ-1-4	TI	X	X	-	-	X	6,91	773
214	14.08.1999	2TZ-2-1	TI	X	X	-	-	X	7,15	1567
215	14.08.1999	2TZ-2-2	TI	X	X	-	-	X	7,59	1066
216	14.08.1999	2TZ-2-3	TI	X	X	-	-	X	7,53	1717
217	14.08.1999	2TZ-2-4	TI	X	X	-	-	X	7,52	3670
218	14.08.1999	2TZ-2-5	TI	X	X	-	-	X	7,45	4750
219	14.08.1999	2TZ-2-6	TI	X	X	-	-	X	7,22	5870
220	14.08.1999	3TZ-1-1	TI	X	X	-	-	X	5,69	541
221	14.08.1999	3TZ-1-2	TI	X	X	-	-	X	5,47	772
222	14.08.1999	3TZ-1-3	TI	X	X	-	-	X	5,74	498
223	14.08.1999	3TZ-1-7	TI	X	X	-	-	X	5,62	839
224	14.08.1999	3TZ-2-1	TI	X	X	-	-	X	5,99	339
225	14.08.1999	3TZ-2-2	TI	X	X	-	-	X	5,38	328

A5-6: continuation.

				Isotopes				Chemistry		
Nr.	date	sample	type	18 O	2 H	3 H	10 Be	anion/cation	pH	LF
226	14.08.1999	3TZ-2-3	TI	X	X	-	-	X	5,83	931
227	14.08.1999	3TZ-2-5	TI	X	X	-	-	X	6,33	377
228	14.08.1999	3TZ-2-6	TI	X	X	-	-	X	6,42	525
229	14.08.1999	3TZ-2-7	TI	X	X	-	-	X	6,49	1480
230	14.08.1999	3TZ-2-8	TI	X	X	-	-	X	7,03	1890
231	14.08.1999	3TZ-3-1	TI	X	X	-	-	X	-	-
232	14.08.1999	3TZ-3-2	TI	X	X	-	-	X	7,45	2530
233	14.08.1999	3TZ-4-2	TI	X	X	-	-	X	7,26	11380
234	14.08.1999	3TZ-4-3	TI	X	X	-	-	X	7,33	10010
235	14.08.1999	3TZ-4-4	TI	X	X	-	-	X	7,06	5620
236	14.08.1999	3TZ-5-1	TI	X	X	-	-	X	7,61	810
237	14.08.1999	3TZ-5-2	TI	X	X	-	-	X	7,33	1127
238	14.08.1999	3TZ-5-4	TI	X	X	-	-	X	7,46	1266
239	14.08.1999	R17-S1	TI	X	X	-	-	X	7,55	1443
240	15.08.1999	LYA-96/04	SW	X	X	X	-	X	7,61	132
241	15.08.1999	LYA-96/11	SW	X	X	X	-	X	7,84	227
242	15.08.1999	LYA-96/12	SW	X	X	X	-	X	7,39	246
243	15.08.1999	LYA-96/13	SW	X	X	X	-	X	8,13	303
244	15.08.1999	TZ-2-4-I1	IW	X	X	-	-	X	-	-
245	15.08.1999	TZ-2-4-I2	IW	X	X	-	-	-	6,66	62
246	15.08.1999	TZ-2-4-I3	IW	X	X	-	-	X	-	-
247	15.08.1999	TZ-2-4-I4	IW	X	X	-	-	-	6,80	50
248	15.08.1999	TZ-2-4-I5	IW	X	X	-	-	X	-	-
249	15.08.1999	TZ-2-4-I6	IW	X	X	-	-	-	6,69	41
250	15.08.1999	TZ-2-4-I7	IW	X	X	-	-	X	-	-
251	15.08.1999	TZ-2-4-I8	IW	X	X	-	-	-	6,31	40
252	15.08.1999	TZ-2-4-I9	IW	X	X	-	-	X	-	-
253	15.08.1999	TZ-2-4-I10	IW	X	X	-	-	-	6,62	41
254	15.08.1999	TZ-2-4-I11	IW	X	X	-	-	X	-	-
255	15.08.1999	TZ-2-4-I12	IW	X	X	-	-	-	6,70	48
256	15.08.1999	TZ-2-4-I13	IW	X	X	-	-	-	-	-
257	15.08.1999	TZ-2-4-I14	IW	X	X	-	-	-	6,65	80
258	15.08.1999	TZ-2-4-I15	IW	X	X	-	-	-	-	-
259	15.08.1999	TZ-2-4-I16	IW	X	X	-	-	-	6,78	79
260	15.08.1999	TZ-2-4-I17	IW	X	X	X	-	-	-	-
261	15.08.1999	TZ-2-4-I18	IW	X	X	-	-	-	6,25	55
262	15.08.1999	TZ-2-4-I19	IW	X	X	-	-	-	-	-
263	15.08.1999	LYA-99/03	RW	X	X	X	-	X	6,43	51
264	16.08.1999	R17-2-I1	IW	X	X	-	-	-	7,21	420
265	16.08.1999	R17-2-I2	IW	X	X	-	-	-	7,83	557
266	16.08.1999	R17-2-I3	IW	X	X	-	-	-	-	-
267	16.08.1999	R17-2-I4	IW	X	X	-	-	-	7,68	644
268	16.08.1999	R17-2-I5	IW	X	X	-	-	-	-	-
269	16.08.1999	R17-2-I6	IW	X	X	-	-	-	7,80	452
270	16.08.1999	R17-2-I7	IW	X	X	-	-	-	-	-
271	16.08.1999	R17-2-I8	IW	X	X	-	-	-	7,97	397
272	16.08.1999	R17-2-I9	IW	X	X	-	-	-	-	-
273	16.08.1999	R17-2-I10	IW	X	X	-	-	-	-	-
274	16.08.1999	R17-2-I11	IW	X	X	-	-	-	-	-
275	16.08.1999	R17-2-I12	IW	X	X	-	-	-	7,94	384
276	16.08.1999	R17-2-I13	IW	X	X	-	-	-	-	-
277	16.08.1999	R17-2-I14	IW	X	X	-	-	-	8,11	427
278	16.08.1999	R17-2-I15	IW	X	X	-	-	X	-	-
279	16.08.1999	R17-2-I16	IW	X	X	-	-	-	7,78	187
280	16.08.1999	R17-2-I17	IW	X	X	-	-	-	-	-
281	16.08.1999	R17-2-I18	IW	X	X	-	-	-	7,94	244
282	16.08.1999	R17-2-I19	IW	X	X	-	-	-	-	-
283	16.08.1999	R17-2-I20	IW	X	X	-	-	-	8,1	301
284	16.08.1999	R17-2-I21	IW	X	X	-	-	-	7,93	406
285	16.08.1999	R17-2-I22	IW	X	X	-	-	-	7,67	237
286	16.08.1999	R17-2-I23	IW	X	X	X	-	-	-	-
287	16.08.1999	R17-2-I24	IW	X	X	-	-	-	7,80	285
288	16.08.1999	R17-2-I25	IW	X	X	-	-	-	-	-
289	16.08.1999	R17-2-I26	IW	X	X	-	-	-	7,89	160
290	16.08.1999	R17-2-I27	IW	X	X	-	-	-	-	-
291	16.08.1999	R17-2-I28	IW	X	X	-	-	-	7,58	937
292	16.08.1999	R17-2-I29	IW	X	X	-	-	-	-	-
293	16.08.1999	R17-2-I30	IW	X	X	-	-	-	7,25	273
294	16.08.1999	R17-2-97-I1	SP	X	X	X	-	X	6,99	429
295	17.08.1999	LYA-99/04	RW	X	X	X	-	X	6,23	42
296	17.08.1999	R1-1-I1	IW	X	X	-	-	-	7,54	150
297	17.08.1999	R1-1-I2	IW	X	X	-	-	-	-	-
298	17.08.1999	R1-1-I3	IW	X	X	-	-	-	-	-
299	17.08.1999	TZ-2-5-I1	IW	X	X	-	-	X	7,93	991
300	17.08.1999	TZ-2-5-I2	IW	X	X	-	-	X	8,07	494

A5-6: continuation.

				Isotopes				Chemistry		
Nr.	date	sample	type	18 O	2 H	3 H	10 Be	anion/cation	pH	LF
301	17.08.1999	TZ-2-5-I3	IW	X	X	-	-	X	8,19	163
302	17.08.1999	TZ-2-5-I4	IW	X	X	-	-	X	7,89	736
303	17.08.1999	TZ-2-5-I5	IW	X	X	-	-	X	8,17	180
304	17.08.1999	TZ-2-5-I6	IW	X	X	-	-	X	7,74	1455
305	17.08.1999	TZ-2-5-I7	IW	X	X	-	-	X	7,60	69
306	17.08.1999	TZ-2-5-I8	IW	X	X	-	-	X	7,55	89
307	17.08.1999	TZ-2-5-I9	IW	X	X	-	-	X	7,62	64
308	17.08.1999	TZ-2-5-I10	IW	X	X	-	-	X	8,08	140
309	17.08.1999	TZ-2-6-I1	IW	X	X	-	-	-	8,08	177
310	17.08.1999	TZ-2-6-I2	IW	X	X	-	-	X	8,03	81
311	18.08.1999	LYA-98/01	GW	X	X	X	-	X	6,51	436
312	18.08.1999	LYA-98/02	GW	X	X	X	-	X	6,42	419
313	18.08.1999	LYA-98/03	GW	X	X	X	-	X	6,06	98
314	18.08.1999	LYA-98/04	GW	X	X	-	-	X	7,11	116
315	18.08.1999	LYA-98/05	GW	X	X	-	-	X	6,21	151
316	18.08.1999	LYA-AL-1	TI	X	X	X	-	-	-	-
317	18.08.1999	LYA-AL-2	TI	X	X	X	-	-	-	-
318	18.08.1999	LYA-AL-3	TI	X	X	-	-	-	-	-
319	18.08.1999	LYA-AL-4	TI	X	X	-	-	-	-	-
320	18.08.1999	LYA-AL-5	TI	X	X	X	-	-	-	-
321	18.08.1999	LYA-96/14	SW	X	X	X	-	X	6,64	303
322	18.08.1999	R17+30-S1	TI	X	X	-	-	X	5,46	4940
323	18.08.1999	R17+30-S2	TI	X	X	-	-	X	6,88	6270
324	18.08.1999	1TZ-1-2	TI	X	X	-	-	X	7,25	1434
325	18.08.1999	1TZ-1-3	TI	X	X	-	-	X	6,94	1570
326	18.08.1999	1TZ-1-4	TI	X	X	-	-	X	6,52	902
327	18.08.1999	1TZ-1-6	TI	X	X	-	-	X	6,90	996
328	18.08.1999	1TZ-2-1	TI	X	X	-	-	X	6,01	779
329	18.08.1999	1TZ-2-3	TI	X	X	-	-	X	7,05	1396
330	18.08.1999	1TZ-3-1	TI	X	X	-	-	X	6,14	334
331	18.08.1999	1TZ-3-2	TI	X	X	-	-	X	6,20	445
332	18.08.1999	1TZ-3-3	TI	X	X	-	-	X	5,61	361
333	19.08.1999	R10-1-I1	IW	X	X	-	-	X	8,15	141
334	19.08.1999	R10-1-I2	IW	X	X	-	-	-	7,69	145
335	19.08.1999	R10-1-I3	IW	X	X	-	-	X	-	-
336	19.08.1999	R10-1-I4	IW	X	X	-	-	-	7,99	118
337	19.08.1999	R10-1-I5	IW	X	X	-	-	X	-	-
338	19.08.1999	R10-1-I6	IW	X	X	-	-	X	7,96	96
339	19.08.1999	R10-1-I7	IW	X	X	-	-	-	-	-
340	19.08.1999	R10-1-I8	IW	X	X	-	-	-	7,33	90
341	19.08.1999	R10-1-I9	IW	X	X	-	-	-	-	-
342	19.08.1999	R10-1-I10	IW	X	X	-	-	X	8,20	171
343	19.08.1999	R10-1-I11	IW	X	X	X	-	-	-	-
344	19.08.1999	R10-1-I12	IW	X	X	-	-	-	7,90	102
345	19.08.1999	R10-1-I13	IW	X	X	-	-	-	-	-
346	19.08.1999	R10-1-I14	IW	X	X	-	-	-	7,47	56
347	19.08.1999	R10-1-I15	IW	X	X	-	-	-	-	-
348	19.08.1999	R10-1-I16	IW	X	X	-	-	-	7,90	138
349	19.08.1999	R10-1-I17	IW	X	X	-	-	-	-	-
350	19.08.1999	R10-1-I18	IW	X	X	-	-	-	8,00	133
351	19.08.1999	R10-1-I19	IW	X	X	-	-	-	-	-
352	19.08.1999	R10-1-I20	IW	X	X	-	-	X	7,77	105
353	19.08.1999	R10-1-I21	IW	X	X	-	-	-	-	-
354	19.08.1999	R10-1-I22	IW	X	X	-	-	-	-	-
355	19.08.1999	R10-1-I23	IW	X	X	-	-	-	-	-
356	19.08.1999	R10-1-I24	IW	X	X	-	-	-	7,43	90
357	19.08.1999	R10-1-I25	IW	X	X	-	-	-	-	-
358	19.08.1999	R10-1-I26	IW	X	X	-	-	X	7,86	106
359	19.08.1999	R10-1-I27	IW	X	X	-	-	-	-	-
360	19.08.1999	R10-1-I28	IW	X	X	-	-	-	7,80	102
361	19.08.1999	R10-1-I29	IW	X	X	-	-	-	-	-
362	19.08.1999	R10-1-I30	IW	X	X	-	-	X	7,26	76
363	19.08.1999	R10-1-I31	IW	X	X	-	-	-	-	-
364	19.08.1999	R10-1-I32	IW	X	X	-	-	-	7,31	111
365	19.08.1999	R10-1-I33	IW	X	X	-	-	-	-	-
366	19.08.1999	R10-1-I34	IW	X	X	-	-	-	7,37	92
367	19.08.1999	R10-1-I35	IW	X	X	-	-	X	-	-
368	19.08.1999	R10-1-I36	IW	X	X	-	-	-	7,43	71
369	19.08.1999	R10-1-I37	IW	X	X	-	-	-	-	-
370	19.08.1999	R10-1-I38	IW	X	X	-	-	-	-	-
371	19.08.1999	R10-1-I39	IW	X	X	-	-	-	7,65	114
372	19.08.1999	R10-1-I40	IW	X	X	-	-	X	7,60	93
373	19.08.1999	R10-1-I41	IW	X	X	-	-	-	-	-
374	19.08.1999	R10-1-I42	IW	X	X	-	-	-	7,85	56
375	19.08.1999	R10-1-I43	IW	X	X	-	-	-	-	-

A5-6: continuation.

				Isotopes				Chemistry		
Nr.	date	sample	type	18 O	2 H	3 H	10 Be	anion/cation	pH	LF
376	19.08.1999	R10-1-I44	IW	X	X	-	-	-	7,80	76
377	19.08.1999	R10-1-I45	IW	X	X	-	-	X	-	-
378	19.08.1999	R10-1-I46	IW	X	X	-	-	-	7,34	91
379	19.08.1999	R10-1-I47	IW	X	X	-	-	-	-	-
380	19.08.1999	R10-1-I48	IW	X	X	-	-	-	7,21	111
381	19.08.1999	R10-1-I49	IW	X	X	-	-	-	-	-
382	19.08.1999	R10-1-I50	IW	X	X	-	-	-	7,40	118
383	19.08.1999	R10-1-I51	IW	X	X	-	-	-	-	-
384	19.08.1999	R10-1-I52	IW	X	X	-	-	-	-	-
385	19.08.1999	R10-1-I53	IW	X	X	-	-	-	-	-
386	19.08.1999	R10-1-I54	IW	X	X	-	-	-	7,64	142
387	19.08.1999	R10-1-I55	IW	X	X	-	-	-	-	-
388	19.08.1999	R10-1-I56	IW	X	X	-	-	-	7,43	88
389	19.08.1999	R10-1-I57	IW	X	X	-	-	-	-	-
390	19.08.1999	R10-2-I1	IW	X	X	-	-	-	-	-
391	19.08.1999	R10-2-I2	IW	X	X	-	-	X	7,68	161
392	19.08.1999	R10-2-I3	IW	X	X	-	-	-	-	-
393	19.08.1999	R10-2-I4	IW	X	X	-	-	X	7,60	299
394	19.08.1999	R10-2-I5	IW	X	X	X	-	-	-	-
395	19.08.1999	R10-2-I6	IW	X	X	-	-	-	8,20	125
396	19.08.1999	R8+50-S14/15	TI	X	X	-	-	X	6,33	511
397	19.08.1999	R8+50-S17	TI	X	X	-	-	X	6,33	511
398	19.08.1999	R8+50-S18	TI	X	X	-	-	-	6,29	282
399	19.08.1999	R8+50-S19	TI	X	X	-	-	-	6,29	282
400	19.08.1999	R8+50-S20/21/22	TI	X	X	-	-	X	6,01	1117
401	19.08.1999	R8+50-S23/24	TI	X	X	-	-	X	5,99	584
402	19.08.1999	R8+50-S25	TI	X	X	-	-	X	5,95	561
403	19.08.1999	R8+50-S26/27	TI	X	X	-	-	X	5,95	561
404	19.08.1999	R8+50-S36	TI	X	X	-	-	-	6,44	1979
405	19.08.1999	R14+40-S1	TI	X	X	-	-	X	5,34	391
406	19.08.1999	R14+40-S3	TI	X	X	-	-	X	5,15	898
407	19.08.1999	R14+40-S4	TI	X	X	-	-	X	5,04	2840
408	19.08.1999	R14+40-S5	TI	X	X	-	-	X	5,27	7370
409	19.08.1999	R22+60-S8	TI	X	X	-	-	-	7,26	1907
410	19.08.1999	R33-A1-15	TI	X	X	-	-	X	7,04	945
411	19.08.1999	R33-A1-16	TI	X	X	-	-	X	7,12	918
412	19.08.1999	R33-A1-17	TI	X	X	-	-	X	7,43	630
413	19.08.1999	R33-A1-18	TI	X	X	-	-	X	7,39	576
414	19.08.1999	R33-A1-19	TI	X	X	-	-	X	7,32	446
415	19.08.1999	R33-A1-21	TI	X	X	-	-	X	5,58	281
416	20.08.1999	R10-1-I58	TI	X	X	X	-	-	-	-
417	20.08.1999	R10-1-Be-1	IW	X	X	-	X	-	-	-
418	20.08.1999	R10-1-Be-2	IW	X	X	-	X	-	-	-
419	20.08.1999	R10-1-Be-3	IW	X	X	-	X	-	-	-
420	20.08.1999	R10-1-Be-4	IW	X	X	-	X	-	-	-
421	20.08.1999	R10-1-Be-5	IW	X	X	-	X	-	-	-
422	20.08.1999	R10-1-Be-6	IW	X	X	-	X	-	-	-
423	20.08.1999	R10-1-Be-7	IW	X	X	-	X	-	-	-
424	20.08.1999	R10-1-Be-8	IW	X	X	-	X	-	-	-
425	20.08.1999	R10-1-Be-9	IW	X	X	-	X	-	-	-
426	20.08.1999	R10-1-Be-10	IW	X	X	-	X	-	-	-
427	20.08.1999	R10-1-E-1	IW	X	X	X	-	X	-	-
428	20.08.1999	R10-1-E-2	IW	X	X	X	-	X	-	-
429	20.08.1999	R10-1-E-3	IW	X	X	X	-	X	-	-
430	20.08.1999	R10-1-E-4	IW	X	X	X	-	X	-	-
431	20.08.1999	R10-1-E-5	IW	X	X	X	-	X	-	-
432	21.08.1999	LYA-99/05	RW	X	X	X	-	X	6,13	50
433	21.08.1999	R22-1-I1	IW	X	X	-	-	X	-	-
434	21.08.1999	R22-1-I2	IW	X	X	-	-	-	8,11	138
435	21.08.1999	R22-1-I3	IW	X	X	-	-	-	8,00	280
436	21.08.1999	LYA-97/03	SP	X	X	X	-	X	6,52	67
437	21.08.1999	LYA-97/04	SP	X	X	X	-	X	6,55	112
438	21.08.1999	LYA-97/05	SP	X	X	X	-	X	6,70	62
439	21.08.1999	LYA-97/06	SP	X	X	X	-	X	6,65	98
440	21.08.1999	LYA-97/07	SP	X	X	X	-	X	6,85	55
441	21.08.1999	R32-1-I1	IW	X	X	X	-	X	5,86	74
442	21.08.1999	R32-2-I1	IW	X	X	X	-	X	6,16	37
443	21.08.1999	R32-2-I2	IW	X	X	-	-	-	-	-
444	21.08.1999	R32-2-I3	IW	X	X	-	-	-	-	-
445	21.08.1999	R32-2-I4	IW	X	X	-	-	-	-	-
446	21.08.1999	R32-2-I5	IW	X	X	-	-	X	-	-
447	21.08.1999	R32-2-I6	IW	X	X	-	-	-	6,07	90
448	21.08.1999	R32-2-I7	IW	X	X	-	-	-	6,69	128
449	21.08.1999	R32-2-I8	IW	X	X	-	-	-	-	-
450	21.08.1999	R32-2-I9	IW	X	X	-	-	-	6,50	93

A5-6: continuation.

				Isotopes				Chemistry		
Nr.	date	sample	type	18 O	2 H	3 H	10 Be	anion/cation	pH	LF
451	21.08.1999	R32-2-I10	IW	X	X	-	-	X	-	-
452	21.08.1999	R32-2-I11	IW	X	X	-	-	-	-	-
453	21.08.1999	R32-2-I12	IW	X	X	-	-	-	5,95	110
454	21.08.1999	R32-2-I13	IW	X	X	-	-	-	-	-
455	21.08.1999	R32-2-I14	IW	X	X	-	-	-	6,38	93
456	21.08.1999	R32-2-I15	IW	X	X	-	-	X	-	-
457	21.08.1999	R32-2-I16	IW	X	X	-	-	-	-	-
458	21.08.1999	R32-2-I17	IW	X	X	-	-	-	6,11	72
459	21.08.1999	R32-2-I18	IW	X	X	-	-	-	-	-
460	21.08.1999	R32-2-I19	IW	X	X	-	-	-	6,21	100
461	21.08.1999	R32-2-I20	IW	X	X	-	-	X	-	-
462	21.08.1999	R32-2-I21	IW	X	X	-	-	-	-	-
463	21.08.1999	R32-2-I22	IW	X	X	-	-	-	5,99	83
464	21.08.1999	R32-2-I23	IW	X	X	-	-	-	-	-
465	21.08.1999	R32-2-I24	IW	X	X	-	-	-	5,78	73
466	21.08.1999	R32-2-I25	IW	X	X	-	-	-	-	-
467	21.08.1999	R32-2-I26	IW	X	X	-	-	-	-	-
468	21.08.1999	R32-2-I27	IW	X	X	-	-	-	6,02	115
469	21.08.1999	R32-2-I28	IW	X	X	-	-	-	-	-
470	21.08.1999	R32-2-I29	IW	X	X	-	-	-	-	-
471	21.08.1999	R32-2-I30	IW	X	X	X	-	X	6,22	48
472	21.08.1999	R32-2-I31	IW	X	X	X	-	X	6,32	37
473	21.08.1999	R32-2-I32	IW	X	X	X	-	X	5,89	145
474	21.08.1999	R32-2-I33	IW	X	X	X	-	-	-	-
475	21.08.1999	R32-2-I34	IW	X	X	X	-	-	-	-
476	22.08.1999	R32-3-I1	IW	X	X	X	-	X	6,20	89
477	22.08.1999	R32-4-I1	IW	X	X	-	-	-	-	-
478	22.08.1999	R32-5-I1	IW	X	X	-	-	-	-	-
479	22.08.1999	R32-5-I2	IW	X	X	-	-	-	6,27	123
480	22.08.1999	LYA-98/06	GW	X	X	-	-	X	5,85	169
481	22.08.1999	LYA-AL-6	TI	X	X	-	-	-	6,56	251
482	23.08.1999	LYA-99/06	RW	X	X	X	-	X	6,03	22
483	17.08.1999	R17-1-Sr-1	IW	X	X	-	-	X	-	-
484	17.08.1999	R17-1-Sr-2	IW	X	X	-	-	X	-	-
485	17.08.1999	R17-2-I31	IW	X	X	-	-	X	-	-
486	17.08.1999	R17-2-I32	IW	X	X	-	-	X	-	-
487	23.08.1999	TZ-3-1-I1	IW	X	X	-	-	X	7,31	114
488	23.08.1999	TZ-3-1-I2	IW	X	X	-	-	-	7,32	101
489	23.08.1999	TZ-3-1-I3	IW	X	X	-	-	-	7,51	232
490	23.08.1999	TZ-3-1-I4	IW	X	X	-	-	-	-	-
491	23.08.1999	TZ-3-1-I5	IW	X	X	-	-	X	7,16	76
492	23.08.1999	TZ-3-1-I6	IW	X	X	-	-	-	-	-
493	23.08.1999	TZ-3-1-I7	IW	X	X	-	-	-	7,10	95
494	23.08.1999	TZ-3-1-I8	IW	X	X	-	-	-	-	-
495	23.08.1999	TZ-3-1-I9	IW	X	X	-	-	-	7,10	80
496	23.08.1999	TZ-3-1-I10	IW	X	X	-	-	X	-	-
497	23.08.1999	TZ-3-1-I11	IW	X	X	-	-	-	-	-
498	23.08.1999	TZ-3-1-I12	IW	X	X	-	-	-	7,24	75
499	23.08.1999	TZ-3-1-I13	IW	X	X	-	-	-	-	-
500	23.08.1999	TZ-3-1-I14	IW	X	X	-	-	-	7,21	78
501	23.08.1999	TZ-3-1-I15	IW	X	X	-	-	-	-	-
502	23.08.1999	TZ-3-1-I16	IW	X	X	-	-	X	7,14	97
503	23.08.1999	TZ-3-1-I17	IW	X	X	-	-	-	-	-
504	23.08.1999	TZ-3-1-I18	IW	X	X	-	-	-	7,19	75
505	23.08.1999	TZ-3-1-I19	IW	X	X	-	-	-	-	-
506	23.08.1999	TZ-3-1-I20	IW	X	X	-	-	-	7,15	89
507	23.08.1999	TZ-3-1-I21	IW	X	X	-	-	X	-	-
508	23.08.1999	TZ-3-1-I22	IW	X	X	-	-	-	8,08	108
509	23.08.1999	TZ-3-1-I23	IW	X	X	-	-	-	7,21	77
510	23.08.1999	TZ-3-1-I24	IW	X	X	-	-	-	7,19	93
511	23.08.1999	TZ-3-1-I25	IW	X	X	-	-	X	7,17	92
512	23.08.1999	TZ-3-1-I26	IW	X	X	-	-	-	-	-
513	23.08.1999	TZ-3-1-I27	IW	X	X	-	-	-	7,18	93
514	23.08.1999	TZ-3-1-I28	IW	X	X	-	-	-	-	-
515	23.08.1999	TZ-3-1-I29	IW	X	X	-	-	-	7,00	72
516	23.08.1999	TZ-3-1-I30	IW	X	X	-	-	-	6,96	96
517	23.08.1999	TZ-3-1-I31	IW	X	X	-	-	-	7,51	1468
518	23.08.1999	TZ-3-1-I32	IW	X	X	-	-	-	7,84	548
519	23.08.1999	TZ-3-1-I33	IW	X	X	-	-	-	7,81	469
520	23.08.1999	TZ-3-1-I34	IW	X	X	-	-	-	7,9	221
521	23.08.1999	TZ-3-1-I35	IW	X	X	-	-	-	7,98	190
522	23.08.1999	TZ-3-1-I36	IW	X	X	X	-	-	6,69	258
523	24.08.1999	LYA-99/07	RW	X	X	X	-	X	5,92	26
524	24.08.1999	R-20-1-I1	IW	X	X	-	-	X	7,11	175
525	24.08.1999	R-20-1-I2	IW	X	X	-	-	-	6,77	63

A5-6: continuation.

				Isotopes				Chemistry		
Nr.	date	sample	type	18 O	2 H	3 H	10 Be	anion/cation	pH	LF
526	24.08.1999	R-20-1-I3	IW	X	X	-	-	-	6,74	70
527	24.08.1999	R-20-1-I4	IW	X	X	-	-	-	-	-
528	24.08.1999	R-20-1-I5	IW	X	X	-	-	X	6,92	111
529	24.08.1999	R-20-1-I6	IW	X	X	-	-	-	-	-
530	24.08.1999	R-20-1-I7	IW	X	X	-	-	-	6,71	68
531	24.08.1999	R-20-1-I8	IW	X	X	-	-	-	-	-
532	24.08.1999	R-20-1-I9	IW	X	X	-	-	-	6,72	55
533	24.08.1999	R-20-1-I10	IW	X	X	-	-	-	7,10	95
534	24.08.1999	R-20-1-I11	IW	X	X	-	-	-	7,19	110
535	24.08.1999	R-20-1-I12	IW	X	X	-	-	-	-	-
536	24.08.1999	R-20-1-I13	IW	X	X	-	-	-	-	-
537	25.08.1999	LYA-96/15	SW	X	X	X	-	X	6,74	316
538	25.08.1999	LYA-99/08	RW	X	X	-	-	-	5,83	104
539	25.08.1999	LYA-96/16	SW	X	X	-	-	-	-	-
540	26.08.1999	LYA-99/09	RW	X	X	X	-	X	6,06	50
541	26.08.1999	LYA-96/17	SW	X	X	X	-	X	8,39	23300
542	26.08.1999	LYA-98/07	GW	X	X	X	-	X	7,01	313
543	26.08.1999	LYA-98/08	GW	X	X	X	-	X	6,42	220
544	26.08.1999	LYA-98/09	GW	X	X	X	-	-	7,02	609
545	26.08.1999	R-19-1-I1	IW	X	X	-	-	-	6,98	138
546	26.08.1999	R-19-1-I2	IW	X	X	-	-	-	7,06	126
547	26.08.1999	R-19-1-I3	IW	X	X	X	-	X	-	-
548	26.08.1999	R-19-1-I4	IW	X	X	-	-	-	7,01	139
549	26.08.1999	R-19-1-I5	IW	X	X	-	-	-	-	-
550	26.08.1999	R-19-1-I6	IW	X	X	-	-	X	6,56	140
551	26.08.1999	LYA-97/08	SP	X	X	X	-	X	6,61	33
552	26.08.1999	LYA-97/09	SP	X	X	X	-	X	6,37	45
553	26.08.1999	R33-A1-13	TI	X	X	-	-	X	6,71	2140
554	26.08.1999	R8+50-S1/2	TI	X	X	-	-	X	6,34	852
555	26.08.1999	R8+50-S3/4	TI	X	X	-	-	X	6,32	652
556	26.08.1999	R8+50-S5/6	TI	X	X	-	-	X	6,06	527
557	26.08.1999	R8+50-S7	TI	X	X	-	-	X	6,21	465
558	26.08.1999	R9+85-S1	TI	X	X	-	-	X	7,13	556
559	26.08.1999	R9+85-S2	TI	X	X	-	-	X	7,15	482
560	26.08.1999	R9+85-S4	TI	X	X	-	-	X	7,37	1154
561	26.08.1999	R9+85-S5	TI	X	X	-	-	X	7,29	880
562	28.08.1999	LYA-99/10	RW	X	X	X	-	X	6,22	70
563	28.08.1999	L-21-1-I1	IW	X	X	-	-	X	5,57	81
564	28.08.1999	L-21-1-I2	IW	X	X	-	-	X	5,72	60
565	28.08.1999	L-21-1-I3	IW	X	X	-	-	X	5,62	61
566	28.08.1999	L-21-1-I4	IW	X	X	X	-	-	-	-
567	28.08.1999	L-21-1-I5	IW	X	X	-	-	X	5,47	50
568	28.08.1999	L-21-1-I6	IW	X	X	-	-	-	-	-
569	28.08.1999	L-21-1-I7	IW	X	X	-	-	-	5,58	45
570	28.08.1999	L-21-1-I8	IW	X	X	-	-	-	-	-
571	28.08.1999	L-21-1-I9	IW	X	X	-	-	-	5,56	58
572	28.08.1999	L-21-1-I10	IW	X	X	-	-	X	5,61	62
573	28.08.1999	L-21-1-I11	IW	X	X	-	-	-	5,75	59
574	28.08.1999	L-21-1-I12	IW	X	X	X	-	-	-	-
575	28.08.1999	L-21-1-I13	IW	X	X	-	-	-	5,52	63
576	28.08.1999	L-21-1-I14	IW	X	X	-	-	-	-	-
577	28.08.1999	L-21-1-I15	IW	X	X	-	-	X	5,78	72
578	28.08.1999	L-21-1-I16	IW	X	X	-	-	-	-	-
579	28.08.1999	L-21-1-I17	IW	X	X	-	-	-	5,74	63
580	28.08.1999	L-21-1-I18	IW	X	X	-	-	-	-	-
581	28.08.1999	L-21-1-I19	IW	X	X	-	-	-	5,87	49
582	28.08.1999	L-21-1-I20	IW	X	X	-	-	X	5,83	45
583	28.08.1999	L-21-1-I21	IW	X	X	-	-	-	5,66	86
584	28.08.1999	L-21-1-I22	IW	X	X	-	-	-	5,80	73
585	28.08.1999	L-21-1-I23	IW	X	X	-	-	X	5,80	69
586	28.08.1999	L-21-1-I24	IW	X	X	-	-	X	5,98	62
587	28.08.1999	L-21-1-I25 (head)	IW	X	X	X	-	X	6,10	140
588	28.08.1999	L-21-1-Be1	IW	X	X	-	X	-	-	-
589	28.08.1999	L-21-1-Be2	IW	X	X	-	X	-	-	-
590	28.08.1999	L-21-1-Be3	IW	X	X	-	X	-	-	-
591	28.08.1999	L-21-1-Be4	IW	X	X	-	X	-	-	-
592	28.08.1999	L-21-1-Be5	IW	X	X	-	X	-	-	-
593	28.08.1999	L-21-1-Be6	IW	X	X	-	X	-	-	-
594	28.08.1999	L-21-1-Be7	IW	X	X	-	X	-	-	-
595	28.08.1999	L-21-1-Be8	IW	X	X	-	X	-	-	-
596	28.08.1999	L-21-1-Be9	IW	X	X	-	X	-	-	-
597	28.08.1999	L-21-1-Be10	IW	X	X	-	X	X	-	-
598	28.08.1999	L-21-1-Be11	IW	X	X	-	X	-	-	-
599	28.08.1999	L-21-1-Be12	IW	X	X	-	X	-	-	-
600	28.08.1999	L-15-1-I1 (head)	IW	X	X	X	-	X	5,64	120

A5-6: continuation.

				Isotopes				Chemistry		
Nr.	date	sample	type	18 O	2 H	3 H	10 Be	anion/cation	pH	LF
601	29.08.1999	L-21-1-I26	IW	X	X	-	-	-	-	-
602	29.08.1999	L-21-1-I27	IW	X	X	-	-	-	-	-
603	29.08.1999	L-21-1-I28	IW	X	X	-	-	-	-	-
604	29.08.1999	L-21-1-I29	IW	X	X	-	-	-	5,68	105
605	29.08.1999	L-21-1-I30	IW	X	X	-	-	-	-	-
606	29.08.1999	L-21-1-I31	IW	X	X	-	-	-	5,67	68
607	29.08.1999	L-21-1-I32	IW	X	X	-	-	-	-	-
608	29.08.1999	L-21-1-I33	IW	X	X	-	-	-	5,52	93
609	29.08.1999	L-2-1-I1	IW	X	X	-	-	X	6,50	121
610	29.08.1999	L-2-1-I2	IW	X	X	-	-	-	-	-
611	29.08.1999	L-2-1-I3	IW	X	X	-	-	-	6,88	127
612	29.08.1999	L-2-1-I4	IW	X	X	-	-	-	-	-
613	29.08.1999	L-2-1-I5	IW	X	X	-	-	-	-	-
614	29.08.1999	L-2-1-I6	IW	X	X	-	-	-	6,73	115
615	29.08.1999	L-2-1-I7	IW	X	X	-	-	-	6,87	172
616	29.08.1999	L-2-1-I8	IW	X	X	-	-	-	-	-
617	29.08.1999	L-2-1-I9	IW	X	X	-	-	-	6,60	66
618	29.08.1999	L-2-1-I10	IW	X	X	-	-	X	-	-
619	29.08.1999	L-2-1-I11	IW	X	X	-	-	-	6,86	122
620	29.08.1999	L-2-1-I12	IW	X	X	-	-	-	-	-
621	29.08.1999	L-2-1-I13	IW	X	X	-	-	-	6,95	80
622	29.08.1999	L-2-1-I14	IW	X	X	-	-	-	-	-
623	29.08.1999	L-2-1-I15 (head)	IW	X	X	X	-	X	6,79	69
624	29.08.1999	LYA-96/18	SW	X	X	X	-	X	7,32	20100
625	29.08.1999	LYA-98/10	GW	X	X	X	-	X	7,15	331
626	30.08.1999	LYA-96/19	SW	X	X	-	-	X	6,39	292
627	30.08.1999	LYA-96/20	SW	X	X	-	-	X	6,24	167
628	30.08.1999	LYA-96/21	SW	X	X	-	-	X	6,13	202
629	30.08.1999	B15-2	TI	X	X	-	-	X	7,37	383
630	30.08.1999	B15-4	TI	X	X	-	-	X	7,09	484
631	30.08.1999	B15-5	TI	X	X	-	-	X	7,01	459
632	30.08.1999	B15-6	TI	X	X	-	-	X	6,56	362
633	30.08.1999	L11-S9	TI	X	X	-	-	X	6,99	1099
634	30.08.1999	LYA-99/11	RW	X	X	X	-	X	5,9	128
635	30.08.1999	LYA-96/22	SW	X	X	X	-	X	6,31	95
636	30.08.1999	LYA-96/23	SW	X	X	X	-	X	7,22	267
637	30.08.1999	LYA-96/24	SW	X	X	X	-	X	6,86	172
638	30.08.1999	LYA-96/25	SW	X	X	X	-	X	7,65	240
639	30.08.1999	LYA-96/26	SW	X	X	X	-	X	7,62	294
640	30.08.1999	LYA-Be-99	RW	X	X	-	X	-	-	-
641	31.08.1999	LYA-99/12	RW	X	X	X	-	X	6,21	35
642	31.08.1999	LYA-97/10	SP	X	X	X	-	X	6,81	428
643	31.08.1999	LYA-97/11	SP	X	X	X	-	X	6,94	765
644	31.08.1999	LYA-97/12	SP	X	X	X	-	X	-	-
645	31.08.1999	LYA-97/13	SP	X	X	X	-	X	7,06	2320
646	31.08.1999	LYA-97/14	SP	X	X	X	-	X	8,06	3100
647	31.08.1999	LYA-97/15	SP	X	X	X	-	X	8,02	3850
648	31.08.1999	LYA-97/16	SP	X	X	X	-	X	7,47	4930
649	31.08.1999	LYA-96/27	SW	X	X	X	-	X	8,5	25800
650	31.08.1999	LYA-98/11	GW	X	X	X	-	X	5,98	122
651	31.08.1999	LYA-98/12	GW	X	X	-	-	-	7.4	1212
652	31.08.1999	LYA-98/13	GW	X	X	-	-	-	6,66	65800
653	31.08.1999	LYA-98/14	GW	X	X	-	-	-	6,35	172
654	31.08.1999	LYA-98/15	GW	X	X	-	-	-	5,78	241
655	01.09.1999	LYA-99/13	RW	X	X	X	-	X	6,13	207
656	01.09.1999	L3-S1	TI	X	X	-	-	-	6,20	2530
657	01.09.1999	L3-S5	TI	X	X	-	-	-	6,94	614
658	01.09.1999	LYA-95/01	SI	X	X	-	-	-	6,52	3270
659	01.09.1999	LYA-95/02	SI	X	X	-	-	-	6,65	2080
660	03.09.1999	L6-I1	IW	X	X	-	-	-	-	-
661	03.09.1999	L6-I2	IW	X	X	-	-	-	-	-
662	03.09.1999	L6-I3	IW	X	X	-	-	-	-	-
663	03.09.1999	L6-I4	IW	X	X	-	-	-	-	-
664	03.09.1999	L6-I5	IW	X	X	-	-	-	-	-
665	03.09.1999	L6-I6	IW	X	X	-	-	-	-	-
666	03.09.1999	L6-I7	IW	X	X	-	-	-	-	-
667	03.09.1999	L6-I8	IW	X	X	-	-	-	-	-
668	03.09.1999	L6-I9	IW	X	X	-	-	-	-	-
669	03.09.1999	L6-I10	IW	X	X	-	-	-	-	-
670	03.09.1999	L6-I11	IW	X	X	-	-	-	-	-

Abbreviations : SP = snow patch; RW = rain water; IW = ice wedge ice; SW = surface water; GW = ground water; SI = sea ice; TI = segregated ice; AL = active layer ice; MW = meltwater.

A5-7: List of bone samples.

samples	Side	Taxon	Skeleton element	Preservation	Type	Locality	Notes
BL-O 1	R	Mammuthus primigenius	tusk	fragment	a	in situ IV TC, boundary ""Kuchchuguy"" /"Ice Complex"	from Volodya
BL-O 2	L	Mammuthus primigenius	tusk	fragment	e	L, shore	trashed
BL-O 3	L	Mammuthus primigenius	tooth	fragment	e	L, shore 5 - 6 km from the camp	trashed
BL-O 4	L	Mammuthus primigenius	tusk	fragment	e	L, shore 5 - 6 km from the camp	trashed
BL-O 5	L	Rangifer tarandus	pelvis	fragment	e	L, shore 5 - 6 km from the camp	trashed
BL-O 6	L	Rangifer tarandus	scapula	fragment	e	L, shore 5 - 6 km from the camp	trashed
BL-O 7	L	Bison priscus	phalanx II		e	L, shore 5 - 6 km from the camp	trashed
BL-O 8	L	Bison priscus	???????????		e	L, shore 5 - 6 km from the camp	trashed
BL-O 9	L	Equus sp.	metatarsale III	fragment	e	L, shore 5 - 6 km from the camp	trashed
BL-O 10	L	Ovibos sp.	cranium	fragment	e	L, shore	trashed
BL-O 11	R	Equus sp.	humerus	distal fragment	b	R, III TC, bone field "O VI"	samples 12,
BL-O 12	R	Mammuthus primigenius	lumbar vertebra		b	R, III TC, bone field "O VI"	13, 14 from
BL-O 13	R	Mammuthus primigenius	2 thorax vertebras ???		b	R, III TC, bone field "O VI"	the same specimen
BL-O 14	R	Mammuthus primigenius	thorax vertebra		b	R, III TC, bone field "O VI"	
BL-O 15	R	Rangifer tarandus	antebrachium		b	R, III TC, bone field "O VI"	juv.
BL-O 16	R	Rangifer tarandus	antler	fragment	b	R, III TC, bone field "O VI"	
BL-O 17	R	Equus sp.	pelvis	fragment	b	R, III TC, bone field "O VI"	
BL-O 18	R	Bison priscus	radius		c	R, I TC	
BL-O 19	R	Rangifer tarandus	tibia	fragment	c	R, I TC	
BL-O 20	R	Mammuthus primigenius	upper molar tooth (M3)	2 fragments	c	R, I TC	
BL-O 21	R	Equus sp.	calcaneus		c	R, I TC	
BL-O 22	R	Equus sp.	radius	distal fragment	c	R, I TC	
BL-O 23	R	Mammuthus primigenius	tusk	fragment	c	R, I TC	C14
BL-O 24	R	Ovibos sp.	humerus	distal fragment	c	R, I TC	
BL-O 25	R	Equus sp.	radius		c	R, I TC	
BL-O 26	R	Rangifer tarandus	shed antler	fragment	c	R, I TC	
BL-O 27	R	Mammuthus primigenius	cranium (ocipitale)	fragment	c	R, I TC	juv., C14
BL-O 28	L	Mammuthus primigenius	ulna (with marrow)	sample cut out	e	shore L	C14
BL-O 29	L	Bison priscus	horn		e	shore L	
BL-O 30	L	Mammuthus primigenius	tusk	fragment	e	shore L	
BL-O 31	L	Rangifer tarandus	sacrum		e	shore L	
BL-O 32	L	Mammuthus primigenius	lower molar tooth (M3)	fragment	e	shore L	
BL-O 33	L	Mammuthus primigenius	pelvis	fragment	e	shore L	

A5-7: continuation.

samples	Side	Taxon	Skeleton element	Preservation	Type	Locality	Notes
BL-O 34	L	Mammuthus primigenius	tusk	fragment	e	shore L	C14
BL-O 35	L	Rangifer tarandus	lumbar vertebra		e	shore L	
BL-O 36	L	Rangifer tarandus	scapula	fragment	e	shore L	
BL-O 37	L	Bison priscus	humerus	distal fragment	e	shore L	trashed
BL-O 38	L	Mammuthus primigenius	tooth	fragment	e	shore L	
BL-O 39	L	Mammuthus primigenius	pelvis	fragment	e	shore L	C14
BL-O 40	L	Bison priscus	ulna		e	shore L	
BL-O 41	L	Equus sp.	astrogalus		e	shore L	
BL-O 42	L	Equus sp.	metatarsale III		e	shore L	
BL-O 43	L	Rangifer tarandus	shed antler		e	shore L	
BL-O 44	L	Panthera spelaea	mandibula	????? ?????	e	shore L, under I TC	
BL-O 45	L	Mammuthus primigenius	cranium	fragment	e	shore L	trashed
BL-O 46	R	Equus sp.	phalanx I		c	R, I TC	
BL-O 47	R	Rangifer tarandus	ulna	damaged	c	R, I TC	
BL-O 48	R	Mammuthus primigenius	tusk	fragment	c	R, I TC	trashed
BL-O 49	R	Mammuthus primigenius	metacarpale I	fragment	b	R III TC, bone field "O VI"	
BL-O 50	R	Equus sp.	femur	distal fragment	b	R III TC, bone field "O VI"	
BL-O 51	R	Large mammal	rib	fragment	b	R III TC, bone field "O VI"	trashed
BL-O 52	R	Mammuthus primigenius	tusk	fragment	b	R III TC, bone field "O VI"	trashed
BL-O 53	R	Bison priscus	metatarsale		b	alas TC, 3 - 4 m above "Kuchchuguy"	
BL-O 54	R	Bison priscus	phalanx I		c	R, alas TC	
BL-O 55	R	Ovibos sp.	?cervical vertebra		c	R, alas TC	
BL-O 56	R	Rangifer tarandus	epistrofeum		c	R, alas TC	
BL-O 57	R	Mammuthus primigenius	pelvis (os ilium)	fragment	c	R, alas TC	juv., C14
BL-O 58	R	Equus sp.	metatarsale III	distal fragment	c	R, III TC	
BL-O 59	R	Mammuthus primigenius	radius	fragment	c	R, III TC	
BL-O 60	R	Rangifer tarandus	cranium	occipital fragment	c	R, III TC	
BL-O 61	R	Equus sp.	calcaneus		c	R, III TC	
BL-O 62	R	Rangifer tarandus	phalanx I		c	R, III TC	
BL-O 63	R	Equus sp.	metatarsale III	deformity	c	R, III TC	
BL-O 64	R	Rangifer tarandus	lumbar vertebra		c	R, III TC	
BL-O 65	R	Equus sp.	phalanx II		c	R, III TC	
BL-O 66	R	Bison priscus	thorax vertebra		c	R, III TC	

A5-7: continuation.

samples	Side	Taxon	Skeleton element	Preservation	Type	Locality	Notes
BL-O 67	L	Mammuthus primigenius	mandible (left stem) with milk teeth dp2 - dp3		e	shore L	juv.
BL-O 68	R	Lepus sp.	cranium	damaged	d	shore R, 100 m (R1)	
BL-O 69	R	Lepus sp.	tibia	distal fragment	c	R, III TC	
BL-O 70	L	Equus sp.	femur		e	L, shore near the camp	
BL-O 71	L	Mammuthus primigenius	tusk	fragment	e	L, shore near the camp	C14
BL-O 72	L	Rangifer tarandus	shed antler		e	L, shore near the camp	
BL-O 73	L	Bison priscus	atlas		e	L, shore near the camp	juv.
BL-O 74	L	Bison priscus	radius	distal fragment	e	L, shore near the camp	
BL-O 75	L	Rangifer tarandus	humerus	distal fragment	e	L, shore near the camp	
BL-O 76	L	Equus sp.	calcaneus	sample damaged	e	L, shore near the camp	
BL-O 77	L	Equus sp.	phalanx I		e	L, shore near the camp	
BL-O 78	L	Rangifer tarandus	metacarpale		e	L, shore near the camp	juv.
BL-O 79	L	Rangifer tarandus	metatarsale	fragment	e	L, shore near the camp	juv.
BL-O 80	L	Ovibos sp.	phalanx I	damaged	e	L, shore near the camp	
BL-O 81	L	Mammuthus primigenius	lower molar tooth (M3) heavily worn		e	L, shore near the camp	
BL-O 82	L	Ovibos sp.	atlas	sample damaged	e	L, shore near the camp	
BL-O 83	L	Bison priscus	femur	fragment	e	L, shore near the camp	trashed
BL-O 84	L	Equus sp.	femur	fragment	e	L, shore near the camp	trashed
BL-O 85	L	Equus sp.	thorax vertebra	sample damaged (2 pieces)	e	L, shore near the camp	
BL-O 86	L	Bison priscus	phalanx II		e	L, shore near the camp	
BL-O 87	L	Bison priscus	phalanx II		e	L, shore near the camp	
BL-O 88	L	Bison priscus	phalanx I		e	L, shore near the camp	
BL-O 89	L	Bison priscus	calcaneus	fragment	e	L, shore near the camp	
BL-O 90	L	Bison priscus	phalanx II		e	L, shore near the camp	
BL-O 91	L	Rangifer tarandus	astrogalus		e	L, shore near the camp	
BL-O 93	L	Rangifer tarandus	shed antler	fragment	e	L, shore near the camp	
BL-O 94	L	Rangifer tarandus	astrogalus		e	L, shore near the camp	
BL-O 95	L	Rangifer tarandus	radius	proximal fragment	e	L, shore near the camp	trashed
BL-O 96	L	Ovibos sp.	metacarpale	distal fragment	e	L, shore near the camp	juv.
BL-O 97	L	Mammalia	bone	fragment	e	L, shore near the camp	
BL-O 98	L	Mammalia	bone	fragment	e	L, shore near the camp	trashed
BL-O 99	L	Rangifer tarandus	tibia	distal fragment	e	L, shore near the camp	

A5-7: continuation.

samples	Side	Taxon	Skeleton element	Preservation	Type	Locality	Notes
BL-O 100	L	Mammuthus primigenius	milk upper tooth (dp2)		e	L, shore near the camp	
BL-O 101	L	Rangifer tarandus	tibia	distal fragment	e	L, shore near the camp	
BL-O 102	L	Lepus sp.	tibia	distal fragment	e	L, shore near the camp	
BL-O 103	L	Rangifer tarandus	carpi radiale		e	L, shore near the camp	
BL-O 104	L	??????????	rib	fragment	e	L, shore near the camp	
BL-O 106	L	Bison priscus	cranium	occipital fragment	e	L, shore near the camp	
BL-O 107	L	Rangifer tarandus	cranium (squamosum)	fragment	e	L, shore near the camp	trashed
BL-O 108	L	Rangifer tarandus	cranium (squamosum)	fragment	e	L, shore near the camp	trashed
BL-O 109	L	Rangifer tarandus	metapodia	distal fragment	e	L, shore near the camp	juv.
BL-O 110	R	Equus sp.	ulna	damaged	a	in situ, II TC, mark 12, altitude 16,8 m	from Lutz
BL-O 111	R	Rangifer tarandus	shed antler	fragment	a	in situ, 0.4m from pseudomorphis (R-32) in alas , altitude 16,8 m	from Hanno
BL-O 112	R	Equus sp.	magnum		a	in situ, II TC, mark 12, altitude 16,8 m	from Lutz
BL-O 113	R	Equus sp.	unciform		a	in situ, II TC, mark 12, altitude 16,8 m	from Lutz
BL-O 114	R	Mammuthus primigenius	upper molar tooth (M3)	fragment	d	R, cape shore	
BL-O 115	R	Rangifer tarandus	humerus	fragment	d	R, cape shore	
BL-O 116	R	Equus sp.	humerus	distal fragment	d	R, cape shore	
BL-O 117	R	Equus sp.	metacarpale III		d	R, cape shore	
BL-O 118	R	Equus sp.	metatarsale III		d	R, cape shore	
BL-O 119	R	Equus sp.	metatarsale III	distal fragment	d	R, cape shore	
BL-O 120	R	Equus sp.	phalanx I		d	R, cape shore	
BL-O 121	R	Rangifer tarandus	thorax vertebra		d	R, cape shore	
BL-O 122	R	Rangifer tarandus	tibia	distal fragment	d	R, cape shore	
BL-O 123	R	Equus sp.	scapula	damaged	d	R, cape shore	
BL-O 124	R	Rangifer tarandus	tibia	distal fragment	d	R, cape shore	
BL-O 125	R	Rangifer tarandus	astrogalus		d	R, cape shore	
BL-O 126	R	Lepus sp.	metapodialis		d	R, cape shore	
BL-O 127	R	Lepus sp.	tibia	distal fragment	d	R, cape shore	
BL-O 128	R	Equus sp.	humerus	distal fragment	d	R, cape shore	juv.
BL-O 129	R	Equus sp.	phalanx I		d	R, cape shore	
BL-O 130	R	Rangifer tarandus	phalanx I		d	R, cape shore	

A5-7: continuation.

samples	Side	Taxon	Skeleton element	Preservation	Type	Locality	Notes
BL-O 131	R	Rangifer tarandus	phalanx I		d	R, cape shore	
BL-O 132	R	Rangifer tarandus	phalanx I		d	R, cape shore	
BL-O 133	R	Rangifer tarandus	phalanx II		d	R, cape shore	
BL-O 134	R	Rangifer tarandus	phalanx I		d	R, cape shore	
BL-O 135	R	Bison priscus	atlas		d	R, cape shore	
BL-O 136	R	Bison priscus	radius	fragment	d	R, cape shore	trashed
BL-O 137	R	Large mammal	?tibia	fragment	d	R, cape shore	trashed
BL-O 138	R	Rangifer tarandus	atlas	fragment	d	R, cape shore	
BL-O 139	R	Mammuthus primigenius	tusk	fragment	d	R, cape shore	trashed
BL-O 140	R	Mammuthus primigenius	tooth	fragment	d	R, cape shore	
BL-O 141	R	Mammuthus primigenius	molar tooth replaced		d	R, cape shore	
BL-O 142	R	Rangifer tarandus	phalanx I		d	R, cape shore	
BL-O 143	R	Rangifer tarandus	phalanx I		d	R, cape shore	
BL-O 144	R	Rangifer tarandus	phalanx I		d	R, cape shore	
BL-O 145	R	Rangifer tarandus	phalanx I		d	R, cape shore	
BL-O 146	R	Rangifer tarandus	phalanx I		d	R, cape shore	
BL-O 147	R	Bison priscus	metatarsale	fragment	d	R, cape shore	trashed
BL-O 148	R	Mammuthus primigenius	tooth	fragment	d	R, cape shore	
BL-O 149	R	Rangifer tarandus	cervical vertebra		d	R, cape shore	
BL-O 150	R	Large mammal	tibia	fragment	d	R, cape shore	trashed
BL-O 151	R	Rangifer tarandus	calcaneus		d	R, cape shore	
BL-O 152	R	Equus sp.	pisiforme		d	R, cape shore	
BL-O 153	R	Rangifer tarandus	phalanx I	distal fragment	d	R, cape shore	
BL-O 154	R	Rangifer tarandus	phalanx III		d	R, cape shore	
BL-O 155	R	Rangifer tarandus	tibia	distal fragment	d	R, cape shore	trashed
BL-O 156	R	Rangifer tarandus	radius	proximal fragment	d	R, cape shore	
BL-O 157	R	Rangifer tarandus	phalanx I		d	R, cape shore	
BL-O 158	R	Rangifer tarandus	phalanx I	proximal fragment	d	R, cape shore	
BL-O 159	R	Canis lupus	astrogalus		d	R, cape shore	
BL-O 160	R	Saiga tatarica	humerus	distal fragment	d	R, cape shore	
BL-O 161	R	Equus sp.	metapodia	distal fragment	d	R, cape shore	trashed
BL-O 162	R	Lepus sp.	humerus	fragment	d	R, cape shore	
BL-O 163	R	Lepus sp.	pelvis		d	R, cape shore	
BL-O 164	R	Mammuthus primigenius	milk tooth	fragment	d	R, cape shore	
BL-O 165	R	Rangifer tarandus	shed antler	fragment	d	R, cape shore	trashed

A5-7: continuation.

samples	Side	Taxon	Skeleton element	Preservation	Type	Locality	Notes
BL-O 166	R	Bison priscus	caudal vertebra	sample damaged	d	R, cape shore	
BL-O 167	R	Equus sp.	metacarpale III	distal fragment	d	R, cape shore	trashed
BL-O 168	R	Bison priscus	pelvis	fragment	d	R, cape shore	trashed
BL-O 169	R	Bison priscus	pelvis	fragment	d	R, cape shore	trashed
BL-O 170	R	Large mammal	cranium	fragment	d	R, cape shore	
BL-O 171	R	Equus sp.	phalanx III	fragment	d	R, cape shore	
BL-O 172	R	Mammal	mandibula	fragment	d	R, cape shore	
BL-O 173	R	Rangifer tarandus	tibia	distal fragment	d	R, cape shore	
BL-O 174	R	Rangifer tarandus	metapodia	distal fragment	d	R, cape shore	
BL-O 175	R	Mammuthus primigenius	tibia	distal fragment	c	R, I TC	?14
BL-O 176	R	Mammuthus primigenius	femur	fragment, ???	c	R, I TC	?14
BL-O 177	R	Mammuthus primigenius	metatarsale II		c	R, I TC	
BL-O 178	R	Mammuthus primigenius	lumbar vertebra	sample damaged	c	R, I TC	?14
BL-O 179	R	Mammuthus primigenius	lumbar vertebra		c	R, I TC	?14
BL-O 180	R	Mammuthus primigenius	thorax vertebra	fragment	c	R, I TC	?14
BL-O 181	R	Mammuthus primigenius	atlas	fragment	c	R, I TC	?14
BL-O 182	R	Mammuthus primigenius	ulna	distal fragment	c	R, I TC	?14
BL-O 183	R	Mammuthus primigenius	metacarpale V		c	R, I TC	?14
BL-O 184	R	Bison priscus	metacarpale	distal fragment	c	R, I TC	
BL-O 185	R	Mammuthus primigenius	femur	fragment	c	R, I TC	?14
BL-O 186	R	Mammuthus primigenius	tusk	fragment	c	R, I TC	?14
BL-O 187	R	Mammuthus primigenius	ulnare		c	R, I TC	
BL-O 188	R	Mammuthus primigenius	thorax vertebra		c	R, I TC	C14
BL-O 189	R	Mammuthus primigenius	metacarpale I		c	R, I TC	
BL-O 190	R	Bison priscus	thorax vertebra		c	R, I TC	
BL-O 191	L	Canis lupus	mandibula (right stem)	fragment	a	in situ, L (L7+60m),altitude 5.5m	
BL-O 192	L	Panthera spelaea	metapodia		a	m	
BL-O 193-1	R	Bison priscus	thorax vertebra		a	in situ, R , "O II", altitude 6 m	
BL-O 193-2	R	Bison priscus	epistropheus		a	in situ, R , "O II", altitude 6 m	
BL-O 193-3	R	Bison priscus	lumbar vertebra		a	in situ, R , "O II", altitude 6 m	samples 193-3,
BL-O 193-4	R	Bison priscus	???????		a	in situ, R , "O II", altitude 6 m	193-4, 193-6
BL-O 193-5	R	Bison priscus	thorax vertebra		a	in situ, R , "O II", altitude 6 m	in natural
BL-O 193-6	R	Bison priscus	lumbar vertebra		a	in situ, R , "O II", altitude 6 m	conjunction
BL-O 193-7	R	Bison priscus	cervical vertebra		a	in situ, R , "O II", altitude 6 m	
BL-O 193-8	R	Bison priscus	thorax vertebra		a	in situ, R , "O II", altitude 6 m	

A5-7: continuation.

samples	Side	Taxon	Skeleton element	Preservation	Type	Locality	Notes
BL-O 193-9	R	Bison priscus	thorax vertebra		a	in situ, R , "O II", altitude 6 m	
BL-O 193-10	R	Bison priscus	thorax vertebra		a	in situ, R , "O II", altitude 6 m	
BL-O 193-11	R	Bison priscus	cervical vertebra		a	in situ, R , "O II", altitude 6 m	
BL-O 193-12	R	Bison priscus	rib	fragment	a	in situ, R , "O II", altitude 6 m	
BL-O 193-13	R	Bison priscus	rib	fragment	a	in situ, R , "O II", altitude 6 m	
BL-O 193-14	R	Bison priscus	rib	fragment	a	in situ, R , "O II", altitude 6 m	
BL-O 193-15	R	Bison priscus	rib	fragment	a	in situ, R , "O II", altitude 6 m	
BL-O 193-16	R	Bison priscus	rib	fragment	a	in situ, R , "O II", altitude 6 m	
BL-O 193-17	R	Bison priscus	vertebra	fragment (3 pieces)	a	in situ, R , "O II", altitude 6 m	
BL-O 193-18	R	Bison priscus	thorax vertebra		a	in situ, R , "O II", altitude 6 m	
BL-O 193-19	R	Bison priscus	thorax vertebra		a	in situ, R , "O II", altitude 6 m	
BL-O 193-20	R	Bison priscus	pelvis	fragment	a	in situ, R , "O II", altitude 6 m	
BL-O 194	R	Bison priscus	femur	fragment (4 pieces)	a	in situ, R , "O I", altitude 7,9 m	juv.
BL-O 195	R	Mammuthus primigenius	tibia	distal fragment	c	R, under "O II"	
BL-O 196	L	Bison priscus	horn sheet		e	L, shore	
BL-O 197	R	Equus sp.	phalanx I		d	R, shore under alas (>R 34)	
BL-O 198	R	Rangifer tarandus	femur	proximal fragment	d	R, shore under alas (>R 34)	
BL-O 199	R	Mammuthus primigenius	tusk	fragment	d	R, shore under alas (>R 34)	trashed
BL-O 200	L	Mammuthus primigenius	and 2 teeth	fragment	e	L, shore 10 km from camp	in Potsdam
BL-O 201	Z	Ovibos sp.	cranium, male		f	????? the river Zimov'e	
BL-O 202	R	Bison priscus	metacarpale		a	in situ, R , "O II"	
O 203		Coelodonta antiqua	mandible (right stem) with 2 teeth			Shirikostan, 10 km norther than Nerpechiy cape	from M. Grigoryev
BL-O 204	L	Bison priscus	horn sheet	fragment	e	L, shore 10 km from camp	
BL-O 205	L	Bison priscus	horn sheet	fragment	e	L, shore	
BL-O 206	R	Equus sp.	mandible (right stem) with teeth P3 - M3	fragment	b	R, on the boundary between alas and IV TC	
BL-O 207	R	Rangifer tarandus	mandibula (left stem) with teeth P2 - M1	fragment	b	R, on the boundary between alas and IV TC	
BL-O 208	R	Mammuthus primigenius	pelvis	fragment	c	R, I TC	C14
BL-O 209	R	Mammuthus primigenius	humerus	distal fragment	c	R, I TC	juv.
BL-O 210	R	Rangifer tarandus	pelvis	fragment	b	R, I TC, bone field "? IV"	
BL-O 211	R	Mammuthus primigenius	tibia	fragment (cut by men)	b	R, I TC, bone field "? IV"	juv., C14
BL-O 212	R	Bison priscus	sacrum	fragment (2 pieces)	b	R, I TC, bone field "? IV"	

A5-7: continuation.

samples	Side	Taxon	Skeleton element	Preservation	Type	Locality	Notes
BL-O 214	R	Equus sp.	tibia	distal fragment	b	R, I TC, bone field "? IV"	
BL-O 215	R	Mammuthus primigenius	lower molar tooth (M3)	fragment	b	R, I TC, bone field "? IV"	
BL-O 216	R	Equus sp.	metapodia	fragment	b	R, I TC, bone field "? IV"	
BL-O 217	R	Mammuthus primigenius	radius	fragment	b	R, I TC, bone field "? IV"	
BL-O 218	R	Equus sp.	tibia	procsimal fragment	b	R, I TC, bone field "? IV"	trashed
BL-O 219	R	Mammuthus primigenius	tusk	fragment	b	R, I TC, bone field "? IV"	C14
BL-O 220	R	Mammuthus primigenius	cranium	fragment	b	R, I TC, bone field "? IV"	
BL-O 221	R	Rangifer tarandus	shed antler	fragment	b	R, I TC, bone field "? IV"	trashed
BL-O 222	R	Equus sp.	femur	procsimal fragment (2 pieces)	b	R, I TC, bone field "? V"	
BL-O 223	R	Equus sp.	tibia		b	R, I TC, bone field "? V"	
BL-O 224	R	Rangifer tarandus	shed antler	fragment	b	R, I TC, bone field "? V"	
BL-O 225	R	Equus sp.	scapula	sample damaged	b	R, I TC, bone field "? V"	
BL-O 226	R	Ovibos sp.	metacarpale		b	R, I TC, bone field "? V"	
BL-O 227	R	Equus sp.	femur	distal fragment	b	R, I TC, bone field "? V"	
BL-O 228	R	Rangifer tarandus	pelvis	fragment	b	R, I TC, bone field "? V"	trashed
BL-O 229	R	Equus sp.	pelvis	fragment	b	R, I TC, bone field "? V"	trashed
BL-O 230	R	Rangifer tarandus	vertebra, ???????	fragment	b	R, I TC, bone field "? V"	
BL-O 231	R	Rangifer tarandus	mandible (right stem) with P4 - M3	fragment	b	R, I TC, bone field "? V"	
BL-O 232	R	Equus sp.	tibia	distal fragment	b	R, I TC, bone field "? V"	
BL-O 233	R	Equus sp.	phalanx I		b	R, I TC, bone field "? V"	
BL-O 234	R	Equus sp.	metatarsale II + metatarsale III		b	R, I TC, bone field "? V"	
BL-O 235	R	Equus sp.	phalanx III		b	R, I TC, bone field "? V"	
BL-O 236	R	Equus sp.	mandibula (left stem) with teeth P4 - M3	heavily worn	b	R, I TC, bone field "? V"	
BL-O 237	R	Bison priscus	scapula	fragment	b	R, I TC, bone field "? V"	
BL-O 238	R	Equus sp.	phalanx I		b	R, I TC, bone field "? V"	
BL-O 240	R	Mammuthus primigenius	tusk	fragment	b	R, I TC, bone field "? V"	C 14
BL-O 241	R	Equus sp.	humerus		b	R, I TC, bone field "? III"	
BL-O 242	R	Bison priscus	radius		b	R, I TC, bone field "? III"	
BL-O 243	R	Equus sp.	calcaneus		b	R, I TC, bone field "? III"	
BL-O 244	R	Equus sp.	pelvis	fragment	b	R, I TC, bone field "? III"	
BL-O 245	R	Bison priscus	lumbar vertebra		b	R, I TC, bone field "? III"	

A5-7: continuation.

samples	Side	Taxon	Skeleton element	Preservation	Type	Locality	Notes
BL-O 246	R	Bison priscus	epistropheus		b	R, I TC, bone field "? III"	
BL-O 247	R	Bison priscus	thorax vertebra		b	R, I TC, bone field "? III"	
BL-O 248	R	Rangifer tarandus	shed antler	fragment	b	R, I TC, bone field "? III"	
BL-O 249	L	Mammuthus primigenius	tusk	damaged	e	L, shore (L I7 + 70 m)	C 14
BL-O 250	L	Mammuthus primigenius	ulna	proximal fragment	e	L, shore (L I7 + 70 m)	C 14
BL-O 251	L	Mammuthus primigenius	tusk	damaged	e	L, shore (L I7 + 70 m)	C 14
BL-O 252	L	Mammuthus primigenius	femur	fragment	e	L, shore under I TC	C 14
BL-O 253	R	Mammuthus primigenius	femur	fragment	d	R, cape shore	C 14
BL-O 254	L	Mammuthus primigenius	ulna	proximal fragment	e	L, shore under I TC	C 14
BL-O 255	L	Mammuthus primigenius	tusk	fragment	e	L, shore 10 km from camp	C 14
BL-O 256	L	Mammuthus primigenius	? femur	fragment	e	L, shore	C 14
BL-O 257	R	Mammuthus primigenius	humerus	distal fragment	d	R, shore	C 14
BL-O 258	R	Mammuthus primigenius	humerus	distal fragment	d	R, shore	C 14
BL-O 259	R	Mammuthus primigenius	femur	4 fragments	d	R, shore	C 14
BL-O 260	L	Coelodonta antiqua	tibia	proximalfragment	e	L, shore	
BL-O 261	R	? Equus sp.	scapula	fragment	c	R, from scree, "Kuchchuguy" altitude ("Kuch." altidude)	trashed
BL-O 262	R	Equus sp.	metacarpale IV		c	R, from scree, "Kuch." altidude	
BL-O 263	R	Lepus sp.	pelvis	fragment	c	R, from scree, "Kuch." altidude	
BL-O 264	R	Equus sp.	pyramidale		c	R, from scree, "Kuch." altidude	
BL-O 265	R	Rangifer tarandus	femur	distal fragment	c	R, from scree, "Kuch." altidude	trashed
BL-O 266	R	Rangifer tarandus	humerus		c	R, from scree, "Kuch." altidude	
BL-O 267	R	Bison priscus	radius	proximal fragment	c	R, from scree, "Kuch." altidude	trashed
BL-O 268	R	Equus sp.	tibia	distal fragment	c	R, from scree, "Kuch." altidude	
BL-O 269	R	Ovibos sp.	calcaneus		c	R, from scree, "Kuch." altidude	
BL-O 270	R	Bison priscus	calcaneus	fragment	c	R, from scree, "Kuch." altidude	
BL-O 271	R	Rangifer tarandus	femur	distal fragment	c	R, from scree, "Kuch." altidude	
BL-O 272	R	Rangifer tarandus	radius	distal fragment	c	R, from scree, "Kuch." altidude	
BL-O 273	R	Mammuthus primigenius	rib	damaged	c	R, from scree, "Kuch." altidude	? 14
BL-O 274	R	Mammuthus primigenius	vertebra	articulation	c	R, from scree, "Kuch." altidude	trashed
BL-O 275	R	Rangifer tarandus	shed antler	fragment	c	R, from scree, "Kuch." altidude	trashed
BL-O 276	R	Equus sp.	metatapcalia III		c	R, from scree, "Kuch." altidude	
BL-O 277	R	Equus sp.	metapodia	fragment	c	R, from scree, "Kuch." altidude	trashed
BL-O 278	R	Mammuthus primigenius	tusk	fragment	c	R, from scree, "Kuch." altidude	trashed
BL-O 279	R	Equus sp.	pelvis	fragment with copulas	c	R, from scree, "Kuch." altidude	

A5-7: continuation.

samples	Side	Taxon	Skeleton element	Preservation	Type	Locality	Notes
BL-O 280	R	Equus sp.	metacarpale III	fragment	c	R, from scree, "Kuch." altidude	
BL-O 281	R	Bison priscus	radius	proximal fragment	c	R, from scree, "Kuch." altidude	
BL-O 282	R	Equus sp.	lower premolar		c	R, from scree, "Kuch." altidude	
BL-O 283	R	Ovibos sp.	humerus	distal fragment	c	R, from scree, "Kuch." altidude	
BL-O 284	R	Equus sp.	tibia		c	R, from scree, "Kuch." altidude	
BL-O 285	R	Mammuthus primigenius	upper molar tooth (M3 or ?M2)	fragment	c	R, from scree, "Kuch." altidude	
BL-O 286	R	Mammuthus primigenius	rib	fragment	c	R, from scree, "Kuch." altidude	? 14
BL-O 287	R	Mammuthus primigenius	scapula	fragment	c	R, from scree, "Kuch." altidude	? 14
BL-O 288	R	Mammuthus primigenius	tusk	fragment	c	R, from scree, "Kuch." altidude	C14
BL-O 289	R	Bison priscus	radius	distal fragment	c	R, from scree, "Kuch." altidude	
BL-O 290	R	Equus sp.	phalanx II		c	R, from scree, "Kuch." altidude	
BL-O 291	R	Rangifer tarandus	pelvis	fragment	c	R, from scree, "Kuch." altidude	trashed
BL-O 292	R	Mammuthus primigenius	cranium	fragment	c	R, II TC	trashed
BL-O 293	R	Ovibos sp.	pelvis	fragment	c	R, II TC	
BL-O 294	R	Equus sp.	pelvis	fragment	c	R, II TC	
BL-O 295	R	Equus sp.	metatarsale III	fragment	c	R, II TC	trashed
BL-O 296	R	Equus sp.	metatarsale III		c	R, II TC	
BL-O 297	R	Equus sp.	radius		c	R, II TC	
BL-O 298	R	Equus sp.	pelvis	fragment	c	R, II TC	trashed
BL-O 299	R	Lepus sp.	metapodia		c	R, II TC	
BL-O 300	R	Lepus sp.	tibia	fragment	c	R, II TC	
BL-O 301	R	Equus sp.	lower molar (M3)		c	R, II TC	juv.
BL-O 302	R	Bison priscus	femur		c	R, II TC	juv.
BL-O 303	R	Bison priscus	humerus		c	R, II TC	
BL-O 304	R	Mammuthus primigenius	tibia	distal fragment	c	R, II TC	C 14
BL-O 305	R	Bison priscus	tibia		c	R, II TC	C 14
BL-O 306	R	Mammuthus primigenius	femur	distal fragment	c	R, II TC	C 14
BL-O 307	R	Lepus sp.	radius	distal fragment	c	R, from ? "Kuchchuguy" altitude	
BL-O 308	R	Mammuthus primigenius	scapula	damaged	c	R, from ? "Kuchchuguy" altitude	C14
BL-O 309	R	Mammuthus primigenius	femur	fragment	b	R, I TC, bone field "? III"	C14
BL-O 310	R	Mammuthus primigenius	pelvis	fragment	c	R, from ? "Kuchchuguy" altitude	C14
BL-O 311	L	Mammuthus primigenius	tusk	fragment	e	L, shore	C14
BL-O 312	R	Mammuthus primigenius	femur	fragment	d	R, shore	C14
BL-O 313	Z	Mammuthus primigenius	humerus		f	? r. Zimov'e, from mammoth' skin	

A5-7: continuation.

samples	Side	Taxon	Skeleton element	Preservation	Type	Locality	Notes
BL-O 314	R	Bison priscus	radius		d	R, shore	juv.
BL-O 315	R	Rangifer tarandus	metatarsal	distal fragment	d	R, shore	
BL-O 316	R	Bison priscus	scapula	proximal fragment	d	R, shore	
BL-O 317	R	Bison priscus	mandible (left stem) with tooth M3		d	R, shore	
BL-O 318	R	Equus sp.	mandibula (right stem) with teeth ?3 -?1		d	R, shore	
BL-O 319	R	Mammuthus primigenius	tooth	fragment	d	R, shore	
BL-O 320	R	Equus sp.	thorax vertebra		d	R, shore	
BL-O 321	R	Equus sp.	lower tooth (P)		d	R, shore	
BL-O 322	R	Equus sp.	pelvis	fragment	d	R, shore	trashed
BL-O 323	R	Equus sp.	metatarsale III	proximal fragment	d	R, shore	
BL-O 324	R	Equus sp.	phalanx I		d	R, shore	juv.
BL-O 325	R	Bison priscus	cranium	occipital fragment	d	R, shore	
BL-O 326	R	Mammuthus primigenius	mandibula	fragment	d	R, shore	juv.
BL-O 327	R	Bison priscus	humerus	distal fragment	d	R, shore	
BL-O 328	R	Equus sp.	metacarpale III		d	R, shore	
BL-O 329	R	Bison priscus	metatarsale	proximal fragment	d	R, shore	
BL-O 330	R	Equus sp.	pelvis	fragment	d	R, shore	trashed
BL-O 331	R	Bison priscus	cranium	fragment	d	R, shore	
BL-O 332	R	Mammuthus primigenius	upper molar tooth (M3 or ?M2)	fragment	d	R, shore	
BL-O 333	R	Rangifer tarandus	femur	fragment	d	R, shore	juv.
BL-O 334	R	Rangifer tarandus	radius	fragment	d	R, shore	juv., trashed
BL-O 335	R	Equus sp.	radius	fragment	d	R, shore	juv.
BL-O 336	R	Ovibos sp.	radius		d	R, shore	juv.
BL-O 337	R	Mammuthus primigenius	calcaneus	sample damaged	d	R, shore	
BL-O 338	R	Equus sp.	radius		d	R, shore	
BL-O 339	R	Bison priscus	pelvis	fragment	d	R, shore	
BL-O 340	R	Ovibos sp.	tibia	distal fragment	d	R, shore	
BL-O 341	R	Rangifer tarandus	calcaneus		d	R, shore	
BL-O 342	R	Rangifer tarandus	astrogalus		d	R, shore	
BL-O 343	R	Mammuthus primigenius	tusk	fragment	d	R, shore	C14
BL-O 344	R	Mammuthus primigenius	pelvis	fragment	d	R, shore	C14
BL-O 345	R	Bison priscus	femur	distal fragment	d	R, shore	

A5-7: continuation.

samples	Side	Taxon	Skeleton element	Preservation	Type	Locality	Notes
BL-O 346	R	Bison priscus	calcaneus	fragment	d	R, shore	
BL-O 347	R	Mammuthus primigenius	tusk	fragment	d	R, shore	C14
BL-O 348	R	Mammuthus primigenius	upper molar tooth (M3)	fragment	d	R, shore	
BL-O 349	R	Equus sp.	unciform		d	R, shore	
BL-O 350	R	Mammuthus primigenius	lumbar vertebra		d	R, shore	C14
BL-O 351	R	Mammuthus primigenius	rib	damaged	d	R, shore	C14
BL-O 352	R	Mammuthus primigenius	tusk	fragment	d	R, shore	C14
BL-O 353	R	Mammuthus primigenius	lower molar tooth (?M3)	damaged	d	R, shore	
BL-O 354	R	Mammuthus primigenius	thorax vertebra	fragment	d	R, shore	C14
BL-O 355	R	Mammuthus primigenius	upper molar tooth (M3)		d	R, shore	
BL-O 356	R	Equus sp.	humerus		d	R, shore	
BL-O 357	R	Bison priscus	pelvis	fragment	d	R, shore	
BL-O 358	R	Mammuthus primigenius	cervical vertebra	fragment	d	R, shore	
BL-O 359	R	Bison priscus	scapula	fragment	d	R, shore	
BL-O 360	R	Ovibos sp.	pelvis	fragment	d	R, shore	
BL-O 361	R	Equus sp.	phalanx I		d	R, shore	
BL-O 362	R	Ovibos sp.	astrogalus		d	R, shore	
BL-O 363	R	Bison priscus	radius	proximal fragment	d	R, shore	
BL-O 364	R	Equus sp.	radius		d	R, shore	
BL-O 365	R	Rangifer tarandus	humerus		d	R, shore	juv.
BL-O 366	R	? Bison priscus	femur	fragment	d	R, shore	trashed
BL-O 367	R	Mammuthus primigenius	lower molar tooth (M2 or M3)	fragment	d	R, shore	
BL-O 368	R	Bison priscus	metacarpale		d	R, shore	
BL-O 369	R	Mammuthus primigenius	upper molar tooth (M3)	fragment	d	R, shore	
BL-O 370	L	Mammuthus primigenius	tusk	fragment	e	L, shore 10 km from camp	C14
BL-O 371	R	Bison priscus	radius	fragment	d	R, shore	
BL-O 372	R	Rangifer tarandus	shed antler	fragment	d	R, shore	
BL-O 373	L	Bison priscus	horn sheet		d	R, shore	
BL-O 374	R	Equus sp.	humerus		d	R, shore	
BL-O 375	R	Mammuthus primigenius	tooth	fragment	d	R, shore	
BL-O 376	R	Coelodonta antiqua	astrogalus		d	R, shore	
BL-O 377	R	Rangifer tarandus	atlas		d	R, shore	
BL-O 378	R	Rangifer tarandus	phalanx I		d	R, shore	
BL-O 379	R	Rangifer tarandus	lumbar vertebra		d	R, shore	

A5-7: continuation.

samples	Side	Taxon	Skeleton element	Preservation	Type	Locality	Notes
BL-O 380	R	Ovibos sp.	humerus	fragment	d	R, shore	juv.
BL-O 381	R	Mammuthus primigenius	cervical vertebra	fragment	d	R, shore	trashed
BL-O 382	R	Rangifer tarandus	lumbar vertebra		d	R, shore	
BL-O 383	R	Mammuthus primigenius	thorax vertebra	fragment	d	R, shore	
BL-O 384	L	Mammuthus primigenius	pelvis	fragment	e	L, shore	
BL-O 385	L	Mammuthus primigenius	tibia	fragment	e	L, shore	C14
BL-O 386	R	Lepus sp.	pelvis		d	R, shore	
BL-O 387	R	Bison priscus	calcaneus	proximal fragment	d	R, shore	
BL-O 388	R	Mammuthus primigenius	upper tooth	fragment	d	R, shore	
BL-O 389	R	Equus sp.	upper molar tooth (M2)		d	R, shore	
BL-O 390	R	Ovibos sp.	humerus	distal fragment	d	R, shore	
BL-O 391	R	Equus sp.	lower molar tooth (M)		d	R, shore	
BL-O 392	R	Rangifer tarandus	metatarsale	distal fragment	d	R, shore	
BL-O 393	R	Large mammal	cranium	fragment	d	R, shore	juv.
BL-O 394	R	Ovibos sp.	vertebra	fragment	d	R, shore	
BL-O 395	R	Mammuthus primigenius	tusk	fragment	d	R, shore	trashed
BL-O 396	R	Equus sp.	upper premolar tooth (P2)		d	R, shore	
BL-O 397	R	Equus sp.	phalanx II		d	R, shore	
BL-O 398	R	Equus sp.	phalanx III		d	R, shore	
BL-O 399	R	Equus sp.	metatarsale III	proximal fragment	d	R, shore	
BL-O 400	R	Bison priscus	phalanx II		d	R, shore	
BL-O 401	R	Lepus sp.	pelvis		d	R, shore	
BL-O 402	R	Bison priscus	lower tooth (M3)		d	R, shore	
BL-O 403	R	Rangifer tarandus	sacrum	fragment	d	R, shore	juv.
BL-O 404	R	Rangifer tarandus	shed antler	fragment	d	R, shore	trashed
BL-O 405	R	Bison priscus or Ovibos sp.	upper premolar teth		d	R, shore	
BL-O 406	R	Rangifer tarandus	astrogalus		d	R, shore	
BL-O 407	R	Ovibos sp.	lower molar tooth (M3)		d	R, shore	
BL-O 408	R	Bison priscus	calcaneus		d	R, shore	
BL-O 409	R	Mammuthus primigenius	ulna	fragment	d	R, shore	C14
BL-O 411	L	Bison priscus	cervical vertebra		e	L, shore	
BL-O 412	L	Mammuthus primigenius	tibia	fragment	e	L, shore	C14, juv.
BL-O 413	L	Coelodonta antiqua	radius		e	L, shore	
BL-O 414	L	Mammuthus primigenius	intermedium		e	L, shore	

A5-7: continuation.

samples	Side	Taxon	Skeleton element	Preservation	Type	Locality	Notes
BL-O 415	L	Equus sp.	lower tooth (M)		e	L, shore	trashed
BL-O 416	L	?????????????	cranium	fragment	e	L, shore	trashed
BL-O 417	L	Rangifer tarandus	metatarsale	proximal fragment	e	L, shore	
BL-O 418	L	Panthera spelaea	tibia		e	L, shore near the camp	
BL-O 419	L	Rangifer tarandus	shed antler	fragment	e	L, shore near the camp	
BL-O 420	L	Rangifer tarandus	metatarsale		e	L, shore near the camp	
BL-O 421	L	Bison priscus	intercarpale		e	L, shore near the camp	
BL-O 422	L	?Carnivora	cervical vertebra		e	L, shore near the camp	trashed
BL-O 423	L	Lepus sp.	calcaneus		e	L, shore near the camp	
BL-O 424	L	? Mammuthus primigenius	tooth	fragment	e	L, shore near the camp	trashed
BL-O 425	L	Mammuthus primigenius	tusk	fragment	e	L	C14
BL-O 426	L	Mammuthus primigenius	tooth		e	L, shore under I TC	
BL-O 427	R	Equus sp.	lower milk tooth (P)		d	R, shore	
BL-O 428	R	Equus sp.	lower tooth (M3)		d	R, shore	
BL-O 429	R	Bison priscus	upper tooth		d	R, shore	
BL-O 430	R	Lepus sp.	pelvis	fragment	d	R, shore	
BL-O 431	R	Lepus sp.	pelvis	fragment	d	R, shore	
BL-O 432	R	Lepus sp.	calcaneus		d	R, shore	
BL-O 433	L	Bison priscus	sacrum	fragment	e	L, shore under I TC	
BL-O 434	L	Ovibos sp.	epistropheus		d	R, shore	
BL-O 435	L	Equus sp.	metacarpale III		d	R, shore	
BL-O 436	L	Equus sp.	metatarsale III		e	L, shore	
BL-O 437	L	Equus sp.	hoof	2 pieces	e	L, shore	
BL-O 438	R	Rangifer tarandus	lumbar vertebra		b	R, boundary alas and IV TC	
BL-O 439	R	Equus sp.	humerus	distal fragment	e	L, shore	
BL-O 440	R	?Ovibos sp.	lumbar vertebra	damaged	e	L, shore	
BL-O 441	R	Equus sp.	phalanx II		e	L, shore	
BL-O 442	R	Rangifer tarandus	cervical vertebra		e	L, shore	juv.
BL-O 443	R	Mammuthus primigenius	tusk	fragment (3 pieces)	c	R, from ? "Kuchchuguy" altitude	C14
BL-O 444	R	Equus sp.	metatarsale III		d	R, shore	
BL-O 445	R	Rangifer tarandus	metatarsale	distal fragment	d	R, shore	juv.
BL-O 446	R	Bison priscus	metatarsale		d	R, shore	
BL-O 447	L	Bison priscus	lumbar vertebra	sample damaged	e	L, shore	
BL-O 448	L	Bison priscus	lumbar vertebra		e	L, shore	

A5-7: continuation.

samples	Side	Taxon	Skeleton element	Preservation	Type	Locality	Notes
BL-O 449	L	Bison priscus	cervical vertebra		e	L, shore	
BL-O 450	L	Bison priscus	cervical vertebra		e	L, shore	
BL-O 451	L	Bison priscus	cervical vertebra		e	L, shore	
BL-O 452	L	Bison priscus	cervical vertebra		e	L, shore	
BL-O 453	L	Ovibos sp.	cervical vertebra		e	L, shore	
BL-O 454	L	Bison priscus	cervical vertebra		e	L, shore	
BL-O 455	L	Mammuthus primigenius	upper molar tooth (M3 or ?M2)	fragment	e	L, shore	
BL-O 456	L	Mammuthus primigenius	upper molar tooth (M2)	fragment	e	L, shore	
BL-O 457	L	Mammuthus primigenius	upper molar tooth (M3 or ?M2)	fragment	e	L, shore	
BL-O 458	L	Mammuthus primigenius	tooth	fragment	e	L, shore	
BL-O 459	L	Equus sp.	metacarpale III	proximal fragment	e	L, shore	
BL-O 460	L	Equus sp.	metacarpale III		e	L, shore	
BL-O 461	L	Equus sp.	metacarpale III		e	L, shore	
BL-O 462	L	Equus sp.	radius	distal fragment	e	L, shore	
BL-O 463	L	Bison priscus	radius		e	L, shore	
BL-O 464	L	Bison priscus	metacarpale	distal fragment	e	L, shore	
BL-O 465	L	Equus sp.	phalanx I		e	L, shore under I TC	
BL-O 466	L	Equus sp.	navuculare		e	L, shore under I TC	
BL-O 467	L	Rangifer tarandus	radius	proximal fragment	e	L, shore under I TC	
BL-O 468	L	Rangifer tarandus	humerus	distal fragment	e	L, shore under I TC	
BL-O 469	L	Mammuthus primigenius	mabdibula	simphis fragment	e	L, shore under I TC	C14
BL-O 470	L	Bison priscus	cervical vertebra		e	L, shore near the camp	
BL-O 471	L	Equus sp.	calcaneus	sample damaged	e	L, shore near the camp	
BL-O 472	L	Equus sp.	metatarsale III	distal fragment	e	L, shore near the camp	
BL-O 473	L	Rangifer tarandus	mabdibula (left stem) with teeth P2 - M3		e	L, shore near the camp	
BL-O 474	L	Equus sp.	thorax vertebra	sample damaged	e	L, shore near the camp	
BL-O 475	L	Rangifer tarandus	lower molar tooth (M3)		e	L, shore	
BL-O 476	L	Mammuthus primigenius	lower molar tooth (M3)	fragment	e	L, shore	
BL-O 477	L	Equus sp.	phalanx		e	L, shore near the camp	
BL-O 478	L	Rangifer tarandus	metacarpale	deformity	e	L, shore near the camp	
BL-O 479	L	Equus sp.	pelvis	fragment	e	L, shore near the camp	
BL-O 480	L	Mammuthus primigenius	femur	fragment	e	L, shore near the camp	trashed

A5-7: continuation.

samples	Side	Taxon	Skeleton element	Preservation	Type	Locality	Notes
BL-O 481	L	Bison priscus	pelvis	fragment	e	L, shore	trashed
BL-O 482	L	Mammuthus primigenius	tusk	fragment	e	L, shore	C 14
BL-O 483	L	Mammuthus primigenius	upper molar tooth (?M1)	fragment	e	L, shore	
BL-O 484	L	Equus sp.	scapula	sample damaged	e	L, shore	
BL-O 485	L	Equus sp.	tibia	distal fragment	e	L, shore	
BL-O 486	L	Equus sp.	astrogalus		e	L, shore	
BL-O 487	L	Equus sp.	metacarpale III	distal fragment	e	L, shore	
BL-O 488	L	Bison priscus	mabdibula	fragment	e	L, shore	
BL-O 489	L	Equus sp.	ulna		e	L, shore	
BL-O 490	L	Bison priscus	humerus	distal fragment	e	L, shore	
BL-O 491	L	Bison priscus	lumbar vertebra		e	L, shore	
BL-O 492	L	Ovibos sp.	atlas	damaged	e	L, shore	
BL-O 493	L	Equus sp.	lumbar vertebra		e	L, shore	
BL-O 494	L	Mammuthus primigenius	tooth replased		e	L, shore	trashed
BL-O 495	L	Bison priscus	cervical vertebra		e	L, shore	
BL-O 496	L	Ovibos sp.	cervical vertebra		e	L, shore	
BL-O 497	L	Bison priscus	cranium with horn	fragment	e	L, shore	
BL-O 498	L	Mammuthus primigenius	tusk	fragment	e	L, shore	C 14
BL-O 499	R	Mammuthus primigenius	tusk	fragment	d	R, shore	C14
BL-O 500	L	Bison priscus	scapula		e	L, shore 10 km from camp	
BL-O 501	L	Mammuthus primigenius	intermedium		e	L, shore	
BL-O 502	L	Mammuthus primigenius	cervical vertebra	fragment	e	L, shore 10 km from camp	C 14
BL-O 503	L	Mammuthus primigenius	scapula	fragment	e	L, shore 10 km from camp	C 14
BL-O 504	L	Mammuthus primigenius	tusk	fragment	e	L, shore	C 14
BL-O 505	L	Mammuthus primigenius	scapula	proximal fragment	e	L, shore	C 14
BL-O 506	L	Mammuthus primigenius	thorax vertebra		e	L, shore	C 14
BL-O 507	L	Mammuthus primigenius	femur	fragment	e	L, shore	C14
BL-O 508	L	Mammuthus primigenius	pelvis	fragment	e	L, shore	C14
BL-O 509	L	Mammuthus primigenius	pelvis	fragment	e	L, shore	C14
BL-O 510	L	Bison priscus	horn		e	L, shore	
BL-O 511	L	Large mammal	limb bone	fragment	e	L, shore 4 - 5 km from the camp	trashed
BL-O 512	L	?Rangifer tarandus	astrogalus		e	L, shore 4 - 5 km from the camp	
BL-O 514	L	Bison priscus	magnum		e	L, shore 4 - 5 km from the camp	
BL-O 515	L	Mammuthus primigenius	tooth	fragment	e	L, shore 4 - 5 km from the camp	
BL-O 516	L	Rangifer tarandus	phalanx I		e	L, shore 4 - 5 km from the camp	

A5-7: continuation.

samples	Side	Taxon	Skeleton element	Preservation	Type	Locality	Notes
BL-O 517	L	Equus sp.	pelvis	fragment	e	L, shore 4 - 5 km from the camp	trashed
BL-O 518	L	Bison priscus	atlas		e	L, shore 4 - 5 km from the camp	
BL-O 519	L	Mammuthus primigenius	humerus	cut out	b	L, III TC, altitude 15 m	C14
BL-O 520	R	Bison priscus	radius		c	R, small TC	
BL-O 521	R	Rangifer tarandus	metacarpale	distal fragment	d	R, shore	
BL-O 522	R	Large mammal	limb bone	fragment	d	R, shore	trashed
BL-O 523	R	Equus sp.	radius	distal fragment	d	R, shore	juv.
BL-O 524	R	Rangifer tarandus	lower premolar tooth (P)		d	R, shore	
BL-O 525	R	Lepus sp.	pelvis	fragment	d	R, shore	
BL-O 526	R	Lepus sp.	calcaneus		d	R, shore	
BL-O 527	L	Equus sp.	pelvis	fragment	e	L, shore 5 - 6 km from the camp	
BL-O 528	L	Equus sp.	metacarpale III	proximal fragment	e	L, shore 5 - 6 km from the camp	
BL-O 529	L	Bison priscus	metacarpale	distal fragment	e	L, shore 5 - 6 km from the camp	
BL-O 530	L	Rangifer tarandus	ulna	fragment	e	L, shore 5 - 6 km from the camp	
BL-O 531	L	Equus sp.	cuneiforme III		e	L, shore 5 - 6 km from the camp	
BL-O 532	L	Equus sp.	phalanx I		e	L, shore 5 - 6 km from the camp	
BL-O 533	L	Ovibos sp.	phalanx I		e	L, shore 5 - 6 km from the camp	
BL-O 534	L	Panthera spelaea	metapodia		e	L, shore 5 - 6 km from the camp	
BL-O 535	L	Equus sp.	cervical vertebra		e	L, shore 5 - 6 km from the camp	
BL-O 536	L	? Ovibos sp.	mandibula	fragment	e	L, shore 5 - 6 km from the camp	
BL-O 537	L	Lepus sp.	metapodia	distal fragment	e	L, shore 5 - 6 km from the camp	
BL-O 538	L	Bison priscus	phalanx II	fragment	e	L, shore 5 - 6 km from the camp	
BL-O 539	L	Ovibos sp.	calcaneus	fragment	e	L, shore 5 - 6 km from the camp	
BL-O 540	L	Equus sp.	phalanx I	fragment	e	L, shore 5 - 6 km from the camp	
BL-O 541	L	Bison priscus	astrogalus		e	L, shore 5 - 6 km from the camp	
BL-O 542	L	Bison priscus	astrogalus		e	L, shore 5 - 6 km from the camp	
BL-O 543	L	Mammuthus primigenius	tooth	fragment	e	L, shore 5 - 6 km from the camp	trashed
BL-O 545	L	Rangifer tarandus	carpi radiale		e	L, shore 5 - 6 km from the camp	
BL-O 546	L	Bison priscus	phalanx II	fragment	e	L, shore 5 - 6 km from the camp	
BL-O 547	L	Equus sp.	sesamoidea phalanx I		e	L, shore 5 - 6 km from the camp	
BL-O 548	L	Equus sp.	phalanx I	fragment	e	L, shore 5 - 6 km from the camp	
BL-O 549	L	?Ovibos sp.	lower tooth	fragment (2 pieces)	e	L, shore 5 - 6 km from the camp	
BL-O 551	L	Equus sp.	pelvis	fragment	e	L, shore 5 - 6 km from the camp	trashed
BL-O 552	L	Rangifer tarandus	tibia	distal fragment	e	L, shore 5 - 6 km from the camp	
BL-O 553	L	Ovibos sp.	thorax vertebra	fragment	e	L, shore 5 - 6 km from the camp	

A5-7: continuation.

samples	Side	Taxon	Skeleton element	Preservation	Type	Locality	Notes
BL-O 554	L	Equus sp.	mandibula	fragment	e	L, shore 5 - 6 km from the camp	trashed
BL-O 555	L	Bison priscus	phalanx III	fragment	e	L, shore 5 - 6 km from the camp	
BL-O 556	L	? Bison priscus	upper premolar tooth		e	L, shore 5 - 6 km from the camp	
BL-O 557	L	Rangifer tarandus	scapula	proximal fragment	e	L, shore 5 - 6 km from the camp	
BL-O 558	L	Equus sp.	astrogalus		e	L, shore 5 - 6 km from the camp	
BL-O 559	L	Bison priscus	calcaneus		e	L, shore 5 - 6 km from the camp	
BL-O 560	L	Rangifer tarandus	thorax vertebra		e	L, shore 5 - 6 km from the camp	juv.
BL-O 561	L	Bison priscus	radius	procsimal fragment	e	L, shore 5 - 6 km from the camp	trashed
BL-O 562	L	Equus sp.	radius	fragment	e	L, shore 5 - 6 km from the camp	juv., trashed
BL-O 563		Bison priscus	astrogalus			L, shore 5 - 6 km from the camp	
BL-O 564	L	Bison priscus	lower tooth		e	L, shore 5 - 6 km from the camp	
BL-O 565	L	? Rangifer tarandus	antler	fragment	e	L, shore 5 - 6 km from the camp	
BL-O 568	L	Equus sp.	sesamoidea phalanx I		e	L, shore 5 - 6 km from the camp	
BL-O 569	L	Rangifer tarandus	pisiforme		e	L, shore 5 - 6 km from the camp	
BL-O 570	L	Equus sp.	phalanx II		e	L, shore 5 - 6 km from the camp	
BL-O 571	L	Ovibos sp.	thorax vertebra	sample cut out	e	L, shore 5 - 6 km from the camp	
BL-O 572	L	Bison priscus	astrogalus	fragment	e	L, shore 5 - 6 km from the camp	
BL-O 573	L	Equus sp.	calcaneus	sample cut out	e	L, shore 5 - 6 km from the camp	
BL-O 574	L	Bison priscus	magnum		e	L, shore 5 - 6 km from the camp	
BL-O 575	L	Ovibos sp.	thorax vertebra		e	L, shore 5 - 6 km from the camp	
BL-O 576	L	Mammuthus primigenius	tusk	fragment	e	L, shore 5 - 6 km from the camp	trashed
BL-O 577	L	Mammuthus primigenius	upper tooth	fragment	e	L, shore 5 - 6 km from the camp	
BL-O 578	L	Mammuthus primigenius	upper tooth	fragment	e	L, shore 5 - 6 km from the camp	
BL-O 579	L	Mammuthus primigenius	tooth	fragment	e	L, shore 5 - 6 km from the camp	
BL-O 580	L	Mammuthus primigenius	tusk	fragment	e	L, shore 5 - 6 km from the camp	trashed
BL-O 581	R	Equus sp.	phalanx I		d	L, shore	juv.
BL-O 582	R	Rangifer tarandus	cervical vertebra		c	R, from scree, "Kuch." altitude	
BL-O 583	R	Rangifer tarandus	vertebra	fragment	a	in situ R, from baydzherakh, R-5	trashed
BL-O 584	R	Bison priscus	radius	2 pieces	a	in situ R, altitude 2m, R4+50	juv.
BL-O 585	R	Mammuthus primigenius	humerus		a	in situ, upper part of small TC between I and II TCs	C14; from Hanno
BL-O 586	L	Mammuthus primigenius	tusk	fragment	e	L, shore	trashed
BL-O 587	L	Rangifer tarandus	metacarpale	sample cut out	e	L, shore	
BL-O 588	L	Equus sp.	phalanx II		e	L, shore	
BL-O 589	L	Equus sp.	tibia	distal fragment	e	L, shore	

A5-7: continuation.

samples	Side	Taxon	Skeleton element	Preservation	Type	Locality	Notes
BL-O 590	L	Mammuthus primigenius	upper molar tooth (M3)		e	L, shore	
BL-O 591	L	Mammuthus primigenius	scapula	proximal fragment	e	L, shore	
BL-O 592	L	Mammuthus primigenius	tusk	fragment	e	L, shore	C 14
BL-O 593	L	Mammuthus primigenius	tooth	fragment	e	L, shore	
BL-O 594	L	Mammuthus primigenius	astrogalus		e	L, shore	
BL-O 595	L	Bison priscus	radius	proximal fragment	e	L, shore	
BL-O 596	L	Bison priscus or Ovibos sp.	upper tooth	fragment	e	L, shore	
BL-O 597	L	Ovibos sp.	epistrofei		e	L, shore	
BL-O 598	L	Bison priscus	metacarpale		e	L, shore	
BL-O 599	Z	Mammuthus primigenius	patella		f	????? r. Zimov'e	from Guido
BL-O 600	Z	Mammuthus primigenius	femur		f	????? r. Zimov'e	from Guido, ?14, juv.
BL-O 601	R	Equus sp.	scapula	fragment	d	R, cape shore	trashed
BL-O 602	R	Bison priscus	metacarpale		d	R, cape shore	
BL-O 603	R	Bison priscus	cranium with horn	fragment	d	R, cape shore	trashed
BL-O 604	R	Bison priscus	??????????		d	R, cape shore	
BL-O 605	R	Rangifer tarandus	humerus	distal fragment	d	R, cape shore	
BL-O 606	R	Equus sp.	phalanx I		d	R, cape shore	
BL-O 607	R	Rangifer tarandus	shed antler	fragment	d	R, cape shore	trashed
BL-O 608	R	Bison priscus	radius	proximal fragment	d	R, cape shore	trashed
BL-O 609	R	Mammuthus primigenius	fibula	fragment	d	R, cape shore	juv.
BL-O 610	R	Bison priscus	thorax vertebra		d	R, cape shore	
BL-O 611	R	Ovibos sp.	cervical vertebra		d	R, cape shore	
BL-O 612	R	Mammuthus primigenius	tibia	fragment	d	R, cape shore	juv.
BL-O 613	R	Mammuthus primigenius	femur	fragment	d	R, cape shore	juv.
BL-O 614	R	?Praeovibos sp.	horn	fragment	d	R, cape shore	
BL-O 615	R	Mammuthus primigenius	metacarpale V		d	R, cape shore	
BL-O 616	R	Mammuthus primigenius	tooth	fragment	d	R, cape shore	
BL-O 617	R	Ovibos sp.	naviculare		d	R, cape shore	
BL-O 618	R	? Mammuthus primigenius	tooth	fragment	d	R, cape shore	trashed
BL-O 619	R	Equus sp.	naviculare		d	R, cape shore	
BL-O 620	R	Rangifer tarandus	phalanx I		d	R, cape shore	
BL-O 621	R	?????????????	bone	fragment	d	R, cape shore	trashed

A5-7: continuation.

samples	Side	Taxon	Skeleton element	Preservation	Type	Locality	Notes
BL-O 622	R	Rangifer tarandus	phalanx II		d	R, cape shore	juv.
BL-O 623	R	Bison priscus	naviculare	fragment	d	R, cape shore	trashed
BL-O 624	R	Rangifer tarandus	astrogalus	fragment	d	R, cape shore	trashed
BL-O 625	R	Rangifer tarandus	tibia	distal fragment	d	R, cape shore	juv.
BL-O 626	R	Rangifer tarandus	upper molar tooth (M)	fragment	d	R, cape shore	
BL-O 627	R	Lepus sp.	humerus	distal fragment	d	R, cape shore	
BL-O 628	L	Bison priscus	humerus	distal fragment	e	L, shore	
BL-O 629	L	Bison priscus	lower tooth (M3)		e	L, shore	
BL-O 630	L	Ovibos sp.	upper tooth (M)		e	L, shore	
BL-O 631	L	Equus sp.	phalanx II		e	L, shore	
BL-O 632	L	Equus sp.	phalanx II		e	L, shore	
BL-O 633	L	Ovibos sp.	cervical vertebra	sample cut out	e	L, shore	
BL-O 634	L	Rangifer tarandus	tibia	distal fragment	e	L, shore	
BL-O 635	L	Rangifer tarandus	humerus	distal fragment	e	L, shore	
BL-O 636	L	Bison priscus	scapula	fragment	e	L, shore	
BL-O 637	L	Bison priscus	scapula	fragment	e	L, shore	
BL-O 638	L	Rangifer tarandus	astrogalus	sample cut out	e	L, shore	
BL-O 639	L	Rangifer tarandus	metacarpale	distal fragment	e	L, shore	
BL-O 640	L	Equus sp.	mandibula	fragment	e	L, shore	trashed
BL-O 641	L	Bison priscus	cervical vertebra	fragment	e	L, shore	
BL-O 642	L	Rangifer tarandus	humerus	distal fragment	e	L, shore	juv.
BL-O 643	L	Equus sp.	pisiforme		e	L, shore	
BL-O 644	L	Ovibos sp.	cervical vertebra		e	L, shore	
BL-O 645	L	Mammuthus primigenius	metacarpale V	fragment	e	L, shore	
BL-O 646	L	Mammuthus primigenius	?tusk	deformity	e	L, shore 10 km from camp	
BL-O 647	L	Bison priscus	cranium with horn	fragment	e	L, shore 10 km from camp	
BL-O 648	L	Bison priscus	radius	proximal fragment	e	L, shore 10 km from camp	
BL-O 649	L	Bison priscus	humerus	fragment	e	L, shore 10 km from camp	
BL-O 650	L	Equus sp.	pelvis	fragment	e	L, shore 10 km from camp	trashed
BL-O 651	L	Bison priscus	humerus	distal fragment	e	L, shore 10 km from camp	
BL-O 652	L	Equus sp.	astrogalus		e	L, shore 10 km from camp	
BL-O 653	L	Equus sp.	astrogalus		e	L, shore 10 km from camp	
BL-O 654	L	Equus sp.	astrogalus		e	L, shore 10 km from camp	
BL-O 655	L	Equus sp.	phalanx II		e	L, shore 10 km from camp	
BL-O 656	L	Equus sp.	phalanx II		e	L, shore 10 km from camp	

A5-7: continuation.

samples	Side	Taxon	Skeleton element	Preservation	Type	Locality	Notes
BL-O 657	L	Ovibos sp.	magnum		e	L, shore 10 km from camp	
BL-O 658	L	Equus sp.	ulna		e	L, shore 10 km from camp	
BL-O 659	L	Mammuthus primigenius	tooth	fragment	e	L, shore 10 km from camp	
BL-O 660	L	Mammuthus primigenius	premolar tooth (heavily worn)	fragment	e	L, shore 10 km from camp	
BL-O 661	L	Mammuthus primigenius	upper molar tooth (M2 or M3)	fragment	e	L, shore 10 km from camp	
BL-O 662	L	Equus sp.	radius		e	L, shore 10 km from camp	
BL-O 663	L	Bison priscus	tibia	distal fragment	e	L, shore 10 km from camp	
BL-O 664	L	Bison priscus	astrogalus		e	L, shore 10 km from camp	
BL-O 665	L	Rangifer tarandus	epistrofei		e	L, shore 10 km from camp	
BL-O 666	L	Mammuthus primigenius	tusk	fragment	e	L, shore 10 km from camp	trashed
BL-O 667	L	Equus sp.	calcaneus	sample damaged	e	L, shore 10 km from camp	
BL-O 668	L	Ovibos sp.	scapula	proximal fragment	e	L, shore 10 km from camp	
BL-O 669	L	Rangifer tarandus	astrogalus		e	L, shore 10 km from camp	
BL-O 670	L	Ovibos sp.	metatarsale	distal fragment	e	L, shore 10 km from camp	
BL-O 671	L	Bison priscus	phalanx II	fragment	e	L, shore 10 km from camp	
BL-O 672	L	Equus sp.	metatarsale III	fragment	e	L, shore 10 km from camp	trashed
BL-O 673	L	Equus sp.	metacarpale III	fragment	e	L, shore 10 km from camp	
BL-O 674	L	Equus sp.	ulna	fragment	e	L, shore 10 km from camp	
BL-O 675	L	Rangifer tarandus	mandibula (right stem) with P4 - M1	fragment	e	L, shore 10 km from camp	
BL-O 676	L	Rangifer tarandus	astrogalus		e	L, shore 10 km from camp	
BL-O 677	L	Ovibos sp.	lower tooth (M)		e	L, shore 10 km from camp	
BL-O 678	L	Equus sp.	phalanx III	fragment	e	L, shore 10 km from camp	
BL-O 679	L	Mammuthus primigenius	tibia	fragment	e	L, shore 10 km from camp	trashed
BL-O 680	L	? Saiga tatarica	thorax vertebra	sample damaged	e	L, shore 10 km from camp	
BL-O 681	L	Ovibos sp.	cranium	fragrnent	e	L, shore 10 km from camp	
BL-O 682	L	Bison priscus	atlas	fragrnent	e	L, shore 10 km from camp	
BL-O 683	L	Equus sp.	metapodia II or IV	distal fragment	e	L, shore 10 km from camp	trashed
BL-O 684	L	Mammuthus primigenius	tibia	distal fragrnent	e	L, shore 10 km from camp	
BL-O 685	R	Mammuthus primigenius	calcaneus	fragment	d	R, cape shore	
BL-O 686	R	Bison priscus	humerus	distal fragment	d	R, cape shore	
BL-O 687	R	Ovibos sp.	cervical? vertebra		d	R, cape shore	
BL-O 688	R	Rangifer tarandus	astrogalus	fragment	d	R, cape shore	trashed

A5-7: continuation.

samples	Side	Taxon	Skeleton element	Preservation	Type	Locality	Notes
BL-O 689	R	Rangifer tarandus	cranium	fragment	d	R, cape shore	
BL-O 690	R	Rangifer tarandus	phalanx II	fragment	d	R, cape shore	
BL-O 691	R	Equus sp.	magnum		d	R, cape shore	
BL-O 692	R	Rangifer tarandus	phalanx I	proximal fragment	d	R, cape shore	
BL-O 693	R	Rangifer tarandus	phalanx III	damaged	d	R, cape shore	
BL-O 694	R	Ovibos sp.	magnum		d	R, cape shore	
BL-O 695	R	? Bison priscus	?pelvis	fragment	d	R, cape shore	trashed
BL-O 696	R	Rangifer tarandus	astrogalus	sample damaged	d	R, cape shore	
BL-O 697	R	Rangifer tarandus	cervical vertebra		d	R, cape shore	juv.
BL-O 698	L	Mammuthus primigenius	ulna	fragment	e	L, shore 10 km from camp	juv.
BL-O 699	L	Bison priscus	lumbar vertebra		e	L, shore 10 km from camp	
BL-O 700	L	Equus sp.	astrogalus		e	L, shore 10 km from camp	
BL-O 701	L	Bison priscus	vertebra	fragment	e	L, shore 10 km from camp	
BL-O 703	L	Bison priscus	metapodia	distal fragment	e	L, shore 10 km from camp	trashed
BL-O 704	L	Rangifer tarandus	naviculare		e	L, shore 10 km from camp	
BL-O 705	L	Rangifer tarandus	phalanx II		e	L, shore 10 km from camp	
BL-O 706	L	Rangifer tarandus	tibia	distal fragment	e	L, shore 10 km from camp	juv.
BL-O 707	L	? Rangifer tarandus	carpi radiale		e	L, shore 10 km from camp	
BL-O 708	L	Ovibos sp.	cranium, brain part, male	fragment	c	L, I TC	
BL-O 709	L	Equus sp.	humerus	distal fragment	c	L, I TC	juv.
BL-O 710	L	Equus sp.	astrogalus		c	L, I TC	
BL-O 711	L	Rangifer tarandus	cervical vertebra		c	L, I TC	
BL-O 712	L	Equus sp.	pelvis	fragment	c	L, I TC	
BL-O 713	L	Equus sp.	femus	fragment	c	L, I TC	trashed
BL-O 714	L	Equus sp.	humerus	fragment	c	L, I TC	juv.
BL-O 715	L	Mammuthus primigenius	tarsale 4-5		c	L, I TC	
BL-O 716	L	Equus sp.	radius	fragment	c	L, I TC	juv.
BL-O 717	L	Ovibos sp.	cervical vertebra		c	L, I TC	
BL-O 718	L	Bison priscus	metapodia	distal fragment	c	L, I TC	
BL-O 719	L	Equus sp.	radius	fragment	c	L, I TC	juv.
BL-O 720	L	Rangifer tarandus	humerus	distal fragment	c	L, I TC	
BL-O 721	L	Bison priscus	astrogalus		c	L, I TC	
BL-O 722	L	Bison priscus	metacarpale	sample damaged	c	L, I TC	juv.
BL-O 723	L	Mammuthus primigenius	atlas		c	L, I TC	
BL-O 724	L	Mammuthus primigenius	femus	fragment	c	L, I TC	juv.

A5-7: continuation.

samples	Side	Taxon	Skeleton element	Preservation	Type	Locality	Notes
BL-O 725	L	Bison priscus	lumbar vertebra		c	L, I TC	
BL-O 726	L	Equus sp.	femus	fragment	c	L, I TC	
BL-O 727	L	Equus sp.	tibia	distal fragment	c	L, I TC	
BL-O 728	L	Equus sp.	humerus	distal fragment	c	L, I TC	
BL-O 729	L	Rangifer tarandus	antebrachium		c	L, I TC	?recent
BL-O 730	L	Rangifer tarandus	humerus	distal fragment	c	L, I TC	
BL-O 731	L	Rangifer tarandus	ulna		c	L, I TC	
BL-O 732	L	Equus sp.	metatarsale III		c	L, I TC	
BL-O 733	L	Equus sp.	antebrachium		c	L, I TC	
BL-O 734	L	Equus sp.	metatarsale III		c	L, I TC	
BL-O 735	L	Equus sp.	tibia		c	L, I TC	
BL-O 736	L	Bison priscus	radius		c	L, I TC	
BL-O 737	L	Ovibos sp.	cervical vertebra		c	L, I TC	
BL-O 738	L	Mammuthus primigenius	metacarpale IV		c	L, I TC	
BL-O 739	L	Bison priscus	astrogalus		c	L, I TC	
BL-O 740	L	Ovibos sp.	naviculare		c	L, I TC	
BL-O 741	L	Rangifer tarandus	epistropheus		c	L, I TC	
BL-O 742	L	Rangifer tarandus	maxilla (left stem) with teeth row (P3 - M3)	fragment	c	L, I TC	
BL-O 743	L	Bison priscus	naviculare		c	L, I TC	
BL-O 744	L	Bison priscus	tibia		e	L, shore	
BL-O 745	L	Mammuthus primigenius	upper molar tooth (?M3)		e	L, shore	
BL-O 746	L	Equus sp.	scapula	fragment	e	L, shore	
BL-O 747	L	Ovibos sp.	tibia	distal fragment	e	L, shore	
BL-O 748	L	Rangifer tarandus	cranium	fragment	e	L, shore	
BL-O 749	L	Bison priscus	cranium	fragment	e	L, shore	
BL-O 750	L	Rangifer tarandus	atlas		e	L, shore	
BL-O 751	L	Equus sp.	magnum		e	L, shore	
BL-O 752	L	Equus sp.	phalanx I		e	L, shore	
BL-O 753	L	Equus sp.	phalanx I		e	L, shore	
BL-O 754	L	Mammuthus primigenius	tooth	fragment	e	L, shore	
BL-O 755	L	Mammuthus primigenius	tooth	fragment	e	L, shore	
BL-O 756	L	Mammuthus primigenius	replaced tooth	fragment	e	L, shore	
BL-O 757	L	Mammuthus primigenius	metacarpale III		e	L, shore	
BL-O 758	L	Equus sp.	astrogalus		e	L, shore	

A5-7: continuation.

samples	Side	Taxon	Skeleton element	Preservation	Type	Locality	Notes
BL-O 759	L	Equus sp.	astrogalus		e	L, shore	
BL-O 760	L	Equus sp.	calcaneus		e	L, shore	
BL-O 761	L	Bison priscus	calcaneus		e	L, shore	
BL-O 762	L	Bison priscus	astrogalus	fragment	e	L, shore	
BL-O 763	L	Ovibos sp.	pelvis	fragment	e	L, shore	
BL-O 764	L	Ovibos sp.	astrogalus		e	L, shore	
BL-O 765	L	Ovibos sp.	cervical vertebra		e	L, shore	
BL-O 766	L	Mammuthus primigenius	pelvis	fragment	e	L, shore	juv., C 14
BL-O 767	L	Bison priscus	phalanx II	fragment	e	L, shore	
BL-O 768	L	Mammuthus primigenius	tooth	fragment	e	L, shore	
BL-O 769	L	Equus sp.	calcaneus	fragment	e	L, shore	trashed
BL-O 770	L	Equus sp.	phalanx I	proximal fragment	e	L, shore	
BL-O 771	L	Rangifer tarandus	radius	distal fragment	e	L, shore	juv.
BL-O 772	L	Rangifer tarandus	shed antler	fragment	e	L, shore	
BL-O 773	L	Bison priscus	calcaneus	fragment	e	L, shore	
BL-O 774	L	Bison priscus	pelvis	fragment	e	L, shore	
BL-O 775	L	Equus sp.	tibia	fragment	e	L, shore	
BL-O 776	L	Ovibos sp.	epistropheus	sample damaged	e	L, shore	
BL-O 777	Z	Equus sp.	metacarpale III		f	r. Zimov'e, shore and flood plane	
BL-O 778	Z	Equus sp.	metacarpale III		f	r. Zimov'e, shore and flood plane	
BL-O 779	Z	Equus sp.	tibia	proximal fragment	f	r. Zimov'e, shore and flood plane	
BL-O 780	Z	Mammuthus primigenius	fibula	distal fragment	f	r. Zimov'e, shore and flood plane	
BL-O 781	Z	Mammuthus primigenius	astrogalus		f	r. Zimov'e, shore and flood plane	
BL-O 782	Z	Mammuthus primigenius	upper molar tooth (?M3)	fragment	f	r. Zimov'e, shore and flood plane	
BL-O 783	Z	Equus sp.	phalanx I		f	r. Zimov'e, shore and flood plane	
BL-O 784	Z	Equus sp.	ulna + radius	proximal fragment	f	r. Zimov'e, shore and flood plane	
BL-O 785	Z	Equus sp.	tibia	distal fragment	f	r. Zimov'e, shore and flood plane	
BL-O 786	Z	Equus sp.	tibia		f	r. Zimov'e, shore and flood plane	
BL-O 787	Z	Equus sp.	phalanx III		f	r. Zimov'e, shore and flood plane	
BL-O 788	Z	Equus sp.	phalanx III	fragment	f	r. Zimov'e, shore and flood plane	
BL-O 789	Z	Equus sp.	upper tooth (M)		f	r. Zimov'e, shore and flood plane	
BL-O 790	Z	Rangifer tarandus	lumbar vertebra		f	r. Zimov'e, shore and flood plane	juv.
BL-O 791	Z	Rangifer tarandus	calcaneus		f	r. Zimov'e, shore and flood plane	
BL-O 792	Z	Rangifer tarandus	calcaneus		f	r. Zimov'e, shore and flood plane	
BL-O 793	Z	Bison priscus	thorax vertebra	???????	f	r. Zimov'e, shore and flood plane	

A5-7: continuation.

samples	Side	Taxon	Skeleton element	Preservation	Type	Locality	Notes
BL-O 794	Z	Rangifer tarandus	pelvis	fragment	f	r. Zimov'e, shore and flood plane	
BL-O 795	Z	Rangifer tarandus	pelvis	fragment	f	r. Zimov'e, shore and flood plane	trashed
BL-O 796	Z	Bison priscus	upper tooth		f	r. Zimov'e, shore and flood plane	
BL-O 797	Z	Mammuthus primigenius	maxilla with milk premolar tooth (dP4)	fragment	f	r. Zimov'e, shore and flood plane	juv.
BL-O 798	Z	Bison priscus	scapula	fragment	f	r. Zimov'e, shore and flood plane	
BL-O 799	L	Rangifer tarandus	tibia	distal fragment (2 pieces)	e	L, shore	
BL-O 800	L	Ovibos sp.	calcaneus	sample damaged	e	L, shore	
BL-O 801	L	Mammuthus primigenius	cranium	fragment	e	L, shore	trashed
BL-O 802	L	Ovibos sp.	tibia	distal fragment	e	L, shore	
BL-O 803	L	Equus sp.	tibia		e	L, shore	
BL-O 804	L	Mammuthus primigenius	thorax vertebra		e	L, shore	C14
BL-O 805	L	Equus sp.	scapula	fragment	e	L, shore	
BL-O 806	L	Rangifer tarandus	spine	thorax fragment (3 vertebras) with copulas	e	L, shore	
BL-O 807	L	Equus sp.	scapula	fragment	e	L, shore	
BL-O 808	L	Ovibos sp.	cervical vertebra	fragment	e	L, shore	
BL-O 809	L	Mammuthus primigenius	molar tooth (M3)	fragment	e	L, shore	
BL-O 810	L	Mammuthus primigenius	lower molar tooth (M3)	sample damaged	e	L, shore	
BL-O 811	L	Mammuthus primigenius	tooth	fragment	e	L, shore	
BL-O 812	L	Mammuthus primigenius	carpale 3		e	L, shore	
BL-O 813	L	Mammuthus primigenius	tusk	fragment	e	L, shore	trashed
BL-O 814	L	Coelodonta antiqua	radius	distal fragment	e	L, shore	
BL-O 815	L	Bison priscus	thorax vertebra		e	L, shore	
BL-O 816	L	Bison priscus	phalanx I		e	L, shore	
BL-O 817	L	Bison priscus	naviculare		e	L, shore	
BL-O 818	L	Bison priscus	sacrum	fragment	e	L, shore	
BL-O 819	L	Ovibos sp.	metacarpale		e	L, shore	
BL-O 820	L	Bison priscus	astrogalus		e	L, shore	
BL-O 821	L	Bison priscus	horn sheet	fragment	e	L, shore	
BL-O 822	L	Mammuthus primigenius	tooth replaced		e	L, shore	
BL-O 823	L	Bison priscus	lumbar vertebra		e	L, shore	
BL-O 824	L	Ovibos sp.	metatarsale	fragment	e	L, shore	

A5-7: continuation.

samples	Side	Taxon	Skeleton element	Preservation	Type	Locality	Notes
BL-O 825	L	Rangifer tarandus	cranium	fragment	e	L, shore	juv.
BL-O 826	L	Rangifer tarandus	metatarsale		e	L, shore	
BL-O 827	L	Rangifer tarandus	tibia (with marrow)	distal fragment	e	L, shore	
BL-O 828	L	?Equus sp.	vertebra	fragment	e	L, shore	trashed
BL-O 829	L	Bison priscus	pelvis	fragment	e	L, shore	
BL-O 830	L	Equus sp.	phalanx I		e	L, shore	
BL-O 831	L	Bison priscus	capri ulnare		e	L, shore	
BL-O 832	L	Ovibos sp.	pelvis	fragment	e	L, shore	trashed
BL-O 833	L	Mammuthus primigenius	pelvis	fragment	e	L, shore	?14
BL-O 834	L	Mammuthus primigenius	scapula	fragment	e	L, shore	?14
BL-O 835	L	Equus sp.	upper milk tooth		e	L, shore	
BL-O 836	L	Ovibos sp.	cranium, female	fragment	e	L, shore under I TC	
BL-O 837	L	Mammuthus primigenius	upper molar tooth (M3)	fragment	e	L, shore under I TC	
BL-O 838	L	Mammuthus primigenius	lower molar tooth (?M3)	fragment	e	L, shore under I TC	
BL-O 839	L	Mammuthus primigenius	tooth	fragment	e	L, shore under I TC	
BL-O 840	L	Mammuthus primigenius	upper molar tooth (M3)	fragment	e	L, shore under I TC	
BL-O 841	L	Equus sp.	tibia	distal fragment	e	L, shore under I TC	
BL-O 842	L	Ovibos sp.	vertebra	fragment	e	L, shore under I TC	
BL-O 843	L	Equus sp.	radius		e	L, shore under I TC	
BL-O 844	L	Equus sp.	humerus	distal fragment	e	L, shore under I TC	
BL-O 845	L	Equus sp.	tibia	distal fragment	e	L, shore under I TC	
BL-O 846	L	Equus sp.	radius	fragment	e	L, shore under I TC	juv.
BL-O 847	L	Equus sp.	femur	fragment	e	L, shore under I TC	juv.
BL-O 848	L	Equus sp.	phalanx II		e	L, shore under I TC	
BL-O 849	L	Bison priscus	phalanx III		e	L, shore under I TC	
BL-O 850	L	Coelodonta antiqua	pelvis	fragment	e	L, shore under I TC	
BL-O 851	L	Bison priscus	metacarpale		e	L, shore under I TC	
BL-O 852	L	Mammuthus primigenius	cranium (jugale)	fragment	e	L, shore under I TC	
BL-O 853	L	Bison priscus	lumbar vertebra		e	L, shore under I TC	
BL-O 854	L	Rangifer tarandus	antler	fragment	e	L, shore under I TC	
BL-O 855	L	Rangifer tarandus	shed antler	fragment	e	L, shore under I TC	
BL-O 856	L	Rangifer tarandus	shed antler	fragment	e	L, shore under I TC	trashed
BL-O 857	L	? Ovibos sp.	atlas	fragment	e	L, shore under I TC	
BL-O 858	L	Equus sp.	mandibula	fragment	e	L, shore under I TC	trashed
BL-O 859	L	Equus sp.	metatarsale III	fragment	e	L, shore under I TC	trashed

A5-7: continuation.

samples	Side	Taxon	Skeleton element	Preservation	Type	Locality	Notes
BL-O 860	L	Ovibos sp.	metatarsale		e	L, shore under I TC	
BL-O 861	L	Rangifer tarandus	phalanx II		e	L, shore under I TC	juv.
BL-O 862	L	Rangifer tarandus	lumbar vertebra	fragment	e	L, shore under I TC	trashed
BL-O 863	L	Equus sp.	metepodia	distal fragment	e	L, shore under I TC	
BL-O 864	Z	Mammuthus primigenius	lumbar vertebra		f	? r. Zimov'e near mammoth' skin	C14
BL-O 865	Z	Mammuthus primigenius	thorax vertebra with copulas		f	? r. Zimov'e near mammoth' skin	C14
BL-O 866	Z	Mammuthus primigenius	thorax vertebra		f	? r. Zimov'e near mammoth' skin	C14
BL-O 867	Z	Mammuthus primigenius	rib	fragment	f	? r. Zimov'e near mammoth' skin	
BL-O 868	Z	Mammuthus primigenius	rib		f	? r. Zimov'e near mammoth' skin	
BL-O 869	Z	Mammuthus primigenius	vertebra	fragment	f	? r. Zimov'e near mammoth' skin	
BL-O 870	Z	Mammuthus primigenius	vertebra	fragment	f	? r. Zimov'e near mammoth' skin	
BL-O 871	Z	Mammuthus primigenius	ulnare		f	? r. Zimov'e near mammoth' skin	
BL-O 872	Z	Mammuthus primigenius	pisiforme		f	? r. Zimov'e near mammoth' skin	
BL-O 873	Z	Mammuthus primigenius	phalanx pasterior		f	? r. Zimov'e near mammoth' skin	
BL-O 874	Z	Bison priscus	scapula	fragment	f	? r. Zimov'e	trashed
BL-O 875		Equus sp.	mandibula	right branch	g	near camp (collected from different unknown localities of B. Lyakhovskiy Island - (c. f. d. u. l.)	
BL-O 876		Equus sp.	cranium	fragment	g	near camp (c. f. d. u. l.)	
BL-O 877		Canis lupus	mandibula (left stem) with 3 teeth		g	near camp (c. f. d. u. l.)	
BL-O 878		Mammuthus primigenius	tusk	damaged	g	near camp (c. f. d. u. l.)	?14
BL-O 879		Mammuthus primigenius	lower molar tooth (?M3)	fragment	g	near camp (c. f. d. u. l.)	
BL-O 880		Mammuthus primigenius	lower molar tooth (M3)	fragment	g	near camp (c. f. d. u. l.)	
BL-O 881		Mammuthus primigenius	upper molar tooth (M2 or M3)	fragment	g	near camp (c. f. d. u. l.)	
BL-O 882		Equus sp.	radius		g	near camp (c. f. d. u. l.)	
BL-O 883		Equus sp.	phalanx III		g	near camp (c. f. d. u. l.)	
BL-O 884		Equus sp.	phalanx II		g	near camp (c. f. d. u. l.)	
BL-O 885		Equus sp.	phalanx II		g	near camp (c. f. d. u. l.)	
BL-O 886		Equus sp.	phalanx II		g	near camp (c. f. d. u. l.)	
BL-O 887		Equus sp.	phalanx II		g	near camp (c. f. d. u. l.)	
BL-O 888		Equus sp.	phalanx II		g	near camp (c. f. d. u. l.)	
BL-O 889		Equus sp.	phalanx I	damaged	g	near camp (c. f. d. u. l.)	

A5-7: continuation.

samples	Side	Taxon	Skeleton element	Preservation	Type	Locality	Notes
BL-O 890		Equus sp.	phalanx I		g	near camp (c. f. d. u. l.)	
BL-O 891		Equus sp.	phalanx I		g	near camp (c. f. d. u. l.)	
BL-O 892		Equus sp.	phalanx I	damaged	g	near camp (c. f. d. u. l.)	
BL-O 893		Equus sp.	phalanx I		g	near camp (c. f. d. u. l.)	
BL-O 894		Equus sp.	phalanx I	damaged	g	near camp (c. f. d. u. l.)	
BL-O 895		Equus sp.	phalanx I		g	near camp (c. f. d. u. l.)	
BL-O 896		Equus sp.	phalanx I		g	near camp (c. f. d. u. l.)	
BL-O 897		Equus sp.	phalanx I		g	near camp (c. f. d. u. l.)	
BL-O 898		Equus sp.	phalanx I		g	near camp (c. f. d. u. l.)	
BL-O 899		Equus sp.	phalanx I		g	near camp (c. f. d. u. l.)	
BL-O 900		Equus sp.	phalanx I		g	near camp (c. f. d. u. l.)	
BL-O 901		Equus sp.	phalanx I		g	near camp (c. f. d. u. l.)	
BL-O 902		Equus sp.	phalanx I		g	near camp (c. f. d. u. l.)	
BL-O 903		Equus sp.	phalanx I		g	near camp (c. f. d. u. l.)	
BL-O 904		Equus sp.	phalanx I		g	near camp (c. f. d. u. l.)	
BL-O 905		Equus sp.	phalanx II		g	near camp (c. f. d. u. l.)	
BL-O 906		Equus sp.	phalanx II		g	near camp (c. f. d. u. l.)	
BL-O 907		Equus sp.	phalanx III		g	near camp (c. f. d. u. l.)	
BL-O 908		Equus sp.	metatarsale IV		g	near camp (c. f. d. u. l.)	
BL-O 909		Equus sp.	metacarpale III		g	near camp (c. f. d. u. l.)	
BL-O 910		Equus sp.	metatarsale III	sample damaged	g	near camp (c. f. d. u. l.)	
BL-O 911		Equus sp.	phalanx I		g	near camp (c. f. d. u. l.)	
BL-O 912		Equus sp.	radius	proximal fragment	g	near camp (c. f. d. u. l.)	
BL-O 913		Bison priscus	metatarsale	fragment	g	near camp (c. f. d. u. l.)	
BL-O 914		Bison priscus	metacarpale	3 samples	g	near camp (c. f. d. u. l.)	
BL-O 915		Ovibos sp.	metacarpale		g	near camp (c. f. d. u. l.)	
BL-O 916		Ovibos sp.	metacarpale		g	near camp (c. f. d. u. l.)	
BL-O 917		Ovibos sp.	metacarpale		g	near camp (c. f. d. u. l.)	
BL-O 918		Ovibos sp.	metatarsale		g	near camp (c. f. d. u. l.)	juv.
BL-O 919		Coelodonta antiqua	tooth		g	near camp (c. f. d. u. l.)	
BL-O 920		Bison priscus	phalanx II		g	near camp (c. f. d. u. l.)	
BL-O 921		Bison priscus	astrogalus		g	near camp (c. f. d. u. l.)	
BL-O 922		Bison priscus	astrogalus		g	near camp (c. f. d. u. l.)	
BL-O 923		Bison priscus	naviculare		g	near camp (c. f. d. u. l.)	
BL-O 924		Ovibos sp.	naviculare		g	near camp (c. f. d. u. l.)	

A5-7: continuation.

samples	Side	Taxon	Skeleton element	Preservation	Type	Locality	Notes
BL-O 925		Ovibos sp.	naviculare		g	near camp (c. f. d. u. l.)	
BL-O 926		Equus sp.	cuboid		g	near camp (c. f. d. u. l.)	
BL-O 927		Equus sp.	radius		g	near camp (c. f. d. u. l.)	
BL-O 928		Bison priscus	phalanx I		g	near camp (c. f. d. u. l.)	
BL-O 929		Ovibos sp.	phalanx I		g	near camp (c. f. d. u. l.)	
BL-O 930		Ovibos sp.	phalanx II		g	near camp (c. f. d. u. l.)	
BL-O 931		Rangifer tarandus	phalanx I		g	near camp (c. f. d. u. l.)	
BL-O 932		Ovibos sp.	astrogalus		g	near camp (c. f. d. u. l.)	
BL-O 933		Rangifer tarandus	astrogalus		g	near camp (c. f. d. u. l.)	
BL-O 934		Rangifer tarandus	astrogalus		g	near camp (c. f. d. u. l.)	
BL-O 935		Rangifer tarandus	astrogalus		g	near camp (c. f. d. u. l.)	
BL-O 936		Rangifer tarandus	astrogalus		g	near camp (c. f. d. u. l.)	
BL-O 937		Lepus sp.	pelvis	fragment	g	near camp (c. f. d. u. l.)	
BL-O 938		Rangifer tarandus	phalanx II		g	near camp (c. f. d. u. l.)	
BL-O 939		Equus sp.	phalanx II		g	near camp (c. f. d. u. l.)	
BL-O 940		Rangifer tarandus	astrogalus		g	near camp (c. f. d. u. l.)	
BL-O 941		Rangifer tarandus	phalanx II		g	near camp (c. f. d. u. l.)	
BL-O 942		Rangifer tarandus	naviculare		g	near camp (c. f. d. u. l.)	
BL-O 943		Equus sp.	magnum		g	near camp (c. f. d. u. l.)	
BL-O 944		Rangifer tarandus	metapodia	distal fragment	g	near camp (c. f. d. u. l.)	
BL-O 945		Rangifer tarandus	carpi ulnare		g	near camp (c. f. d. u. l.)	
BL-O 946		Rangifer tarandus	astrogalus	fragment	g	near camp (c. f. d. u. l.)	
BL-O 947		Bison priscus	phalanx II		g	near camp (c. f. d. u. l.)	
BL-O 948		Bison priscus	ulna		g	near camp (c. f. d. u. l.)	
BL-O 949		Mammuthus primigenius	metatarsale I		g	near camp (c. f. d. u. l.)	
BL-O 950		Mammuthus primigenius	metatarsale II	sample damaged	g	near camp (c. f. d. u. l.)	
BL-O 951		Equus sp.	atlas		g	near camp (c. f. d. u. l.)	
BL-O 952		Mammuthus primigenius	tooth replaced	fragment	g	near camp (c. f. d. u. l.)	
BL-O 953		Mammuthus primigenius	tooth	fragment	g	near camp (c. f. d. u. l.)	
BL-O 954		Mammuthus primigenius	tooth replaced	fragment	g	near camp (c. f. d. u. l.)	
BL-O 955		Mammuthus primigenius	tooth	fragment	g	near camp (c. f. d. u. l.)	trashed
BL-O 956		Mammuthus primigenius	lower milk tooth	fragment	g	near camp (c. f. d. u. l.)	
BL-O 957		Mammuthus primigenius	tooth	fragment	g	near camp (c. f. d. u. l.)	trashed
BL-O 958		Equus sp.	upper tooth (M2)		g	near camp (c. f. d. u. l.)	
BL-O 959		Equus sp.	lower tooth (M3)		g	near camp (c. f. d. u. l.)	

A5-7: continuation.

samples	Side	Taxon	Skeleton element	Preservation	Type	Locality	Notes
BL-O 960		Mammuthus primigenius	lower premolar milk tooth (dp3)	fragment	g	near camp (c. f. d. u. l.)	
BL-O 961		? Mammuthus primigenius	tooth	fragment	g	near camp (c. f. d. u. l.)	trashed
BL-O 962		Lepus sp.	radius		g	near camp (c. f. d. u. l.)	
BL-O 963		Bison priscus	upper tooth		g	near camp (c. f. d. u. l.)	
BL-O 964		Bison priscus or Ovibos sp.	upper premolar tooth (P2)		g	near camp (c. f. d. u. l.)	
BL-O 965		Rangifer tarandus	upper premolar tooth (P2)	heavily worn	g	near camp (c. f. d. u. l.)	
BL-O 966		Rangifer tarandus	upper tooth (M)	heavily worn	g	near camp (c. f. d. u. l.)	
BL-O 967		Ovibos sp.	tooth	fragment	g	near camp (c. f. d. u. l.)	
BL-O 968		Equus sp.	incisor		g	near camp (c. f. d. u. l.)	
BL-O 969		Rangifer tarandus	upper molar tooth (M)		g	near camp (c. f. d. u. l.)	
BL-O 970		Rangifer tarandus	upper premolar tooth	fragment	g	near camp (c. f. d. u. l.)	trashed
BL-O 971	L	Bison priscus	cervical vertebra		e	L, shore	
BL-O 972	Z	Mammuthus primigenius	patella		f	? r. Zimov'e near mammoth' skin	at Lutz
BL-O 973	L	Mammuthus primigenius	tooth	fragment	e	L, shore	trashed
BL-O 974	L	Mammuthus primigenius	vertebra	fragment	e	L, shore	trashed
BL-O 975	L	Mammuthus primigenius	tooth	fragment	e	L, shore 10 km from camp	trashed
BL-O 976	L	Mammuthus primigenius	tooth	fragment	e	L, shore 10 km from camp	trashed
BL-O 977	L	Mammuthus primigenius	tooth	fragment	e	L, shore 10 km from camp	trashed
BL-O 978	L	Mammuthus primigenius	tooth	fragment	e	L, shore 10 km from camp	trashed
BL-O 979	L	Mammuthus primigenius	tooth	fragment	e	L, shore 10 km from camp	trashed
BL-O 980	L	Mammuthus primigenius	tooth	fragment	e	L, shore 10 km from camp	trashed
BL-O 981	L	Mammuthus primigenius	tooth	fragment	e	L, shore 10 km from camp	trashed
BL-O 982	L	Rangifer tarandus	cranium	fragment	e	L, shore 10 km from camp	trashed
BL-O 983	L	Rangifer tarandus	cranium	fragment	e	L, shore	trashed
BL-O 984	L	Ovibos sp.	cranium	fragment	e	L, shore	trashed
BL-O 985	L	Mammuthus primigenius	tooth	fragment	e	L, shore	trashed
BL-O 986	L	Mammuthus primigenius	tooth	fragment	e	L, shore	trashed
BL-O 987	L	Mammuthus primigenius	tooth	fragment	e	L, shore	trashed
BL-O 988	L	Mammuthus primigenius	tooth	fragment	e	L, shore	trashed
BL-O 989	L	Mammuthus primigenius	tooth	fragment	e	L, shore	trashed
BL-O 990	L	Mammuthus primigenius	tooth	fragment	e	L, shore	trashed
BL-O 991	L	Mammuthus primigenius	tooth	fragment	e	L, shore	trashed

A5-7: continuation.

samples	Side	Taxon	Skeleton element	Preservation	Type	Locality	Notes
BL-O 992	L	Mammuthus primigenius	tooth	fragment	e	L, shore	trashed
BL-O 993	L	Mammuthus primigenius	tusk	fragment	e	L, shore	trashed
BL-O 994	L	Mammuthus primigenius	tusk	fragment	e	L, shore	trashed
BL-O 995	R	Rangifer tarandus	femur	proximal fragment	d	R, cape shore	trashed
BL-O 996	L	Mammuthus primigenius	tibia		e	L, shore near the camp	trashed
BL-O 997	R	Mammuthus primigenius	tooth		d	R, shore under I TC	
BL-O 998	L	Mammuthus primigenius	tusk	fragment	d	R, shore under I TC	trashed
BL-O 999	L	Equus sp.	incisor		e	L, shore near the camp	
BL-O 1000	R	Large mammal	limb bone	fragment	a	in situ, R, stream 14\1 (R-14), "Olyor"	
BL-O 1001	L	Small mammals	different parts of skeleton		e	L, shore 10 km from camp	
BL-O 1002	L	Bison priscus	tooth	fragment	e	L, shore	
BL-O 1003	L	Clangula hyemalis	cranium	sample damaged	e	L, shore	
BL-O 1004	L	Bison priscus	horn core		e	L, shore	trashed
BL-O 1005	L	Bison priscus	thorax vertebra		e	L, shore	trashed
BL-O 1006	L	Mammuthus primigenius	scapula			L, in log (on surface)	trashed
BL-O 1007	L	Mammuthus primigenius	scapula			L, in log (on surface)	trashed
BL-O 1008	L	Mammuthus primigenius	calcaneus		e	L, shore under II TC	trashed
BL-O 1009	L	Equus sp.	thorax vertebra		e	L, shore under II TC	trashed
BL-O 1010	L	Bison priscus	radius	fragment	e	L, shore under II TC	trashed
BL-O 1011	L	Mammuthus primigenius	scapula		e	L, shore under I TC	trashed
BL-O 1012	L	Mammuthus primigenius	calcaneus		e	L, shore under I TC	trashed
BL-O 1013	L	Mammuthus primigenius	tusk		e	L, shore	trashed
BL-O 1014	L	Mammuthus primigenius	tusk	fragment	e	L, shore	trashed
BL-O 1015	L	Mammuthus primigenius	molar tooth		e	L, shore	trashed
BL-O 1016	L	Bison priscus	lumbar vertebra	fragment	e	L, shore	
BL-O 1017		Rangifer tarandus	maxilla with teeth P4 - M2	fragment		shore	
BL-O 1018		Mammuthus primigenius	humerus			shore	?14
BL-O 1019	R	Lepus sp.	cranium		d	R, shore	

A5-8: List of small fossil samples (rodents, insects, ostracodes, seeds).

sample		site	altitude (m, a.s.l.)	Sediment description
1. "Olyor" deposits				
R-3		R-17+30m	3,2	Silt, grey, with gross-grained sand, rock debris and rubble
R-1		R-17+30m	3,3	Sand, gross-grained, strong ferriginous, loose, with rock debris (ca. 50 mm)
R-2		R-17+30m	3,6	Sand, brownish-grey, gross-grained,strong ferriginous, loose, with rock debris
R-5		R-14+30m	4	Silt, grey, with peat inclusions, with fragment of mammal limb bone
R-4		R-17	4,2	Silt, grey, with rock debris and plant detritus beds
R-6		R-14+30m	4,4	Silt, grey, with peat inclusions, plant detritus beds, rock debris
B-2		R-17	4,5	grey silt with few gravel
	OS-4	R-17	4,8	yellowish-brown silt with gravel and peat lenses
2. "Kuchchuguy" subaerial deposits				
B-1	OS-1	R--17	5,2	yellowish-grey sandy silt with grass roots
	OS-2	R--17	5,5	yellowish-grey sandy silt with grass roots
	OS-3	R--17	5,8	yellowish-grey sandy silt with grass roots
	OS-9	R-6	0,4	grey silt with few grass roots
	OS-8	R-6	0,7	grey silt with few grass roots
B-3	OS-5	R-6	1	yellowish-grey sandy silt with grass roots
	OS-6	R-6	1,3	yellowish-grey sandy silt with grass roots
	OS-7	R-6	1,7	yellowish-grey sandy silt with grass roots
	OS-10	R-6	2	yellowish-grey sandy silt with grass roots
B-5	OS-11	R-6	2,3	yellowish-grey sandy silt with grass roots
	OS-12	R-6	2,5	yellowish-grey sandy silt with grass roots
	OS-13	R-6	2,8	yellowish-grey sandy silt with grass roots
	OS-14	R-6	3,1	yellowish-grey sandy silt with grass roots
	OS-15	R-6	4	yellowish-grey sandy silt with grass roots
	OS-16	R-6	4,3	yellowish-grey sandy silt with grass roots
	OS-17	R-6	4,6	yellowish-grey sandy silt with grass roots
	OS-18	R-6	4,9	yellowish-grey sandy silt with grass roots
B-4	OS-19	R-6	5,2	yellowish-grey sandy silt with grass roots
	OS-20	R-6	5,5	yellowish-grey sandy silt with grass roots
	OS-21	R-6	5,8	yellowish-grey sandy silt with grass roots

A5-8: continuation.

sample		site	altitude (m, a.s.l.)	Sediment description
	OS-22	R-6	6,1	yellowish-grey sandy silt with grass roots
	OS-23	R-6	6,4	yellowish-grey sandy silt with grass roots
	OS-24	R-6	6,7	yellowish-grey sandy silt with grass roots
B-11	OS-44	R-18	12,6	yellowish-grey sandy silt with few grass roots
	OS-45	R-18	12,9	yellowish-grey sandy silt with few grass roots
3. "Kuchchuguy" subaqual deposits				
B-13	OS-49	R-22	1,2	grey and yellowish-grey sandy silt with few grass roots
	OS-50	R-22	1,5	grey and yellowish-grey sandy silt with few grass roots
B-14	OS-51	R-22	2,4	yellowish-grey sandy silt
	OS-52	R-22	2,7	yellowish-grey sandy silt
B-18	OS-58	L-11	3,5	yellowish-grey sandy silt
	OS-59	L-11	3,8	yellowish-grey sandy silt
4. "Krest-yuryach" deposits				
B-15	OS-53	R-22	2,5	grey silt with plant detritus in ice wedges pseudomorhism
	OS-54	R-22	2,8	grey silt with plant detritus in ice wedges pseudomorhism
B-16	OS-55	R-22	4	grey clayey silt with fresh-water shells
B-17	OS-56	L-11	4	grey silt with plant detritus in ice wedges pseudomorhism
	OS-57	L-11	4,3	grey silt with plant detritus in ice wedges pseudomorhism
B-19	OS-60	L-11	7	grey clayey silt with fresh-water shells
	OS-61	L-11	7,3	grey clayey silt with fresh-water shells
5." Ice complex" deposits (yedoma)				
	OS-25	R-5	14,2	grey sandy silt with grass roots and plant detritus
B-6	OS-26	R-5	14,5	grey sandy silt with grass roots and plant detritus
	OS-27	R-5	14,8	grey sandy silt with grass roots and plant detritus
	OS-28	R-5	15,1	grey sandy silt with grass roots and plant detritus
	OS-29	R-5	16,4	grey sandy silt with grass roots and plant detritus
	OS-30	R-5	16,7	grey sandy silt with grass roots and plant detritus
B-7	OS-31	R-5	17	yellowish-grey sandy silt with grass roots
	OS-32	R-5	17,3	yellowish-grey sandy silt with grass roots
	OS-33	R-5	17,6	yellowish-grey sandy silt with grass roots

A5-8: continuation.

sample		site	altitude (m, a.s.l.)	Sediment description
	OS-34	R-5	17,9	yellowish-grey sandy silt with grass roots
B-8	OS-35	R-4	21,4	grey silt
	OS-36	R-18	12,9	grey silt with grass roots
B-9	OS-37	R-18	13,2	grey silt with grass roots
	OS-38	R-18	13,5	grey silt with grass roots
	OS-39	R-18	16,5	grey silt with grass roots
B-10	OS-40	R-18	16,8	yellowish-grey silt with grass roots
	OS-41	R-18	17,1	yellowish-grey silt with grass roots
	OS-42	R-18	17,4	yellowish-grey silt with grass roots
	OS-43	R-18	17,7	yellowish-grey silt with grass roots
B-12	OS-46	R-18	22,3	grey silt with grass roots
	OS-47	R-18	22,5	grey silt with grass roots
	OS-48	R-18	22,8	grey silt with grass roots
6. Holocene deposits, alas				
B-22	OS-64	L-17	6,7	grey silt with peat lenses
B-20	OS-62	L-17	8,5	plant detritus and twigs of large shrubs
B-21	OS-63	L-17	13,5	grey silt with peat lenses
7. Holocene deposits, river terrace				
B-23	OS-65	L-0	1	yellowish-grey sand with plant detritus
B-24	OS-66	L-0	1,5	
B-25	OS-67	L-0	2,3	grey sand and silt with plant detritus
recent				
B-0		L-0	0	modern sediment (subface sample)

Index "B" - samples screened with 0.5 mm mesh. Index "R" - samples screened with 1,0 mm mesh.
Index "OS" - seeds samples

A5-9: List of peat samples for botanical analysis.

Sample	Material	Site	Altitude	Deposits
BL-R-T1	Peat, dark-brown, slightly compressed	side R, R 8+60m, stream 8/2	~ 1.4 - 1.6m	Upper "Olyorian", upper part
BL-R-T2	Peat, dark-brown, tightly compressed	side R, R 8+60m, stream 8/3	~ 1.0 - 1.4m	Upper "Olyorian", lower part
BL-L-T3	Peat, brownish-red, slightly compressed	side L, L34+40m		Ice complex deposits, basal part
BL-L-T4	Peat, brownish-red, slightly compressed	side L, L 50m	~10 - 12m	"Subaquatic Kuchchuguy"
BL-L-T5	Peat, brownish-red, slightly compressed	side L, L 50m	~10 - 12m	"Subaquatic Kuchchuguy"
BL-R-T6	Peat, dark-brown, tightly compressed	side L		Holocene deposits

A5-10: List of mollusc samples.

Sample	Material	Site	Altitude	Deposits
BL-R-M1	Bivalvia	site R, R 41+50m	1,8 m	"Krest-Yuryakh"
BL-R-M2	Bivalvia and Gastropoda	site R, R 22+30m		"Krest-Yuryakh"
BL-R-M3	Bivalvia and Gastropoda	site R	shore, R21-R24	
BL-R-M4	Bivalvia	site R, R-32		"Krest-Yuryakh"
BL-R-M5	Bivalvia	side R	shore	?"Krest-Yuryakh"
BL-R-M6	Bivalvia and Gastropoda		shore	?"Krest-Yuryakh"

A5-11: List of samples for paleomagnetics.

Sample number	Locality	Sediment description	Altitude (m a.s.l.)	Position	Number, condition (melting or frozen)
Pm 1	R-17+30	Aleurite, grey, with abundant thin rootlets, solid, dry	4	lower part of "Kuchchuguy"	5 melting
Pm 1 (monolithe)	R-17+30	Aleurite, grey, with abundant thin rootlets, solid, dry	4	lower part of "Kuchchuguy"	1 monolithe melting
Pm 2	R-17+30	Aleurite, light brown with small rock debris, rare	3,7	upper part "Olyor"	6 melting
Pm 3	R-17+30	Aleurite, light brown, with small rock debris. rare	3,5	upper part "Olyor"	6 melting
Pm 4	R-8+50	Aleurite, brownish-grey, plated	2,5	upper part "Olyor"	6 melting and 2 frozen
Pm 5	R-8+50	Aleurite, light brown with small rock debris, rare and pebble, rare	2,8	upper part "Olyor"	6 melting
Pm 6	R-8+50	Aleurite, light brown, with small rock debris, rare	3,1	upper part "Olyor"	6 melting
Pm 7	R-8+50	Aleurite, grey, with small rock debris rare	3,5	upper part "Olyor"	6 melting
Pm 8	R-8+50	Aleurite, grey, with abundant thin rootlets, dry	4,2	lower part of "Kuchchuguy"	6 melting
Pm 9	R-17+85	Aleurite, grey, with small rock debris, rare	2,3	upper part "Olyor"	6 frozen
Pm 10	R-17+85	Aleurite, grey ,with small rock debris, rare	2,4	upper part "Olyor"	6 frozen

A5-12: Description of soil profiles.

Type: Permafrost alluvial layered poorly developed (primitive) soil
Pit 23.20.08.99
terrace 1: 1 km from the mouth of Zimov'e river (by the river)
Vegetation: *Poa alpigena* 30 %; more than anything; some dead leaves of cereals

I	0-23 cm	Loam, strong muddy, greyish-rusty-brown with dirty-grey spots (gleyed), slowly boundary of alive and dead roots, average amount of allochthonous plant remains; wet; lamination is only visible in frozen material by allochthonous plant remains; homogeneous grain size composition; rough boundary, weakly fuzzy; a crack with rusty streak from this horizon toward to the bottom; squeezed.
II	23-39 cm	Loamy sand, muddy; dirty-bluish-grey with many black spots of semi-decayded vegetation; more or less stratified by plant remains, homogeneous grain size composition; rusty fissures and horizon boundaries.
III	39-46 cm	3 interlayers: 1) Loamy sand, muddy rusty-grey-brown, rust spreads on it from a crack - 1.5 cm; 2) muddy sand + loam, the same colour, as 1) - 2 cm; 3) Loamy sand bluish-grey, muddy, similar to II - 3.5 cm.; all interlayers are moist.
IV	46-52 cm	Sand, well stratified, various grain size composition (fine up coarse sand), light-rusty, moist, interlayers with organic matter.
V	52-56 cm	Loamy sand, muddy; dirty-bluish-grey with many black spots of semi-decayded vegetation; more or less stratified by plant remains, homogeneous grain size composition; rusty fissures and horizon boundaries, moist.
VI	56-64 cm	Sand, well stratified, various grain size composition (fine to coarse sand, with debris), light-rusty, moist, interlayers with organic matter.
VII	64-73 cm	Loamy sand dark - bluish-grey, with less plant remains than II, moist.

Permafrost is lower - the soil with a small amount of ice.

Pit 101.22.08.99
45 m from sea shore
Vegetation: *Poa alpigena* 40 %, *Stellaria humifusa* 5 %.

I	0-26 cm	Loamy sand, dirty-grey with gleyed, rusty spots, wet, plant remains (thin roots in a common mass, clusters and discontinuous interlayers).
II	26-39 cm	coarse sand with debris (about 40 %), yellow with rusty shade, wet, plant remains - separate black slices of roots.
III	39-48cm	Loamy sand with large grains of sand, middle muddy, brownish-grey, stratified, thixotropic, wet, average amount of plant remains
IV	48-56 cm	Loamy sand bluish-steel-grey with rusty films on cracks, wet - moist, average amount of plant remains.

Subtype: Permafrost alluvial sod-gley; Pit 108.
Vegetation: Mosses (alive 5 %, black dead 2 %, green mostly dead 40 %), Cereal 40, *Stellaria humifusa* 2-3 %, *Cochlearia* un.

Ao	0-1 cm	Dead remains of plants.
AotA1	1-7 cm	Very dense netting of roots, plant remains between the roots, treated by frost, wet.
Bg '	7-15 cm	Loamy sand, muddy, bluish-grey with rusty spots, moist; less netting of alive and dead roots than in AotA1, any cut off chunk (the block hold the form).
G	15-33 cm	Loamy sand with separate sand clusters; Gleyic horizon, bluish-steel colour with rusty streaks on separate cracks; moist; many plant remains, but they do not hold loamy sand as a monolith.
	33-37 cm	Interlayer of various mainly coarse sands with unrounded debris, yellowish-grey, slightly rusty; moist more wet.

Permafrost is lower (grey loamy sand), there is a little ice.

A5-12: continuation

Type: Permafrost alluvial peat-gley soils; Pit 9

Vegetation: Mosses 98 %, cereals + sedges 40 %, Herbs (*Chrysosplenium alternifolium, Pedicularis sudetica* ssp. *albolabiata*) 1%

To	0-3 cm	Dark - brown dead mosses.
T1	3-8 cm	Peat, brown, poorly muddy, interlocked by roots, without any lamination probably,
T2	8-13 cm	Peat light-brown, moss-grassy, muddy, interlocked by the roots.
Tg	13-17 cm	Peat bluish-brown, muddy, poorly sanded, moss-grassy.
Gt	17-29 cm	Loamy sand, muddy up to loam, grey, many grass remains.

Permafrost is deeper.

Subtype: Permafrost peatish-gley; Pit 18.

Tv	0-1 cm	Alive mosses.
T2	1-2 cm	Brown peat, destroyed by permafrost, almost without mud and roots.
T2G	2-8 cm	Brown peat and mud dirty-grey between a dense netting of thick roots; moist.
GT	8-18 cm	Loamy sand - loam, strong muddy and peaty, dense netting of shallow alive roots, moist,many plant remains.
Gt	18-32 cm	Loam, dirty-grey with rusty streaks and spots. Moist, water oozes on cracks; many plant remainsl.
G	32-42 cm	Loam, bluish-grey with separate rusty spots, many plant remains.

Permafrost is lower - soil with a great many of ice (large streaks).

Type: Permafrost effused; Pit 1.9.08.99

Top of a hill.

Nano-relief: diameter of mounds is 20-50 cm, height is about 10 cm. There is a lot of lemming holes in cracks.

Mounds: Vascular plants 40 %, Lichens 80 %, mosses shallow, pressed to soil, covered by lichens 5 %, *Salix polaris* 20 %, *S. glauca* 2-3 %, Cereals (*Alopecurus alpinus* etc.) 15 %, Herbs (*Senecio atropurpureus, Pedicularis*) 5 %.

Cracks: Lichens 15 %, Mosses higher and noticeable 50 %, *Salix polaris* + *S. glauca* 10, Herbs (*Saxifraga hieracifolia, Potentilla hyparctica, ranunculus* sp.) 5 %.

Pit-hole: the bottom is absolutely even, ice occures under a crack or mound indipendent of the position.

1a a mound

	0-0.5 cm	Crust of mosses and lichens.
A0T1 [2]	0.5-3 cm	Dense sod , with dark - brown peat, wet, netting by roots.
Bg	3-15 cm	Loam, yellowish-grey, structured (fine grains) to non structured; wet.
hcr	15-18 cm	Spot of cryoturbated humus: loam, dark - brown-grey, wet.
CG	18-34 cm	Loam, heavier than Bg, dirty - bluish-grey with light-rusty streaks and spots, thixotropic, a vertical expansion is moved; wet, on contact with permafrost, moist; a few of plant remains.

Permafrost is lower.

1b a crack

	0-0.3 cm	Crust of mosses and lichens.
AT2	0.3-11 cm	Peat dark-brown, partially mineralised, loose: the knife enters easily, on boundary with Bg strongly loosened (almost up to a hollow), wet, is pierced by roots; sinuous boundary , streaks of pea on a crack .
Bg	11-17 cm	Loam, yellowish-grey with grey shade, small spot of humus. At vertical expansion is moved apart by stratums; wet, but not enough for alive roots.
CG [Cg ']	17-36 cm	Loam, heavier, than Bg, dirty-bluish-grey with light-rusty streaks and spots, thixotropic, at vertical expansion is moved apart by stratums. Wet, on contact with permafrost is moist. A very small amount of plant remains.

Permafrost is lower.

A5-12: continuation

Description of paleo sols
Section R 17
samples: 2-12, 20-30, 45-55, 60-75, 80-90, 95-105, 115-125, 145-155
Vegetation: Cereals 60 %, Herbs (*Cochlearia* 20 %, *Papaver lapponicumun*).

Av	0-1 cm	Dense sod.
A1g '	1-19 cm	Loamy sand, brown - grey, homogeneous (particles of peat, plant rests, particles of mosses, saved greenish colour), it is bad stratified (bent in different directions, variable thickness, small clusters of peat), rusty spots of the incorrect form; compressed, thawed. On cracks more friable and more peat. Rough boundary with underlying horizon, bent-tongue, but clear, weakly gleyed, non-peaty stratums.
Bg "	19-59 cm	Loamy sand, dusty, yellowish-grey, bad stratified. Stratums go is not consent general slope of a surface and slope of horizons (declination to the opposite direction). Lenses both clusters of peat and loamy sand with the large contents of plant rests. In the bulk loamy sand - thin roots. Rusting on courses of the roots. A gleyed by vague stratums and in a nuance of colour. Transition rough, but clear.
A1g " buried	59-78 cm	Loamy sand dusty, on colour is very similar to A1g ', but more gleyed (the general steel nuance), bad stratified (stratums are bent in different directions, variable thickness, small clusters of peat), rusty spots of the incorrect form. Compressed, thawn. The boundary light crooked, but clear. Rusty fil on the contact of two horizons . wood.
Bg' buried	78-91 cm	Loamy sand dusty, yellowish-grey tinged with blue. Dimply layer, film of rusting in various directions (on any internal cracks). It is not enough of plant rests. Frozen, ice streak are not visible.
G buried	91-112 cm	Loamy sand dusty, bluish-grey, frozen, thin, light bent schlieren of ice, general declination of them corresponds to declination of a surface and horizons; more plant rests than in B buried; boundary rough, leaked-spotty, noticeable on colouring.
112-143 cm		Loamy sand dusty, yellowish-grey, non-gleying, frozen, schlieren thiner, ice is less, than in G buried, the general declination schlieren corresponds to declination of a surface and horizons.
The olior 143-lower 200 cm		Hashed thickness, grey and yellow spots, loamy-sandy filler, rock debris, clusters of sand.

A5-12: continuation

Section R18/1.
samples: 0-12, 12-24, 24-33, 33-40, 40-49, 49-63, 63-85, 85-110, 110-130, 130-155, 155-184, 190-220, 230-260
TFK - „test for a knife" - the depth of penetration of a knife into rock.

B	0-12 cm	Brownish-grey with buried bands more humused and brown. Colouring is very rough (more grey and yellowish diffuse spots), brown small roots are visible in more humused bands . Isolated points of a rusting on courses of the roots. It is not enough of plant rests. TFK = 9.5 cm.
Cg "	12-24 cm	More gleyed and stratified. The layer is more grey and more yellow bands. Grey colour is both in horizontally prolated spots. Subhorizontal small crack is grey - brown, humused,The brown small roots are visible. It is not so much plant rests in remaining parts of horizon a little, so small-sized. TFK = 7 cm.
A buried	24-33 cm	Most humused horizon, is brown - grey, stratified, diffuse interlayers of yellowish-grey colour. Plant rests are average amount. TFK = 10 cm.
B buried	33-40 cm	Yellow-grey, structured: very - very small-sized grains, a little larger then poppy-seeds. TFK = 11.5 cm
G buried	40-49 cm	Loamy sand, muddy up to loam, dirty - grey, stratified. It is not enough of plant rests, but there are interlayers a plenty of very small-sized roots. Above horizon a thin dash line of a rusting. TFK = 12 cm.
	49-63 cm	Strangely enough, is similar to B buried, but meet both non-structured clusters; more humused on contact with permafrost. TFK = 8 cm.
	63-184 cm	The frozen rocks are lower. There are grey - brown humused discontinuous bands under declination 45degrees and more on a yellowish-grey background. Their greatest amount and density is observed on a depth 110-130 cm. There is almost a spot (sloping - striped) here. All this plot(site) under small declination to the sea is intersected by more icy, than main rock, small bands. It is appreciable 'poppy-seed' structure. All this is loamy sand. Well noticeable icy bands go on depthes: 68, 84, 93, 116-119, 142, 160 and is lower 184 cm (about it below).
	184-188 cm	Ice band with frozen inside it plant rests.
	188-230 cm	Loamy sand frozen, almost without vegetation and humus spots.
	230-280 cm	Loamy sand frozen with an interesting structure: the denudation looks as the mutton wool, been matted by horizontal bands. Humus is not noticeably.

R18/2 Soils
samples: 0-11, 11-22, 22-27, 27-40, further through 10 cm.
High baydjarakh with a flat apex
vegetation: mosses low 20 %, Cereals (*Alopecurus, Poa*) 5-8 %, Oxyria 1 %, *Papaver lapponicum* un.

A1	0-22 cm	Greyish-brown, clusters of peat.
B	22-27 cm	Greyish-yellow, stratified.
G	27-40 cm	Precise stratified, and the stratums are bent downwards, into cracks. Bluish-grey and yellow - grey laminas.
A	40-50 cm	Humus horizon. Probably, in the not infringed condition it was above-permafrost a stratum of accumulation of a humus. Brown - grey.
	50-410 cm	Uniform thikness of loamy sand with diffuse light noticeable broad bands more grey (humused) and more yellow colour. Light icy. On depthes 60-70, 90-120, 140-160 cm the bands are traced is grey - dark blue of points (Vivianite?).

A5-13: List of samples collected by the Bykovsky team at the upper part of MKh main section in 1999.

Sample No.	Height a.s.l., m	Depth in local profile, m	Sediment sample (all samples taken from frozen sediment)			Pollen sample (taken from the sediment sample before drying)		Macrofossil sample (all samples taken from freshly melted and undisplaced sediment)			Sampling date
			Description	Cryo-structure	Melted water removed, ml	No.	Description	No.	Method	Original volume	
1	2	4	5	6	7	9	11	12	13	14	15
Site: Baydzherakh "H" ("Hans"), Stn. 745, 10 m SE of 1999 landmark R5 39.2 m a.s.l. (ca 1998 RP 4.4), top level of actively destroyed b-khs, capped by modern soil on the top Yedoma surface											
MKh99-1	37,6	1,6	Peat inclusions in silt, close to ice wedge		250	MKh99-1P					23.8
MKh99-2	37,1	2,1	Silt with high ice content among peat "hummocks", squeezed up along the ice wedge margin	Reticulated lens-like	525	MKh99-2P					23.8
MKh99-3	37	2,2	Peat inclusions in silt and ice	Clear ice inclusions	250	MKh99-3P	peat				17.8
MKh99-3aC	36,7	2.4- 2.6	Autochthonous peat (sphagnum, sedges) in "hummocks"					MKh99-3aC	Melted in fabric bag, dried, no screening	ca 4 litres	17.8
MKh99-4	36,4	2,8	Silt with high ice content beneath the peat core of the b-kh	Lens-like	520	MKh99-4P	grass roots (few)				17.8
MKh99-5	35,3	3,9	Fine- and medium sand, intercalating with silt lenses	Massive	200	MKh99-5P	grass roots (few)				17.8
MKh99-5oS	35,3	3,9	Sand and silt					MKh99-5oS	Water-screened, sieve 0.5 mm	ca 8 litres	14.8
MKh99-5S	35,3		Sand and silt w/small bone fragments and insects					MKh99-5S	Floatation, then heavy fraction water-screened, sieve 0.5 mm	ca 8 litres	17.8

A5-13: continuation.

1	2	4	5	6	7	9	11	12	13	14	15
MKh99-5aS	34,8	4.3-4.5	Sand and silt w/small bone fragments and insects					MKh99-5aS	Floatation, then heavy fraction water-screened, sieve 0.5 mm	ca 5 litres	17.8
MKh99-6	34,1	5,1	Fine- and medium sand, intercalating with silt lenses	Massive, with thick (1-2 cm) horizontal ice bands	200	MKh99-6P	grass roots (few)				17.8
MKh99-6S	34,1	5.0-5.2						MKh99-6S	Floatation, then heavy fraction water-screened, sieve 0.5 mm	15 litres	17.8
MKh99-7	34	5,2	Fine- and medium sand, intercalating with silt lenses	Massive, with thick (1-2 cm) horizontal ice bands	350	MKh99-7P	grass roots				19.8
MKh99-8	33,3	5,9	Silt with high ice content	Lens-like	300	MKh99-8P	grass roots in branches + woody sticks				19.8
MKh99-9	32,6	6,6	Silt with high ice content	Lens-like, reticulated	425	MKh99-9P	grass roots + woody sticks				19.8
Site: Baydzherakh "E" ("Erdel"), Stn. 780, under the 1999 landmark R6 38.7 m a.s.l. (ca 1998 RP 4.6), top level of actively destroyed b-khs, capped by modern soil on the top Yedoma surface											
MKh99-22	31,8	6,9	Silt with high ice content	Lens-like, with numerous small and some large lenses	450	MKh99-22P	grass roots (few)				1.9
MKh99-22aS	31,3	7.3-7.6	Ice-rich silt with thread-like rootlets and soft (rotten ?) woody roots					MKh99-22aS		10 litres	1.9
MKh99-23	31	7,7	Silt with high ice content	Banded, alteration of lens-like and massive	350	MKh99-23P					1.9

A5-13: continuation.

1	2	4	5	6	7	9	11	12	13	14	15
MKh99-24	30,3	8,4	Silt with high ice content	Banded, alteration of lens-like and massive	300	MKh99-24P					1.9
Site: Baydzherakh "V" ("Vanya"), Stn. 745, 9 m below landmark R5 39.2 m a.s.l. (ca 1998 RP 4.4), and directly below b-kh "H", separated from it by an ice wedge, parallel to the cliff; second level of b-khs from the top											
MKh99-10	30,2	9	Silt with high ice content	Lens-like	150	MKh99-10P	grass roots + woody sticks				19.8
MKh99-11	29,5	9,7	Sandy silt with small woody twigs and very few grass roots (top of paleosol "V")	Massive	25	MKh99-11P	woody sticks only				19.8
MKh99-12	28,8	10,4	Silty sand, very rich with plant organic - grass roots, twigs (yellow inside), small woody sticks - "paleosol" V.	Massive	50	MKh99-12P	grass roots + woody sticks				19.8
MKh99-12aC	28,8	10,4	Silty sand, very rich with plant organic - grass roots, twigs (yellow inside), small woody sticks - "paleosol" V.					MKh99-12aC	Floatation, then heavy fraction poured into fabric bag and dried; no sieve used.	ca 5 litres	19.8
MKh99-13	28,2	11,0	Silt with high ice content	Lens-like with thick (up to 2 cm) ice bands	250	MKh99-13P	grass roots				20.8
MKh99-14	27,5	11,7	Silt with high ice content and numerous grass rootlets	Lens-like	485	MKh99-14P	grass roots				20.8
Site: Baydzherakh "L" ("Lyosha"), Stn. 745, 12 m below landmark R5 39.2 m a.s.l., continuing b-kh "V"downwards.											
MKh99-14aS	27,0	12.1-12.4	Silty sand					MKh99-14aS	Floatation, then heavy fraction water-screened, sieve 0.5 mm	12 litres	26.8
MKh99-15	26,7	12,5	Sandy silt with small woody twigs and grass roots (top of paleosol "L")		300	MKh99-15P	grass roots in branches + woody sticks				20.8
MKh99-16	26,2	13,0	Silt rich with numerous grass rootlets and small stems - paleosol "L"		260	MKh99-16P	grass roots + small stems				21.8

A5-13: continuation.

1	2	4	5	6	7	9	11	12	13	14	15
MKh99-16æ	26,2	12.7-13.0	Silt rich with numerous grass rootlets and small stems - paleosol "L"					MKh99-16æ	Floatation, then heavy fraction poured into fabric bag and dried; no sieve used.	12 litres	21.8
MKh99-17	25,8	13,4	Silt	Banded, alteration of lens-like and massive	60	MKh99-17P	grass roots, twigs, and woody sticks				21.8
Site: Baydzherakh "M" ("Maloy"), Stn. 750, 14 m below landmark R5 39.2 m a.s.l., and 10 m E from b-kh "L".											21.8
MKh99-18aS	25,4	13.7-13.9	Sandy silt with small woody twigs (above paleosol "M")					MKh99-18aS	Floatation, then heavy fraction water-screened, sieve 0.5 mm	5 litres	1.9
MKh99-18	24,7	14,5	Sandy silt with small woody twigs and grass roots (top of paleosol "M")	Massive, alternating with lens-like	160	MKh99-18P	grass roots + small stems				21.8
MKh99-19	23,9	15,3	Silt with high ice content	Lens-like	350	MKh99-19P					21.8
Site: Baydzherakh "F" ("Final"), Stn. 775, 15-16 m below landmark R6 38.7 m a.s.l., and 30 m E from b-kh "M".											
MKh99-20	23,3	15,9	Silt with numerous grass rootlets, lower part of "paleosol" "F"	Massive, alternating with lens-like	320	MKh99-20P					21.8
MKh99-21	22,5	16,7	Silt with high ice content	Lens-like	475	MKh99-21P					21.8
Site: Baydzherakh "Ma1" ("Mammoth 1"), Stn.900, 155 m SE of landmark R5 (ca 1998 RP 4.9), 36 m a.s.l. (old elevation 34.5 revised), the top level of baydzherakhs, partially eroded from above)											
MKh99-25S	33,5	2,5	Silt with grass rootlets around the baby mammoth skull	Massive				MKh99-25S	Water-screened, sieve 0.5 mm	2 liters	4.9
Site: Baydzherakh "Ma2" ("Mammoth 2"), Stn. 900, 155 m SE of landmark R5, 36 m a.s.l., right below baydzherakh M1											
MKh99-26S	28,0	8,0	Sandy silt					MKh99-26S	Melted and dried in fabric bag, no sieve used	2 litres	4.9

A5-14: The composition of the mammal bone collection (Bykovsky Peninsula, 1999).

Taxon	Total		Mam.-Khayata		Shore and bar		Holocene shore	Shore and bar between the 2nd and 3rd creeks
	n	%	n	%	n	%	n	n
Lepus sp. - hare	11	3,9	1	5,9	10	4,2		
Canis sp. - wolf	2	0,7		0,0	2	0,8		
Phoca sp. - seal (recent)	5	1,8		0,0	3	1,3	2	
Mammuthus primigenius (Blum.) - woolly mammoth	114	40,6	6	35,3	100	41,8	4	4
Equus caballus L. - small horse	81	28,8	1	5,9	71	29,7	7	2
Equus sp. - large horse	3	1,1	1	5,9	2	0,8		
Equus sp. - very large horse	1	0,4		0,0	1	0,4		
Rangifer tarandus (L.) - reindeer	31	11,0	4	23,5	23	9,6	3	1
Ovibos sp. - muskox	7	2,5		0,0	5	2,1		2
Bison priscus (Boj.) - bison	21	7,5	2	11,8	19	7,9		
Not identified	5	1,8	2	11,8	3	1,3		
TOTAL	**281**	**100**	**17**	**100**	**239**	**100**	**16**	**9**

A5-15: Mammal bones, found in 1999 within the Mamontova Khayata cliff (Bykovsky Peninsula).

Data-base No.	Field label	Taxon	Skeleton element	Preservation	Loc. type (*)	Locality	Elevation (a.s.l.)
1	2	3	4	5	6	7	8
1	M9-1	Mammuthus primigenius (Blum.)	femur juv.	damaged	b	MKh, ca Stn. 910, base of active slope, in mud	13-15 m
2	M9-2	Rangifer tarandus (L.)	shed antler	fragment	b	MKh, ca Stn. 940, in mud	13-15 m
3	M9-3	Rangifer tarandus (L.)	femur	fragment damaged	b	MKh, ca Stn. 960, in mud flow beneath baydzherakh	18-20 m
4	M9-4	Bison priscus (Boj.)	metatarsal	complete	b	MKh, ca Stn.460, 20 m NW from RP 5.5, in mud	25-26 m
5	M9-5	Rangifer tarandus (L.)	radius	complete	b	MKh, Stn.700, ca 10 m SE from R 4, surface of seaside slope of a baydzherakh under destruction	29 m
6	M9-6	Equus sp. (large)	tibia	fragment damaged	b	MKh, ca Stn.910, landslide of a baydzherakh	29 m
7	M9-7	Mammuthus sp.	astragalus juv.	damaged	b	MKh, ca Stn. 800	25-30 m
8	M9-8	Bison priscus (Boj.)	vertebris thoraic	complete	c	MKh, ca Stn. 300, on the grass over the first old circus	ca 8 m
9	M9-9	Mammuthus primigenius (Blum.)	fibula juv.	damaged	b	MKh, ca Stn. 650	25-27 m
10	M9-10	Lepus sp.	tibia	complete	a	MKh, Stn.900, depth 8.2 (+3.2 m from R5)	28 m
11	M9-11	Mammuthus primigenius (Blum.)	humerus juv.	damaged	b	MKh, Stn.900, depth 8.2 (+3.2 m from R5) (possibly from baydzh. Ma1)	28 m ca
12	M9-12	?	rib	fragment	b	MKh, Stn.900, depth 8.2 (+3.2 m from R5) (possibly from baydzh. Ma1)	28 m ca
13	M9-13	Rangifer ? Alces ?	shed antler	fragment	a	MKh, Stn.900, depth 0.8 m (top peat)	35.2 m
14	M9-14	Mammuthus primigenius (Blum.)	skull juv	damaged	a	MKh, Stn.900, depth 2.5 m from top, N side of Baydzh. Ma1	33.5 m
15	M9-15	Mammuthus primigenius (Blum.)	skull juv	fragment	a	MKh, Stn.900, depth 2.5 m from top (E side of baydzh. Ma1)	33.5 m
16	M9-16	?	rib	fragment	b	MKh, Stn.900, depth	

German-Russian Expedition POLAR URAL '99

A contribution to the EC-project EURASIAN ICE SHEETS

by Wolf-Dieter Hermichen, Anette Gierlichs, Frank Wischer and
Dmitry Bolshiyanov

Wolf-Dieter Hermichen, Frank Wischer : Alfred Wegener Institute for Polar and Marine Research, Research Department Potsdam, PO Box 600149, D14401 Potsdam, Germany
Anette Gierlichs: : Alfred Wegener Institute for Polar and Marine Research, Columbusstraße, D-27568 Bremerhaven
Dmitry Bolshiyanov: Arctic and Antarctic Research Institute (AARI), Bering St. 38, 199397 St. Petersburg, Russia

1. Introduction

(W.-D. Hermichen, D. Bolshiyanov)

Since 1998 the lake sediment group of AWI-Potsdam is involved in the research project 'Eurasian Ice Sheets' supported by the Commission of the European communities (ENV 4-CT97-0563) which is run by 6 groups from Bergen University (N), Geological Survey of Finland, Geological Survey of Norway, Lund University (S), Alfred Wegener Institute Bremerhaven-Potsdam (D), and by the University of Wales (Centre for Glaciology Aberystwyth, GB) in co-operation with Russian scientific groups.
After Svendsen (1997) the major scientific objectives of the project are:
1. To reconstruct from field observations and remote sensing the glacial and climate history of the Eurasian Arctic for the last glacial cycle, especially for the period 20,000-18,000 yrs BP.
>Mapping of the Weichselian/Valdaian maximum ice sheet extent and associated ice-marginal features;
>Establishing a chronology for the last glacial maximum (LGM) in the different sectors of the Russian mainland; reconstructing former ice-flow directions and interactions between the different ice sheets and domes during the LGM;
>Reconstruction of the periglacial environment during the Late-Weichselian, including ice-dammed lakes and vegetation.
2. Numerical modelling of ice sheets and their sensivity to climatic change.
The contribution of the AWI is focused onto studies of sediment sequences from lake basins of the area Polar Urals-Pechora Basin.
Based on former Russian-German co-operation in paleoenvironmental research in the Siberian Arctic (e.g. Melles, 1994; Melles, Hagedorn, Bolshiyanov, 1997), a joint AARI-AWI expedition to the Polar Urals - "PolarUral-99"- was agreed, aiming to the coring of bottom sediments from Lake Lyadhej-To (68°15'N, 65°45'E, c. 150 m a.s.l.) and Lake Bol'shoe Shchuch'e (67°54'N, 66°18'E, c. 120 m a.s.l.).
On the base of a survey, made in August 1998 (Hermichen and Wischer, 1999), coring on Lake Lyadhej-To was performed in April 1999 from the lake ice cover by the AWI-group.
In the course of 10 days 45 meters were cored at 3 stations. The cores represent the complete lacustrine sediment sequence, including the uppermost part of the basal till-like layer.
Contemporarily, the limnological-geomorphological survey of the Lake Bol'shoe Shchuch'e and its surroundings was done by the AARI-group (see section 4).

2. Expedition itinerary

(W.-D. Hermichen)

Participants,
With respect to different working places the expedition team consistsed of 2 groups:

Group "Shchuch'e":
Bolshiyanov, Dmitry (geographer)- AARI St.Petersburg
Pavlov, Maxim (student of geography) - St.Petersburg State University;
Group "Lyadhej-To":
Gierlichs, Anette (geophysicist, PhD-student) - AWI Bremerhaven
Hermichen, Wolf-Dieter (geophysicist) - AWI Potsdam
Müller, Gerald (technician) - AWI Potsdam
Wischer, Frank (geologist, PhD-student) - AWI Potsdam
Ippolitov, Valery (general assistant) - Agency VICAAR St.Petersburg
Minnekhonov, Viktor (driver) - Company Polyarnouralgeologiya Vorkuta
Pizhashov, Sergey (driver) - Company Polyarnouralgeologiya Vorkuta

Course of the expedition

The German part of the logistical preparation of 'PolarUral-99' was carried out by the expedition staff in Potsdam and Bremerhaven in January-February 1999, supported by the AWI-logistics department.
Within the Russian Federation, people from AARI St. Petersburg, Agency VICAAR St. Petersburg and Company Polyarnouralgeologiya Vorkuta, kindly supported the expedition.

February 23. - 28: Shipping of the expedition equipment (20 ft-container, 4250 kg) fromBremerhaven/Hafenlager to St. Petersburg/South Customs Post by truck.
March 1 - 12: Customs clearance in St. Petersburg/South Customs Post.
March 15 - April 12: Shipping of the container from St. Petersburg to Vorkuta by railway.
March 29 – April 1: Train journey of Bolshiyanov, Ippolitov and Pavlov the from St. Petersburg to Vorkuta.
April 7 – 9: Flight of the German participants from Berlin to Vorkuta via St. Petersburg - Syktyvkar.
April 1 – 12: Preparation to the expedition in Vorkuta including preparation of thesledge-tractor train, purchase of food supplies, acquaintance with information about the survey area in the archives of Polyarnouralgeologiya.
April 13: Flight (MI-8) of 2 groups to Lake Bol'shoe Shchuch'e (Bolshiyanov, Pavlov) and to Lake Lyadhej-To (Gierlichs, Hermichen, Wischer).
April 16 - 18: Journey of the sledge-tractor train from Vorkuta to Lake Lyadhhej-To (Müller, Ippolitov, Minnekhonov, Pizhashov).

April 13-22:	Hydrological and geomorphological studies in the valley of Lake Bol'shoe Shchuch'e, bottom lacustrine sediment sampling.
April 14 - 22:	Ramaq-GPR (ground penetrating radar) survey on Lake Lyadhhej-To.
April 19 - 29:	Sediment coring at 3 sites on Lake Lyadhhej-To
April 23:	Evacuation of the group from Lake Shchuch 'e by MI-8, airborne visual geomorphological observations along the route from Lake Shchuch'e to Lake Lyadhej-To. Bolshiyanov, Pavlov and Gierlichs return to Vorkuta.
April 24 - 27:	Bolshiyanov, Pavlov and Gierlichs fly to St. Petersburg via Syktyvkar.
April 30 - May 01:	Journey of the sledge-tractor train from Lake Lyadhhej-To to the Vorkuta-base of Polyarnouralgeologiya (Hermichen, Müller, Wischer, Ippolitov, Minnekhonov, and Pizhashov)
May 02 - 09:	Loading of the expedition container in Vorkuta, completion of all administrative activities, dispatch of the container with cargo to St. Petersburg by railway (Ippolitov).
May 03 - 07:	Return of Hermichen, Müller and Wischer to Germany (by railway to St. Petersburg via Vologda).
May 10:	Departure of the expedition container from Vorkuta and flight of Ippolitov to St. Petersburg. End of the expedition
May 25:	Arrival of of the expedition container in St. Petersburg/ South Customs Post.
June 13 - 17:	Shipping of the expedition container from St. Petersburg to Bremerhaven/Hafenlager by truck.

3. Coring of bottom sediments on Lake Lyadhej-To

(A. Gierlichs, W.-D. Hermichen, and F. Wischer)

3.1 Working area

Lake Lyadhej-To is located at the western foothills of the Polar Urals (68°15'N, 65°45'E, 150 m a.s.l.), inside the hypothetical southern limit of the last glaciation. Field investigations indicate that the Lyadhej-To may be carved into bedrock, and therefore it seemed to be well suited for achieving a long continuous sedimentary record since the last deglacation. Today it is situated in a tundra-landscape. Numerous smaller (presumably thermokarst-/glaciokarst-) lakes surround it.

Geomorphological evidence for a (presumably early- to mid-Weichselian) Kara-ice sheet margin was found c. 25 km to the south of the study site: Endmoraines (deposited at an altitude of c. 550 m a.s.l.) indicating glacier lobes having invaded into some valleys of the northernmost Ural mountains (Astakhov et al., 1999).

But, there are also alternative conclusions from geomorphological studies, pointing to a local glaciation of the Polar Urals in Weichselian time (see section 4 of this report).

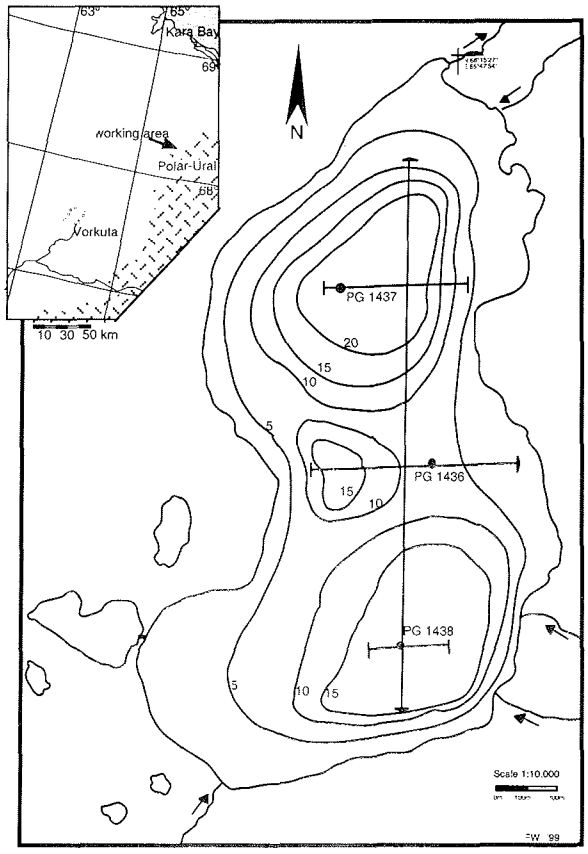

Fig 1: Bathymetric map of Lake Lyadhej-To, based on former measurements and radar-profiling. Depth contours are given in meters. Coring sites are marked by dots, GPR profiles by straight lines.

Geometry of the lake basin

Lake Lyadhej-To is ca. 2.5 km long and 1.5 km wide. It is divided into a southern and a northern basin, which are up to 26 m and 21 m deep, respectively. Main inflows are three rivulets in the

south, whereas a minor inflow and the outflow are situated in the north of the lake (see fig.1)
The lake has a shallow shoreline, only in the south there is a steep slope with a height of approximately 15 m.

Hydrology
The lake is mesotrophic to oligotrophic, ice-free in summer. In April 1999 it was covered by ice, 1.9 m thick. Temperature of the water column was slightly above 0°C without distinct changes. At the beginning of August 1998 the uppermost 5m had a temperature of 16°C, a gradual decrease to 11°C occurred in depths between 5 m and 15 m which was followed by a slighter decrease to 9°C at the bottom. Dissolved oxygen values vary between 9 and 10.8 mg /l. The conductivity is low with values between 45 and 67 µScm/1, the water is neutral to slightly basic (pH 7.4 to 8.3).

3.2 Survey of bottom sediments in Lake Lyadhej-To using ground-penetrating radar (GPR)

(A. Gierlichs)

Only little was known about the geometry of the lake basin and about its sediment prior to the fieldwork. That's why a survey with a RAMAC/GPR system was performed on the snow-covered lake ice to map the water depth and the sediment-thickness and to get information on the hardrock surface topography beneath the bottom sediments.

Equipment and measurements
The RAMAC/GPR system is a digital ground penetrating radar system with true 16 bit A/D converter. The maximum number of samples is variable. We chose 2048 sampling points.
In this survey 25 MHz antennae were used with an offset of 4 meters. Because the profiles had to be recorded on foot on the lake ice - external-triggering using keyboard, the spacing of the recorded traces was 4 meters, too.
Profiles with a maximum length of 1000 meters were recorded. The signal itself was stacked 2048 times for noise reduction and signal enhancement. The water depth was about 25 meters maximum. With a velocity of sound in water of ca. 30 m/µs and with an assumed velocity of sediments of 200 m/µs, a recording length of 2000 ns was chosen. So it was possible to record signals also from deeper areas of the sediments. Five transections of the lake were measured; especially the deepest parts of the two basins and the ridge between them were the points of interest. At the deepest parts of the lake the layering of the sediments assumed to be undisturbed.
CMP measurements give velocity-information about the 'C'ommon 'M'id 'P'oint between the transmitter and receiver antennae. Two CMP measurements for velocity information were recorded at the ridge, where the water depth was well known. The distance between the antennae was increased to 30 m symmetric for each trace and the signal was stacked 4096 times.

Data processing:
The profiles were pre-processed with the software GRADIX in the field camp, to determine the best coring sites. Traces were filtered and printed using an AGC with a window length of 48 ns. The CMP measurement show three main reflectors (fig. 2): The first at 290 ns with a velocity of 220 m/µs, the second at 510 ns with a velocity of 510 m/µs and the third at 630 ns with a velocity of 110 m/µs. With this information it is possible to estimate the thickness of the sediments in the basins. The reflections and velocity information of deeper areas are not discussed here, because the main aspect is the thickness of the sediments.

Results:
The signal between 0 and 200 ns at the southern basin (Profile 1/Fig.3) and between 0 and 250 ns at the northern basin (Profile 2/Fig.4) shows the ice on the sea surface. In the deepest part of the southern basin the sediment layers are approximately 4 meters thick (profile 1). In the northern basin the received signals indicate about 8 meters of sediments (profile 2). The data in between shows the water column of the lake. Internal structures of the sediments are not resolved. Profile 3 (Fig.5) was measured on the ridge of Lake Lyadhej-To. Unfortunately the profile missed the ridge in the eastern part of the profile. The profile starts at the western shore of the lake. Traces 1 to 18 show ice from 0 to 200 ns. The water depth increases from west to east and the ice and the sediments can be resolved. The structure of the sediments between 600 ns and 1100 ns of traces 1-25 and 40-60 is unusual. It is not yet clear, whether this structure is artificial or not. The sediments have a thickness of about 12 meters (250 ns). The data quality is good along the whole profile. The next profile starts at the southern point and ends at the camp on the ridge in the middle of the lake (Profile 4/Fig.6). The points, at which profile 1 and profile 3 intersect profile 4 are marked in the plots. Profile 1 is not exactly at the deepest point of the southern basin, whereas profile 3 is right on the top of the ridge. The penetration of the signal into the sediment-layer on the ridge is about 500 ns. Around trace 180 several reflections with a total traveltime of 800 ns - 900 ns are detected. The signal at the slope of the ridge, between trace 100 and 130, looks quite strange - it is not yet clear, if this is a result of a technical problem. The horizontal signal between 600 ns and 700 ns, which can be correlated at all traces, seems to be the multiple of the ice cover of the lake. Profile 5a+b (Figs. 7, 8) starts at the ridge and ends in the northern part of the lake. Here, the sediments of the ridge are also detected quite well. Reflections of the sediments were found with a total traveltime of 700 ns for the traces 1-40. The reflections from deeper parts at the beginning of profile 5a are probably artificial. These signals, which move parallel and slightly upwards, are recorded again around trace 20 with a total traveltime of 600 ns to 1100 ns. Between traces 40 and 80 a multiple of the lake bottom can be seen at 900 ns. The multiple at 600 - 700 ns is recorded again in profile 5b. The profile starts at the camp and ends in the northern part of the lake and shows decreasing sediment thickness with increasing waterdepth. It is not yet clear,

whether this results from the energy loss of the signal due to bad coupling. At the deepest part of the northern basin the intersecting point with profile 2 is marked again in the plot.
Profile 2 gives also new information about the topography of the lake. The deepest part of this basin was expected to be more eastern. The new information about the water depth of the northern basin and about the sediment coverage is shown in profile 2. The signal of the western slope of the ridge - trace 1 - 20, between 300 ns and 800 ns - is probably an effect of a temporary malfunction of the antenna. This did not occur in other parts of the profile. The thickness of the sediments here varies between 200 - 150 ns. The deepest point of this profile shows less sediment than the shallower parts like the profiles mentioned before. The multiple, often seen between 600 ns and 700 ns on other profiles, is missing completely.

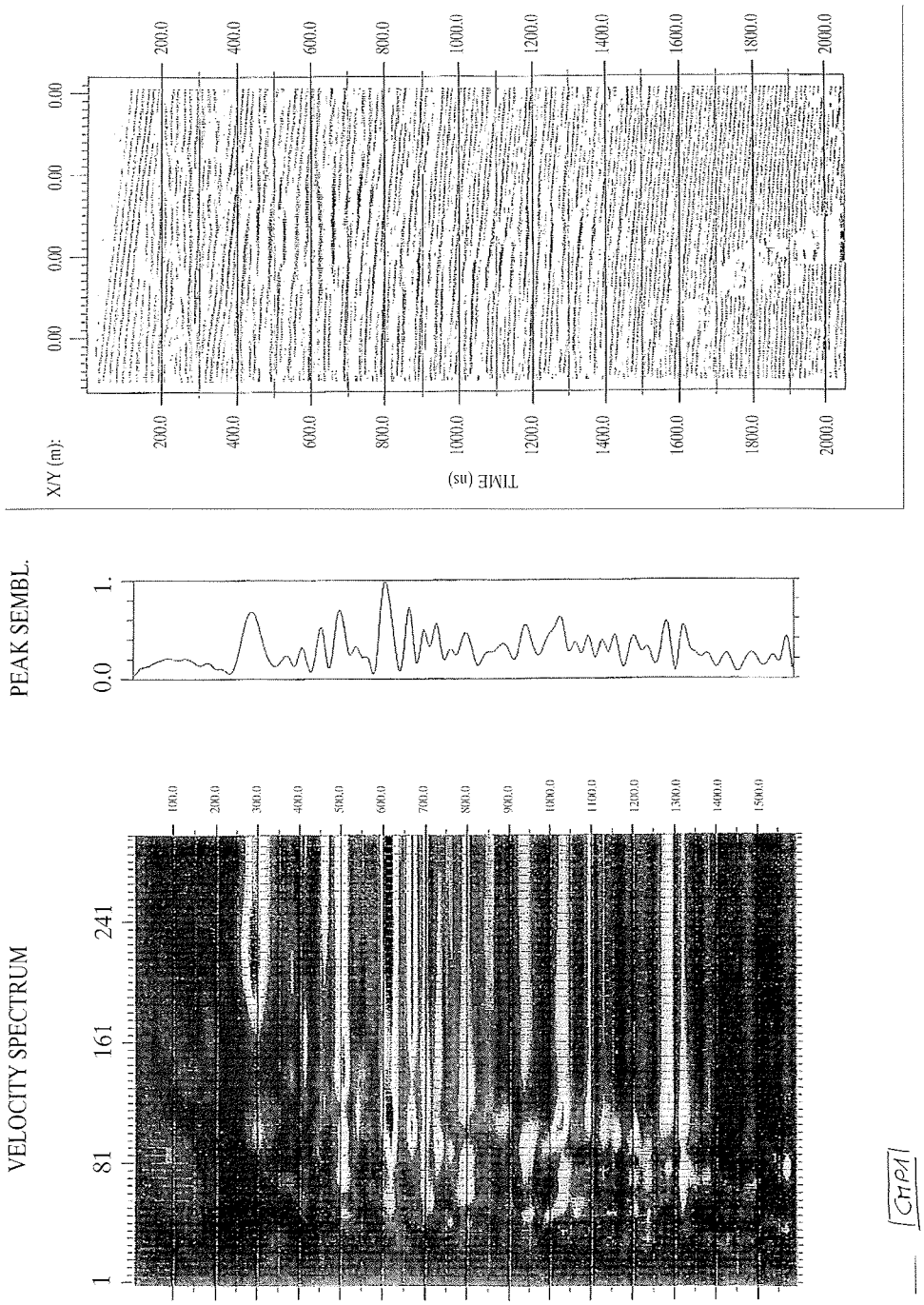

Fig. 2: Results of CMP-Measurements at Position 1

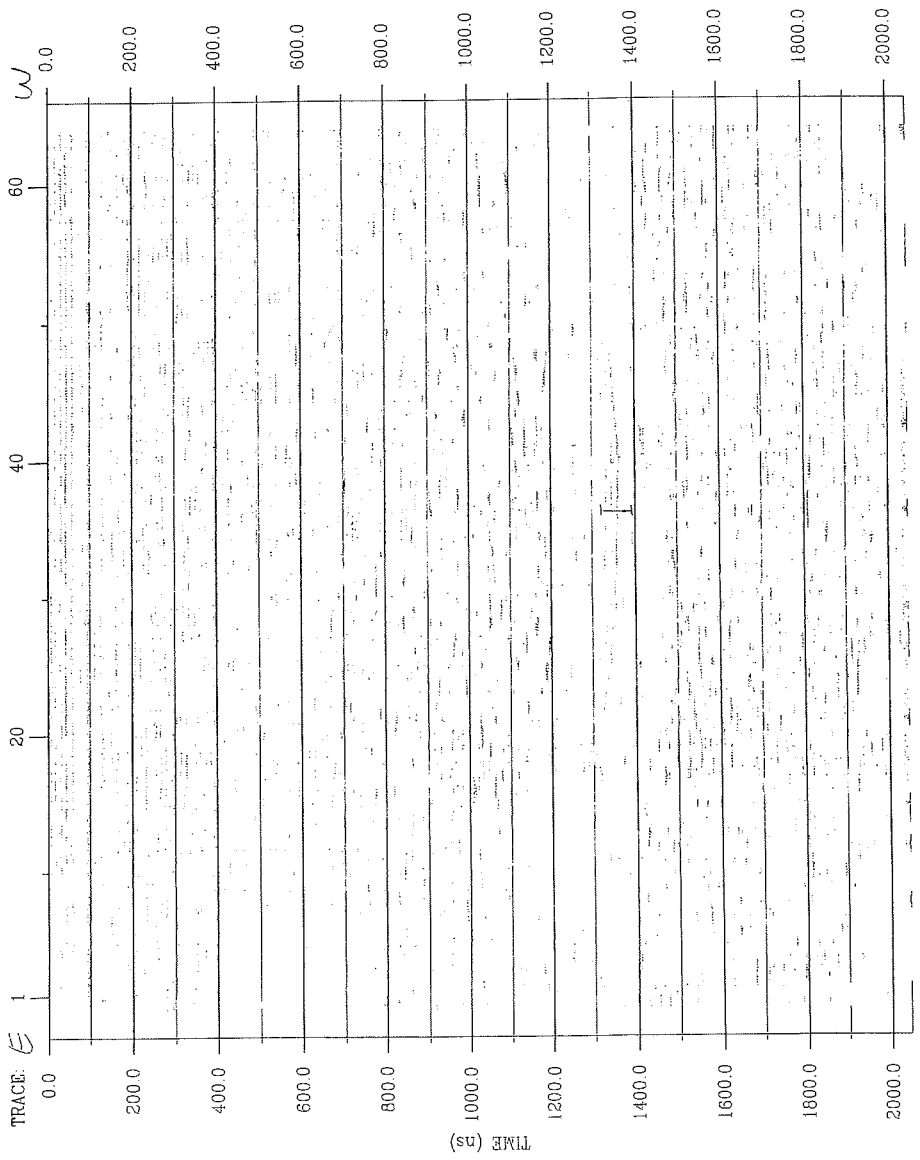

Fig 3:GPR-Profile 1

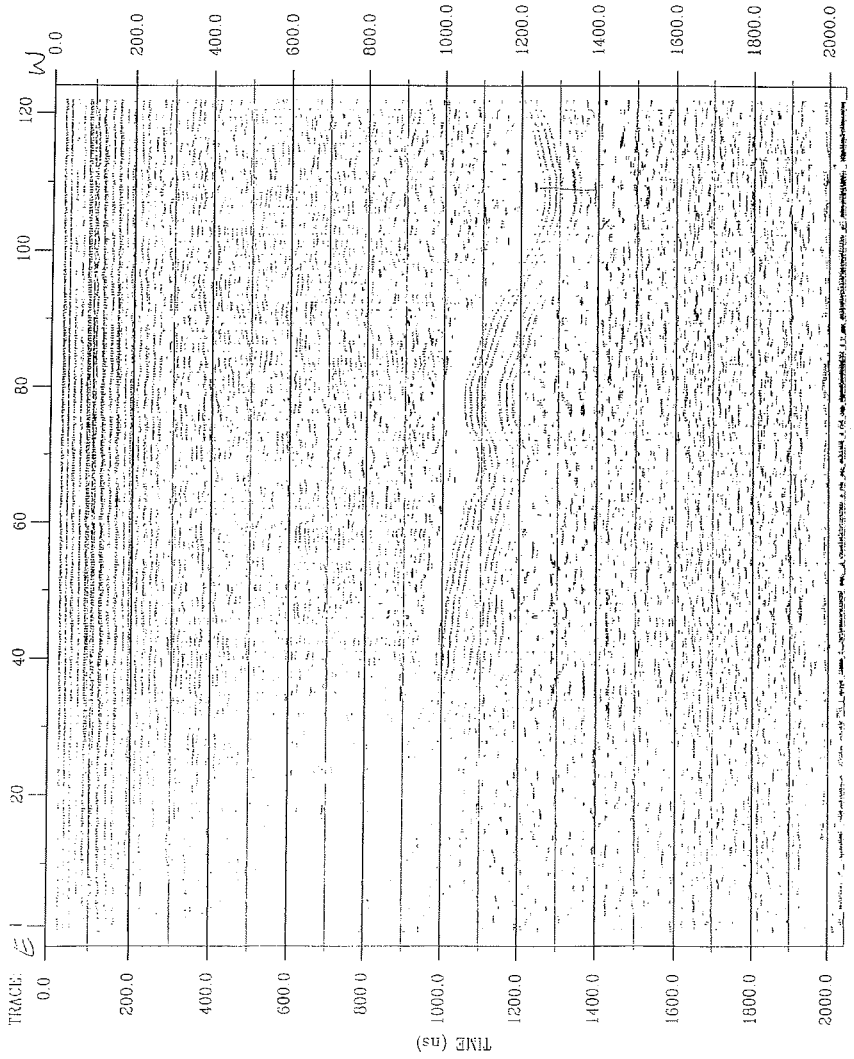

Fig 4:GPR-Profile 2

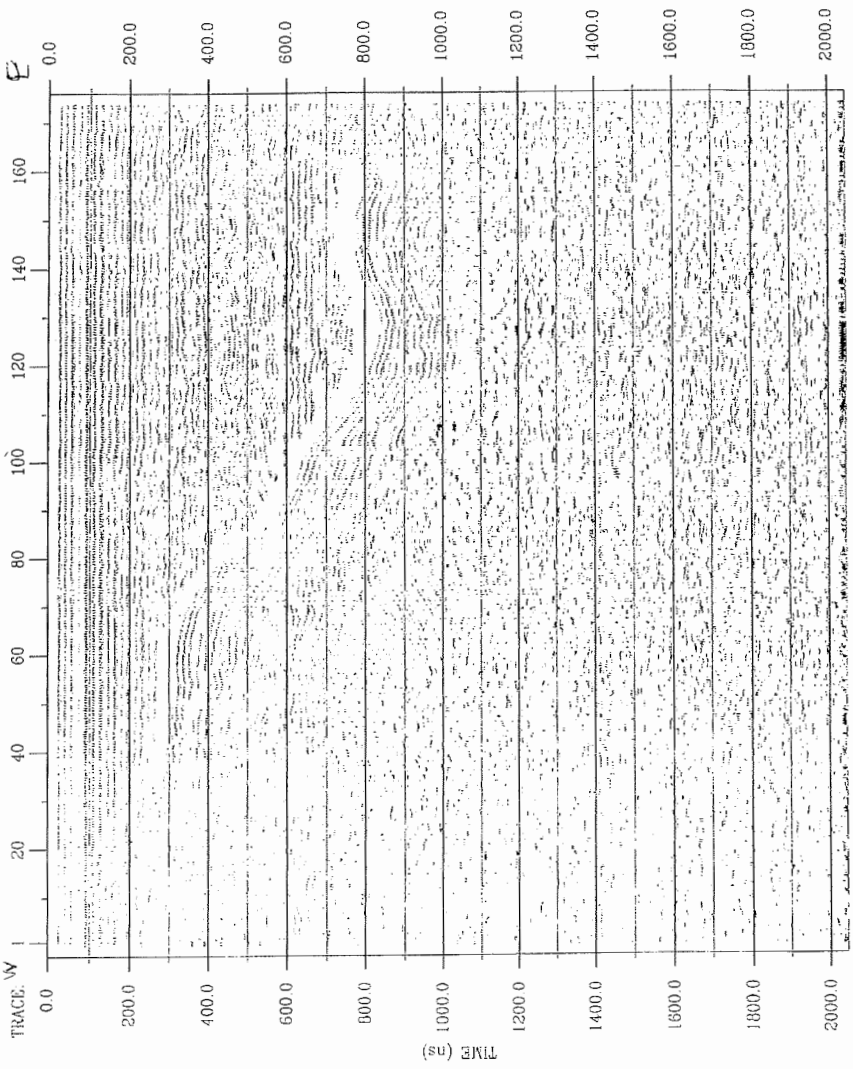

Fig 5:GPR-Profile 3

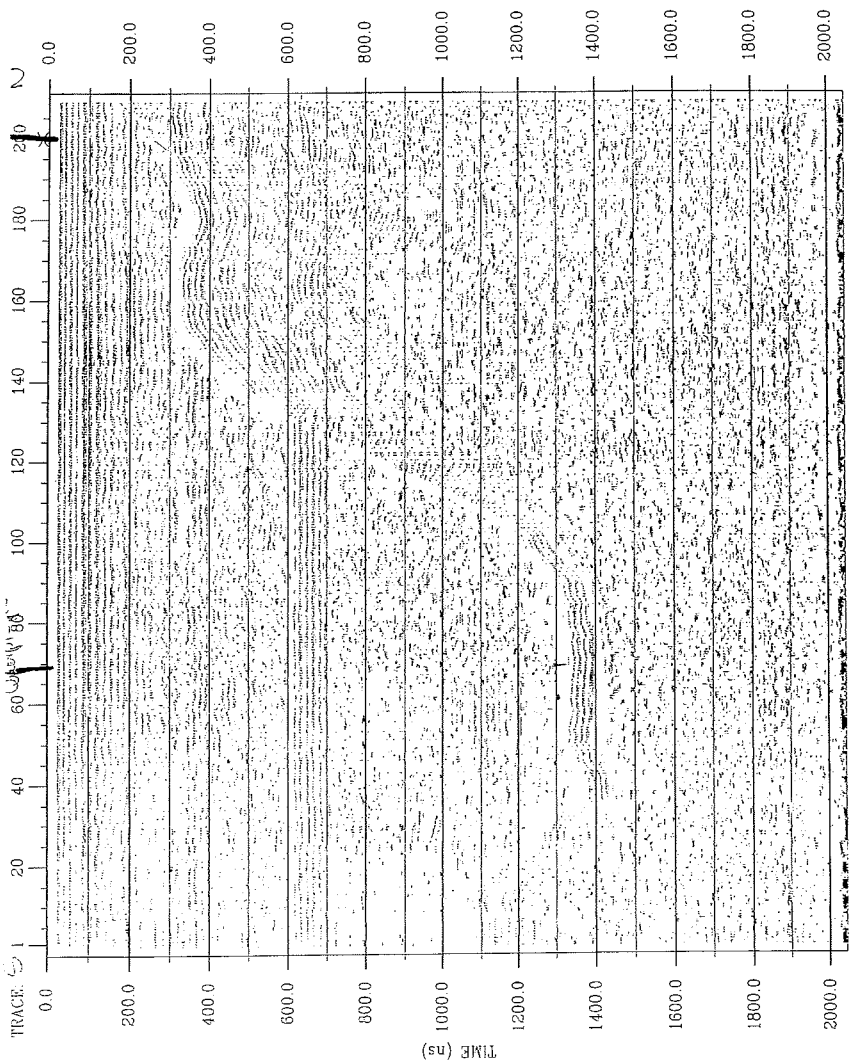

Fig 6:GPR-Profile 4

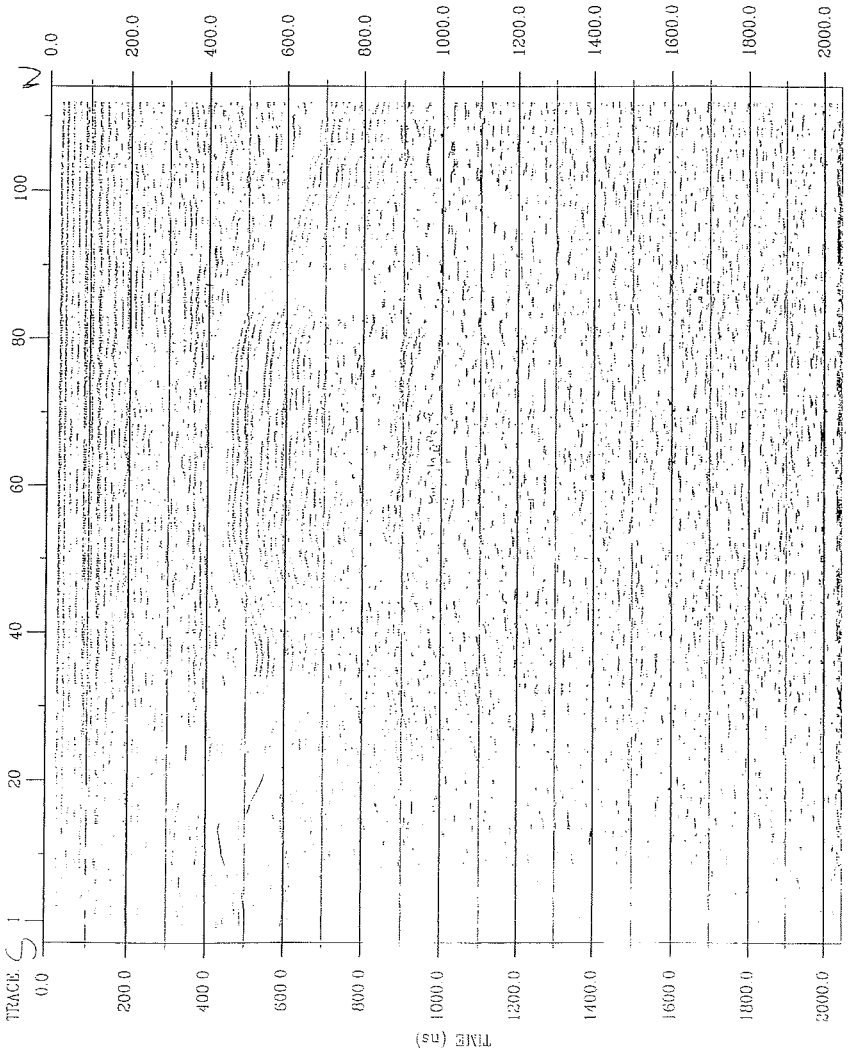

Fig 7:GPR-Profile 5a

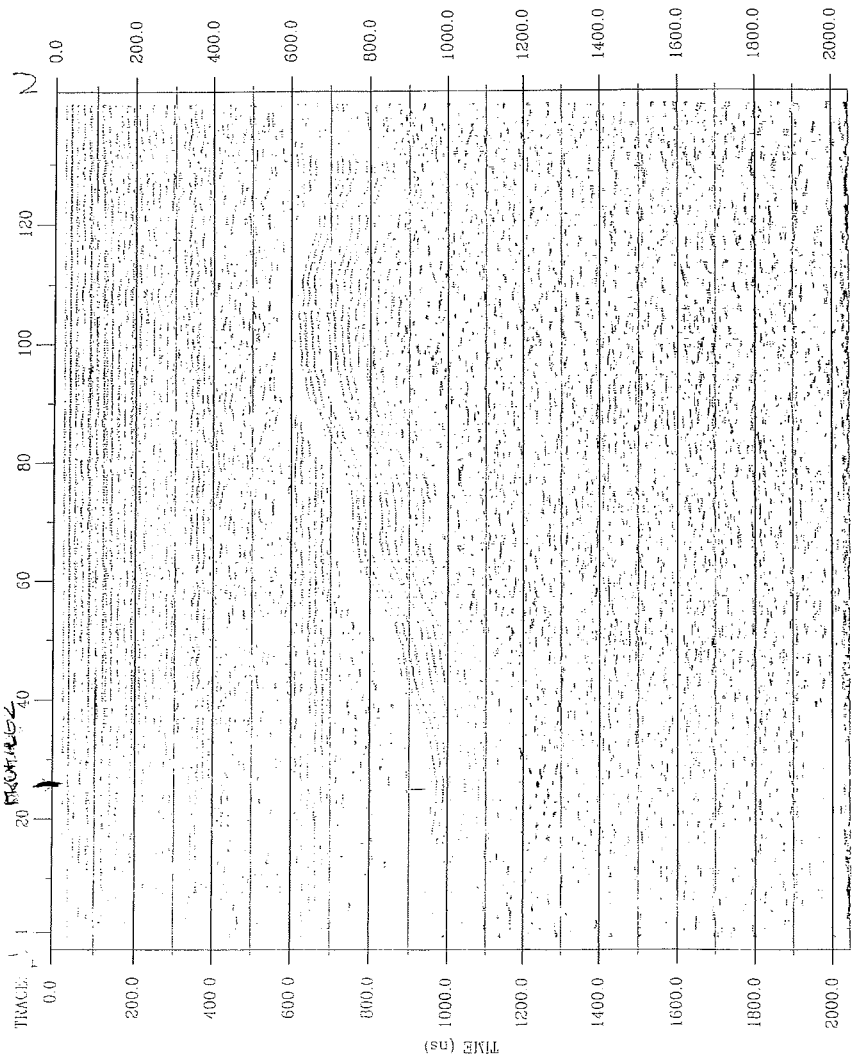

Fig 8:GPR-Profile 5b

Conclusion:
The RAMAC/GPR system is a good opportunity for pre-surveying frozen lakes to determine coring sites. Although air temperature was often below -15°C, it was possible to measure a total of c. 4.5 km with a good penetration of the sediments. Due to logistic problems, the antenna had to be moved on foot. Moving the antennae with a snowmobile on sledges is a more advanced way of GPR-profiling, well established in other parts of polar research. Continuous measurements and longer profiles could be recorded using internal triggering. The icy surface of the lake caused some damage to the antennae so that they did not work reliably on all parts of the profiles. Fortunately they could be repaired during the expedition.
The drilling results correspond quite well with the predicted sediment thickness derived from radar measurements. In the southern basin 4 meters of lacustrine sediments were expected and 7.8 meters were recovered. In the northern basin 8 meters thickness was predicted, and 7.0 meters were found. Beside the information on the thickness of the sediments, the topography of the lake bottom was also measured. Former measurements were corrected using the new information given from the radar profiles. Unfortunately the conditions for the measurements were not optimal, otherwise the whole lake could have been surveyed with GPR. The survey with the 25 MHz antenna gives an idea of sediment structures below the lake bottom and the topography of the lake bottom itself. With maximum water depth of 25 m and a lacustrine sediment thickness of 8 m Lake Lyadhej-To is an optimum-testing site for high-resolution GPR. Using 50 MHz and 100 MHz antennae would give detailed information on internal structures of the sediment section.

3.3 Coring: Equipment and procedures
(F. Wischer)

Coring was carried out through holes in the 1.9-m thick ice cover, using a tripod with hand-operated winches. A special tent protected the working site.
Two types of coring devices were used - both equipped with a plastic liner (inner diameter 60mm) to take in the sediment column.
A light gravity corer was applied for the sampling of soft near-surface sediments. It is able to recover a maximum core length of 55 cm.
Longer sediment cores were obtained with a piston corer; a manually operated hammer (20kg) supplies the penetration of the corer. The maximum recovery with every employment is 3 m, limited by the length of liner. However, deeper situated sediment can also be sampled, because the start of the coring process is controlled by release of the piston at a defined depth of the corer. The piston is fixed in the lower tube aperture during the way of the corer through the water column and the overlaying sediments. Therefore, it is possible to obtain a sediment sequence of more than 20 m by matching overlapping cored sequences.
A detailed description of coring technique is given by Melles et al. (1994).

After recovering the piston corer from the water, it was immediately transported to the heated field station to avoid freezing. The cores were cut into segments of a length ≤100 cm, sealed airtight and labelled. Before sealing the visible sediment was described roughly.
Finally, the cores were stored in thermoboxes at a temperature >0°C.

3.4 Field description of the sediment columns

(F. Wischer)

Sediment coring was started at site PG 1436 (see fig.1 and table, given below) on top of the underwater-plateau at a water depth of 7 m. The sediment recovery was 7.6 m.
Thanks to the results of GPR profiling (which indicated unstratified sediments with a thickness > 25 m), we decided to stop the coring at site PG 1436.
Two more promising sites could be located by GPR: PG 1437 in the northern and PG 1438 in the southern basins. At site PG 1437 11.8m could be obtained at a water depth of 21.7 m, coring at PG 1438 resulted in a core of 10 m (water depth 24.4 m).
Due to the covering plastic tubes the sediments could be described only roughly:
At sites PG 1437 (northern basin) and PG 1438 (southern basin) an unstratified, poorly sorted, consolidated diamicton occurs at the base, which was interpreted as a moraine, deposited during the last glacier advance.
The uppermost seven meters of PG 1437 consist of laminated and stratified clayey silts (or silty clays) of dark greyish to black colour, which are rich in organic remains. They were interpreted as limnic sediments, reflecting the complete post-glacial lake history.
Site PG 1438 contains comparable sediments between 6.5 m and 0 m. The sequence between 8.0 m and 6.5 m consists of partly stratified sands with some clay layers and can be interpreted as a state of low autochthonous biomass production in the lake.
The sediment succession of PG 1436 is comparable to the other sections only in the top three meters. The deeper parts consist of poorly sorted, partly stratified clastic sediments, which may have been deposited by a mass flow, e. g. by a landslide or a mudflow from a nearby mountain valley, as field observations suggest.

Table: Bottom sediment cores recovered from Lake Lyadhej-To.
Positions determined by GPS. GC: gravity corer, PC: piston corer

Core No.	Position		Locality	Water depth (m)	Date	Gear	Recovery (cm)
	Latitude	Longitude					
1436 -1	68°14.709 N	65°47.197 E	Central Plateau	7.0	20.04.	PC 0	-247
-2					20.04.	PC 237	-507
-3					20.04.	PC 457	-577
-4					22.04.	PC 457	-613
-5					22.04.	PC 557	-757
1437 -1	68°15.060 N	65°47.120 E	Northern Basin	21.7	23.04.	GC 0	-35
-2					24.04.	PC 0	-252
-3					24.04.	PC 212	-503
-4					25.04.	PC 462	-742
-5					25.04.	PC 712	-999
-6					26.04.	PC 962	-1179
1438 -1	68°14.493 N	65°46.880 E	Southern Basin	24.4	28.04.	PC 0	-293
-2					28.04.	PC 250	-543
-3					29.04.	PC 500	-794
-4					29.04.	PC 816	-1000
1439 -1	68°14.493 N	65°46.880 E	Southern Basin	24.4	29.04.	GC 0	-39

4. Studies on Lake Bol'shoe Shchuch'e

(D. Bol'shiyanov & M. Pavlov)

4.1. Weather conditions during the survey on the lake

The air temperature in the central part of Lake Bol'shoe Shchuch'e (measured 2-3 times a day by an aspiration psychrometer) gradually increased from April 13 until April 21. On April 21, a sharp warming occurred and on April 22, the temperature was above 0°C (Fig. 9). After that it became cold again, and cold weather persisted until May.

The wind regime in the lake basin was determined by its orientation. Of 10 observation days, the northwesterly wind was blowing for 7 days, the southeasterly wind continued for two days and on one day the wind was absent. In the night from April 21 to 22, wind gusts with the speed of up to 20 m/s unstable in direction were observed frequently breaking loose from the western basin slope and generating vortices of the tornado type. The living tent was displaced, overturned and broken by one of such vortices.

4.2. Lake depth measurement

The depths in the lake were measured using a lead. The holes through the ice were drilled by a hand drill. A longitudinal and a cross profiles were made on which the depths were measured at 17 points (Fig. 10). The largest depth measured was 136 m. This coincides precisely with the maximum lake depth measured by the previous investigators (Kemmerich, 1961).
The lake basin has an elongated shape. Its length is 13 km and the average width is 1 km. The measurements revealed that the basin has steep slopes and a flat bottom at a depth between 120 to 136 m (Figs. 11 and 12).

4.3. Water temperature measurements

The water temperature was measured using a pair of deep-water reversible thermometers TG-1 with the help of a hydrological winch. The first measurement series was made on April 15 at a point with the coordinates: 67°53.912'N, 66°17.695'E. The second series of measurements was undertaken on April 21 in the hole in ice after sampling bottom sediments cores. The hole was located 50 m to the northeast of the point of first series of measurements. Figure 13 presents the curves of water temperature distribution by depth constructed after introducing necessary corrections to the temperature measured. The same data are presented in the table. As can be seen from the figure and the table, the data differ very seriously. It is unlikely that they reflect natural changes in the temperature regime of the lake. The curve plotted from temperature measurements on April 21 seems to be more preferable as it corresponds to water temperature measurements in the same lake area made by N.G.Oberman (Polyarnouralgeologiya) on April 24-25, 1977.

Table: Water temperature distribution with depth

measurement no 1		measurement no 2	
Depth, m	Temperature, °C	Depth, m	Temperature, °C
5	0,58	5	1,22
25	0,31	10	1,24
40	0,73	25	1,52
53	1,08	30	1,65
105	1,53	50	1,85
120	1,49	100	2,03
122	1,53	117	2,12
124	1,65	121,5	2,14
125	1,67	123,5	2,28
		125,5	2,21

4.4. Sampling of bottom sediment cores

Sampling of bottom sediments was performed using a GOIN ground corer, 1.5 m long, from the same hole in ice that was later used for measuring water temperature. For lowering and recovery of the sampler, a hydrological winch was used. After sampling from the hole, the corer was immediately brought to the living tent for avoiding sediment freezing at the ambient air temperature of –15 to –16°C. The temperature of the upper and lower core portions was measured by a thermometer stuck into the sediment before the core was extracted from the corer. After that the core was described, divided into samples or packed entirely to plastic tubes.

Six cores of bottom sediments of Lake Bol'shoe Shchuch'e were collected:

Core 1 – 59 cm thick (preserved completely)
Core 2 – 58 cm (preserved completely)
Core 3 – 60.5 cm (divided into samples, 2 cm each, a total of 29 samples)
Core 4 – 33 cm (divided into samples, 2 cm each, a total of 16 samples)
Core 5 – 44.5 cm (preserved completely)
Core 6 – 56 cm (preserved completely)

Table: Results of sediment temperature measurement.

Core No.	Surface temp. (°C)	Bottom temp. (°C)	Note
1	2,1	2,4	
2	1,2	3,7	The foot temperature is overestimated as a result of hot water treatment of the corer end
3	1,2	2,4	The foot temperature is overestimates as a result of hot water treatment of the corer end
4	1,5	2,3	
5	1,3	1,4	
6	1,6	2,0	

Core 6 was subjected to analysis under the laboratory conditions. After it was extracted from the corer, it was cut into two halves and dried. The lithological features are revealed for visual studies only at a specific sediment moisture state. In the dry or wet form the sediment looks uniform. At a specific stage of sediment drying, varves are evident. They consist of silt-clay material deposited in winter and silt deposited in summer. A large lake depth and a non-uniform sedimentation regime throughout the year guarantee the formation of a pair of layers – winter and summer during the year. The thickness of the pair of layers in the sediment studied varies between 0.3 to 1.2 mm comprising 1 mm on average. In addition, the sediment contains sand and

gravel interlayers up to several mm thick. They are rhythmically deposited in the water bodies.
As shown by the studies of varved clays of current sub-glacial water bodies in the Arctic (Bolshiyanov, 1985) and in the Antarctic (Bolshiyanov et al., 1991), the sandy-gravel interlayers in the strata of bottom sediments serve as evidence of the catastrophic events of the detrital material discharge to the lakes due to snow-ice mass melting periodically accumulating in the lake basins. At the time of their degradation, a large amount of water is released during a short time resulting in erosion and transport of detrital material to the accumulation basins.
Counting the varves and determining the location of sand-gravel interlayers in the section allows determining an approximate time of the catastrophic events. The spore-pollen studies also allow specifying the glaciation periods connected with local climate cooling. After counting the pairs of layers and ice interlayers dividing them, samples for spore-pollen analysis and of organic matter for radiocarbon dating were collected. Figure 14 presents the structure of cores 5 and 6 and the sampling intervals. From the diagram in Figure 15 one can determine the time of deposition of sand interlayers in the lake that probably resulted from the discharge of a large quantity of detrital material to the lake and from melting of small glaciers and firn.

4.5. Geomorphological observations in the valley of Lake Bol'shoe Shchuch'e and along the route to Lake Lyadhhey-To

The valley of Lake Bol'shoe Shchuch'e is a geomorphological expression of the Earth's crust fault. The strike of the "Shchuch'e" fault is NW –323°. This direction corresponds to the direction of the main lineaments in this area. The directions of the main lineaments were measured over the 9750 km^2 area using the 1:500 000 scale map. A rose-diagram of lineaments was plotted (Fig. 16) where two directions dominate: NE - 42° and NW - 315°.
The northern half of the lake basin is cut by an anticlinal massive comprised of slates, quartzite-sandstone and effusive rocks of Bedamelskaya suite of the upper Proterozoic-Cambrian. Along the western slope of the basin these rocks are displaced northwestward over 8 km compared with the eastern slope. The entire western slope and the southern half of the eastern slope are comprised of the Ordovician slates, siltstone, sandstone and conglomerates. At the slopes of the southern part of the lake, dikes of gabbro-diabase outcrop to the surface.
A cross-profile of the valley is trapezoidal - steep straight slopes and a flat bottom. The asymmetry of the lake basin slope is expressed in a steeper and straight western slope and in the eastern slope complicated with erosion entrenchments. The asymmetry is due to the rock bedding features.
The rocks outstripped at the western slope have incidence up to 70° along the 65° azimuth, i.e. in conformity with the slope. The rocks at the eastern slope dip at the 20° angles to the southeast - 110°, i.e. across the strike. An asymmetry of the lake basin morphology is also expressed in the meridional direction. The slopes and watershed of the southern part of the basin are much lower. The highest marks of the Proterozoic-Cambrian massive in the northern

area are up to 1223 m whereas in the southern area the watershed heights reach only 500-580 m. Cirques are present at the western slope of the tectonic basin. At the eastern slope, the erosion grooves in the upper parts of the slopes, combine into funnel-shaped systems of dry valleys. The asymmetry in the basin morphology is also reflected in vegetation. The osier shrubs in the northern half of the lake reach the 500-600 m heights at the eastern eroded slope. At the western straight talus slope, the osier shrubs have no place to fasten and reach only the 300 m height. In the southern half of the basin at the eastern slope, larch reaches the 170-180 m height above the lake level.
In the southern area of the basin, the terraces at the heights of 120-170 and 50 m above the lake level are clearly pronounced. There is a terrace 7-10 m above the water level on both lakeshores in the accumulative debris cones and at the bedrock slope. Its width is up to 25-30 m and the surface is comprised of the rounded pebble and is covered by vegetation (moss, lichen and wild rosemary). The lowest terrace which points to the increased lake level stand in the past is located at the 3 m height above the water level.
The morphology of the Lake Bol'shoe Shchuch'e basin and the absence of accumulation of ice deposits indicates that the glaciers, which partly occupied it, did not mechanically reworked the relief significantly. The lake terraces probably formed as a result of lake being dammed by mountain glaciers.
Airborne visual observations undertaken during the flight to Lake Lyadhey-To revealed that the formation of the glacial relief features in the valleys of the northern slope of the Polar Urals was rather caused by the local mountain glaciers. Thus, a described bend of the glacial ridges upward the Polar Urals valleys could be due not to the penetration of the Kara ice shield to the Urals valleys as described by Astakhov et al. (1999) but to other causes. Figure 17 depicts such a ridge that served as the main proof of the Kara ice shield advance from the north to the mountains up to a height of 560 m (Astakhov et al., 1999). As can be seen in this figure, there is a ring structure eastward in the next valley of Lake Ochety whose formation was caused by melting of dead ice buried by glacial deposits. The center of this structure has a sink with a lake (Fig. 17-a). The slopes of this structure were completely preserved and that is why it looks as a ring. The margin of the first "Kara" moraine bending southward could also be determined by ice melting in the center of the accumulated glacial deposits. A concave relief of this feature and the lake left from ice melting indicates this. The slope and erosion processes shade the northern part of the ring structure. An explicitly pronounced southward arch is also worked in addition by current nivation processes that are clearly marked by the firn preserved during summer under the northern arch slope. Thus, the Kara origin of these glacial deposits cannot be attributed to only the direction of the end moraine orientation. There are other mechanisms that result in the formation of such features.

References

Astakhov, V.I., Svendsen, J.I., Matiouchkov, A., Mangerud, J., Maslenikova, O., and Tveranger, J. (1999): Marginal formation of the last Kara and Barents ice sheets in Northern European Russia. - Boreas, vol. 28, π 1, p. 23-45.

Bolshiyanov, D.Yu. (1985): Sedimentation in the modern sub-glacial lake (by the example of Lake Izmenchivoye, Severnaya Zemlya archipelago). – Vestnik LGU, V. 7, Issue 1, p. 43-50.

Bolshiyanov, D.Yu., Verkulich S., Pushina Z., Kirienko E. (1991): Some features of the Late Pleistocen and Holocen history of the Bunger Hills (East Antarctica).- Proceedings Intern. 6-th Symp. Antarctic Earth Sciences, Tokyo, 1991, p. 101-106.

Hermichen, W.-D. & F. Wischer (1999): Eurasian ice sheets: Expedition to the Lake Lyadhej-To (Polar Urals). In: Rachold, V. (editor), Berichte zur Polarforschung 315: 261-268.

Kemmerich, A.O. (1961): Hydrography of the North, Sub-Polar and Polar Urals. Moscow, 139 p.

Melles, M. (Editor) (1994): The expeditions NORILSK/TAYMYR 1993. Berichte zur Polarforschung 148: 3-25.

Melles, M., Kulbe, T., Overduin, P.P., Verkulich, S. (1994): The Expedition Bunger Oasis 1993/94 of the AWI Research Unit Potsdam. In Melles, M. (ed.): The Expeditions Norilsk/Taymyr 1993 and Bunger Oasis 1993/94 of the AWI- Research Unit Potsdam. Berichte zur Polarforschung, 148:27-80.

Melles, M., B. Hagedorn and D. Bolshiyanov (1997): Russian-German Cooperation - The expedition TAYMYR/SEVERNAYA ZEMLYA 1996. Berichte zur Polarforschung 237, 169 p.

Svendsen, J.I. (1997): Ice sheets and climate in the Eurasian Arctic at the last glacial maximum (EURASIAN ICE SHEETS). Research proposal submitted to the Comission of the European Communities. University of Bergen. 55 p.

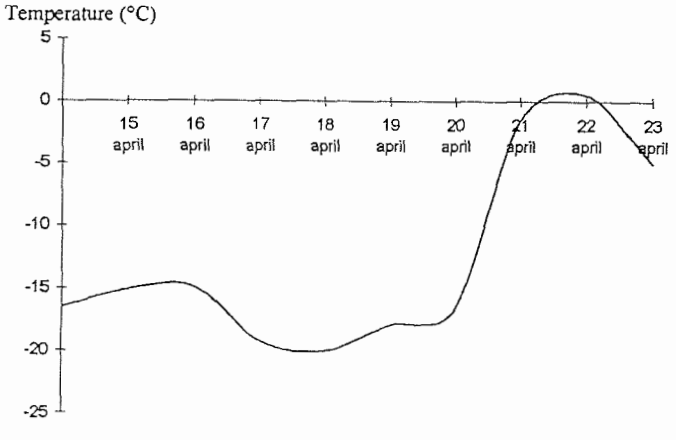

Fig. 9: Daily average temperature on Lake Bol'shoe Shchuch'e

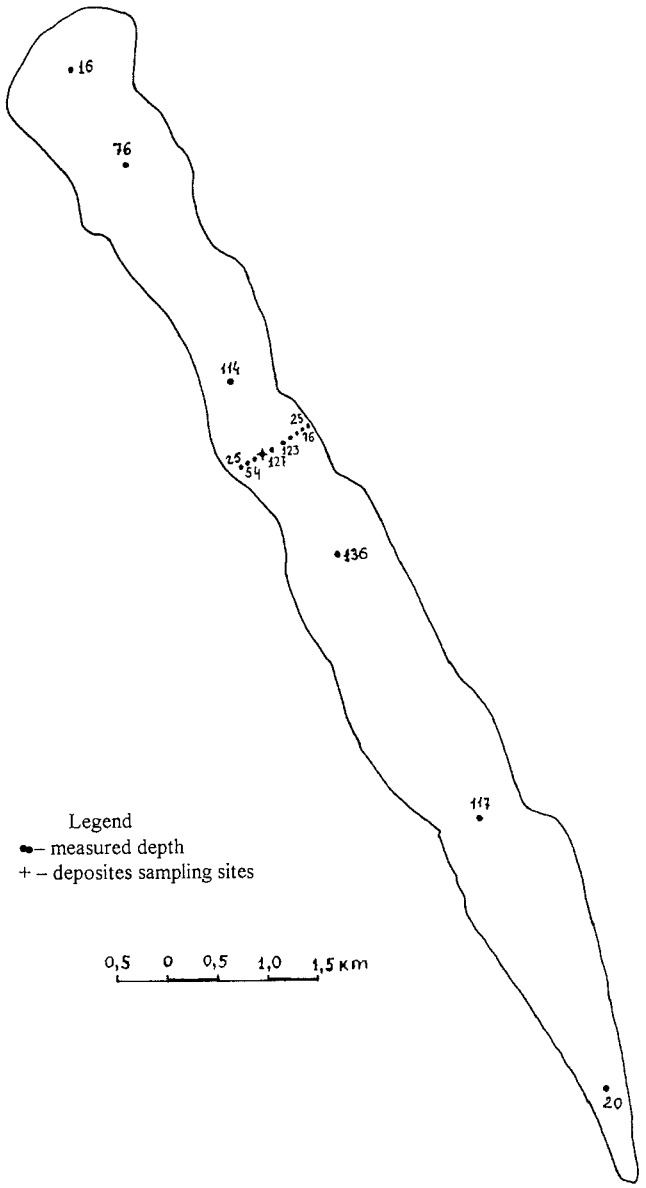

Fig. 10: Stationsof bathymetric measurements on Lake Bol'shoe Shchuch'e

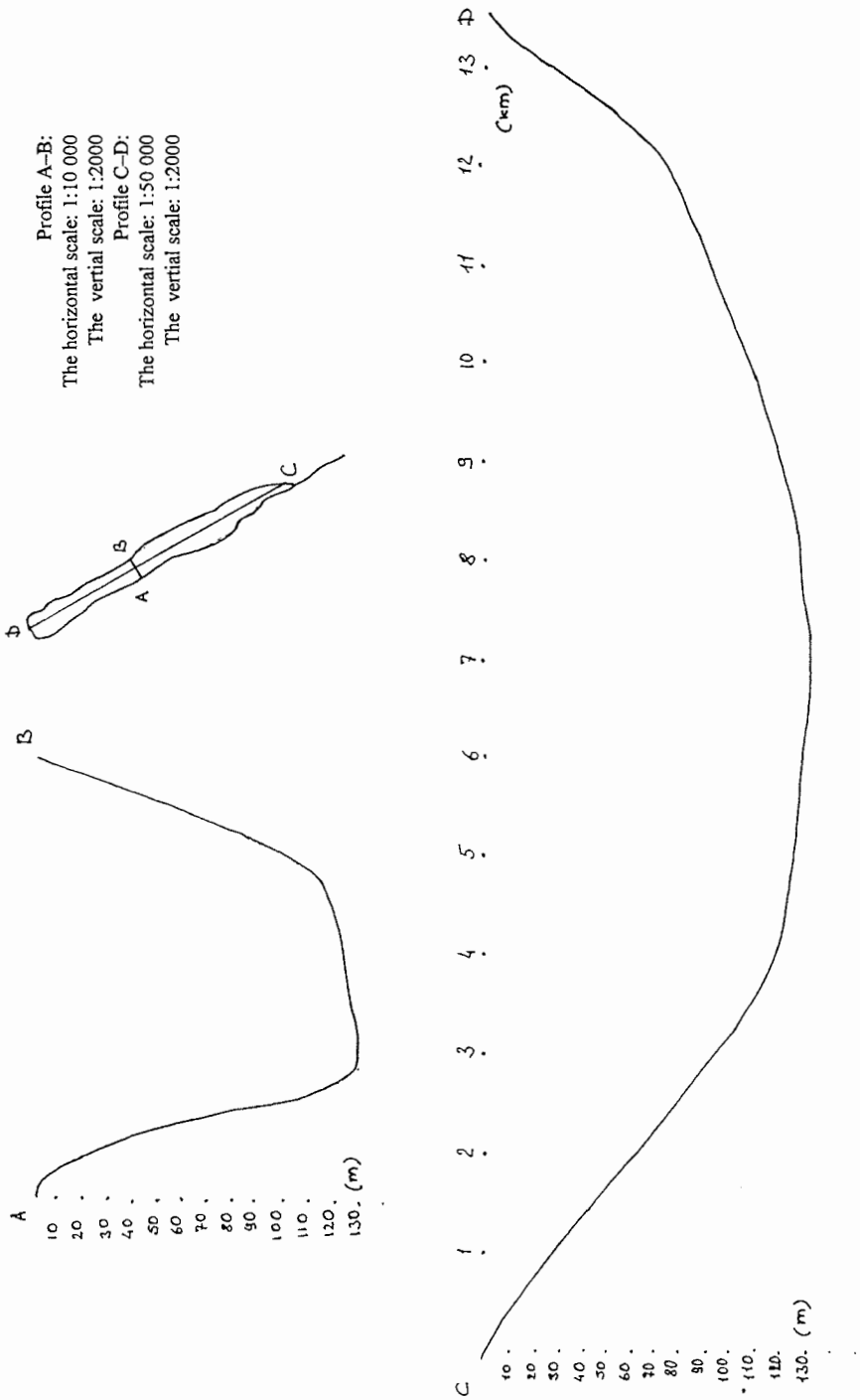

Fig. 11: Sections AB and CD through the basin of Lake Bol'shoe Shchuch'e

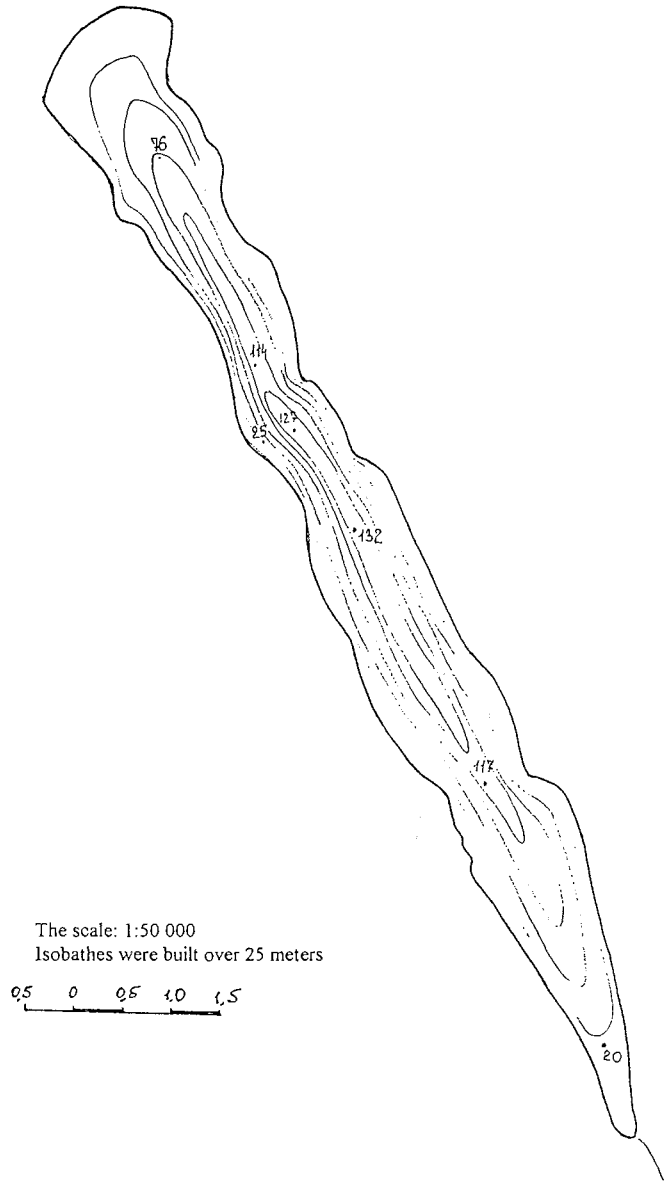

Fig. 12: Bathymetric map of Lake Bol'shoe Shchuch'e

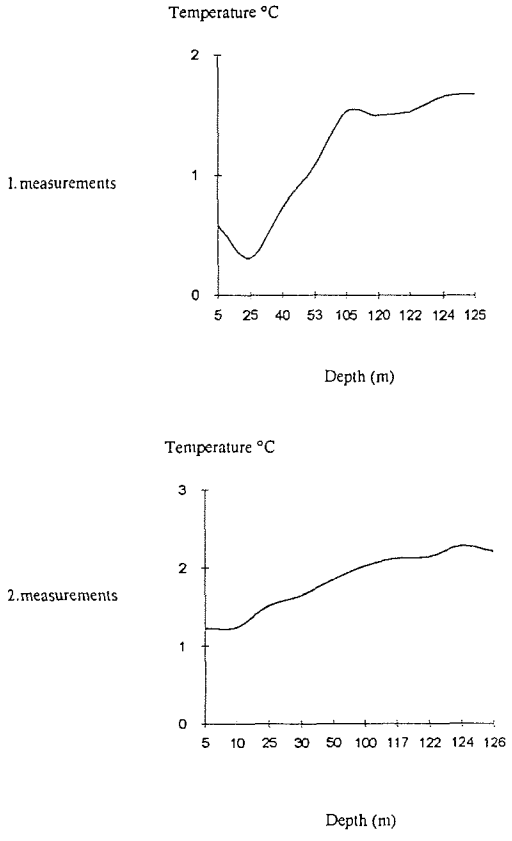

Fig. 13: Water temperature profile, Lake Bol'shoe Shchuch'e (April, 21, 1999)

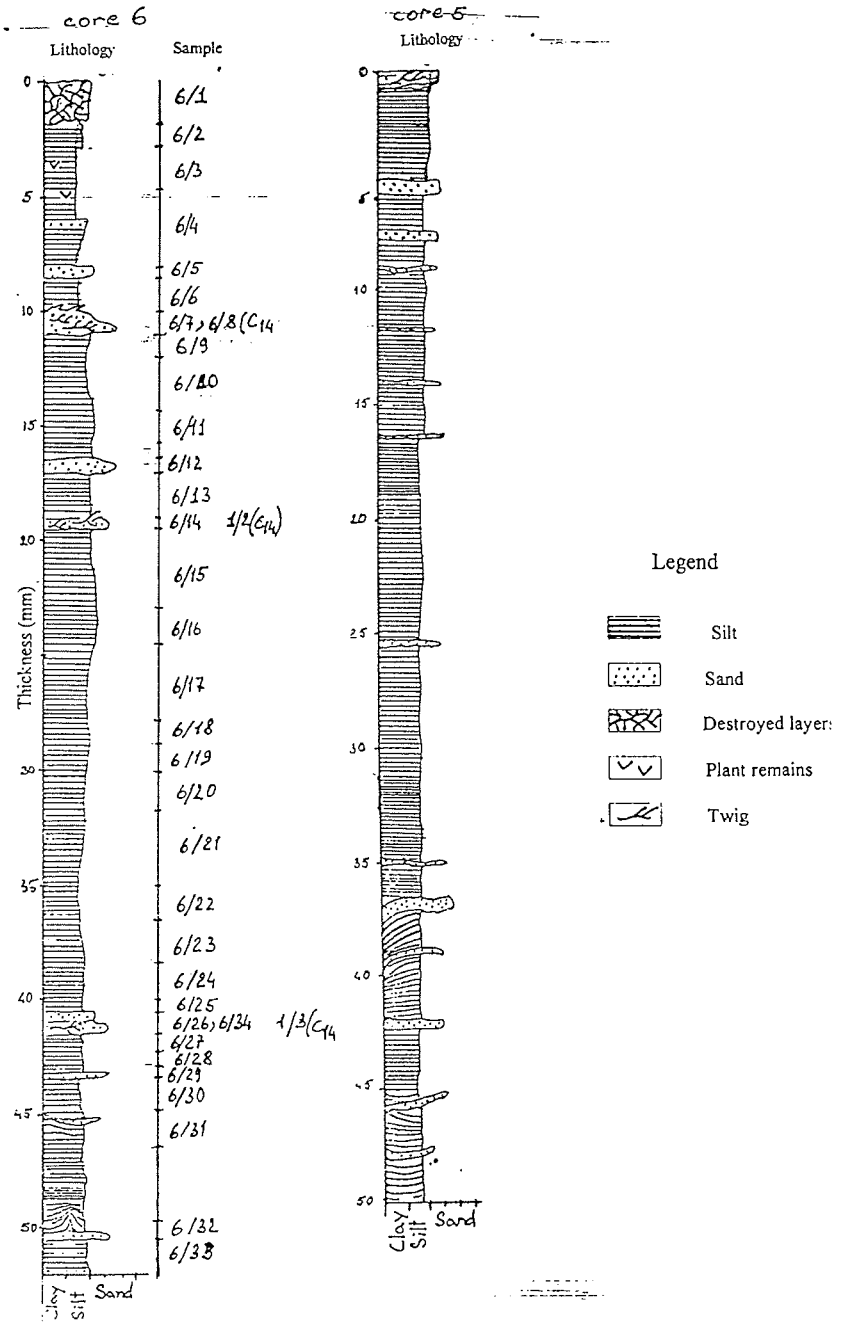

Fig. 14: Lake Bol'shoe Shchuch'e, bottom sediment sequences and subsamples (cores 5/right side , core 6/left side).

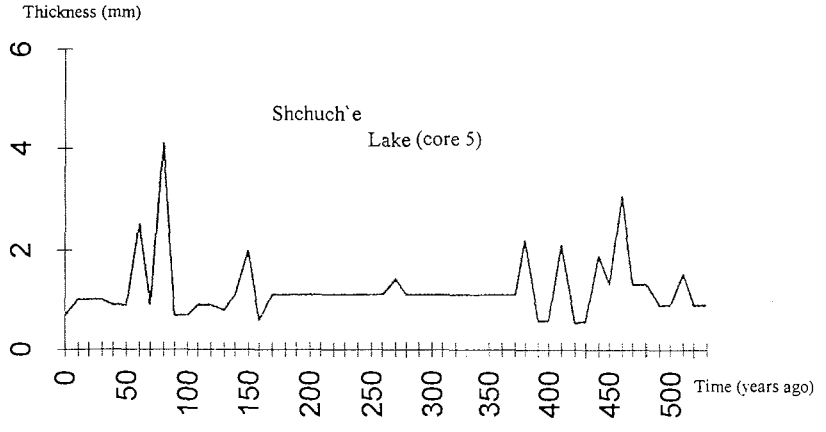

Fig. 15: Sedimentation rates, Lake Bol'shoe Shchuch'e, core 5.

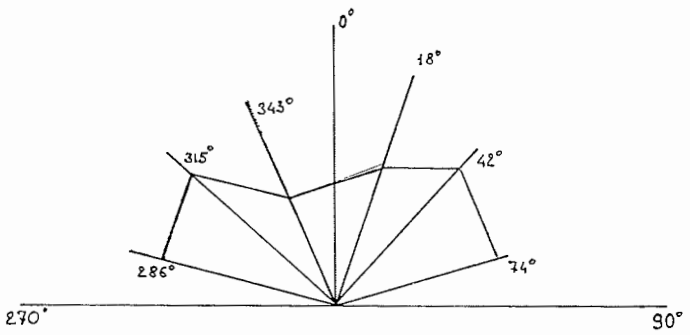

Fig. 16: Rose-diagramm of lineaments in the area of Lake Bol'shoe Shchuch'e

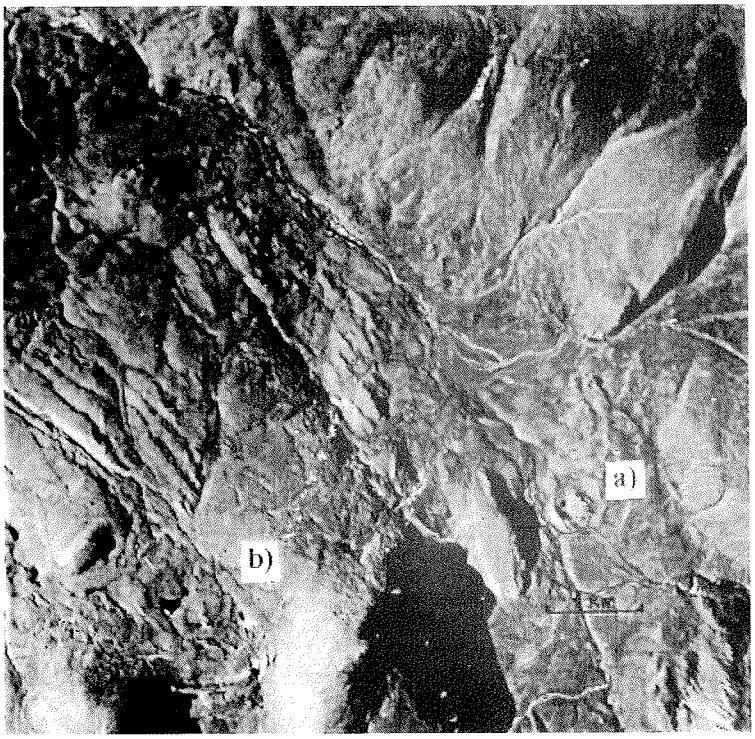

Fig. 17: Air-photograph (N - top) of the northwestern slope of the Polar Urals with morainic features discussed in the text.

Folgende Hefte der Reihe „Berichte zur Polarforschung“ sind bisher erschienen:

* **Sonderheft Nr. 1/1981** – „Die Antarktis und ihr Lebensraum“
Eine Einführung für Besucher – Herausgegeben im Auftrag von SCAR
* **Heft Nr. 1/1982** – „Die Filchner-Schelfeis-Expedition 1980/81“
zusammengestellt von Heinz Kohnen
* **Heft Nr. 2/1982** – „Deutsche Antarktis-Expedition 1980/81 mit FS „Meteor“
First International BIOMASS Experiment (FIBEX) – Liste der Zooplankton- und Mikronektonnetzfänge
zusammengestellt von Norbert Klages
* **Heft Nr. 3/1982** – „Digitale und analoge Krill-Echolot-Rohdatenerfassung an Bord des Forschungsschiffes ‚Meteor‘“ (im Rahmen von FIBEX 1980/81, Fahrtabschnitt ANT III), von Bodo Morgenstern

Heft Nr. 4/1982 – „Filchner-Schelfeis-Expedition 1980/81“
Liste der Planktonfänge und Lichtstärkemessungen
zusammengestellt von Gerd Hubold und H. Eberhard Drescher
* **Heft Nr. 5/1982** – “Joint Biological Expedition on RRS ‘John Biscoe’, February 1982“
by G. Hempel and R. B. Heywood
* **Heft Nr. 6/1982** – „Antarktis-Expedition 1981/82 (Unternehmen ‚Eiswarte‘)“
zusammengestellt von Gode Gravenhorst

Heft Nr. 7/1982 – „Marin-Biologisches Begleitprogramm zur Standorterkundung 1979/80 mit MS ‚Polarsirkel‘ (Pre-Site Survey)“ – Stationslisten der Mikronekton- und Zooplanktonfänge sowie der Bodenfischerei
zusammengestellt von R. Schneppenheim

Heft Nr. 8/1983 – “The Post-Fibex Data Interpretation Workshop“
by D. L. Cram and J.-C. Freytag with the collaboration of J. W. Schmidt, M. Mall, R. Kresse, T. Schwinghammer
* **Heft Nr. 9/1983** – “Distribution of some groups of zooplankton in the inner Weddell Sea in summer 1979/80“
by I. Hempel, G. Hubold, B. Kaczmaruk, R. Keller, R. Weigmann-Haass

Heft Nr. 10/1983 – „Fluor im antarktischen Ökosystem“ – DFG-Symposium November 1982
zusammengestellt von Dieter Adelung

Heft Nr. 11/1983 – “Joint Biological Expedition on RRS ‘John Biscoe’, February 1982 (II)“
Data of micronecton and zooplankton hauls, by Uwe Piatkowski

Heft Nr. 12/1983 – „Das biologische Programm der ANTARKTIS-I-Expedition 1983 mit FS ‚Polarstern‘“
Stationslisten der Plankton-, Benthos- und Grundschleppnetzfänge und Liste der Probennahme an Robben und Vögeln, von H. E. Drescher, G. Hubold, U. Piatkowski, J. Plötz und J. Voß
* **Heft Nr. 13/1983** – „Die Antarktis-Expedition von MS ‚Polarbjörn‘ 1982/83“ (Sommerkampagne zur Atka-Bucht und zu den Kraul-Bergen), zusammengestellt von Heinz Kohnen
* **Sonderheft Nr. 2/1983** – „Die erste Antarktis-Expedition von FS ‚Polarstern‘ (Kapstadt, 20. Januar 1983 – Rio de Janeiro, 25. März 1983)“, Bericht des Fahrtleiters Prof. Dr. Gotthilf Hempel

Sonderheft Nr. 3/1983 – „Sicherheit und Überleben bei Polarexpeditionen“
zusammengestellt von Heinz Kohnen
* **Heft Nr. 14/1983** – „Die erste Antarktis-Expedition (ANTARKTIS I) von FS ‚Polarstern‘ 1982/83“
herausgegeben von Gotthilf Hempel

Sonderheft Nr. 4/1983 – “On the Biology of Krill *Euphausia superba*“ – Proceedings of the Seminar and Report of the Krill Ecology Group, Bremerhaven 12. - 16. May 1983, edited by S. B. Schnack

Heft Nr. 15/1983 – “German Antarctic Expedition 1980/81 with FRV ‘Walther Herwig’ and RV ‘Meteor’“ – First International BIOMASS Experiment (FIBEX) – Data of micronekton and zooplankton hauls
by Uwe Piatkowski and Norbert Klages

Sonderheft Nr. 5/1984 – “The observatories of the Georg von Neumayer Station“, by Ernst Augstein

Heft Nr. 16/1984 – “FIBEX cruise zooplankton data“
by U. Piatkowski, I. Hempel and S. Rakusa-Suszczewski
* **Heft Nr. 17/1984** – Fahrtbericht (cruise report) der ‚Polarstern‘-Reise ARKTIS I, 1983“
von E. Augstein, G. Hempel und J. Thiede

Heft Nr. 18/1984 – „Die Expedition ANTARKTIS II mit FS ‚Polarstern‘ 1983/84“,
Bericht von den Fahrtabschnitten 1, 2 und 3, herausgegeben von D. Fütterer

Heft Nr. 19/1984 – „Die Expedition ANTARKTIS II mit FS ‚Polarstern‘ 1983/84“,
Bericht vom Fahrtabschnitt 4, Punta Arenas-Kapstadt (Ant-II/4), herausgegeben von H. Kohnen

Heft Nr. 20/1984 – „Die Expedition ARKTIS II des FS ‚Polarstern‘ 1984, mit Beiträgen des FS ‚Valdivia‘ und des Forschungsflugzeuges ‚Falcon 20‘ zum Marginal Ice Zone Experiment 1984 (MIZEX)“
von E. Augstein, G. Hempel, J. Schwarz, J. Thiede und W. Weigel

Heft Nr. 21/1985 – “Euphausiid larvae in plankton from the vicinity of the Antarctic Penisula, February 1982“ by Sigrid Marschall and Elke Mizdalski

Heft Nr. 22/1985 – “Maps of the geographical distribution of macrozooplankton in the Atlantic sector of the Southern Ocean“ by Uwe Piatkowski

Heft Nr. 23/1985 – „Untersuchungen zur Funktionsmorphologie und Nahrungsaufnahme der Larven des Antarktischen Krills *Euphausia superba* Dana“ von Hans-Peter Marschall

Heft Nr. 24/1985 – „Untersuchungen zum Periglazial auf der König-Georg-Insel Südshetlandinseln/ Antarktika. Deutsche physiogeographische Forschungen in der Antarktis. – Bericht über die Kampagne 1983/84" von Dietrich Barsch, Wolf-Dieter Blümel, Wolfgang Flügel, Roland Mäusbacher, Gerhard Stäblein, Wolfgang Zick

* **Heft Nr. 25/1985** – „Die Expedition ANTARKTIS III mit FS ‚Polarstern' 1984/1985" herausgegeben von Gotthilf Hempel.

* **Heft Nr. 26/1985** – "The Southern Ocean"; A survey of oceanographic and marine meteorological research work by Hellmer et al.

* **Heft Nr. 27/1986** – „Spätpleistozäne Sedimentationsprozesse am antarktischen Kontinentalhang vor Kapp Norvegia, östliche Weddell-See" von Hannes Grobe

Heft Nr. 28/1986 – „Die Expedition ARKTIS III mit ‚Polarstern' 1985 mit Beiträgen der Fahrtteilnehmer, herausgegeben von Rainer Gersonde

* **Heft Nr. 29/1986** – „5 Jahre Schwerpunktprogramm ‚Antarktisforschung' der Deutschen Forschungsgemeisnchaft." Rückblick und Ausblick. Zusammengestellt von Gotthilf Hempel, Sprecher des Schwerpunktprogramms

Heft Nr. 30/1986 – "The Meteorological Data of the Georg-von-Neumayer-Station for 1981 and 1982" by Marianne Gube and Friedrich Obleitner

* **Heft Nr. 31/1986** – „Zur Biologie der Jugendstadien der Notothenioidei (Pisces) an der Antarktischen Halbinsel" von A. Kellermann

* **Heft Nr. 32/1986** – „Die Expedition ANTARKTIS IV mit FS ‚Polarstern' 1985/86" mit Beiträgen der Fahrtteilnehmer, herausgegeben von Dieter Fütterer

Heft Nr. 33/1987 – „Die Expedition ANTARKTIS-IV mit FS ‚Polarstern' 1985/86 – Bericht zu den Fahrtabschnitten ANT-IV/3-4" von Dieter Karl Fütterer

Heft Nr. 34/1987 – „Zoogeographische Untersuchungen und Gemeinschaftsanalysen an antarktischen Makroplankton" von U. Piatkowski

Heft Nr. 35/1987 – „Zur Verbreitung des Meso- und Makrozooplanktons in Oberflächenwasser der Weddell See (Antarktis)" von E. Boysen-Ennen

Heft Nr. 36/1987 – „Zur Nahrungs- und Bewegungsphysiologie von *Salpa thompsoni* und *Salpa fusiformis*" von M. Reinke

Heft Nr. 37/1987 – "The Eastern Weddell Sea Drifting Buoy Data Set of the Winter Weddell Sea Project (WWSP)" 1986 by Heinrich Hoeber und Marianne Gube-Lehnhardt

Heft Nr. 38/1987 – "The Meteorological Data of the Georg von Neumayer Station for 1983 and 1984" by M. Gube-Lenhardt

Heft Nr. 39/1987 – „Die Winter-Expedition mit FS ‚Polarstern' in die Antarktis (ANT V/1-3)" herausgegeben von Sigrid Schnack-Schiel

Heft Nr. 40/1987 – "Weather and Synoptic Situation during Winter Weddell Sea Project 1986 (ANT V/2) July 16 - September 10, 1986" by Werner Rabe

Heft Nr. 41/1988 – „Zur Verbreitung und Ökologie der Seegurken im Weddellmeer (Antarktis)" von Julian Gutt

Heft Nr. 42/1988 – "The zooplankton community in the deep bathyal and abyssal zones of the eastern North Atlantic" by Werner Beckmann

* **Heft Nr. 43/1988** – "Scientific cruise report of Arctic Expedition ARK IV/3" Wissenschaftlicher Fahrtbericht der Arktis-Expedition ARK IV/3, compiled by Jörn Thiede

* **Heft Nr. 44/1988** – "Data Report for FV 'Polarstern' Cruise ARK IV/1, 1987 to the Arctic and Polar Fronts" by Hans-Jürgen Hirche

Heft Nr. 45/1988 – „Zoogeographie und Gemeinschaftsanalyse des Makrozoobenthos des Weddellmeeres (Antarktis)" von Joachim Voß

Heft Nr. 46/1988 – "Meteorological and Oceanographic Data of the Winter-Weddell-Sea Project 1986 (ANT V/3)" by Eberhard Fahrbach

Heft Nr. 47/1988 – „Verteilung und Herkunft glazial-mariner Gerölle am Antarktischen Kontinentalrand des östlichen Weddellmeeres" von Wolfgang Oskierski

Heft Nr. 48/1988 – „Variationen des Erdmagnetfeldes an der GvN-Station" von Arnold Brodscholl

* **Heft Nr. 49/1988** – „Zur Bedeutung der Lipide im antarktischen Zooplankton" von Wilhelm Hagen

* **Heft Nr. 50/1988** – „Die gezeitenbedingte Dynamik des Ekström-Schelfeises, Antarktis" von Wolfgang Kobarg

Heft Nr. 51/1988 – „Ökomorphologie notothenliider Fische aus dem Weddellmeer, Antarktis" von Werner Ekau

Heft Nr. 52/1988 – „Zusammensetzung der Bodenfauna in der westlichen Fram-Straße" von Dieter Piepenburg

* **Heft Nr. 53/1988** – „Untersuchungen zur Ökologie des Phytoplanktons im südöstlichen Weddellmeer (Antarktis) im Jan./Febr. 1985" von Eva-Maria Nöthig

Heft Nr. 54/1988 – „Die Fischfauna des östlichen und südlichen Weddellmeeres: geographische Verbreitung, Nahrung und trophische Stellung der Fischarten" von Wiebke Schwarzbach

Heft Nr. 55/1988 – "Weight and length data of zooplankton in the Weddell Sea in austral spring 1986 (Ant. V/3)" by Elke Mizdalski

Heft Nr. 56/1989 – "Scientific cruise report of Arctic expeditions ARK IV/1, 2 & 3" by G. Krause, J. Meinke und J. Thiede

Heft Nr. 57/1989 – „Die Expedition ANTARKTIS V mit FS ‚Polarstern' 1986/87"
Bericht von den Fahrtabschnitten ANT V/4-5 von H. Miller und H. Oerter

* **Heft Nr. 58/1989** – „Die Expedition ANTARKTIS VI mit FS ‚Polarstern' 1987/88"
von D. K. Fütterer

Heft Nr. 59/1989 – „Die Expedition ARKTIS V/1a, 1b und 2 mit FS ‚Polarstern' 1988"
von M. Spindler

Heft Nr. 60/1989 – „Ein zweidimensionales Modell zur thermohalinen Zirkulation unter dem Schelfeis"
von H. H. Hellmer

Heft Nr. 61/1989 – "Die Vulkanite im westlichen und mittleren Neuschwabenland,
Vestfjella und Ahlmannryggen, Antarktika" von M. Peters

* **Heft Nr. 62/1989** – "The Expedition ANTARKTIS VII/1 and 2 (EPOS I) of RV 'Polarstern'
in 1988/89", by I. Hempel

Heft Nr. 63/1989 – „Die Eisalgenflora des Weddellmeeres (Antarktis): Artenzusammensetzung und Biomasse
sowie Ökophysiologie ausgewählter Arten" von Annette Bartsch

Heft Nr. 64/1989 – "Meteorological Data of the G.-v.-Neumayer-Station (Antarctica)" by L. Helmes

Heft Nr. 65/1989 – "Expedition Antarktis VII/3 in 1988/89" by I. Hempel, P. H. Schalk, V. Smetacek

Heft Nr. 66/1989 – „Geomorphologisch-glaziologische Detailkartierung
des arid-hochpolaren Borgmassivet, Neuschwabenland, Antarktika" von Karsten Brunk

Heft Nr. 67/1990 – "Identification key and catalogue of larval Antarctic fishes",
edited by Adolf Kellermann

Heft Nr. 68/1990 – "The Expedition Antarktis VII/4 (Epos leg 3) and VII/5 of RV 'Polarstern' in 1989",
edited by W. Arntz, W. Ernst, I. Hempel

Heft Nr. 69/1990 – „Abhängigkeiten elastischer und rheologischer Eigenschaften des Meereises vom
Eisgefüge", von Harald Hellmann

* **Heft Nr. 70/1990** – „Die beschalten benthischen Mollusken (Gastropoda und Bivalvia) des
Weddellmeeres, Antarktis", von Stefan Hain

Heft Nr. 71/1990 – „Sedimentologie und Paläomagnetik an Sedimenten der Maudkuppe (Nordöstliches
Weddellmeer)", von Dieter Cordes

Heft Nr. 72/1990 – "Distribution and abundance of planktonic copepods (Crustacea) in the Weddell Sea
in summer 1980/81", by F. Kurbjeweit and S. Ali-Khan

Heft Nr. 73/1990 – „Zur Frühdiagenese von organischem Kohlenstoff und Opal in Sedimenten des südlichen
und östlichen Weddellmeeres", von M. Schlüter

Heft Nr. 74/1990 – „Expeditionen ANTARKTIS-VIII/3 und VIII/4 mit FS ‚Polarstern' 1989"
von Rainer Gersonde und Gotthilf Hempel

Heft Nr. 75/1991 – „Quartäre Sedimentationsprozesse am Kontinentalhang des Süd-Orkey-Plateaus im
nordwestlichen Weddellmeer (Antarktis)", von Sigrun Grünig

Heft Nr. 76/1990 – „Ergebnisse der faunistischen Arbeiten im Benthal von King George Island
(Südshetlandinseln, Antarktis)", von Martin Rauschert

Heft Nr. 77/1990 – „Verteilung von Mikroplankton-Organismen nordwestlich der Antarktischen Halbinsel
unter dem Einfluß sich ändernder Umweltbedingungen im Herbst", von Heinz Klöser

Heft Nr. 78/1991 – „Hochauflösende Magnetostratigraphie spätquartärer Sedimente arktischer
Meeresgebiete", von Norbert R. Nowaczyk

Heft Nr. 79/1991 – „Ökophysiologische Untersuchungen zur Salinitäts- und Temperaturtoleranz
antarktischer Grünalgen unter besonderer Berücksichtigung des β-Dimethylsulfoniumpropionat
(DMSP) - Stoffwechsels", von Ulf Karsten

Heft Nr. 80/1991 – „Die Expedition ARKTIS VII/1 mit FS ‚Polarstern' 1990",
herausgegeben von Jörn Thiede und Gotthilf Hempel

Heft Nr. 81/1991 – „Paläoglaziologie und Paläozeanographie im Spätquartär am Kontinentalrand des
südlichen Weddelmeeres, Antarktis", von Martin Melles

Heft Nr. 82/1991 – „Quantifizierung von Meereseigenschaften: Automatische Bildanalyse von
Dünnschnitten und Parametisierung von Chlorophyll- und Salzgehaltsverteilungen", von Hajo Eicken

Heft Nr. 83/1991 – „Das Fließen von Schelfeisen - numerische Simulationen
mit der Metholde der finiten Differenzen", von Jürgen Determann

Heft Nr. 84/1991 – „Die Expedition ANTARKTIS-VIII/1-2, 1989 mit der Winter Weddell Gyre Study
der Forschungsschiffe ‚Polarstern' und ‚Akademik Fedorov'", von Ernst Augstein,
Nikolai Bagriantsev und Hans Werner Schenke

Heft Nr. 85/1991 – „Zur Entstehung von Unterwassereis und das Wachstum und die Energiebilanz
des Meereises in der Atka Bucht, Antarktis", von Josef Kipfstuhl

* **Heft Nr. 86/1991** – „Die Expedition ANTARKTIS-VIII mit FS ‚Polarstern' 1989/90. Bericht vom
Fahrtabschnitt ANT-VIII/5", von Heinz Miller und Hans Oerter

Heft Nr. 87/1991 – "Scientific cruise reports of Arctic expeditions ARK VI/1-4 of RV 'Polarstern'
in 1989", edited by G. Krause, J. Meincke & H. J. Schwarz

Heft Nr. 88/1991 – „Zur Lebensgeschichte dominanter Copepodenarten (*Calanus finmarchicus,
C. glacialis, C. hyperboreus, Metridia longa*) in der Framstraße", von Sabine Diel

Heft Nr. 89/1991 – „Detaillierte seismische Untersuchungen am östlichen Kontinentalrand des Weddell-Meeres vor Kapp Norvegia, Antarktis", von Norbert E. Kaul

Heft Nr. 90/1991 – „Die Expedition ANTARKTIS-VIII mit FS ‚Polarstern' 1989/90. Bericht von den Fahrtabschnitten ANT-VIII/6-7", herausgegeben von Dieter Karl Fütterer und Otto Schrems

Heft Nr. 91/1991 – "Blood physiology and ecological consequences in Weddell Sea fishes (Antarctica)", by Andreas Kunzmann

Heft Nr. 92/1991 – „Zur sommerlichen Verteilung des Mesozooplanktons im Nansen-Becken, Nordpolarmeer", von Nicolai Mumm

Heft Nr. 93/1991 – „Die Expedition ARKTIS VII mit FS ‚Polarstern', 1990. Bericht vom Fahrtabschnitt ARK VII/2", herausgegeben von Gunther Krause

Heft Nr. 94/1991 – „Die Entwicklung des Phytoplanktons im östlichen Weddellmeer (Antarktis) beim Übergang vom Spätwinter zum Frühjahr", von Renate Scharek

Heft Nr. 95/1991 – „Radioisotopenstratigraphie, Sedimentologie und Geochemie jungquartärer Sedimente des östlichen Arktischen Ozeans", von Horst Bohrmann

Heft Nr. 96/1991 – „Holozäne Sedimentationsentwicklung im Scoresby Sund, Ost-Grönland", von Peter Marienfeld

Heft Nr. 97/1991 – „Strukturelle Entwicklung und Abkühlungsgeschichte von Heimefrontfjella (Westliches Dronning Maud Land/Antarktika)", von Joachim Jacobs

Heft Nr. 98/1991 – „Zur Besiedlungsgeschichte des antarktischen Schelfes am Beispiel der Isopoda (Crustacea, Malacostraca)", von Angelika Brandt

* **Heft Nr. 99/1992** – "The Antarctic ice sheet and environmental change: a three-dimensional modelling study", by Philippe Huybrechts

* **Heft Nr. 100/1992** – „Die Expeditionen ANTARKTIS IX/1-4 des Forschungsschiffes ‚Polarstern' 1990/91" herausgegeben von Ulrich Bathmann, Meinhard Schulz-Baldes, Eberhard Fahrbach, Victor Smetacek und Hans-Wolfgang Hubberten

Heft Nr. 101/1992 – „Wechselbeziehungen zwischen Schwermetallkonzentrationen (Cd, Cu, Pb, Zn) im Meerwasser und in Zooplanktonorganismen (Copepoda) der Arktis und des Atlantiks", von Christa Pohl

Heft Nr. 102/1992 – „Physiologie und Ultrastruktur der antarktischen Grünalge *Prasiola crispa ssp. antarctica* unter osmotischem Streß und Austrocknung", von Andreas Jacob

* **Heft Nr. 103/1992** – „Zur Ökologie der Fische im Weddellmeer", von Gerd Hubold

Heft Nr. 104/1992 – „Mehrkanalige adaptive Filter für die Unterdrückung von multiplen Reflexionen in Verbindung mit der freien Oberfläche in marinen Seismogrammen", von Andreas Rosenberger

Heft Nr. 105/1992 – "Radiation and Eddy Flux Experiment 1991 *(REFLEX I)*", von Jörg Hartmann, Christoph Kottmeier und Christian Wamser

Heft Nr. 106/1992 – „Ostracoden im Epipelagial vor der Antarktischen Halbinsel - ein Beitrag zur Systematik sowie zur Verbreitung und Populationsstruktur unter Berücksichtigung der Saisonalität", von Rüdiger Kock

* **Heft Nr. 107/1992** – „ARCTIC '91: Die Expedition ARK-VIII/3 mit FS ‚Polarstern' 1991", von Dieter K. Fütterer

Heft Nr. 108/1992 – „Dehnungsbeben an einer Störungszone im Ekström-Schelfeis nördlich der Georg-von-Neumayer-Station, Antarktis. – Eine Untersuchung mit seismologischen und geodätischen Methoden", von Uwe Nixdorf.

* **Heft Nr. 109/1992** – „Spätquartäre Sedimentation am Kontinentalrand des südöstlichen Weddellmeeres, Antarktis", von Michael Weber.

* **Heft Nr. 110/1992** – „Sedimentfazies und Bodenwasserstrom am Kontinentalhang des nordwestlichen Weddellmeeres", von Isa Brehme.

Heft Nr. 111/1992 – „Die Lebensbedingungen in den Solekanälchen des antarktischen Meereises", von Jürgen Weissenberger.

Heft Nr. 112/1992 – „Zur Taxonomie von rezenten benthischen Foraminiferen aus dem Nansen Becken, Arktischer Ozean", von Jutta Wollenburg.

Heft Nr. 113/1992 – „Die Expedition ARKTIS VIII/1 mit FS ‚Polarstern' 1991", herausgegeben von Gerhard Kattner.

* **Heft Nr. 114/1992** – „Die Gründungsphase deutscher Polarforschung, 1865 - 1875", von Reinhard A. Krause.

Heft Nr. 115/1992 – "Scientific Cruise Report of the 1991 Arctic Expedition ARK VIII/2 of RV 'Polarstern' (EPOS II)", by Eike Rachor.

Heft Nr. 116/1992 – "The Meteorological Data of the Georg-von-Neumayer-Station (Antarctica) for 1988, 1989, 1990 and 1991", by Gert König-Langlo.

Heft Nr. 117/1992 – „Petrogenese des metamorphen Grundgebirges der zentralen Heimefrontfjella (westliches Dronning Maud Land / Antarktis)", von Peter Schulze.

Heft Nr. 118/1993 – „Die mafischen Gänge der Shackleton Range / Antarktika: Petrographie, Geochemie, Isotopengeochemie und Paläomagnetik", von Rüdiger Hotten.

* **Heft Nr. 119/1993** – „Gefrierschutz bei Fischen der Polarmeere", von Andreas P. A. Wöhrmann.

* **Heft Nr. 120/1993** – "East Siberian Arctic Region Expedition '92: The Laptev Sea - its Significance for Arctic Sea-Ice Formation and Transpolar Sediment Flux", by D. Dethleff, D. Nürnberg, E. Reimnitz, M. Saarso and Y. P. Sacchenko. – "Expedition to Novaja Zemlja and Franz Josef Land with RV. 'Dalnie Zelentsy'", by D. Nürnberg and E. Groth.

* **Heft Nr. 121/1993** – „Die Expedition ANTARKTIS X/3 mit FS ‚Polarstern' 1992", herausgegeben von Michael Spindler, Gerhard Dieckmann und David Thomas

Heft Nr. 122/1993 – „Die Beschreibung der Korngestalt mit Hilfe der Fourier-Analyse: Parametrisierung der morphologischen Eigenschaften von Sedimentpartikeln", von Michael Diepenbroek.

* **Heft Nr. 123/1993** – „Zerstörungsfreie hochauflösende Dichteuntersuchungen mariner Sedimente", von Sebastian Gerland.

Heft Nr. 124/1993 – „Umsatz und Verteilung von Lipiden in arktischen marinen Organismen unter besonderer Berücksichtigung unterer trophischer Stufen", von Martin Graeve.

Heft Nr. 125/1993 – „Ökologie und Respiration ausgewählter arktischer Bodenfischarten", von Christian F. von Dorrien.

Heft Nr. 126/1993 – „Quantitative Bestimmung von Paläoumweltparametern des Antarktischen Oberflächenwassers im Spätquartier anhand von Transferfunktionen mit Diatomeen", von Ulrich Zielinski

* **Heft Nr. 127/1993** – „Sedimenttransport durch das arktische Meereis: Die rezente lithogene und biogene Materialfracht", von Ingo Wollenburg.

Heft Nr. 128/1993 – "Cruise ANTARKTIS X/3 of RV 'Polarstern': CTD-Report", von Marek Zwierz.

Heft Nr. 129/1993 – „Reproduktion und Lebenszyklen dominanter Copepodenarten aus dem Weddellmeer, Antarktis", von Frank Kurbjeweit

Heft Nr. 130/1993 – „Untersuchungen zu Temperaturregime und Massenhaushalt des Filchner-Ronne-Schelfeises, Antarktis, unter besonderer Berücksichtigung von Anfrier- und Abschmelzprozessen", von Klaus Grosfeld

Heft Nr. 131/1993 – „Die Expedition ANTARKTIS X/5 mit FS ‚Polarstern' 1992", herausgegeben von Rainer Gersonde

Heft Nr. 132/1993 – „Bildung und Abgabe kurzkettiger halogenierter Kohlenwasserstoffe durch Makroalgen der Polarregionen", von Frank Laturnus

Heft Nr. 133/1994 – "Radiation and Eddy Flux Experiment 1993 *(REFLEX II)*", by Christoph Kottmeier, Jörg Hartmann, Christian Wamser, Axel Bochert, Christof Lüpkes, Dietmar Freese and Wolfgang Cohrs

* **Heft Nr. 134/1994** – "The Expedition ARKTIS-IX/1", edited by Hajo Eicken and Jens Meincke

Heft Nr. 135/1994 – „Die Expeditionen ANTARKTIS X/6-8", herausgegeben von Ulrich Bathmann, Victor Smetacek, Hein de Baar, Eberhard Fahrbach und Gunter Krause

Heft Nr. 136/1994 – „Untersuchungen zur Ernährungsökologie von Kaiserpinguinen *(Aptenodytes forsteri)* und Königspinguinen *(Aptenodytes patagonicus)*", von Klemens Pütz

• **Heft Nr. 137/1994** – „Die känozoische Vereisungsgeschichte der Antarktis", von Werner U. Ehrmann

Heft Nr. 138/1994 – „Untersuchungen stratosphärischer Aerosole vulkanischen Ursprungs und polarer stratosphärischer Wolken mit einem Mehrwellenlängen-Lidar auf Spitzbergen *(79° N, 12° E)*", von Georg Beyerle

Heft Nr. 139/1994 – „Charakterisierung der Isopodenfauna (Crustacea, Malacostraca) des Scotia-Bogens aus biogeographischer Sicht: Ein multivariater Ansatz", von Holger Winkler.

Heft Nr. 140/1994 – „Die Expedition ANTARKTIS X/4 mit FS ‚Polarstern' 1992", herausgegeben von Peter Lemke

Heft Nr. 141/1994 – „Satellitenaltimetrie über Eis – Anwendung des GEOSAT-Altimeters über dem Ekströmisen, Antarktis", von Clemens Heidland

Heft Nr. 142/1994 – "The 1993 Northeast Water Expedition. Scientific cruise report of RV 'Polartstern' Arctic cruises ARK IX/2 and 3, USCG 'Polar Bear' cruise NEWP and the NEWLand expedition", edited by Hans-Jürgen Hirche and Gerhard Kattner

Heft Nr. 143/1994 – „Detaillierte refraktionsseismische Untersuchungen im inneren Scoresby Sund Ost-Grönland", von Notker Fechner

Heft Nr. 144/1994 – "Russian-German Cooperation in the Siberian Shelf Seas: Geo-System Laptev Sea", edited by Heidemarie Kassens, Hans-Wolfgang Hubberten, Sergey M. Pryamikov and Rüdiger Stein

• **Heft Nr. 145/1994** – "The 1993 Northeast Water Expedition. Data Report of RV ‚Polarstern' Arctic Cruises IX/2 and 3", edited by Gerhard Kattner and Hans-Jürgen Hirche.

Heft Nr. 146/1994 – "Radiation Measurements at the German Antarctic Station Neumayer 1982 - 1992", by Torsten Schmidt and Gerd König-Langlo.

Heft Nr. 147/1994 – „Krustenstrukturen und Verlauf des Kontinentalrandes im Weddell-Meer / Antarktis", von Christian Hübscher.

• **Heft Nr. 148/1994** – "The expeditions NORILSK/TAYMYR 1993 and BUNGER OASIS 1993/94 of the AWI Research Unit Potsdam", edited by Martin Melles.

** **Heft Nr. 149/1994** – „Die Expedition ARCTIC '93. Der Fahrtabschnitt ARK-IX/4 mit FS ‚Polarstern' 1993", herausgegeben von Dieter K. Fütterer.

Heft Nr. 150/1994 – „Der Energiebedarf der Pygoscelis-Pinguine: eine Synopse", von Boris M. Culik.

Heft Nr. 151/1994 – "Russian-German Cooperation: The Transdrift I Expedition to the Laptev Sea", edited by Heidemarie Kassens and Valeriy Y. Karpiy.

Heft Nr. 152/1994 – „Die Expedition ANTARKTIS-X mit FS ‚Polarstern' 1992. Bericht von den Fahrtabschnitten / ANT-X / 1a und 2", herausgegeben von Heinz Miller.

Heft Nr. 153/1994 – „Aminosäuren und Huminstoffe im Stickstoffkreislauf polarer Meere", von Ulrike Hubberten.

Heft Nr. 154/1994 – "Regional and seasonal variability in the vertical distribution of mesozooplankton in the Greenland Sea", by Claudio Richter.

Heft Nr. 155/1995 – „Benthos in polaren Gewässern", herausgegeben von Christian Wiencke und Wolf Arntz.

Heft Nr. 156/1995 – "An adjoint model for the determination of the mean oceanic circulation, air-sea fluxes and mixing coefficients", by Reiner Schlitzer.

Heft Nr. 157/1995 – „Biochemische Untersuchungen zum Lipidstoffwechsel antarktischer Copepoden", von Kirsten Fahl.

** **Heft Nr. 158/1995** – „Die Deutsche Polarforschung seit der Jahrhundertwende und der Einfluß Erich von Drygalskis", von Cornelia Lüdecke.

* **Heft Nr. 159/1995** – "The distribution of $\partial^{18}O$ in the Arctic Ocean: Implications for the freshwater balance of the halocline and the sources of deep and bottom waters", by Dorothea Bauch.

* **Heft Nr. 160/1995** – „Rekonstruktion der spätquartären Tiefenwasserzirkulation und Produktivität im östlichen Südatlantik anhand von benthischen Foraminiferenvergesellschaftungen", von Gerhard Schmiedl.

Heft Nr. 161/1995 – „Der Einfluß von Salinität und Lichtintensität auf die Osmolytkonzentrationen, die Zellvolumina und die Wachstumsraten der antarktischen Eisdiatomeen *Chaetoceros sp.* und *Navicula sp.* unter besonderer Berücksichtigung der Aminosäure Prolin", von Jürgen Nothnagel.

Heft Nr. 162/1995 – „Meereistransportiertes lithogenes Feinmaterial in spätquartären Tiefseesedimenten des zentralen östlichen Arktischen Ozeans und der Framstraße", von Thomas Letzig.

Heft Nr. 163/1995 – „Die Expedition ANTARKTIS-XI/2 mit FS ‚Polarstern' 1993/94", herausgegeben von Rainer Gersonde.

Heft Nr. 164/1995 – „Regionale und altersabhängige Variation gesteinsmagnetischer Parameter in marinen Sedimenten der Arktis", von Thomas Frederichs.

Heft Nr. 165/1995 – „Vorkommen, Verteilung und Umsatz biogener organischer Spurenstoffe: Sterole in antarktischen Gewässern", von Georg Hanke.

Heft Nr. 166/1995 – „Vergleichende Untersuchungen eines optimierten dynamisch-thermodynamischen Meereismodells mit Beobachtungen im Weddellmeer", von Holger Fischer.

* **Heft Nr. 167/1995** – „Rekonstruktionen von Paläo-Umweltparametern anhand von stabilen Isotopen und Faunen-Vergesellschaftungen planktischer Foraminiferen im Südatlantik", von Hans-Stefan Niebler

Heft Nr. 168/1995 – „Die Expedition ANTARKTIS XII mit FS ‚Polarstern' 1993/94. Bericht von den Fahrtabschnitten ANT XII/1 und 2", herausgegeben von Gerhard Kattner und Dieter Karl Fütterer

Heft Nr. 169/1995 – „Medizinische Untersuchung zur Circadianrhythmik und zum Verhalten bei Überwinterern auf einer antarktischen Forschungsstation", von Hans Wortmann

Heft-Nr. 170/1995 – DFG-Kolloquium: Terrestrische Geowissenschaften -- Geologie und Geophysik der Antarktis.

Heft Nr. 171/1995 – „Strukturentwicklung und Petrogenese des metamorphen Grundgebirges der nördlichen Heimfrontfjella (westliches Dronning Maud Land/Antarktika)", von Wilfried Bauer.

Heft Nr. 172/1995 – „Die Struktur der Erdkruste im Bereich des Scoresby Sund, Ostgrönland: Ergebnisse refraktionsseismischer und gravimetrischer Untersuchungen", von Holger Mandler.

Heft Nr. 173/1995 – „Paläozoische Akkretion am paläopazifischen Kontinentalrand der Antarktis in Nordvictorialand – P-T-D-Geschichte und Deformationsmechanismen im Bowers Terrane", von Stefan Matzer.

Heft Nr. 174/1995 – "The Expedition ARKTIS-X/2 of RV 'Polarstern' in 1994", edited by Hans-W. Hubberten

Heft Nr. 175/1995 – "Russian-German Cooperation: The Expedition TAYMYR 1994", edited by Christine Siegert and Gmitry Bolshiyanov.

* **Heft Nr. 176/1995** – "Russian-German Cooperation: Laptev Sea System", edited by Heidemarie Kassens, Dieter Piepenburg, Jörn Thiede, Leonid Timokhov, Hans-Wolfgang Hubberten and Sergey M. Priamikov.

Heft Nr. 177/1995 – „Organischer Kohlenstoff in spätquartären Sedimenten des Arktischen Ozeans: Terrigener Eintrag und marine Produktivität", von Carsten J. Schubert

Heft Nr. 178/1995 – "Cruise ANTARKTIS XII/4 of RV 'Polarstern' in 1995: CTD-Report", by Jüri Sildam.

Heft Nr. 179/1995 – „Benthische Foraminiferenfaunen als Wassermassen-, Produktions- und Eisdriftanzeiger im Arktischen Ozean", von Jutta Wollenburg.

Heft Nr. 180/1995 – „Biogenopal und biogenes Barium als Indikatoren für spätquartäre Produktivitätsänderungen am antarktischen Kontinentalhang, atlantischer Sektor", von Wolfgang J. Bonn.

Heft Nr. 181/1995 – „Die Expedition ARKTIS X/1 des Forschungsschiffes ‚Polarstern' 1994", herausgegeben von Eberhard Fahrbach.

Heft Nr. 182/1995 – "Laptev Sea System: Expeditions in 1994", edited by Heidemarie Kassens.

Heft Nr. 183/1996 – „Interpretation digitaler Parasound Echolotaufzeichnungen im östlichen Arktischen Ozean auf der Grundlage physikalischer Sedimenteigenschaften", von Uwe Bergmann.

Heft Nr. 184/1996 – "Distribution and dynamics of inorganic nitrogen compounds in the troposphere of continental, coastal, marine and Arctic areas", by Maria Dolores Andrés Hernández.

Heft Nr. 185/1996 – „Verbreitung und Lebensweise der Aphroditen und Polynoiden (Polychaeta) im östlichen Weddellmeer und im Lazarevmeer (Antarktis)", von Michael Stiller.

Heft Nr. 186/1996 – "Reconstruction of Late Quaternary environmental conditions applying the natural radionuclides ^{230}Th, ^{10}Be, ^{231}Pa and ^{238}U: A study of deep-sea sediments from the eastern sector of the Antarctic Circumpolar Current System", by Martin Frank.

Heft Nr. 187/1996 – "The Meteorological Data of the Neumayer Station (Antarctica) for 1992, 1993 and 1994", by Gert König-Langlo and Andreas Herber.

Heft Nr. 188/1996 – „Die Expedition ANTARKTIS-XI/3 mit FS ‚Polarstern' 1994", herausgegeben von Heinz Miller und Hannes Grobe.

Heft Nr. 189/1996 – „Die Expedition ARKTIS-VII/3 mit FS ‚Polarstern' 1990", herausgegeben von Heinz Miller und Hannes Grobe

Heft Nr. 190/1996 – "Cruise report of the Joint Chilean-German-Italian Magellan ‚Victor Hensen' Campaign in 1994", edited by Wolf Arntz and Matthias Gorny.

Heft Nr. 191/1996 – „Leitfähigkeits- und Dichtemessung an Eisbohrkernen", von Frank Wilhelms.

Heft Nr. 192/1996 – „Photosynthese-Charakteristika und Lebensstrategie antarktischer Makroalgen", von Gabriele Weykam.

Heft Nr. 193/1996 – „Heterogene Reaktionen von N_2O_5 und Hbr und ihr Einfluß auf den Ozonabbau in der polaren Stratosphäre", von Sabine Seisel.

Heft Nr. 194/1996 – „Ökologie und Populationsdynamik antarktischer Ophiuroiden (Echinodermata)", von Corinna Dahm.

Heft Nr. 195/1996 – „Die planktische Foraminifere *Neogloboquadrina pachyderma* (Ehrenberg) im Weddellmeer, Antarktis", von Doris Berberich.

Heft Nr. 196/1996 – „Untersuchungen zum Beitrag chemischer und dynamischer Prozesse zur Variabilität des stratosphärischen Ozons über der Arktis", von Birgit Heese

Heft Nr. 197/1996 – "The Expedition ARKTIS-XI/2 of 'Polarstern' in 1995", edited by Gunther Krause.

Heft Nr. 198/1996 – „Geodynamik des Westantarktischen Riftsystems basierend auf Apatit-Spaltspuranalysen", von Frank Lisker.

Heft Nr. 199/1996 – "The 1993 Northeast Water Expedition. Data Report on CTD Measurements of RV 'Polarstern' Cruises ARKTIS IX/2 and 3", by Gerion Budéus and Wolfgang Schneider.

Heft Nr. 200/1996 – "Stability of the Thermohaline Circulation in analytical and numerical models", by Gerrit Lohmann.

Heft Nr. 201/1996 – „Trophische Beziehungen zwischen Makroalgen und Herbivoren in der Potter Cove (King George-Insel, Antarktis)", von Katrin Iken.

Heft Nr. 202/1996 – „Zur Verbreitung und Respiration ökologisch wichtiger Bodentiere in den Gewässern um Svalbard (Arktis)", von Michael K. Schmid.

* **Heft Nr. 203/1996** – „Dynamik, Rauhigkeit und Alter des Meereises in der Arktis – Numerische Untersuchungen mit einem großskaligen Modell", von Markus Harder.

Heft Nr. 204/1996 – „Zur Parametrisierung der stabilen atmosphärischen Grenzschicht über einem antarktischen Schelfeis", von Dörthe Handorf.

Heft Nr. 205/1996 – "Textures and fabrics in the GRIP ice core, in relation to climate history and ice deformation", by Thorsteinn Thorsteinsson.

Heft Nr. 206/1996 – „Der Ozean als Teil des gekoppelten Klimasystems: Versuch der Rekonstruktion der glazialen Zirkulation mit verschieden komplexen Atmosphärenkomponenten", von Kerstin Fieg.

Heft Nr. 207/1996 – „Lebensstrategien dominanter antarktischer Oithonidae (Cyclopoida, Copepoda) und Oncaeidae (Poecilostomatoida, Copepoda) im Bellingshausenmeer", von Cornelia Metz.

Heft Nr. 208/1996 – „Atmosphäreneinfluß bei der Fernerkundung von Meereis mit passiven Mikrowellenradiometern", von Christoph Oelke.

Heft Nr. 209/1996 – „Klassifikation von Radarsatellitendaten zur Meereiserkennung mit Hilfe von LIne-Scanner-Messungen", von Axel Bochert.

Heft Nr. 210/1996 – „Die mit ausgewählten Schwämmen (Hexactinellida und Demospongiae) aus dem Weddellmeer, Antarktis, vergesellschaftete Fauna", von Kathrin Kunzmann.

Heft Nr. 211/1996 – "Russian-German Cooperation: The Expedition TAYMYR 1995 and the Expedition KOLYMA 1995", by Dima Yu. Bolshiyanov and Hans-W. Hubberten.

Heft Nr. 212/1996 – "Surface-sediment composition and sedimentary processes in the central Arctic Ocean and along the Eurasian Continental Margin", by Ruediger Stein, Gennadij I. Ivanov, Michael A. Levitan, and Kirsten Fahl.

Heft Nr. 213/1996 – „Gonadenentwicklung und Eiproduktion dreier *Calanus*-Arten (Copepoda): Freilandbeobachtungen, Histologie und Experimente", von Barbara Niehoff

Heft Nr. 214/1996 – „Numerische Modellierung der Übergangszone zwischen Eisschild und Eisschelf", von Christoph Mayer.

Heft Nr. 215/1996 – „Arbeiten der AWI-Forschungsstelle Potsdam in Antarktika, 1994/95", herausgegeben von Ulrich Wand.

Heft Nr. 216/1996 – „Rekonstruktion quartärer Klimaänderungen im atlantischen Sektor des Südpolarmeeres anhand von Radiolarien", von Uta Brathauer.

Heft Nr. 217/1996 – „Adaptive Semi-Lagrange-Finite-Elemente-Methode zur Lösung der Flachwassergleichungen: Implementierung und Parallelisierung", von Jörn Behrens.

Heft Nr. 218/1997 – "Radiation and Eddy Flux Experiment 1995 (REFLEX III)", by Jörg Hartmann, Axel Bochert, Dietmar Freese, Christoph Kottmeier, Dagmar Nagel and Andreas Reuter.

Heft Nr. 219/1997 – „Die Expedition ANTARKTIS-XII mit FS ‚Polarstern' 1995. Bericht vom Fahrtabschnitt ANT-XII/3, herausgegeben von Wilfried Jokat und Hans Oerter.

Heft Nr. 220/1997 – „Ein Beitrag zum Schwerefeld im Bereich des Weddellmeeres, Antarktis. Nutzung von Altimetermessungen des GEOSAT und ERS-1", von Tilo Schöne.

Heft Nr. 221/1997 – „Die Expeditionen ANTARKTIS-XIII/1-2 des Forschungsschiffes ‚Polarstern' 1995/96", herausgegeben von Ulrich Bathmann, Mike Lukas und Victor Smetacek.

Heft Nr. 222/1997 – "Tectonic Structures and Glaciomarine Sedimentation in the South-Eastern Weddell Sea from Seismic Reflection Data", by László Oszkó.

Heft Nr. 223/1997 – „Bestimmung der Meereisdicke mit seismischen und elektromagnetisch-induktiven Verfahren", von Christian Haas.

Heft Nr. 224/1997 – „Troposphärische Ozonvariationen in Polarregionen", von Silke Wessel.

Heft Nr. 225/1997 – „Biologische und ökologische Untersuchungen zur kryopelagischen Amphipodenfauna des arktischen Meereises", von Michael Poltermann.

Heft Nr. 226/1997 – "Scientific Cruise Report of the Arctic Expedition ARK-XI/1 of RV 'Polarstern' in 1995", edited by Eike Rachor.

Heft Nr. 227/1997 – „Der Einfluß kompatibler Substanzen und Kryoprotektoren auf die Enzyme Malatdehydrogenase (MDH) und Glucose-6-phosphat-Dehydrogenase (G6P-DH) aus *Acrosiphonia arcta* (Chlorophyta) der Arktis", von Katharina Kück.

Heft Nr. 228/1997 – „Die Verbreitung epibenthischer Mollusken im chilenischen Beagle-Kanal", von Katrin Linse.

Heft Nr. 229/1997 – „Das Mesozooplankton im Laptevmeer und östlichen Nansen-Becken - Verteilung und Gemeinschaftsstrukturen im Spätsommer", von Hinrich Hanssen.

Heft Nr. 230/1997 – „Modell eines adaptierbaren, rechnergestützten, wissenschaftlichen Arbeitsplatzes am Alfred-Wegener-Institut für Polar- und Meeresforschung", von Lutz-Peter Kurdelski

Heft Nr. 231/1997 – „Zur Ökologie arktischer und antarktischer Fische: Aktivität, Sinnesleistungen und Verhalten", von Christopher Zimmermann

Heft Nr. 232/1997 – „Persistente chlororganische Verbindungen in hochantarktischen Fischen", von Stephan Zimmermann

Heft Nr. 233/1997 – „Zur Ökologie des Dimethylsulfoniumpropionat (DMSP)-Gehaltes temperierter und polarer Phytoplanktongemeinschaften im Vergleich mit Laborkulturen der Coccolithophoride *Emiliania huxleyi* und der antarktischen Diatomee *Nitzschia lecointei*", von Doris Meyerdierks.

Heft Nr. 234/1997 – „Die Expedition ARCTIC '96 des FS ‚Polarstern' (ARK XIII) mit der Arctic Climate System Study (ACSYS)", von Ernst Augstein und den Fahrtteilnehmern.

Heft Nr. 235/1997 – „Polonium-210 und Blei-219 im Südpolarmeer: Natürliche Tracer für biologische und hydrographische Prozesse im Oberflächenwasser des Antarktischen Zirkumpolarstroms und des Weddellmeeres", von Jana Friedrich

Heft Nr. 236/1997 – "Determination of atmospheric trace gas amounts and corresponding natural isotopic ratios by means of ground-based FTIR spectroscopy in the high Arctic", by Arndt Meier.

Heft Nr. 237/1997 – "Russian-German Cooperation: The Expedition TAYMYR/SEVERNAYA ZEMLYA 1996", edited by Martin Melles, Birgit Hagedorn and Dmitri Yu. Bolshiyanov

Heft Nr. 238/1997 – "Life strategy and ecophysiology of Antarctic macroalgae", by Iván M. Gómez.

Heft Nr. 239/1997 – „Die Expedition ANTARKTIS XIII/4-5 des Forschungsschiffes ‚Polarstern' 1996", herausgegeben von Eberhard Fahrbach und Dieter Gerdes.

Heft Nr. 240/1997 – „Untersuchungen zur Chrom-Speziation in Meerwasser, Meereis und Schnee aus ausgewählten Gebieten der Arktis", von Heide Giese.

Heft Nr. 241/1997 – "Late Quaternary glacial history and paleoceanographic reconstructions along the East Greenland continental margin: Evidence from high-resolution records of stable isotopes and ice-rafted debris", by Seung-Il Nam.

Heft Nr. 242/1997 – "Thermal, hydrological and geochemical dynamics of the active layer at a continuous permafrost site, Taymyr Peninsula, Siberia", by Julia Boike.

Heft Nr. 243/1997 – „Zur Paläoozeanographie hoher Breiten: Stellvertreterdaten aus Foraminiferen", von Andreas Mackensen.

Heft Nr. 244/1997 – "The Geophysical Observatory at Neumayer Station, Antarctica, Geomagnetic and seismological observations in 1995 and 1996", by Alfons Eckstaller, Thomas Schmidt, Viola Graw, Christian Müller and Johannes Rogenhagen.

Heft Nr. 245/1997 – „Temperaturbedarf und Biogeographie mariner Makroalgen - Anpassung mariner Makroalgen an tiefe Temperaturen, von Bettina Bischoff-Bäsmann.

Heft Nr. 246/1997 – „Ökologische Untersuchungen zur Fauna des arktischen Meereises", von Christine Friedrich.

Heft Nr. 247/1997 – „Entstehung und Modifizierung von marinen gelösten organischen Substanzen", von Berit Kirchhoff.

Heft Nr. 248/1997 – "Laptev Sea System: Expeditions in 1995", edited by Heidemarie Kassens.

Heft Nr. 249/1997 – "The Expedition ANTARKTIS XIII/3 (EASIZ I) of RV 'Polarstern' to the eastern Weddell Sea in 1996", edited by Wolf Arntz and Julian Gutt.

Heft Nr. 250/1997 – „Vergleichende Untersuchungen zur Ökologie und Biodiversität des Mega-Epibenthos der Arktis und Antarktis", von Adreas Starmans.

Heft Nr. 251/1997 – „Zeitliche und räumliche Verteilung von Mineralvergesellschaftungen in spätquartären Sedimenten des Arktischen Ozeans und ihre Nützlichkeit als Klimaindikatoren während der Glazial/Interglazial-Wechsel", von Christoph Vogt.

Heft Nr. 252/1997 – „Solitäre Ascidien in der Potter Cove (King George Island, Antarktis). Ihre ökologische Bedeutung und Populationsdynamik", von Stephan Kühne.

Heft Nr. 253/1997 – "Distribution and role of microprotozoa in the Southern Ocean", by Christine Klaas.

Heft Nr. 254/1997 – „Die spätquartäre Klima- und Umweltgeschichte der Bunger-Oase, Ostantarktis", von Thomas Kulbe

Heft Nr. 255/1997 – "Scientific Cruise Report of the Arctic Expedition ARK-XIII/2 of RV 'Polarstern' in 1997", edited by Ruediger Stein and Kirsten Fahl.

Heft Nr. 256/1998 – „Das Radionuklid Tritium im Ozean: Meßverfahren und Verteilung von Tritium im Südatlantik und im Weddellmeer", von Jürgen Sültenfuß.

Heft Nr. 257/1998 – „Untersuchungen der Saisonalität von atmosphärischem Dimethylsulfid in der Arktis und Antarktis", von Christoph Kleefeld.

Heft Nr. 258/1998 – „Bellingshausen- und Amundsenmeer: Entwicklung eines Sedimentationsmodells", von Frank-Oliver Nitsche.

Heft Nr. 259/1998 – "The Expedition ANTARKTIS-XIV/4 of RV 'Polarstern' in 1997", by Dieter K. Fütterer.

* **Heft Nr. 260/1998** – „Die Diatomeen der Laptevsee (Arktischer Ozean): Taxonomie und biogeographische Verbreitung", von Holger Cremer

Heft Nr. 261/1998 – „Die Krustenstruktur und Sedimentdecke des Eurasischen Beckens, Arktischer Ozean: Resultate aus seismischen und gravimetrischen Untersuchungen", von Estella Weigelt.

Heft Nr. 262/1998 – "The Expedition ARKTIS-XIII/3 of RV 'Polarstern' in 1997", by Gunther Krause.

Heft Nr. 263/1998 – „Thermo-tektonische Entwicklung von Oates Land und der Shackleton Range (Antarktis) basierend auf Spaltspuranalysen", von Thorsten Schäfer.

Heft Nr. 264/1998 – „Messungen der stratosphärischen Spurengase ClO, HCl, O_3, N_2O, H_2O und OH mittels flugzeuggetragener Submillimeterwellen-Radiometrie", von Joachim Urban.

Heft Nr. 265/1998 – „Untersuchungen zu Massenhaushalt und Dynamik des Ronne Ice Shelfs, Antarktis", von Astrid Lambrecht.

Heft Nr. 266/1998 – "Scientific Cruise Report of the Kara Sea Expedition of RV 'Akademic Boris Petrov' in 1997", edited by Jens Matthiessen and Oleg Stepanets.

Heft Nr. 267/1998 – „Die Expedition ANTARKTIS-XIV mit FS ‚Polarstern' 1997. Bericht vom Fahrtabschnitt ANT-XIV/3", herausgegeben von Wilfried Jokat und Hans Oerter.

Heft Nr. 268/1998 – „Numerische Modellierung der Wechselwirkung zwischen Atmosphäre und Meereis in der arktischen Eisrandzone", von Gerit Birnbaum.

Heft Nr. 269/1998 – "Katabatic wind and Boundary Layer Front Experiment around Greenland (KABEG '97)", by Günther Heinemann.

Heft Nr. 270/1998 – "Architecture and evolution of the continental crust of East Greenland from integrated geophysical studies", by Vera Schlindwein.

Heft Nr. 271/1998 – "Winter Expedition to the Southwestern Kara Sea - Investigations on Formation and Transport of Turbid Sea-Ice", by Dirk Dethleff, Per Loewe, Dominik Weiel, Hartmut Nies, Gesa Kuhlmann, Christian Bahe and Gennady Tarasov.

Heft Nr. 272/1998 – „FTIR-Emissionsspektroskopische Untersuchungen der arktischen Atmosphäre", von Edo Becker.

Heft Nr. 273/1998 – „Sedimentation und Tektonik im Gebiet des Agulhas Rückens und des Agulhas Plateaus (‚SETA-RAP')", von Gabriele Uenzelmann-Neben.

Heft Nr. 274/1998 – "The Expedition ANTARKTIS XIV/2", by Gerhard Kattner.

Heft Nr. 275/1998 – „Die Auswirkung der 'NorthEastWater'-Polynya auf die Sedimentation von NO-Grönland und Untersuchungen zur Paläo-Ozeanographie seit dem Mittelweichsel", von Hanne Notholt.

Heft Nr. 276/1998 – „Interpretation und Analyse von Potentialfelddaten im Weddellmeer, Antarktis: der Zerfall des Superkontinents Gondwana", von Michael Studinger.

Heft Nr. 277/1998 – „Koordiniertes Programm Antarktisforschung". Berichtskolloquium im Rahmen des Koordinierten Programms „Antarktisforschung mit vergleichenden Untersuchungen in arktischen Eisgebieten", herausgegeben von Hubert Miller.

Heft Nr. 278/1998 – „Messung stratosphärischer Spurengase über Ny-Ålesund, Spitzbergen, mit Hilfe eines bodengebundenen Mikrowellen-Radiometers", von Uwe Raffalski.

Heft Nr. 279/1998 – "Arctic Paleo-River Discharge (APARD). A New Research Programme of the Arctic Ocean Science Board (AOSB)", edited by Ruediger Stein.

Heft Nr. 280/1998 – „Fernerkundungs- und GIS-Studien in Nordostgrönland" von Friedrich Jung-Rothenhäusler.

Heft Nr. 281/1998 – „Rekonstruktion der Oberflächenwassermassen der östlichen Laptevsee im Holozän anhand von aquatischen Palynomorphen", von Martina Kunz-Pirrung.

Heft Nr. 282/1998 – "Scavenging of ^{231}Pa and ^{230}Th in the South Atlantic: Implications for the use of the $^{231}Pa/^{230}Th$ ratio as a paleoproductivity proxy", by Hans-Jürgen Walter.

Heft Nr. 283/1998 – „Sedimente im arktischen Meereis - Eintrag, Charakterisierung und Quantifizierung", von Frank Lindemann.

Heft Nr. 284/1998 – „Langzeitanalyse der antarktischen Meereisbedeckung aus passiven Mikrowellendaten", von Christian H. Thomas.

Heft Nr. 285/1998 – „Mechanismen und Grenzen der Temperaturanpassung beim Pierwurm *Arenicola marina* (L.)", von Angela Sommer.

Heft Nr. 286/1998 – „Energieumsätze benthischer Filtrierer der Potter Cove (King George Island, Antarktis)", von Jens Kowalke.

Heft Nr. 287/1998 – "Scientific Cooperation in the Russian Arctic: Research from the Barents Sea up to the Laptev Sea", edited by Eike Rachor.

Heft Nr. 288/1998 – „Alfred Wegener. Kommentiertes Verzeichnis der schriftlichen Dokumente seines Lebens und Wirkens", von Ulrich Wutzke.

Heft Nr. 289/1998 – "Retrieval of Atmospheric Water Vapor Content in Polar Regions Using Spaceborne Microwave Radiometry", by Jungang Miao.

Heft Nr. 290/1998 – „Strukturelle Entwicklung und Petrogenese des nördlichen Kristallingürtels der Shackleton Range, Antarktis: Proterozoische und Ross-orogene Krustendynamik am Rand des Ostantarktischen Kratons", von Axel Brommer.

Heft Nr. 291/1998 – „Dynamik des arktischen Meereises - Validierung verschiedener Rheologieansätze für die Anwendung in Klimamodellen", von Martin Kreyscher.

Heft Nr. 292/1998 – „Anthropogene organische Spurenstoffe im Arktischen Ozean, Untersuchungen chlorierter Biphenyle und Pestizide in der Laptevsee, technische und methodische Entwicklungen zur Probenahme in der Arktis und zur Spurenstoffanalyse", von Sven Utschakowski.

Heft Nr. 293/1998 – „Rekonstruktion der spätquartären Klima- und Umweltgeschichte der Schirmacher Oase und des Wohlthat Massivs (Ostantarktika)", von Markus Julius Schwab.

Heft Nr. 294/1998 – „Besiedlungsmuster der benthischen Makrofauna auf dem ostgrönländischen Kontinentalhang", von Klaus Schnack.

Heft Nr. 295/1998 – „Gehäuseuntersuchungen an planktischen Foraminiferen hoher Breiten: Hinweise auf Umweltveränderungen während der letzten 140.000 Jahre", von Harald Hommers.

Heft Nr. 296/1998 – "Scientific Cruise Report of the Arctic Expedition ARK-XIII/1 of RV 'Polarstern' in 1997", edited by Michael Spindler, Wilhelm Hagen and Dorothea Stübing.

Heft Nr. 297/1998 – „Radiometrische Messungen im arktischen Ozean - Vergleich von Theorie und Experiment", von Klaus-Peter Johnsen.

Heft Nr. 298//1998 – "Patterns and Controls of CO_2 Fluxes in Wet Tundra Types of the Taimyr Peninsula, Siberia - the Contribution of Soils and Mosses", by Martin Sommerkorn.

Heft Nr. 299/1998 – "The Potter Cove coastal ecosystem, Antarctica. Synopsis of research performed within the frame of the Argentinean-German Cooperation at the Dallmann Laboratory and Jubany Station (Kind George Island, Antarctica, 1991 - 1997)", by Christian Wiencke, Gustavo Ferreyra, Wolf Arntz & Carlos Rinaldi.

Heft Nr. 300/1999 – "The Kara Sea Expedition of RV 'Akademik Boris Petrov' 1997: First Results of a Joint Russian-German Pilot Study", edited by Jens Matthiessen, Oleg V. Stepanets, Ruediger Stein, Dieter K. Fütterer, and Eric M. Galimov.

Heft Nr. 301/1999 – "The Expedition ANTARKTIS XV/3 (EASIZ II)", edited by Wolf E. Arntz and Julian Gutt.

Heft Nr. 302/1999 – „Sterole im herbstlichen Weddellmeer (Antarktis): Großräumige Verteilung, Vorkommen und Umsatz", von Anneke Mühlebach.

Heft Nr. 303/1999 – „Polare stratosphärische Wolken: Lidar-Beobachtungen, Charakterisierung von Entstehung und Entwicklung", von Jens Biele.

Heft Nr. 304/1999 – „Spätquartäre Paläoumweltbedingungen am nördlichen Kontinentalrand der Barents- und Kara-See. Eine Multi-Parameter-Analyse", von Jochen Knies.

Heft Nr. 305/1999 – "Arctic Radiation and Turbulence Interaction Study (ARTIST)", by Jörg Hartmann, Frank Albers, Stefania Argentini, Axel Bochert, Ubaldo Bonafé, Wolfgang Cohrs, Alessandro Conidi, Dietmar Freese, Teodoro Georgiadis, Alessandro Ippoliti, Lars Kaleschke, Christof Lüpkes, Uwe Maixner, Giangiuseppe Mastrantonio, Fabrizio Ravegnani, Andreas Reuter, Giuliano Trivellone and Angelo Viola.

Heft Nr. 306/1999 – "German-Russian Cooperation: Biogeographic and biostratigraphic investigations on selected sediment cores from the Eurasian continental margin and marginal seas to analyze the Late Quaternary climatic variability", edited by Robert R. Spielhagen, Max S. Barash, Gennady I. Ivanov, and Jörn Thiede.

Heft Nr. 307/1999 – „Struktur und Kohlenstoffbedarf des Makrobenthos am Kontinentalhang Ostgrönlands", von Dan Seiler.

Heft Nr. 308/1999 – "ARCTIC '98: The Expedition ARK-XIV/1a of RV 'Polarstern' in 1998", edited by Wilfried Jokat.

Heft Nr. 309/1999 – „Variabilität der arktischen Ozonschicht: Analyse und Interpretation bodengebundener Millimeterwellenmessungen", von Björn-Martin Sinnhuber.

Heft Nr. 310/1999 – „Rekonstruktion von Meereisdrift und terrigenem Sedimenteintrag im Spätquartär: Schwermineralassoziationen in Sedimenten des Laptev-See-Kontinentalrandes und des zentralen Arktischen Ozeans", von Marion Behrends.

Heft Nr. 311/1999 – „Parameterisierung atmosphärischer Grenzschichtprozesse in einem regionalen Klimamodell der Arktis", von Christoph Abegg.

Heft Nr. 312/1999 – „Solare und terrestrische Strahlungswechselwirkung zwischen arktischen Eisflächen und Wolken", von Dietmar Freese.

Heft Nr. 313/1999 – "Snow accumulation on Ekströmisen, Antarctica", by Elisabeth Schlosser, Hans Oerter and Wolfgang Graf.

Heft Nr. 314/1999 – „Die Expedition ANTARKTIS XV/4 des Forschungsschiffes ‚Polarstern' 1998", herausgegeben von Eberhard Fahrbach.

Heft Nr. 315/1999 – "Expeditions in Siberia in 1998", edited by Volker Rachold.

Heft Nr. 316/1999 – „Die postglaziale Sedimentationsgeschichte der Laptewsee: schwermineralogische und sedimentpetrographische Untersuchungen", von Bernhard Peregovich.

Heft-Nr. 317/1999 – „Adaption an niedrige Temperaturen: Lipide in Eisdiatomeen", von Heidi Lehmal.

Heft-Nr. 318/1999 – „Effiziente parallele Lösungsverfahren für elliptische partielle Differentialgleichungen in der numerischen Ozeanmodellierung", von Natalja Rakowsky.

Heft-Nr. 319/1999 – "The Ecology of Arctic Deep-Sea Copepods (Euchaetidae and Aetideidae). Aspects of their Distribution, Trophodynamics and Effect on the Carbon Flux", by Holger Auel.

Heft-Nr. 320/1999 – "Modellstudien zur arktischen stratosphärischen Chemie im Vergleich mit Meßdaten", von Veronika Eyring.

Heft-Nr. 321/1999 – "Analyse der optischen Eigenschaften des arktischen Aerosols", von Dagmar Nagel.

Heft-Nr. 322/1999 – "Messungen des arktischen stratosphärischen Ozons: Vergleich der Ozonmessungen in Ny-Ålesund, Spitzbergen, 1997 und 1998", von Jens Langer.

Heft-Nr. 323/1999 – "Untersuchung struktureller Elemente des südöstlichen Weddellmeeres / Antarktis auf der Basis mariner Potentialfelddaten", von Uwe F. Meyer.

Heft-Nr. 324/1999 – "Geochemische Verwitterungstrends eines basaltischen Ausgangsgesteins nach dem spätpleistozänen Gletscherrückzug auf der Taimyrhalbinsel (Zentralsibirien) - Rekonstruktion an einer sedimentären Abfolge des Lama Sees", von Stefanie K. Harwart.

Heft-Nr. 325/1999 – "Untersuchungen zur Hydrologie des arktischen Meereises - Konsequenzen für den kleinskaligen Stofftransport", von Johannes Freitag.

Heft-Nr. 326/1999 – "Die Expedition ANTARKTIS XIV/2 des Forschungsschiffes 'Polarstern' 1998", herausgegeben von Eberhard Fahrbach.

Heft-Nr. 327/1999 – "Gemeinschaftsanalytische Untersuchungen der Harpacticoidenfauna der Magellanregion, sowie erste similaritätsanalytische Vergleiche mit Assoziationen aus der Antarktis", von Kai Horst George.

Heft-Nr. 328/1999 – "Rekonstruktion der Paläo-Umweltbedingungen am Laptev-See-Kontinentalrand während der beiden letzten Glazial/Interglazial-Zyklen anhand sedimentologischer und mineralogischer Untersuchungen", von Claudia Müller.

Heft-Nr. 329/1999 – "Räumliche und zeitliche Variationen atmosphärischer Spurengase aus bodengebundenen Messungen mit Hilfe eines Michelson interferometers", von Justus Notholt.

Heft-Nr. 330/1999 – "The 1998 Danish-German Excursion to Disko Island, West Greenland", edited by Angelika Brandt, Helge A. Thomsen, Henning Heide-Jørgensen, Reinhard M. Kristensen and Hilke Ruhberg.

Heft-Nr. 331/1999 – "Poseidon" Cruise No. 243 (Reykjavik - Greenland - Reykjavik, 24 August - 11 September 1998): Climate change and the Viking-age fjord environment of the Eastern Settlement, sw Greenland", by Gerd Hoffmann, Antoon Kuijpers, and Jörn Thiede.

Heft-Nr. 332/1999 – "Modeling of marine biogeochemical cycles with an emphasis on vertical particle fluxes", by Regina Usbeck.

Heft-Nr. 333/1999 – "Die Tanaidaceenfauna des Beagle-Kanals und ihre Beziehungen zur Fauna des antarktischen Festlandsockels", von Anja Schmidt.

Heft-Nr. 334/1999 – "D-Aminosäuren als Tracer für biogeochemische Prozesse im Fluß-Schelf-Ozean-System der Arktis", von Hans Peter Fitznar.

Heft-Nr. 335/1999 – "Ökophysiologische Ursachen der limitierten Verbreitung reptanter decapoder Krebse in der Antarktis", von Markus Frederich.

Heft-Nr. 336/1999 – "Ergebnisse der Untersuchung des grönländischen Inlandeises mit dem elektromagnetischen Reflexionsverfahren in der Umgebung von NGRIP", von Fidan Göktas.

Heft-Nr. 337/1999 – "Paleozoic and mesozoic tectono-thermal history of central Dronning Maud Land, East Antarctica, – evidence from fission-track thermochronology", by Stefanie Meier.

Heft-Nr. 338/1999 – "Probleme hoher Stoffwechselraten bei Cephalopoden aus verschiedenen geographischen Breiten", von Susanne Zielinski.

Heft-Nr. 339/1999 – "The Expedition ARKTIS XV/1", edited by Gunther Krause.

Heft-Nr. 340/1999 – "Microbial Properties and Habitats of Permafrost Soils on Taimyr Peninsula, Central Siberia", by Nicolé Schmidt.

Heft-Nr. 341/1999 – "Photoacclimation of phytoplankton in different biogeochemical provinces of the Southern Ocean and its significance for estimating primary production", by Astrid Bracher.

Heft-Nr. 342/1999 – "Modern and Late Quaternary Depositional Environment of the St. Anna Trough Area, Northern Kara Sea", edited by Ruediger Stein, Kirsten Fahl, Gennadij I. Ivanov, Michael A. Levitan, and Gennady Tarasov.

Heft-Nr. 343/1999 – "ESF-IMPACT Workshop/Oceanic impacts: mechanisms and environmental perturbations, 15-17 April 1999 in Bremerhaven", edited by Rainer Gersonde and Alexander Deutsch.

Heft-Nr. 344/1999 – "Die Klimageschichte der hohen nördlichen Breiten seit dem mittleren Miozän: Hinweise aus sedimentologischen-tonmineralogischen Analysen (ODP Leg 151, zentrale Framstraße)", von Amelie Winkler.

Heft-Nr. 345/1999 – "Kurzfristige Klimaschwankungen im Scotiameer und Ergebnisse zur Kalbungsgeschichte der Antarktis während der letzten 200000 Jahre", von Annette Hofmann.

Heft-Nr. 346/2000 – "Glazialmarine Sedimentationsentwicklung am westantarktischen Kontinentalrand im Amundsen- und Bellingshausenmeer - Hinweise auf Paläoumweltveränderungen während der quartären Klimazyklen", von Claus-Dieter Hillenbrand.

Heft-Nr. 347/2000 – "Zur Ökologie des Phytoplanktons im arktischen Laptevmeer - ein jahreszeitlicher Vergleich", von Kirsten Tuschling.

Heft-Nr. 348/2000 – "Untersuchungen zum Fettstoffwechsel des Südlichen See-Elefanten *(Mirounga leonina L.)* in der Antarktis", von Sven Ramdohr.

Heft-Nr. 349/2000 – "Licht- und Temperatureinfluß auf den enzymatischen Oxidationsschutz der antarktischen Eisdiatomee *Entomoneis kufferathii* Manguin", von Raimund Schriek.

Heft-Nr. 350/2000 – "Die Expedition ARKTIS XV/3 des Forschungsschiffes 'Polarstern' 1999", herausgegeben von Ursula Schauer.

Heft-Nr. 351/2000 – "Dissolution kinetics of biogenic silica in marine environments", by Dirk Rickert.

Heft-Nr. 352/2000 – "Geometrie und Kinematik des tertiären Deckenbaus im West Spitzbergen Falten- und Überschiebungsgürtel, Brøggerhalvøya, Svalbard", von Kerstin Saalmann.

Heft-Nr. 353/2000 – "Zur Ökologie der Benthos-Foraminiferen der Potter Cove (King George Island, Antarktis)", von Michaela Mayer.

Heft-Nr. 354/2000 – "Expeditions in Siberia in 1999", edited by Volker Rachold.

* vergriffen / out of print.
** nur noch beim Autor / only from the author.